

ELEVENTH EDITION



Brenner & Rector's THE KIDNEY

ALAN S.L. YU | GLENN M. CHERTOW | VALÉRIE A. LUYCKX
PHILIP A. MARSDEN | KARL SKORECKI | MAARTEN W. TAAL

EY

VALÉRIE A. LUYCKX
MAARTEN W. TAAL

VOLUME ONE

VOLUME TWO

2-Volume Set

ELEVENTH EDITION



Brenner & Rector's
THE KIDNEY

VOLUME ONE

ALAN S.L. YU, MB, BChir

Harry Statland and Solon Summerfield Professor of Medicine
Director, Division of Nephrology and Hypertension and the Jared Grantham Kidney Institute
University of Kansas Medical Center
Kansas City, Kansas

GLENN M. CHERTOW, MD, MPH

Norman S. Coplon/Satellite Healthcare Professor of Medicine
Department of Medicine
Division of Nephrology
Stanford University School of Medicine
Palo Alto, California

VALÉRIE A. LUYCKX, MBBCh, MSc

Affiliate Lecturer
Renal Division
Brigham and Women's Hospital
Harvard Medical School
Boston, Massachusetts;
Institute of Biomedical Ethics and the History of Medicine
University of Zürich
Zürich, Switzerland

PHILIP A. MARSDEN, MD

Professor of Medicine
Elisabeth Hofmann Chair in Translational Research
Oreopoulos-Baxter Division Director of Nephrology
University of Toronto
Toronto, Ontario, Canada

KARL SKORECKI, MD, FRCP(C), FASN

Dean, Azrieli Faculty of Medicine
Bar-Ilan University
Safed, Israel

MAARTEN W. TAAL, MBChB, MMed, MD, FCP(SA), FRCP

Department of Renal Medicine
Royal Derby Hospital
Derby, United Kingdom;
Centre for Kidney Research and Innovation
Division of Medical Sciences and Graduate Entry Medicine
School of Medicine
University of Nottingham
Nottingham, United Kingdom

Special Assistant to the Editors

WALTER G. WASSER, MD

Attending Physician, Division of Nephrology
Mayanei HaYeshua Medical Center
Bnei Brak, Israel;
Rambam Health Care Campus
Haifa, Israel



ELSEVIER

Elsevier
1600 John F. Kennedy Blvd.
Ste 1800
Philadelphia, PA 19103-2899

BRENNER & RECTOR'S THE KIDNEY, ELEVENTH EDITION

Set ISBN: 978-0-323-53265-5
Volume 1 ISBN: 978-0-323-75933-5
Volume 2 ISBN: 978-0-323-75934-2

Copyright © 2020 by Elsevier, Inc. All rights reserved.

No part of this publication may be reproduced or transmitted in any form or by any means, electronic or mechanical, including photocopying, recording, or any information storage and retrieval system, without permission in writing from the publisher. Details on how to seek permission, further information about the Publisher's permissions policies and our arrangements with organizations such as the Copyright Clearance Center and the Copyright Licensing Agency, can be found at our website: www.elsevier.com/permissions.

This book and the individual contributions contained in it are protected under copyright by the Publisher (other than as may be noted herein).

Notice

Practitioners and researchers must always rely on their own experience and knowledge in evaluating and using any information, methods, compounds or experiments described herein. Because of rapid advances in the medical sciences, in particular, independent verification of diagnoses and drug dosages should be made. To the fullest extent of the law, no responsibility is assumed by Elsevier, authors, editors or contributors for any injury and/or damage to persons or property as a matter of products liability, negligence or otherwise, or from any use or operation of any methods, products, instructions, or ideas contained in the material herein.

Previous editions copyrighted 2016, 2012, 2008, 2004, 2000, 1996, 1991, 1986, 1981, and 1976.

Library of Congress Control Number: 2019934877

Senior Content Strategist: Nancy Anastasi Duffy
Senior Content Development Specialist: Joanie Milnes
Publishing Services Manager: Julie Eddy
Senior Project Manager: Rachel E. McMullen
Design Direction: Renee Duenow

Printed in Canada

Last digit is the print number: 9 8 7 6 5 4 3 2 1



Working together
to grow libraries in
developing countries

www.elsevier.com • www.bookaid.org

Dedicated to

Barry M. Brenner, MD

*our mentor and role model, whose vision continues to challenge and inspire us
and to*

Joan Ryan

for her patient stewardship of The Kidney through three wonderful editions

Contributors

Andrew Advani, BSc, MBChB (Hons), PhD, FRCP(UK), FASN

Associate Professor of Medicine
University of Toronto;
St. Michael's Hospital
Toronto, Ontario, Canada

Todd Alexander, MD, PhD

Pediatric Nephrologist and Professor
Department of Paediatrics
University of Alberta
Edmonton, Alberta, Canada

Michael Allon, MD

Professor of Medicine
Division of Nephrology
University of Alabama at Birmingham
Birmingham, Alabama

Gerald B. Appel, MD

Professor of Clinical Medicine
Department of Medicine
Columbia University Medical Center
New York, New York

Suheir Assady, MD, PhD

Director, Department of Nephrology and Hypertension
Rambam Health Care Campus
Haifa, Israel

Colin Baigent, BMBCh, MA, MSc, FRCP, FFPH

Professor of Epidemiology
Nuffield Department of Population Health
University of Oxford
Oxford, Great Britain

George L. Bakris, MD

Professor and Director
American Heart Association Comprehensive Hypertension
Center
Department of Medicine
University of Chicago Medicine
Chicago, Illinois

Marisa Battistella, PharmD

Associate Professor
University Health Network/Leslie Dan Faculty of
Pharmacy
University of Toronto,
Toronto, Ontario, Canada

Srinivasan Beddhu, MD

Professor of Internal Medicine
Department of Internal Medicine
University of Utah School of Medicine
Salt Lake City, Utah

Aminu K. Bello, MD, PhD

Assistant Professor/Nephrologist
Department of Medicine
University of Alberta
Edmonton, Alberta, Canada

Theresa J. Berndt, MD

Assistant Professor of Medicine
Division of Nephrology and Hypertension
Mayo Clinic College of Medicine
Rochester, Minnesota

John F. Bertram, BSc, PhD, DSc

Biomedicine Discovery Institute
Development and Stem Cells Program
Department of Anatomy and Developmental Biology
Monash University
Clayton, Victoria, Australia

Vivek Bhalla, MD

Assistant Professor
Medicine/Nephrology
Stanford University School of Medicine
Stanford, California

Daniel G. Bichet, MD

Professor
Department of Medicine and Physiology
University of Montreal;
Nephrologist
Department of Medicine
Hôpital du Sacré-Coeur de Montréal
Montréal, Québec, Canada

Boris Bikbov, MD, PhD

Researcher
Department of Renal Medicine
Istituto di Ricerche Farmacologiche Mario Negri IRCCS
Ranica, Bergamo, Italy

Detlef Bockenhauer, MD, PhD

Professor
Department of Renal Medicine
University College London;
Doctor
Department of Nephrology
Great Ormond Street Hospital for Children
London, Great Britain

Alain Bonnardeaux, MD, PhD

Full Professor
Department of Medicine
Université de Montréal
Montréal, Québec, Canada

Josée Bouchard, MD, FRCPC

Associate Professor of Medicine
Department of Nephrology
Hôpital du Sacré-Coeur de Montréal
University of Montréal
Montréal, Québec, Canada

Richard M. Breyer, PhD

Professor
Division of Nephrology and Hypertension
Vanderbilt University School of Medicine
Nashville, Tennessee

Stefan Broer, PhD

Research School of Biology
Australian National University
Canberra, Australian Capital Territory, Australia

Carlo Brugnara, MD

Department of Laboratory Medicine
Boston Children's Hospital
Boston, Massachusetts

Catherine R. Butler, MD

Fellow
Department of Medicine, Division of Nephrology
University of Washington
Seattle, Washington

Héloïse Cardinal, MD, PhD

Associate Professor, Division of Nephrology
Department of Medicine
Université de Montréal
Montréal, Québec, Canada

Juan Jesús Carrero, Pharm, PhD Pharm, PhD Med, MBA

Professor
Department of Medical Epidemiology and Biostatistics
Karolinska Institutet
Stockholm, Sweden

Daniel C. Cattran, MD

Professor of Medicine
Department of Medicine
University Health Network;
Senior Scientist
Toronto General Research Institute
University Health Network
Toronto, Ontario, Canada

Tak Mao Daniel Chan, MBBS, MD

Chief of Nephrology
Department of Medicine
University of Hong Kong, Queen Mary Hospital
Hong Kong, Hong Kong

Tara I. Chang, MD, MS

Associate Professor of Medicine
Division of Nephrology
Stanford University
Palo Alto, California

Glenn M. Chertow, MD, MPH

Norman S. Coplon/Satellite Healthcare Professor of
Medicine
Department of Medicine
Division of Nephrology
Stanford University School of Medicine
Palo Alto, California

Andrew A. Chin, MD

Division of Nephrology
Department of Internal Medicine
University of California, Davis School of Medicine
Sacramento, California

Yeoungjee Cho, MBBS(hons), FRACP, PhD

Consultant Nephrologist
Nephrology
Princess Alexandra Hospital;
Clinical Trialist
Australasian Kidney Trials Network
University of Queensland
Brisbane, Queensland, Australia

Michel Chonchol, MD

Professor of Medicine
Division of Renal Diseases and Hypertension
University of Colorado Denver Anschutz Medical Center
Aurora, Colorado

Marta Christov, MD, PhD

Assistant Professor of Medicine
Westchester Medical Center and New York Medical
College
Valhalla, New York

William L. Clapp, MD

Professor of Pathology, Director of Renal Pathology
Department of Pathology, Immunology and Laboratory
Medicine
University of Florida College of Medicine
Gainesville, Florida

Rachel Becker Cohen, MD

Institute of Pediatric Nephrology
Shaare Zedek Medical Center;
Hadassah-Hebrew University School of Medicine
Jerusalem, Israel

Kelsey Connelly, MD

Faculty of Medicine
University of Manitoba
Winnipeg, Manitoba, Canada

H. Terence Cook, MB BS, FRCPath

Professor of Renal Pathology
Department of Medicine
Imperial College
London, Great Britain

Josef Coresh, MD, PhD

Professor
Epidemiology, Medicine and Biostatistics
Johns Hopkins University;
Director
G.W. Comstock Center for Public Health and Prevention
Johns Hopkins Bloomberg School of Public Health
Baltimore, Maryland

Ricardo Correa-Rotter, MD

Head
Department of Nephrology and Mineral Metabolism
Instituto Nacional de Ciencias Médicas y Nutrición
Salvador Zubirán
Mexico City, Mexico

Shawn E. Cowper, MD

Associate Professor of Dermatology and Pathology
Department of Dermatology
Yale University
New Haven, Connecticut

Vivette D. D'Agati, MD

Professor of Pathology
Columbia University College of Physicians and Surgeons;
Director, Renal Pathology Laboratory
Columbia University Medical Center
New York, New York

Kevin Damman, MD, PhD

Doctor
Department of Cardiology
University Medical Center Groningen
Groningen, The Netherlands

Mogamat Razeen Davids, MBChB, FCP(SA), MMed

Professor
Division of Nephrology, Department of Medicine
Stellenbosch University and Tygerberg Hospital
Cape Town, South Africa

Sara Davison, BSc, MD, MSc

Chief of Nephrology
Department of Medicine
University of Alberta
Edmonton, Alberta, Canada

Aleksander Denic, MD

Division of Nephrology and Hypertension
Mayo Clinic
Rochester, Minnesota

Bradley M. Denker, MD

Associate Professor of Medicine
Department of Medicine
Harvard Medical School;
Clinical Chief
Renal Division
Beth Israel Deaconess Medical Center;
Chief of Nephrology
Harvard Vanguard Medical Associates
Boston, Massachusetts

Thomas A. Depner, BS, MD

Division of Nephrology
Department of Internal Medicine
University of California, Davis School of Medicine
Sacramento, California

Thomas D. DuBose, Jr., MD

Professor Emeritus of Medicine
Wake Forest School of Medicine
Winston-Salem, North Carolina

Vinay A. Duddalwar, MD, FRCR

Professor of Radiology and Urology
Department of Radiology
Keck School of Medicine, University of Southern
California
Los Angeles, California

Kai-Uwe Eckardt, MD

Professor of Medicine
Director of the Medical Department,
Division of Nephrology and Internal Intensive Care
Medicine
Charité–Universitätsmedizin Berlin
Berlin, Germany

William J. Elliott, MD, PhD

Professor of Preventive Medicine, Internal Medicine and
Pharmacology
Pacific Northwest University of Health Sciences;
Head, Division of Pharmacology
Pacific Northwest University of Health Sciences
Yakima, Washington

David H. Ellison, MD

Professor
Department of Internal Medicine
Division of Nephrology and Hypertension
Oregon Health & Science University
Portland, Oregon

Ronald J. Falk, MD

Nan and Hugh Cullman Eminent Professor
 Chair, Department of Medicine
 Director, UNC Kidney Center
 Chapel Hill, North Carolina

Robert Andrew Fenton, BSc, MSc, PhD

Professor of Molecular Cell Biology
 Department of Biomedicine
 Aarhus University
 Aarhus, Denmark

Alessia Fornoni, MD, PhD

Professor of Medicine and Chief
 Division of Nephrology and Hypertension
 University of Miami Miller School of Medicine;
 Director
 Katz Family Drug Discovery Center
 Miami, Florida

Benjamin S. Freedman, PhD

Assistant Professor
 Department of Pathology (Adjunct) and Department of
 Medicine
 Division of Nephrology, Kidney Research Institute, and
 Institute for Stem Cell and Regenerative Medicine
 University of Washington School of Medicine
 Seattle, Washington

Yaakov Frishberg, MD

Institute of Pediatric Nephrology
 Shaare Zedek Medical Center;
 Hebrew University Hadassah School of Medicine
 Jerusalem, Israel

Jørgen Frøkiaer, MD, DMSci

Department of Clinical Medicine
 Aarhus University
 Aarhus, Denmark

John W. Funder, MD, PhD, FRCP, FRACP

Distinguished Scholar
 Hudson Institute and Monash University
 Clayton, Victoria, Australia

Amit X. Garg, MD

Professor
 Division of Nephrology Department of Medicine
 Western University
 Institute for Clinical Evaluative Sciences
 London, Ontario, Canada

Marc Ghannoum, MD

Associate Professor of Medicine
 University of Montreal, Verdun Hospital
 Montréal, Québec, Canada

Mohammed Benghanem Gharbi, MD

Nephrology Department
 Faculty of Medicine and Pharmacy of Casablanca
 University Hassan II of Casablanca
 Casablanca, Morocco

Richard E. Gilbert, MBBS, PhD, FRACP, FACP, FRCPC

Professor
 Department of Medicine
 University of Toronto;
 Head
 Division of Endocrinology
 St. Michael's Hospital
 Toronto, Ontario, Canada

Richard J. Glasscock, MD

Emeritus Professor
 Department of Medicine
 Geffen School of Medicine at UCLA
 Los Angeles, California

Nimrit Goraya, MD

Assistant Professor
 Division of Nephrology and Hypertension,
 Program Director
 Nephrology Fellowship Program
 Baylor Scott and White Health
 Temple, Texas

Morgan E. Grams, MD, PhD

Associate Professor
 Division of Nephrology
 Johns Hopkins University
 Baltimore, Maryland

Per Henrik Groop, MD, DMSc, FRCPE

Professor
 Clinicum
 University of Helsinki;
 Chief Physician
 Abdominal Center Nephrology
 Helsinki University Hospital
 Helsinki, Finland

Steven Habbous, MD

Department of Epidemiology and Biostatistics
 Western University
 London, Ontario, Canada

Yoshio N. Hall, MD, MS

Associate Professor
 Department of Medicine/Nephrology
 University of Washington;
 Investigator
 Kidney Research Institute | Medicine
 University of Washington
 Seattle, Washington

Mitchell L. Halperin, MD, FRCPC, FRS

Emeritus Professor of Medicine
 Department of Medicine/Nephrology
 St. Michaels Hospital
 University of Toronto
 Toronto, Ontario, Canada

L. Lee Hamm, MD

Senior Vice President and Dean
Tulane University School of Medicine
New Orleans, Louisiana

Peter C. Harris, PhD

Professor of Medicine and Biochemistry and Molecular Biology
Division of Nephrology and Hypertension
Mayo Clinic
Rochester, Minnesota

Raymond C. Harris, MD

Ann and Roscoe R. Robinson Professor of Medicine
Department of Medicine
Vanderbilt University School of Medicine
Nashville, Tennessee

Richard Haynes, MB, BCh, MRCP(UK)

Clinical Research Fellow
Nuffield Department of Population Health
University of Oxford;
Honorary Consultant Nephrologist
Oxford Kidney Unit
Oxford University Hospitals NHS Trust
Oxford, Great Britain

Marie Josée Hébert, MD

Professor
Vice-Rector of Research
Shire Chair in Nephrology, Transplantation and Renal Regeneration
Department of Medicine
Université de Montréal
Montréal, Québec, Canada

William G. Herrington, MA, MBBS, MD, MRCP

Associate Professor and MRC-Kidney Research UK
Professor David Kerr Clinician Scientist
MRC Population Health Research Unit
Nuffield Department of Population Health
Oxford, Great Britain

Ewout J. Hoorn, MD, PhD

Nephrologist and Associate Professor
Department of Internal Medicine, Division of Nephrology & Transplantation
Erasmus Medical Center
Rotterdam, The Netherlands

Thomas H. Hostetter, MD

Professor of Medicine and Vice Chairman for Research
Case Western Reserve University School of Medicine
Cleveland, Ohio

Susie L. Hu, MD

Associate Professor of Medicine
Medicine, Division of Kidney Disease and Hypertension
Warren Alpert Medical School of Brown University
Providence, Rhode Island

Tobias B. Huber, MD

Professor
Department of Medicine
University Medical Center Hamburg-Eppendorf
Hamburg, Germany

Hossein Jadvar, MD

Associate Professor of Radiology
Department of Radiology
Keck School of Medicine, University of Southern California
Los Angeles, California

Edgar A. Jaimes, MD

Chief, Renal Service
Department of Medicine
Memorial Sloan Kettering Cancer Center
New York, New York

Sarbjit Vanita Jassal, MD, MB, MRCP(UK), FRCPC

Staff Nephrologist and Director, Geriatric Dialysis Program
Division of Nephrology
University Health Network;
Professor of Medicine
University of Toronto
Toronto, Ontario, Canada

J. Charles Jennette, MD

Kenneth M. Brinkhous Distinguished Professor and Chair
Department of Pathology and Laboratory Medicine
School of Medicine;
Chief of Pathology and Laboratory Medicine Services,
UNC Hospitals;
Executive Director, UNC Nephropathology Division
University of North Carolina at Chapel Hill
Chapel Hill, North Carolina

David W. Johnson, MBBS (Hons), PhD, DMed(Res), FRACP, FASN

Director of Nephrology
Department of Nephrology
Princess Alexandra Hospital;
Deputy Chair
Australasian Kidney Trials Network
Brisbane, Queensland, Australia

Kamel S. Kamel, MD, FRCP(C)

St. Michael's Hospital
University of Toronto
Toronto, Ontario, Canada

S. Ananth Karumanchi, MD

Professor of Medicine
Director, Renovascular Research
Cedars-Sinai Medical Center
Los Angeles, California

David Kavanagh, MD, PhD

Professor of Complement Therapeutics
National Renal Complement Therapeutics Centre
Newcastle University
Newcastle upon Tyne, Great Britain

Frieder Keller, MD, Prof. Dr. Med.

Internal Medicine
University Hospital
Ulm, Germany

Christine J. Ko, MD

Professor of Dermatology and Pathology
Yale University
New Haven, Connecticut

Harbir Singh Kohli, MD, DM

Professor
Department of Nephrology
Post Graduate Institute of Medical Education and Research
Chandigarh, Union Territory, India

Jay L. Koyner, MD

Associate Professor of Medicine
Department of Medicine
Section of Nephrology
University of Chicago
Chicago, Illinois

Jordan Kreidberg, MD, PhD

Division of Nephrology
Boston Children's Hospital
Harvard Medical School
Boston, Massachusetts

Anoushka Krishnan, MBBS, FRACP

Department of Nephrology
Sir Charles Gairdner Hospital,
Perth, Western Australia, Australia

Rajiv Kumar, MD

Ruth and Vernon Taylor Professor of Medicine,
Biochemistry and Molecular Biology,
Distinguished Medical Investigator,
Chair Emeritus
Division of Nephrology and Hypertension
Mayo Clinic College of Medicine
Rochester, Minnesota

Gabrielle Lafreniere, MD, FRCPC

Assistant Professor of Medicine
Université Laval;
Geriatrician
Division of Geriatrics
Centre Hospitalier Universitaire de Québec
Québec, Quebec, Canada

Ngan N. Lam, MD, MSc

Doctor
Department of Medicine, Nephrology
University of Alberta
Edmonton, Alberta, Canada

Martin J. Landray, PhD FRCP

Professor of Medicine and Epidemiology
Clinical Trial Service Unit & Epidemiological Studies Unit
Nuffield Department of Population Health
Oxford, Great Britain

Harold E. Layton, PhD

Professor
Department of Mathematics
Duke University
Durham, North Carolina

Timmy Lee, MD, MSPH

Associate Professor of Medicine
Department of Medicine
University of Alabama at Birmingham
Birmingham, Alabama

Colin R. Lenihan, MB BCh BAO, PhD

Clinical Associate Professor
Department of Nephrology
Stanford University
Palo Alto, California

Krista L. Lentine, MD, PhD

Professor of Medicine
Center for Abdominal Transplantation
Saint Louis University
St. Louis, Missouri

Andrew S. Levey, MD

Chief Emeritus
William B. Schwartz Division of Nephrology
Tufts Medical Center;
Professor of Medicine
Dr. Gerald J. and Dorothy R. Friedman Professor Emeritus
Tufts University School of Medicine
Boston, Massachusetts

Adeera Levin, BSc, MD, FRCPC

Professor
Department of Medicine (Nephrology)
University of British Columbia;
Director
BC Provincial Renal Agency
Vancouver, British Columbia, Canada

Christoph Licht, MD

Pediatric Nephrologist
Department of Paediatrics
Senior Associate Scientist
Program in Cell Biology
Research Institute
The Hospital for Sick Children
Professor
Department of Paediatrics
University of Toronto
Toronto, Ontario, Canada

Bengt Lindholm, MD, PhD

Adjunct Professor
 Divisions of Baxter Novum and Renal Medicine
 Karolinska Institutet
 Stockholm, Sweden

Kathleen Liu, MD, PhD, MAS

Assistant Professor
 Divisions of Nephrology and Critical Care Medicine,
 University of California, San Francisco
 San Francisco, California

Valérie A. Luyckx, MBBCh, MSc

Affiliate Lecturer
 Renal Division
 Brigham and Women's Hospital
 Harvard Medical School
 Boston, Massachusetts;
 Institute of Biomedical Ethics and the History of Medicine
 University of Zürich
 Zürich, Switzerland

David A. Maddox, PhD

Professor
 Department of Internal Medicine
 University of South Dakota Sanford School of Medicine;
 Senior Research Scientist (WOC)
 Research & Development
 Sioux Falls VA Health Care System
 Sioux Falls, South Dakota

Yoshiro Maezawa, MD, PhD

Department of Clinical Cell Biology & Medicine
 Chiba University Graduate School of Medicine
 Chiba, Japan

Gary R. Matzke, BS Pharm, PharmD

Professor Emeritus
 Pharmacotherapy and Outcomes Science
 School of Pharmacy, Virginia Commonwealth University
 Richmond, Virginia

Ivan D. Maya, MD

Associate Professor
 Department of Medicine
 University of Central Florida
 Orlando, Florida

Sharon E. Maynard, MD

Associate Professor
 Department of Medicine
 Lehigh Valley Health Network
 University of South Florida Morsani College of Medicine
 Allentown, Pennsylvania

James A. McCormick, MD

Associate Professor
 Department of Medicine
 Division of Nephrology and Hypertension
 Oregon Health and Science University
 Portland, Oregon

Alicia Ann McDonough, PhD

Professor
 Integrative Anatomical Sciences
 Department of Cell and Neurobiology
 Keck School of Medicine, University of Southern
 California
 Los Angeles, California

John J.V. McMurray, BSc(Hons), MB ChB(Hons), MD, FESC, FACC, FAHA

British Heart Foundation Cardiovascular Research Centre
 University of Glasgow
 Glasgow, Scotland, Great Britain

Rajnish Mehrotra, MBBS, MD, MS

Section Head, Nephrology
 Harborview Medical Center;
 Division of Nephrology
 University of Washington
 Seattle, Washington

Timothy W. Meyer, MD

Professor
 Department of Medicine
 Stanford University
 Stanford, California;
 Staff Physician
 Department of Medicine
 VA Palo Alto HCS
 Palo Alto, California

Catherine Meyer-Schvesinger, MD

Professor
 Institute of Cellular and Integrative Physiology
 University Medical Center Hamburg-Eppendorf
 Hamburg, Germany

Orson W. Moe, MD

Professor
 Department of Internal Medicine
 Division of Nephrology
 UT Southwestern Medical Center;
 Director
 Charles and Jane Pak Center for Mineral Metabolism and
 Clinical Research
 UT Southwestern Medical Center
 Dallas, Texas

Karen M. Moritz, BSc, MSc, PhD

Child Health Research Centre and School of Biomedical
 Sciences
 The University of Queensland
 St. Lucia, Australia

Alvin H. Moss, MD

Director
Center for Health Ethics and Law
West Virginia University;
Professor of Medicine
Department of Medicine
Section of Geriatrics, Palliative Medicine and Hospice
West Virginia University
Morgantown, West Virginia

David B. Mount, MD

Clinical Chief
Renal Division
Brigham and Women's Hospital
Boston, Massachusetts

Karen A. Munger, PhD

Chief, Research and Development
Sioux Falls VA Health Care System;
Associate Professor of Medicine
Department of Internal Medicine
University of South Dakota
Sioux Falls, South Dakota

Behzad Najafian, MD

Associate Professor
Department of Pathology
University of Washington
Seattle, Washington

Luis Gabriel Navar, PhD

Professor and Chairman
Department of Physiology
Tulane University
New Orleans, Louisiana

Robert G. Nelson, MD, PhD

Senior Investigator
Chief, Chronic Kidney Disease Section
Phoenix Epidemiology and Clinical Research Branch
National Institute of Diabetes and Digestive and Kidney
Diseases
Phoenix, Arizona

Lindsay E. Nicolle, MD

Professor Emeritus
Department of Internal Medicine
University of Manitoba
Winnipeg, Manitoba, Canada

Sanjay K. Nigam, MD

Nancy Kaehr Chair in Research
Pediatrics, Medicine and Cellular Molecular Medicine
University of California, San Diego
La Jolla, California

Mark Douglas Okusa, MD

Professor of Medicine, Chief, Division of Nephrology
Department of Medicine
University of Virginia
Charlottesville, Virginia

Paul M. Palevsky, MD

Chief, Renal Section
VA Pittsburgh Healthcare System;
Professor of Medicine and Clinical & Translational
Science
Renal-Electrolyte Division
Department of Medicine
University of Pittsburgh
Pittsburgh, Pennsylvania

Suetonia C. Palmer, MB ChB, PhD, FRACP

Doctor
Department of Medicine
University of Otago Christchurch
Christchurch, New Zealand

Suzanne L. Palmer, MD

Professor of Radiology
Department of Radiology
Keck School of Medicine, University of Southern
California
Los Angeles, California

Chirag R. Parikh, MD, PhD

Director, Division of Nephrology
Ronald Peterson Professor of Medicine
Johns Hopkins School of Medicine
Baltimore, Maryland

David Pearce, MD

Professor
Department of Medicine
Division of Nephrology
Department of Cellular and Molecular Pharmacology
University of California San Francisco
San Francisco, California

Aldo J. Peixoto, MD

Professor of Medicine
Department of Internal Medicine (Nephrology)
Yale University School of Medicine;
Clinical Chief, Section of Nephrology
Department of Internal Medicine
Yale University School of Medicine
New Haven, Connecticut

William F. Pendergraft III, MD, PhD

Assistant Professor of Medicine
Division of Nephrology and Hypertension
Department of Medicine
University of North Carolina School of Medicine
Cambridge, Massachusetts

Mark A. Perazella, MD, MS

Professor of Medicine
Section of Nephrology
Yale University School of Medicine;
Director, Acute Dialysis Services
Yale-New Haven Hospital
New Haven, Connecticut

Norberto Perico, MD

Istituto di Ricerche Farmacologiche Mario Negri IRCCS
Bergamo, Italy

Martin R. Pollak, MD

Division of Nephrology
Beth Israel Deaconess Medical Center
Harvard Medical School
Boston, Massachusetts

Didier Portilla, MD

Professor
Department of Medicine
University of Virginia
Charlottesville, Virginia

Susan E. Quaggin, MD

Doctor
Feinberg Cardiovascular Research Institute
Northwestern University
Chicago, Illinois

Jai Radhakrishnan, MD, MS

Professor of Medicine at Columbia University Medical Center
Division of Nephrology, Department of Medicine
Columbia University Medical Center;
Clinical Chief
Division of Nephrology
New York Presbyterian Hospital
New York, New York

Rawi Ramadan, MD

Director, Medical Transplantation Unit
Department of Nephrology and Hypertension
Rambam Health Care Campus
Haifa, Israel

Heather N. Reich, MD, CM, PhD, FRCPC

Nephrologist, Clinician Scientist
Department of Nephrology
University Health Network;
Associate Professor
Gabor Zellerman Chair in Nephrology Research
Department of Medicine
University of Toronto
Toronto, Ontario, Canada

Andrea Remuzzi, MD

Istituto di Ricerche Farmacologiche Mario Negri IRCCS
Bergamo, Italy

Giuseppe Remuzzi, MD, FRCP

Istituto di Ricerche Farmacologiche Mario Negri IRCCS
Bergamo, Italy;
L. Sacco
Department of Biomedical and Clinical Sciences
University of Milan
Milan, Italy

Leonardo V. Riella, MD, PhD

Associate Physician
Brigham and Women's Hospital;
Assistant Professor of Medicine
Department of Medicine
Harvard Medical School
Boston, Massachusetts

Miquel C. Riella, MD, PhD

Professor of Medicine
Department of Medicine
Catholic University of Parana, Brazil;
Professor of Medicine
Department of Medicine
Evangelic School of Medicine
Curitiba, Brazil

Choni Rinat III, MD

Institute of Pediatric Nephrology
Shaare Zedek Medical Center;
Hadassah-Hebrew University School of Medicine
Jerusalem, Israel

Darren M. Roberts, BPharm, MBBS, PhD, FRACP

Visiting Medical Officer
NSW Poisons Information Centre
Sydney Children's Hospital Network;
Staff Specialist
Renal Medicine and Clinical Pharmacology and
Toxicology
St Vincent's Hospital;
Conjoint Associate Professor
University of New South Wales
Sydney, New South Wales, Australia

Norman D. Rosenblum, MD

Paediatric Nephrologist
Department of Paediatrics
The Hospital for Sick Children;
Senior Scientist
Program in Developmental and Stem Cell Biology
The Hospital for Sick Children;
Professor
Department of Paediatrics
University of Toronto
Toronto, Ontario, Canada

Mitchell H. Rosner, MD

Professor of Medicine
Chair, Department of Medicine
University of Virginia Health System
Charlottesville, Virginia

Andrew D. Rule, MD

Division of Nephrology and Hypertension
Mayo Clinic
Rochester, Minnesota

Ernesto Sabath, MD

Department of Natural Sciences
Universidad Autonoma de Queretaro
Queretaro, Mexico

Manish K. Saha, MD

Assistant Professor of Medicine
 Division of Nephrology and Hypertension
 Department of Medicine
 UNC Kidney Center
 University of North Carolina, Chapel Hill
 Chapel Hill, North Carolina

Khashayar Sakhaee, MD

Laura Kim Pak Professor in Mineral Metabolism Research
 BeutiControl Cosmetics Inc.;
 Professor in Mineral Metabolism and Osteoporosis
 Chief, Division of Mineral Metabolism
 University of Texas, Southwestern Medical Center
 Dallas, Texas

Vinay Sakhija, MD

Director of Nephrology and Transplant Medicine
 Max Hospital
 Mohali, Punjab, India

Alan D. Salama, MBBS, PhD, FRCP

UCL Centre for Nephrology
 Royal Free Hospital
 London, United Kingdom

Jeff M. Sands, MD

Juha P. Kokko Professor of Medicine and Physiology
 Medicine—Renal Division
 Emory University
 Atlanta, Georgia

Anjali Bhatt Saxena, MD

Director of Peritoneal Dialysis
 Department of Internal Medicine
 Division of Nephrology
 Santa Clara Valley Medical Center
 San Jose, California;
 Clinical Assistant Professor of Medicine
 Department of Internal Medicine
 Stanford University
 Stanford, California

Johannes Schlöndorff, MD

Division of Nephrology
 Beth Israel Deaconess Medical Center
 Harvard Medical School
 Boston, Massachusetts

Rizaldy Paz Scott, MS, PhD

Research Assistant Professor
 Feinberg School of Medicine
 Northwestern University
 Chicago, Illinois

Neil Sheerin, BSc, MBBS, PhD, FRCP

Professor of Nephrology
 Institute of Cellular Medicine
 National Renal Complement Therapeutics Centre
 Newcastle University
 Newcastle upon Tyne, Great Britain

Prableen Singh, MD

Associate Professor of Medicine
 Division of Nephrology and Hypertension
 University of California San Diego & VA San Diego
 Healthcare System
 San Diego, California

Karl Skorecki, MD, FRCP(C), FASN

Dean, Azrieli Faculty of Medicine
 Bar-Ilan University
 Safed, Israel

Itzchak N. Slotki, MD

Director
 Division of Adult Nephrology
 Shaare Zedek Medical Center;
 Associate Professor of Medicine
 Hadassah Hebrew University of Jerusalem
 Jerusalem, Israel

Miroslaw J. Smogorzewski, MD, PhD

Associate Professor of Medicine
 Division of Nephrology
 Department of Medicine
 University of Southern California, Keck School of
 Medicine
 Los Angeles, California

William E. Smoyer, MD

Vice President and Director
 Center for Clinical and Translational Research
 Nationwide Children's Hospital;
 Professor
 Department of Pediatrics
 The Ohio State University
 Columbus, Ohio

Stuart M. Sprague, DO

Chairperson, Division of Nephrology and Hypertension
 Department of Medicine
 NorthShore University Health System
 Evanston, Illinois;
 Clinical Professor of Medicine
 Department of Medicine
 University of Chicago Pritzker School of Medicine
 Chicago, Illinois

Peter Stenvinkel, MD, PhD, FENA

Professor
 Department of Renal Medicine
 CLINTEC
 Stockholm, Sweden

Jason R. Stubbs, MD

Associate Professor of Medicine
 Division of Nephrology and Hypertension
 The Kidney Institute
 University of Kansas Medical Center
 Kansas City, Kansas

Maarten W. Taal, MBChB, MMed, MD, FCP(SA), FRCP
 Department of Renal Medicine
 Royal Derby Hospital
 Derby, United Kingdom;
 Centre for Kidney Research and Innovation
 Division of Medical Sciences and Graduate Entry Medicine
 School of Medicine
 University of Nottingham
 Nottingham, United Kingdom

Manjula Kurella Tamura, MD, MPH
 Professor
 Department of Medicine/Nephrology
 Stanford University
 Palo Alto, California

Jane C. Tan, MD, PhD
 Department of Medicine
 Stanford University
 Stanford, California

Navdeep Tangri, MD, FRCPC, PhD
 University of Manitoba
 Department of Medicine
 Chronic Disease Innovation Centre, Seven Oaks General Hospital
 Winnipeg, Manitoba, Canada

Stephen C. Textor, MD
 Professor of Medicine
 Division of Nephrology and Hypertension
 Mayo Clinic
 Rochester, Minnesota

Ravi I. Thadhani, MD, MPH
 Chair, Department of Biomedical Sciences
 Cedars-Sinai Medical Center
 Los Angeles, California

Scott Culver Thomson, MD
 Professor
 Department of Medicine
 University of California;
 Chief of Nephrology Section
 Department of Medicine
 VA San Diego Healthcare System
 San Diego, California

Kathryn Tinckam, MD, MMSc
 Associate Professor
 Division of Nephrology
 Departments of Medicine and Laboratory Medicine & Pathobiology
 University of Toronto
 Toronto, Ontario, Canada

Vicente E. Torres, MD, PhD
 Professor of Medicine
 Division of Nephrology and Hypertension
 Mayo Clinic
 Rochester, Minnesota

Volker Vallon, MD
 Professor
 Division of Nephrology & Hypertension
 Departments of Medicine & Pharmacology
 University of California San Diego & VA San Diego Healthcare System
 San Diego, California

Joseph G. Verbalis, MD
 Professor
 Department of Medicine
 Georgetown University
 Washington, DC;
 Chief
 Department of Endocrinology and Metabolism
 Georgetown University Hospital
 Washington, Maryland

Jill W. Verlander, DVM
 Scientist
 Division of Nephrology, Hypertension, and Renal Transplantation
 University of Florida College of Medicine;
 Director
 College of Medicine Electron Microscopy Core Facility
 University of Florida
 Gainesville, Florida

Ron Wald, MDCM, MPH
 Staff Nephrologist
 Division of Nephrology
 Department of Medicine
 Li Ka Shing Knowledge Institute of St. Michael's Hospital and the University of Toronto;
 Institute for Clinical Evaluative Sciences
 Toronto, Ontario, Canada

I. David Weiner, MD
 Professor of Medicine and Physiology and Functional Genomics
 Division of Nephrology, Hypertension and Transplantation
 University of Florida College of Medicine;
 Section Chief
 Nephrology and Hypertension Section
 NF/SGVHS
 Gainesville, Florida

Steven D. Weisbord, MD, MSc
 Staff Physician
 Renal Section
 VA Pittsburgh Healthcare System;
 Associate Professor of Medicine and Clinical and Translational Science
 Renal-Electrolyte Division
 University of Pittsburgh School of Medicine
 Pittsburgh, Pennsylvania

Robert H. Weiss, MD
 Professor
 Department of Nephrology
 University of California, Davis
 Davis, California

Donald Everett Wesson, MD, MBA

President, Baylor Scott and White Health and Wellness Center
Department of Internal Medicine
Baylor Scott and White Health;
Professor of Medicine
Department of Internal Medicine
Texas A&M College of Medicine
Dallas, Texas

David C. Wheeler, MB ChB, MD

Professor of Kidney Medicine
Centre for Nephrology, Division of Medicine
University College London
London, Great Britain

Christopher S. Wilcox, MD, PhD

Chief
Department of Nephrology and Hypertension
Georgetown University Medical Center
Washington, DC

Jane Y. Yeun, MD

Division of Nephrology
Department of Internal Medicine
University of California, Davis School of Medicine
Sacramento, California;
Veterans Affairs Sacramento Health Care System
Mather Field, California

Brian Young, MD

Health Sciences Associate Clinical Professor
Division of Nephrology
Department of Internal Medicine, Division of Nephrology
University of California, Davis Medical Center
Sacramento, California

Alan S.L. Yu, MB, BChir

Harry Statland and Solon Summerfield Professor of Medicine
Director, Division of Nephrology and Hypertension and the Jared Grantham Kidney Institute
University of Kansas Medical Center
Kansas City, Kansas

Ming-Zhi Zhang, MD

Associate Professor
Department of Medicine
Vanderbilt University
Nashville, Tennessee

Preface

Welcome to the 11th edition of Brenner & Rector's *The Kidney*. Like the summer Olympic games, which it generally precedes by a few months, the emergence of each new edition of *The Kidney* follows a 4-year cycle, which is short enough to keep up with major advances in the field, but just long enough to complete the arduous editorial process. The purpose of this book remains unchanged from what Barry M. Brenner and Floyd C. Rector, Jr. conceived originally in 1973; namely to serve as a compendium of nephrology, from basic science to clinical diagnosis and treatment of kidney disease. The intended audience, now truly international, includes medical students, residents, nephrology fellows and practitioners, adult and pediatric renal scientists, and anyone else fascinated by the mysteries of the kidney. For those of us belonging to a certain generation, the *raison d'être* for *The Kidney* needs no justification. We grew up with it, considering it the definitive text of nephrology. But the modern era of medicine has been marked by a proliferation of readily accessible online digital tools that promise timely and partially digested answers to highly focused questions, catering to trainees and young physicians accustomed to the rapid pace of the modern digital age, and to established, harried clinicians with limited time for reading. While these tools are invaluable, and I confess that I, too, use them on occasion, there is clearly a place for a more considered exposition of the many complex topics in nephrology, that has both breadth and depth, combining intellectual rigor with the excitement of fresh discoveries.

The 11th edition, as with the previous two, is now edited by an international team of editors, a monumental task that remarkably was once managed singlehandedly by Barry M. Brenner. To introduce fresh perspective, we have added a new editor to the team, Valérie A. Luyckx from University of Zürich and the Brigham and Women's Hospital in Boston, a world-renowned expert in global health and management of kidney disease in underserved populations, and an advisor to the International Society of Nephrology and the World Health Organization on global health-related ethics issues. Almost one third of the chapters in this edition have been rewritten by new authors. In addition, we commissioned four entirely new chapters that address emerging areas in nephrology and are written by authoritative experts in those areas, namely "Cardiorenal Syndromes," "Supportive Care in Advanced Kidney Disease," "Considerations in Live Kidney Donation," and "Global Challenges and Initiatives in Kidney Health." To enhance the reader experience, we have introduced a listing of "Key Points" that appear at the beginning of the chapters, to summarize and highlight the important

new information. In addition, some of the chapters that are focused on physiology have "Clinical Relevance" boxes to highlight points in the text that have specific relevance to clinical practice.

While some of us will look forward to the tactile experience of opening the two physical volumes of this new edition when it comes out, many of our readers will inevitably prefer the convenience of perusing our enhanced eBook online. These readers will be rewarded with additional material absent from the print version (a necessity so as to avoid occupational injury while removing from the shelf), including the full list of references for every chapter, board review-style multiple choice questions to encourage active learning and help prepare for certification or recertification, and periodic updates to the content, all of which are fully searchable.

Needless to say, an undertaking of this magnitude requires the combined effort of countless individuals. First and foremost, on behalf of the entire editorial team I would like to express deep gratitude to the 184 authors of the chapters in this edition, all of whom committed time out of their busy schedules as clinicians, scientists, and academic leaders to contribute to this project. I wish to thank my fellow editors, Glenn Chertow, Valérie Luyckx, Phil Marsden, Karl Skorecki, and Maarten Taal for their sterling work, and for entrusting me with the leadership of this edition. I also thank Walter Wasser, who has now come to our rescue twice, at short notice, to assist the editorial team finalize manuscripts, both for this edition and the previous one. All of us, in turn, are grateful to the many staff at Elsevier for shepherding this project along. Joan Ryan, a veteran of many editions of *The Kidney*, was superb as our senior content development specialist, until she had to take a leave of absence and Joanie Milnes graciously stepped in to take over. Nancy Duffy, and before her Maureen Ianuzzi, served expertly as our content strategist, and Rachel McMullen served as our senior project manager.

I would like to thank my family, as well as my trainees, colleagues, and coworkers at the University of Kansas Medical Center, for their patience during the past two years, during which this project consumed far too much of my attention and took me away from spending time with them. Finally, I would like to thank Barry M. Brenner, whose spirit of scientific rigor and exacting intellectual standards continue to guide *The Kidney*. I hope that readers will share our excitement in this new edition and savor all that it has to offer.

Alan S.L. Yu, MB, BChir
Kansas City, Kansas

Embryology of the Kidney

Rizaldy Paz Scott | Yoshiro Maezawa | Jordan Kreidberg |
Susan E. Quaggin

CHAPTER OUTLINE

MAMMALIAN KIDNEY DEVELOPMENT, 2

MODEL SYSTEMS TO STUDY KIDNEY
DEVELOPMENT, 8

GENETIC ANALYSIS OF MAMMALIAN
KIDNEY DEVELOPMENT, 15

MOLECULAR GENETICS OF
NEPHROGENESIS, 22

KEY POINTS

- The development of the kidney relies on reciprocal signaling and inductive interactions between neighboring cells.
- Epithelial cells that comprise the tubular structures of the kidney are derived from two distinct cell lineages: the ureteric epithelia lineage that branches and gives rise to collecting ducts and the nephrogenic mesenchyme lineage that undergoes mesenchyme to epithelial transition to form connecting tubules, distal tubules, the loop of Henle, proximal tubules, parietal epithelial cells, and podocytes.
- Nephrogenesis and nephron endowment requires an epigenetically regulated balance between nephron progenitor self-renewal and epithelial differentiation.
- The timing of incorporation of nephron progenitor cells into nascent nephrons predicts their positional identity within the highly patterned mature nephron.
- Stromal cells and their derivatives coregulate ureteric branching morphogenesis, nephrogenesis, and vascular development.
- Endothelial cells track the development of the ureteric epithelia and establish the renal vasculature through a combination of vasculogenic and angiogenic processes.
- Collecting duct epithelia have an inherent plasticity enabling them to switch between principal and intercalated cell identities.

MAMMALIAN KIDNEY DEVELOPMENT

ANATOMIC OVERVIEW OF THE MAMMALIAN KIDNEY

The kidney is a sophisticated, highly vascularized organ that plays a central role in overall body homeostasis. In humans, the kidneys filter as much as 180 liters of blood per day, receiving as much as ~20% of the total cardiac output. Renal filtration of blood removes metabolic waste products (e.g., urea, ammonia, and by-products of bile from the liver) as urine while concomitantly adjusting the levels of water, electrolytes, and pH of tissue fluids. Additionally, the kidneys regulate blood pressure via the renin-angiotensin-aldosterone system, secrete erythropoietin that stimulates erythrocyte production, and contribute to the activation of vitamin D to control calcium and phosphate balance.

The filtration function of the kidneys is accomplished by basic units called nephrons (Fig. 1.1). Humans on average have 1 million nephrons per adult kidney but the range of total nephrons is highly variable across human populations.⁴ Each mouse kidney may contain up to 12,000–16,000 nephrons depending on the strain.⁵ This wide range in nephron number is influenced by genetic background, fetal nutrition and environment, and maturity at birth.^{6,7} Nephron endowment can be clinically important as markedly reduced nephron numbers raises the susceptibility risk to hypertension and chronic kidney disease.^{1–3,8,9} At the core of the nephron is the renal corpuscle or glomerulus (see Fig. 1.1). The glomerulus consists of a porous and highly convoluted capillary bed composed of highly fenestrated glomerular endothelial cells. These glomerular capillaries are circumscribed by morphologically elaborate and interdigitating cells called podocytes. These capillaries are further structurally supported by pericytes

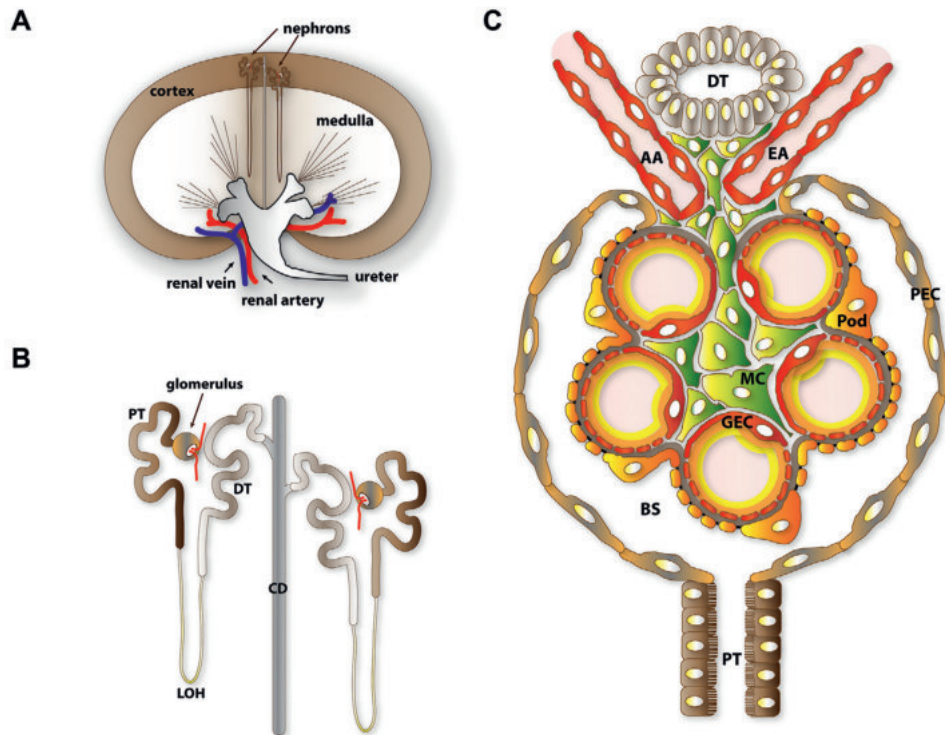


Fig. 1.1 Anatomic organization of the kidney. (A) Spatial distribution of nephron within the metanephric kidney. Glomeruli, the filtration compartments of the nephrons, are found in the cortex. (B) Segmental structure of nephrons. The vascularized glomerulus is found at the proximal end and is connected through a series of renal tubules where urinary filtrate composition is refined through resorption and secretion. (C) Cellular organization of the glomeruli. AA, Afferent arteriole; BS, Bowman space; CD, Collecting duct; DT, distal tubule; EA, efferent arteriole; GEC, glomerular endothelial cell; LOH, loop of Henle; MC, mesangial cell; PEC, parietal epithelial cell; Pod, podocyte; PT, proximal tubule. Reproduced with permission from Scott RP, Quaggin SE. The cell biology of renal filtration. *J Cell Biol.* 2015;209:100–210.

called mesangial cells. Blood filtration occurs through this capillary tuft, generating primary urine that collects within the Bowman capsule, an enclosure formed by parietal epithelial cells. From the Bowman capsule, urine drains through a series of tubules starting with the proximal tubules, the loop of Henle, the distal tubules, and the collecting ducts. These tubules are responsible for dynamic resorption and secretion processes that help recycle filtered small molecules; they also adjust water, electrolyte, and acid–base balance by fine-tuning the composition of the final urine output before it exits the ureter and is excreted via the bladder. Supporting the main functions of the nephrons are interstitial fibroblasts and a heterogeneous network of extraglomerular vasculature.

DEVELOPMENT OF THE UROGENITAL SYSTEM

The vertebrate kidney derives from the intermediate mesoderm of the urogenital ridge, a structure found along the posterior wall of the abdomen in the developing fetus.^{10,11} Mammalian kidneys develop in three successive stages, generating three distinct excretory structures known as the pronephros, the mesonephros, and the metanephros (Fig. 1.2). The pronephros and mesonephros are vestigial structures in mammals and degenerate before birth; the metanephros is the definitive mammalian kidney. The early stages of kidney development are required for the development of the adrenal glands and gonads that also form within the urogenital ridge. Furthermore, many of the signaling pathways and genes that play important roles in the metanephric kidney appear to play parallel roles during the development of the pronephros

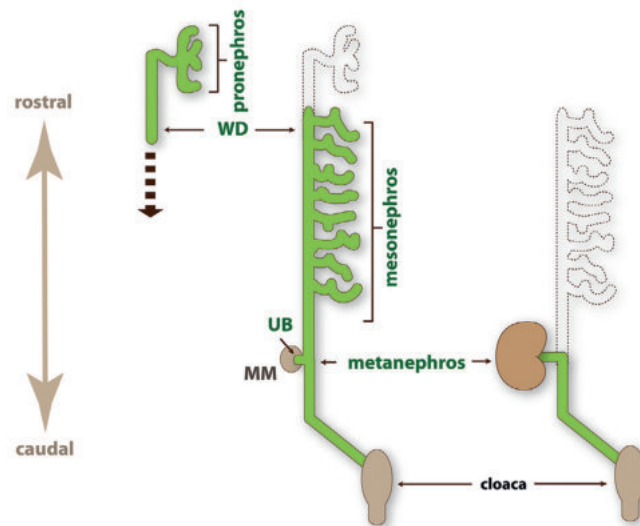


Fig. 1.2 Three stages of mammalian kidney development. The pronephros and mesonephros develop in a rostral-to-caudal direction and the tubules are aligned adjacent to the wolffian or nephric duct (WD). The metanephros develops from an outgrowth of the distal end of the wolffian duct known as the ureteric bud epithelium (UB) and a cluster of cells known as the metanephric mesenchyme (MM). The pronephros and mesonephros are vestigial structures in mice and humans and are regressed by the time the metanephros is well developed.

and mesonephros. The pronephros consists of pronephric tubules and the pronephric duct (also known as the precursor to the wolffian duct) and develops from the rostral-most region of the urogenital ridge at 22 days of gestation in humans and 8 days post coitum (embryonic stage E8) in mice (Table 1.1). Throughout the rest of this chapter, most timelines of kidney development are with reference to the mouse. The pronephros serves as the principal excretory organ of the larval stages of fishes and amphibians. The mesonephros develops caudal to the pronephric tubules in the midsection of the urogenital ridge. The mesonephros becomes the functional excretory apparatus in lower vertebrates (adult fish and amphibians) and may perform a filtering function during embryonic life in mammals. Prior to its degeneration, endothelial, peritubular myoid, and steroidogenic cells from the mesonephros migrate into the adjacent adrenogonadal primordia, which ultimately form the adrenal gland and gonads.¹² Abnormal mesonephric migration leads to gonadal dysgenesis, a fact that underscores the intricate association between these organ systems during development and explains the common association of gonadal and renal defects in congenital syndromes.^{13,14}

DEVELOPMENT OF THE METANEPHROS

The metanephros is the third and final stage, representing the definitive adult kidney of higher vertebrates. It results from a series of reciprocal inductive interactions that occur between the metanephric mesenchyme (MM) and

the epithelial ureteric bud (UB) at the caudal end of the urogenital ridge. The UB is first visible as an outgrowth at the distal end of the wolffian duct approximately between the fourth and fifth week of gestation in humans or E10.5 in mice. The MM becomes histologically distinct from the surrounding mesenchyme and is found adjacent to the UB. Upon invasion of the MM by the UB, signals from the MM cause the UB to branch into a T-tubule (at around E11.5 in mice) and then to undergo iterative dichotomous branching, giving rise to the urinary collecting duct system (Fig. 1.3). Simultaneously, the UB sends reciprocal signals to the MM, which is induced to condense along the surface of the bud. Following condensation, a subset of MM cells aggregates adjacent and inferior to the tips of the branching UB. These collections of cells, known as pretubular aggregates, undergo mesenchymal-to-epithelial conversion to become the renal vesicle (Fig. 1.4).

URETERIC BRANCHING MORPHOGENESIS

The collecting duct system is composed of hundreds of tubules through which the filtrate produced by the nephrons is conducted out of the kidney, to the ureter, and then to the bladder. Water and salt resorption and excretion, ammonia transport, and H⁺ ion secretion required for acid–base homeostasis also occur in the collecting ducts, under different regulatory mechanisms, and using different transporters and channels than are active along tubular portions of the nephron. The collecting ducts are all derived from the original

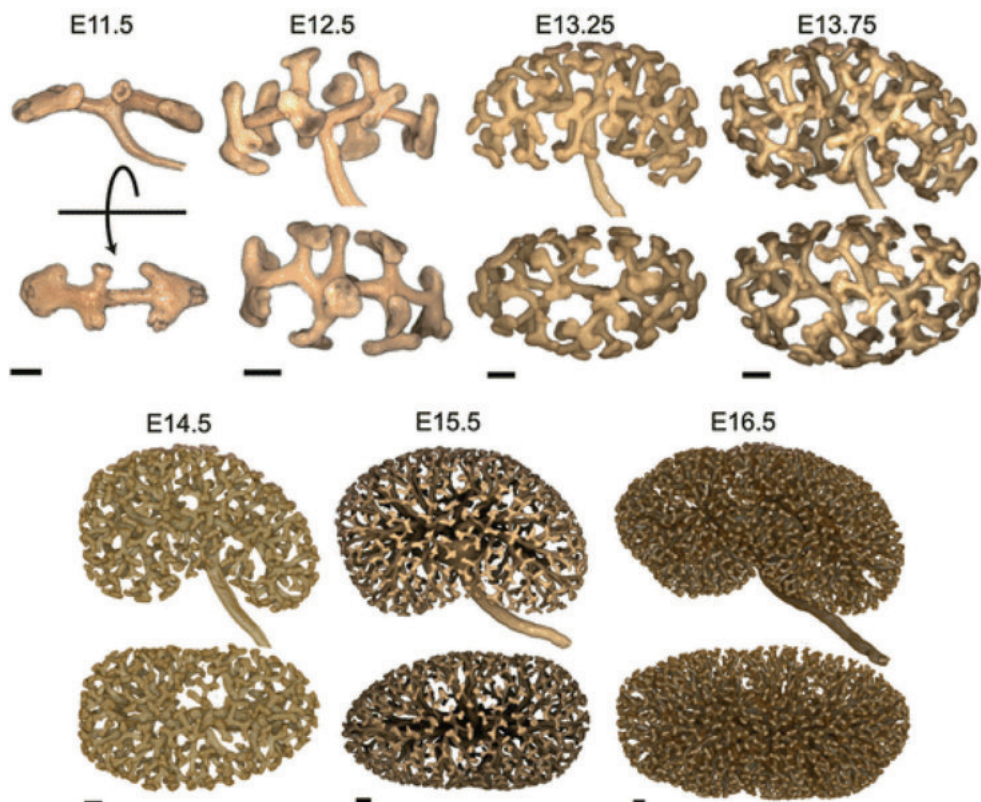


Fig. 1.3 Ureteric branching morphogenesis. Rapid reiterative branching of the UB within a 5-day period in mice as imaged with a pan-cytokeratin antibody using optical projection tomography. By E16.5, the renal pelvis, formed by the widening and coalescence of the earliest branches of the ureteric tree, is already apparent. Reproduced with permission from Short KM, Smuth I. Imaging, analyzing and interpreting branching morphogenesis in the developing kidney. *Results Probl Cell Differ*. 2017;60:233–256.

Table 1.1 Timelines of Human and Mouse Kidney Development

| Stage/Event | Human ^a | Mouse ^b |
|---------------------------------|--------------------|--------------------|
| Pronephros | | |
| • Emergence | 22nd day | E9 |
| • Disappearance by | 25th day | E10 |
| Mesonephros | | |
| • Emergence | 24th day | E10 |
| • Disappearance by | 16th week | E14 |
| Metanephros | | |
| • Ureteric bud induction | 28th–32nd day | E10.5 |
| • Nephrogenesis | 44th day | E13 |
| • Glomerulogenesis | 8th–9th week | E14 |
| • Cessation of nephrogenesis | 36th week | P3 |
| Gestation (Total Length) | 40 weeks | 19–21 days |

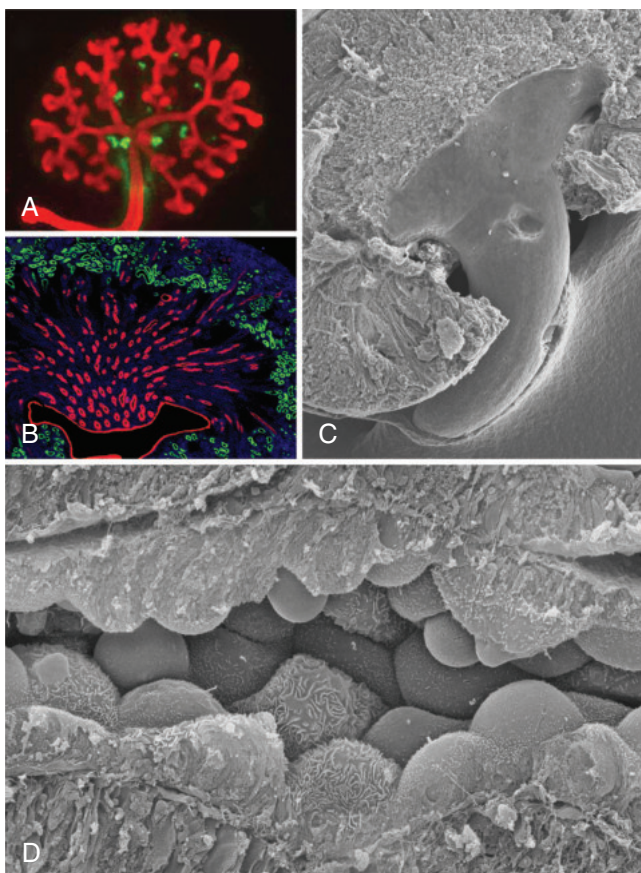
^aHuman timelines refer to gestational periods.^bMouse timelines are indicated as either embryonic days post coitum (E) or postnatal (P).

Fig. 1.4 The collecting duct system. The branching ureteric epithelia gives rise to the collecting duct system. (A) E12.5 mouse embryonic kidney explant grown for 2 days and (B) neonatal mouse kidney section stained for the ureteric epithelium and collecting ducts (pan-cytokeratin, red) and proximal tubules (Lotus lectin, green). (C) Scanning electron micrograph of a hemisected adult mouse kidney showing the funnel-shaped renal papilla. (D) Scanning electron micrograph of a collecting duct showing smooth principal cells and reticulated intercalated cells.

UB (Fig. 1.5). Whereas each nephron is an individual unit separately induced and originating from a distinct pretubular aggregate, the collecting ducts are the product of branching morphogenesis from the UB. Considerable remodeling is involved in forming collecting ducts from branches of the UB.¹⁵ The branching is highly patterned, with the first several rounds of branching being somewhat symmetric, followed by additional rounds of asymmetric branching, in which a main trunk of the collecting duct continues to extend toward the nephrogenic zone, while smaller buds branch as they induce new nephrons within the nephrogenic zone. Originally, the UB derivatives are branching within a surrounding mesenchyme. Ultimately, they form a funnel-shaped structure in which cone-shaped groupings of ducts or papillae sit within a funnel or calyx that drains into the ureter. The mouse kidney has a single papilla and calyx, whereas a human kidney has 8 to 10 papillae, each of which drains into a minor calyx, with several minor calyces draining into a smaller number of major calyces.

DEVELOPMENT OF THE NEPHRON

The renal vesicle undergoes patterned segmentation and proceeds through a series of morphologic changes that include gradual recruitment of mesenchymal progenitors to form the glomerulus and components of the nephrogenic tubules from the proximal convoluted tubule, the loop of Henle, and the distal tubule. The renal vesicles undergo differentiation, passing through morphologically distinct stages starting from the comma-shaped and proceeding to the S-shaped body, capillary loop, and mature stage, each step involving precise proximal-to-distal patterning and structural transformations (see Fig. 1.4). Remarkably, this process is repeated 600,000 to 1 million times in each developing human kidney as new nephrons are sequentially born at the tips of the UB throughout fetal life.

The glomerulus develops from the most proximal end of the renal vesicle that is furthest from the UB tip.^{16,17} Distinct cell types of the glomerulus can first be identified in the S-shaped stage, where presumptive podocytes appear as a columnar-shaped epithelial cell layer. A vascular cleft develops and separates the presumptive podocyte layer from more distal cells that will form the proximal tubule. Parietal epithelial cells differentiate and flatten to form the Bowman capsule, a structure that surrounds the urinary space and is continuous with the proximal tubular epithelium. Concurrently, endothelial cells migrate into the vascular cleft. Together with podocytes, the endothelial cells produce the glomerular basement membrane, a major component of the mature filtration barrier. Initially the podocytes are connected by intercellular tight junctions at their apical surface.¹⁸ As glomerulogenesis proceeds, the podocytes flatten and spread out to cover the increased surface area of the growing glomerular capillary bed. They develop microtubular-based primary processes and actin-based secondary foot processes.^{19–21} Foot processes of neighboring podocytes interdigitate and elongate. As podocytes mature, intercellular epithelial tight junctions linking become restricted to the basal aspect of the podocyte, relocate from the cell body to the foot processes, and are eventually replaced by a modified adherens junction-like structure known as the slit diaphragm.^{18,22} The slit diaphragms are signaling hubs serving as the final layer of the glomerular filtration barrier.²³ Mesangial cell ingrowth follows

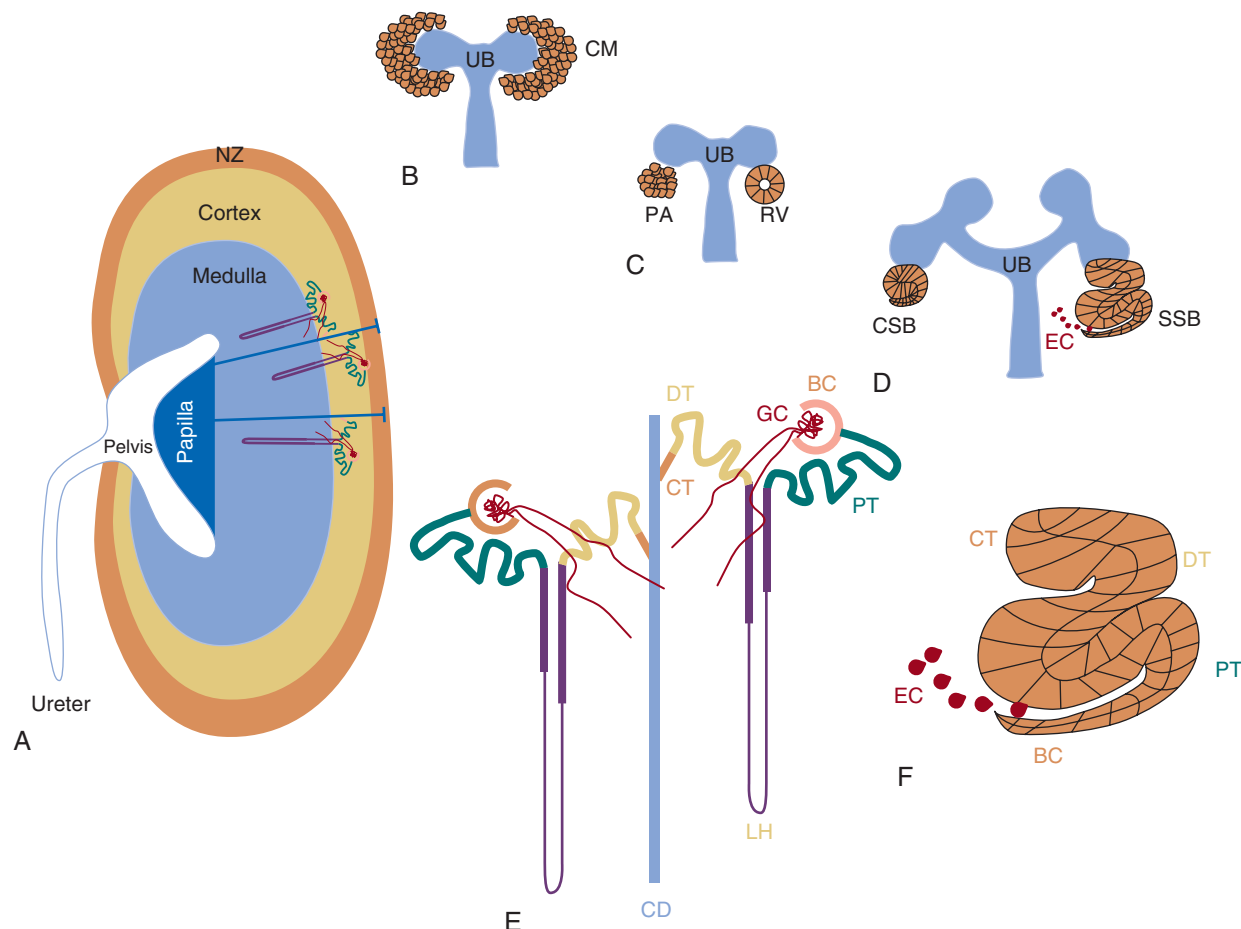


Fig. 1.5 Overview of nephrogenesis. (A) Gross kidney histoarchitecture. (B–E) As described in the text, reciprocal interaction between the ureteric bud and metanephric mesenchyme results in a series of well-defined morphologic stages leading to formation of the nephron, including the branching of the UB epithelium and the epithelialization of the metanephric mesenchyme into a highly patterned nephron. (F) Distinctive segmentation of the S-shaped body defines the patterning of the nephron. BC, Bowman capsule; CD, collecting duct; CM, cap mesenchyme; CSB, comma-shaped body; CT, connecting tubule; DT, distal tubule; EC, endothelial cells; LH, loop of Henle; NZ, nephrogenic zone; PA, pretubular aggregate; PT, proximal tubule; SSB, S-shaped body; UB, ureteric bud.

the migration of endothelial cells and is required for development and patterning of the capillary loops that are found in normal glomeruli. The endothelial cells also flatten considerably and capillary lumens are formed due to apoptosis of a subset of endothelial cells.²⁴ At the capillary loop stage, glomerular endothelial cells develop fenestrae, which are semipermeable transcellular pores common in capillary beds exposed to high hemodynamic flux.

In the mature stage glomerulus, the podocytes, fenestrated endothelial cells, and intervening glomerular basement membrane comprise the filtration barrier that separates the urinary from the blood space. Together, these components provide a size- and charge-selective barrier that permits free passage of small solutes and water but prevents the loss of larger molecules such as proteins. The mesangial cells are found between the capillary loops where they are required to provide ongoing structural support to the capillaries and possess smooth-muscle cell-like characteristics that have the capacity to contract, which may account for some of the dynamic properties of the glomerulus. The tubular portion of the nephron becomes segmented in a proximal–distal order, into the proximal convoluted tubule, the descending and ascending loops of Henle, and distal convoluted tubule.

The distal tubule is contiguous with the collecting duct, a derivative of the UB. Imaging and fate mapping studies reveal that this interconnection results from the invasion of the UB by cells from the distal segments of nascent nephrons (around the S-shaped body stage).²⁵

Although all segments of the nephron are present at birth and filtration occurs prior to birth, maturation of the tubule continues in the postnatal period. Increased expression levels of transporters, switches in transporter isoforms, alterations in paracellular transport mechanisms, and permeability and biophysical properties of tubular membranes have all been observed to occur postnatally.²⁶ These observations emphasize the importance of considering the developmental stage of the nephron in interpretation of renal transport and may explain the age of onset of symptoms in inherited transport disorders.

THE NEPHROGENIC ZONE

After the first few rounds of branching of the UB, and the concomitant induction of nephrons from the MM, the kidney subdivides into two major compartments: an outer region called the cortex and an inner region called the medulla. The glomeruli and proximal and distal tubules localize within

the cortex, together with the distal part of the nephron that connects directly to the collecting ducts. The loop of Henle and the rest of the collecting duct network comprise the epithelial structures found in the medulla. Kidney growth and nephrogenesis occurs in a radial fashion with new branches of the ureteric tree and newer nephrons added at the outermost periphery of the developing cortex which is called the nephrogenic zone. The nephrogenic zone is morphologically identifiable as a narrow band beneath the renal capsule where the branching UB tips are found together with nascent nephrons (pretubular aggregates, renal vesicles, comma-shaped bodies, and S-shaped bodies) and self-renewing nephron progenitors. Within the developing kidney, the most mature nephrons are found in the innermost layers of the cortex, and the most immature nephrons in the most peripheral regions. The nephrogenic zone, therefore, represents an active site of nephrogenesis. The nephrogenic zone progressively thins out with the gradual depletion of nephrogenic precursors and disappears once the remaining nephron progenitors have completely epithelialized.

RENAL STROMA AND INTERSTITIAL CELL POPULATIONS

For decades in classic embryologic studies of kidney development, emphasis has been placed on the reciprocal inductive signals between MM and UB. However, in recent years, interest in the stromal cell as a key regulator of nephrogenesis has arisen.^{17,27–29} Stromal cells also derive from the MM but are not induced to condense by the UB. Two distinct populations of stromal cells have been described: cortical stromal cells exist as a thin layer beneath the renal capsule while medullary stromal cells populate the interstitial space between the collecting ducts and tubules (Fig. 1.6). Cortical stromal cells also surround the MM condensates and provide signals required for UB branching and patterning of the developing kidney. Disruption or loss of these stromal cells leads to impairment of UB branching, reduction in nephron number, disrupted nephron patterning with failure of cortical-medullary boundary formation, and maldevelopment of the renal vasculature. A reciprocal signaling loop from the UB exists to properly pattern stromal cell populations. Loss of these UB-derived signals leads to a buildup of stromal cells beneath the capsule that are several layers thick. As nephrogenesis proceeds, stromal cells differentiate into peritubular interstitial cells and pericytes that are required for vascular remodeling and the production of extracellular matrix responsible for proper nephric formation.²⁹ These cells migrate from their position around the condensates to areas between the developing nephrons within the medulla.

THE RENAL VASCULATURE

The microcirculations of the kidney include the specialized glomerular capillary system responsible for production of the ultrafiltrate, and the vasa recta bundles and peritubular capillaries involved in the countercurrent mechanism for urine osmoregulation (Fig. 1.7). Vasculogenesis and angiogenesis have been described as two distinct processes in blood vessel formation (Fig. 1.8). Vasculogenesis is the de novo differentiation of previously nonvascular endothelial cell precursors into structures that resemble capillary beds, whereas angiogenesis refers to sprouting from these early beds to form mature vessel structures, including arteries,

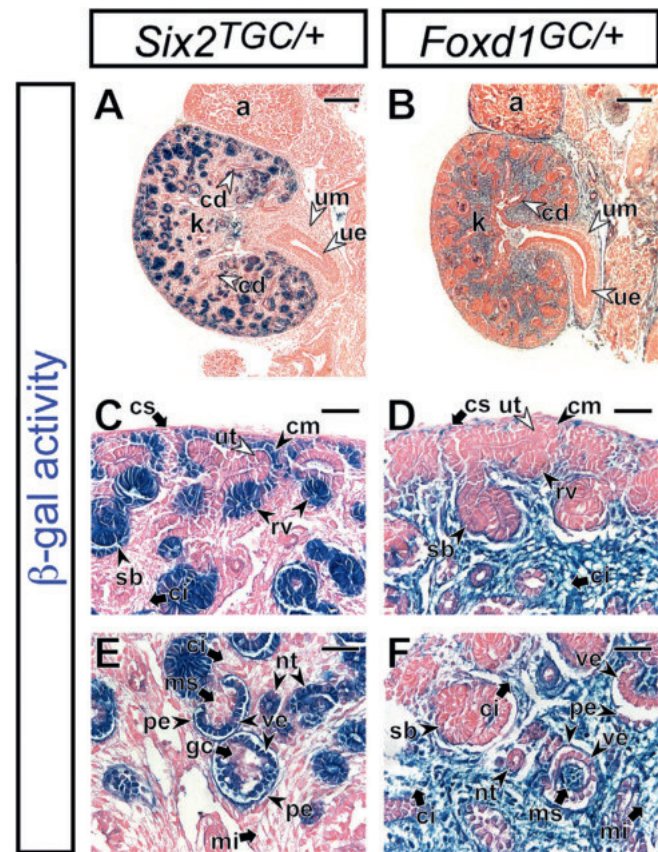


Fig. 1.6 The nephrogenic and stromal mesenchyme. Lineage tracing analysis in E14.5 mouse kidneys showing nephrogenic derivatives of *Six2*-expressing condensing mesenchyme (A, C, and E) and the *Foxd1*-expressing stromal mesenchyme (B, D, and F), stained for β -galactosidase activity (blue). a, Adrenal gland; cd, collecting duct; ci, renal cortical interstitium; cm, cap mesenchyme; cs, renal cortical stroma; gal, galactosidase; gc, glomerular capillary; k, kidney; mi, renal medullary interstitium; ms, mesangium; nt, nephrogenic tubule; pe, parietal epithelium; rv, renal vesicle; sb, S-shaped body; ue, ureter epithelium; um, ureter mesenchyme; ut, ureteric tip; ve, visceral epithelium (podocyte). Reproduced with permission from Kobayashi A, Mugford JW, Krautzberger Am, et al. Identification of a multipotent self-renewing stromal progenitor population during mammalian kidney organogenesis. *Stem Cell Reports*. 2014;3:650–662.

veins, and capillaries. Both processes are involved in development of the renal vasculature. At E11.5 in mice, the UB is tracked by a primitive vessel that elaborates in synchrony with both UB branching and nephrogenesis. A rich capillary network is identifiable by E12.5 while the presence of endothelial cell-containing glomeruli becomes apparent at E14.5.

Transplantation experiments support a model where endogenous endothelial progenitors within the MM give rise to renal vessels *in situ* through angiogenesis, although the origin of large blood vessels is still not clear.^{30–35} At E13, capillaries form networks around the developing nephric tubules and by E14, the hilar artery and first-order interlobar renal artery branches can be identified. These branches will form the corticomedullary arcades and interlobular arteries that branch from these arcades. Further branching produces the glomerular afferent arterioles. From E13.5 onward, endothelial cells migrate into the vascular cleft of developing glomeruli, where they undergo differentiation to form the

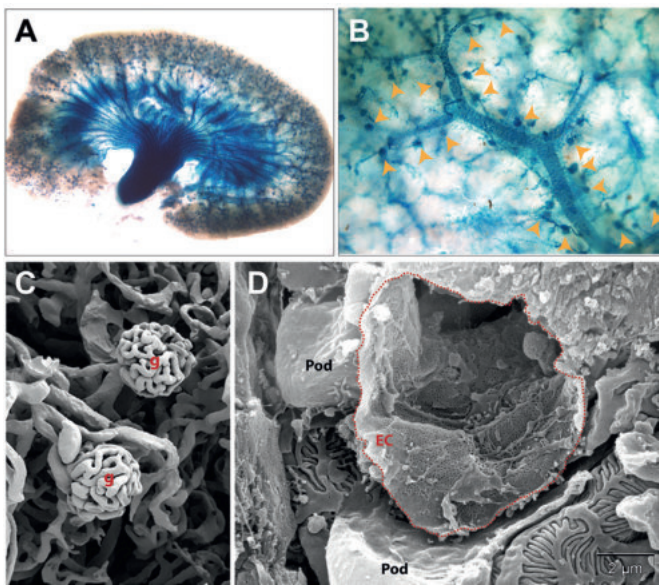


Fig. 1.7 The renal vasculature. (A) Visualization of the renal vascular network in a reporter mouse strain expressing prokaryotic β -galactosidase through the promoter of the vascular-specific phosphatase gene *Ptprb*. (B) Higher magnification of the renal cortex in (A) showing endothelial cell distribution in glomeruli (yellow arrowheads), arterioles, peritubular capillaries, and arcuate arteries. (C) Corrosion resin cast of the renal vasculature revealing the highly convoluted assembly of the glomerular capillaries (g). (D) Scanning electron micrograph of a glomerulus with an exposed endothelial lumen (dashed outline) revealing fenestrations. EC, Endothelial cell; Pod, podocytes. Corrosion cast electron micrograph courtesy Fred Hossler, Department of Anatomy and Cell Biology, East Tennessee State University.

glomerular capillary loops. The efferent arterioles carry blood away from the glomerulus to a system of fenestrated peritubular capillaries that are in close contact with the adjacent tubules and receive filtered water and solutes reabsorbed from the filtrate.³⁶ These capillaries have few pericytes. In comparison, the vasa rectae, which surround the medullary tubules and are involved in urinary concentration, are also fenestrated but have more pericytes. They arise from the efferent arterioles of deep glomeruli.³⁷ The peritubular capillary system surrounding the proximal tubules is well developed in the late fetal period, whereas the vasa rectae mature 1 to 3 weeks postnatally.

MODEL SYSTEMS TO STUDY KIDNEY DEVELOPMENT

THE KIDNEY ORGAN CULTURE SYSTEM

From the late 1950s, the method of growing mouse embryonic kidneys as floating cultures on top of filters (Fig. 1.9), a technique pioneered by Clifford Grobstein and improved by Lauri Saxen, accelerated the advancement of the kidney developmental biology field. This classic method, which remains widely in use to this day, has the advantages that the kidney explants are cultivated within an easily manipulated, controlled environment, and there is a possibility of visualizing the pattern of kidney growth by real-time fluorescence microscopy. Although vascularization and functional

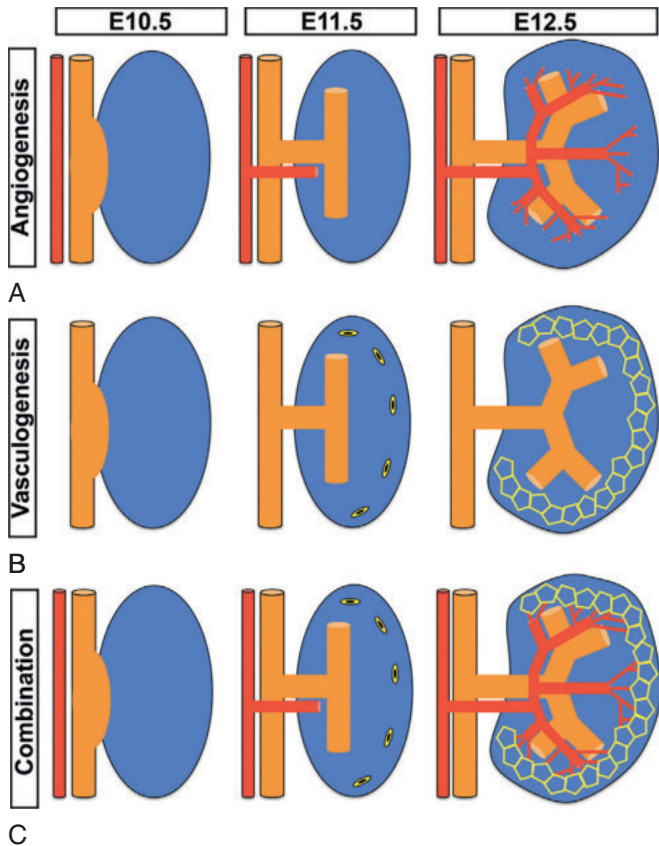


Fig. 1.8 Angiogenesis and vasculogenesis in renal vascular development. Schematic overview of early development of the renal vasculature. (A) Angiogenesis generates major blood vessels through sprouting and branching of pioneer vessels (red) that follow the branching ureteric bud (brown). (B) Scattered endothelial progenitor cells (yellow) are distinctly present as early as E11.5 at the periphery of the developing metanephric kidney (blue). These sporadic endothelial cells coalesce and organize into a primitive capillary plexus (yellow) by E12.5. (C) Major vessels formed via angiogenesis and capillaries that arise by vasculogenesis become interconnected to establish the elaborate renal vascular network. Adapted from Stolz DB, Sims-Lucas S. Unwrapping the origins and roles of the renal endothelium. *Pediatr Nephrol*. 2015;30:865–872.

maturity is largely restricted in embryonic kidney explants, in vitro cultured kidneys display remarkable recapitulation of ureteric branching and epithelialization and segmental patterning of the MM (Fig. 1.10). Historically, kidney explant cultures provided crucial proof for the principle of reciprocal tissue induction in organogenesis. It was used to demonstrate that the UB and the MM exchange inductive cues, driving branching morphogenesis of the UB and epithelialization of the MM.^{10,38}

As originally shown by Grobstein, Saxen, and colleagues, the two major components of the metanephric kidney, the MM and the UB, could be separated from each other, and the isolated mesenchyme could be induced to form nephron-like tubules by a selected set of other embryonic tissues, the best example of which is the embryonic neural tube.^{10,38} When the neural tube is used to induce the separated mesenchyme, there is terminal differentiation of the mesenchyme into tubules, but not significant tissue expansion. In contrast, intact metanephric rudiments can grow more extensively,

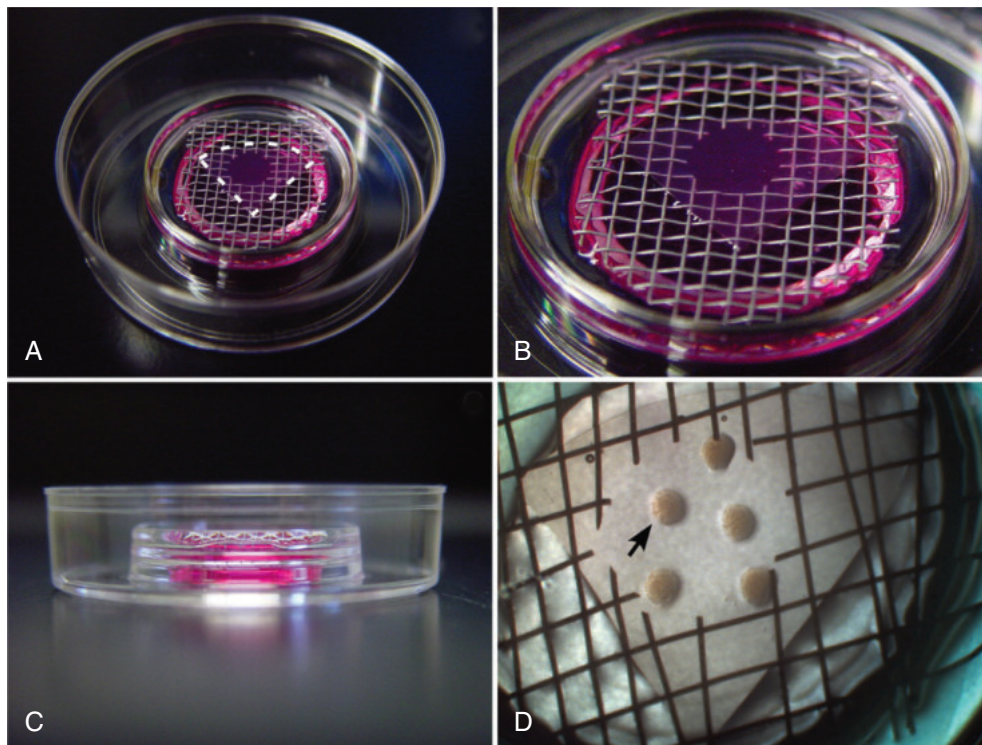


Fig. 1.9 Metanephric organ explants. (A, B) Top and (C) lateral view of a kidney organ culture. Embryonic kidney explants are grown at the air-growth medium interface on top of a floating porous polycarbonate filter (dashed lines in A) supported on a metal mesh. (D) Kidneys grown after 4 days of culture. Reproduced with permission from Cold Spring Harbor Protocols.⁷⁴¹

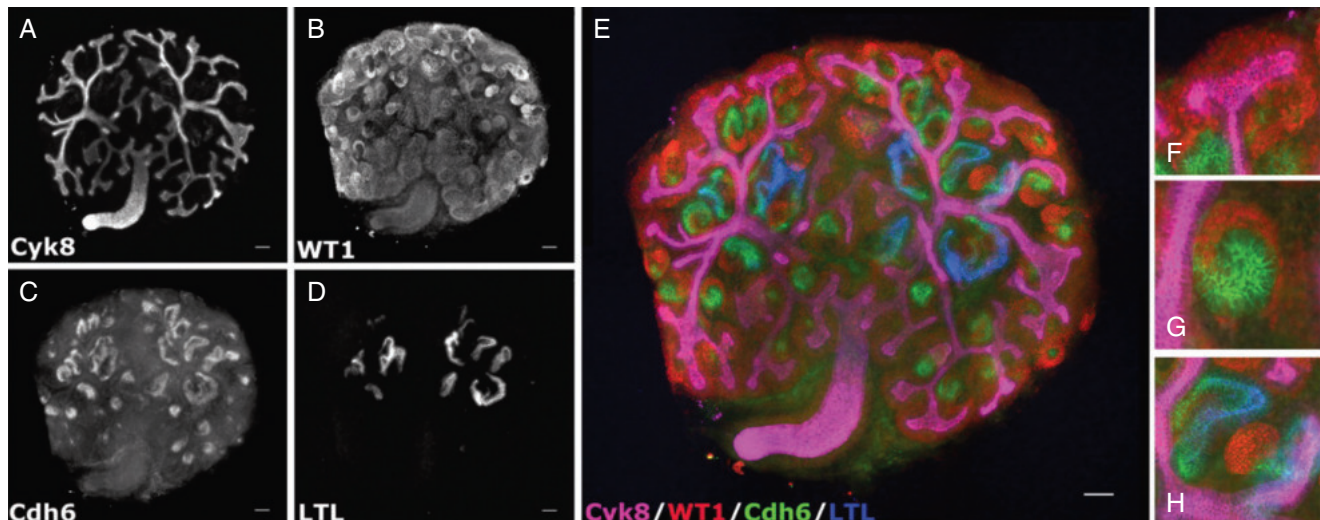


Fig. 1.10 Recapitulation of branching and nephrogenesis in renal explant cultures. (A) Ureteric tree stained for cytokeratin 8 (Cyk8). (B) Condensed metanephric mesenchyme stained for WT1. (C) Epithelial derivatives of the metanephric mesenchyme stained for E-cadherin (Cdh1). (D) Proximal tubules stained with *Lotus tetragonolobus* lectin (LTL). (E) Merged image of A–D. (F) WT1-expressing cells represent the nephron progenitor cells that surround the UB. (G) Cdh1-expression marks the mesenchyme-to-epithelial transformation of nephron progenitor cells. (H) Early patterning of nascent nephrons along a proximodistal axis. Reproduced with permission from Cold Spring Harbor Protocols.⁷⁴¹

displaying both sustained UB branching and early induction of nephrons even when cultured for a week. The isolated mesenchyme experiment has proven useful in the analysis of renal agenesis phenotypes, where there is no outgrowth of the UB. In these cases, the mesenchyme can be placed in contact with the neural tube to determine whether it has the intrinsic ability to differentiate. Most often, when renal agenesis is due to the mutation of a transcription factor,

tubular induction is not rescued by the neural tube, as could be predicted for transcription factors, which would be expected to act in a cell-autonomous fashion.³⁹ In the converse situation, in which renal agenesis is caused by loss of a gene function in the UB (e.g., *Emx2*), it is usually possible for the embryonic neural tube to induce tubule formation in isolated mesenchymes.⁴⁰ Therefore the organ culture induction assay can be used to test hypotheses concerning whether a particular

gene is required in the UB or the MM. Recently, as chemical inhibitors specific for various signal transduction pathways have been synthesized and become available, it has been possible to add these to organ cultures and observe effects that are informative about the roles of specific pathways in development of the kidney. Examples are the use of drugs to block the ERK/MAP kinase, PI3K/Akt, Notch signaling, and Wnt signaling pathways in renal explant cultures.^{41–45} Synthetic antisense oligonucleotides and small interfering or silencing RNA (siRNA) have also been successfully used to inhibit gene expression in kidney organ cultures.^{45–55}

GENETIC MOUSE MODELS

Many of the genetic pathways regulating many aspects of development are strongly conserved between mice and humans. Due to the relative ease of manipulating the genome of the mouse, its small size, and shorter gestation period, the mouse has become the primary model organism for the study of mechanism of human development and diseases. Anatomic and functional features of the human kidney are for the most part highly similar in the mouse, albeit at a smaller scale, while a number of genes identified as essential for normal mouse kidney development are also known to be associated with congenital anomalies of the kidney and urinary tract (CAKUT) and other kidney diseases.^{56–58}

The wealth of our understanding of metanephric kidney development over the past two decades is owed to the harnessing of homologous gene recombination to introduce targeted mutations and novel alleles into specific genes in cultured mouse embryonic stem cells. This paved the way for the creation of numerous genetically engineered mice that have become highly valuable tools for the study of renal developmental biology and the etiology of certain genetic diseases of the kidneys and the urinary tract (Table e1.2). The technology is applied in many ways. In its simplest is the creation of null mutations within the germline that generate gene knockout mouse models. The limitation of this method is that certain genes are essential for early development and their inactivation in the germline can cause premature lethality, thus precluding the analysis of the function of those genes in organogenesis. A novel improvement to this is the use of a conditional gene-targeting strategy, allowing for the creation of conditional alleles. This involves introducing small recognition sites for recombinase enzymes of which the Cre recombinase is the most routine now (Fig. 1.11). A conditional “floxed” allele of the target gene locus is created by incorporating two *loxP* sites within two separate introns, flanking the exons that can be excised or recombined. In principle, normal transcription from the locus is expected prior to recombination of the floxed allele and should effectively promote a wild type phenotype. The Cre recombinase itself is engineered under the control of a tissue-specific promoter. Breeding between tissue-specific transgenic Cre animals and those harboring a conditional allele for a particular gene ultimately results in a cell- or tissue-type specific inactivation of the gene of interest. This strategy has also been refined in some cases, so that the Cre expression is also temporally regulated by the use of a drug such as doxycycline or tamoxifen. A number of Cre lines are now available to target genes specifically within different subpopulations of renal cells and progenitors. The transgenic Cre lines driven by the *Hoxb7*,

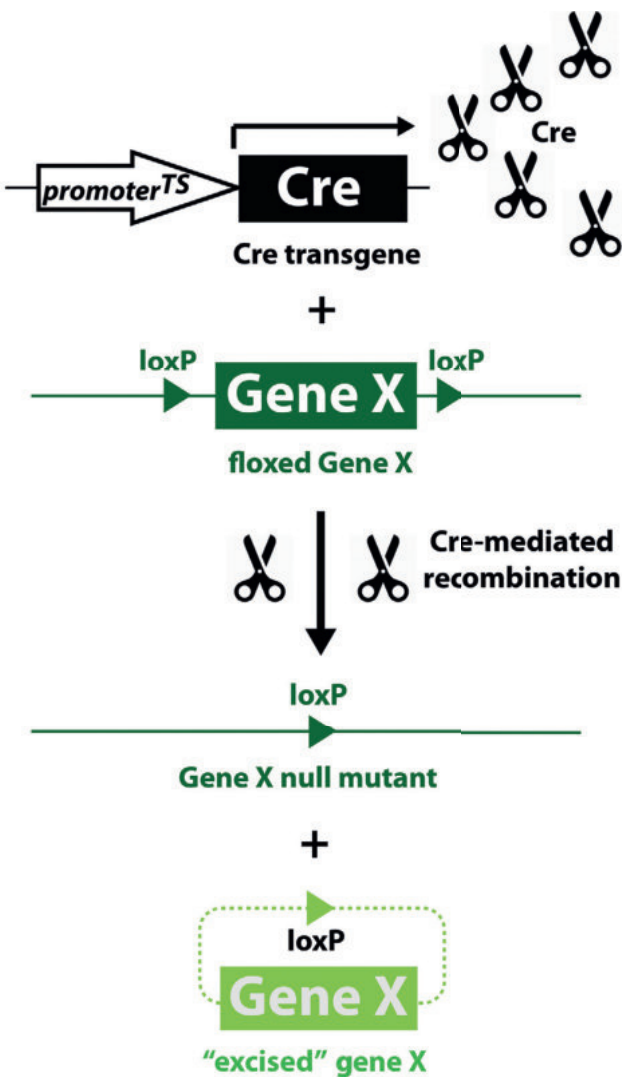


Fig. 1.11 Cre-lox homologous gene recombination system. Simplified overview of Cre recombinase-mediated homologous recombination for generation of tissue-specific conditional null mutations of a target gene. Cre recombinase expression is engineered to be driven under the control of tissue specific promoter (*promoter^{TS}*). The target gene (or typically certain exons within the target chromosomal locus) are flanked with *loxP* sites (recognition sites for Cre recombinase). Cre activity in specific cell types mediates the excision of the *loxP*-flanked (floxed) target gene, creating a null allele.

Six2, *Foxd1*, and *Nphs2* promoters are among the most highly cited gene excision drivers for targeted genetic inactivation in the ureteric, nephrogenic, stromal, and podocyte cell lineages.^{59–64} Lately, the introduction of the more precise CRISPR-Cas9 gene editing tool, an ingenious application of the adaptive immune response of prokaryotes against bacteriophages, is facilitating the way researchers create customized mutant cells and animal models to study various aspects of renal development (Fig. 1.12).^{65–68}

The discovery of new kidney-relevant genes or signaling pathways has also been achieved by random chemical mutagenesis in mice. The alkylating agent N-ethyl-N-nitrosourea (ENU) is routinely used to introduce random point mutations in mouse spermatogonia. The introduced mutations can result in loss or gain of function and are either recessive or

Table e1.2 Summary of Knockout and Transgenic Models for Kidney Development

| Gene Mutation or Knockout | Phenotype | Associated Human Diseases | References |
|---|---|---|---|
| Renal Agenesis | | | |
| <i>Celsr1</i> | Renal agenesis, hydronephrosis | Spina bifida, unilateral renal agenesis, hydronephrosis | 331 |
| <i>Ctnnb1</i> (β -catenin) | Renal agenesis or severe renal hypoplasia, premature differentiation of UB epithelia (UB-selective) | Mental retardation, multiple cancers, eye defects | 181, 185 |
| <i>Emx2</i> | Renal agenesis | Schizencephaly (cerebral cleft abnormalities) | 40 |
| <i>Emx2, Pax2</i> | Duplicated kidneys and ureter, ureteral obstruction | CAKUT, VUR | 531 |
| <i>Esrp1</i> | Renal agenesis, renal hypoplasia | | 532 |
| <i>Etv4, Etv5</i> | Renal agenesis or severe renal hypodysplasia | | 210, 212 |
| <i>Eya1</i> | Renal agenesis | Branchiootorenal syndrome (brachial fistulae, deafness) | 136, 150 |
| <i>Fgf9, Fgf20</i> | Renal agenesis | | 305 |
| <i>Fgf10, Gdnf, Gfra1</i> | Renal agenesis | | 222 |
| <i>Fgfr1, Fgfr2</i> | Renal agenesis (MM-selective) | | 304 |
| <i>Fras1, Frem1, Frem2</i> | UB failure, defect of GDNF expression | Fraser syndrome (cryptophthalmos, syndactyly, CAKUT); Manitoba-oculo-tricho-anal (MOTA) syndrome | 165, 166, 225, 227, 228 |
| <i>Gata3</i> | Renal agenesis, gonad dysgenesis (null mutation) | Hypoparathyroidism, sensorineural deafness, and renal dysplasia (HDRS) syndrome; autoimmune disease | 179, 180, 182, 183 |
| <i>Gdf11</i> <i>Gdnf, Gfra1, Ret</i> | UB failure, skeletal defects Renal agenesis or rudimentary kidneys, aganglionic megacolon | Hirschsprung disease, Multiple endocrine neoplasm type IIA/B (MEN2A/MEN2B), and familial medullary thyroid carcinoma (FMTC) | 145, 533 142–144, 148, 161, 164, 534–537 |
| <i>Gen1</i> | Renal agenesis, duplex kidneys, hydronephrosis, ureteral obstruction | | 538 |
| <i>Gli3</i> | Renal agenesis, severe renal agenesis, absence of renal medulla and papilla | Pallister-Hall (PH) syndrome (polydactyly, imperforate anus, abnormal kidneys, defects in the gastrointestinal tract, larynx, and epiglottis) | 265, 266 |
| <i>Greb11</i> <i>Grem1</i> <i>Ghrl2</i> | Renal agenesis Renal agenesis; apoptosis of the MM Occasional unilateral renal agenesis, CD barrier dysfunction, diabetes insipidus | CAKUT Autosomal dominant deafness, ectodermal dysplasia | 539–541 146 542, 543 |
| <i>Grip1</i> | Renal agenesis | Fraser syndrome (cryptophthalmos, syndactyly, CAKUT) | 229–231 |
| <i>Hnf1b</i> | Renal agenesis, renal hypoplasia, hydronephrosis, duplex kidneys | CAKUT, diabetes mellitus, renal cysts, renal carcinoma | 544 |
| <i>Hoxa11, Hoxd11</i> | Distal limbs, vas deferens | Radio-ulnar synostosis with amegakaryocytic thrombocytopenia | 545 |
| <i>Hs2st1</i> | Lack of UB branching and mesenchymal condensation | | 546 |
| <i>Isl1</i> | Renal agenesis, renal hypoplasia, hydronephrosis (MM-selective) | | 547 |
| <i>Itga8</i> ($\alpha 8$ Integrin) | Renal agenesis, renal hypodysplasia | Fraser syndrome (cryptophthalmos, syndactyly, CAKUT) | 169 |

Continued on following page

Table e1.2 Summary of Knockout and Transgenic Models for Kidney Development (Cont'd)

| Gene Mutation or Knockout | Phenotype | Associated Human Diseases | References |
|--|--|---|--------------------|
| <i>Itgb1</i> ($\beta 1$ Integrin) | Renal agenesis, disrupted UB branching, hypoplastic collecting duct system (collecting duct-selective); podocyte dedifferentiation (podocyte-selective) | Fraser syndrome (cryptophthalmos, syndactyly, CAKUT) | 177, 548, 549 |
| <i>Kif26b</i> | Renal agenesis, failed UB attraction to the MM | | 167 |
| <i>Lamc1</i> | UB failure, delayed nephrogenesis, water transport defects | | 232 |
| <i>Lhx1</i> (<i>Lim1</i>) | Renal agenesis (null mutant); renal hypoplasia, UB branching defect, hydronephrosis, distal ureter obstruction (UB-selective); arrested nephrogenesis, nephron patterning defects (MM-selective) | Mayer-Rokitansky-Küster-Hauser (MRKH) syndrome (müllerian duct agenesis) | 141, 550, 551 |
| <i>Lrp4</i> | Delayed UB induction, failed MM induction, syndactyly, oligodactyly | Cenani-Lenz syndrome | 552–555 |
| <i>Mark2</i> (<i>Par1b</i>), <i>Mark3</i> (<i>Par1a</i>) | Renal hypoplasia, proximal tubule dilation, immature glomeruli | | 556 |
| <i>Npnt</i> | Delayed UB association with the MM | | 168 |
| <i>Osr1</i> | Lack of MM, adrenal gland, gonads, defects in formation of pericardium and atrial septum | | 137, 149, 281, 282 |
| <i>Pax2</i> | Renal hypoplasia, VUR | CAKUT, VUR, optic nerve colobomas | 46, 47 |
| <i>Pax2</i> , <i>Pax8</i> | Defect in intermediate mesoderm transition, failure of pronephric duct formation | CAKUT, VUR, optic nerve colobomas | 557 |
| <i>Pbx1</i> | Unilateral renal agenesis, expansion of nephrogenic precursors | CAKUT, hearing loss, abnormal ears | 357, 558–560 |
| <i>Ptf1a</i> | Failure of UB induction, anal atresia, persistent cloaca, skeletal malformation | Pancreatic and cerebellar agenesis; diabetes mellitus | 561–563 |
| <i>Rara</i> , <i>Rarb</i> | Renal hypoplasia, dysplasia, hydronephrosis, skeletal and multiple visceral abnormalities | | 14, 17, 88 |
| <i>Sall1</i> | Renal agenesis, severe renal hypodysplasia | Townes-Brock syndrome (anal, renal, limb, ear anomalies) | 140, 564 |
| <i>Shh</i> | Bilateral or unilateral renal agenesis, unilateral ectopic dysplastic kidney, defective ureteral stromal differentiation | Vertebral defects, anal atresia, cardiac defects, tracheoesophageal fistula, renal anomalies, and limb abnormalities (VACTERL) syndrome | 59 |
| <i>Six1</i> | Lack of UB branching and mesenchymal condensation | Branchiootorenal syndrome | 136, 150 |
| <i>Sox8</i> , <i>Sox9</i> | Renal genesis, renal hypoplasia | Campomelic dysplasia (limb and skeletal defects, abnormal gonad development) | 565 |
| <i>Tln1</i> , <i>Tln2</i> | Renal agenesis | | 566 |
| <i>Wnt5a</i> | Renal agenesis, renal dysplasia, duplex kidneys, hydronephrosis | CAKUT | 567–569 |
| <i>Wt1</i> | Renal and gonadal agenesis, severe lung, heart, spleen, adrenal, and mesothelial abnormalities | Wilms tumor, aniridia, genitourinary abnormalities, and retardation (WAGR) syndrome; Denys–Drash syndrome | 39, 48, 437, 438 |
| Hypoplasia/Dysplasia/Low Nephron Mass | | | |
| <i>Adams1</i> | Hypoplasia of the renal medulla, hydronephrosis | | 319, 321 |
| <i>Adams1</i> , <i>Adams4</i> | Hypoplasia of the renal medulla, hydronephrosis | | 570 |

Table e1.2 Summary of Knockout and Transgenic Models for Kidney Development (Cont'd)

| Gene Mutation or Knockout | Phenotype | Associated Human Diseases | References |
|-----------------------------------|---|--|--------------------|
| <i>Agtr2</i> | Various collecting duct defects | CAKUT | 257, 422, 423 |
| <i>Ald1a2 (Raldh2)</i> | Renal hypoplasia, hydronephrosis, ectopic ureter | | 182 |
| <i>Bmp1ra (Alk3)</i> | Hypoplasia of renal medulla, fewer UB branches (UB-selective) | Juvenile polyposis syndrome | 254 |
| <i>Bmp4</i> | Severe renal hypodysplasia | Microphthalmia, orofacial cleft | 242 |
| <i>Bmp7</i> | Renal hypoplasia, reduced MM survival | | 294 |
| <i>Cask</i> | Renal hypoplasia and dysplasia, premature depletion of nephrogenic precursor cells | Microcephaly, mental retardation | 308, 571 |
| <i>Cdc42</i> | Renal hypoplasia, oligonephronia, defects in mesenchyme to epithelial transition (CM-selective) | | 355, 572 |
| <i>Cfl1</i> | Renal hypodysplasia, ureter duplication | | 573 |
| <i>Chd4 (Mi-2β)</i> | Renal hypodysplasia | Sifrim-Hitz-Weiss syndrome (autosomal dominant intellectual disability disorder with variable congenital defects in cardiac, skeletal, and urogenital systems) | 318, 574 |
| <i>Ctnnb1 (β-catenin)</i> | Severely hypoplastic kidney, lack of nephrogenic zone and S-shaped body (CM-selective) | Mental retardation, multiple cancers, eye defects | 289 |
| <i>Dchs1, Dchs2</i> | Renal hypoplasia, impaired ureteric branching, expansion of nephrogenic precursor zone | Van Maldergem syndrome 1—periventricular nodular heterotopia, intellectual disability, deafness, renal hypoplasia, tracheal anomalies, and skeletal dysplasia | 353, 356, 575 |
| <i>Dicer1</i> | Renal hypoplasia, dysplasia, cysts (UB-selective); renal hypoplasia characterized by premature termination of nephrogenesis (MM-selective) | | 576, 577 |
| <i>Dkk1</i> | Overgrown renal papilla (renal tubule and collecting duct restricted) | | 250 |
| <i>Dlg1</i> | Renal hypoplasia and dysplasia, premature depletion of nephrogenic precursor cells | | 308, 571 |
| <i>Dstn (Destrin)</i> | Renal hypodysplasia, ureter duplication | | 573 |
| <i>Egfr</i> | Hypoplasia of the renal papilla, moderate polyuria and urine concentration defects | | 248 |
| <i>Egln1 (Phd2), Egln3 (Phd3)</i> | Renal hypoplasia, oligonephronia, abnormal postnatal nephron formation, glomerulosclerosis (stroma-specific) | Familial erythrocytosis; abnormally high EPO levels; high altitude adaptation hemoglobin (HALAH) | 578 |
| <i>Esrrg</i> | Agenesis of renal papilla | | 53 |
| <i>Fat4</i> | Renal hypoplasia, impaired ureteric branching, failed nephrogenesis (mesenchyme-to-epithelial transition), expansion of nephrogenic precursor zone (stroma-selective) | Van Maldergem syndrome 2 (VMLDS2): dysmorphic faces, tracheomalacia, microtia, intellectual disability, and skeletal dysplasia | 352, 353, 356, 575 |
| <i>Fgf7</i> | Small kidneys, reduction in nephron number | | 253 |
| <i>Fgf8</i> | Renal dysplasia, arrested nephrogenesis at pretubular aggregate stage (MM-selective) | Kallmann syndrome, hypogonadism | 286, 287 |

Continued on following page

Table e1.2 Summary of Knockout and Transgenic Models for Kidney Development (Cont'd)

| Gene Mutation or Knockout | Phenotype | Associated Human Diseases | References |
|------------------------------------|---|---|-------------------|
| <i>Fgf10</i> | Renal hypoplasia, multiorgan developmental defects, including the lungs, limb, thyroid, pituitary and salivary glands | | 252 |
| <i>Fgfr1, Fgfr2</i> | Renal agenesis (MM-selective) | | 304 |
| <i>Fgfr2</i> | Renal hypoplasia, hydronephrosis (UB-selective) | | 60 |
| <i>Foxc2</i> | Renal hypoplasia | Lymphedema-distichiasis syndrome | 237, 579 |
| <i>Foxd1</i> | Accumulation of undifferentiated CM, attenuated UB branching, stromal patterning defects | | 28, 341, 343 |
| <i>Frs2</i> | Mild renal hypoplasia (UB-selective) | | 580 |
| <i>Fzd4, Fzd8</i> | Impaired UB branching, renal hypoplasia | | 581 |
| <i>Hdac1, Hdac2</i> | Renal hypoplasia, renal dysplasia, arrest of nephrogenesis at the renal vesicle stage | | 582, 583 |
| <i>Lats1, Lats2</i> | Renal hypoplasia, impaired UB-branching and UB tip specification, impaired nephrogenesis and renal interstitial differentiation | | 354, 584 |
| <i>Lgr4</i> | Severe renal hypoplasia and oligonephronia; renal cysts | Aniridia-genitourinary anomalies; mental retardation | 585, 586 |
| <i>Lmx1b</i> | Renal dysplasia, skeletal abnormalities | Nail-patella syndrome | 435, 442 |
| <i>Map2k1 (Mek2), Map2k (Mek1)</i> | Renal hypodysplasia, megaureter | Cardiofaciocutaneous syndrome | 208 |
| <i>Mdm2</i> | Renal hypoplasia and dysplasia, severely impaired UB branching and nephrogenesis (UB-selective); depletion of nephrogenic precursors (MM-selective) | | 587, 588 |
| <i>Mf2</i> | Renal hypoplasia, oligonephronia | | 589 |
| <i>Mitf</i> | Oligonephronia | Microphthalmia, Waardenburg syndrome type 2A | 590 |
| <i>Nf2</i> | Renal hypoplasia, renal dysplasia | | 584 |
| <i>Notch1, Notch2</i> | Loss of nephron derivatives, nephron segmentation defects | Alagille syndrome (cholestatic liver disease, cardiac disease, kidney dysplasia, renal cysts, renal tubular acidosis) | 293 |
| <i>Pbx1</i> | Reduced UB branching, expansion of nephrogenic precursors, delayed mesenchyme-to-epithelial transformation, dysgenesis of adrenal gland and gonads | | 357, 558 |
| <i>Plxnb2</i> | Renal hypoplasia and ureter duplication | | 591 |
| <i>Pou3f3 (Brn1)</i> | Impaired development of distal tubules, loop of Henle, and macula densa; distal nephron–patterning defect | | 320 |
| <i>Prr</i> | Renal hypoplasia, renal dysplasia, oligonephronia | | 592, 593 |
| <i>Psen1, Psen2</i> | Severe renal hypoplasia, severe defects in nephrogenesis | | 594 |
| <i>Ptgs2</i> | Oligonephronia | | 595 |
| <i>Rbpj</i> | Severe renal hypoplasia, oligonephronia, loss of proximal nephron segments, tubular cysts (MM-selective) | | 596, 597 |
| <i>Sall1</i> | Severe renal hypoplasia, cystic dysplasia of nephrogenic derivatives (tubules and glomeruli) | Townes-Brocks branchiootorenal-like syndrome | 358 |

Table e1.2 Summary of Knockout and Transgenic Models for Kidney Development (Cont'd)

| Gene Mutation or Knockout | Phenotype | Associated Human Diseases | References |
|--|---|--|--------------------|
| <i>Shp2</i> | Severe impairment of UB branching, renal hypoplasia | | 207 |
| <i>Six1</i> | Hydronephrosis, hydroureter, abnormal development of ureteral smooth muscle | | 361 |
| <i>Six2</i> | Renal hypoplasia and premature depletion of nephrogenic precursors (homozygous loss); increased UB branching and augmentation of nephron endowment (haploinsufficiency) | | 278, 337 |
| <i>Tbx18</i> | Hydronephrosis, hydroureter, abnormal development of ureteral smooth muscle | | 359, 361 |
| <i>Tfap2b</i> | MM failure, craniofacial and skeletal defects | | 598 |
| <i>Trp53 (p53)</i> | Oligonephronia, precocious depletion of nephrogenic precursors | Multiple cancers | 599 |
| <i>Trps1</i> | Impaired UB branching, renal hypoplasia | Trichorhinophalangeal syndrome (skeletal defects) | 600 |
| <i>Vangl2</i> | Impaired UB branching and renal hypoplasia | Neural tube defects | 332 |
| <i>Wnt4</i> | Failure of MM induction | | 289 |
| <i>Wnt7b</i> | Complete absence of medulla and renal papilla (UB-selective) | | 245 |
| <i>Wnt9b</i> | Vestigial kidney, failure of MM induction; cystic kidney (CD-selective) | | 135, 325 |
| <i>Wnt11</i> | Impaired ureteric branching, renal hypoplasia | | 211 |
| <i>Yap</i> | Renal hypoplasia renal dysplasia, hydronephrosis, severe disruption of UB branching (UB-selective), oligonephronia, defects in mesenchyme to epithelial transition (CM-selective) | Coloboma, hearing impairment, cleft palate, cognitive deficit, hematuria | 355, 572, 584 |
| Mislocalized or Ectopic UB/Increased UB Branching | | | |
| <i>Bmp4</i> | Duplex ureter, hydroureter, renal hypodysplasia | Microphthalmia, orofacial cleft | 242 |
| <i>Cer1</i> | Increased ureteric branching, altered spatial organization of ureteric branches | | 601 |
| <i>Cfl1</i> | Renal hypodysplasia, ureter duplication | | 573 |
| <i>Foxc1</i> | Duplex kidneys, ectopic ureters, hydronephrosis, hydroureter | | 237 |
| <i>Gata3</i> | Ectopic ureteric budding, duplex kidneys, hydroureter (UB-selective) | Hypoparathyroidism, sensorineural deafness, and renal dysplasia (HDRS) syndrome; autoimmune disease (rheumatoid arthritis) | 179, 180, 182, 183 |
| <i>Hnf1b, Pax2</i> | Renal hypoplasia, duplex kidneys, ectopic ureters, megaureter, hydronephrosis | CAKUT | 602 |
| <i>Hspb11 (Ift25)</i> | Duplex kidneys | | 603 |
| <i>Ift27</i> | Duplex kidneys | | 603 |
| <i>Lzts2</i> | Duplex kidneys/ureters, hydronephrosis, hydroureter | | 604 |
| <i>Plxnb1</i> | Increased ureteric branching | | 605 |
| <i>Plxnb2</i> | Renal hypoplasia and ureter duplication | | 591 |
| <i>Robo2</i> | Increased UB branching | CAKUT, VUR | 238, 239 |

Continued on following page

Table e1.2 Summary of Knockout and Transgenic Models for Kidney Development (Cont'd)

| Gene Mutation or Knockout | Phenotype | Associated Human Diseases | References |
|----------------------------------|--|---|-------------------|
| <i>Ror2</i> | Duplex ureter, hydronephrosis | Skeletal dysplasia, shortened limbs, brachydactyly, facial dysmorphia (brachydactyly, type B1, Robinow syndrome) | 569, 606 |
| <i>Sema3a</i> | Increased ureteric branching (UB-selective) | | 50 |
| <i>Slit2</i> | Increased UB branching | CAKUT, VUR | 238, 239 |
| <i>Spry1</i> | Supernumerary UBs, multiple ureters | | 87, 218 |
| <i>Wnt5a</i> | Duplex ureter, hydronephrosis | Robinow syndrome (skeletal dysplasia, shortened limbs, brachydactyly, facial dysmorphia) | 569, 606 |
| Renal Cysts | | | |
| <i>Angpt1, Angpt2</i> | Interstitial medullary cysts, urinary concentration defects | | 407 |
| <i>Aqp11</i> | Abnormal vacuolization of proximal tubules; polycystic kidneys | | 607 |
| <i>Arhgap35 (GRLF1)</i> | Glomerular cysts | | 73 |
| <i>Bcl2</i> | Renal hypoplasia and cysts | | 608 |
| <i>Bicc1</i> | Polycystic kidneys | | 609 |
| <i>Bpck</i> | Polycystic kidneys, hydrocephalus | Meckel syndrome 3 | 610 |
| <i>Erbb4</i> | Renal cysts (overexpression in renal tubules) | | 611 |
| | Dilated and mispolarized tubules, increased renal fibrosis (renal tubule deletion) | | |
| <i>Fat4</i> | Renal cysts, disrupted hair cell organization in inner ear | Van Maldergem syndrome (mental retardation, abnormal craniofacial features, deafness, limb malformations, renal hypoplasia) | 330, 612 |
| | | | |
| <i>Glis3</i> | Polycystic kidney, neonatal diabetes | Congenital hypothyroidism, diabetes mellitus, hepatic fibrosis, congenital glaucoma | 613, 614 |
| <i>Gpc3</i> | Disorganized tubules and medullary cysts | Simpson-Golabi-Behmel syndrome | 615–617 |
| <i>Hnf1b</i> | Polycystic kidney disease (tubule-selective) | CAKUT, diabetes mellitus, renal cysts, renal carcinoma | 326, 329, 544 |
| <i>Ift88 (Orpk)</i> | Polycystic kidneys; defective left-right asymmetric patterning | ARPKD | 618, 619 |
| <i>Ilk</i> | Medullary cysts (stroma-specific) | | 620 |
| <i>Invs</i> | Polycystic kidneys, inverted viscera | Nephronophthisis | 621, 622 |
| <i>Kif3A</i> | Polycystic kidney disease (tubule-selective) | | 623 |
| <i>Mafb (Kreisler)</i> | Decreased glomeruli, cysts, and tubular dysgenesis | Musculoaponeurotic fibrosarcoma | 624, 625 |
| <i>Mks1</i> | Renal hypoplasia and cysts | Meckel syndrome (multicystic dysplasia, neural tube defect) | 626 |
| <i>Pkd1, Pkd2</i> | Renal cysts | ADPKD, ARPKD | 627 |
| <i>Pten</i> | Abnormal ureteric bud branching, cysts (UB-selective) | Cowden disease, Bannayan-Riley-Ruvalcaba syndrome, various tumors | 209 |
| <i>Sall1</i> | Nephrogenic tubule and glomerular cysts (stroma specific) | Townes-Brocks branchiootorenal-like syndrome | 358 |
| <i>Taz</i> | Polycystic kidneys, emphysema | | 628, 629 |
| <i>Tek (Tie2)</i> | Interstitial medullary cysts, urinary concentration defects | Cutaneous and mucosal venous malformation, congenital glaucoma | 407 |
| <i>Vhl</i> | Renal cysts (tubule-selective) | Von Hippel-Lindau syndrome | 630 |
| <i>Xylt2</i> | Polycystic kidneys and liver | | 631 |
| <i>Zeb2</i> | Glomerular cysts | Mowat-Wilson syndrome (Hirschsprung disease with associated mental retardation) | 632 |

Table e1.2 Summary of Knockout and Transgenic Models for Kidney Development (Cont'd)

| Gene Mutation or Knockout | Phenotype | Associated Human Diseases | References |
|---|--|--|--------------------|
| Later Phenotypes (Tubular, Vascular, and Glomerular Defects) | | | |
| <i>Ace</i> | Atrophy of renal papillae, vascular thickening and hypertrophy, perivascular inflammation | Chronic systemic hypotension | 258, 259 |
| <i>Actn4</i> | Glomerular developmental defects, FSGS | SRNS | 451, 452 |
| <i>Adam10</i> | Loss of principal cells of the CD, hydronephrosis, polyuria | Alzheimer disease; reticulate acropigmentation of Kitamura | 271 |
| <i>Agt</i> | Atrophy of renal papillae, vascular thickening and hypertrophy, perivascular inflammation | Chronic systemic hypotension | 256, 427 |
| <i>Agtr1a (AT1A)</i> | Hypertrophy of juxtaglomerular apparatus and expansion of renin cell progenitors, mesangial cell hypertrophy | Chronic systemic hypotension | 633 |
| <i>Agtr1a/Agtr1b (AT1A/AT1B)</i> | Atrophy of renal papillae, vascular thickening and hypertrophy, perivascular inflammation | Chronic systemic hypotension | 261 |
| <i>Ampd</i> | Podocyte foot process effacement, proteinuria | Minimal change nephropathy | 634 |
| <i>Angpt1</i> | Simplification and <i>dilation</i> of glomerular capillaries; detachment of glomerular endothelium from the GBM; loss of mesangial cells; loss of ascending vasa recta (compound deletion with <i>Angpt2</i>) | | 382, 407 |
| <i>Angpt2</i> | Cortical peritubular capillary abnormalities (null allele); apoptosis of glomerular capillaries, proteinuria (transgenic overexpression); loss of ascending vasa recta (compound deletion with <i>Angpt1</i>) | | 390, 391, 407 |
| <i>Arhgdia (RhoGDIα)</i> <i>Bmp7</i> | Podocyte effacement and proteinuria Hypoplastic kidney, impaired maturation of nephron, reduced proximal tubules (podocyte-selective) | SRNS, FSGS | 77, 80, 635 398 |
| <i>Cd151</i> | Podocyte foot process effacement, disorganized GBM, tubular cystic dilation | Nephropathy (FSGS) associated with pretribial epidermolysis bullosa and deafness | 636, 637 |
| <i>Cd2ap</i> <i>Cdc42</i> | Podocyte effacement, proteinuria Congenital nephrosis; impaired formation of podocyte foot processes (podocyte-selective) | FSGS | 484 474 |
| <i>Cmas</i> | Congenital nephrosis; impaired formation of podocyte foot processes, defective sialylation | | 638 |
| <i>Col4a1, Col4a3, Col4a4, Col4a5</i> | Disorganized GBM, proteinuria | Alport syndrome | 639–642 |
| <i>Coq6</i> | Nephrotic syndrome and deafness | SRNS, FSGS, sensorineural deafness | 462, 643 |
| <i>Crb2</i> <i>Crk1, Crk2, CrkL</i> | Podocyte effacement and proteinuria Albuminuria, altered podocyte cytoarchitecture (podocyte-selective) | SRNS, FSGS | 644 645 |
| <i>Cxcl12 (SDF1), Cxcr4, Cxcr7</i> | Petechial hemorrhage in the kidneys, glomerular aneurysm, fewer glomerular fenestrations, reduced mesangial cells, podocyte foot process effacement, mild renal hypoplasia | WHIM (warts, hypogammaglobulinemia, infections, and myelokathexis) syndrome | 401, 402, 646 |

Continued on following page

Table e1.2 Summary of Knockout and Transgenic Models for Kidney Development (Cont'd)

| Gene Mutation or Knockout | Phenotype | Associated Human Diseases | References |
|-----------------------------------|--|--|-------------------|
| <i>Dicer1</i> | Podocyte damage, albuminuria, end-stage renal failure (podocyte-selective); reduced renin production, renal vascular abnormalities, striped fibrosis (renin cell-selective) | Pleuropulmonary blastoma | 430, 492–494 |
| <i>Dnm1, Dnm2 (Dynamin 1/2)</i> | Podocyte foot process effacement and proteinuria (podocyte-selective) | | 647 |
| <i>Dot1l</i> | Increased intercalated at the expense of principal CD cells; polyuria | | 275, 277 |
| <i>Efnb1 (Ephrin B1)</i> | Podocyte foot process effacement and proteinuria (podocyte-selective) | | 648 |
| <i>Efnb2 (Ephrin B2)</i> | Dilation of glomerular capillaries | | 396 |
| <i>Egln1 (Phd2), Egln3 (Phd3)</i> | Renal hypoplasia, oligonephronia, abnormal postnatal nephron formation, abnormally elevated erythropoietin production, dilation of renal blood vessels, glomerulosclerosis (stroma-specific) | Familial erythrocytosis; abnormally high EPO levels; high altitude adaptation hemoglobin (HALAH) | 578 |
| <i>Elf5</i> | Paucity in principal CD cells | | 274 |
| <i>Fat1</i> | Foot process fusion, failure of foot process formation, proteinuria | SRNS, FSGS, hematuria with neurologic defects; glioblastoma, colorectal cancer, head and neck cancer | 459, 649 |
| <i>Fermt2 (Kindlin-2)</i> | Rac1 hyperactivation, podocyte effacement and proteinuria | | 650 |
| <i>Flt1 (Vegfr1)</i> | Nephrotic syndrome | | 491 |
| <i>Foxc1 and Foxc2</i> | Impaired podocyte differentiation, dilated glomerular capillary loop, poor mesangial migration; proteinuria and glomerulosclerosis | Anterior segment dysgenesis/ Axenfeld-Rieger syndrome (iris hypoplasia and defective cornea); lymphedema-distichiasis syndrome (lower limb swelling and extra eyelashes) | 83, 651, 652 |
| <i>Foxi1</i> | Tubular acidosis; absence of CD intercalated cells | Tubular acidosis and deafness | 268, 269 |
| <i>Fyn</i> | Podocyte foot process effacement, abnormal slit diaphragms, proteinuria | | 478, 653 |
| <i>Gata3</i> | Impaired maintenance of mesangial cells, dilation of glomerular capillaries, glomerulosclerosis and mesangial matrix expansion, proteinuria | | 654 |
| <i>Gnas (Gαs)</i> | FSGS, mesangial expansion, proteinuria, urinary concentration defect (renin cell-specific) | Pseudohypoparathyroidism, McCune-Albright syndrome, endocrine tumors | 655, 656 |
| <i>Gne (Mnk)</i> | Hyposialylation defect, foot process effacement, GBM splitting, proteinuria and hematuria | | 657 |
| <i>Grhl2</i> | Occasional unilateral renal agenesis, CD barrier dysfunction, diabetes insipidus | Autosomal dominant deafness, ectodermal dysplasia | 542, 543 |
| <i>Ilk</i> | Nephrotic syndrome (podocyte-selective); collecting duct obstruction (UB-selective) | | 236, 482 |
| <i>Insr</i> | Podocyte effacement, GBM alteration, proteinuria (podocyte-selective) | Diabetic nephropathy | 658 |
| <i>Itga3 (Integrin α3)</i> | Reduced UB branching, glomerular defects, poor foot process formation | | 249, 251 |
| <i>Itga6 (Integrin α6)</i> | Collecting duct dilation and dysplasia | Epidermolysis bullosa, collecting duct dysplasia | 659 |

Table e1.2 Summary of Knockout and Transgenic Models for Kidney Development (Cont'd)

| Gene Mutation or Knockout | Phenotype | Associated Human Diseases | References |
|-------------------------------------|--|---|--------------------|
| <i>Itgb1</i> (<i>Integrin β1</i>) | Podocyte loss, capillary and mesangial degeneration, glomerulosclerosis (podocyte-selective) | | 548, 549 |
| <i>Itgb4</i> (<i>Integrin β4</i>) | CD dilation and dysplasia | Epidermolysis bullosa | 659 |
| <i>Kdr</i> (<i>Flik1/Vegfr2</i>) | Thrombotic microangiopathy, ascites; renal papilla dysplasia, urine concentration defects, loss of peritubular papillary capillaries (stroma specific) | Capillary infantile hemangioma | 345, 377 |
| <i>Kirrel</i> (<i>Neph1</i>) | Abnormal slit diaphragm function, FSGS | | 82 |
| <i>Lama5</i> | Defective glomerulogenesis, abnormal GBM, poor podocyte adhesion, loss of mesangial cells | | 233 |
| <i>Lamb2</i> | Proteinuria prior to the onset of foot process effacement | Pierson syndrome | 234, 660 |
| <i>Lmx1b</i> | Impaired differentiation of podocytes, cytoskeletal disruption in podocytes | Nail-patella syndrome | 661–663 |
| <i>Mafb</i> (<i>Kreisler</i>) | Abnormal podocyte differentiation | | 434 |
| <i>Magi2</i> | Podocyte effacement and proteinuria | SRNS, FSGS | 664–666 |
| <i>Mib1</i> | Loss of principal CD cells, polyuria, urine concentration defects, sodium wasting, hydronephrosis | Left ventricular noncompaction | 272 |
| <i>Mpp5</i> (<i>Pals1</i>) | Tubular cysts, podocyte effacement, and proteinuria | | 667 |
| <i>Mpv17</i> | Nephrotic syndrome | | 668 |
| <i>Mtor</i> | Proteinuria, podocyte autophagy defects (podocyte-selective) | | 669 |
| <i>Myo1E</i> | Podocyte foot process effacement and proteinuria | SRNS | 458, 670, 671 |
| <i>Nck1, Nck2</i> | Failure of foot process formation (podocyte-selective) | | 64 |
| <i>Nid1</i> | Abnormal GBM | | 672 |
| <i>Notch1, Notch2</i> | Lack of glomerular endothelial and mesangial cells (standard knockout); lack of podocytes and proximal tubular cells (MM-selective); impaired nephrogenesis (cap mesenchyme-selective) | Alagille syndrome (cholestatic liver disease, cardiac disease, kidney dysplasia, renal cysts, renal tubular acidosis) | 362, 363, 597, 673 |
| <i>Nphs1</i> (<i>Nephrin</i>) | Absent slit diaphragms, podocyte effacement, proteinuria | Congenital nephrosis of the Finnish type, childhood-onset steroid-resistant nephritic syndrome, childhood- and adult-onset FSGS | 444 |
| <i>Nphs2</i> (<i>Podocin</i>) | Congenital nephrosis, FSGS, vascular defects | SRNS, FSGS | 443, 674 |
| <i>Npnt</i> | Mislocalization of $\alpha 8\beta 1$ integrin, mesangial hyperproliferation and sclerosis (nephron and podocyte specific deletion) | | 675 |
| <i>Nrp1</i> | Glomerular aneurysm, impaired mesangial development, glomerulosclerosis | | 510 |
| <i>Par1a, Par1b</i> | Proximal tubule dilation and immature glomeruli | | 556 |
| <i>Pdgfb, Pdgfrb</i> | Lack of mesangial cells, ballooned glomerular capillary loop | | 508, 509 |
| <i>Pik3c3</i> (<i>Vps34</i>) | FSGS, defects in vesicular trafficking (podocyte-selective) | | 676, 677 |
| <i>Podxl</i> | Podocyte effacement, reduced glomerular capillary fenestrae, abnormal GBM, anuria | Congenital FSGS, omphalocele, and microcoria | 678, 679 |

Continued on following page

Table e1.2 Summary of Knockout and Transgenic Models for Kidney Development (Cont'd)

| Gene Mutation or Knockout | Phenotype | Associated Human Diseases | References |
|---|--|---|------------------------|
| <i>Prkci</i> (<i>aPKCλ/ι</i>) | Defect of podocyte foot processes, nephrotic syndrome (podocyte-selective) | | 472, 473 |
| <i>Ptpro</i> (<i>GLEPP1</i>) | Broadened podocyte foot processes with altered interdigitation patterns | SRNS | 657, 680 |
| <i>Rab3A</i> | Albuminuria, disorganization of podocyte foot process structure | | 681 |
| <i>Rbpj</i> | Decreased renal arterioles, absence of mesangial cells, and depletion of renin cells (stromal cell-selective) Reduction in juxtaglomerular cells, impaired renin synthesis (renin cell-selective) Loss of principal CD cells (UB-specific) | | 274, 364, 432 |
| <i>Rhpn1</i> | FSGS, podocyte foot process effacement, GBM thickening | | 464 |
| <i>Robo2</i> | Abnormal pattern of podocyte foot process interdigitation, focal effacement of foot processes, proteinuria | CAKUT, VUR | 682 |
| <i>Scl5a2</i> (<i>SGLT2</i>) | Elevated urinary excretion of glucose, calcium, and magnesium | Glucosuria | 683 |
| <i>Sh3gl1</i> , <i>Sh3gl2</i> , <i>Sh3gl3</i> (<i>Endophilin 1/2/3</i>) | Podocyte foot process effacement and proteinuria, neuronal defects | | 647 |
| <i>Sirpa</i> | Irregular podocyte foot process interdigitation, mild proteinuria | | 684 |
| <i>Sox4</i> | Oligonephronia, podocyte effacement, GBM defects (MM-selective) | | 685 |
| <i>Sox17</i> , <i>Sox18</i> | Vascular insufficiency in kidneys and liver; ischemic atrophy of renal and hepatic parenchyma; defective postnatal a | HLT (hypotrichosis-lymphedema-telangiectasia) syndrome (hair, vascular, and lymphatic disorder) | 403, 406 |
| <i>Sv2b</i> | Podocyte foot process effacement and proteinuria | | 686 |
| <i>Synj1</i> | Podocyte foot process effacement and proteinuria; neuronal defects | | 647 |
| <i>Tcf21</i> (<i>Pod1</i>) | Lung and cardiac defects, sex reversal and gonadal dysgenesis, vascular defects, disruption in UB branching, impaired podocyte differentiation, dilated glomerular capillary, poor mesangial migration | | 13, 339, 440 |
| <i>Tek</i> (<i>Tie2</i>) | Loss of ascending vasa recta and medullary capillary plexus, urinary concentration defects | Cutaneous and mucosal venous malformations, congenital glaucoma | 407 |
| <i>Tfcp2l1</i> | Loss of CD intercalated cells | | 273 |
| <i>Tjp1</i> (<i>ZO-1</i>) | Podocyte effacement and proteinuria | | 687 |
| <i>Trp63</i> (<i>TP63</i>) | Loss of CD intercalated cells | ADULT (acro-dermato-ungual-lacrimal-tooth) syndrome; limb-mammary syndrome | 270 |
| <i>Trpc6</i> | Protected from angiotensin-mediated or proteinuria or complement-dependent glomerular injury (null mutation); podocyte foot process effacement and proteinuria (transgenic overexpression in the podocyte lineage) | SRNS, FSGS | 460, 489, 490, 688–691 |
| <i>Vangl2</i> | Immature and poorly branched glomerular tuft | Neural tube defects | 332 |

Table e1.2 Summary of Knockout and Transgenic Models for Kidney Development (Cont'd)

| Gene Mutation or Knockout | Phenotype | Associated Human Diseases | References |
|----------------------------------|---|----------------------------------|--------------------|
| <i>Vegfa</i> | Endotheliosis, disruption of glomerular filtration barrier formation, nephrotic syndrome (podocyte-selective); peritubular capillary rarefaction and polycythemia (tubule-specific) | | 375, 376, 378, 692 |
| <i>Vhl</i> | Glomerulonephritis (podocyte-selective) | Von Hippel-Lindau syndrome | 400 |
| <i>Wasl (N-wasp)</i> | Podocyte effacement, proteinuria | | 693 |
| <i>Wnt7b</i> | Impaired development medullary microvasculature | | 694 |
| <i>Wnt11</i> | Glomerular cysts | | 695 |

ADPKD, Autosomal dominant polycystic kidney disease; ARPKD, autosomal recessive polycystic kidney disease; CAKUT, congenital anomalies of the kidney and urinary tract; CD, collecting duct; CM, cap mesenchyme; FSGS, focal segmental glomerulosclerosis; GBM, glomerular basement membrane; GDNF, glial cell-derived neurotrophic factor; MM, metanephric mesenchyme; SRNS, steroid-resistant nephrotic syndrome; UB, ureteric bud; VUR, vesicoureteral reflux.

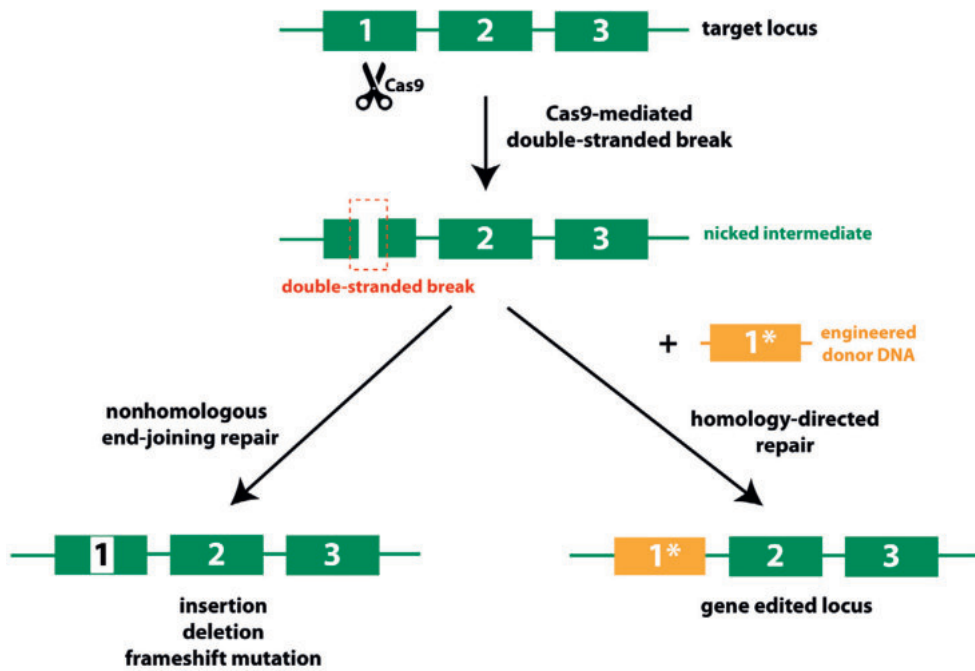


Fig. 1.12 Gene editing using the CRISPR-Cas9 system. Simplified overview for targeted introduction of mutations using the CRISPR-Cas9 system. Site-specific cleavage of a target gene locus with the Cas9 endonuclease creates a double-strand DNA break. The nicked target gene can be repaired by an error-prone, nonhomologous repair mechanism resulting in nucleotide insertion, deletion, or frameshift mutations. Introduction of a homologous engineered donor DNA results in a homologous substitution into the target locus which then results in a precisely edited gene.

dominant. Breeding of ENU-injected male mice results in offspring that can then be screened for various renal phenotypes (e.g., dysplasia, cysts, proteinuria) and heritability.^{69–71} Some examples of genes whose relevance to kidney development functions was revealed from ENU mutagenesis include *Arhgap23* (ciliogenesis and glomerular cyst defects), *Six1* (renal hypoplasia), *Scl5a2 (SGLT2)* (glucosuria), *Pou3f3 (Brn1)* (oligonephronia and smaller loop of Henle), and *Aqp11* (proximal tubule vacuolation and cysts).^{72–74}

Significant innovations in high-throughput gene sequencing are also facilitating the identification of monogenic mutations associated with heritable kidney diseases.^{75,76} Putative disease-causing genes identified from genome-wide association studies can then be validated in corresponding gene-targeted mouse models. Similarly, a gene whose mutation has been identified to cause kidney maldevelopment and dysfunction in mice can be investigated for incidence of mutations across the human genome (e.g., *Arhgdia* in nephrotic syndrome).^{77–80} Other genome-wide approaches that have led to the discovery of novel genes in kidney development and disease include gene trap consortia^{81,82} and genome-wide transcriptome and proteome projects.^{83–85}

IMAGING AND LINEAGE TRACING STUDIES

Reporter mouse lines are animal models engineered to express transgenes encoding an enzyme (e.g., bacterial β-galactosidase or firefly luciferase) or fluorescent protein tag in a cell lineage-specific manner (Fig. 1.13). In the simplest model, a single transgene comprising the reporter coding region is placed downstream of a cell-specific promoter. Such a model is useful to identify and follow distinct cell lineages where the chosen promoter is active. *Hoxb7-EGFP* is the first

fluorescent transgene developed to visualize renal development.⁸⁶ Enhanced green fluorescent protein (EGFP), placed under the control of the *Hoxb7* promoter, specifically labels the wolffian duct and the ureteric epithelial lineage. *Hoxb7-EGFP* has therefore proven to be invaluable in studying the rates and pattern of ureteric branching morphogenesis and ureteral development, including disruption of these events in the context of particular mutant backgrounds.^{60,87–89} An alternative model uses two separate transgenes, namely a cell-specific Cre driver and an independent reporter transgene (e.g., R26R). With the R26R reporter model, β-galactosidase transgene expression is switched on by a Cre-mediated removal of an upstream stop codon.⁹⁰ Inducible reporter systems incorporate genetic regulatory elements that allow for both cell-specific promoter- and drug-dependent activation of the reporter gene. The most commonly used strategies for controlled transgene expression in mice are the Tet-operon/repressor bi-transgenic and the estrogen-receptor ligand binding domain (Cre-ERT2) systems. These inducible reporter systems allow for timed pulse labeling of cell lineages, resulting in permanent tagging of progenitor cells and their direct derivatives. Inducible reporter systems have become valuable tools for the mapping of cell fates. Inducible reporter systems have been used to establish that the *Six2⁺* cells are the progenitors of all epithelial structures of the mature nephron.⁶¹ In some cases, the Cre transgene is engineered with an associated fluorophore expression cassette under the control of a shared promoter, thus allowing easy identification of cells with targeted gene mutations. A wide variety of reporter and Cre transgenes (see Table e1.2) are now available to characterize the development and organization of multiple compartments of the kidney.

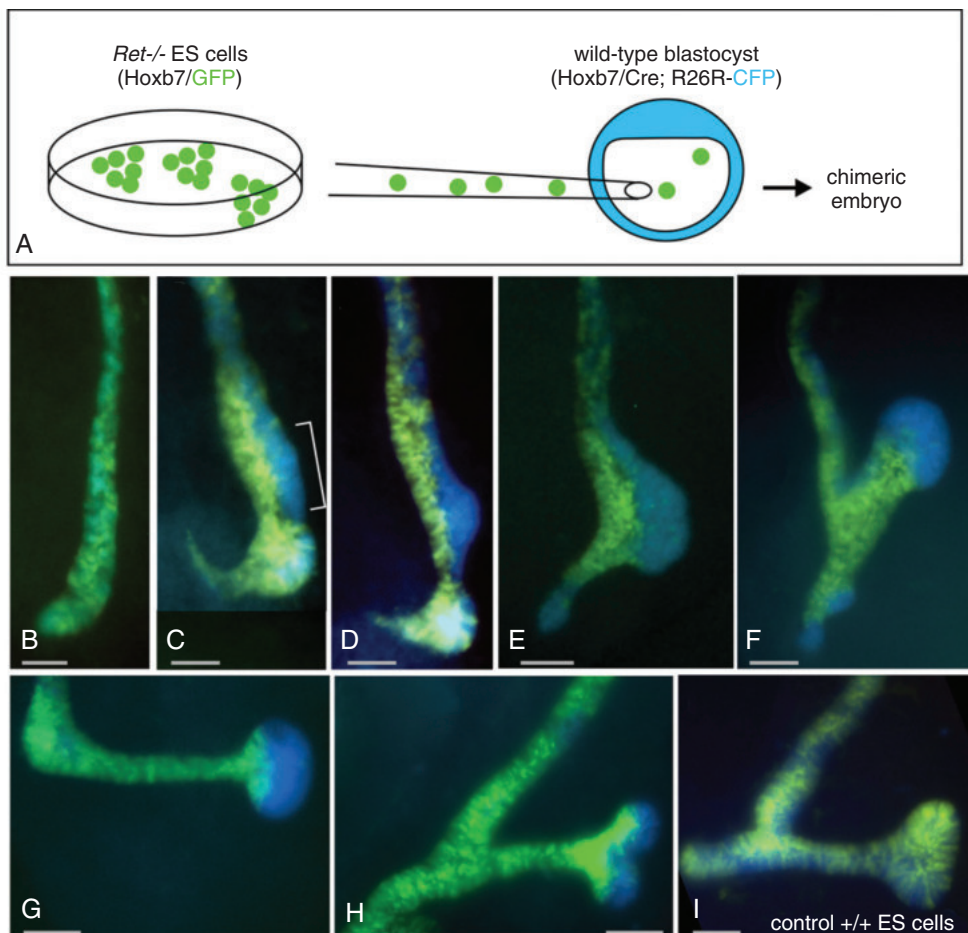


Fig. 1.13 Cell fate tracing through genetic expression of fluorophores. Segregation of *Ret*-deficient cells in the outgrowth and branching of the ureteric bud (UB). (A) *Ret*-null embryonic stem cells (ES) expressing *Hoxb7-GFP* were mixed with a wild-type transgenic blastocyst (*Hoxb7-Cre; R26R-CFP*). This generates chimeric animals in which *Ret*-null cells exhibit green fluorescent protein (GFP) fluorescence, while wild-type UB cells express cyan fluorescent protein (CFP). (B) At E9.5, *Ret*-null epithelial cells are intermingled with wild-type cells in the wolffian duct (WD). (C) At E10, when the dorsal side of the WD begins to swell, the region where UB will emerge becomes enriched with CFP-expressing but not *Ret*-null cells. (D, E) At around E10.5 dpc, the UB is exclusively formed by wild-type cells. (F) Upon elongation of the UB at E11, the bulbous distal tip of the UB is formed by wild-type cells but the *Ret*-null cells begin to contribute to the trailing trunk structure. (G, H) During the initial branching of the UB at around E11.5, *Ret*-null cells are excluded from the distal ampullary UB tips. (I) In contrast, control cells expressing *Ret* and GFP contribute to the whole branching UB structure. *dpc*, Days post coitum. Reproduced with permission from *Developmental Cell*.¹⁸⁶

Reporter mice expressing fluorescent tags also come in handy for segregation and isolation of particular cell types on the basis of fluorescence, facilitating global gene expression analysis, elucidation of transcriptional regulatory networks, and epigenetic interactions that orchestrate particular morphogenetic events (Table 1.3). Purified single or bulk populations of fluorescence-tagged cells can be used for high-throughput discovery of transcriptomes, genome-wide DNA-binding protein interactions, histone modifications, and nucleosome complexes through revolutionary next-generation DNA sequencing methods such as RNA-seq (RNA sequencing) and ChIP-seq (chromatin immunoprecipitation sequencing).^{91–93}

NONMAMMALIAN MODEL SYSTEMS FOR KIDNEY DEVELOPMENT

Organisms separated by millions of years of evolution from humans still provide useful models to study the genetic basis and function of mammalian kidney development. This stems

from the fact that all of these organisms possess excretory organs designed to remove metabolic wastes from the body, and that genetic pathways involved in other aspects of invertebrate development may serve as templates to dissect pathways in mammalian kidney development. In support of the latter argument, elucidation of the genetic interactions and molecular mechanism of the Kirrel (Neph1) orthologue and nephrin-like molecules SYG1 and SYG2 in synapse formation in the soil nematode *Caenorhabditis elegans* is providing major clues to the function of these genes in glomerular and slit diaphragm formation and function in mammals.⁹⁴

The excretory organs of invertebrates differ greatly in their structure and complexity and range in size from a few cells in *C. elegans*, to several hundred cells in *Drosophila*, to the more recognizable kidneys in amphibians, birds, and mammals. In *C. elegans*, the excretory system consists of a single large H-shaped excretory cell, a pore cell, a duct cell, and a gland cell.^{95,96} *C. elegans* provides many benefits as a model system: the availability of powerful genetic tools

Table 1.3 Mouse Strains for Conditional Gene Targeting and Lineage Marking of Cells

| Gene Promoter | Cre | rtTA | Cre-ERT2 | Fluorescent Reporter | Renal Expression | Extrarenal Expression | Reference |
|-----------------------------|-----|------|----------|----------------------|--|--|---------------------|
| <i>11Hsd2</i> | ✓ | | | ✓ | Principal cells of collecting duct, connecting tubules | Amygdala, cerebellum, colon, ovary, uterus, epididymis salivary glands | 696 |
| <i>Aqp2</i> | ✓ | | ✓ | | Principal cells of collecting duct | Testis, vas deferens | 697 |
| <i>Atp6v1b1</i> | ✓ | | | ✓ | Collecting ducts (intercalated cells), connecting tubule | | 698, 699 |
| <i>Bmp7</i> | ✓ | | ✓ | ✓ | Cap mesenchyme | | 700 |
| <i>Cdh16 (Ksp-Cadherin)</i> | ✓ | | ✓ | | Renal tubules, collecting ducts, ureteric bud, wolffian duct, mesonephros | Müllerian duct | 701, 702 |
| <i>Cited1</i> | | | ✓ | ✓ | Cap mesenchyme | | 703 |
| <i>Emx1</i> | ✓ | | ✓ | ✓ | Renal tubules (proximal and distal tubules) | Cerebral cortex, thymus | 704 |
| <i>Foxd1</i> | ✓ | | ✓ | ✓ | Stromal cells | | 705 |
| <i>Gdnf</i> | | | ✓ | ✓ | Cap mesenchyme | | 706 |
| <i>Ggt1</i> | ✓ | | | | Cortical tubules | | 707 |
| <i>Hoxb6</i> | ✓ | | ✓ | | Metanephric mesenchyme | Lateral mesoderm, limb buds | 547, 708 |
| <i>Hoxb7</i> | ✓ | ✓ | | ✓ | Ureteric bud, wolffian duct, collecting ducts, distal ureter | Spinal cord, dorsal root ganglia | 59 |
| <i>Kap</i> | ✓ | | | | Proximal tubules | Brain | 709, 710 |
| <i>Klf3</i> | | | ✓ | | Collecting ducts | Gonads | GUDMAP ^a |
| <i>Nphs1</i> | ✓ | ✓ | | ✓ | Podocytes | Brain | 711, 712 |
| <i>Nphs2</i> | ✓ | ✓ | ✓ | | Podocytes | | 713 |
| <i>Osr1</i> | ✓ | | ✓ | ✓ | Metanephric mesenchyme | Intermediate mesoderm | 714, 715 |
| <i>Osr2</i> | ✓ | | | | Condensing metanephric mesenchyme; glomeruli | Palatal mesenchyme | 716 |
| <i>Pax2</i> | ✓ | | | ✓ | Pronephric duct, wolffian duct, ureteric bud, cap mesenchyme | Inner ear, midbrain, cerebellum, olfactory bulb | 717 |
| <i>Pax3</i> | ✓ | | | | Metanephric mesenchyme | | |
| <i>Pax8</i> | ✓ | ✓ | ✓ | ✓ | Renal tubules (proximal and distal tubules) and collecting ducts (Tet-On inducible system) | Neural tube, neural crest | 713, 718, 719 |
| <i>Pck1</i> | ✓ | | ✓ | ✓ | Proximal tubules | Liver | 630 |
| <i>Pdgfb</i> | | | ✓ | | Endothelium | Systemic vascular endothelium | 722 |
| <i>Pdgfrb</i> | ✓ | ✓ | ✓ | ✓ | Mesangial cells, vascular smooth muscles | Pericytes, vascular smooth muscles | 396, 510, 723 |
| <i>Prox1</i> | ✓ | | ✓ | ✓ | Ascending vasa rectae, lymphatic vessels | Systemic lymphatic vasculature | 724–726 |
| <i>Rarb</i> | ✓ | | | ✓ | Metanephric mesenchyme | | 550 |
| <i>Ren1</i> | ✓ | | ✓ | ✓ | Juxtaglomerular cells, afferent arterioles, mesangial cells | Adrenal gland, testis, sympathetic ganglia | 420 |
| <i>Ret</i> | | | ✓ | | Urteric bud, collecting ducts | Dorsal root ganglion, neural crest | 727 |
| <i>Sall1</i> | | | ✓ | | Metanephric mesenchyme (tamoxifen-inducible system) | Limb buds, central nervous system, heart | 728 |
| <i>Six2</i> | ✓ | ✓ | ✓ | ✓ | Cap mesenchyme | | 61 |
| <i>Slc22a6</i> | | | ✓ | | Proximal tubules | | 721 |
| <i>Slc5a2</i> | ✓ | | | | Proximal tubules | | 729 |
| <i>Sox18</i> | | | ✓ | | Cortical and medullary vasculature | Blood vessel and precursor of lymphatic endothelial cells | 730–732 |

Continued on following page

Table 1.3 Mouse Strains for Conditional Gene Targeting and Lineage Marking of Cells (Cont'd)

| Gene Promoter | Cre | rtTA | Cre-ERT2 | Fluorescent Reporter | Renal Expression | Extrarenal Expression | Reference |
|---------------------|-----|------|----------|----------------------|--|--|---------------|
| <i>Spin3</i> | ✓ | | | | Medullary tubules (distal or connecting tubules?) | Mesonephric tubules, pancreas, lung, liver, gastrointestinal tract | 718, 719, 733 |
| <i>T (Brachury)</i> | ✓ | | ✓ | | Whole kidney (both ureteric bud and metanephric mesenchyme) | Pan-mesodermal | 286 |
| <i>Tbx18</i> | ✓ | | | | Ureteral mesenchyme | Heart, limb buds | 734 |
| <i>Tcf21</i> | ✓ | | | | Metanephric mesenchyme, cap mesenchyme, podocytes, stromal cells | Epicardium, lung mesenchyme, gonad, spleen, adrenal gland | 246 |
| <i>Tek</i> | ✓ | ✓ | ✓ | ✓ | Endothelium | Systemic vasculature endothelium | 735–737 |
| <i>Tie1</i> | ✓ | ✓ | | | Endothelium | Systemic vasculature endothelium | 738 |
| <i>Umod</i> | ✓ | | ✓ | | Thick ascending limbs of loops of Henle | Testis, brain | 739 |
| <i>Wnt4</i> | ✓ | | ✓ | ✓ | Renal vesicles, nascent nephrons (comma- and S-shaped bodies) | Lungs, developing gonads | 61, 740 |

^aGenitourinary Development and Molecular Anatomy Project (GUDMAP); <http://www.gudmap.org>.

Cre (noninducible Cre recombinase transgene); rtTA (reverse tetracycline transactivator, tetracycline inducible expression system); Cre-ERT2 (Cre-estrogen receptor ligand binding domain fusion transgene, tamoxifen-inducible expression system); fluorescent reporter (promoter-driven expression of a fluorescent protein such as green fluorescent protein and its variants.)

including “mutants by mail,” a short life and reproductive cycle, a publicly available genome sequence and resource database (<http://www.wormbase.org>), the ease of performing genetic enhancer-suppressor screens in worms, and the fact that they share many genetic pathways with mammals. Major contributions in our understanding of the function of polycystic and cilia-related genes have been made from studying *C. elegans*. The *Pkd1* and *Pkd2* homologues, *LOV1* and *LOV2* of *C. elegans*, are involved in cilia development and mating behavior.^{97,98} Strides in understanding the function of the slit diaphragm have also been made from *C. elegans* as described earlier.

Similar to *C. elegans*, the relative ease of large-scale genetic screens and phenotypic characterization in *Drosophila* makes it another valuable complimentary model for understanding the genetic basis of developmental processes. The excretory system of *Drosophila* consists of two parts, the nephrocytes and the malpighian tubules, which are functionally analogous to podocytes and renal tubules, respectively. A fundamental difference from vertebrate kidneys is that the nephrocytes and malpighian tubules are not physically connected. Nephrocytes either surround the heart (epicardial nephrocytes) or the esophagus (garland cells) and have elaborate membrane invaginations that closely resemble the glomerular filtration barrier. Remarkably, mutations of *Drosophila* homologs of genes known to be essential to form slit diaphragms and maintain podocyte functions also impair nephrocyte morphology and filtration functions.^{99–103} Similarly, conserved genes have been identified that regulate normal patterning and function of Malpighian tubules and vertebrate renal tubules.^{104–109} Functional readouts such as impaired

nephrocyte filtration or uptake of tracers, ultrastructural analysis, and mortality screens can be executed efficiently in *Drosophila*, which can facilitate the characterization of novel gene functions that are vital for renal filtration.^{110–112}

The pronephros is the functional kidney of the larva of some fishes (with the exception of jawless fishes which only develop the pronephros) and amphibians, while the mesonephros serve as the kidney in adults of these aquatic animals. The pronephros of the zebrafish (*Danio rerio*) larva consists of two tubules connected to a fused, single, midline glomerulus. The zebrafish pronephric glomerulus expresses many of the same genes found in mammalian glomeruli (e.g., *Vegfa*, *Nphs1*, *Nphs2*, and *Wt1*) and contain podocytes and fenestrated endothelial cells.¹¹³ Advantages to the zebrafish as a model system include its short reproductive cycle, transparency of the larvae with easy visualization of defects in pronephric development without sacrificing the organism, the availability of the genome sequence, the ability to rapidly knockdown gene function using morpholino oligonucleotides, and the ability to perform functional studies of filtration using fluorescently tagged labels of varying sizes.¹¹⁴ These features make zebrafish amenable to both forward and reverse genetic screens. Currently, multiple labs perform knockdown screens of mammalian homologs and genome-wide mutagenesis screens in zebrafish in order to study renal function. The pronephros of the clawed frog *Xenopus laevis* has also been used as a simple model to study early events in nephrogenesis.^{115,116} Similar to the fish, the pronephros of the clawed frog consists of a single glomus, paired tubules, and a duct. The fact that *X. laevis* embryos develop rapidly outside the body (all major organ systems are formed by 6 days of age),

the ease of injecting DNA, mRNA, and protein, ability to perform grafting, and in vitro culture experiments establish the frog as a valuable model system to dissect early inductive and patterning cues.^{117,118} The availability of transgenic zebrafish and *Xenopus* lines that express the fluorescent protein EGFP in pronephric and mesonephric kidneys provide an opportunity to visualize real-time kidney development and function.^{119–121}

STEM CELL DERIVED KIDNEY ORGANOIDS

The discovery that a combination of small molecules and cytokines can effectively induce human pluripotent stem cells (hPSCs) to develop into intermediate mesoderm laid the groundwork for ingenious in vitro methods to generate kidney organoid cultures in which most fundamental processes in early renal development are recapitulated.^{65,122–128} These hPSC-derived kidney organoids can form many renal structures, including the glomerulus, proximal tubule, loop of Henle, distal tubule, collecting ducts, interstitium, and a primitive endothelial network. Gene editing of hPSCs through CRISPR-Cas9 technology (see Fig. 1.12) provides a unique opportunity for a time- and cost-effective strategy to interrogate novel gene functions relevant to embryonic kidney development.^{66,129–131} One particular example is the study of epithelial cyst pathogenesis in kidney organoids from polycystin-deficient hPSCs.⁶⁵ Although their use in renal replacement therapy remains to be realized, kidney organoids have immediate practical application in high-throughput screening of drugs for nephrotoxicity.¹³²

GENETIC ANALYSIS OF MAMMALIAN KIDNEY DEVELOPMENT

INTERACTION OF THE URETERIC BUD AND THE METANEPHRIC MESENCHYME

The classic studies with the organ culture system that started in the 1950s provided an extensive framework that formed the basis for further studies of organ development.^{38,133,134} These elegant studies demonstrated that the epithelialization of the MM requires a UB-derived factor which we now know as Wnt9b.¹³⁵ However, the modern era of studies on the early development of the kidney began with the observation of renal agenesis phenotypes in gene-targeted or knockout mice, the earliest among these being the knockout of several transcription factors, including the *Wt1*, *Pax2*, *Eya1*, *Osr1* (*Odd1*), *Six1*, *Sall1*, *Lhx1* (*Lim1*), and *Emx2*.^{39,40,47,136–141} The knockout of genes for several secreted signaling molecules such as GDNF (glial cell line-derived neurotrophic factor), GDF11 (growth differentiation factor 11), gremlin, and the receptors Ret and GFRα1 also resulted in renal agenesis, at least in the majority of embryos.^{142–148}

Clinical Relevance

Perturbation of cell-cell communication during embryonic kidney development can have wide-ranging detrimental consequences, including renal agenesis, CAKUT, proteinuria, kidney cysts, defective urine osmoregulation, acidosis, and predisposition to hypertension and chronic kidney diseases.

EARLY LINEAGE DETERMINATION OF THE METANEPHRIC MESENCHYME

In most embryos exhibiting renal agenesis, an appropriately localized putative MM is often uninhabited by a UB outgrowth. Two exceptions are the *Osr1* (*Odd1*)- and *Eya1*-mutant embryos, where this distinct patch of MM is absent, suggesting that *Osr1* and *Eya1* represent early determinants of the MM (Fig. 1.14). Together, the phenotypes of these knockout mice have provided an initial molecular hierarchy of early kidney development.^{136,149} *Osr1* marks the intermediate mesoderm from which the mesenchymal cells within the mesonephric and metanephric kidney are derived and is subsequently downregulated upon epithelial differentiation. Mice lacking *Osr1* do not form the MM and do not express several other factors required for metanephric kidney formation, including *Eya1*, *Six2*, *Pax2*, *Sall1*, or *Gdnf*.¹⁴⁹

Eya1-mediated specification of the MM cell fate is thought to occur via interaction with another transcription factor, *Six1*. *EYA1* and *SIX1* mutations are found in humans with branchiootochal (BOR) syndrome.¹⁵⁰ It is now known through in vitro experiments that *Eya1* and *Six1* form a regulatory complex that appears to be involved in transcriptional regulation.^{151,152} Interestingly, *Eya1* was shown to have an intrinsic phosphatase activity that regulates the activation of the *Eya1/Six1* complex.^{152,153} Moreover, *Eya* and *Six* family genes are coexpressed in several tissues in mammals, *Xenopus* and *Drosophila*, further supporting a functional interaction between these genes.^{136,138,139,154,155} Direct transcriptional targets of this complex appear to include the pro-proliferative factor *Myc*.¹⁵² In the *Eya1*-deficient urogenital ridge the putative MM is completely absent.¹⁵⁶ Consistent with this finding, *Six1* is either absent or poorly expressed in the presumptive location of the MM of *Eya1*-null embryos.^{152,154–156} *Eya1* is expressed in the *Six1*-null mesenchyme, suggesting that *Eya1* is upstream of *Six1*.^{138,139}

The transcription factor *Wt1* is another essential regulator of early MM development. *Wt1* expression is weak in the uninduced MM but increases in the condensed cap mesenchyme surrounding the branching UB tips. *Wt1* expression remains throughout nephrogenesis but eventually becomes restricted to the presumptive podocytes at the proximal end of the S-shaped nephron. Mature podocytes continue to express *Wt1* at high levels. Genetic loss of *Wt1* in mice prevents UB outgrowth and causes apoptosis of the MM, whereas human mutations of *WT1* have been linked to renal tumors.^{39,157} Among the numerous identified transcriptional targets of *Wt1* known to be required for kidney development are *Bmp7*, *Pax2*, and *Sall1*.⁴⁸ More recently, it has been shown that *Wt1* regulates antagonistic fibroblast growth factor (FGF) and bone morphogenetic protein (BMP)/SMAD (contraction of homologous Sma and MAD genes of worms and fruitflies) signaling pathways, effectively promoting the proliferation and survival of the MM.^{158,159} The absence of *Wt1* significantly downregulates the expression of the genes for several FGF ligands, including *Fgf8*, *Fgf10*, *Fgf16*, and *Fgf20*, which support mesenchymal proliferation.^{48,159} Furthermore, *Wt1* deficiency in nephron progenitors leads to specific loss of *Gas1*, a gene encoding for an extracellular glycosphingolipid-tethered protein that modulates PI3K-Akt signaling downstream of FGFs.¹⁵⁸ The impairment of FGF signaling upon loss of *Wt1* is exacerbated by the upregulation of BMP/SMAD signaling,

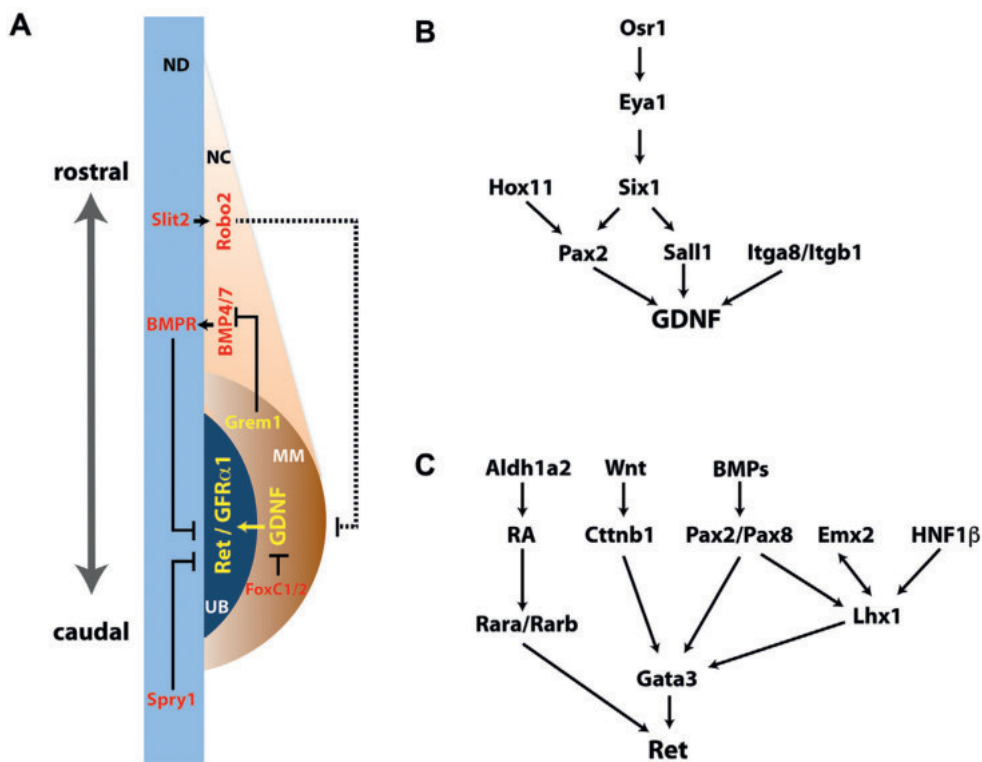


Fig. 1.14 Genetic interactions during early metanephric kidney development. (A) Regulatory interactions that control the strategically localized expression of glial cell-derived neurotrophic factor (GDNF) and Ret and the subsequent induction of the ureteric bud. The anterior part of GDNF expression is restricted by Foxc1/2 and Slit2/Robo2 signaling. Spry1 suppresses the postreceptor activity of Ret. BMP4/7-BMPR signaling inhibits the response to GDNF, an effect counteracted by Grem1. Genetic regulatory network that controls the expression of (B) GDNF and (C) Ret. *BMPR*, Bone morphogenetic protein receptor; *MM*, metanephric mesenchyme; *NC*, nephrogenic cord; *ND*, nephric duct; *UB*, ureteric bud.

which promotes apoptosis.¹⁵⁹ This is thought to occur through the loss of *Bmp4* expression, a direct target of *Wt1*, which inhibits BMP4 signaling.

URETERIC BUD INDUCTION

In many cases of renal agenesis, a failure of the GDNF-Ret signaling axis has been identified.¹⁶⁰ GDNF, a member of the TGF- β superfamily and secreted by the MM, activates the Ret-GFR α 1 receptor complex that is expressed by cells of the nephric duct and the UB. Activation of the Ret tyrosine kinase is of central importance to UB induction. Most mutant embryos lacking *Gdnf*, *Ret*, or *Cfra1* exhibit partial or complete renal agenesis due to severe impairment of UB induction while exogenous GDNF is sufficient to induce sprouting of ectopic buds from the nephric duct.^{142–144,148,161–164} Consistently, other genes linked to renal agenesis are known to regulate the normal expression of GDNF. These include transcription factors (e.g., *Eya1*, *Pax2*, *Six1*, *Hox11* paralogues, and *Sall1*) and proteins required to stimulate or maintain GDNF expression (e.g., GDF11, Kif26b, nephronectin, $\alpha\beta1$ -integrin, and *Fras1*) (see Fig. 1.14).^{136,139,140,145,165–173}

As described earlier, *Eya1* mutants fail to form the MM. *Pax2* is a transcriptional regulator of the paired box family and is expressed widely during the development of both UB and mesenchymal components of the urogenital system.¹⁷⁰ In *Pax2*-null embryos, *Eya1*, *Six1* and *Sall1* are expressed,¹⁵⁶ suggesting that *Eya1* and *Six1* are likely upstream of *Pax2*. Through a combination of molecular and in vivo studies, it

has been demonstrated that *Pax2* appears to act as a transcriptional activator of *Gdnf* and regulates the expression of *Ret*.^{171,174} *Pax2* also appears to regulate kidney formation through epigenetic control as it is involved in the assembly of a histone H3–lysine 4 methyltransferase complex through the ubiquitously expressed nuclear factor PTIP, which regulates histone methylation.¹⁷⁵ The *Hox* genes are conserved in all metazoans and specify positional information along the body axis. *Hox11* paralogues include *Hoxa11*, *Hoxc11*, and *Hoxd11*. Mice carrying mutations in any one of these genes do not have kidney abnormalities; however, triple-mutant mice for these genes demonstrate a complete absence of metanephric kidney induction.¹⁷² Interestingly, in this mutant, the formation of condensing MM and the expression of *Eya1*, *Pax2*, and *Wt1* remain unperturbed, suggesting that *Hox11* is not upstream of these factors. Although there seems to be some hierarchy, *Eya1*, *Pax2*, and *Hox11* appear to form a complex to coordinately regulate the expression of *Gdnf*.¹⁷⁶

Sall1 indirectly controls the expression of GDNF. *Sall1* is necessary for the expression of the kinesin *Kif26b* by the MM cells.¹⁶⁷ In the absence of either *Sall1* or *Kif26b*, the nephronectin receptor $\alpha\beta1$ -integrin expressed by the MM mesenchyme is downregulated. The loss of *Sall1*, *Kif26b*, *Itga8* ($\alpha 8$ integrin), *Itgb1* ($\beta 1$ -integrin), and *Npnt* (nephronectin) compromises the adhesion of the MM cells to the UB tips, ultimately causing loss of *Gdnf* expression and failure of UB outgrowth.^{168,169,177} The absence of *Fras1*, an extracellular matrix protein linked to Fraser syndrome, which is expressed

selectively in the UB epithelium and nascent epithelialized nephrons but not the MM, causes loss of *Gdnf* expression.¹⁶⁵ *Fras1* likely regulates MM induction and GDNF expression via multiple signaling pathways. *Fras1* deficiency results in downregulation of *Gdf11*, *Hox11*, *Six2*, and *Itga8*, and an increase in *Bmp4*, which altogether cooperatively controls *Gdnf* expression.¹⁶⁵

GENES REQUIRED BY THE URETERIC BUD

Several components of the genetic network supporting the development of the nephric duct and the UB have been identified (see Fig. 1.14). *Pax2* and *Pax8* are required to maintain the expression of *Lhx1*.¹⁷⁸ *Pax2*, *Pax8*, and *Lhx1* altogether likely coordinate the expression of *Gata3*, which is necessary for elongation of the nephric duct.¹⁷⁹ *Gata3* and *Emx2*, which are required for the expression of *Ret* in the nephric duct, are both regulated by β-catenin (*Ctnnb1*), an effector of the canonical Wnt signaling pathway.^{40,180,181} Acting likely in parallel with *Gata3* to maintain *Ret* expression in the UB is *Aldh1a2* (*Raldh2*), a gene in the retinoic acid synthesis pathway.¹⁸² Surprisingly, this genetic regulatory hierarchy cannot fully account for the distinctive phenotypes arising from the mutation of each individual gene, suggesting that additional important components of the nephric duct genetic network have yet to be identified. Nephric duct specification fails in *Pax2/Pax8* mutants but not in the case of *Lhx1* deficiency, where only the caudal portion of the nephric duct degenerates.¹⁷⁸ The absence of *Gata3* or *Aldh1a2* causes misguided elongation of the nephric duct, terminating into either blind-ended ureters or abnormal connections between the bladder and urethra.¹⁷⁹ The curtailed caudal growth of the nephric duct when either *Lhx1* or *Gata3* is lost prevents the formation of the first UB and consequently causes renal agenesis.^{179,183,184} The absence of *Aldh1a2* leads to the formation of ectopic ureters and hydronephrotic kidneys.¹⁸² *Emx2* deficiency does not prevent caudal extension of the nephric duct toward the presumptive MM but the evagination of the UB is aborted, thereby resulting in renal agenesis.⁴⁰ Without β-catenin, nephric duct cells undergo precocious differentiation into collecting duct epithelia.¹⁸⁵ *Ret* does not affect the nephric duct fate but has importance in later UB development and insertion of the nephric duct to the cloaca.^{162,182,186} Identification of additional targets of *Pax2*, *Pax8*, *Lhx1*, *Gata3*, and β-catenin are necessary in order to fully understand these seemingly disparate mutant phenotypes.

UB induction and subsequent branching requires a unique spatial organization of *Ret* signaling. The bulbous UB tip is a region enriched with proliferative ureteric epithelial cells, in contrast to the emerging stalk regions of the developing ureteric tree.^{41,187} It is now well appreciated that receptor tyrosine kinase signaling primarily through *Ret* is key to the proliferation of UB tip epithelia. Exogenous GDNF supplemented in explanted embryonic kidneys can cause expansion of the UB tip region toward the source of the ligand.^{187–189} ERK kinase activation is prominent within the ampullary UB terminals where *Ret* expression is elevated.⁴¹ Consistently, chimera analysis in mice reveals that *Ret*-deficient cells do not contribute to the formation of the UB tips.¹⁶² Altogether, these studies underscore the importance of strategic levels of *Ret* expression and activation of proliferative signaling pathways in the stereotypical sculpting of the nascent collecting duct network.

A ligand-receptor complex formed by GDNF, GFRα1, and *Ret* is necessary for autophosphorylation of *Ret* on its intracellular tyrosines (see Fig. 1.12). A number of downstream adaptor molecules and effectors have been identified to interact with active phosphorylated *Ret*, including Grb2, Grb7, Grb10, ShcA, Frs2, PLCγ1, Shp2, Src, and Dok adaptor family members (Dok4/5/6).^{190–201} These downstream *Ret* effectors altogether are likely contributors to the activation of the Ras/SOS/ERK and PI3K/Akt pathways supporting the proliferation, survival, and migratory behavior of the UB epithelium.^{41,43,202} Knock-in mutations of the interaction site for Shc/Frs2/Dok adaptors on the short isoform of *Ret* lead to the formation of rudimentary kidneys.^{203–206} Specific mutation of the PLCγ1 docking site on *Ret* leads to renal dysplasia and ureter duplications.²⁰³ The loss of *Shp2* and the upstream ERK regulators *Map2k1* (*Mek2*) and *Map2k2* (*Mek1*) in the UB lineage also cause severe renal hypoplasia phenocopying that is observed in occasional *Ret*-deficient kidneys.^{207,208} UB-specific inactivation of *Pten*, a target of the PI3K/Akt pathway, disrupts UB branching.²⁰⁹ Taken together, these findings underscore the significance of *Ret* signaling in normal UB branching.

A number of transcriptional targets of *Ret* activation in microdissected UB stimulated with GDNF have been elucidated (Fig. 1.15).²¹⁰ Among these are *Ret* itself and *Wnt11*, which stimulates *Gdnf* expression in the MM,²¹¹ suggesting that a positive feedback loop exists for the GDNF-*Ret* signaling pathway. *Ret* activation also positively regulates the ETS transcription factors *Etv4* and *Etv5*, which are also necessary for normal UB branching morphogenesis. *Etv4*-null homozygous mutants and compound heterozygous mutants for *Etv4* and *Etv5* manifest severe renal hypoplasia or renal agenesis, suggesting that these transcription factors are indispensable targets of *Ret* for proper UB development.²¹⁰ In chimeric animals, *Etv4/Etv5*-deficient cells, like *Ret*-deficient cells, fail to integrate within the UB tip domain.^{162,212}

The gene *Sprouty* was identified as a general antagonist of receptor tyrosine kinases and was discovered for inhibiting the FGF and EGF signaling pathways that pattern the *Drosophila* airways, wings, and ovarian follicles.^{213–215} Of the four mammalian *Sprouty* homologues, *Spry1*, *Spry2*, and *Spry4* are expressed in developing kidneys.²¹⁶ *Spry1* is expressed strongly at the UB tips, whereas *Spry2* and *Spry4* are found in both the UB and the MM.²¹⁷ *Sprouty* molecules are thought to uncouple receptor tyrosine kinases with the activation of ERK pathways either through competitive binding with the Grb2/SOS complex or the kinase Raf, effectively repressing ERK activation. Interestingly, *Spry1* expression is distinctively upregulated upon GDNF activation of *Ret*.²¹⁰ This suggests that *Ret* activates a negative feedback mechanism via *Spry1* in order to control activated ERK levels and modulate cell proliferation in the UB. Studies on *Spry1* knockout mice reveal some intriguing facets about *Ret* dependence of UB induction and branching.^{87,218–222} *Spry1* deficiency leads to ectopic UB induction and it can rescue renal development in the absence of either GDNF or *Ret*.^{222,223} Germline inactivation of *Spry2* does not overtly affect renal development but can rescue renal hypoplasia in mice engineered to express *Ret* mutants impaired in activating the Ras/ERK pathway.²¹⁷ The transcriptional targets of *Ret*, such as *Etv4*, *Etv5*, and *Wnt11*, are retained in *Gdnf/Spry1* or *Ret/Spry1* compound null mutants.^{222,223} These findings indicate that *Ret* signaling is not absolutely required for UB development. In fact,

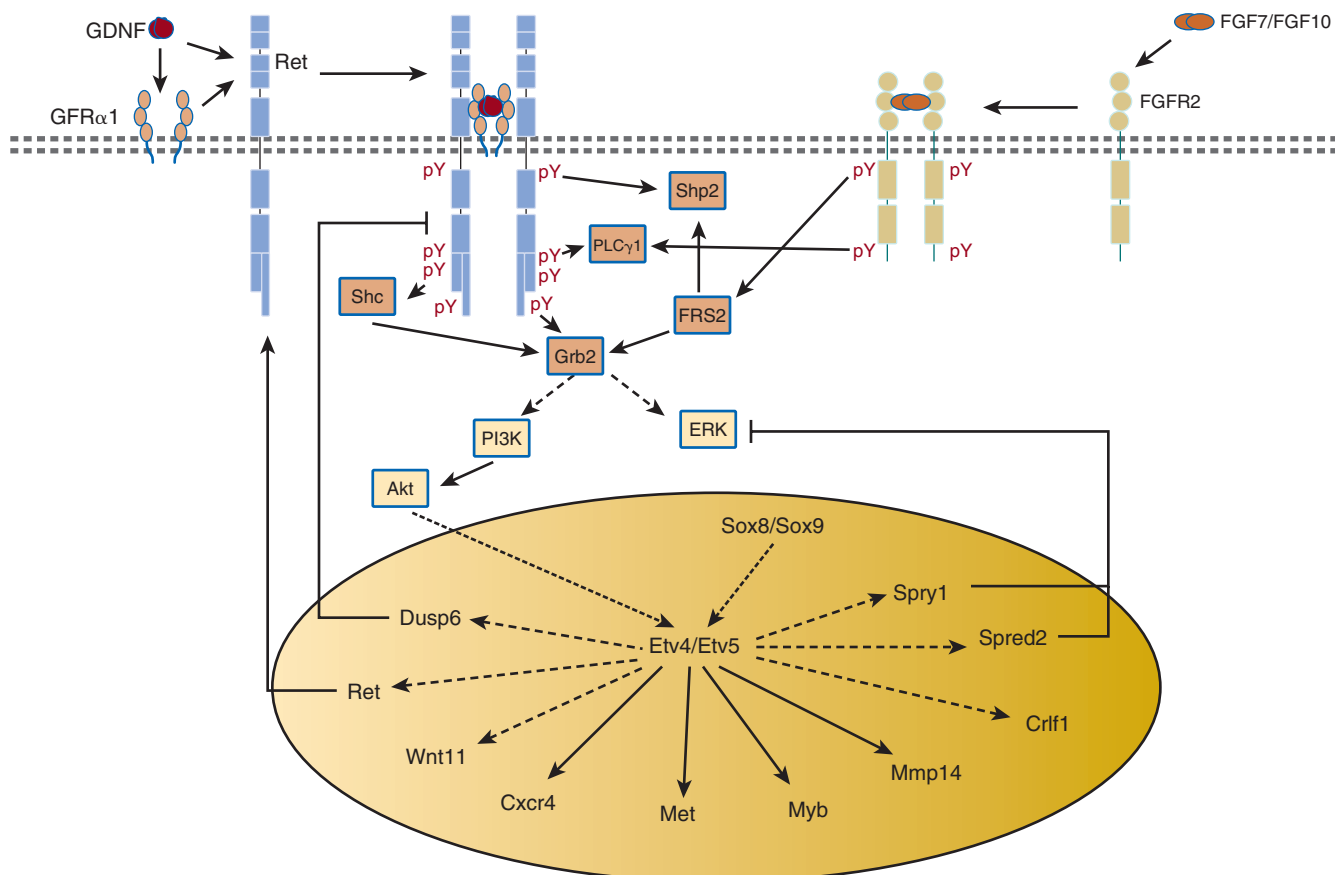


Fig. 1.15 Ret signaling pathway. Ret is activated and becomes autophosphorylated on intracellular tyrosine residues upon association with glial cell-derived neurotrophic factor (*GDNF*) and *GFR α 1*. Signaling molecules such as *Grb2*, *Shc*, *FRS2*, *PLC γ 1*, and *Shp2* bind directly to the phosphorylated tyrosine residues within the intracellular domain of Ret. Recruitment of *Shc*, *FRS2*, and *Grb2* leads to activation of ERK and PI3K/Akt pathways. *GDNF*-Ret signaling leads to the specific activation of a host of genes, some of which are strongly dependent on the upregulation of the transcription factors *Etv4* and *Etv5* (solid arrows). *Etv4*/*Etv5* activation requires activation of the PI3K/Akt but not the ERK pathway. *Sox8* and *Sox9* are believed to act in parallel to reinforce transcriptional responses to *GDNF*-Ret engagement. Some of these pathways are shared with the *FGF7/10*-*FGFR2* receptor signaling system. *Spry1* and *Spred2* negatively regulate ERK signaling, whereas *Dusp6* likely mitigates the dephosphorylation of the Ret receptor, thus acting as part of a negative feedback regulatory loop.

signaling via *FGF10* and *FGFR2* receptors is sufficient for renal development despite the absence of *GDNF* or *Ret*, provided *Spry1* is inactivated. Nevertheless, patterns of renal branching are distinctively altered in *Gdnf/Spry1* and *Gdnf//Ret* compound mutants with UB tips often displaying more heterogeneous shapes and orientation. These indicate that there remain some distinctive roles of *GDNF*-*Ret* signaling that cannot be fully compensated by *FGF10*/*FGFR2* during UB development.

ADHESION PROTEINS IN EARLY KIDNEY DEVELOPMENT

A current theme in cell biology is that growth factor signaling often occurs coordinately with signals from the extracellular matrix transduced by adhesion receptors such as members of the integrin family. The $\alpha 8\beta 1$ integrin complex is expressed by cells of the MM interacting with the novel ligand nephronectin (*Npnt*) expressed specifically by UB cells.^{169,224} In most *Itga8* ($\alpha 8$ integrin) mutant embryos, UB outgrowth is arrested upon contact with the MM.¹⁶⁹ In a small portion of embryos, this block is overcome, and a single, usually hypoplastic, kidney develops. Knockout mice for *Npnt* exhibit

renal agenesis or severe hypoplasia.¹⁶⁸ Thus the interaction of $\alpha 8\beta 1$ integrin with nephronectin must have an important role in the continued growth of the UB toward the MM. Both *Itga8* and *Npnt* knockout phenotypes appear to result from a reduction in *Gdnf* expression.¹⁶⁸ The attraction of the UB to the mesenchyme is also governed by the maintenance of proper cell–cell adhesion within mesenchymal cells. *Kif26b*, a kinesin specifically expressed in the MM, is important for tight condensation of mesenchymal cells.¹⁶⁷ Genetic inactivation of *Kif26b* results in renal agenesis resulting from impaired UB induction. In *Kif26b*-mutant mice, the compact aggregation of mesenchymal cells is compromised, resulting in distinctive loss of polarized expression of integrin $\alpha 8$ and severe downregulation of *Gdnf* expression. Hence, dysregulation of mesenchymal cell adhesion causes the failure to attract and induce the ureteric epithelia. Genetic evidence further shows that nephronectin localization at the basement membrane of the UB is critical for *Gdnf* expression by the MM. Genetic inactivation of basement membrane proteins associated with Fraser syndrome (*Fras1*, *Frem1/Qbrick*, and *Frem2*) lead to renal agenesis characterized by severe downregulation of *Gdnf* expression.^{165,166,225–228} On the basis of interaction of

nephronectin with *Fras1*, *Frem1*, and *Frem2*, it has been proposed that the *Fras1*/*Frem1*/*Frem2* ternary complex anchor nephronectin to the UB basement membrane, thus stabilizing engagement with $\alpha 8\beta 1$ integrin expressed by the MM (Fig. 1.16).²²⁵ *Grip1*, a PDZ-domain protein known to interact with *Fras1*, is required to localize the *Fras1*/*Frem1*/*Frem2* complex on the basal aspect of the UB epithelium.²²⁹ *Grip1* mutations phenocopy Fraser syndrome, including renal agenesis, thus further highlighting the importance of the strategic localization of nephronectin on the UB surface towards the opposing MM.^{229–231}

The establishment of epithelial basement membranes during metanephric kidney development involves the stage-specific assembly of different laminin α and β subunits with

a common laminin $\gamma 1$ subunit. The UB-specific inactivation of the gene *Lamc1*, which encodes for laminin $\gamma 1$, leads to impaired UB induction and branching, ultimately causing either renal agenesis or hypomorphic kidneys with water transport deficits.²³² *Lamc1* deficiency prevents the formation of basement membranes, causing downregulation of both growth factor (GDNF, Wnt11, and FGF2) and integrin-based signaling. This highlights another example of how signaling through the extracellular matrix intersects with growth factor signaling to influence morphogenesis. The importance of basement membrane assembly in the development of other renal structures is emphasized by genetic studies on the genes *Lama5* and *Lamb2*, which encode for laminins $\alpha 5$ and $\beta 2$, respectively. Loss of *Lama5* causes either renal agenesis or

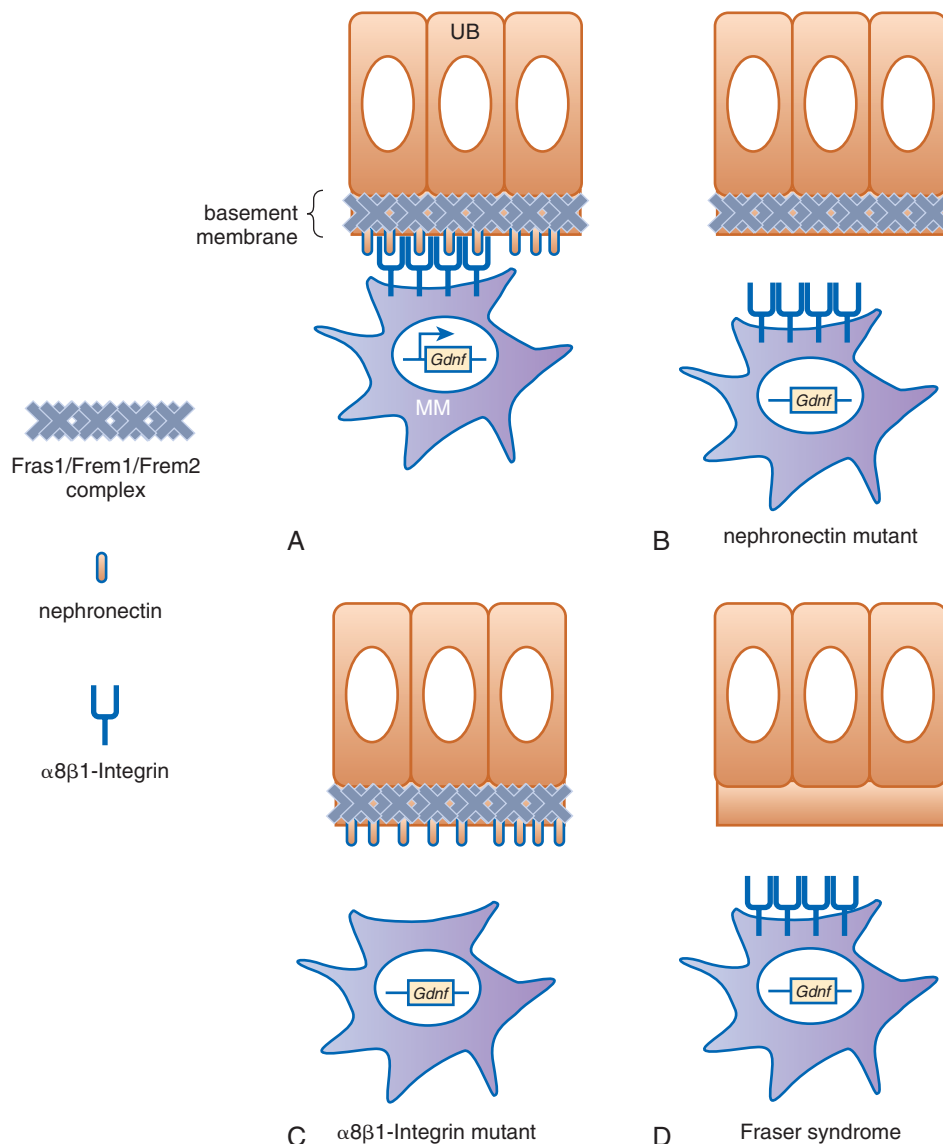


Fig. 1.16 Molecular model of renal defect in Fraser syndrome. (A) Adhesion to the ureteric bud (UB) epithelium positively regulates the expression of glial cell-derived neurotrophic factor (GDNF) by the metanephric mesenchyme (MM). Adhesion and GDNF expression are impaired in the absence of (B) nephronectin (expressed by the UB), (C) $\alpha 8\beta 1$ integrin (expressed by the MM), (D) or the *Fras1*/*Frem1*/*Frem2* complex. *Fras1*, *Frem1*, and *Frem2* are implicated in Fraser syndrome, and are believed to coordinate anchor nephronectin to the UB basement membrane and stabilize the conjugation with $\alpha 8\beta 1$ integrin. Modified from Kiyosumi, Takeichi M, Nakano I, et al.: Basement membrane assembly of the integrin $\alpha 8\beta 1$ ligand nephronectin requires Fraser syndrome-associated proteins. *J Cell Biol.* 2012;197:677–689.

disruption of glomerulogenesis, whereas deficiency for *Lamb2* leads to a defective glomerular filtration barrier.^{233,234}

The UB branching program is stereotypically organized such that the proliferative UB epithelial cells are largely confined to the bulbous UB tips, whereas cell division is dampened within the elongated nonbranching UB stalks of the growing ureteric tree. TROP2/Tacstd2, an adhesion molecule related to EpCAM, is expressed prominently in the UB stalks where it colocalizes with collagen-1.²³⁵ TROP2, unlike EpCAM, which is expressed throughout the UB tree, is not expressed at the UB ampullary tips. Consistently, dissociated and sorted UB cells expressing high levels of TROP2 are nonproliferative and express low levels of *Ret*, *Gfra1*, and *Wnt11*, which are notable UB tip markers. Elevated expression of TROP2 is also associated with poor attachment of epithelial cells to collagen matrix and suppression of cell spreading and motility, thus emphasizing the importance of this adhesion molecule in negative regulation of UB branching and the sculpting of the nascent collecting duct network. The formation of patent lumens within epithelial tubules of the kidney is also dependent on coordinated cell adhesion. $\beta 1$ Integrin is tethered to the actin cytoskeleton via a ternary complex formed between integrin-like kinase (ILK) and parvin. ILK has been shown to be important in mediating cell cycle arrest and cell contact inhibition in the collecting duct epithelia.²³⁶ The targeted ablation of the *Ilk* gene in the UB did not cause remarkable defects in UB branching but eventually caused postnatal lethality due to obstruction of collecting ducts arising from dysregulated intraluminal cell proliferation. Thus cell adhesion molecules may suppress cell division to regulate distinctive aspects of renal branching and tubulogenesis.

POSITIONING OF THE URETERIC BUD

A crucial aspect of kidney development that is of great relevance to renal and urological congenital defects in humans relates to the positioning of the UB (see Fig. 1.14). Incorrect positioning of the bud, or duplication of the bud, results in abnormally shaped kidneys and incorrect insertion of the ureter into the bladder, with a resultant ureteral reflux that can predispose to infection and scarring of the kidneys and urological tract.

Foxc1 is a transcription factor of the Forkhead family, expressed in the intermediate mesoderm and the MM adjacent to the wolffian duct. In the absence of *Foxc1*, the expression of GDNF adjacent to the wolffian duct is less restricted than in wild type embryos. *Foxc1* deficiency results in ectopic UBs, hypoplastic kidneys, and duplicated ureters.²³⁷ Additional molecules that regulate the location of UB outgrowth are Slit2 and Robo2, signaling molecules best known for their role in axon guidance in the developing nervous system. Slit2 is a secreted factor, and Robo2 is its cognate receptor. Slit2 is mainly expressed in the Wolffian duct, whereas Robo2 is expressed in the mesenchyme.²³⁸ UBs form ectopically in embryos deficient in either *Slit2* or *Robo2*, similar to the *Foxc1* mutant. However, in contrast to the *Foxc1* phenotype, none of the ureters in *Slit2/Robo2* mutants failed to undergo the normal remodeling that results in insertion in the bladder.²³⁸ Instead, the ureters remained connected to the nephric duct in *Slit2* or *Robo2* mutants. The domain of *Gdnf* expression is expanded anteriorly in the absence of either *Slit2* or *Robo2*. Indeed, mutations in *Robo2* have been identified in patients

with vesicoureteral junction defects and vesicoureteral reflux.²³⁹ The expression of *Pax2*, *Eya1*, *Foxc1*, and *Six2*, all thought to regulate *Gdnf* expression, was not dramatically different in the absence of *Slit2* or *Robo2*, suggesting that Slit2-Robo2 signaling was not upstream of these genes. Instead, recent findings strongly suggest that Slit2-Robo2 signaling, as in other systems, acts as a repulsive guidance cue.²⁴⁰ Consistent with this are findings that *Slit2* is most strongly expressed at an increasing gradient, at regions more anterior from the normal site of UB induction. Thus the absence of *Robo2* most likely compromises normal separation of the wolffian duct from the nephrogenic mesenchyme, ultimately broadening the nephrogenic zone and provoking ectopic UB induction.

Spry1, as described earlier in this chapter, negatively regulates the Ras/Erk signaling pathway and is expressed strongly in the posterior wolffian duct and the UB tips.²⁴¹ Embryos lacking *Spry1* develop supernumerary UBs, but unlike mutants of *Foxc1*, *Slit2*, or *Robo2* they do not display changes in *Gdnf* expression.²¹⁸ The phenotype of *Spry1* mutants can be rescued by reducing the *Gdnf* expression dosage.²¹⁸ *Spry1* deletion also rescues the renal agenesis defect in mice lacking either *Ret* or *Gdnf*.²²² Consistently, renal agenesis and severe renal hypoplasia in mice expressing *Ret* specifically mutated on a tyrosine phosphorylation site known to couple with the Ras/ERK pathway can be reversed in the absence of *Spry1*.²²³ Thus *Spry1* appears to regulate UB induction sites by dampening receptor tyrosine kinase-dependent proliferative signaling.

Another negative regulator of branching is BMP4, which is expressed in the mesenchyme surrounding the wolffian duct. *Bmp4* heterozygous mutants have duplicated ureters, and, in organ culture, BMP4 blocks the induction of ectopic UBs by GDNF-soaked beads.²⁴² Furthermore, knockout of *Grem1*, which encodes for the secreted BMP inhibitor Gremlin, causes renal agenesis, supporting a role for BMP in the suppression of UB formation.²⁴³

FORMATION OF THE COLLECTING DUCT SYSTEM

The overall shape, structure, and size of the kidneys are largely guided by the stereotypical branching of the UB and the subsequent patterning of the collecting duct system. During late gestation, past embryonic stage E15.5 in the mouse, the trunks of the UB tree undergo extensive elongation to establish the array of collecting ducts found in the renal medulla and papilla. The radial arrangement of elongated collecting ducts together with the loops of Henle (derived from the nephrogenic mesenchyme) establishes the corticomедullary axis by which nephron distributions are patterned. After birth, further elongation of the newly formed collecting duct network is partly responsible for the postnatal growth of the kidney.

Elongation of the collecting duct involves oriented cell division characterized by the parallel alignment of the mitotic spindle of proliferating ductal epithelia with the longitudinal axis of the duct.²⁴⁴ Oriented cytokinesis, therefore, guarantees that the daughter cells contribute to lengthening of the duct with minimal effect on tubular lumen diameter. The renal medulla and pelvis are nonexistent in mice lacking *Wnt7b*.²⁴⁵ Notably, the collecting ducts and loops of Henle are stubbier due to reorientation of cell division toward a radial instead of a longitudinal axis. *Wnt7b* expression is restricted within

the nonbranching stalk of the ureteric tree and is absent in the ampullary UB tips. Failed development of the renal medullary and papillary regions is also recapitulated in mice where *Ctnnb1* is ablated in the renal stroma, suggesting that Wnt7b activates the canonical β -catenin-dependent Wnt signaling pathway involving the ureteric epithelia and the surrounding stroma.^{245–247} However, the relevant reverse signal from the interstitial stroma to the collecting duct that drives oriented cell division in the duct epithelia remains unknown.

The normal development of the collecting ducts is also dependent on cell survival cues provided by diverse ligands, such as Wnt7b, EGF, HGF, and interactions with the extracellular matrix.^{245,248,249} Papillary collecting ducts display higher incidences of apoptosis in mice lacking Wnt7b or EGFR.^{245,248} Conversely, loss of Dkk1 (Dickkopf1), a secreted antagonist of Wnt7b, results in overgrowth of the renal papilla.²⁵⁰ Conditional inactivation of *Dkk1* using the *Pax8-Cre* transgene (expressed in renal tubules and the collecting ducts) causes increased proliferation of papillary epithelial cells. The HGF-receptor Met, $\alpha 3\beta 1$ integrin (*Itga3/Itgb1*), and laminin $\alpha 5$ (*Lama5*) are all required to maintain the expression of Wnt7b, and thus likely support the viability of collecting duct cells.^{177,249,251}

Poor development of the renal medulla and papilla are also observed in mutant mice lacking *Fgf7*, *Fgf10*, *Fgfr2*, *Bmp1ra* (*Alk3*), the components of the renin-angiotensin system, *Shh* (Sonic hedgehog), or the orphan nuclear steroid hormone receptor gene *Esrng*. FGF7 and FG10 are the cognate ligands of FGFR2. Renal hypoplasia is observed when *Fgfr2* is conditionally removed from the ureteric lineage and is more severe than in mutants lacking *Fgf7* or *Fgf10*, suggesting that these related ligands may have some functional redundancy in the development of the UB and collecting ducts.^{60,252,253} Kidneys lacking *Bmp1ra* show an attenuated phosphorylation of SMAD1, an effector of the BMP and TGF β ligands, and a concomitant increase in Myc and β -catenin levels.²⁵⁴ Although the significance of these results is not clear, the elevated expression of β -catenin indicates a novel crosstalk between BMP and Wnt signaling pathways in collecting ducts. Signaling through angiotensin is relevant to both early UB branching and the morphogenesis of medullary collecting ducts.²⁵⁵ Genetic inactivation of angiotensinogen, its processing enzyme ACE, and its target angiotensin-II AT1R receptors (*Agtr1a* and *Agtr1b*) results in similar phenotypes characterized by hypoplastic kidneys with modestly sized renal papillae.^{256–261} Furthermore, the postnatal growth and survival of renal papilla grown ex vivo are dependent on the presence of AT1R.²⁶² Interestingly, in cultures of renal papilla explants, angiotensin appears to regulate the Wnt7b, FGF7, and $\alpha 3\beta 1$ integrin signaling pathways such that the loss of endogenous angiotensin or pharmacologic inhibition of AT1R causes significant dampening of the expression of *Wnt7b*, *Fgf7*, *Ctnnb1*, *Itga3*, and *Itgb1*.²⁶² *Shh* is expressed in the more distal derivatives of the UB, the medullary collecting ducts, and the ureter.²⁶³ The germline deletion of *Shh* results in either bilateral renal agenesis or a single ectopic dysplastic kidney.^{263,264} It has been shown that *Shh* controls the expression of early inductive and patterning genes (*Pax2* and *Sall1*), cell cycle regulators (*Mycn* and *Cnd1*), and signaling effectors of the Hedgehog pathway (*Gli1* and *Gli2*). Interestingly, genetic removal of *Gli3* in an *Shh*-null background restores the expression of *Pax2*, *Sall1*, *Cnd1*, *Mycn*, *Gli1*, and *Gli2*,

providing physiologic proof for the role of *Gli3* as a repressor of the Shh pathway in renal development.²⁶⁴ Frameshift mutations resulting in truncation of the expressed Gli3 protein are linked to Pallister-Hall syndrome and the presence of hydronephrosis and hydroureter in both humans and mice.^{265,266} *Esrng* has a strong and localized expression within collecting duct epithelia later in gestation and its inactivation in mice causes complete aplasia of the renal medulla and papillae. However, the ligand of *Esrng* remains to be identified and little is known regarding its downstream targets.

The mature collecting duct epithelia consist of two major cell subtypes: the abundant principal cells which strongly express the aquaporins, ion channels, and pumps mediating Na $^+$ and K $^+$ transport; and the fewer intercalated cells which are responsible for secretion of protons and bicarbonate ions (see Fig. 1.14). A third collecting duct cell subtype, now called the transition cell, has been recently identified and coexpresses principal and intercalated cell-specific genes.²⁶⁷ Fate mapping analyses in an *Aqp2-Cre* and *Atp6v1b1-Cre* fluorescent reporter mouse line estimate that principal cells constitute ~60% of collecting duct epithelia, while intercalated cells and transition cells constitute ~30% and ~10%, respectively. Genetic studies suggest a cell type plasticity among collect duct epithelia with gene mutations identified as leading to disproportionate increase in one cell at the expense of the other with detrimental consequences in the maintenance of fluid, electrolyte, and acid balance.^{267–272} Lineage tracing analyses indicate that both principal and intercalated cells can dynamically switch fates, transforming into an intermediate cell type, the transition cell.²⁶⁷ Gene expression analyses implicate the Notch signaling pathway as an important regulator of collecting duct cell composition and patterning. Intercalated cells strongly express the Notch ligand *Jag1*, whereas principal cells express the Notch2 receptor.^{267,273} Genetic induction of Notch signaling within collecting ducts in adult mice notably increased the amount of *Aqp2* $^+$ principal cells while the number of *Atp6v1b1* $^+$ intercalated cells decreased in parallel, without altering the number of transition cells.²⁶⁷ Similarly, loss of the transcription factors *Tfcp2l1*, *Foxi1*, or the p53-related *Trp63* results in the paucity of intercalated cells.^{268,269} *Tfcp2l1* induces the expression of intercalated cell-specific genes including *Jag1* and *Atp6v1b1*.²⁷³ It has been proposed that Notch activation in the UB suppresses *Foxi1*, while the identification of putative Trp63 binding sites in the promoters of several Notch ligands suggests that Trp63 may repress Notch signaling. Conversely, inhibition of Notch signaling in ureteric epithelia leads to a disproportionate predominance of intercalated cells at the expense of principal cells, and the onset of polyuria, urinary concentration defects, and hydronephrosis.^{271,272,274} A specific target of Notch signaling in principal cells is the transcription factor *Elf5*, which positively regulates expression of principal cell-specific genes *Aqp2* and *Avpr2*.²⁷⁴ One other identified epigenetic regulator of principal cell fate is the histone methyltransferase encoded by *Dot1l*, which normally represses the aquaporin gene *Aqp5* and the intercalated cell-specific gene *Atp6v1b1*.^{275–277} *Dot1l* deficiency elevates the expression of both *Aqp5*, whose product interferes with cell surface localization of the principal cell-specific aquaporin *Aqp2* while concomitantly promoting the acquisition of intercalated cell traits with the upregulation of *Atp6v1b1*.

MOLECULAR GENETICS OF NEPHROGENESIS

EPITHELIALIZATION OF THE METANEPHRIC MESENCHYME

The generation of a sufficient number of nephrons requires a highly regulated balance between the expansion of progenitor compartments and the commitment toward epithelial fate to become renal vesicles. This has important clinical implications as the impaired renewal of nephron precursors or their perturbed differentiation can ultimately cause a wide range of renal pathologies due to significant paucity of functional nephrons. Signaling through Wnt, FGF, the BMP family of ligands, and Fat4 have been identified as important regulators of the delicate balance between progenitor self-renewal and differentiation.

All nephrogenic structures (podocytes, parietal epithelial cells, proximal tubules, loop of Henle, distal tubules, and the connecting tubule directly conjoined with the collecting duct) descend from a common progenitor pool that expresses the transcription factor *Six2*.⁶¹ *Six2* expression is notably elevated in the cap mesenchyme that condenses adjacent to the UB and is downregulated once this cap mesenchyme organizes into pretubular aggregates. It is now recognized that *Six2* activity is required to keep these nephron progenitor cells in a naïve, proliferative precursor state.^{61,278} *Six2* has been demonstrated to function as both a transcriptional activator that promotes cell cycling and proliferation, and as part of a repressor complex silencing differentiation-related genes.^{279,280} *Six2* can synergize with *Sall1*, to promote transcription of genes relevant to progenitor status (e.g., *Wt1*, *Eya1*, and *Gdnf*). *Six2* and *Sall1* also co-occupy promoters of their own genes, thus acting as positive feedback regulators of progenitor fate. *Six2* also interacts with *Osr1*, *Tcf* (Lef), and *Aes* (Groucho/TLE) to form a repressor complex that antagonizes expression of genes related to epithelialization (e.g., *Fgf8* and *Wnt4*).^{281,282} Complete loss of *Six2* causes premature ectopic formation of renal vesicles at E12.5 and the untimely depletion of nephron precursors.^{61,278} In contrast, overexpression of *Six2* prevented epithelialization of the cap mesenchyme.²⁷⁸

Six2⁺ nephron progenitors respond to stimulation with the UB-secreted factor *Wnt9b* and transition into epithelial renal vesicles.²⁸³ During the transition from cap mesenchyme to renal vesicles, expressions of a second Wnt family member *Wnt4* and an FGF family member *Fgf8* are activated. Canonical Wnt signaling involving β-catenin–dependent gene transcription is necessary and sufficient for the early inductive actions of *Wnt9b* and *Wnt4*, although it is also known that *Wnt4* can activate a noncanonical alternative pathway during the final phase of nephrogenic epithelialization.^{284–289} The interaction between *Six2*- and Wnt-signaling pathways appears to be intricately dosage- and context-dependent.^{280,282,283} When *Six2* expression remains high, Wnt signaling promotes progenitor renewal.²⁹⁰ In this situation, the stabilization of β-catenin promotes the association of *Six2* downstream target Myc with β-catenin, favoring precursor proliferation.^{283,291} However, with a sustained canonical Wnt-signaling pathway, β-catenin accumulates and displaces *Aes* converting the *Tcf* complex into a differentiation driver.²⁸⁰ The stabilization of

β-catenin eventually interferes with *Six2* expression, thus attenuating *Six2* expression. Notch signaling is required to prime nephron progenitors for differentiation and contributes to the silencing of *Six2* expression.²⁹² All nephron segments fail to form when Notch signaling is lost within the *Six2⁺* precursor lineage.²⁹³

The growth factor BMP7 is also required for the formation of the nephrogenic compartment.^{294–296} Activation of the Jnk pathway mediates the proliferative effect of BMP7 in uncommitted nephron precursors.^{297,298} BMP7, through activation of the p38-MAPK, causes upregulation of the transcriptional repressor *Trps1*.²⁹⁹ Loss of *Trps1* severely impairs the formation of renal vesicles. It has been speculated that *Trps1* may indirectly relieve repression of *Cdh1* expression. Additionally, BMP7-dependent phosphorylation and nuclear translocation of SMAD1/5/8 is required for *Wnt9b*-induced epithelialization.³⁰⁰ Thus BMP7 has dual essential roles in promoting both progenitor replenishment and priming for epithelialization. How these pathways integrate with *Six2*-dependent signaling complexes remains poorly understood. BMP signaling could either positively or negatively modulate β-catenin signaling. In other systems, SMAD proteins can associate and synergize with β-catenin and Tcf.³⁰¹ BMP signaling can also activate the PTEN pathway, which indirectly suppresses β-catenin activity.^{302,303}

The FGFs FGF2, FGF8, FGF9, and FGF20, and their cognate receptors FGFR1 and FGFR2, are essential to form nephrons. Compound loss of FGFR1 and FGFR2 in the MM leads to renal agenesis.³⁰⁴ FGF9 and FGF20 are required to maintain the multipotency and proliferative state of nephron precursors.³⁰⁵ FGF2 is required for the condensation of the cap mesenchyme.³⁰⁶ FGF8 is not needed for the formation of renal vesicles but is required for the survival of the newly formed nephrogenic epithelia. Renal vesicles lacking *Fgf8* fail to express *Wnt4* and *Lhx1*, and do not progress into S-shaped intermediate nephrons.^{286,287} Potential downstream targets of FGFR1/FGFR2 relevant to nephrogenesis are the closely related MAGUK family proteins encoded by the genes *Cask* and *Dlg1*.³⁰⁷ The absence of *Cask* and *Dlg1* causes impaired proliferation and cell death in nephron precursors, with a distinctive dampening of the Ras/ERK signaling pathway.³⁰⁸ *Fgf8* expression is severely attenuated when both *Cask* and *Dlg1* are absent. Moreover, *Cask/Dlg1* deficiency causes the formation of a loose cluster of cap mesenchyme around the UB. As *Dlg1* has been implicated in the directed migration of Schwann cells,^{309,310} it is tempting to speculate that *Cask* and *Dlg1* may play a supportive role in the UB-directed condensation of the cap mesenchyme.

NEPHRON SEGMENTATION AND TUBULOGENESIS

The mature nephron is a highly compartmentalized structure with individual segments having distinguishable molecular, cellular, and anatomic attributes. Nephron segments are organized along a proximal-distal axis, from the most proximal renal corpuscle or glomerulus, followed by the proximal tubule, the loop of Henle, the distal tubule, and the most distal connecting tubule that links directly to the UB-derived collecting duct. The segmental patterning of nephrons involves a complex series of events instructed by inductive cues between neighboring cells and controlled by epigenetic

signaling mechanisms. A variety of human diseases result from the mispatterning of nephrons.³¹¹

Elegant imaging studies combined with high-throughput single-cell gene expression analysis demonstrate that nephron patterning is determined as early as the recruitment of mesenchymal nephron progenitors from the cap mesenchyme.³¹² Recent evidence indicates that renal vesicle arises not from a single event in time. Instead, nephron progenitors progressively incorporate into the nascent nephrons, with the timing of their recruitment predicting their acquisition of proximal–distal fates (i.e., initial recruits commit to distal fates while the last recruits contribute to the formation of more proximal fates) (Fig. 1.17).

By the renal vesicle stage, gene expression asymmetry highlights an early establishment of proximal and distal domains. Genes such as *Fgf8*, *Lhx1*, *Dll1*, *Dkk1*, *Hnf1b*, *Sox9*, and *Pou3f3* are markedly elevated in the distal portion of the renal vesicles, whereas *Wt1*, *Foxc2*, and *Mafb* are largely restricted in the proximal end.^{57,313} Some genes are expressed in both regions, such as *Wnt4*, *Jag1*, *Cdh6*, and *Ccnd1*, albeit nonuniformly and more elevated in the distal domain.³¹³ By the S-shaped body stage, nephron segmentation has become more evident, with several more marker genes having distinctively regionalized expression patterns.

As the earliest nephron precursors that interact with the UB become destined to acquire distal fates, it can be speculated that localized Wnt9b signaling orients the proximal–distal axis. Interestingly, in chick mesonephros, overexpression of Wnt3 in the coelomic lining redirects the glomerular development farthest away from the coelomic

lining while the distal nephron occasionally become fused with the coelomic lining.³¹⁴ During nephrogenesis, a gradient of β -catenin activity is established along the nephron's longitudinal axis with the highest β -catenin activity found in the distal end, progressively decreasing towards the proximal end.⁴⁵ Although β -catenin is absolutely required to initiate nephron induction, its activity must be attenuated in order to complete an epithelial differentiation program.²⁸⁹ Indeed, a β -catenin gradient is already established within renal vesicles and a persistent constitutive activation of β -catenin prevents epithelialization.^{45,289} In organ cultures, pharmacologic manipulation of β -catenin activity can alter proximal and distal fate acquisition. Attenuation of β -catenin activity accelerates glomerular development. Conversely, augmentation of β -catenin activity favors the expression of *Lgr5*, a marker of distal fate, while repressing proximal identity. Additionally, it has been identified that modulation of β -catenin activity involves an integration of Wnt, Notch, and BMP signaling pathways.

Although many genes are now known as marking nephron segments, only a few other genes and pathways have been characterized that strongly influence proximal versus distal fate determination. Loss of *Hnf1b* in the nephrogenic precursors causes marked loss of proximal and median domain markers at the S-shaped body stage, causing the formation of immature and cystic glomeruli connected to the collecting duct by a severely truncated renal tubule.^{315–317} A mutation in *Sall1* that prevents Sall1-NuRD interaction downregulates the distal marker *Lgr5*, and specifically impairs the development of the loop of Henle and distal tubules.³¹⁸ Other genes

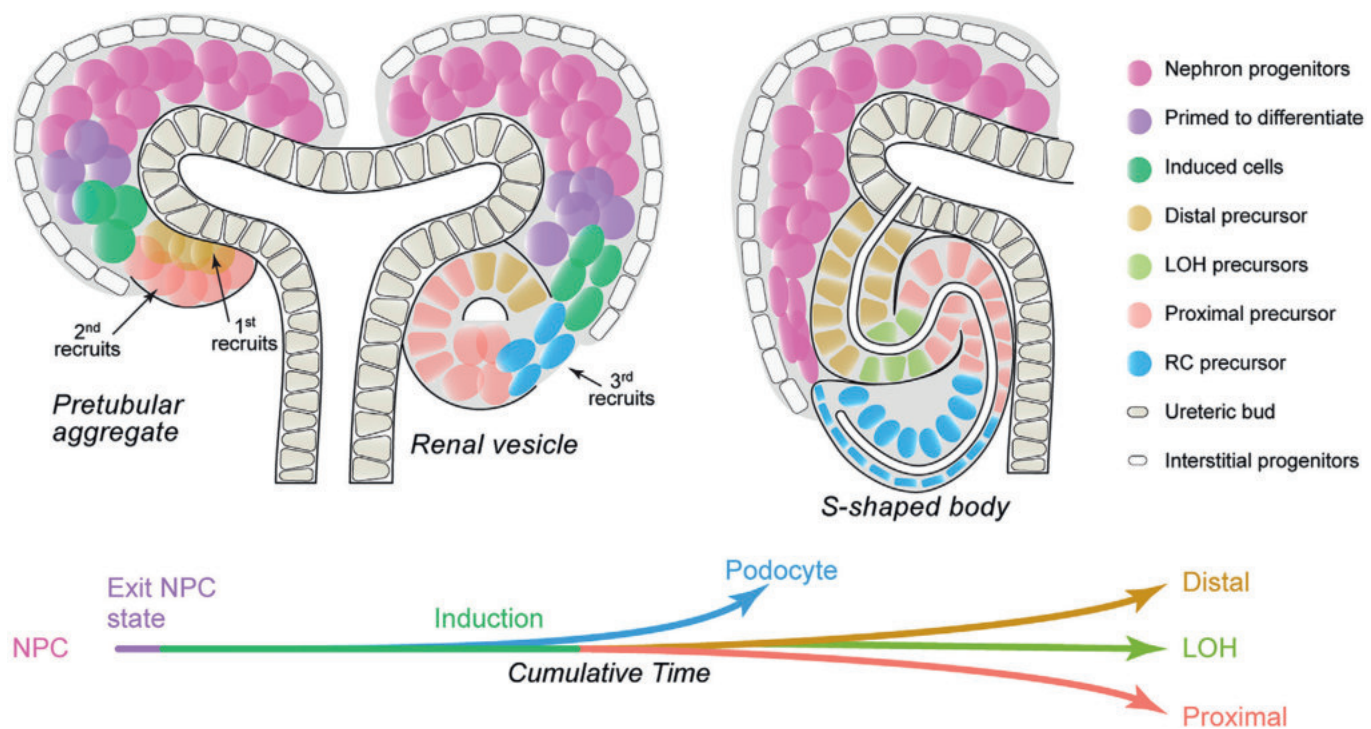


Fig. 1.17 Gradual recruitment of progenitor cells during nephrogenesis. Early recruited nephron progenitors clustering around the ureteric bud give rise to pretubular aggregates. New progenitors continue to be recruited and incorporate to the proximal end of the renal vesicle. Distal, medial, and proximal domains are established by the S-shaped body stage. *NPC*, Nephron progenitor cell; *LOH*, loop of Henle; *RC*, renal corpuscle. Adapted from Lindström NO, De Sena Brandine G, Tran T, et al. Progressive recruitment of mesenchymal progenitors reveals a time-dependent process of cell fate acquisition in mouse and human nephrogenesis. *Dev Cell* 2018;45:651–660.

required to generate distal tubules and the loop of Henle are *Pou3f3* and *Adams1*.^{319–321}

In addition to cell differentiation, the spatial orientation of cells is essential for tubule elongation and morphogenesis. In epithelia, cells are uniformly organized along an apical–basal plane of polarity. However, in addition, cells in most tissues require positional information in the plane perpendicular to the apical–basal axis. This type of polarization is referred to as planar cell polarity and is critical for the morphogenesis of metazoans.^{322,323} Using cell lineage analysis and close examination of the mitotic axis of dividing cells, it has been shown that the lengthening of renal tubules is associated with mitotic orientation of cells along the tubule axis, demonstrating intrinsic planar cell polarity.²⁴⁴ Dysregulation of oriented cell division can give rise to cysts due to abnormal widening of tubule diameters.³²⁴ To date, molecules implicated in planar cell polarity and nephrogenic tubule elongation include *Wnt9b*, *Hnf1b*, *Pkhd1*, *Fat4*, *Celsr1*, and *Vangl2*.^{244,246,325–332}

CESSATION OF NEPHROGENESIS

Nephrogenesis is a time-limited event that is not reactivated postinjury to the kidneys of humans and mice at adulthood. The last wave of nephrogenesis is observed around the 36th wave of gestation in humans and shortly after birth in mice.^{333,334} Cessation of nephron generation is characterized by the exhaustion of nephron progenitor cells and the completion of epithelial differentiation of the remaining nephrogenic precursor. Although various morphologic and molecular changes occurring at this time have been characterized in mouse kidneys, the exact trigger is not fully understood.^{333,335,336}

In mice, the nephrogenic zone progressively shrivels after birth and is replaced by mature tubules by P6. The precursor markers *Six2* and *Cited1* are significantly downregulated at P2 and are undetectable by P3, concomitant with the disappearance of the cap mesenchyme. Multiple newly induced nephrons are found associated with each UB tip at P3 that are no longer found at P7. Ureteric branching also ends between birth and P3 accompanied by a significant reduction of *Ret* and *Wnt11* and loss of the UB ampullary shape.^{333,335} In contrast, *Wnt9b* expression in the UB remains high even at P4, consistent with findings that the UB tips isolated from P3 kidneys remain competent in promoting survival and inducing epithelialization of recombined mesenchyme taken from embryonic kidneys.³³³ This strongly argues against the possibility that weakened trophic support from the UB contributes to the progressive decline of the nephrogenic precursor population and is supported by the rarity of apoptosis within the postnatal nephrogenic zone. *Foxd1* expression is also downregulated by P3, but given the expansion of the cap mesenchyme in *Foxd1*- or stroma-deficient kidneys, it is unlikely that postnatal loss of the *Foxd1*⁺ stromal compartment provokes the abrupt halting of nephrogenesis.³³³ There is also no evidence that nephrogenic progenitors have switched to stromal fates. Instead, what is now apparent is that the remaining cap mesenchyme becomes globally committed to epithelialize. Interestingly, when nephron progenitor proliferation is enhanced and kidney size is increased as seen in *Six2* haploinsufficient mice, the timing of nephrogenesis cessation is unaltered.³³⁷

Two opposing factors appear more likely to contribute to the termination of nephrogenesis: (1) a rapid decline in the proliferation rate of the *Six2*⁺ cell compartment, which was observed between E15.5 and P0; and (2) an acceleration of nephrogenic differentiation postnatally.^{333,335} One model proposed posits that the novel spatial relationship between cell types in the kidney around birth (as compared to early embryonic stages) dramatically alters the molecular context of the nephrogenic niche, thus shifting the balance between progenitor self-renewal and commitment to differentiation.^{335,336,338} Another proposed model argues that increased oxygen tension after birth, which turns on the expression of glycolysis-related genes, could act as an active trigger that ends nephrogenesis.³³⁶ However, this latter model, although applicable in mice, may not be a shared mechanism in humans where nephrogenesis ceases before parturition. A thorough understanding of the mechanism of nephrogenesis cessation is necessary to better assess the potential of regenerative therapies for the kidney.

MOLECULAR GENETICS OF THE STROMAL CELL LINEAGE

The maintenance of reiterative ureteric branching and nephron induction largely accounts for the growth and enlargement of embryonic kidneys. Genetic studies reveal that interstitial stroma provide additional inductive cues that regulate UB branching and nephrogenesis (Fig. 1.18). These studies also underscore the pivotal role played by the stroma in establishing the stereotypical radial patterning of the kidney. In embryonic kidneys, the stroma is organized into two distinct zones: an outer stromal region within the nephrogenic zone expressing the winged helix transcription factor *Foxd1*, and a deeper region expressing the basic-helix-loop–helix (bHLH) transcription factor *Tcf21* (*Pod1*).^{28,29,339,340} Without either *Foxd1* or *Tcf21*, UB branching and nephrogenesis are notably impaired, resulting in a distinctive perturbation of the corticomедullary renal histoarchitecture.^{28,29,339}

The most prominent features of the genetic loss of *Foxd1* include the thickening of the renal capsule and the formation of large metanephric mesenchymal condensates.^{28,341} The morphologically altered renal capsule in *Foxd1*-mutant kidneys has notably lost expression of *Aldh1a2* (*Raldh2*) and *Sfrp1* (a regulator of Wnt signaling), and is abnormally interspersed with endothelial cells and *Bmp4*-positive cells.³⁴¹ The identity of these *Bmp4*-expressing cells populating the renal capsule in *Foxd1*-deficient kidneys is unknown, although they are clearly distinct from the presumptive medullary stroma based on lineage tracing for *Foxd1*-promoter expression. As BMP4 is a known chemotactic agent for endothelial cells,³⁴² it is very likely that the ectopic *Bmp4*-positive cells account for the presence of endothelial cells within the broadened renal capsule of *Foxd1*-mutant kidneys. The accumulation of the cap mesenchyme is also likely contributed in part by ectopic *Bmp4* signaling in the absence of *Foxd1* because *Bmp4* has been shown to antagonize epithelialization of the cap mesenchyme.³⁴² Transcriptome analysis reveals that the gene *Dcn*, which encodes for the collagen-binding proteoglycan decorin, is a specific target that is repressed by *Foxd1* in the cortical interstitium.³⁴³ *Dcn* expression is normally localized within the medullary stroma but is normally absent in the cortical stroma of wild type kidneys. In the absence of *Foxd1*, *Dcn*

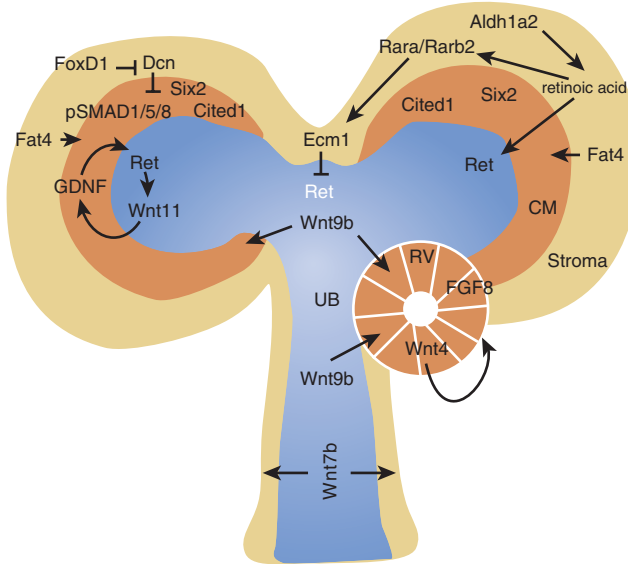


Fig. 1.18 Tripartite inductive interactions regulating ureteric branching and nephrogenesis. Six2 and Cited1 are expressed in the self-renewing nephron progenitors within the cap mesenchyme (CM) surrounding the ureteric bud (UB). The UB tip domains express high levels of Ret, which is activated by glial cell-derived neurotrophic factor (GDNF) from the surrounding CM. Wnt11 is upregulated in response to Ret activation and stimulates GDNF synthesis in the CM. Wnt9b expressed by the UB, and Fat4 by the Foxd1-positive stroma are required to initiate nephrogenesis from a subset of the CM. This results in the formation of a transient renal vesicle (RV) expressing FGF8 and Wnt4, factors that sustain epithelialization. The stroma expresses Aldh1a2, a gene required for retinoic acid synthesis, and genes for the retinoic acid receptors (*Rara* and *Rarb*). Retinoic acid signaling stimulates elevated expression of Ret in the UB tip domain while at the same time suppressing Ret expression via *Rara/Rarb2* and *Ecm1* in the stroma to initiate bifurcation of the UB tip to generate new branches. Foxd1 in the cortical stroma also represses *Dcn*, thus relieving the *Dcn*-mediated suppression of BMP7-dependent signaling, which results in phosphorylation of SMAD1/5/8 (pSMAD1/5/8) and epithelialization of the cap mesenchyme.

becomes abundantly expressed in the presumptive cortical stromal region. Functional cell-culture-based assays and epithelialization assays of mesenchymal aggregates reveal that *Dcn* inhibits Bmp7 signaling and mesenchyme-to-epithelial transformation. The antagonistic effect of *Dcn* on epithelial differentiation is further enhanced in vitro when the mesenchymal aggregates are grown in collagen IV, thus recapitulating the persistence of the cap mesenchyme as seen in *Foxd1*-mutant kidneys where both *Dcn* and collagen IV are upregulated in the cortical interstitium. These findings are corroborated by the partial rescue of the *Foxd1*-null phenotype through genetic inactivation of *Dcn*. Fate mapping studies also reveal that the *Foxd1*⁺ stromal mesenchyme are the precursors of renal mural cells (renin cells, smooth muscle cells, pericytes, perivascular fibroblasts, and glomerular mesangial cells) and endothelial cells comprising peritubular capillaries.^{32,33,344,345}

Tcf21 is expressed in the medullary stroma as well as in the condensing MM.^{33,340} *Tcf21* is also expressed in a number of differentiated renal cell types that derive from these mesenchymal cells and include developing and mature podocytes of the renal glomerulus, cortical and medullary peritubular

interstitial cells, pericytes surrounding small renal vessels, and adventitial cells surrounding larger blood vessels (see Fig. 1.6).²⁴⁶ The defect in nephrogenesis observed in *Tcf21*-null mice is similar to the defect seen in *Foxd1* knockout mice, with a disruption of branching morphogenesis with an associated arrest and delay in nephrogenesis.^{339,341,346} Interestingly, as with *Foxd1*, *Tcf21* also represses *Dcn*, although the significance of *Dcn* upregulation in *Tcf21*-null mutant mice has not been formally addressed.³⁴⁷ The analysis of chimeric mice that are derived from *Tcf21*-mutant embryonic stem cells and GFP-expressing embryos demonstrated both cell autonomous and noncell-autonomous roles for *Tcf21* in nephrogenesis.³⁴⁶ Most strikingly, the glomerulogenesis defect is rescued by the presence of wild type stromal cells (i.e., mutant cells will epithelialize and form nephrons normally as long as they are surrounded by wild-type stromal cells). In addition, there is a cell-autonomous requirement for *Tcf21* in stromal mesenchymal cells to allow differentiation into interstitial and pericyte cell lineages of the cortex and medulla as *Tcf21*-null cells were unable to contribute to these populations.

Although many of the defects in the *Tcf21*-mutant kidneys phenocopy those seen in the *Foxd1*-mutant kidneys, there are important differences. Kidneys from *Tcf21*-null mice have vascular anomalies and defective pericyte differentiation that were not reported in *Foxd1*-mutant mice.^{339,346} These differences might result from the broader domain of *Tcf21* expression, which also includes the condensing mesenchyme, podocytes, and medullary stromal cells, in addition to the stromal cells that surround the condensates. In contrast to *Foxd1*, *Tcf21* is not highly expressed in the thin rim of stromal cells found immediately beneath the capsule, suggesting that *Foxd1* and *Tcf21* might mark early and late stromal cell lineages, respectively, with overlap in the stroma that surrounds the condensates.²⁹ However, definitive co-labeling studies to address this issue have not been performed. As both *Tcf21* and *Foxd1* are transcription factors, it is interesting to speculate that they might interact or regulate the expression of a common stromal “inducing factor.”

Retinoids secreted by the renal stroma are also recognized as important for the maintenance of a high level of *Ret* receptor expression in the UB tip, promoting the proliferation of UB epithelial cells and the growth of the ureteric tree.^{17,348–350} The defective UB branching seen in *Foxd1*-null mutants is most likely a direct consequence of the loss of cortical expression of *Aldh1a2*, a gene involved in retinol synthesis.³⁴¹ More recently, it has been shown that renal stroma immediately around the UB tips is also important in regulating the bifurcation of the tips and the creation of new UB branches.³⁵¹ Autocrine retinoid signaling in the stromal cells juxtaposed to the UB tips stimulates the expression of extracellular matrix 1 (*Ecm1*). *Ecm1* is specifically expressed at the UB cleft, where it suppresses and restricts *Ret* expression domains within the UB tips. In the absence of *Ecm1*, *Ret* expression in the UB tips broadens, effectively attenuating UB branching due to impaired formation of UB bifurcation clefts. Thus stromal retinoids promote and confine *Ret* expression domains and more likely cell proliferation patterns within the UB tips.

Recent studies provide valuable insight on how stroma-based signaling intersects with UB-derived inductive cues to promote proper differentiation of the nephrogenic mesenchyme.^{352–356} When the stromal lineage is selectively annihilated by

Foxd1-Cre-driven expression of diphtheria toxin, the zone of condensing mesenchymal cells capping the UBs is abnormally broadened while the development of pretubular aggregates is strongly hindered. This reiterates findings from the *Foxd1*-null mice suggesting that regulation of nephrogenesis involves a crosstalk between stroma and UB-derived inductive signals. In particular, it was shown that Fat4-dependent Hippo signaling initiated by the stroma integrates with canonical Wnt signaling derived from the ureteric lineage in order to balance the nephron precursor propagation and differentiation. The absence of Fat4 in the stromal compartment or its ligands Dchs1 and Dchs2 from the cap mesenchyme phenocopies the expansion of the nephrogenic precursor domain and failed epithelial differentiation of nephron progenitors seen in stroma-deficient kidneys.^{353,356} It was postulated that Fat4, acting through the Hippo pathway, promotes the differentiation of the epithelial transition of nephrogenic precursors.^{353–356} This was further reiterated by the rescue of the depletion of nephrogenic precursors by *Fat4* deficiency in *Wnt9b* knockouts.³⁵² Interestingly, the loss of Vangl2, a signaling partner of Fat4 known to regulate renal tubular diameter, fails to rescue the loss of nephron progenitors in *Wnt9b* knockouts, suggesting that Fat4-mediated signaling during early differentiation of nephrogenic precursors is likely independent of the planar cell polarity pathway.^{350,352} Transcriptional regulation of stroma-dependent restriction of nephron progenitor expansion involves the transcription factors *Sall1*, *Foxd1*, and *Pbx1*.^{28,341,357} More importantly, *Sall1* is likely a major upstream regulator of many of the stroma functions as *Sall1* binds directly to several stroma-related gene loci, including *Fat4*, *Dcn*, *Pbx1*, *Tcf21*, *Meis1*, and *Hoxd10*.³⁵⁸ Loss of *Sall1* in the stroma downregulates *Fat4* expression and results in an excess of *Six2⁺* nephron precursors.

The T-box transcription factor *Tbx18* is strongly expressed during early urogenital tract development in the ureteral mesenchyme and a subset of kidney stromal mesenchyme originating from *Foxd1* positive precursor cells.^{359,360} Later in renal development, *Tbx18* expression is also found in the renal capsule, vascular smooth muscle cells, pericytes, mesangial cells, and the mesenchyme surrounding the renal papillae and calyces.³⁶⁰ The most overt phenotype of *Tbx18*-inactivation is the onset of hydronephrosis and hydroureter as a result of impaired development of the ureteral smooth muscle cells.^{359,361} This underscores the importance of *Tbx18* in the normal differentiation of the ureteral mesenchyme. A more recent detailed phenotypic characterization of *Tbx18*-null mutant kidneys reveals an additional significance of this transcription factor in the overall development of the renal vasculature.³⁶⁰ The branching and overall density of the renal vasculature are notably reduced in the absence of *Tbx18*. *Tbx18* is also specifically required in the normal development of the glomerular microvasculature. Loss of *Tbx18* causes significant oligonephronia and dilation of glomerular capillaries. These vascular phenotypes likely result from the degeneration of the stromal mesenchyme adjacent to the developing vasculature and the failure to sustain the proliferation of mesangial precursors.

Mice carrying a hypomorphic allele of *Notch2* that is missing two epidermal growth factor (EGF) motifs are born with a reduced number of glomeruli that lack both endothelial and mesangial cells, as discussed in the section on nephron segmentation.^{362,363} The downstream Notch signaling target,

Rbpj, has also been described as crucial for the proper development of the renal vasculature and the glomerular mesangium. Conditional inactivation of *Rbpj* in the *Foxd1*-expressing stromal lineage leads to profound renal maldevelopment and early postnatal death.³⁶⁴ *Rbpj* deficiency in the renal stroma results in poor branching and simplification of the renal vascular network. *Rbpj* conditional mutant kidneys have a greater proportion of larger vessels and a concomitant reduction in microvascular density. Glomeruli are dilated and lack mesangial cells in *Rbpj* conditional knockouts. Furthermore, loss of *Rbpj* results in loss of renin cells, abnormal thickening of blood vessels, and renal fibrosis. Altogether, these studies highlight the distinctive significance of Notch signaling within the stromal mesenchyme in the establishment and organization of the renal vasculature.

MOLECULAR GENETICS OF VASCULAR FORMATION

Although we now have a comprehensive if not complete understanding of the mechanisms underlying ureteric branching and nephrogenesis, we still know little how the complex vascularization of the kidney is coordinated with epithelial and stromal development. During kidney development, the formation and elaborate patterning of an arterial, venous, and capillary blood vascular network involves a combination of both vasculogenesis and angiogenesis (see Fig. 1.8). In addition, lymphangiogenesis underlies the development of the lymphatic vasculature from veins. The major renal vessels align close to the branching UB and likely elaborate through angiogenesis into large-caliber afferent and efferent distributaries.³³ Vasculogenesis in the kidney likely arises from sporadic endothelial cells within the MM that organize to form a primitive vascular network and then give rise to most of the peritubular capillaries.^{32,365,33} Additionally, vasculogenesis within the S-shaped nephron intermediates establishes the glomerular capillaries.^{34,35,366,367}

Grafting studies demonstrate that transplanted embryonic kidneys can become vascularized from the invasion of host-derived extrinsic blood vessels.^{368,369} However, more recent fate mapping studies provide compelling evidence for the existence of endogenous endothelial precursors within the kidney.^{31–35} Cultured mouse embryonic kidneys contain a heterogeneous intrinsic pool of endothelial cells that express the endothelial-specific markers Kdr, Cd31, and Cd146.³³ As early as E11.5 embryonic stage in the mouse, *Kdr⁺* cells are readily identifiable as either single-cell clusters or primitive capillaries. The primitive capillaries consist of *Cd31⁺/Cd146⁺* cells, whereas the single cells predominantly express *Cd146⁺* but not *Cd31*. At E12.5, *Cd31⁺* cells have formed an elaborate chain-like network, including being found adjacent to *Pax2⁺* cap mesenchyme while singular *Cd146⁺* cells have become scarce. Lineage tracing analysis demonstrates that a subset of endogenous renal endothelial cells that give rise to peritubular capillaries but not glomerular endothelial cells are derived from *Foxd1⁺* stromal cells.^{32,33}

Isolated E11.5, E12.5, and E13.5 kidneys, and also cultured E11.5 kidneys, produce VEGF-A, a potent factor known to promote vascularization.³³ Indeed, the pharmacologic inhibition of VEGFR signaling completely abolishes the establishment of endothelial cell networks in cultured embryonic kidney explants, suggesting that VEGF-A signaling is essential

for renal vascular development. More recent imaging studies reveal that kidney vascularization is initiated at E11 in the mouse, when systemic vessels from embryonic circulation circumscribe around the UB.^{370,371} From E13.5, the endothelial network surrounds the cap mesenchyme and UB in a cyclical manner by which endothelia form across and in close contact with the bifurcating UB, which begs the question as to whether endothelial development coregulate ureteric branching. It is, however, easily conceivable that given the importance of oxygen levels in nephrogenesis,^{372–374} the intimate integration of the renal vascular plexus, which carries oxygen-delivering erythrocytes, is essential for nephron maturation.

Conditional gene targeting experiments and cell-selective deletion of *Vegfa* from podocytes demonstrates that VEGF-A signaling is required for formation and maintenance of the glomerular filtration barrier.^{375,376} Glomerular endothelial cells express VEGFR2 as they migrate into the vascular cleft. Although a few endothelia migrate into the developing glomeruli of *Vegfa* podocyte conditional knockout mutants (likely due to a small amount of VEGF-A produced by presumptive podocytes at the S-shaped stage of glomerular development prior to Cre-mediated genetic deletion), the endothelia fail to develop fenestrations and rapidly disappear, leaving capillary “ghosts” (Fig. 1.19). Deletion of a single *Vegfa* allele from podocytes leads to glomerular endothelial

defects known as endotheliosis, a phenomenon involving hypertrophy of glomerular endothelial cells and loss of fenestrations (endotheliosis), progressing to capillary occlusion and thrombosis (thrombotic microangiopathy).³⁷⁵ Inactivation of *Vegfr2* phenocopies endotheliosis and thrombotic microangiopathy, indicating that VEGFA primarily signals through VEGFR2 in supporting the development and maintenance of the glomerular endothelium.³⁷⁷ As the dose of *Vegfa* decreased, the associated endothelial phenotypes became more severe. Upregulation of the major 164 angiogenic VEGF-A isoform in developing podocytes of transgenic mice led to massive proteinuria and collapse of the glomerular tuft by 5 days of age. Taken together, these results show a requirement for VEGF-A for development and maintenance of the specialized glomerular endothelia and demonstrate a major paracrine signaling function for VEGF-A in the glomerulus. Furthermore, tight regulation of the dose of VEGF-A is essential for proper formation of the glomerular capillary system. The molecular basis and mechanism of dosage sensitivity is unclear at present and is particularly intriguing given the documented inducible regulation of VEGF-A by hypoxia-inducible factors (HIFs) at a transcriptional level. Despite this, it is clear that *in vivo*, a single *Vegfa* allele is unable to compensate for loss of the other. Similarly, VEGF-A signaling is essential for the development of the

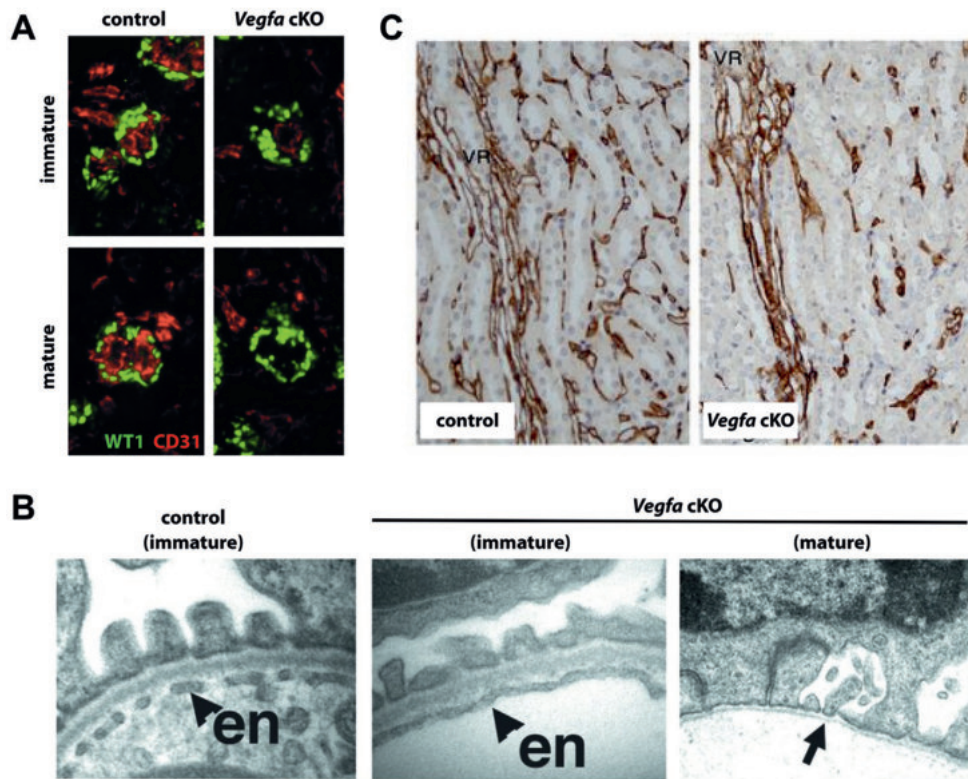


Fig. 1.19 VEGF-A is essential for the development of the glomerular and peritubular capillaries. (A) *Vegfa* inactivation in podocytes leads to recruitment of fewer endothelial cells in the glomerulus which are subsequently lost. Podocytes and endothelial cells are stained with WT1 (green) and CD31 (red), respectively. (B) Transmission electron micrograph showing that in podocyte-specific *Vegfa* knockouts, the glomerular endothelium (*en*) lack fenestrae (arrowheads) and eventually detach leaving the glomerular basement membrane bare (arrow). (C) *Vegfa* ablation in renal tubules leads to a significant reduction in peritubular capillaries (stained brown for CD34). VR, Vasa recta. Panels (A) and (B) were adapted from Eremina V, et al. Glomerular-specific alterations of VEGF-A expression lead to distinct congenital and acquired renal diseases. *J Clin Invest.* 2003;111:707–716. Panel (C) adapted from Dimke H. Tubulovascular cross-talk by vascular endothelial growth factor A maintains peritubular microvasculature in kidney. *J Am Soc Nephrol.* 2014;26:1027–1038.

peritubular capillaries. Ablation of *Vegfa* in renal tubules did not cause gross histologic disturbance in the kidney but lead to a dramatic reduction of peritubular capillaries and an abnormal elevation in renal erythropoietin production (see Fig. 1.19).³⁷⁸ This uncovered an important tubulo vascular crosstalk involved in the promotion of erythrocyte development by the kidney.

A second major receptor tyrosine kinase (RTK) signaling pathway required for maturation of developing blood vessels is the angiopoietin–Tie signaling system. Angiopoietin 1 (*Angpt1*) stabilizes newly formed blood vessels and is associated with loss of vessel plasticity and concurrent recruitment of pericytes or vascular support cells to the vascular wall.³⁷⁹ The molecular switch or pathway leading to vessel maturation through the activation of Tie2 (encoded by the gene *Tek*, the major receptor for *Angpt1*) is not known and appears to be independent of the platelet-derived growth factor (PDGF) signaling system that is required for pericyte recruitment. The importance of *Angpt1* in promoting the development of the renal microvasculature was first suggested based on observations that exogenous *Angpt1* enhances the growth of interstitial capillaries in mouse metanephric organ cultures.³⁸⁰ Because *Angpt1*-null mice perish embryonically at around E12.5, the in vivo role of *Angpt1* during renal development was gleaned using an inducible knockout strategy.^{381,382} Ablation of *Angpt1* deletion at around E10.5 results in general dilation of renal blood vessels, including the glomerular capillaries sometimes observed as simplified single enlarged loops.³⁸² A marked reduction of mesangial cells was also observed in *Angpt1*-deficient mutants. Without *Angpt1*, a few endothelial cells are seen detached from the glomerular basement membrane. In contrast, it is proposed that angiopoietin 2 (*Angpt2*) functions as a context-dependent antagonist of the Tie2 receptor.^{383,384} Consistent with this hypothesis is the fact that overexpression of *Angpt2* in transgenic mice results in a phenotype similar to the *Angpt1* or *Tek* knockout mice. *Angpt1*, *Angpt2*, Tie2, and the orphan receptor Tie1 are all expressed in the developing kidney.^{385–389} Whereas, *Angpt1* is quite broadly expressed in condensing mesenchyme, podocytes, and tubular epithelial cells, *Angpt2* is more restricted to pericytes and smooth muscle cells surrounding cortical and large vessels as well as in the mesangium. *Angpt2*-null mice are viable but exhibit defects in peritubular cortical capillary development.³⁹⁰ Podocyte-specific overexpression of *Angpt2* causes proteinuria and increased apoptosis in glomerular capillaries.³⁹¹ Both angiopoietin ligands function in concert with VEGF-A, although the precise degree of crosstalk between these pathways is still under investigation. VEGF-A and *Angpt2*, for example, have been shown to cooperate in promoting endothelial sprouting. Chimeric studies showed that Tie1 is required for the development of the glomerular capillary system because *Tie1*-null cells fail to incorporate in the glomerular endothelium.³⁹²

Renal vascular development also relies on a third tyrosine kinase–dependent signaling mediated by ephrins and Eph family receptors, which are better known for their involvement in axon guidance and specification of arterial and venous cell fates.^{393,394} Ephrins and their cognate receptors are expressed widely during renal development. Overexpression of *Ephb4* leads to defects in glomerular arteriolar formation, whereas conditional deletion of *Efnb2* (*EphrinB2*) from perivascular smooth muscle cells and mesangial cells leads to glomerular vascular abnormalities.^{395,396} How this occurs

is not entirely clear as *Efnb2* has a dynamic pattern of expression in the developing glomerulus, beginning in podocyte precursors and rapidly switching to glomerular endothelial cells and mesangial cells.³⁹⁷

Dysregulation of BMP within the podocyte compartment also results in glomerular vascular defects. Overexpression of BMP4 leads to defects in endothelial and mesangial recruitment, whereas overexpression of noggin, a natural BMP2 antagonist, leads to collapse of the glomerular tuft.^{398,399} *Bmp4* haploinsufficiency, on the other hand, leads to dysplastic kidneys and glomerular cysts with collapsed capillary tufts.³⁹⁹ Additional studies are required to fully understand the role of this family of growth factors in glomeruli.

An additional pathway that is likely to play a role in glomerular endothelial development and perhaps of the entire renal vasculature is the SDF1-CXCR4 axis. CXCR4, a G-protein–coupled chemokine receptor, is strongly expressed in endothelial cells. SDF1 (encoded by the gene *Cxcl12*), the only known ligand for CXCR4, is expressed in a dynamic segmental pattern in podocytes and later in the mesangial cells of the glomerulus.⁴⁰⁰ Embryonic deletion of either *Cxcl12* or *Cxcr4* does not preclude nephrogenesis but results in the defective formation of blood vessels, notably an abnormal patterning of the renal vasculature and the development of a simplified and dilated glomerular capillary tuft.⁴⁰¹ Genetic loss of CXCR7, which is thought to act as a decoy receptor for SDF1, interestingly phenocopies defective development seen in SDF1 and CXCR4-mutant mice. Unlike CXCR4, CXCR7 is specifically expressed by podocytes and not endothelial cells.⁴⁰² It has been proposed that CXCR7, acting as a scavenger receptor, establishes an SDF1 morphogen gradient preventing feedback inhibition of CXCR4 receptor expression in target cells such as the endothelium. Consistent with this, inactivation of *Cxcr7* distinctively causes downregulation of *Cxcr4* expression in the renal cap mesenchyme and the glomerular tuft. Thus the spatial regulation of SDF1-CXCR4 signaling appears to be important for the normal development of the glomerular vasculature.

Two transcription factors belonging to the large Sry-related HMG box (Sox) gene family, named *Sox17* and *Sox18*, have distinctive and overlapping expression in vascular endothelial cells.⁴⁰³ Complete loss of *Sox17* is embryonic lethal in mice due to endodermal dysmorphogenesis.⁴⁰⁴ In mice, *Sox18* ablation results in a mild coat defect but does not cause cardiovascular abnormalities.⁴⁰⁵ Nevertheless, a point mutation in *SOX18* in humans has been implicated in HLT (hypotrichosis-lymphedema-telangiectasia) syndrome, which affects hair, lymph, and blood vessel vasculature.⁴⁰⁶ The more severe consequence of the human *SOX18* mutation compared to the null mutation in mice was suggested to be due to a dominant-negative effect. *Sox17*, however, shows haploinsufficiency in a homozygous *Sox18* background, affecting neovascularization in kidneys, liver, and the reproductive system and causing early postnatal lethality.⁴⁰³ Kidneys from *Sox17/Sox18* double-null mutant mice have hypoplastic and atrophying medullary regions. In these compound *Sox17/Sox18* mutants, the radiating outer medullary vascular bundles of the vasa recta are missing without apparent abnormalities in the inner medullary or cortical regions. These defects within the outer medullary region result in variable degrees of hydronephrosis. Interestingly, midgestational loss of both *Angpt1* and *Angpt2* ligands or their cognate receptor Tie2 leads to rarefaction of the medullary capillary plexus and

the absence of outer medullary vascular bundles, particularly the fenestrated ascending vasa recta, leading to urinary concentration defects and interstitial fluid retention that culminates in the formation of interstitium-derived medullary cysts (Fig. 1.20).⁴⁰⁷ This raises an intriguing possibility that Sox17 and Sox18 pathways either converge or intersect with Angpt1/Angpt2-Tie2 signaling in coordinating late-stage angiogenesis in kidneys.

A least understood component of the renal vasculature are the lymphatic vessels. Similar to other organs, the renal lymphatics play important roles in interstitial fluid homeostasis and the regulation of the immune response. Lymphatic vessels have been identified surrounding the renal artery in the hilum, in the arcuate and interlobular arteries in the cortex, and are also found in the renal capsule.^{408–410} These lymphatic

vessels are known to express the hyaluronan receptor Lyve1.^{407,411} The medulla was previously thought to lack lymphatic vessels. However, more recently a study of angiopoietin-Tie2 signaling in the kidney reveals that the ascending vasa rectae represent hybrid vessels that express markers of both blood (*Cd34*, *Emcn*, *Pecam1*, and *Plvap*) and lymphatic endothelial cells (*Prox1* and *Vegfr3*) (see Fig. 1.19).⁴⁰⁷ This underscores a novel lymphatic circuit for the drainage of medullary interstitial fluid as part of the osmoregulation of urine. VEGF-C signaling via the receptor VEGFR3 is essential for lymphangiogenesis.^{412–415} *Vegfr3* deficiency in adult mice causes the extravasation of fibrinogen into the renal interstitium.⁴¹⁶ How the renal lymphatic vasculature is particularly remodeled upon inactivation of VEGF-C/VEGFR3 signaling remains unknown.

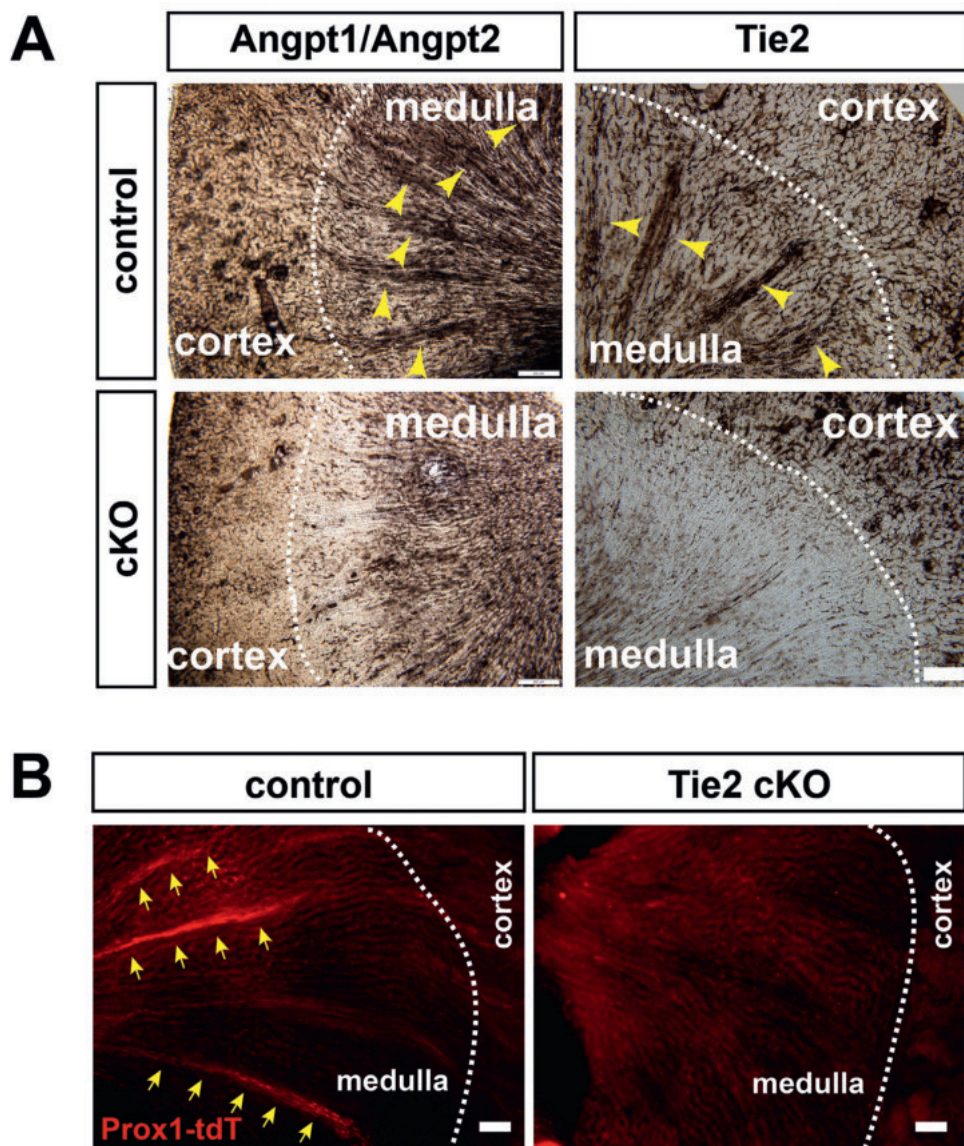


Fig. 1.20 Ascending vasa recta development depends on angiopoietin-Tie2 signaling. (A) Midgestational (E16.5) loss of both Angpt1 and Angpt2 or their cognate receptor Tie2 (Tek) leads to loss of vasa recta bundles (yellow arrowheads) in the outer renal medulla, particularly the ascending vasa rectae. (B) Ascending vasa rectae are novel lymphatic-like vessels expressing the lymphatic-specific Prox1 transcription factor as seen in transgenic reporter mice expressing the fluorophore tdTomato under the control of the *Prox1* promoter. *Prox1-tdT*⁺ vascular bundles representing the ascending vasa rectae are absent in kidneys of Tie2-deficient mouse mutants. *cKO*, Conditional knockout; *Prox1-tdT*, *Prox1-tdTomato* transgene. Adapted with permission from Kenig-Kozlovsky, Scott RP, Onay T, et al. Ascending vasa recta are angiopoietin/Tie2-dependent lymphatic-like vessels. *J Am Soc Nephrol*. 2018;29:1097–1107.

RENIN CELLS AND THE JUXTAGLOMERULAR APPARATUS

The juxtaglomerular apparatus consists of cells that line the afferent arteriole, the macula densa cells of the distal tubule, and the extraglomerular mesangial cells that are in contact with intraglomerular mesangium.⁴¹⁷ Renin-expressing cells may be seen in arterioles in early mesonephric kidneys in 5-week human fetuses and in metanephric kidneys by week 8, at a stage prior to hemodynamic flow changes within the kidney, and are derived from *Foxd1*-expressing stromal mesenchyme.⁴¹⁸ Renin-expressing cells reside within the MM and give rise not only to juxtaglomerular cells but also to mesangial cells.^{419,420}

The only known substrate for renin, angiotensinogen, is converted to angiotensin I and angiotensin II by angiotensin-converting enzyme (ACE).⁴²¹ The renin–angiotensin–aldosterone axis is required for normal renal development. In humans, the use of ACE inhibitors during pregnancy has been associated with congenital defects including renal anomalies.^{422,423} Two subtypes of angiotensin receptors exist: AT1 receptors are responsible for most of the classically recognized functions of the renin–angiotensin system (RAS), including pressor effects and aldosterone release mediated through angiotensin; functions of the type 2 receptors have been more difficult to characterize, but generally seem to oppose the actions of the AT1 receptors.⁴²⁴ Genetic deletion of angiotensinogen or ACE results in hypotension and defects in formation of the renal papilla and pelvis.^{256–259} Humans have one *AT1* gene whereas mice have two: *Agtr1a* and *Agtr1b*. Mice carrying a knockout for either AT1 receptor alone exhibit no major defects,^{425,426} whereas combined deficiency phenocopies the angiotensinogen and ACE phenotypes.^{260,261} Although AT2 receptor (*Agtr2*) expression is markedly upregulated in the embryonic kidney, genetic deletion of the AT2 receptor does not cause major impairment of renal development.^{427,428} However, an association between *Agtr2*-deficiency and malformations of the collecting duct system, including vesicoureteral reflux and ureteropelvic junction obstruction, has been reported.⁴²⁹

MicroRNAs (miRNAs) are regulatory RNAs that act as antisense posttranscriptional repressors by binding the 3' untranslated region of target mRNAs. Eukaryotes express hundreds of miRNAs that can regulate thousands of mRNAs, and they have been shown to play an important role in development and disease, including in differentiation, signaling pathways, proliferation, apoptosis, and tumorigenicity. Dicer1 is an endoribonuclease that processes precursor miRNAs. Deletion of *Dicer1* from renin-expressing cells results in severely reduced number of juxtaglomerular cells, reduced renin production, and lower blood pressure. The kidney develops severe vascular abnormalities and striped fibrosis along the affected blood vessels, suggesting that miRNAs are required for normal morphogenesis and function of the kidney.⁴³⁰

Gene promoter analysis indicates that renin expression is dependent on the Notch signaling pathway. The intracellular domain of Notch (NIC) and the transcription factor *Rbpj* bind and cooperatively stimulate reporter gene expression from the renin promoter.⁴³¹ Genetic studies, however, indicate that Notch signaling has a broader role in the juxtaglomerular apparatus.⁴³² The conditional ablation of *Rbpj* in renin cells results in severe paucity of juxtaglomerular cells with

consequential decrease in overall renin expression and the development of lower blood pressure. Lack of increase in apoptosis in *Rbpj* conditional mutant kidneys suggests that *Rbpj* may have altered the cell fate specification of renin cell precursors.

PODOCYTE DEVELOPMENT

Presumptive podocytes are located at the proximal end of the S-shaped body, lining the emerging vascular cleft (Fig. 1.21). Immature podocytes are simple columnar epithelia expressing E-cadherin (Fig. 1.22). Postmitotic mature podocytes, on the other hand, normally lose E-cadherin expression and atypically express vimentin, an intermediate filament protein more common among mesenchymal cells but absent in most epithelial cells. The most distinctive morphologic feature of a fully differentiated podocyte is its arborized and stellate appearance (Fig. 1.22). Podocytes ensheathe the glomerular capillaries with their foot processes, effectively forming the final layer of the glomerular filtration barrier. Foot processes emanating from adjacent podocytes interdigitate in *trans* and form a unique and porous intercellular junction called the slit diaphragm through which primary urinary filtrate passes. Three-dimensional reconstruction of podocyte ultrastructure obtained by block-face scanning electron microscopy reveals the morphologic transformation of podocytes during development and the formation of interdigitating foot processes.^{22,433} Columnar-shaped immature podocytes are linked by tight and adherens junctions that progressively migrate from the apical to the basal side. Once the junctional complex has descended close to the basement membrane, podocytes begin to flatten, spread, and interdigitate with short primitive foot processes underneath the junctions. As the primitive processes grow, the tight and adherens junctions relocate from the cell body to between the processes forming the immature foot processes. Finally, the junctional complexes are gradually replaced with slit diaphragms, resulting in mature foot processes.

The transcription factors *Wt1*, *Tcf21*, *Mafb*, *Foxc2*, and *Lmx1b* are highly expressed by developing podocytes and are important for the elaboration of podocyte foot processes and the establishment of slit diaphragms.* Complete loss of *Wt1* leads to renal agenesis.³⁹ However, specific loss of a *Wt1* splice isoform results in poor development of podocyte foot processes.⁴³⁶ The *Wt1*-null phenotype in mice can also be rescued using a yeast artificial chromosome containing the human *WT1* gene and, depending on the level of expression of *WT1*, the mice developed a range of glomerular pathologies ranging from crescentic glomerulonephritis to mesangial sclerosis, clinical features observed in Denys-Drash syndrome arising from a mutant *WT1* allele in humans.⁴³⁷ Transgenic mice expressing a Denys-Drash–mutant *Wt1* allele under the regulation of a podocyte-specific promoter also developed glomerular disease with abnormalities observed in the adjacent endothelium.⁴³⁸ Genome-wide analysis of the *Wt1* targets in podocytes reveals that *Wt1* autoregulates its own transcription and acts as master regulator of a complex transcriptional network that regulates podocyte development, structure, and function, including transcription factors (*Lmx1b*, *Tcf21*, *Mafb*,

*References 39, 83, 339, 340, 434, and 435.

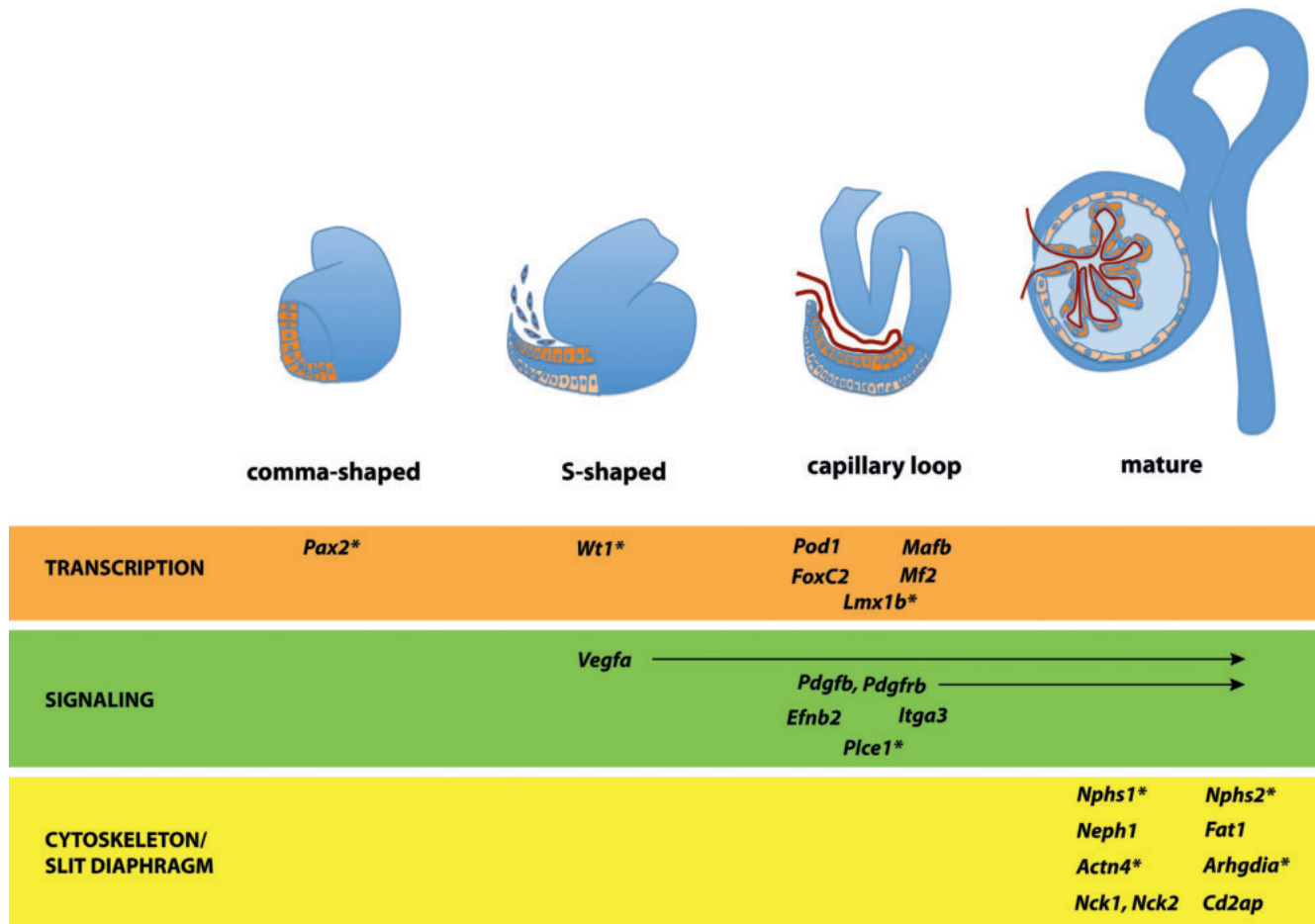


Fig. 1.21 Molecular basis of glomerular development. Key factors are shown along with the time point where major effects were observed in knockout or transgenic mouse studies. Many factors play roles at more than one time point. Genes identified as mutated in patients with glomerular disease are marked by asterisks.

*Tead1, Foxc1, and Foxc2) and genes strongly linked to podocyte dysfunction and nephrotic diseases (*Actn4, Arhgap24, Cd2ap, Col4a3, Col4a4, Lamb2, Nphs1, Nphs2, and Plice1*).⁴³⁹ Inactivation of *Lmx1b*, *Tcf21*, *Mafb*, and *Foxc2* causes podocytes to remain as cuboidal epithelia and failure to spread on the glomerular capillary bed.^{83,339,434,440} *Tcf21* likely acts upstream of *Mafb* as the latter is downregulated in *Tcf21*-null mice.⁴³⁴ Loss of *Mafb* and *Lmx1b* reduces the expression of *Nphs1* (nephrin) and *Nphs2* (podocin), whereas the absence of *Foxc2* causes the specific downregulation of *Nphs2* and $\alpha 3\alpha 4\alpha 5$ (IV) collagen.^{83,434,441} *Lmx1b* mutations are linked to nail-patella syndrome in humans, with a subset of affected individuals manifesting nephrotic disease.^{435,442} *Wt1, Tcf21, Mafb, Foxc2* and *Lmx1b* are expressed from the S-shape stage onward and remain constitutively expressed in adult glomeruli. Proteinuria develops from loss of these genes, thus underscoring the importance of normal podocyte maturation in the establishment of the glomerular filtration barrier.*

Genetic studies have also led to the identification of structural proteins crucial for normal podocyte function and the integrity of the glomerular filtration barrier. The seminal discoveries of the causal link between nephrotic diseases and mutations in podocyte-specific genes *Nphs1* and *Nphs2* set the stage for vigorous investigations that led to the appreciation of the key importance of podocytes in renal filtration.^{443,444}

Mutations in *Nphs1*, the gene that encodes for the protein nephrin, are associated with congenital nephropathy of the Finnish variety (CNF), a serious condition that requires early renal replacement therapy.⁴⁴⁴ Glomeruli obtained from infants affected by CNF are devoid of slit diaphragms. Nephrin, a huge transmembrane adhesion molecule with multiple immunoglobulin-like motifs, was shown to be a structural component of the slit diaphragm. *Nphs2*, whose product is the intracellular membrane-bound protein podocin, and is the first gene identified as being linked to steroid-resistant nephrotic syndrome (SRNS).⁴⁴³ Podocin, which interacts with nephrin in cholesterol-rich membrane microdomains (also called lipid rafts), is also a vital and indispensable component of the slit diaphragm.^{445–449} A number of other genes specifically expressed by podocytes have been associated with proteinuric diseases, including *Cd2ap, Kirrel (Neph1), Fat1, Actn4, Tpc6, Myo1e, Arhgap24, Arhgdia, Rhpn1, Inf2, Coq2, Coq6, Plice1, and APOL1*.^{77,78,80,82,450–464} The products of these genes are either integral parts of the slit diaphragm complex or direct interacting partners of the complex, while the remainder are important in regulating the development, viability, cytoskeleton, and distinctive morphology of podocytes (Fig. 1.23).

The topologic organization of slit diaphragm components remains unknown, but it is likely that the larger adhesion molecules nephrin and Fat1 could be bridging juxtaposed

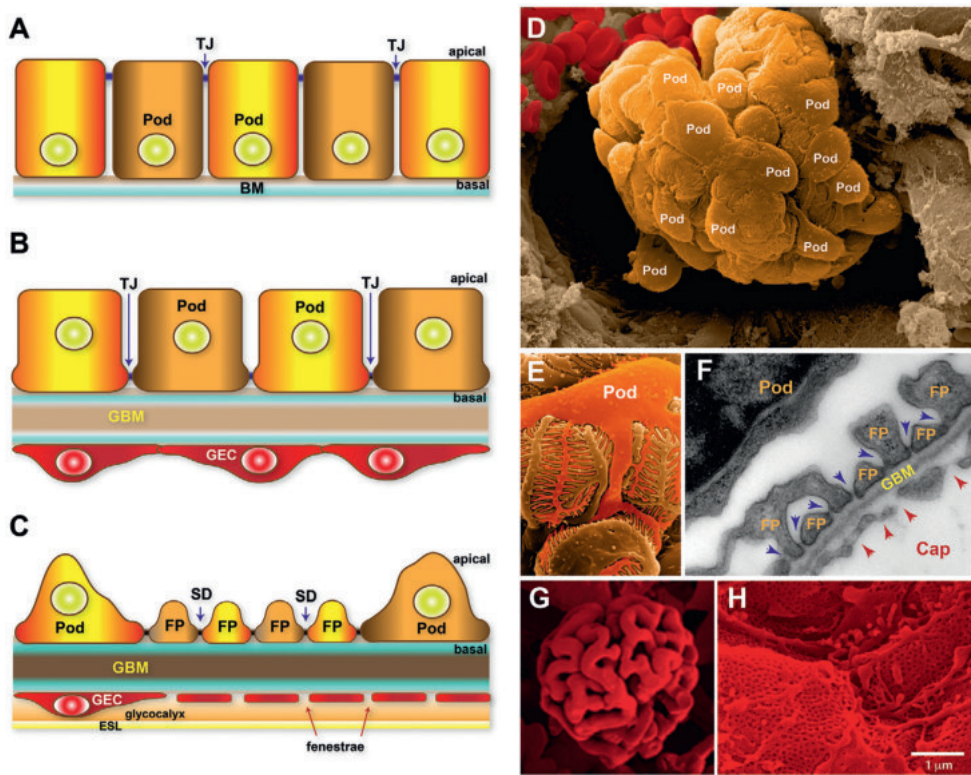


Fig. 1.22 Maturation of the glomerular filtration barrier. (A) In S-shaped bodies, presumptive podocytes (*Pod*) are columnar epithelial cells conjoined by apically localized tight junctions (*TJ*). (B) At the capillary loop stage, the basement membranes (*BM*) of podocytes and glomerular endothelial cells (*GEC*) fuse forming the glomerular basement membrane (*GBM*). During this stage, the podocytes begin to spread, and their cell junctions relocate more basally. (C) As the glomerulus matures, podocytes lose their cuboidal morphology and have developed elaborate foot processes (*FP*) that interdigitate with processes from neighboring podocytes. The podocyte cell junctions have been transformed into slit diaphragms (*SD*) that link juxtaposed FPs. GECs also flatten, develop fenestrae, and become covered by a glycocalyx that, together with absorbed plasma components, form the endothelial cell surface layer (*ESL*). The *GBM* is now a unified *BM* between podocytes and the *GECs*. (D) Scanning electron micrograph (SEM) of a cracked glomerulus exposing the capillary tuft covered by podocytes (gold). (E) Higher magnification view of a podocyte *in situ* revealing the elaborate FPs interdigitated with FPs from other podocytes. (F) Transmission electron micrograph of a glomerulus showing the *SD* (blue arrows) between interdigitating FPs and the endothelial fenestrae (red arrows) on the opposite side of the *GBM* (Cap, glomerular capillary lumen). (G) SEM of a resin cast of the renal vasculature demonstrating the highly convoluted glomerular capillary tuft. (Courtesy of Fred E. Hossler, East Tennessee State University). (H) A view inside an exposed glomerular endothelial lumen showing its highly fenestrated surface. Adapted from Scott RP, Quaggin SE. Formation and maintenance of a functional glomerulus. In Little, M. H. (ed.). *Kidney Development, Disease, Repair and Regeneration*. San Diego: Academic Press; 2016.

foot processes (see Fig. 1.22).^{459,465–467} Smaller adhesion molecules within the slit diaphragms such as Neph1, Neph3, and P-cadherin may more likely associate in *cis* (within the same foot process surface).^{468–470} Nephrin and the related protein Neph1 are known to interact with the polarity complex proteins Par3, Par6, and aPKC λ/γ , indicating a coregulation between the polarized cell structure of podocytes and the compartmentalized assembly of the slit diaphragm complex along the foot processes.⁴⁷¹ Conditional inactivation in podocytes of aPKC λ/γ or the small GTPase Cdc42, which positively regulates the Par3/Par6/ aPKC λ/γ complex, causes proteinuria characterized by abnormal pseudo-slit diaphragms formed between effaced foot processes (Fig. 1.24).^{472–474} It has also been shown that inactivation of aPKC λ/γ can specifically inhibit the localization of nephrin to the cell surface.⁴⁷⁵

Terminal foot processes of podocytes are longitudinally supported by parallel bundles of actin, setting them apart from the larger primary processes that have a microtubule-based backbone.²¹ The stereotypical response of podocytes to injury either through chemical insults or a detrimental gene mutation is effacement of foot processes. In effaced foot processes, the actin cytoskeleton has been remodeled

into a mesh-like network of randomly oriented filaments.⁴⁷⁶ Genetic and biochemical studies provide evidence that the slit diaphragm is functionally coupled to the actin cytoskeleton, and that perturbation of this relationship results in compromised renal filtration and proteinuric disease. Nck adaptor molecules (Nck1 and Nck2) are known to link tyrosine kinase receptors to signaling molecules that regulate the actin cytoskeleton. Podocytes lacking *Nck1* and *Nck2* are effaced and form abnormal slit diaphragms.⁶⁴ Cell culture studies reveal that clustered nephrin is phosphorylated at its cytoplasmic tail by the kinase Fyn, creating distinctive phosphotyrosine sites where Nck1 and Nck2 adaptors can bind directly. The association between nephrin and Nck adaptors consequently recruits N-WASP and the Arp2/3 protein complex to mediate localized polymerization of actin.^{64,477} Loss of Fyn causes congenital nephrosis, whereas podocyte-specific inactivation of *Wasl*, the gene encoding for N-WASP, leads to proteinuric disease.^{478,479} It is also very likely that Nck adaptors can mediate the adhesion of podocytes to the glomerular basement membrane by virtue of their ability to interact with the PINCH–ILK–integrin complex.^{480–482} Cdc42, in addition to its role in podocyte polarization, has also been shown to be

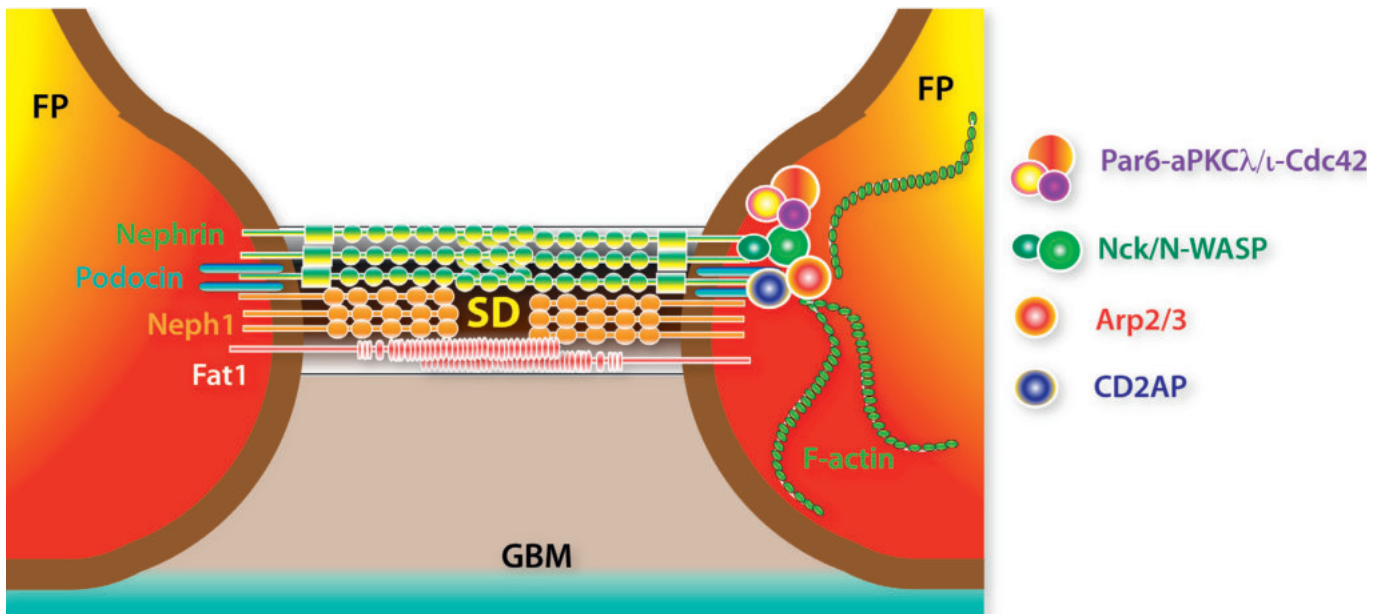


Fig. 1.23 Structural overview of the slit diaphragm. An oversimplified diagram depicting the major adhesion receptors comprising the SD and how they are possibly integrated with the actin cytoskeleton of podocyte foot processes. FP, Podocyte foot process; SD, slit diaphragm; GBM, glomerular basement membrane. Adapted from Scott RP, Quaggin SE. Formation and maintenance of a functional glomerulus. In Little, M. H. (ed.). *Kidney Development, Disease, Repair and Regeneration*. San Diego: Academic Press; 2016.

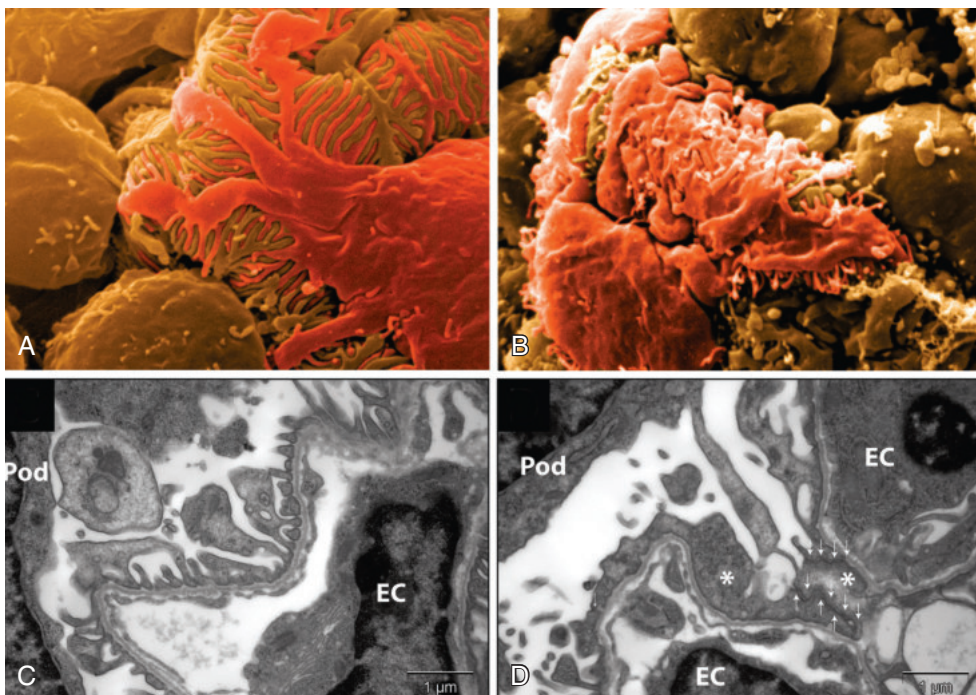


Fig. 1.24 Cdc42 is required for normal podocyte development. (A, B) False-colored scanning electron micrographs of glomeruli from neonatal kidneys: (A) wild-type control podocytes showing normal interdigitated foot processes; and (B) Cdc42-deficient mutant podocytes showing total effacement of foot processes. (C, D) Transmission electron micrographs of sectioned glomeruli: (C) wild-type control showing regularly interdigitating foot processes and basolateral slit diaphragms; and (D) podocyte-specific Cdc42-deficient mutant showing mislocalized cell junctions (arrows) between effaced foot processes (asterisk). EC, Endothelial cell; Pod, podocyte. Adapted from Scott RP, Hawley SP, Ruston J, et al. Podocyte-specific loss of Cdc42 leads to congenital nephropathy. *J Am Soc Nephrol*. 2012;23:1149–1154.

required for the coupling of actin polymerization to nephrin. CD2AP, a molecule known to stabilize actin microfilaments, is also indispensable in podocytes.^{483–485} Mutations in *Actn4*, *Arhgdia*, *Arhgap24*, *Inf2*, and *Myo1e*, whose protein products are established regulators of the actin cytoskeleton, are also

implicated in pathologic transformation of podocytes and proteinuric diseases.^{77,78,80,451–453,455–458}

It has been proposed that the slit diaphragm likely functions in mechanotransduction in podocytes, allowing them to modulate renal filtration in response to hemodynamic changes

within the glomerular microenvironment.^{486,487} *MEC-2*, the *C. elegans* homologue of podocin, is a component of the touch receptor complex coupled to the ion channel MEC-4/MEC-10.⁴⁸⁸ Loss of *MEC-2* in worms leads to insensitivity to touch.⁴⁸⁸ In podocytes, the ion channel *Trpc6* forms an integral component of the slit diaphragm directly interacting with podocin.⁴⁸⁷ In diverse cell types such as myocytes, cochlear hair cells, and sensory neurons, the *Trpc6* channel opening is gated by mechanical stimuli. Human mutations in *TRPC6* have been strongly linked to proteinuria.^{486,489,490}

A novel lipid-dependent signaling pathway involving the VEGF receptor Flt1 (VEGFR1) has been described recently as crucial for the regulation of podocyte actin cytoskeleton and the maintenance of slit diaphragms. Genetic removal of *Flt1* from podocytes leads to foot process effacement and proteinuria.⁴⁹¹ Intriguingly, a kinase-inactive mutant of Flt1 is able to support normal podocyte development and function. In vivo, Flt1 is cleaved, releasing a soluble ectodomain (sFlt1). The secreted sFlt1 has been shown to act as an autocrine factor in podocytes, associating with glycosphingolipids, and mediating podocyte cell adhesion, nephrin phosphorylation, and actin polymerization. It has been proposed that sFlt1 may function physiologically to stabilize the slit diaphragms and the attachment of podocytes to the glomerular basement membrane.

Three groups generated mice carrying a podocyte-specific deletion of *Dicer1*, thereby interfering with the production of functional miRNAs.^{492–494} Podocyte-specific *Dicer1* knockout mice develop albuminuria by 3 weeks of age and rapidly

progress to end-stage renal failure by approximately 6 weeks. A number of potential miRNA targets were identified, but their functional significance in the podocyte *in vivo* is yet unknown.

From all of these studies, it follows that intrinsic proteins and functions of podocytes play a key role in the development and maintenance of the permselective properties of the glomerular filtration barrier. Podocytes also function as vasculature support cells producing VEGF-A and other angiogenic growth factors. It is likely that endothelial cells also produce hitherto unknown trophic factors that promote terminal differentiation and survival of podocytes.

GLOMERULAR BASEMENT MEMBRANE DEVELOPMENT

The mature glomerular basement membrane (GBM) is a fusion of the extracellular matrices (ECM) of podocytes and glomerular endothelial cells. The GBM is a highly organized and compositionally complex matrix whose abundant components include collagens (types I, IV, VI, and XVIII), laminins ($\alpha 5$, $\beta 2$, and $\gamma 1$), nidogen-1, heparan sulfate proteoglycans (agrin and perlecan), and tubulointerstitial nephritis antigen-like protein (Fig. 1.25).^{495–497} The GBM is an essential part of the glomerular filtration barrier, functioning as an intermediary sieving matrix and a sink for secreted trophic and signaling factors, as well as mediating cellular communication between the glomerular endothelium and podocytes. Furthermore, adhesive cell-ECM interactions among the

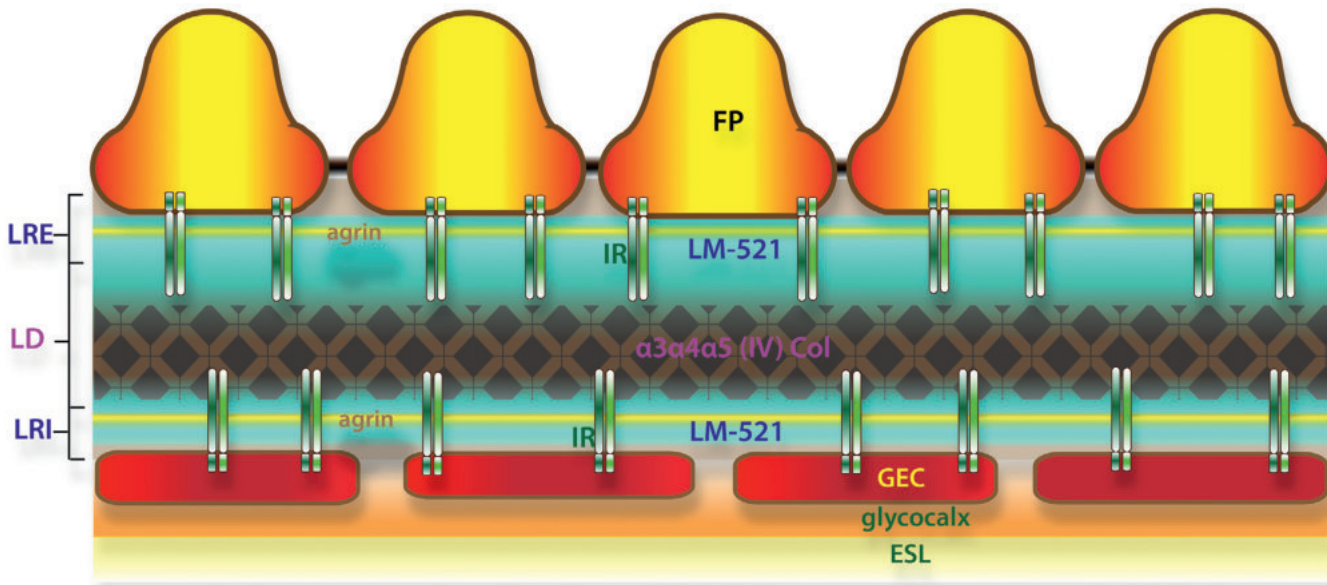


Fig. 1.25 Stratified organization of the glomerular basement membrane. A model of the organization of a mature GBM. The laminin complex LM-521 (pale cyan) and agrin (yellow) form two distinct layers underneath the basal aspects of podocytes and GECs. $\alpha 3\alpha 4\alpha 5$ -Type IV collagens (hatched brown area) are more centrally distributed but are thought to be closer to the GEC. The laminin and type IV collagen complexes have significant overlap. Epitope mapping of integrin- $\beta 1$ suggests that integrin receptors (IR) on podocytes are normally separate and less likely to interact with the type IV collagens in the mature human GBM. The morphologically distinct layers of the GBM in transmission electron micrographs are roughly demarcated. ESL, Endothelial surface layer; FP, podocyte foot process; GBM, glomerular basement membrane; GEC, glomerular endothelial cell; LD, lamina densa; LM, laminin; LRE, lamina rare externa; LRI, lamina rara interna. Based on STORM imaging by Suleiman HL, Zhang L, Roth R, et al. Nanoscale protein architecture of the kidney glomerular basement membrane. *Elife* 2013;2:e01149. Adapted from Scott RP, Quaggin SE. Formation and maintenance of a functional glomerulus. In Little MH (ed.). *Kidney Development, Disease, Repair and Regeneration*. San Diego: Academic Press; 2016.

GBM, the podocytes, and the glomerular endothelial cells maintain the structural integrity of the glomerular filtration barrier.

Among the major components of the GBM, type IV collagens and laminins have been shown to be the most indispensable, highlighted by proteinuric kidney diseases such as Alport syndrome, Goodpasture disease, and Pierson syndrome. Alport syndrome is linked to a growing list of mutations in the genes *COL4A3*, *COL4A4*, and *COL4A5* encoding for type IV collagen subunits $\alpha 3$, $\alpha 4$, and $\alpha 5$, respectively.^{498,499} Maturation of the GBM requires the replacement of juvenile $\alpha 1\alpha 1\alpha 2$ with $\alpha 3\alpha 4\alpha 5$ type IV collagen trimers, a developmental switch improving the structural resilience of the GBM.⁵⁰⁰ In Alport syndrome, the assembly of heterotrimeric $\alpha 3\alpha 4\alpha 5$ type IV collagen complex is compromised while the $\alpha 1\alpha 1\alpha 2$ type IV collagen complexes persists. Because $\alpha 3\alpha 4\alpha 5$ type IV collagen trimers constitute about half the total proteins in the mature GBM, it is not surprising that Alport syndrome GBM is severely distorted.⁵⁰¹ The importance of type IV collagens in the GBM is further underscored in Goodpasture disease, an autoimmune disorder targeting $\alpha 3$ type IV collagen subunit.⁵⁰² In Pierson syndrome, mutations in *LAMB2* encoding the laminin $\beta 2$ subunit impair the assembly of the laminin complex LM-521 (a trimer formed among laminin- $\alpha 5$, - $\beta 2$, and - $\gamma 1$ subunits).^{503,504} Deformation of the GBM and proteinuria results from loss of *Lamb2* and *Lama5* (laminin- $\alpha 5$) in mice.^{234,505–507}

DEVELOPMENT OF THE MESANGIUM

Mesangial cells grow into the developing glomerulus and come to sit between the capillary loops. Gene deletion studies have demonstrated a critical role for PDGF-B/PDGFR- β signaling in this process (Fig. 1.26). Deletion of the *Pdgfb* gene, which is expressed by glomerular endothelia, or the PDGFR- β receptor gene (*Pdgfrb*), which is expressed by mesangial cells, results in glomeruli with a single balloon-like capillary loop, instead of the intricately convoluted glomerular capillaries of wild-type kidneys. Furthermore, the glomeruli contain no mesangial cells.⁵⁰⁸ Endothelial-cell-specific deletion of *Pdgfb* results in the same glomerular phenotype and shows that production of PDGF-B by the endothelium is required for mesangial migration.⁵⁰⁹ PDGF-B-dependent recruitment of mesangial cells into nascent glomeruli also requires the coreceptor neuropilin-1 (Nrp1).⁵¹⁰ *Nrp1*-deficiency within the *Pdgfrb⁺*-cell lineage in mice phenocopies glomerular aneurysm seen upon loss of either *Pdgfb* or *Pdgfrb* (Fig. 1.27). In vitro, mesangial cell chemotaxis, but not cell proliferation and survival in response to PDGF-B, strongly requires the mesangial expression of *Nrp1*. Furthermore, loss of the mesangium resulting from *Nrp1* ablation results in the delamination of the glomerular endothelium and inward buckling of the GBM. These findings altogether underscore the key supportive role of the mesangium for the development and maintenance of a highly convoluted glomerular capillary tuft. Indeed, targeted injury to the mesangium, either with snake venom or with antibodies against *Thy1*, results in secondary damage to the glomerular endothelium and glomerular aneurysms.^{511–515} Mesangial cells and the matrix they produce are required to pattern the glomerular capillary system. Loss of podocyte-derived factors such as VEGF-A also leads to failure of mesangial cell ingrowth, likely through the primary loss of endothelial cells and failure of PDGF-B signaling.³⁷⁶

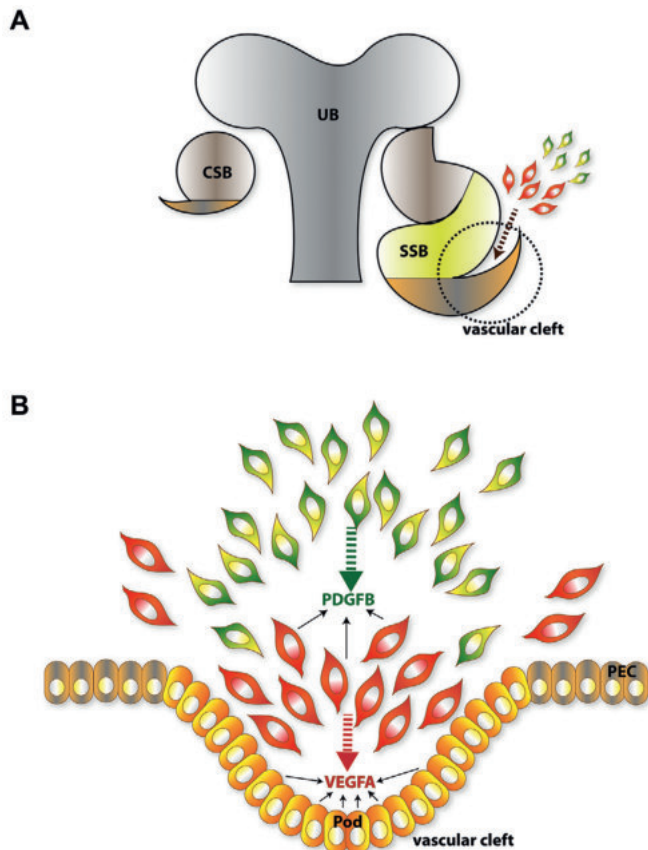


Fig. 1.26 Sequential recruitment of endothelial and mesangial cells into the developing glomerulus. (A) The glomerulus forms around the vascular cleft at the proximal end of S-shaped intermediate nephrons. (B) Within the vascular cleft, presumptive podocytes (*Pod*) secrete VEGFA that attracts VEGFR2-expressing angioblasts (red), which are the precursors of GECs. The angioblasts are followed by mesangial cell precursors expressing PDGFR- β (green), which are attracted by PDGFB secreted by the endothelial cells. *UB*, Ureteric bud; *CSB*, comma-shaped body; *PEC*, parietal epithelial cell; *SSB*, S-shaped body. Adapted from Scott RP, Quaggin SE. Formation and maintenance of a functional glomerulus. In Little MH (ed.). *Kidney Development, Disease, Repair and Regeneration*. San Diego: Academic Press; 2016.

A number of other knockouts demonstrate defects in both vascular development and mesangial cell ingrowth. Loss of the transcription factors *Tcf21* and *Foxc2* causes defective migration of mesangial cells.^{83,339} Mesangial abnormalities in *Tcf21*- and *Foxc2*-deficient mice are poorly understood in terms of mesangium-specific transcriptional targets of *Tcf21* and *Foxc2*. Nevertheless, these mutant phenotypes highlight the importance of crosstalk between cell compartments within the glomerulus.

DEVELOPMENT OF THE BOWMAN CAPSULE

The outermost cells of the proximal end of the S-shaped nascent nephron are the presumptive parietal epithelial cells that eventually form the Bowman capsule that enclose the glomerular tuft and where primary urinary filtrate collects. Similar to podocytes, parietal precursors are originally cuboidal epithelial cells that progressively flatten and become

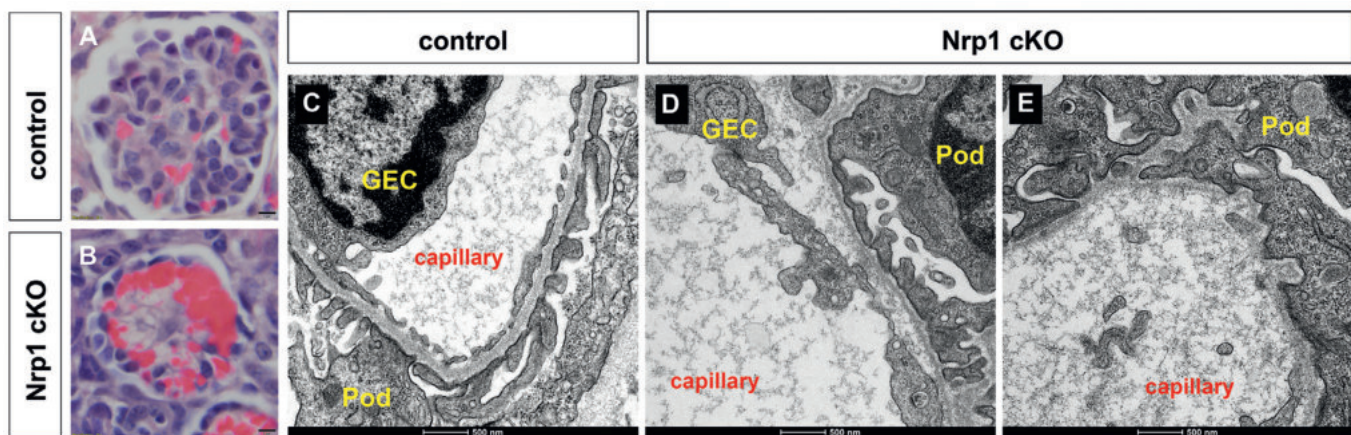


Fig. 1.27 Nrp1 is required for mesangial cell recruitment in the glomerulus. (A, B) Hypocellularity and glomerular aneurysm due to the absence of the mesangium in Nrp1-deficient mice. Representative histological sections of normal control (A) and *Nrp1* conditional knockout (*cKO*)-mutant kidneys. (C–E) Transmission electron micrographs of glomeruli showing the delamination (D) or complete detachment (E) of the glomerular endothelium from the glomerular basement membrane in *Nrp1*-*cKO* kidneys. In the absence of *Nrp1* in the *Pdgfrb*⁺ lineage, the glomerular endothelium has impaired development of fenestrae. GEC, Glomerular endothelial cell; Pod, podocyte. Adapted from Bartlett CS, Scott RP, Carota IA, et al. Glomerular mesangial recruitment and function require the co-receptor neuropilin-1. *Am J Physiol Renal Physiol*. 2017;313:F1232–F1242.

squamous. Parietal epithelia express the proteins claudin-1 (*Cldn1*) and claudin-2 (*Cldn2*) that form part of tight junctions, which help contain urinary filtrate.^{516,517} Parietal epithelial cells like podocytes express *Wt1*, although at a reduced level. Whether this differential level of *Wt1* expression affects cell fate commitment to either the podocyte or parietal cell lineage warrants further investigation. *WT1* is known to attenuate canonical Wnt signaling through an epigenetic mechanism that suppresses *Ctnnb1* expression.⁵¹⁸ Specific loss of *Ctnnb1* in nephrogenic epithelia from the S-shaped stage causes the formation of glomerular cysts where the Bowman capsule lacks parietal epithelia and are instead formed by podocytes containing notably containing foot processes and slit diaphragms.⁵¹⁹ Parietal cell specification is therefore strongly dependent on canonical Wnt-β-catenin signaling, which sets it apart from podocytes where *Ctnnb1* expression is dispensable.⁵²⁰ In the absence of parietal epithelial cells, glomerular capillaries develop poorly while the mislocalized *Vegfa*-expressing podocytes cause formation of ectopic capillaries next to the abnormal Bowman capsule.⁵¹⁹ It can therefore be inferred that parietal epithelial cells may function in compartmentalizing the podocyte–glomerular endothelial cell crosstalk, ensuring that glomerular endothelial cells form a well elaborated capillary tuft covered by an adequate number of podocytes.

NEURAL DEVELOPMENT

Renal vascular tone and urinary functions are regulated by a dense neural network in the kidney that relays bidirectional signals to the brain.⁵²¹ Glomerular filtration rate, renal blood flow, tubular resorption of fluid, electrolytes, and urinary solutes, as well as the secretion of renin, are regulated by sympathetic innervations of the glomeruli, renal tubules and blood vessels.⁵²² Over the past decade, the renal sympathetic innervation has attracted considerable attention after it has been recognized that persistently elevated renal sympathetic nerve activity contributes to the pathogenesis of renal hypertension.^{523,524} In particular, it has been shown that surgical

excision of sympathetic input to the kidneys can alleviate refractory hypertension.^{525,526} The distribution of afferent and efferent nerves to the kidney has been partially mapped but the developmental program involved in establishing them is largely unknown.^{527–529} Fate mapping and molecular studies specifically addressing the origin and development of renal nerves have yet to be reported, although many lessons have been learned about guidance pathways in play in both neural and vascular development in other systems. Neurons, like early blood vessels, appear to closely track the branching UB in cultured embryonic kidneys.^{33,370,530} It can be speculated that the sympathetic innervation and vascularization of the kidney are coordinately synchronized with better known inductive events between the UB and the MM.

Complete reference list available at ExpertConsult.com.

KEY REFERENCES

5. Short KM, Combes AN, Lefevre J, et al. Global quantification of tissue dynamics in the developing mouse kidney. *Dev Cell*. 2014;29:188–202.
10. Saxen L. *Organogenesis of the Kidney*. Cambridge: Cambridge University Press; 1987.
41. Grobstein C. Trans-filter induction of tubules in mouse metanephrogenic mesenchyme. *Exp Cell Res*. 1956;10:424–440.
48. Lindstrom NO, Lawrence ML, Burn SF, et al. Integrated beta-catenin, BMP, PTEN, and Notch signaling patterns the nephron. *Elife*. 2015;3:e04000.
59. Lindstrom NO, McMahon JA, Guo J, et al. Conserved and divergent features of human and mouse kidney organogenesis. *J Am Soc Nephrol*. 2018;29:785–805.
64. Kobayashi A, Valerius MT, Mugford JW, et al. Six2 defines and regulates a multipotent self-renewing nephron progenitor population throughout mammalian kidney development. *Cell Stem Cell*. 2008;3:169–181.
65. Kobayashi A, Mugford JW, Krautberger AM, et al. Identification of a multipotent self-renewing stromal progenitor population during mammalian kidney organogenesis. *Stem Cell Reports*. 2014;3:650–662.
136. Carroll TJ, Park JS, Hayashi S, et al. Wnt9b plays a central role in the regulation of mesenchymal to epithelial transitions underlying organogenesis of the mammalian urogenital system. *Dev Cell*. 2005;9:283–292.

143. Moore MW, Klein RD, Farinas I, et al. Renal and neuronal abnormalities in mice lacking GDNF. *Nature*. 1996;382:76–79.
144. Pichel JG, Shen L, Sheng HZ, et al. Defects in enteric innervation and kidney development in mice lacking GDNF. *Nature*. 1996;382:73–76.
145. Sanchez MP, Silos-Santiago I, Friesen J, et al. Renal agenesis and the absence of enteric neurons in mice lacking GDNF. *Nature*. 1996;382:70–73.
162. Schuchardt A, D’Agati V, Larsson-Blomberg L, et al. Defects in the kidney and enteric nervous system of mice lacking the tyrosine kinase receptor Ret. *Nature*. 1994;367:380–383.
165. Vega QC, Worby CA, Lechner MS, et al. Glial cell line-derived neurotrophic factor activates the receptor tyrosine kinase RET and promotes kidney morphogenesis. *Proc Natl Acad Sci U S A*. 1996;93:10657–10661.
187. Chi X, Michos O, Shakya R, et al. Ret-dependent cell rearrangements in the Wolffian duct epithelium initiate ureteric bud morphogenesis. *Dev Cell*. 2009;17:199–209.
212. Majumdar A, Vainio S, Kispert A, et al. Wnt11 and Ret/Gdnf pathways cooperate in regulating ureteric branching during metanephric kidney development. *Development*. 2003;130:3175–3185.
219. Basson MA, Akbulut S, Watson-Johnson J, et al. Sprouty1 is a critical regulator of GDNF/RET-mediated kidney induction. *Dev Cell*. 2005;8:229–239.
223. Michos O, Cebrion C, Hyink D, et al. Kidney development in the absence of Gdnf and Sprouty requires Fgf10. *PLoS Genet*. 2010;6:e100809.
225. Brandenberger R, Schmidt A, Linton J, et al. Identification and characterization of a novel extracellular matrix protein nephronectin that is associated with integrin alpha8beta1 in the embryonic kidney. *J Cell Biol*. 2001;154:447–458.
239. Griesammer U, Le M, Plumpp AS, et al. SLIT2-mediated ROBO2 signaling restricts kidney induction to a single site. *Dev Cell*. 2004;6:709–717.
246. Yu J, Carroll TJ, Rajagopal J, et al. A Wnt7b-dependent pathway regulates the orientation of epithelial cell division and establishes the cortico-medullary axis of the mammalian kidney. *Development*. 2009;136:161–171.
258. Niimura F, Labosky PA, Kakuchi J, et al. Gene targeting in mice reveals a requirement for angiotensin in the development and maintenance of kidney morphology and growth factor regulation. *J Clin Invest*. 1995;96:2947–2954.
268. Park J, Shrestha R, Qiu C, et al. Single-cell transcriptomics of the mouse kidney reveals potential cellular targets of kidney disease. *Science*. 2018;360:758–763.
274. Werth M, Schmidt-Ott KM, Leete T, et al. Transcription factor TFCP2L1 patterns 2604 cells in the mouse kidney collecting ducts. *Elife*. 2017;6.
279. Self M, Lagutin OV, Bowling B, et al. Six2 is required for suppression of nephrogenesis and progenitor renewal in the developing kidney. *EMBO J*. 2006;25:5214–5228.
281. Park JS, Ma W, O’Brien LL, et al. Six2 and Wnt regulate self-renewal and commitment of nephron progenitors through shared gene regulatory networks. *Dev Cell*. 2012;23:637–651.
283. Xu J, Liu H, Park JS, et al. Osr1 acts downstream of and interacts synergistically with Six2 to maintain nephron progenitor cells during kidney organogenesis. *Development*. 2014;141:1442–1452.
284. Karner CM, Das A, Ma Z, et al. Canonical Wnt9b signaling balances progenitor cell expansion and differentiation during kidney development. *Development*. 2011;138:1247–1257.
285. Tamigawa S, Wang H, Yang Y, et al. Wnt4 induces nephronic tubules in metanephric mesenchyme by a non-canonical mechanism. *Dev Biol*. 2011;352:58–69.
286. Stark K, Vainio S, Vassileva G, et al. Epithelial transformation of metanephric mesenchyme in the developing kidney regulated by Wnt-4. *Nature*. 1994;372:679–683.
290. Park JS, Valerius MT, McMahon AP. Wnt/beta-catenin signaling regulates nephron induction during mouse kidney development. *Development*. 2007;134:2533–2539.
293. Chung E, Deacon P, Marable S, et al. Notch signaling promotes nephrogenesis by downregulating Six2. *Development*. 2016;143:3907–3913.
294. Chung E, Deacon P, Park JS. Notch is required for the formation of all nephron segments and primes nephron progenitors for differentiation. *Development*. 2017;144:4530–4539.
313. Lindstrom NO, De Sena Brandine G, Tran T, et al. Progressive recruitment of mesenchymal progenitors reveals a time-dependent process of cell fate acquisition in mouse and human nephrogenesis. *Dev Cell*. 2018;45:651–660, e654.
326. Karner CM, Chirumamilla R, Aoki S, et al. Wnt9b signaling regulates planar cell polarity and kidney tubule morphogenesis. *Nat Genet*. 2009;41:793–799.
331. Saburi S, Hester I, Fischer E, et al. Loss of Fat4 disrupts PCP signaling and oriented cell division and leads to cystic kidney disease. *Nat Genet*. 2008;40:1010–1015.
334. Hartman HA, Lai HL, Patterson LT. Cessation of renal morphogenesis in mice. *Dev Biol*. 2007;310:379–387.
336. Rumballe BA, Georgas KM, Combes AN, et al. Nephron formation adopts a novel spatial topology at cessation of nephrogenesis. *Dev Biol*. 2011;360:110–122.
353. Das A, Tamigawa S, Karner CM, et al. Stromal-epithelial crosstalk regulates kidney progenitor cell differentiation. *Nat Cell Biol*. 2013;15:1035–1044.
354. Bagherie-Lachidam M, Reginensi A, Pan Q, et al. Stromal Fat4 acts non-autonomously with Dchs1/2 to restrict the nephron progenitor pool. *Development*. 2015;142:2564–2573.
357. Mao Y, Francis-West P, Irvine KD. Fat4/Dchs1 signaling between stromal and cap mesenchyme cells influences nephrogenesis and ureteric bud branching. *Development*. 2015;142:2574–2585.
371. Munro DAD, Hohenstein P, Davies JA. Cycles of vascular plexus formation within the nephrogenic zone of the developing mouse kidney. *Sci Rep*. 2017;7:3273.
372. Daniel E, Azizoglu DB, Ryan AR, et al. Spatiotemporal heterogeneity and patterning of developing renal blood vessels. *Angiogenesis*. 2018.
376. Eremina V, Sood M, Haigh J, et al. Glomerular-specific alterations of VEGF-A expression 2819 lead to distinct congenital and acquired renal diseases. *J Clin Invest*. 2003;111:707–716.
379. Dimke H, Sparks MA, Thomson BR, et al. Tubulovascular cross-talk by vascular endothelial growth factor maintains peritubular microvasculature in kidney. *J Am Soc Nephrol*. 2014.
433. Ichimura K, Kakuta S, Kawasaki Y, et al. Morphological process of podocyte development revealed by block-face scanning electron microscopy. *J Cell Sci*. 2017;130:132–142.
443. Boute N, Gribouval O, Roselli S, et al. NPHS2, encoding the glomerular protein podocin, is mutated in autosomal recessive steroid-resistant nephrotic syndrome. *Nat Genet*. 2000;24:349–354.
444. Kestila M, Lenkkeri U, Mannikko M, et al. Positionally cloned gene for a novel glomerular protein—nephrin—is mutated in congenital nephrotic syndrome. *Mol Cell*. 1998;1:575–582.
497. Suleiman H, Zhang L, Roth R, et al. Nanoscale protein architecture of the kidney glomerular basement membrane. *Elife*. 2013;2:e01149.
508. Lindahl P, Hellstrom M, Kalen M, et al. Paracrine PDGF-B/PDGF-Rbeta signaling controls mesangial cell development in kidney glomeruli. *Development*. 1998;125:3313–3322.
509. Bjarnegard M, Enge M, Norlin J, et al. Endothelium-specific ablation of PDGFB leads to pericyte loss and glomerular, cardiac and placental abnormalities. *Development*. 2004;131:1847–1857.

REFERENCES

- Zandi-Nejad K, Luyckx VA, Brenner BM. Adult hypertension and kidney disease: the role of fetal programming. *Hypertension*. 2006;47:502–508.
- Luyckx VA, Brenner BM. Low birth weight, nephron number, and kidney disease. *Kidney Int Suppl*. 2005;S68–S77.
- Rossing P, Tarnow L, Nielsen FS, et al. Low birth weight. A risk factor for development of diabetic nephropathy? *Diabetes*. 1995;44:1405–1407.
- Bertram JF, Douglas-Denton RN, Diouf B, et al. Human nephron number: implications for health and disease. *Pediatr Nephrol*. 2011;26:1529–1533.
- Short KM, Combes AN, Lefevre J, et al. Global quantification of tissue dynamics in the developing mouse kidney. *Dev Cell*. 2014;29:188–202.
- Wang X, Garrett MR. Nephron number, hypertension, and CKD: physiological and genetic insight from humans and animal models. *Physiol Genomics*. 2017;49:180–192.
- Gurusinghe S, Tambay A, Sethna CB. Developmental origins and nephron endowment in hypertension. *Front Pediatr*. 2017;5:151.
- Puelles VG, Hoy WE, Hughson MD, et al. Glomerular number and size variability and risk for kidney disease. *Curr Opin Nephrol Hypertens*. 2011;20:7–15.
- Gross ML, Amann K, Ritz E. Nephron number and renal risk in hypertension and diabetes. *J Am Soc Nephrol*. 2005;16(suppl 1):S27–S29.
- Saxen L. *Organogenesis of the Kidney*. Cambridge: Cambridge University Press; 1987.
- James RG, Schultheiss TM. Patterning of the avian intermediate mesoderm by lateral plate and axial tissues. *Dev Biol*. 2003;253:109–124.
- Capel B, Albrecht KH, Washburn LL, et al. Migration of mesonephric cells into the mammalian gonad depends on Sry. *Mech Dev*. 1999;84:127–131.
- Cui S, Ross A, Stallings N, et al. Disrupted gonadogenesis and male-to-female sex reversal in Podl knockout mice. *Development*. 2004;131:4095–4105.
- Mendelsohn C, Lohnes D, Decimo D, et al. Function of the retinoic acid receptors (RARs) during development (II). Multiple abnormalities at various stages of organogenesis in RAR double mutants. *Development*. 1994;120:2749–2771.
- Osatanhondh V, Potter EL. Development of human kidney as shown by microdissection. III. Formation and interrelationship of collecting tubules and nephrons. *Arch Pathol*. 1963;76:290–302.
- Kreidberg JA. Podocyte differentiation and glomerulogenesis. *J Am Soc Nephrol*. 2003;14:806–814.
- Batourina E, Gim S, Bello N, et al. Vitamin A controls epithelial/mesenchymal interactions through Ret expression. *Nat Genet*. 2001;27:74–78.
- Reeves W, Caulfield JP, Farquhar MG. Differentiation of epithelial foot processes and filtration slits: sequential appearance of occluding junctions, epithelial polyanion, and slit membranes in developing glomeruli. *Lab Invest*. 1978;39:90–100.
- Drenckhahn D, Franke RP. Ultrastructural organization of contractile and cytoskeletal proteins in glomerular podocytes of chicken, rat, and man. *Lab Invest*. 1988;59:673–682.
- Andrews PM, Bates SB. Filamentous actin bundles in the kidney. *Anat Rec*. 1984;210:1–9.
- Ichimura K, Kurihara H, Sakai T. Actin filament organization of foot processes in rat podocytes. *J Histochem Cytochem*. 2003;51:1589–1600.
- Ichimura K, Miyazaki N, Sadayama S, et al. Three-dimensional architecture of podocytes revealed by block-face scanning electron microscopy. *Sci Rep*. 2015;5:8993.
- Grahammer F, Schell C, Huber TB. The podocyte slit diaphragm—from a thin grey line to a complex signalling hub. *Nat Rev Nephrol*. 2013.
- Fierlbeck W, Liu A, Coyle R, et al. Endothelial cell apoptosis during glomerular capillary lumen formation in vivo. *J Am Soc Nephrol*. 2003;14:1349–1354.
- Kao RM, Vasilyev A, Miyawaki A, et al. Invasion of distal nephron precursors associates with tubular interconnection during nephrogenesis. *J Am Soc Nephrol*. 2012;23:1682–1690.
- Baum M, Quigley R, Satlin L. Maturational changes in renal tubular transport. *Curr Opin Nephrol Hypertens*. 2003;12:521–526.
- Bard J. A new role for the stromal cells in kidney development. *Bioessays*. 1996;18:705–707.
- Hatini V, Huh SO, Herzlinger D, et al. Essential role of stromal mesenchyme in kidney morphogenesis revealed by targeted disruption of Winged Helix transcription factor BF-2. *Genes Dev*. 1996;10:1467–1478.
- Levinson R, Mendelsohn C. Stromal progenitors are important for patterning epithelial and mesenchymal cell types in the embryonic kidney. *Semin Cell Dev Biol*. 2003;14:225–231.
- Robert B, St John PL, Hyink DP, et al. Evidence that embryonic kidney cells expressing flk-1 are intrinsic, vasculogenic angioblasts. *Am J Physiol*. 1996;271:F744–F753.
- Hu Y, Li M, Gothert JR, et al. Hemovascular progenitors in the kidney require sphingosine-1-phosphate receptor 1 for vascular development. *J Am Soc Nephrol*. 2016;27:1984–1995.
- Sims-Lucas S, Schaefer C, Bushnell D, et al. Endothelial progenitors exist within the kidney and lung mesenchyme. *PLoS ONE*. 2013;8:e65993.
- Halt KJ, Parssinen HE, Junnila SM, et al. CD146(+) cells are essential for kidney vasculature development. *Kidney Int*. 2016;90:311–324.
- Hyink DP, Abrahamson DR. Origin of the glomerular vasculature in the developing kidney. *Semin Nephrol*. 1995;15:300–314.
- Hyink DP, Tucker DC, St John PL, et al. Endogenous origin of glomerular endothelial and mesangial cells in grafts of embryonic kidneys. *Am J Physiol*. 1996;270:F886–F899.
- Pallone TL, Chunhua C. Renal cortical and medullary microcirculations: structure and function. In: Alpern RJ, Moe OW, Caplan MJ, eds. *Seldin and Giebisch's The Kidney*. Vol. 1. London: Academic Press; 2013:803–857.
- Kriz W, Bachmann S. Pre- and postglomerular arterioles of the kidney. *J Cardiovasc Pharmacol*. 1985;7(suppl 3):S24–S30.
- Grobstein C. Inductive epitheliomesenchymal interaction in cultured organ rudiments of the mouse. *Science*. 1953;118:52–55.
- Kreidberg JA, Sariola H, Loring JM, et al. WT-1 is required for early kidney development. *Cell*. 1993;74:679–691.
- Miyamoto N, Yoshida M, Kuratani S, et al. Defects of urogenital development in mice lacking Emx2. *Development*. 1997;124:1653–1664.
- Fisher CE, Michael L, Barnett MW, et al. Erk MAP kinase regulates branching morphogenesis in the developing mouse kidney. *Development*. 2001;128:4329–4338.
- Cheng HT, Miner JH, Lin M, et al. Gamma-secretase activity is dispensable for mesenchyme-to-epithelium transition but required for podocyte and proximal tubule formation in developing mouse kidney. *Development*. 2003;130:5031–5042.
- Tang MJ, Cai Y, Tsai SJ, et al. Ureteric bud outgrowth in response to RET activation is mediated by phosphatidylinositol 3-kinase. *Dev Biol*. 2002;243:128–136.
- Kuure S, Popsueva A, Jakobson M, et al. Glycogen synthase kinase-3 inactivation and stabilization of beta-catenin induce nephron differentiation in isolated mouse and rat kidney mesenchymes. *J Am Soc Nephrol*. 2007;18:1130–1139.
- Lindstrom NO, Lawrence ML, Burn SF, et al. Integrated beta-catenin, BMP, PTEN, and Notch signalling patterns the nephron. *Elife*. 2015;3:e04000.
- Rothenpieler UW, Dressler GR. Pax-2 is required for mesenchyme-to-epithelium conversion during kidney development. *Development*. 1993;119:711–720.
- Torres M, Gomez-Pardo E, Dressler GR, et al. Pax-2 controls multiple steps of urogenital development. *Development*. 1995;121:4057–4065.
- Hartwig S, Ho J, Pandey P, et al. Genomic characterization of Wilms' tumor suppressor 1 targets in nephron progenitor cells during kidney development. *Development*. 2010;137:1189–1203.
- Tufro A. Morpholino-mediated gene knockdown in mammalian organ culture. *Methods Mol Biol*. 2012;886:305–309.
- Tufro A, Teichman J, Woda C, et al. Semaphorin3a inhibits ureteric bud branching morphogenesis. *Mech Dev*. 2008;125:558–568.
- Unbekandt M, Davies JA. Dissociation of embryonic kidneys followed by reaggregation allows the formation of renal tissues. *Kidney Int*. 2010;77:407–416.
- Davies JA, Unbekandt M. siRNA-mediated RNA interference in embryonic kidney organ culture. *Methods Mol Biol*. 2012;886:295–303.
- Berry R, Harewood L, Pei L, et al. Esrrg functions in early branch generation of the ureteric bud and is essential for normal development of the renal papilla. *Hum Mol Genet*. 2011;20:917–926.
- Lee WC, Hough MT, Liu W, et al. Dact2 is expressed in the developing ureteric bud/collecting duct system of the kidney and controls morphogenetic behavior of collecting duct cells. *Am J Physiol Renal Physiol*. 2010;299:F740–F751.

37.e2 SECTION I – NORMAL STRUCTURE AND FUNCTION

55. Sakai T, Larsen M, Yamada KM. Fibronectin requirement in branching morphogenesis. *Nature*. 2003;423:876–881.
56. Lindstrom NO, McMahon JA, Guo J, et al. Conserved and divergent features of human and mouse kidney organogenesis. *J Am Soc Nephrol*. 2018;29:785–805.
57. Lindstrom NO, Tran T, Guo J, et al. Conserved and divergent molecular and anatomic features of human and mouse nephron patterning. *J Am Soc Nephrol*. 2018;29:825–840.
58. Nicolaou N, Renkema KY, Bongers EM, et al. Genetic, environmental, and epigenetic factors involved in CAKUT. *Nat Rev Nephrol*. 2015;11:720–731.
59. Yu J, Carroll TJ, McMahon AP. Sonic hedgehog regulates proliferation and differentiation of mesenchymal cells in the mouse metanephric kidney. *Development*. 2002;129:5301–5312.
60. Zhao H, Kegg H, Grady S, et al. Role of fibroblast growth factor receptors 1 and 2 in the ureteric bud. *Dev Biol*. 2004;276:403–415.
61. Kobayashi A, Valerius MT, Mugford JW, et al. Six2 defines and regulates a multipotent self-renewing nephron progenitor population throughout mammalian kidney development. *Cell Stem Cell*. 2008;3:169–181.
62. Kobayashi A, Mugford JW, Krautberger AM, et al. Identification of a multipotent self-renewing stromal progenitor population during mammalian kidney organogenesis. *Stem Cell Reports*. 2014;3:650–662.
63. Moeller MJ, Sanden SK, Soofi A, et al. Podocyte-specific expression of cre recombinase in transgenic mice. *Genesis*. 2003;35:39–42.
64. Jones N, Blasutig IM, Eremina V, et al. Nck adaptor proteins link nephrin to the actin cytoskeleton of kidney podocytes. *Nature*. 2006;440:818–823.
65. Freedman BS, Brooks CR, Lam AQ, et al. Modelling kidney disease with CRISPR-mutant kidney organoids derived from human pluripotent epiblast spheroids. *Nat Commun*. 2015;6:8715.
66. Kim YK, Refaeli I, Brooks CR, et al. Gene-edited human kidney organoids reveal mechanisms of disease in podocyte development. *Stem Cells*. 2017;35:2366–2378.
67. Forbes TA, Howden SE, Lawlor K, et al. Patient-iPSC-derived kidney organoids show functional validation of a ciliopathic renal phenotype and reveal underlying pathogenetic mechanisms. *Am J Hum Genet*. 2018;102:816–831.
68. Kim EY, Yazdizadeh Shotorbani P, Dryer SE. Trpc6 inactivation confers protection in a model of severe nephrosis in rats. *J Mol Med*. 2018.
69. Bakey Z, Bihoreau MT, Piedagnel R, et al. The SAM domain of ANKS6 has different interacting partners and mutations can induce different cystic phenotypes. *Kidney Int*. 2015;88:299–310.
70. Rathkolb B, Tran TV, Klempert M, et al. Large-scale albuminuria screen for nephropathy models in chemically induced mouse mutants. *Nephron Exp Nephrol*. 2005;100:e143–e149.
71. Aigner B, Rathkolb B, Herbach N, et al. Screening for increased plasma urea levels in a large-scale ENU mouse mutagenesis project reveals kidney disease models. *Am J Physiol Renal Physiol*. 2007;292:F1560–F1567.
72. Bosman EA, Quint E, Fuchs H, et al. Catweasel mice: a novel role for Six1 in sensory patch development and a model for branchio-oto-renal syndrome. *Dev Biol*. 2009;328:285–296.
73. Stewart K, Gaitan Y, Shafer ME, et al. A point mutation in p190A RhoGAP affects ciliogenesis and leads to glomerulocystic kidney defects. *PLoS Genet*. 2016;12:e1005785.
74. Tchekneva EE, Khuchua Z, Davis LS, et al. Single amino acid substitution in aquaporin 11 causes renal failure. *J Am Soc Nephrol*. 2008;19:1955–1964.
75. Vivante A, Hildebrandt F. Exploring the genetic basis of early-onset chronic kidney disease. *Nat Rev Nephrol*. 2016;12:133–146.
76. Renkema KY, Stokman MF, Giles RH, et al. Next-generation sequencing for research and diagnostics in kidney disease. *Nat Rev Nephrol*. 2014;10:433–444.
77. Gee HY, Saisawat P, Ashraf S, et al. ARHGDIA mutations cause nephrotic syndrome via defective RHO GTPase signaling. *J Clin Invest*. 2013;123:3243–3253.
78. Gupta IR, Baldwin C, Auguste D, et al. ARHGDIA: a novel gene implicated in nephrotic syndrome. *J Med Genet*. 2013;50:330–338.
79. Shibata S, Nagase M, Yoshida S, et al. Modification of mineralocorticoid receptor function by Rac1 GTPase: implication in proteinuric kidney disease. *Nat Med*. 2008;14:1370–1376.
80. Togawa A, Miyoshi J, Ishizaki H, et al. Progressive impairment of kidneys and reproductive organs in mice lacking Rho GDIalpha. *Oncogene*. 1999;18:5373–5380.
81. Stanford WL, Cohn JB, Cordes SP. Gene-trap mutagenesis: past, present and beyond. *Nat Rev Genet*. 2001;2:756–768.
82. Donoviel DB, Freed DD, Vogel H, et al. Proteinuria and perinatal lethality in mice lacking NEPH1, a novel protein with homology to NEPHRIN. *Mol Cell Biol*. 2001;21:4829–4836.
83. Takemoto M, He L, Norlin J, et al. Large-scale identification of genes implicated in kidney glomerulus development and function. *EMBO J*. 2006;25:1160–1174.
84. Yoshida Y, Miyamoto M, Bo X, et al. Overview of kidney and urine proteome databases. *Contrib Nephrol*. 2008;160:186–197.
85. Miyamoto M, Yoshida Y, Taguchi I, et al. In-depth proteomic profiling of the normal human kidney glomerulus using two-dimensional protein prefractionation in combination with liquid chromatography-tandem mass spectrometry. *J Proteome Res*. 2007;6:3680–3690.
86. Srinivas S, Goldberg MR, Watanabe T, et al. Expression of green fluorescent protein in the ureteric bud of transgenic mice: a new tool for the analysis of ureteric bud morphogenesis. *Dev Genet*. 1999;24:241–251.
87. Basson MA, Watson-Johnson J, Shakya R, et al. Branching morphogenesis of the ureteric epithelium during kidney development is coordinated by the opposing functions of GDNF and Sprouty1. *Dev Biol*. 2006;299:466–477.
88. Batourina E, Tsai S, Lambert S, et al. Apoptosis induced by vitamin A signaling is crucial for connecting the ureters to the bladder. *Nat Genet*. 2005;37:1082–1089.
89. Watanabe T, Costantini F. Real-time analysis of ureteric bud branching morphogenesis in vitro. *Dev Biol*. 2004;271:98–108.
90. Soriano P. Generalized lacZ expression with the ROSA26 Cre reporter strain. *Nat Genet*. 1999;21:70–71.
91. Wade JT. Mapping transcription regulatory networks with ChIP-seq and RNA-seq. *Adv Exp Med Biol*. 2015;883:119–134.
92. Park PJ. ChIP-seq: advantages and challenges of a maturing technology. *Nat Rev Genet*. 2009;10:669–680.
93. Brunskill EW, Park JS, Chung E, et al. Single cell dissection of early kidney development: multilineage priming. *Development*. 2014;141:3093–3101.
94. Shen K, Fetter RD, Bargmann CI. Synaptic specificity is generated by the synaptic guidepost protein SYG-2 and its receptor, SYG-1. *Cell*. 2004;116:869–881.
95. Nelson FK, Albert PS, Riddle DL. Fine structure of the *Caenorhabditis elegans* secretory-excretory system. *J Ultrastruct Res*. 1983;82:156–171.
96. Barr MM. *Caenorhabditis elegans* as a model to study renal development and disease: sexy cilia. *J Am Soc Nephrol*. 2005;16:305–312.
97. Barr MM, DeModena J, Braun D, et al. The *Caenorhabditis elegans* autosomal dominant polycystic kidney disease gene homologs *lov-1* and *pkl-2* act in the same pathway. *Curr Biol*. 2001;11:1341–1346.
98. Simon JM, Sternberg PW. Evidence of a mate-finding cue in the hermaphrodite nematode *Caenorhabditis elegans*. *Proc Natl Acad Sci U S A*. 2002;99:1598–1603.
99. Weavers H, Prieto-Sanchez S, Grawe F, et al. The insect nephrocyte is a podocyte-like cell with a filtration slit diaphragm. *Nature*. 2009;457:322–326.
100. Zhuang S, Shao H, Guo F, et al. Sns and Kirre, the *Drosophila* orthologs of Nephrin and Neph1, direct adhesion, fusion and formation of a slit diaphragm-like structure in insect nephrocytes. *Development*. 2009;136:2335–2344.
101. Helmstaedter M, Luthy K, Godel M, et al. Functional study of mammalian Neph proteins in *Drosophila melanogaster*. *PLoS ONE*. 2012;7:e40300.
102. Hochapfel F, Denk L, Mendl G, et al. Distinct functions of Crumbs regulating slit diaphragms and endocytosis in *Drosophila* nephrocytes. *Cell Mol Life Sci*. 2017;74:4573–4586.
103. Fu Y, Zhu JY, Richman A, et al. A *Drosophila* model system to assess the function of human monogenic podocyte mutations that cause nephrotic syndrome. *Hum Mol Genet*. 2017;26:768–780.
104. Denholm B. Shaping up for action: the path to physiological maturation in the renal tubules of *Drosophila*. *Organogenesis*. 2013;9:40–54.
105. Dow JA, Romero MF. *Drosophila* provides rapid modeling of renal development, function, and disease. *Am J Physiol Renal Physiol*. 2010;299:F1237–F1244.
106. Miller J, Chi T, Kapahi P, et al. *Drosophila melanogaster* as an emerging translational model of human nephrolithiasis. *J Urol*. 2013;190:1648–1656.
107. Weavers H, Skaer H. Tip cells act as dynamic cellular anchors in the morphogenesis of looped renal tubules in *Drosophila*. *Dev Cell*. 2013;27:331–344.

108. Weavers H, Skaer H. Tip cells: master regulators of tubulogenesis? *Semin Cell Dev Biol.* 2014;31:91–99.
109. Liu X, Kiss I, Lengyel JA. Identification of genes controlling malpighian tubule and other epithelial morphogenesis in *Drosophila melanogaster*. *Genetics.* 1999;151:685–695.
110. Helmstaedter M, Huber TB, Hermle T. Using the *Drosophila* nephrocyte to model podocyte function and disease. *Front Pediatr.* 2017;5:262.
111. Helmstaedter M, Simons M. Using *Drosophila* nephrocytes in genetic kidney disease. *Cell Tissue Res.* 2017;369:119–126.
112. Zhang F, Zhao Y, Han Z. An in vivo functional analysis system for renal gene discovery in *Drosophila* pericardial nephrocytes. *J Am Soc Nephrol.* 2013;24:191–197.
113. Majumdar A, Drummond IA. Podocyte differentiation in the absence of endothelial cells as revealed in the zebrafish avascular mutant, *cloche*. *Dev Genet.* 1999;24:220–229.
114. Drummond IA. Kidney development and disease in the zebrafish. *J Am Soc Nephrol.* 2005;16:299–304.
115. Kyuno J, Masse K, Jones EA. A functional screen for genes involved in *Xenopus* pronephros development. *Mech Dev.* 2008;125:571–586.
116. Krneta-Stankic V, DeLay BD, Miller RK. *Xenopus*: leaping forward in kidney organogenesis. *Pediatr Nephrol.* 2017;32:547–555.
117. Jones EA. *Xenopus*: a prince among models for pronephric kidney development. *J Am Soc Nephrol.* 2005;16:313–321.
118. DeLay BD, Krneta-Stankic V, Miller RK. Technique to target microinjection to the developing *Xenopus* kidney. *J Vis Exp.* 2016.
119. Zhou W, Boucher RC, Bollig F, et al. Characterization of mesonephric development and regeneration using transgenic zebrafish. *Am J Physiol Renal Physiol.* 2010;299:F1040–F1047.
120. Diep CQ, Ma D, Deo RC, et al. Identification of adult nephron progenitors capable of kidney regeneration in zebrafish. *Nature.* 2011;470:95–100.
121. Corkins ME, Hanania HL, Krneta-Stankic V, et al. Transgenic *Xenopus laevis* line for in vivo labeling of nephrons within the kidney. *Genes (Basel).* 2018;9.
122. Mae SI, Shono A, Shiota F, et al. Monitoring and robust induction of nephrogenic intermediate mesoderm from human pluripotent stem cells. *Nat Commun.* 2013;4:1367.
123. Araoka T, Mae S, Kurose Y, et al. Efficient and rapid induction of human iPSCs/ESCs into nephrogenic intermediate mesoderm using small molecule-based differentiation methods. *PLoS ONE.* 2014;9:e84881.
124. Takasato M, Er PX, Chiu HS, et al. Kidney organoids from human iPS cells contain multiple lineages and model human nephrogenesis. *Nature.* 2015;526:564–568.
125. Takasato M, Little MH. A strategy for generating kidney organoids: Recapitulating the development in human pluripotent stem cells. *Dev Biol.* 2016;420:210–220.
126. Morizane R, Bonventre JV. Generation of nephron progenitor cells and kidney organoids from human pluripotent stem cells. *Nat Protoc.* 2017;12:195–207.
127. Yamaguchi S, Morizane R, Homma K, et al. Generation of kidney tubular organoids from human pluripotent stem cells. *Sci Rep.* 2016;6:38353.
128. Takasato M, Little MH. Making a kidney organoid using the directed differentiation of human pluripotent stem cells. *Methods Mol Biol.* 2017;1597:195–206.
129. Higashijima Y, Hirano S, Nangaku M, et al. Applications of the CRISPR-Cas9 system in kidney research. *Kidney Int.* 2017;92:324–335.
130. Singh P, Schimenti JC, Bolcun-Filas E. A mouse geneticist's practical guide to CRISPR applications. *Genetics.* 2015;199:1–15.
131. Garreta E, Gonzalez F, Montserrat N. Studying kidney disease using tissue and genome engineering in human pluripotent stem cells. *Nephron.* 2017.
132. Rookmaaker MB, Schutgens F, Verhaar MC, et al. Development and application of human adult stem or progenitor cell organoids. *Nat Rev Nephrol.* 2015;11:546–554.
133. Auerbach R, Grobstein C. Inductive interaction of embryonic tissues after dissociation and reaggregation. *Exp Cell Res.* 1958;15:384–397.
134. Grobstein C. Morphogenetic interaction between embryonic mouse tissues separated by a membrane filter. *Nature.* 1953;172:869–870.
135. Carroll TJ, Park JS, Hayashi S, et al. Wnt9b plays a central role in the regulation of mesenchymal to epithelial transitions underlying organogenesis of the mammalian urogenital system. *Dev Cell.* 2005;9:283–292.
136. Xu PX, Adams J, Peters H, et al. Eya1-deficient mice lack ears and kidneys and show abnormal apoptosis of organ primordia. *Nat Genet.* 1999;23:113–117.
137. Wang Q, Lan Y, Cho ES, et al. Odd-skipped related 1 (Odd 1) is an essential regulator of heart and urogenital development. *Dev Biol.* 2005;288:582–594.
138. Laclef C, Souil E, Demignon J, et al. Thymus, kidney and craniofacial abnormalities in Six 1 deficient mice. *Mech Dev.* 2003;120:669–679.
139. Xu PX, Zheng W, Huang L, et al. Six1 is required for the early organogenesis of mammalian kidney. *Development.* 2003;130:3085–3094.
140. Nishinakamura R, Matsumoto Y, Nakao K, et al. Murine homolog of SALL1 is essential for ureteric bud invasion in kidney development. *Development.* 2001;128:3105–3115.
141. Shawlot W, Behringer RR. Requirement for Lim1 in head-organizer function. *Nature.* 1995;374:425–430.
142. Moore MW, Klein RD, Farinas I, et al. Renal and neuronal abnormalities in mice lacking GDNF. *Nature.* 1996;382:76–79.
143. Pichel JG, Shen L, Sheng HZ, et al. Defects in enteric innervation and kidney development in mice lacking GDNF. *Nature.* 1996;382:73–76.
144. Sanchez MP, Silos-Santiago I, Frisen J, et al. Renal agenesis and the absence of enteric neurons in mice lacking GDNF. *Nature.* 1996;382:70–73.
145. Esquela AF, Lee SJ. Regulation of metanephric kidney development by growth/differentiation factor 11. *Dev Biol.* 2003;257:356–370.
146. Michos O, Panman L, Vintersten K, et al. Gremlin-mediated BMP antagonism induces the epithelial-mesenchymal feedback signaling controlling metanephric kidney and limb organogenesis. *Development.* 2004;131:3401–3410.
147. Schuchardt A, D'Agati V, Larsson-Blomberg L, et al. RET-deficient mice: an animal model for Hirschsprung's disease and renal agenesis. *J Intern Med.* 1995;238:327–332.
148. Cacalano G, Farinas I, Wang LC, et al. GFRalpha1 is an essential receptor component for GDNF in the developing nervous system and kidney. *Neuron.* 1998;21:53–62.
149. James RG, Kamei CN, Wang Q, et al. Odd-skipped related 1 is required for development of the metanephric kidney and regulates formation and differentiation of kidney precursor cells. *Development.* 2006;133:2995–3004.
150. Buller C, Xu X, Marquis V, et al. Molecular effects of Eya1 domain mutations causing organ defects in BOR syndrome. *Hum Mol Genet.* 2001;10:2775–2781.
151. Ikeda K, Watanabe Y, Ohto H, et al. Molecular interaction and synergistic activation of a promoter by Six, Eya, and Dach proteins mediated through CREB binding protein. *Mol Cell Biol.* 2002;22:6759–6766.
152. Li X, Oghi KA, Zhang J, et al. Eya protein phosphatase activity regulates Six1-Dach-Eya transcriptional effects in mammalian organogenesis. *Nature.* 2003;426:247–254.
153. Tootle TL, Silver SJ, Davies EL, et al. The transcription factor Eyes absent is a protein tyrosine phosphatase. *Nature.* 2003;426:299–302.
154. Fougerousse F, Durand M, Lopez S, et al. Six and Eya expression during human somitogenesis and MyoD gene family activation. *J Muscle Res Cell Motil.* 2002;23:255–264.
155. Pandur PD, Moody SA. *Xenopus* Six1 gene is expressed in neurogenic cranial placodes and maintained in the differentiating lateral lines. *Mech Dev.* 2000;96:253–257.
156. Sajithlal G, Zou D, Silvius D, et al. Eya 1 acts as a critical regulator for specifying the metanephric mesenchyme. *Dev Biol.* 2005;284:323–336.
157. Hastie ND. Wilms' tumour 1 (WT1) in development, homeostasis and disease. *Development.* 2017;144:2862–2872.
158. Kann M, Bae E, Lenz MO, et al. WT1 targets Gas1 to maintain nephron progenitor cells by modulating FGF signals. *Development.* 2015;142:1254–1266.
159. Motamedi FJ, Badro DA, Clarkson M, et al. WT1 controls antagonistic FGF and BMP-pSMAD pathways in early renal progenitors. *Nat Commun.* 2014;5:4444.
160. Bouchard M. Transcriptional control of kidney development. *Differentiation.* 2004;72:295–306.
161. Schuchardt A, D'Agati V, Larsson-Blomberg L, et al. Defects in the kidney and enteric nervous system of mice lacking the tyrosine kinase receptor Ret. *Nature.* 1994;367:380–383.
162. Shakya R, Watanabe T, Costantini F. The role of GDNF/Ret signaling in ureteric bud cell fate and branching morphogenesis. *Dev Cell.* 2005;8:65–74.
163. Vainio S, Muller U. Inductive tissue interactions, cell signaling, and the control of kidney organogenesis. *Cell.* 1997;90:975–978.

37.e4 SECTION I – NORMAL STRUCTURE AND FUNCTION

164. Vega QC, Worby CA, Lechner MS, et al. Glial cell line-derived neurotrophic factor activates the receptor tyrosine kinase RET and promotes kidney morphogenesis. *Proc Natl Acad Sci USA*. 1996;93:10657–10661.
165. Pitera JE, Scambler PJ, Woolf AS. Fras1, a basement membrane-associated protein mutated in Fraser syndrome, mediates both the initiation of the mammalian kidney and the integrity of renal glomeruli. *Hum Mol Genet*. 2008;17:3953–3964.
166. Vrontou S, Petrou P, Meyer BI, et al. Fras1 deficiency results in cryptophthalmos, renal agenesis and blebbed phenotype in mice. *Nat Genet*. 2003;34:209–214.
167. Uchiyama Y, Sakaguchi M, Terabayashi T, et al. Kif26b, a kinesin family gene, regulates adhesion of the embryonic kidney mesenchyme. *Proc Natl Acad Sci U S A*. 2010;107:9240–9245.
168. Linton JM, Martin GR, Reichardt LF. The ECM protein nephronectin promotes kidney development via integrin alpha8beta1-mediated stimulation of Gdnf expression. *Development*. 2007;134:2501–2509.
169. Muller U, Wang D, Denda S, et al. Integrin alpha8beta1 is critically important for epithelial-mesenchymal interactions during kidney morphogenesis. *Cell*. 1997;88:603–613.
170. Dressler GR, Deutsch U, Chowdhury K, et al. Pax2, a new murine paired-box-containing gene and its expression in the developing excretory system. *Development*. 1990;109:787–795.
171. Brophy PD, Ostrom L, Lang KM, et al. Regulation of ureteric bud outgrowth by Pax2-dependent activation of the glial derived neurotrophic factor gene. *Development*. 2001;128:4747–4756.
172. Wellik DM, Hawkes PJ, Capecchi MR. Hox11 paralogous genes are essential for metanephric kidney induction. *Genes Dev*. 2002;16:1423–1432.
173. Kobayashi H, Kawakami K, Asashima M, et al. Six1 and Six4 are essential for Gdnf expression in the metanephric mesenchyme and ureteric bud formation, while Six1 deficiency alone causes mesonephric-tubule defects. *Mech Dev*. 2007;124:290–303.
174. Clarke JC, Patel SR, Raymond RM Jr, et al. Regulation of c-Ret in the developing kidney is responsive to Pax2 gene dosage. *Hum Mol Genet*. 2006;15:3420–3428.
175. Patel SR, Kim D, Levitan I, et al. The BRCT-domain containing protein PTIP links PAX2 to a histone H3, lysine 4 methyltransferase complex. *Dev Cell*. 2007;13:580–592.
176. Gong KQ, Yellowitz AR, Sun H, et al. A Hox-Eya-Pax complex regulates early kidney developmental gene expression. *Mol Cell Biol*. 2007;27:7661–7668.
177. Wu W, Kitamura S, Truong DM, et al. Beta1-integrin is required for kidney collecting duct morphogenesis and maintenance of renal function. *Am J Physiol Renal Physiol*. 2009;297:F210–F217.
178. Bouchard M, Souabni A, Mandler M, et al. Nephric lineage specification by Pax2 and Pax8. *Genes Dev*. 2002;16:2958–2970.
179. Grote D, Souabni A, Busslinger M, et al. Pax 2/8-regulated Gata 3 expression is necessary for morphogenesis and guidance of the nephric duct in the developing kidney. *Development*. 2006;133:53–61.
180. Grote D, Boualia SK, Souabni A, et al. Gata3 acts downstream of beta-catenin signaling to prevent ectopic metanephric kidney induction. *PLoS Genet*. 2008;4:e1000316.
181. Bridgewater D, Cox B, Cain J, et al. Canonical WNT/beta-catenin signaling is required for ureteric branching. *Dev Biol*. 2008;317:83–94.
182. Chia I, Grote D, Marcotte M, et al. Nephric duct insertion is a crucial step in urinary tract maturation that is regulated by a Gata3-Raldh2-Ret molecular network in mice. *Development*. 2011;138:2089–2097.
183. Lim KC, Lakshmanan G, Crawford SE, et al. Gata3 loss leads to embryonic lethality due to noradrenaline deficiency of the sympathetic nervous system. *Nat Genet*. 2000;25:209–212.
184. Pedersen A, Skjøng C, Shawlot W. Lim 1 is required for nephric duct extension and ureteric bud morphogenesis. *Dev Biol*. 2005;288:571–581.
185. Marose TD, Merkel CE, McMahon AP, et al. Beta-catenin is necessary to keep cells of ureteric bud/Wolffian duct epithelium in a precursor state. *Dev Biol*. 2008;314:112–126.
186. Chi X, Michos O, Shakya R, et al. Ret-dependent cell rearrangements in the Wolffian duct epithelium initiate ureteric bud morphogenesis. *Dev Cell*. 2009;17:199–209.
187. Michael L, Davies JA. Pattern and regulation of cell proliferation during murine ureteric bud development. *J Anat*. 2004;204:241–255.
188. Pepicelli CV, Kispert A, Rowitch DH, et al. GDNF induces branching and increased cell proliferation in the ureter of the mouse. *Dev Biol*. 1997;192:193–198.
189. Sainio K, Suvanto P, Davies J, et al. Glial-cell-line-derived neurotrophic factor is required for bud initiation from ureteric epithelium. *Development*. 1997;124:4077–4087.
190. Alberti L, Borrello MG, Ghizzoni S, et al. Grb2 binding to the different isoforms of Ret tyrosine kinase. *Oncogene*. 1998;17:1079–1087.
191. Arighi E, Alberti L, Torriti F, et al. Identification of Shc docking site on Ret tyrosine kinase. *Oncogene*. 1997;14:773–782.
192. Borrello MG, Alberti L, Arighi E, et al. The full oncogenic activity of Ret/ptc2 depends on tyrosine 539, a docking site for phospholipase Cgamma. *Mol Cell Biol*. 1996;16:2151–2163.
193. Borrello MG, Pelicci G, Arighi E, et al. The oncogenic versions of the Ret and Trk tyrosine kinases bind Shc and Grb2 adaptor proteins. *Oncogene*. 1994;9:1661–1668.
194. Crowder RJ, Enomoto H, Yang M, et al. Dok-6, a Novel p62 Dok family member, promotes Ret-mediated neurite outgrowth. *J Biol Chem*. 2004;279:42072–42081.
195. Grimm J, Sachs M, Britsch S, et al. Novel p62dok family members, dok-4 and dok-5, are substrates of the c-Ret receptor tyrosine kinase and mediate neuronal differentiation. *J Cell Biol*. 2001;154:345–354.
196. Kurokawa K, Iwashita T, Murakami H, et al. Identification of SNT/FRS2 docking site on RET receptor tyrosine kinase and its role for signal transduction. *Oncogene*. 2001;20:1929–1938.
197. Melillo RM, Barone MV, Lupoli G, et al. Ret-mediated mitogenesis requires Src kinase activity. *Cancer Res*. 1999;59:1120–1126.
198. Melillo RM, Santoro M, Ong SH, et al. Docking protein FRS2 links the protein tyrosine kinase RET and its oncogenic forms with the mitogen-activated protein kinase signaling cascade. *Mol Cell Biol*. 2001;21:4177–4187.
199. Pandey A, Duan H, Di Fiore PP, et al. The Ret receptor protein tyrosine kinase associates with the SH2-containing adapter protein Grb10. *J Biol Chem*. 1995;270:21461–21463.
200. Pandey A, Liu X, Dixon JE, et al. Direct association between the Ret receptor tyrosine kinase and the Src homology 2-containing adapter protein Grb7. *J Biol Chem*. 1996;271:10607–10610.
201. Perrinjaquet M, Vilar M, Ibanez CF. Protein-tyrosine phosphatase SHP2 contributes to GDNF neurotrophic activity through direct binding to phospho-Tyr687 in the RET receptor tyrosine kinase. *J Biol Chem*. 2010;285:31867–31875.
202. Tang MJ, Worley D, Sanicola M, et al. The RET-glial cell-derived neurotrophic factor (GDNF) pathway stimulates migration and chemoattraction of epithelial cells. *J Cell Biol*. 1998;142:1337–1345.
203. Jain S, Encinas M, Johnson EM Jr, et al. Critical and distinct roles for key RET tyrosine docking sites in renal development. *Genes Dev*. 2006;20:321–333.
204. Jain S, Knoten A, Hoshi M, et al. Organotypic specificity of key RET adaptor-docking sites in the pathogenesis of neurocristopathies and renal malformations in mice. *J Clin Invest*. 2010;120:778–790.
205. Jijiwa M, Fukuda T, Kawai K, et al. A targeting mutation of tyrosine 1062 in Ret causes a marked decrease of enteric neurons and renal hypoplasia. *Mol Cell Biol*. 2004;24:8026–8036.
206. Wong A, Bogni S, Kotka P, et al. Phosphotyrosine 1062 is critical for the in vivo activity of the Ret9 receptor tyrosine kinase isoform. *Mol Cell Biol*. 2005;25:9661–9673.
207. Willecke R, Heuberger J, Grossmann K, et al. The tyrosine phosphatase Shp2 acts downstream of GDNF/Ret in branching morphogenesis of the developing mouse kidney. *Dev Biol*. 2011;360:310–317.
208. Ihermann-Hella A, Lume M, Miinalainen IJ, et al. Mitogen-activated protein kinase (MAPK) pathway regulates branching by remodeling epithelial cell adhesion. *PLoS Genet*. 2014;10:e1004193.
209. Kim D, Dressler GR. PTEN modulates GDNF/RET mediated chemotaxis and branching morphogenesis in the developing kidney. *Dev Biol*. 2007;307:290–299.
210. Lu BC, Cebrian C, Chi X, et al. Etv4 and Etv5 are required downstream of GDNF and Ret for kidney branching morphogenesis. *Nat Genet*. 2009;41:1295–1302.
211. Majumdar A, Vainio S, Kispert A, et al. Wnt11 and Ret/Gdnf pathways cooperate in regulating ureteric branching during metanephric kidney development. *Development*. 2003;130:3175–3185.
212. Kuure S, Chi X, Lu B, et al. The transcription factors Etv4 and Etv5 mediate formation of the ureteric bud tip domain during kidney development. *Development*. 2010;137:1975–1979.
213. Kramer S, Okabe M, Hacohen N, et al. Sprouty: a common antagonist of FGF and EGF signaling pathways in Drosophila. *Development*. 1999;126:2515–2525.

214. Hacohen N, Kramer S, Sutherland D, et al. Sprouty encodes a novel antagonist of FGF signaling that patterns apical branching of the Drosophila airways. *Cell*. 1998;92:253–263.
215. Reich A, Sapir A, Shilo B. Sprouty is a general inhibitor of receptor tyrosine kinase signaling. *Development*. 1999;126:4139–4147.
216. Zhang S, Lin Y, Itaranta P, et al. Expression of Sprouty genes 1, 2 and 4 during mouse organogenesis. *Mech Dev*. 2001;109:367–370.
217. Miyamoto R, Jijiwa M, Asai M, et al. Loss of Sprouty2 partially rescues renal hypoplasia and stomach hypoganglionosis but not intestinal aganglionosis in Ret Y1062F mutant mice. *Dev Biol*. 2011;349:160–168.
218. Basson MA, Akbulut S, Watson-Johnson J, et al. Sproutyl is a critical regulator of GDNF/RET-mediated kidney induction. *Dev Cell*. 2005;8:229–239.
219. Chi L, Zhang S, Lin Y, et al. Sprouty proteins regulate ureteric branching by coordinating reciprocal epithelial Wnt11, mesenchymal Gdnf and stromal Fgf7 signalling during kidney development. *Development*. 2004;131:3345–3356.
220. Chi X, Hadjantonakis AK, Wu Z, et al. A transgenic mouse that reveals cell shape and arrangement during ureteric bud branching. *Genesis*. 2009;47:61–66.
221. Gross I, Morrison DJ, Hyink DP, et al. The receptor tyrosine kinase regulator Sproutyl is a target of the tumor suppressor WT1 and important for kidney development. *J Biol Chem*. 2003;278:41420–41430.
222. Michos O, Cebrion C, Hyink D, et al. Kidney development in the absence of Gdnf and Spryl requires Fgf10. *PLoS Genet*. 2010;6:e1000809.
223. Rozen EJ, Schmidt H, Dolcet X, et al. Loss of Sproutyl rescues renal agenesis caused by Ret mutation. *J Am Soc Nephrol*. 2009;20:255–259.
224. Brandenberger R, Schmidt A, Linton J, et al. Identification and characterization of a novel extracellular matrix protein nephronectin that is associated with integrin alpha8beta1 in the embryonic kidney. *J Cell Biol*. 2001;154:447–458.
225. Kiyozumi D, Takeichi M, Nakano I, et al. Basement membrane assembly of the integrin alpha8beta1 ligand nephronectin requires Fraser syndrome-associated proteins. *J Cell Biol*. 2012;197:677–689.
226. Saisawat P, Tasic V, Vega-Warner V, et al. Identification of two novel CAKUT-causing genes by massively parallel exon resequencing of candidate genes in patients with unilateral renal agenesis. *Kidney Int*. 2012;81:196–200.
227. Alazami AM, Shaheen R, Alzahrani F, et al. FREM1 mutations cause bifid nose, renal agenesis, and anorectal malformations syndrome. *Am J Hum Genet*. 2009;85:414–418.
228. Kiyozumi D, Sugimoto N, Sekiguchi K. Breakdown of the reciprocal stabilization of QBRICK/Frem1, Fras1, and Frem2 at the basement membrane provokes Fraser syndrome-like defects. *Proc Natl Acad Sci USA*. 2006;103:11981–11986.
229. Takamiya K, Kostourou V, Adams S, et al. A direct functional link between the multi-PDZ domain protein GRIP1 and the Fraser syndrome protein Fras1. *Nat Genet*. 2004;36:172–177.
230. Schanze D, Kayserili H, Satkin BN, et al. Fraser syndrome due to mutations in GRIP1—clinical phenotype in two families and expansion of the mutation spectrum. *Am J Med Genet A*. 2014;164A:837–840.
231. Vogel MJ, van Zon P, Brueton L, et al. Mutations in GRIP1 cause Fraser syndrome. *J Med Genet*. 2012;49:303–306.
232. Yang DH, McKee KK, Chen ZL, et al. Renal collecting system growth and function depend upon embryonic gamma laminin expression. *Development*. 2011;138:4535–4544.
233. Miner JH, Li C. Defective glomerulogenesis in the absence of laminin alpha5 demonstrates a developmental role for the kidney glomerular basement membrane. *Dev Biol*. 2000;217:278–289.
234. Noakes PG, Miner JH, Gautam M, et al. The renal glomerulus of mice lacking s-laminin/laminin beta 2: nephrosis despite molecular compensation by laminin beta 1. *Nat Genet*. 1995;10:400–406.
235. Tsukahara Y, Tanaka M, Miyajima A. TROP2 expressed in the trunk of the ureteric duct regulates branching morphogenesis during kidney development. *PLoS ONE*. 2011;6:e28607.
236. Smeeton J, Zhang X, Bulus N, et al. Integrin-linked kinase regulates p38 MAPK-dependent cell cycle arrest in ureteric bud development. *Development*. 2010;137:3233–3243.
237. Kume T, Deng K, Hogan BL. Murine forkhead/winged helix genes Foxc1 (Mfl) and Foxc2 (Mfh1) are required for the early organogenesis of the kidney and urinary tract. *Development*. 2000;127:1387–1395.
238. Grieshammer U, Le M, Plump AS, et al. SLIT2-mediated ROBO2 signaling restricts kidney induction to a single site. *Dev Cell*. 2004;6:709–717.
239. Lu W, van Erde AM, Fan X, et al. Disruption of ROBO2 is associated with urinary tract anomalies and confers risk of vesicoureteral reflux. *Am J Hum Genet*. 2007;80:616–632.
240. Wainwright EN, Wilhelm D, Combes AN, et al. ROBO2 restricts the nephrogenic field and regulates Wolffian duct-nephrogenic cord separation. *Dev Biol*. 2015;404:88–102.
241. Kim HJ, Bar-Sagi D. Modulation of signalling by Sprouty: a developing story. *Nat Rev Mol Cell Biol*. 2004;5:441–450.
242. Miyazaki Y, Oshima K, Fogo A, et al. Bone morphogenetic protein 4 regulates the budding site and elongation of the mouse ureter. *J Clin Invest*. 2000;105:863–873.
243. Michos O, Goncalves A, Lopez-Rios J, et al. Reduction of BMP4 activity by gremlin 1 enables ureteric bud outgrowth and GDNF/WNT11 feedback signalling during kidney branching morphogenesis. *Development*. 2007;134:2397–2405.
244. Fischer E, Legue E, Doyen A, et al. Defective planar cell polarity in polycystic kidney disease. *Nat Genet*. 2006;38:21–23.
245. Yu J, Carroll TJ, Rajagopal J, et al. A Wnt7b-dependent pathway regulates the orientation of epithelial cell division and establishes the cortico-medullary axis of the mammalian kidney. *Development*. 2009;136:161–171.
246. Maezawa Y, Binnie M, Li C, et al. A new Cre driver mouse line, Tcf21/Podl-Cre, targets metanephric mesenchyme. *PLoS ONE*. 2012;7:e40547.
247. Boivin FJ, Bridgewater D. β -Catenin in stromal progenitors controls medullary stromal development. *Am J Physiol Renal Physiol*. 2018;314:F1177–F1187.
248. Zhang Z, Pasquet E, Hueber PA, et al. Targeted inactivation of EGF receptor inhibits renal collecting duct development and function. *J Am Soc Nephrol*. 2010;21:573–578.
249. Liu Y, Chattopadhyay N, Qin S, et al. Coordinate integrin and c-Met signalling regulate Wnt gene expression during epithelial morphogenesis. *Development*. 2009;136:843–853.
250. Pietila I, Ellwanger K, Railo A, et al. Secreted Wnt antagonist Dickkopf-1 controls kidney papilla development coordinated by Wnt-7b signalling. *Dev Biol*. 2011;353:50–60.
251. Kreidberg JA, Donovan MJ, Goldstein SL, et al. Alpha 3 beta 1 integrin has a crucial role in kidney and lung organogenesis. *Development*. 1996;122:3537–3547.
252. Ohuchi H, Hori Y, Yamasaki M, et al. FGF10 acts as a major ligand for FGF receptor 2 IIIb in mouse multi-organ development. *Biochem Biophys Res Commun*. 2000;277:643–649.
253. Qiao J, Uzzo R, Obara-Ishihara T, et al. FGF-7 modulates ureteric bud growth and nephron number in the developing kidney. *Development*. 1999;126:547–554.
254. Hartwig S, Bridgewater D, Di Giovanni V, et al. BMP receptor ALK3 controls collecting system development. *J Am Soc Nephrol*. 2008;19:117–124.
255. Yosypiv IV. Renin-angiotensin system in ureteric bud branching morphogenesis: implications for kidney disease. *Pediatr Nephrol*. 2013.
256. Kim HS, Krege JH, Kluckman KD, et al. Genetic control of blood pressure and the angiotensinogen locus. *Proc Natl Acad Sci U S A*. 1995;92:2735–2739.
257. Niimura F, Labosky PA, Kakuchi J, et al. Gene targeting in mice reveals a requirement for angiotensin in the development and maintenance of kidney morphology and growth factor regulation. *J Clin Invest*. 1995;96:2947–2954.
258. Krege JH, John SW, Langenbach LL, et al. Male-female differences in fertility and blood pressure in ACE-deficient mice. *Nature*. 1995;375:146–148.
259. Esther CR Jr, Howard TE, Marino EM, et al. Mice lacking angiotensin-converting enzyme have low blood pressure, renal pathology, and reduced male fertility. *Lab Invest*. 1996;74:953–965.
260. Tsuchida S, Matsusaka T, Chen X, et al. Murine double nullizygotes of the angiotensin type 1A and 1B receptor genes duplicate severe abnormal phenotypes of angiotensinogen nullizygotes. *J Clin Invest*. 1998;101:755–760.
261. Oliverio MI, Kim HS, Ito M, et al. Reduced growth, abnormal kidney structure, and type 2 (AT2) angiotensin receptor-mediated blood pressure regulation in mice lacking both AT1A and AT1B receptors for angiotensin II. *Proc Natl Acad Sci U S A*. 1998;95:15496–15501.

262. Song R, Preston G, Khalili A, et al. Angiotensin II regulates growth of the developing papillae ex vivo. *Am J Physiol Renal Physiol.* 2012;302:F1112–F1120.
263. Chiang C, Litigutong Y, Lee E, et al. Cyclopia and defective axial patterning in mice lacking Sonic hedgehog gene function. *Nature.* 1996;383:407–413.
264. Hu MC, Mo R, Bhella S, et al. GLI3-dependent transcriptional repression of Gli1, Gli2 and kidney patterning genes disrupts renal morphogenesis. *Development.* 2006;133:569–578.
265. Kang S, Graham JM Jr, Olney AH, et al. GLI3 frameshift mutations cause autosomal dominant Pallister-Hall syndrome. *Nat Genet.* 1997;15:266–268.
266. Bose J, Grotewold L, Ruther U. Pallister-Hall syndrome phenotype in mice mutant for Gli3. *Hum Mol Genet.* 2002;11:1129–1135.
267. Park J, Shrestha R, Qiu C, et al. Single-cell transcriptomics of the mouse kidney reveals potential cellular targets of kidney disease. *Science.* 2018;360:758–763.
268. Enerback S, Nilsson D, Edwards N, et al. Acidosis and deafness in patients with recessive mutations in FOXI1. *J Am Soc Nephrol.* 2018;29:1041–1048.
269. Blomqvist SR, Vidarsson H, Fitzgerald S, et al. Distal renal tubular acidosis in mice that lack the forkhead transcription factor Foxi1. *J Clin Invest.* 2004;113:1560–1570.
270. El-Dahr SS, Li Y, Liu J, et al. p63+ ureteric bud tip cells are progenitors of intercalated cells. *JCI Insight.* 2017;2.
271. Guo Q, Wang Y, Tripathi P, et al. Adam10 mediates the choice between principal cells and intercalated cells in the kidney. *J Am Soc Nephrol.* 2015;26:149–159.
272. Jeong HW, Jeon US, Koo BK, et al. Inactivation of Notch signaling in the renal collecting duct causes nephrogenic diabetes insipidus in mice. *J Clin Invest.* 2009;119:3290–3300.
273. Werth M, Schmidt-Ott KM, Leete T, et al. Transcription factor TFCP2L1 patterns cells in the mouse kidney collecting ducts. *Elife.* 2017;6.
274. Grassmeyer J, Mukherjee M, deRiso J, et al. Elf5 is a principal cell lineage specific transcription factor in the kidney that contributes to Aqp2 and Avpr2 gene expression. *Dev Biol.* 2017;424:77–89.
275. Wu H, Chen L, Zhou Q, et al. Aqp2-expressing cells give rise to renal intercalated cells. *J Am Soc Nephrol.* 2013;24:243–252.
276. Wu H, Chen L, Zhang X, et al. Aqp5 is a new transcriptional target of Dot1a and a regulator of Aqp2. *PLoS ONE.* 2013;8:e53342.
277. Xiao Z, Chen L, Zhou Q, et al. Dot1l deficiency leads to increased intercalated cells and upregulation of V-ATPase B1 in mice. *Exp Cell Res.* 2016;344:167–175.
278. Self M, Lagutin OV, Bowling B, et al. Six2 is required for suppression of nephrogenesis and progenitor renewal in the developing kidney. *EMBO J.* 2006;25:5214–5228.
279. Kanda S, Tanigawa S, Ohmori T, et al. Sall1 maintains nephron progenitors and nascent nephrons by acting as both an activator and a repressor. *J Am Soc Nephrol.* 2014;25:2584–2595.
280. Park JS, Ma W, O'Brien LL, et al. Six2 and Wnt regulate self-renewal and commitment of nephron progenitors through shared gene regulatory networks. *Dev Cell.* 2012;23:637–651.
281. Xu J, Liu H, Chai OH, et al. Osrl1 interacts synergistically with Wt1 to regulate kidney organogenesis. *PLoS ONE.* 2016;11:e0159597.
282. Xu J, Liu H, Park JS, et al. Osrl1 acts downstream of and interacts synergistically with Six2 to maintain nephron progenitor cells during kidney organogenesis. *Development.* 2014;141:1442–1452.
283. Karner CM, Das A, Ma Z, et al. Canonical Wnt9b signaling balances progenitor cell expansion and differentiation during kidney development. *Development.* 2011;138:1247–1257.
284. Tanigawa S, Wang H, Yang Y, et al. Wnt4 induces nephronic tubules in metanephric mesenchyme by a non-canonical mechanism. *Dev Biol.* 2011;352:58–69.
285. Stark K, Vainio S, Vassileva G, et al. Epithelial transformation of metanephric mesenchyme in the developing kidney regulated by Wnt4. *Nature.* 1994;372:679–683.
286. Perantoni AO, Timofeeva O, Naillat F, et al. Inactivation of FGF8 in early mesoderm reveals an essential role in kidney development. *Development.* 2005;132:3859–3871.
287. Grieshammer U, Cebrion C, Ilagan R, et al. FGF8 is required for cell survival at distinct stages of nephrogenesis and for regulation of gene expression in nascent nephrons. *Development.* 2005;132:3847–3857.
288. Burn SF, Webb A, Berry RL, et al. Calcium/NFAT signalling promotes early nephrogenesis. *Dev Biol.* 2011;352:288–298.
289. Park JS, Valerius MT, McMahon AP. Wnt/beta-catenin signaling regulates nephron induction during mouse kidney development. *Development.* 2007;134:2533–2539.
290. Ramalingam H, Fessler AR, Das A, et al. Disparate levels of beta-catenin activity determine nephron progenitor cell fate. *Dev Biol.* 2018;440:13–21.
291. Pan X, Karner CM, Carroll TJ. Myc cooperates with beta-catenin to drive gene expression in nephron progenitor cells. *Development.* 2017;144:4173–4182.
292. Chung E, Deacon P, Marable S, et al. Notch signaling promotes nephrogenesis by downregulating Six2. *Development.* 2016;143:3907–3913.
293. Chung E, Deacon P, Park JS. Notch is required for the formation of all nephron segments and primes nephron progenitors for differentiation. *Development.* 2017;144:4530–4539.
294. Dudley AT, Lyons KM, Robertson EJ. A requirement for bone morphogenetic protein-7 during development of the mammalian kidney and eye. *Genes Dev.* 1995;9:2795–2807.
295. Luo G, Hofmann C, Bronckers AL, et al. BMP-7 is an inducer of nephrogenesis, and is also required for eye development and skeletal patterning. *Genes Dev.* 1995;9:2808–2820.
296. Tomita M, Asada M, Asada N, et al. Bmp7 maintains undifferentiated kidney progenitor population and determines nephron numbers at birth. *PLoS ONE.* 2013;8:e73554.
297. Blank U, Brown A, Adams DC, et al. BMP7 promotes proliferation of nephron progenitor cells via a JNK-dependent mechanism. *Development.* 2009;136:3557–3566.
298. Muthukrishnan SD, Yang X, Friesel R, et al. Concurrent BMP7 and FGF9 signalling governs AP-1 function to promote self-renewal of nephron progenitor cells. *Nat Commun.* 2015;6:10027.
299. Gai Z, Zhou G, Itoh S, et al. Trps1 functions downstream of Bmp7 in kidney development. *J Am Soc Nephrol.* 2009;20:2403–2411.
300. Brown AC, Muthukrishnan SD, Guay JA, et al. Role for compartmentalization in nephron progenitor differentiation. *Proc Natl Acad Sci USA.* 2013;110:4640–4645.
301. Labbe E, Letamendia A, Attisano L. Association of Smads with lymphoid enhancer binding factor 1/T cell-specific factor mediates cooperative signaling by the transforming growth factor-beta and wnt pathways. *Proc Natl Acad Sci USA.* 2000;97:8358–8363.
302. Persad S, Troussard AA, McPhee TR, et al. Tumor suppressor PTEN inhibits nuclear accumulation of beta-catenin and T cell/lymphoid enhancer factor 1-mediated transcriptional activation. *J Cell Biol.* 2001;153:1161–1174.
303. He XC, Zhang J, Tong WG, et al. BMP signaling inhibits intestinal stem cell self-renewal through suppression of Wnt/beta-catenin signaling. *Nat Genet.* 2004;36:1117–1121.
304. Poladja DP, Kish K, Kutay B, et al. Role of fibroblast growth factor receptors 1 and 2 in the metanephric mesenchyme. *Dev Biol.* 2006;291:325–339.
305. Barak H, Huh SH, Chen S, et al. FGF9 and FGF20 maintain the stemness of nephron progenitors in mice and man. *Dev Cell.* 2012;22:1191–1207.
306. Perantoni AO, Dove LF, Karavanova I. Basic fibroblast growth factor can mediate the early inductive events in renal development. *Proc Natl Acad Sci USA.* 1995;92:4696–4700.
307. Caruana G. Genetic studies define MAGUK proteins as regulators of epithelial cell polarity. *Int J Dev Biol.* 2002;46:511–518.
308. Ahn SY, Kim Y, Kim ST, et al. Scaffolding proteins DLG1 and CASK cooperate to maintain the nephron progenitor population during kidney development. *J Am Soc Nephrol.* 2013;24:1127–1138.
309. Cotter L, Ozcelik M, Jacob C, et al. Dlg1-PTEN interaction regulates myelin thickness to prevent damaging peripheral nerve overmyelination. *Science.* 2010;328:1415–1418.
310. Etienne-Manneville S, Manneville JB, Nicholls S, et al. Cdc42 and Par6-PKCzeta regulate the spatially localized association of Dlg1 and APC to control cell polarization. *J Cell Biol.* 2005;170:895–901.
311. Allanson JE, Hunter AG, Mettler GS, et al. Renal tubular dysgenesis: a not uncommon autosomal recessive syndrome: a review. *Am J Med Genet.* 1992;43:811–814.
312. Lindstrom NO, De Sena Brandine G, Tran T, et al. Progressive recruitment of mesenchymal progenitors reveals a time-dependent process of cell fate acquisition in mouse and human nephrogenesis. *Dev Cell.* 2018;45:651–660.e4.
313. Georgas K, Rumballe B, Valerius MT, et al. Analysis of early nephron patterning reveals a role for distal RV proliferation in fusion to the

- ureteric tip via a cap mesenchyme-derived connecting segment. *Dev Biol.* 2009;332:273–286.
314. Schneider J, Arraf AA, Grinstein M, et al. Wnt signaling orients the proximal-distal axis of chick kidney nephrons. *Development.* 2015;142:2686–2695.
315. Massa F, Garbay S, Bouvier R, et al. Hepatocyte nuclear factor 1beta controls nephron tubular development. *Development.* 2013;140: 886–896.
316. Heliot C, Desgrange A, Buisson I, et al. HNF1B controls proximal-intermediate nephron segment identity in vertebrates by regulating Notch signalling components and Irx1/2. *Development.* 2013;140:873–885.
317. Naylor RW, Przepiorski A, Ren Q, et al. HNF1beta is essential for nephron segmentation during nephrogenesis. *J Am Soc Nephrol.* 2013;24:77–87.
318. Basta JM, Robbins L, Denner DR, et al. A Sall1-NuRD interaction regulates multipotent nephron progenitors and is required for loop of Henle formation. *Development.* 2017;144:3080–3094.
319. Mittaz L, Ricardo S, Martinez G, et al. Neonatal calyceal dilation and renal fibrosis resulting from loss of Adamts-1 in mouse kidney is due to a developmental dysgenesis. *Nephrol Dial Transplant.* 2005;20:419–423.
320. Nakai S, Sugitani Y, Sato H, et al. Crucial roles of Brn1 in distal tubule formation and function in mouse kidney. *Development.* 2003;130:4751–4759.
321. Mittaz L, Russell DL, Wilson T, et al. Adamts-1 is essential for the development and function of the urogenital system. *Biol Reprod.* 2004;70:1096–1105.
322. Seifert JR, Mlodzik M. Frizzled/PCP signalling: a conserved mechanism regulating cell polarity and directed motility. *Nat Rev Genet.* 2007;8:126–138.
323. Zallen JA. Planar polarity and tissue morphogenesis. *Cell.* 2007;129:1051–1063.
324. Bacallao RL, McNeill H. Cystic kidney diseases and planar cell polarity signaling. *Clin Genet.* 2009;75:107–117.
325. Karner CM, Chirumamilla R, Aoki S, et al. Wnt9b signaling regulates planar cell polarity and kidney tubule morphogenesis. *Nat Genet.* 2009;41:793–799.
326. Verdeguer F, Le Corre S, Fischer E, et al. A mitotic transcriptional switch in polycystic kidney disease. *Nat Med.* 2010;16:106–110.
327. Ma Z, Gong Y, Patel V, et al. Mutations of HNF1beta inhibit epithelial morphogenesis through dysregulation of SOCS-3. *Proc Natl Acad Sci U S A.* 2007;104:20386–20391.
328. Hiesberger T, Shao X, Gourley E, et al. Role of the hepatocyte nuclear factor-1beta (HNF1beta) C-terminal domain in Pkh1 (ARPKD) gene transcription and renal cystogenesis. *J Biol Chem.* 2005;280:10578–10586.
329. Gresh L, Fischer E, Reimann A, et al. A transcriptional network in polycystic kidney disease. *EMBO J.* 2004;23:1657–1668.
330. Saburi S, Hester I, Fischer E, et al. Loss of Fat4 disrupts PCP signaling and oriented cell division and leads to cystic kidney disease. *Nat Genet.* 2008;40:1010–1015.
331. Brzoska HL, d'Esposito AM, Kolatsi-Joannou M, et al. Planar cell polarity genes Celsr1 and Vangl2 are necessary for kidney growth, differentiation, and rostrocaudal patterning. *Kidney Int.* 2016;90:1274–1284.
332. Yates LL, Papakrivopoulou J, Long DA, et al. The planar cell polarity gene Vangl2 is required for mammalian kidney-branching morphogenesis and glomerular maturation. *Hum Mol Genet.* 2010;19:4663–4676.
333. Hartman HA, Lai HL, Patterson LT. Cessation of renal morphogenesis in mice. *Dev Biol.* 2007;310:379–387.
334. Hinchliffe SA, Sargent PH, Howard CV, et al. Human intrauterine renal growth expressed in absolute number of glomeruli assessed by the disector method and Cavalieri principle. *Lab Invest.* 1991;64: 777–784.
335. Rumballe BA, Georgas KM, Combes AN, et al. Nephron formation adopts a novel spatial topology at cessation of nephrogenesis. *Dev Biol.* 2011;360:110–122.
336. Brunskill EW, Lai HL, Jamison DC, et al. Microarrays and RNA-Seq identify molecular mechanisms driving the end of nephron production. *BMC Dev Biol.* 2011;11:15.
337. Combes AN, Wilson S, Phipson B, et al. Haploinsufficiency for the Six2 gene increases nephron progenitor proliferation promoting branching and nephron number. *Kidney Int.* 2018;93:589–598.
338. Hendry C, Rumballe B, Moritz K, et al. Defining and redefining the nephron progenitor population. *Pediatr Nephrol.* 2011;26:1395–1406.
339. Quaggin SE, Schwartz L, Cui S, et al. The basic-helix-loop-helix protein pod1 is critically important for kidney and lung organogenesis. *Development.* 1999;126:5771–5783.
340. Quaggin SE, Vanden Heuvel GB, Igashira P. Pod-1, a mesoderm-specific basic-helix-loop-helix protein expressed in mesenchymal and glomerular epithelial cells in the developing kidney. *Mech Dev.* 1998;71:37–48.
341. Levinson RS, Batourina E, Choi C, et al. Foxd1-dependent signals control cellularity in the renal capsule, a structure required for normal renal development. *Development.* 2005;132:529–539.
342. Valdimarsdottir G, Goumans MJ, Rosendahl A, et al. Stimulation of Id1 expression by bone morphogenetic protein is sufficient and necessary for bone morphogenetic protein-induced activation of endothelial cells. *Circulation.* 2002;106:2263–2270.
343. Fetting JL, Guay JA, Karolak MJ, et al. FOXD1 promotes nephron progenitor differentiation by repressing decorin in the embryonic kidney. *Development.* 2014;141:17–27.
344. Sequeira-Lopez ML, Lin EE, Li M, et al. The earliest metanephric arteriolar progenitors and their role in kidney vascular development. *Am J Physiol Regul Integr Comp Physiol.* 2015;308:R138–R149.
345. Mukherjee E, Maringer K, Papke E, et al. Endothelial marker-expressing stromal cells are critical for kidney formation. *Am J Physiol Renal Physiol.* 2017;313:F611–F620.
346. Cui S, Schwartz L, Quaggin SE. Pod1 is required in stromal cells for glomerulogenesis. *Dev Dyn.* 2003;226:512–522.
347. Cui S, Li C, Ema M, et al. Rapid isolation of glomeruli coupled with gene expression profiling identifies downstream targets in Pod1 knockout mice. *J Am Soc Nephrol.* 2005;16:3247–3255.
348. Mendelsohn C, Batourina E, Fung S, et al. Stromal cells mediate retinoid-dependent functions essential for renal development. *Development.* 1999;126:1139–1148.
349. Moreau E, Vilar J, Lelievre-Pegorier M, et al. Regulation of c-ret expression by retinoic acid in rat metanephros: implication in nephron mass control. *Am J Physiol.* 1998;275:F938–F945.
350. Vilar J, Gilbert T, Moreau E, et al. Metanephros organogenesis is highly stimulated by vitamin A derivatives in organ culture. *Kidney Int.* 1996;49:1478–1487.
351. Paroly SS, Wang F, Spraggan L, et al. Stromal protein ecm1 regulates ureteric bud patterning and branching. *PLoS ONE.* 2013;8:e84155.
352. Das A, Tanigawa S, Karner CM, et al. Stromal-epithelial crosstalk regulates kidney progenitor cell differentiation. *Nat Cell Biol.* 2013;15:1035–1044.
353. Bagherie-Lachidan M, Reginensi A, Pan Q, et al. Stromal Fat4 acts non-autonomously with Dchs1/2 to restrict the nephron progenitor pool. *Development.* 2015;142:2564–2573.
354. McNeill H, Reginensi A, Lats1/2 regulate Yap/Taz to control nephron progenitor epithelialization and inhibit myofibroblast formation. *J Am Soc Nephrol.* 2017;28:852–861.
355. Reginensi A, Scott RP, Gregorietta A, et al. Yap- and Cdc42-dependent nephrogenesis and morphogenesis during mouse kidney development. *PLoS Genet.* 2013;9:e1003380.
356. Mao Y, Francis-West P, Irvine KD. Fat4/Dchs1 signaling between stromal and cap mesenchyme cells influences nephrogenesis and ureteric bud branching. *Development.* 2015;142:2574–2585.
357. Schnabel CA, Godin RE, Cleary ML. Pbx1 regulates nephrogenesis and ureteric branching in the developing kidney. *Dev Biol.* 2003;254:262–276.
358. Ohmori T, Tanigawa S, Kaku Y, et al. Sall1 in renal stromal progenitors non-cell autonomously restricts the excessive expansion of nephron progenitors. *Sci Rep.* 2015;5:15676.
359. Airik R, Bussen M, Singh MK, et al. Tbx18 regulates the development of the ureteral mesenchyme. *J Clin Invest.* 2006;116:663–674.
360. Xu J, Nie X, Cai X, et al. Tbx18 is essential for normal development of vasculature network and glomerular mesangium in the mammalian kidney. *Dev Biol.* 2014;391:17–31.
361. Nie X, Sun J, Gordon RE, et al. SIX1 acts synergistically with TBX18 in mediating ureteral smooth muscle formation. *Development.* 2010;137:755–765.
362. McCright B. Notch signaling in kidney development. *Curr Opin Nephrol Hypertens.* 2003;12:5–10.
363. McCright B, Gao X, Shen L, et al. Defects in development of the kidney, heart and eye vasculature in mice homozygous for a hypomorphic Notch2 mutation. *Development.* 2001;128:491–502.

364. Lin EE, Sequeira-Lopez ML, Gomez RA. RBP-J in FOXD1+ renal stromal progenitors is crucial for the proper development and assembly of the kidney vasculature and glomerular mesangial cells. *Am J Physiol Renal Physiol.* 2014;306:F249–F258.
365. Schmidt-Ott KM, Chen X, Paragas N, et al. c-kit delineates a distinct domain of progenitors in the developing kidney. *Dev Biol.* 2006;299:238–249.
366. Gao X, Chen X, Taglienti M, et al. Angioblast-mesenchyme induction of early kidney development is mediated by Wt1 and Vegfa. *Development.* 2005;132:5437–5449.
367. Ballermann BJ. Glomerular endothelial cell differentiation. *Kidney Int.* 2005;67:1668–1671.
368. Sariola H, Ekblom P, Lehtonen E, et al. Differentiation and vascularization of the metanephric kidney grafted on the chorioallantoic membrane. *Dev Biol.* 1983;96:427–435.
369. Ekblom P. Formation of basement membranes in the embryonic kidney: an immunohistological study. *J Cell Biol.* 1981;91:1–10.
370. Munro DAD, Hohenstein P, Davies JA. Cycles of vascular plexus formation within the nephrogenic zone of the developing mouse kidney. *Sci Rep.* 2017;7:3273.
371. Daniel E, Azizoglu DB, Ryan AR, et al. Spatiotemporal heterogeneity and patterning of developing renal blood vessels. *Angiogenesis.* 2018.
372. Buchholz B, Schley G, Eckardt KU. The impact of hypoxia on nephrogenesis. *Curr Opin Nephrol Hypertens.* 2016;25:180–186.
373. Hemker SL, Sims-Lucas S, Ho J. Role of hypoxia during nephrogenesis. *Pediatr Nephrol.* 2016;31:1571–1577.
374. Rymer C, Paredes J, Halt K, et al. Renal blood flow and oxygenation drive nephron progenitor differentiation. *Am J Physiol Renal Physiol.* 2014;307:F337–F345.
375. Eremina V, Sood M, Haigh J, et al. Glomerular-specific alterations of VEGF-A expression lead to distinct congenital and acquired renal diseases. *J Clin Invest.* 2003;111:707–716.
376. Eremina V, Cui S, Gerber H, et al. Vascular endothelial growth factor a signaling in the podocyte-endothelial compartment is required for mesangial cell migration and survival. *J Am Soc Nephrol.* 2006;17:724–735.
377. Sison K, Eremina V, Baelde H, et al. Glomerular structure and function require paracrine, not autocrine, VEGF-VEGFR-2 signaling. *J Am Soc Nephrol.* 2010;21:1691–1701.
378. Dimke H, Sparks MA, Thomson BR, et al. Tubulovascular cross-talk by vascular endothelial growth factor a maintains peritubular microvasculature in kidney. *J Am Soc Nephrol.* 2014.
379. Suri C, Jones PF, Patan S, et al. Requisite role of angiopoietin-1, a ligand for the TIE2 receptor, during embryonic angiogenesis [see comments]. *Cell.* 1996;87:1171–1180.
380. Kolatsi-Joannou M, Li XZ, Suda T, et al. Expression and potential role of angiopoietins and Tie-2 in early development of the mouse metanephros. *Dev Dyn.* 2001;222:120–126.
381. Suri C, Jones PF, Patan S, et al. Requisite role of angiopoietin-1, a ligand for the TIE2 receptor, during embryonic angiogenesis. *Cell.* 1996;87:1171–1180.
382. Jeansson M, Gawlik A, Anderson G, et al. Angiopoietin-1 is essential in mouse vasculature during development and in response to injury. *J Clin Invest.* 2011;121:2278–2289.
383. Maisonneuve PC, Suri C, Jones PF, et al. Angiopoietin-2, a natural antagonist for Tie2 that disrupts in vivo angiogenesis [see comments]. *Science.* 1997;277:55–60.
384. Augustin HG, Breier G. Angiogenesis: molecular mechanisms and functional interactions. *Thromb Haemost.* 2003;89:190–197.
385. Yuan HT, Suri C, Yancopoulos GD, et al. Expression of angiopoietin-1, angiopoietin-2, and the Tie-2 receptor tyrosine kinase during mouse kidney maturation. *J Am Soc Nephrol.* 1999;10:1722–1736.
386. Woolf AS, Yuan HT. Angiopoietin growth factors and Tie receptor tyrosine kinases in renal vascular development. *Pediatr Nephrol.* 2001;16:177–184.
387. Yuan HT, Suri C, Landon DN, et al. Angiopoietin-2 is a site-specific factor in differentiation of mouse renal vasculature. *J Am Soc Nephrol.* 2000;11:1055–1066.
388. Satchell SC, Harper SJ, Mathieson PW. Angiopoietin-1 is normally expressed by periendothelial cells. *Thromb Haemost.* 2001;86:1597–1598.
389. Satchell SC, Harper SJ, Tooke JE, et al. Human podocytes express angiopoietin 1, a potential regulator of glomerular vascular endothelial growth factor. *J Am Soc Nephrol.* 2002;13:544–550.
390. Pitera JE, Woolf AS, Gale NW, et al. Dysmorphogenesis of kidney cortical peritubular capillaries in angiopoietin-2-deficient mice. *Am J Pathol.* 2004;165:1895–1906.
391. Davis B, Dei Cas A, Long DA, et al. Podocyte-specific expression of angiopoietin-2 causes proteinuria and apoptosis of glomerular endothelia. *J Am Soc Nephrol.* 2007;18:2320–2329.
392. Partanen J, Puri MC, Schwartz L, et al. Cell autonomous functions of the receptor tyrosine kinase TIE in a late phase of angiogenic capillary growth and endothelial cell survival during murine development. *Development.* 1996;122:3013–3021.
393. Gerety SS, Anderson DJ. Cardiovascular ephrinB2 function is essential for embryonic angiogenesis. *Development.* 2002;129:1397–1410.
394. Wang HU, Anderson DJ. Eph family transmembrane ligands can mediate repulsive guidance of trunk neural crest migration and motor axon outgrowth. *Neuron.* 1997;18:383–396.
395. Andres AC, Munarini N, Djonov V, et al. EphB4 receptor tyrosine kinase transgenic mice develop glomerulopathies reminiscent of aglomerular vascular shunts. *Mech Dev.* 2003;120:511–516.
396. Foo SS, Turner CJ, Adams S, et al. Ephrin-B2 controls cell motility and adhesion during blood-vessel-wall assembly. *Cell.* 2006;124:161–173.
397. Takahashi T, Takahashi K, Gerety S, et al. Temporally compartmentalized expression of ephrin-B2 during renal glomerular development. *J Am Soc Nephrol.* 2001;12:2673–2682.
398. Kazama I, Mahoney Z, Miner JH, et al. Podocyte-derived BMP7 is critical for nephron development. *J Am Soc Nephrol.* 2008;19:2181–2191.
399. Ueda H, Miyazaki Y, Matsusaka T, et al. Bmp in podocytes is essential for normal glomerular capillary formation. *J Am Soc Nephrol.* 2008;19:685–694.
400. Ding M, Cui S, Li C, et al. Loss of the tumor suppressor Vhlh leads to upregulation of Cxcr4 and rapidly progressive glomerulonephritis in mice. *Nat Med.* 2006;12:1081–1087.
401. Takabatake Y, Sugiyama T, Kohara H, et al. The CXCL12 (SDF-1)/CXCR4 axis is essential for the development of renal vasculature. *J Am Soc Nephrol.* 2009;20:1714–1723.
402. Haegel S, Einer C, Thiele S, et al. CXC chemokine receptor 7 (CXCR7) regulates CXCR4 protein expression and capillary tuft development in mouse kidney. *PLoS ONE.* 2012;7:e42814.
403. Matsui T, Kanai-Azuma M, Hara K, et al. Redundant roles of Sox17 and Sox18 in postnatal angiogenesis in mice. *J Cell Sci.* 2006;119:3513–3526.
404. Kanai-Azuma M, Kanai Y, Gad JM, et al. Depletion of definitive gut endoderm in Sox17-null mutant mice. *Development.* 2002;129:2367–2379.
405. Pennisi D, Bowles J, Nagy A, et al. Mice null for sox18 are viable and display a mild coat defect. *Mol Cell Biol.* 2000;20:9331–9336.
406. Irrthum A, Devriendt K, Chitayat D, et al. Mutations in the transcription factor gene SOX18 underlie recessive and dominant forms of hypothrochosis-lymphedema-telangiectasia. *Am J Hum Genet.* 2003;72:1470–1478.
407. Kenig-Kozlofsky Y, Scott RP, Onay T, et al. Ascending vasa recta are angiopoietin/Tie2-dependent lymphatic-like vessels. *J Am Soc Nephrol.* 2018;29:1097–1107.
408. Bell RD, Keyl MJ, Shrader FR, et al. Renal lymphatics: the internal distribution. *Nephron.* 1968;5:454–463.
409. Holmes MJ, O'Morchoe PJ, O'Morchoe CC. Morphology of the intrarenal lymphatic system. Capsular and hilar communications. *Am J Anat.* 1977;149:333–351.
410. Kriz W, Dieterich HJ. [The lymphatic system of the kidney in some mammals. Light and electron microscopic investigations]. *Z Anat Entwicklungsgesch.* 1970;131:111–147 [in German].
411. Lee HW, Qin YX, Kim YM, et al. Expression of lymphatic endothelium-specific hyaluronan receptor LYVE-1 in the developing mouse kidney. *Cell Tissue Res.* 2011;343:429–444.
412. Karkkainen MJ, Haiko P, Sainio K, et al. Vascular endothelial growth factor C is required for sprouting of the first lymphatic vessels from embryonic veins. *Nat Immunol.* 2004;5:74–80.
413. Veikkola T, Jussila L, Makinen T, et al. Signalling via vascular endothelial growth factor receptor-3 is sufficient for lymphangiogenesis in transgenic mice. *EMBO J.* 2001;20:1223–1231.
414. Makinen T, Jussila L, Veikkola T, et al. Inhibition of lymphangiogenesis with resulting lymphedema in transgenic mice expressing soluble VEGF receptor-3. *Nat Med.* 2001;7:199–205.
415. Nurmi H, Saharinen P, Zarkada G, et al. VEGF-C is required for intestinal lymphatic vessel maintenance and lipid absorption. *EMBO Mol Med.* 2015;7:1418–1425.

416. Heinolainen K, Karaman S, D'Amico G, et al. VEGFR3 modulates vascular permeability by controlling VEGF/VEGFR2 signaling. *Circ Res*. 2017;120:1414–1425.
417. Schnermann J, Homer W. Smith Award lecture. The juxtaglomerular apparatus: from anatomical peculiarity to physiological relevance. *J Am Soc Nephrol*. 2003;14:1681–1694.
418. Song R, Lopez M, Yosypiv IV. Foxd1 is an upstream regulator of the renin-angiotensin system during metanephric kidney development. *Pediatr Res*. 2017;82:855–862.
419. Starke C, Betz H, Hickmann L, et al. Renin lineage cells repopulate the glomerular mesangium after injury. *J Am Soc Nephrol*. 2015;26:48–54.
420. Sequeira Lopez ML, Pentz ES, Nomasa T, et al. Renin cells are precursors for multiple cell types that switch to the renin phenotype when homeostasis is threatened. *Dev Cell*. 2004;6:719–728.
421. Husain A, Graham R. *Enzymes and Receptors of the Renin-Angiotensin System: Celebrating a Century of Discovery*. Sidney: Harwood Academic; 2000.
422. Cooper WO, Hernandez-Diaz S, Arbogast PG, et al. Major congenital malformations after first-trimester exposure to ACE inhibitors. *N Engl J Med*. 2006;354:2443–2451.
423. Friberg P, Sundelin B, Bohman SO, et al. Renin-angiotensin system in neonatal rats: induction of a renal abnormality in response to ACE inhibition or angiotensin II antagonism. *Kidney Int*. 1994;45:485–492.
424. Timmermans PB, Wong PC, Chiu AT, et al. Angiotensin II receptors and angiotensin II receptor antagonists. *Pharmacol Rev*. 1993;45:205–251.
425. Ito M, Oliverio MI, Mannon PJ, et al. Regulation of blood pressure by the type 1A angiotensin II receptor gene. *Proc Natl Acad Sci U S A*. 1995;92:3521–3525.
426. Sugaya T, Nishimatsu S, Tanimoto K, et al. Angiotensin II type 1a receptor-deficient mice with hypotension and hyperreninemia. *J Biol Chem*. 1995;270:18719–18722.
427. Ichiki T, Labosky PA, Shiota C, et al. Effects on blood pressure and exploratory behaviour of mice lacking angiotensin II type-2 receptor. *Nature*. 1995;377:748–750.
428. Hein L, Barsh GS, Pratt RE, et al. Behavioural and cardiovascular effects of disrupting the angiotensin II type-2 receptor in mice. *Nature*. 1995;377:744–747.
429. Nishimura H, Yerkes E, Hohenfellner K, et al. Role of the angiotensin type 2 receptor gene in congenital anomalies of the kidney and urinary tract, CAKUT, of mice and men. *Mol Cell*. 1999;3:1–10.
430. Sequeira-Lopez ML, Weatherford ET, Borges GR, et al. The microRNA-processing enzyme dicer maintains juxtaglomerular cells. *J Am Soc Nephrol*. 2010;21:460–467.
431. Pan L, Glenn ST, Jones CA, et al. Activation of the rat renin promoter by HOXD10.PBX1b.PREP1, Ets-1, and the intracellular domain of notch. *J Biol Chem*. 2005;280:20860–20866.
432. Castellanos Rivera RM, Monteagudo MC, et al. Transcriptional regulator RBPJ regulates the number and plasticity of renin cells. *Physiol Genomics*. 2011;43:1021–1028.
433. Ichimura K, Kakuta S, Kawasaki Y, et al. Morphological process of podocyte development revealed by block-face scanning electron microscopy. *J Cell Sci*. 2017;130:132–142.
434. Sadl V, Jin F, Yu J, et al. The mouse Kreisler (Krmll/MafB) segmentation gene is required for differentiation of glomerular visceral epithelial cells. *Dev Biol*. 2002;249:16–29.
435. Chen H, Lun Y, Ovchinnikov D, et al. Limb and kidney defects in Lmx1b mutant mice suggest an involvement of LMX1B in human nail patella syndrome. *Nat Genet*. 1998;19:51–55.
436. Hammes A, Guo JK, Lutsch G, et al. Two splice variants of the Wilms' tumor 1 gene have distinct functions during sex determination and nephron formation. *Cell*. 2001;106:319–329.
437. Moore AW, McInnes L, Kreidberg J, et al. YAC complementation shows a requirement for *Wt1* in the development of epicardium, adrenal gland and throughout nephrogenesis. *Development*. 1999;126:1845–1857.
438. Natoli TA, Liu J, Eremina V, et al. A mutant form of the Wilms' tumor suppressor gene *WT1* observed in Denys-Drash syndrome interferes with glomerular capillary development. *J Am Soc Nephrol*. 2002;13:2058–2067.
439. Kann M, Ettou S, Jung YL, et al. Genome-wide analysis of Wilms' tumor 1-controlled gene expression in podocytes reveals key regulatory mechanisms. *J Am Soc Nephrol*. 2015;26:2097–2104.
440. Maezawa Y, Onay T, Scott RP, et al. Loss of the podocyte-expressed transcription factor Tcf21/Pod1 results in podocyte differentiation defects and FSGS. *J Am Soc Nephrol*. 2014;25:2459–2470.
441. Suleiman H, Heudobler D, Raschta AS, et al. The podocyte-specific inactivation of Lmx1b, Ldb1 and E2a yields new insight into a transcriptional network in podocytes. *Dev Biol*. 2007;304:701–712.
442. Dreyer SD, Zhou G, Baldini A, et al. Mutations in LMX1B cause abnormal skeletal patterning and renal dysplasia in nail patella syndrome. *Nat Genet*. 1998;19:47–50.
443. Boute N, Gribouval O, Roselli S, et al. NPHS2, encoding the glomerular protein podocin, is mutated in autosomal recessive steroid-resistant nephrotic syndrome. *Nat Genet*. 2000;24:349–354.
444. Kestila M, Lenkkeri U, Mannikko M, et al. Positionally cloned gene for a novel glomerular protein—nephrin—is mutated in congenital nephrotic syndrome. *Mol Cell*. 1998;1:575–582.
445. Holzman LB, St John PL, Kovari IA, et al. Nephrin localizes to the slit pore of the glomerular epithelial cell. *Kidney Int*. 1999;56:1481–1491.
446. Huber TB, Kottgen M, Schilling B, et al. Interaction with podocin facilitates nephrin signaling. *J Biol Chem*. 2001;276:41543–41546.
447. Huber TB, Simons M, Hartleben B, et al. Molecular basis of the functional podocin-nephrin complex: mutations in the NPHS2 gene disrupt nephrin targeting to lipid raft microdomains. *Hum Mol Genet*. 2003;12:3397–3405.
448. Ruotsalainen V, Ljungberg P, Wartiovaara J, et al. Nephrin is specifically located at the slit diaphragm of glomerular podocytes. *Proc Natl Acad Sci U S A*. 1999;96:7962–7967.
449. Schwarz K, Simons M, Reiser J, et al. Podocin, a raft-associated component of the glomerular slit diaphragm, interacts with CD2AP and nephrin. *J Clin Invest*. 2001;108:1621–1629.
450. Tzur S, Rosset S, Shemer R, et al. Missense mutations in the APOL1 gene are highly associated with end stage kidney disease risk previously attributed to the MYH9 gene. *Hum Genet*. 2010;128:345–350.
451. Kaplan JM, Kim SH, North KN, et al. Mutations in ACTN4, encoding alpha-actinin-4, cause familial focal segmental glomerulosclerosis. *Nat Genet*. 2000;24:251–256.
452. Kos CH, Le TC, Sinha S, et al. Mice deficient in alpha-actinin-4 have severe glomerular disease. *J Clin Invest*. 2003;111:1683–1690.
453. Yao J, Le TC, Kos CH, et al. Alpha-actinin-4-mediated FSGS: an inherited kidney disease caused by an aggregated and rapidly degraded cytoskeletal protein. *PLoS Biol*. 2004;2:e167.
454. Ashworth S, Teng B, Kaufeld J, et al. Cofilin-1 inactivation leads to proteinuria—studies in zebrafish, mice and humans. *PLoS ONE*. 2010;5:e12626.
455. Boyer O, Benoit G, Gribouval O, et al. Mutations in INF2 are a major cause of autosomal dominant focal segmental glomerulosclerosis. *J Am Soc Nephrol*. 2011;22:239–245.
456. Brown EJ, Schlondorff JS, Becker DJ, et al. Mutations in the formin gene INF2 cause focal segmental glomerulosclerosis. *Nat Genet*. 2010;42:72–76.
457. Akilesh S, Suleiman H, Yu H, et al. Arhgap24 inactivates Rac1 in mouse podocytes, and a mutant form is associated with familial focal segmental glomerulosclerosis. *J Clin Invest*. 2011;121:4127–4137.
458. Krendel M, Kim SV, Willinger T, et al. Disruption of myosin 1e promotes podocyte injury. *J Am Soc Nephrol*. 2009;20:86–94.
459. Ciani L, Patel A, Allen ND, et al. Mice lacking the giant protocadherin mFAT1 exhibit renal slit junction abnormalities and a partially penetrant cyclopia and anophthalmia phenotype. *Mol Cell Biol*. 2003;23:3575–3582.
460. Reiser J, Polu KR, Moller CC, et al. TRPC6 is a glomerular slit diaphragm-associated channel required for normal renal function. *Nat Genet*. 2005;37:739–744.
461. Diomedi-Camassei F, Di Giandomenico S, Santorelli FM, et al. COQ2 nephropathy: a newly described inherited mitochondrialopathy with primary renal involvement. *J Am Soc Nephrol*. 2007;18:2773–2780.
462. Heeringa SF, Chernin G, Chaki M, et al. COQ6 mutations in human patients produce nephrotic syndrome with sensorineural deafness. *J Clin Invest*. 2011;121:2013–2024.
463. Hinkes B, Wiggins RC, Gbadegesin R, et al. Positional cloning uncovers mutations in PLCE1 responsible for a nephrotic syndrome variant that may be reversible. *Nat Genet*. 2006;38:1397–1405.
464. Lal MA, Andersson AC, Katayama K, et al. Rhophilin-1 is a key regulator of the podocyte cytoskeleton and is essential for glomerular filtration. *J Am Soc Nephrol*. 2014.

37.e10 SECTION I – NORMAL STRUCTURE AND FUNCTION

465. Khoshnoodi J, Sigmundsson K, Ofverstedt LG, et al. Nephrin promotes cell-cell adhesion through homophilic interactions. *Am J Pathol.* 2003;163:2337–2346.
466. Wartiovaara J, Ofverstedt LG, Khoshnoodi J, et al. Nephrin strands contribute to a porous slit diaphragm scaffold as revealed by electron tomography. *J Clin Invest.* 2004;114:1475–1483.
467. Inoue T, Yaoita E, Kurihara H, et al. FAT is a component of glomerular slit diaphragms. *Kidney Int.* 2001;59:1003–1012.
468. Brasch J, Harrison OJ, Honig B, et al. Thinking outside the cell: how cadherins drive adhesion. *Trends Cell Biol.* 2012;22:299–310.
469. Gerke P, Huber TB, Sellin L, et al. Homodimerization and heterodimerization of the glomerular podocyte proteins nephrin and NEPH1. *J Am Soc Nephrol.* 2003;14:918–926.
470. Heikkila E, Ristola M, Havana M, et al. Trans-interaction of nephrin and Neph1/Neph3 induces cell adhesion that associates with decreased tyrosine phosphorylation of nephrin. *Biochem J.* 2011;435:619–628.
471. Hartleben B, Schweizer H, Lubben P, et al. Neph-Nephrin proteins bind the Par3-Par6-atypical protein kinase C (aPKC) complex to regulate podocyte cell polarity. *J Biol Chem.* 2008;283:23033–23038.
472. Hirose T, Satoh D, Kurihara H, et al. An essential role of the universal polarity protein, aPKClambda, on the maintenance of podocyte slit diaphragms. *PLoS ONE.* 2009;4:e4194.
473. Huber TB, Hartleben B, Winkelmann K, et al. Loss of podocyte aPKClambda/iota causes polarity defects and nephrotic syndrome. *J Am Soc Nephrol.* 2009;20:798–806.
474. Scott RP, Hawley SP, Ruston J, et al. Podocyte-specific loss of cdc42 leads to congenital nephropathy. *J Am Soc Nephrol.* 2012;23:1149–1154.
475. Satoh D, Hirose T, Harita Y, et al. aPKClambda maintains the integrity of the glomerular slit diaphragm through trafficking of nephrin to the cell surface. *J Biochem.* 2014;156:115–128.
476. Shirato I, Sakai T, Kimura K, et al. Cytoskeletal changes in podocytes associated with foot process effacement in Masugi nephritis. *Am J Pathol.* 1996;148:1283–1296.
477. Verma R, Kovari I, Soofi A, et al. Nephrin ectodomain engagement results in Src kinase activation, nephrin phosphorylation, Nck recruitment, and actin polymerization. *J Clin Invest.* 2006;116:1346–1359.
478. Verma R, Wharram B, Kovari I, et al. Fyn binds to and phosphorylates the kidney slit diaphragm component Nephrin. *J Biol Chem.* 2003;278:20716–20723.
479. Schell C, Baumhakl L, Salou S, et al. N-WASP is required for stabilization of podocyte foot processes. *J Am Soc Nephrol.* 2013.
480. Tu Y, Li F, Goicoechea S, et al. The LIM-only protein PINCH directly interacts with integrin-linked kinase and is recruited to integrin-rich sites in spreading cells. *Mol Cell Biol.* 1999;19:2425–2434.
481. Dai C, Stoltz DB, Bastacky SI, et al. Essential role of integrin-linked kinase in podocyte biology: bridging the integrin and slit diaphragm signaling. *J Am Soc Nephrol.* 2006;17:2164–2175.
482. El-Aouni C, Herbach N, Blattner SM, et al. Podocyte-specific deletion of integrin-linked kinase results in severe glomerular basement membrane alterations and progressive glomerulosclerosis. *J Am Soc Nephrol.* 2006;17:1334–1344.
483. Yaddanapudi S, Altintas MM, Kistler AD, et al. CD2AP in mouse and human podocytes controls a proteolytic program that regulates cytoskeletal structure and cellular survival. *J Clin Invest.* 2011;121:3965–3980.
484. Shih NY, Li J, Karpitskii V, et al. Congenital nephrotic syndrome in mice lacking CD2-associated protein. *Science.* 1999;286:312–315.
485. Kim JM, Wu H, Green G, et al. CD2-associated protein haploinsufficiency is linked to glomerular disease susceptibility. *Science.* 2003;300:1298–1300.
486. Schermer B, Benzing T. Lipid-protein interactions along the slit diaphragm of podocytes. *J Am Soc Nephrol.* 2009;20:473–478.
487. Huber TB, Schermer B, Benzing T. Podocin organizes ion channel-lipid supercomplexes: implications for mechanosensation at the slit diaphragm. *Nephron Exp Nephrol.* 2007;106:e27–e31.
488. Huang M, Gu G, Ferguson EL, et al. A stomatin-like protein necessary for mechanosensation in *C. elegans*. *Nature.* 1995;378:292–295.
489. Winn MP, Conlon PJ, Lynn KL, et al. A mutation in the TRPC6 cation channel causes familial focal segmental glomerulosclerosis. *Science.* 2005;308:1801–1804.
490. Heeringa SF, Moller CC, Du J, et al. A novel TRPC6 mutation that causes childhood FSGS. *PLoS ONE.* 2009;4:e7771.
491. Jin J, Sison K, Li C, et al. Soluble FLT1 binds lipid microdomains in podocytes to control cell morphology and glomerular barrier function. *Cell.* 2012;151:384–399.
492. Ho J, Ng KH, Rosen S, et al. Podocyte-specific loss of functional microRNAs leads to rapid glomerular and tubular injury. *J Am Soc Nephrol.* 2008;19:2069–2075.
493. Harvey SJ, Jarad G, Cunningham J, et al. Podocyte-specific deletion of dicer alters cytoskeletal dynamics and causes glomerular disease. *J Am Soc Nephrol.* 2008;19:2150–2158.
494. Shi S, Yu L, Chiu C, et al. Podocyte-selective deletion of dicer induces proteinuria and glomerulosclerosis. *J Am Soc Nephrol.* 2008;19:2159–2169.
495. Byron A, Randles MJ, Humphries JD, et al. Glomerular cell cross-talk influences composition and assembly of extracellular matrix. *J Am Soc Nephrol.* 2014;25:953–966.
496. Lennon R, Byron A, Humphries JD, et al. Global analysis reveals the complexity of the human glomerular extracellular matrix. *J Am Soc Nephrol.* 2014;25:939–951.
497. Suleiman H, Zhang L, Roth R, et al. Nanoscale protein architecture of the kidney glomerular basement membrane. *Elife.* 2013;2:e01149.
498. Kruegel J, Rubel D, Gross O. Alport syndrome—insights from basic and clinical research. *Nat Rev Nephrol.* 2013;9:170–178.
499. Savige J. Alport syndrome: its effects on the glomerular filtration barrier and implications for future treatment. *J Physiol.* 2014;592:4013–4023.
500. Miner JH, Sanes JR. Collagen IV alpha 3, alpha 4, and alpha 5 chains in rodent basal laminae: sequence, distribution, association with laminins, and developmental switches. *J Cell Biol.* 1994;127:879–891.
501. Candiello J, Cole GJ, Halfter W. Age-dependent changes in the structure, composition and biophysical properties of a human basement membrane. *Matrix Biol.* 2010;29:402–410.
502. Cui Z, Zhao MH. Advances in human antiglomerular basement membrane disease. *Nat Rev Nephrol.* 2011;7:697–705.
503. Matejas V, Hinkes B, Alkandari F, et al. Mutations in the human laminin beta2 (LAMB2) gene and the associated phenotypic spectrum. *Hum Mutat.* 2010;31:992–1002.
504. Zenker M, Aigner T, Wendler O, et al. Human laminin beta2 deficiency causes congenital nephrosis with mesangial sclerosis and distinct eye abnormalities. *Hum Mol Genet.* 2004;13:2625–2632.
505. Goldberg S, Adair-Kirk TL, Senior RM, et al. Maintenance of glomerular filtration barrier integrity requires laminin alpha5. *J Am Soc Nephrol.* 2010;21:579–586.
506. Kikkawa Y, Miner JH. Molecular dissection of laminin alpha 5 in vivo reveals separable domain-specific roles in embryonic development and kidney function. *Dev Biol.* 2006;296:265–277.
507. Shannon MB, Patton BL, Harvey SJ, et al. A hypomorphic mutation in the mouse laminin alpha5 gene causes polycystic kidney disease. *J Am Soc Nephrol.* 2006;17:1913–1922.
508. Lindahl P, Hellstrom M, Kalen M, et al. Paracrine PDGF-B/PDGF-Rbeta signaling controls mesangial cell development in kidney glomeruli. *Development.* 1998;125:3313–3322.
509. Bjarnegard M, Enge M, Norlin J, et al. Endothelium-specific ablation of PDGFB leads to pericyte loss and glomerular, cardiac and placental abnormalities. *Development.* 2004;131:1847–1857.
510. Bartlett CS, Scott RP, Carota IA, et al. Glomerular mesangial cell recruitment and function require the co-receptor neuropilin-1. *Am J Physiol Renal Physiol.* 2017;313:F1232–F1242.
511. Barnes JL, Hevey KA, Hastings RR, et al. Mesangial cell migration precedes proliferation in Habu snake venom-induced glomerular injury. *Lab Invest.* 1994;70:460–467.
512. Nakao N, Hiraiwa N, Yoshiki A, et al. Tenascin-C promotes healing of Habu-snake venom-induced glomerulonephritis: studies in knockout congenic mice and in culture. *Am J Pathol.* 1998;152:1237–1245.
513. Wnuk M, Hlushchuk R, Tuffin G, et al. The effects of PTK787/ZK22258, an inhibitor of VEGFR and PDGFRbeta pathways, on intussusceptive angiogenesis and glomerular recovery from Thy1.1 nephritis. *Am J Pathol.* 2011;178:1899–1912.
514. Ichimura K, Kurihara H, Sakai T. Involvement of mesangial cells expressing alpha-smooth muscle actin during restorative glomerular remodeling in Thy-1.1 nephritis. *J Histochem Cytochem.* 2006;54:1291–1301.
515. Ichimura K, Stan RV, Kurihara H, et al. Glomerular endothelial cells form diaphragms during development and pathologic conditions. *J Am Soc Nephrol.* 2008;19:1463–1471.
516. Gharib SA, Pippin JW, Ohse T, et al. Transcriptional landscape of glomerular parietal epithelial cells. *PLoS ONE.* 2014;9:e105289.
517. Ohse T, Chang AM, Pippin JW, et al. A new function for parietal epithelial cells: a second glomerular barrier. *Am J Physiol Renal Physiol.* 2009;297:F1566–F1574.

518. Akpa MM, Iglesias DM, Chu LL, et al. Wilms tumour suppressor, WT1, suppresses epigenetic silencing of the beta-catenin gene. *J Biol Chem.* 2014;290:2279–2288.
519. Grouls S, Iglesias DM, Wentzzenen N, et al. Lineage specification of parietal epithelial cells requires beta-catenin/Wnt signaling. *J Am Soc Nephrol.* 2012;23:63–72.
520. Dai C, Stoltz DB, Kiss LP, et al. Wnt/beta-catenin signaling promotes podocyte dysfunction and albuminuria. *J Am Soc Nephrol.* 2009;20:1997–2008.
521. Sata Y, Head GA, Denton K, et al. Role of the sympathetic nervous system and its modulation in renal hypertension. *Front Med (Lausanne).* 2018;5:82.
522. Kumagai H, Oshima N, Matsuura T, et al. Importance of rostral ventrolateral medulla neurons in determining efferent sympathetic nerve activity and blood pressure. *Hypertens Res.* 2012;35:132–141.
523. Sata Y, Kawada T, Shimizu S, et al. Predominant role of neural arc in sympathetic baroreflex resetting of spontaneously hypertensive rats. *Circ J.* 2015;79:592–599.
524. Grassi G, Mark A, Esler M. The sympathetic nervous system alterations in human hypertension. *Circ Res.* 2015;116:976–990.
525. Schlaich MP, Sobotka PA, Krum H, et al. Renal sympathetic-nerve ablation for uncontrolled hypertension. *N Engl J Med.* 2009;361:932–934.
526. Krum H, Schlaich M, Whitbourn R, et al. Catheter-based renal sympathetic denervation for resistant hypertension: a multicentre safety and proof-of-principle cohort study. *Lancet.* 2009;373:1275–1281.
527. Barajas L, Liu L, Powers K. Anatomy of the renal innervation: intrarenal aspects and ganglia of origin. *Can J Physiol Pharmacol.* 1992;70:735–749.
528. McKenna OC, Angelakos ET. Adrenergic innervation of the canine kidney. *Circ Res.* 1968;22:345–354.
529. Mulder J, Hokfelt T, Kneuepfer MM, et al. Renal sensory and sympathetic nerves reinnervate the kidney in a similar time-dependent fashion after renal denervation in rats. *Am J Physiol Regul Integr Comp Physiol.* 2013;304:R675–R682.
530. Sariola H, Holm K, Henke-Fahle S. Early innervation of the metanephric kidney. *Development.* 1988;104:589–599.
531. Boualia SK, Gaitan Y, Murawski I, et al. Vesicoureteral reflux and other urinary tract malformations in mice compound heterozygous for Pax2 and Emx2. *PLoS ONE.* 2011;6:e21529.
532. Bebee TW, Sims-Lucas S, Park JW, et al. Ablation of the epithelial-specific splicing factor Esrp1 results in ureteric branching defects and reduced nephron number. *Dev Dyn.* 2016;245:991–1000.
533. McPherron AC, Lawler AM, Lee SJ. Regulation of anterior/posterior patterning of the axial skeleton by growth/differentiation factor 11. *Nat Genet.* 1999;22:260–264.
534. Srinivas S, Wu Z, Chen CM, et al. Dominant effects of RET receptor misexpression and ligand-independent RET signaling on ureteric bud development. *Development.* 1999;126:1375–1386.
535. Jing S, Wen D, Yu Y, et al. GDNF-induced activation of the ret protein tyrosine kinase is mediated by GDNFR-alpha, a novel receptor for GDNF. *Cell.* 1996;85:1113–1124.
536. Schuchardt A, D'Agati V, Pachnis V, et al. Renal agenesis and hypodysplasia in ret-k mutant mice result from defects in ureteric bud development. *Development.* 1996;122:1919–1929.
537. Enomoto H, Araki T, Jackman A, et al. GFR alpha1-deficient mice have deficits in the enteric nervous system and kidneys. *Neuron.* 1998;21:317–324.
538. Wang H, Zhang C, Wang X, et al. Disruption of Gen1 causes congenital anomalies of the kidney and urinary tract in mice. *Int J Biol Sci.* 2018;14:10–20.
539. Brophy PD, Rasmussen M, Parida M, et al. A gene implicated in activation of retinoic acid receptor targets is a novel renal agenesis gene in humans. *Genetics.* 2017;207:215–228.
540. Sanna-Cherchi S, Khan K, Westland R, et al. Exome-wide association study identifies GREB1L mutations in congenital kidney malformations. *Am J Hum Genet.* 2017;101:789–802.
541. De Tomasi L, David P, Humbert C, et al. Mutations in GREB1L cause bilateral kidney agenesis in humans and mice. *Am J Hum Genet.* 2017;101:803–814.
542. Hinze C, Ruffert J, Walentin K, et al. GRHL2 is required for collecting duct epithelial barrier function and renal osmoregulation. *J Am Soc Nephrol.* 2018;29:857–868.
543. Aue A, Hinze C, Walentin K, et al. A grainyhead-like 2/Ovo-like 2 pathway regulates renal epithelial barrier function and lumen expansion. *J Am Soc Nephrol.* 2015;26:2704–2715.
544. Desgrange A, Heliot C, Skovorodkin I, et al. HNF1B controls epithelial organization and cell polarity during ureteric bud branching and collecting duct morphogenesis. *Development.* 2017;144:4704–4719.
545. Patterson LT, Pembaur M, Potter SS. Hoxa11 and Hoxd11 regulate branching morphogenesis of the ureteric bud in the developing kidney. *Development.* 2001;128:2153–2161.
546. Bullock SL, Fletcher JM, Beddington RS, et al. Renal agenesis in mice homozygous for a gene trap mutation in the gene encoding heparan sulfate 2-sulfotransferase. *Genes Dev.* 1998;12:1894–1906.
547. Kaku Y, Ohmori T, Kudo K, et al. Islet1 deletion causes kidney agenesis and hydronephrosis resembling CAKUT. *J Am Soc Nephrol.* 2013;24:1242–1249.
548. Kanasaki K, Kanda Y, Palmsten K, et al. Integrin beta1-mediated matrix assembly and signaling are critical for the normal development and function of the kidney glomerulus. *Dev Biol.* 2008;313:584–593.
549. Pozzi A, Jarad G, Moeckel GW, et al. Beta1 integrin expression by podocytes is required to maintain glomerular structural integrity. *Dev Biol.* 2008;316:288–301.
550. Kobayashi A, Kwan KM, Carroll TJ, et al. Distinct and sequential tissue-specific activities of the LIM-class homeobox gene Lim1 for tubular morphogenesis during kidney development. *Development.* 2005;132:2809–2823.
551. Ledig S, Brucker S, Barresi G, et al. Frame shift mutation of LHX1 is associated with Mayer-Rokitansky-Kuster-Hauser (MRKH) syndrome. *Hum Reprod.* 2012;27:2872–2875.
552. Kariminejad A, Stollfuss B, Li Y, et al. Severe Cenani-Lenz syndrome caused by loss of LRP4 function. *Am J Med Genet A.* 2013;161A:1475–1479.
553. Karner CM, Dietrich MF, Johnson EB, et al. Lrp4 regulates initiation of ureteric budding and is crucial for kidney formation—a mouse model for Cenani-Lenz syndrome. *PLoS ONE.* 2010;5:e10418.
554. Khan TN, Klar J, Ali Z, et al. Cenani-Lenz syndrome restricted to limb and kidney anomalies associated with a novel LRP4 missense mutation. *Eur J Med Genet.* 2013;56:371–374.
555. Li Y, Pawlik B, Elcioglu N, et al. LRP4 mutations alter Wnt/beta-catenin signaling and cause limb and kidney malformations in Cenani-Lenz syndrome. *Am J Hum Genet.* 2010;86:696–706.
556. Akchurin O, Du Z, Ramkellawan N, et al. Partitioning-defective 1a/b depletion impairs glomerular and proximal tubule development. *J Am Soc Nephrol.* 2016;27:3725–3737.
557. Narlis M, Grote D, Gaitan Y, et al. Pax2 and Pax8 regulate branching morphogenesis and nephron differentiation in the developing kidney. *J Am Soc Nephrol.* 2007;18:1121–1129.
558. Schnabel CA, Selleri L, Cleary ML. Pbx1 is essential for adrenal development and urogenital differentiation. *Genesis.* 2003;37:123–130.
559. Le Tanno P, Breton J, Bidart M, et al. PBX1 haploinsufficiency leads to syndromic congenital anomalies of the kidney and urinary tract (CAKUT) in humans. *J Med Genet.* 2017;54:502–510.
560. Heidet L, Moriniere V, Henry C, et al. Targeted exome sequencing identifies PBX1 as involved in monogenic congenital anomalies of the kidney and urinary tract. *J Am Soc Nephrol.* 2017;28:2901–2914.
561. Vlangos CN, Siuniak AN, Robinson D, et al. Next-generation sequencing identifies the Danforth's short tail mouse mutation as a retrotransposon insertion affecting Ptfla expression. *PLoS Genet.* 2013;9:e1003205.
562. Semba K, Araki K, Matsumoto K, et al. Ectopic expression of Ptfla induces spinal defects, urogenital defects, and anorectal malformations in Danforth's short tail mice. *PLoS Genet.* 2013;9:e1003204.
563. Mesrobian HG, Sulik KK. Characterization of the upper urinary tract anatomy in the Danforth spontaneous murine mutation. *J Urol.* 1992;148:752–755.
564. Sato A, Kishida S, Tanaka T, et al. Sall1, a causative gene for Townes-Brocks syndrome, enhances the canonical Wnt signaling by localizing to heterochromatin. *Biochem Biophys Res Commun.* 2004;319:103–113.
565. Reginensi A, Clarkson M, Neirijnck Y, et al. SOX9 controls epithelial branching by activating RET effector genes during kidney development. *Hum Mol Genet.* 2011;20:1143–1153.
566. Mathew S, Palamuttam RJ, Mernaugh G, et al. Talin regulates integrin beta1-dependent and -independent cell functions in ureteric bud development. *Development.* 2017;144:4148–4158.
567. Pietila I, Prunskaita-Hyyrylainen R, Kaisto S, et al. Wnt5a deficiency leads to anomalies in ureteric tree development, tubular epithelial cell organization and basement membrane integrity pointing to a role in kidney collecting duct patterning. *PLoS ONE.* 2016;11:e0147171.

37.e12 SECTION I – NORMAL STRUCTURE AND FUNCTION

568. Yun K, Ajima R, Sharma N, et al. Non-canonical Wnt5a/Ror2 signaling regulates kidney morphogenesis by controlling intermediate mesoderm extension. *Hum Mol Genet.* 2014;23:6807–6814.
569. Qi X, Okinaka Y, Nishita M, et al. Essential role of Wnt5a-Ror1/Ror2 signaling in metanephric mesenchyme and ureteric bud formation. *Genes Cells.* 2016;21:325–334.
570. Boerboom D, Lafond JF, Zheng X, et al. Partially redundant functions of Adamsl and Adams4 in the perinatal development of the renal medulla. *Dev Dyn.* 2011;240:1806–1814.
571. Naim E, Bernstein A, Bertram JF, et al. Mutagenesis of the epithelial polarity gene, discs large 1, perturbs nephrogenesis in the developing mouse kidney. *Kidney Int.* 2005;68:955–965.
572. Elias BC, Das A, Parekh DV, et al. Cdc42 regulates epithelial cell polarity and cytoskeletal function during kidney tubule development. *J Cell Sci.* 2015;128:4293–4305.
573. Kuure S, Cebrion C, Machingo Q, et al. Actin depolymerizing factors cofilin1 and destin are required for ureteric bud branching morphogenesis. *PLoS Genet.* 2010;6:e1001176.
574. Denner DR, Rauchman M. Mi-2/NuRD is required in renal progenitor cells during embryonic kidney development. *Dev Biol.* 2013;375:105–116.
575. Mao Y, Mulvaney J, Zakaria S, et al. Characterization of a Dchs1 mutant mouse reveals requirements for Dchs1-Fat4 signaling during mammalian development. *Development.* 2011;138:947–957.
576. Nagalakshmi VK, Ren Q, Pugh MM, et al. Dicer regulates the development of nephrogenic and ureteric compartments in the mammalian kidney. *Kidney Int.* 2011;79:317–330.
577. Chu JV, Sims-Lucas S, Bushnell DS, et al. Dicer function is required in the metanephric mesenchyme for early kidney development. *Am J Physiol Renal Physiol.* 2014;306:F764–F772.
578. Kobayashi H, Liu J, Urrutia AA, et al. Hypoxia-inducible factor prolyl-4-hydroxylation in FOXD1 lineage cells is essential for normal kidney development. *Kidney Int.* 2017;92:1370–1383.
579. Pepper MS. Literature watch. FOXC2 haploinsufficient mice are a model for human autosomal dominant lymphedema-distichiasis syndrome. *Lymphat Res Biol.* 2003;1:245–249.
580. Sims-Lucas S, Cullen-McEwen L, Eswarakumar VP, et al. Deletion of Frs2alpha from the ureteric epithelium causes renal hypoplasia. *Am J Physiol Renal Physiol.* 2009;297:F1208–F1219.
581. Ye X, Wang Y, Rattner A, et al. Genetic mosaic analysis reveals a major role for frizzled 4 and frizzled 8 in controlling ureteric growth in the developing kidney. *Development.* 2011;138:1161–1172.
582. Chen S, Yao X, Li Y, et al. Histone deacetylase 1 and 2 regulate Wnt and p53 pathways in the ureteric bud epithelium. *Development.* 2015;142:1180–1192.
583. Liu H, Chen S, Yao X, et al. Histone deacetylases 1 and 2 regulate the transcriptional programs of nephron progenitors and renal vesicles. *Development.* 2018;145.
584. Reginensi A, Enderle L, Gregorieff A, et al. A critical role for NF2 and the Hippo pathway in branching morphogenesis. *Nat Commun.* 2016;7:12309.
585. Kato S, Matsubara M, Matsuo T, et al. Leucine-rich repeat-containing G protein-coupled receptor-4 (LGR4, Gpr48) is essential for renal development in mice. *Nephron Exp Nephrol.* 2006;104:e63–e75.
586. Yi T, Weng J, Siwko S, et al. LGR4/GPR48 inactivation leads to aniridia-genitourinary anomalies-mental retardation syndrome defects. *J Biol Chem.* 2014;289:8767–8780.
587. Hilliard SA, Yao X, El-Dahr SS. Mdm2 is required for maintenance of the nephrogenic niche. *Dev Biol.* 2014;387:1–14.
588. Hilliard S, Aboudeneh K, Yao X, et al. Tight regulation of p53 activity by Mdm2 is required for ureteric bud growth and branching. *Dev Biol.* 2011;353:354–366.
589. Kume T, Deng K, Hogan BL. Minimal phenotype of mice homozygous for a null mutation in the forkhead/winged helix gene, Mf2. *Mol Cell Biol.* 2000;20:1419–1425.
590. Phelep A, Laouari D, Bharti K, et al. MITF-A controls branching morphogenesis and nephron endowment. *PLoS Genet.* 2017;13:e1007093.
591. Peralta N, Jakobson M, Ola R, et al. Sema4C-Plexin B2 signalling modulates ureteric branching in developing kidney. *Differentiation.* 2011;81:81–91.
592. Song R, Preston G, Ichihara A, et al. Deletion of the prorenin receptor from the ureteric bud causes renal hypodysplasia. *PLoS ONE.* 2013;8:e63835.
593. Song R, Preston G, Kidd L, et al. Prorenin receptor is critical for nephron progenitors. *Dev Biol.* 2016;409:382–391.
594. Wang P, Pereira FA, Beasley D, et al. Presenilins are required for the formation of comma- and S-shaped bodies during nephrogenesis. *Development.* 2003;130:5019–5029.
595. Norwood VF, Morham SG, Smithies O. Postnatal development and progression of renal dysplasia in cyclooxygenase-2 null mice. *Kidney Int.* 2000;58:2291–2300.
596. Bonegio RG, Beck LH, Kahlon RK, et al. The fate of Notch-deficient nephrogenic progenitor cells during metanephric kidney development. *Kidney Int.* 2011;79:1099–1112.
597. Cheng HT, Kim M, Valerius MT, et al. Notch2, but not Notch1, is required for proximal fate acquisition in the mammalian nephron. *Development.* 2007;134:801–811.
598. Moser M, Pscherer A, Roth C, et al. Enhanced apoptotic cell death of renal epithelial cells in mice lacking transcription factor AP-2beta. *Genes Dev.* 1997;11:1938–1948.
599. Li Y, Liu J, Li W, et al. p53 enables metabolic fitness and self-renewal of nephron progenitor cells. *Development.* 2015;142:1228–1241.
600. Gui T, Sun Y, Gai Z, et al. The loss of Trps1 suppresses ureteric bud branching because of the activation of TGF-beta signaling. *Dev Biol.* 2013;377:415–427.
601. Chi L, Saarela U, Railo A, et al. A secreted BMP antagonist, Cer1, fine tunes the spatial organization of the ureteric bud tree during mouse kidney development. *PLoS ONE.* 2011;6:e27676.
602. Paces-Fessy M, Fabre M, Lesaulnier C, et al. Hnf1b and Pax2 cooperate to control different pathways in kidney and ureter morphogenesis. *Hum Mol Genet.* 2012;21:3143–3155.
603. Desai PB, San Agustin JT, Stuck MW, et al. Ift25 is not a cystic kidney disease gene but is required for early steps of kidney development. *Mech Dev.* 2018.
604. Peng Y, Clark C, Luong R, et al. The leucine zipper putative tumor suppressor 2 protein LZTS2 regulates kidney development. *J Biol Chem.* 2011;286:40331–40342.
605. Korostylev A, Worzfeld T, Deng S, et al. A functional role for semaphorin 4D/plexin B1 interactions in epithelial branching morphogenesis during organogenesis. *Development.* 2008;135:3333–3343.
606. Nishita M, Qiao S, Miyamoto M, et al. Role of Wnt5a-Ror2 signaling in morphogenesis of the metanephric mesenchyme during ureteric budding. *Mol Cell Biol.* 2014;34:3096–3105.
607. Morishita Y, Matsuzaki T, Hara-chikuma M, et al. Disruption of aquaporin-11 produces polycystic kidneys following vacuolization of the proximal tubule. *Mol Cell Biol.* 2005;25:7770–7779.
608. Veis DJ, Sorenson CM, Shutter JR, et al. Bcl-2-deficient mice demonstrate fulminant lymphoid apoptosis, polycystic kidneys, and hypopigmented hair. *Cell.* 1993;75:229–240.
609. Tran U, Zakin L, Schweickert A, et al. The RNA-binding protein bicaudal C regulates polycystin 2 in the kidney by antagonizing miR-17 activity. *Development.* 2010;137:1107–1116.
610. Cook SA, Collin GB, Bronson RT, et al. A mouse model for Meckel syndrome type 3. *J Am Soc Nephrol.* 2009;20:753–764.
611. Veikkolainen V, Naillat F, Railo A, et al. ErbB4 modulates tubular cell polarity and lumen diameter during kidney development. *J Am Soc Nephrol.* 2012;23:112–122.
612. Cappello S, Gray MJ, Badouel C, et al. Mutations in genes encoding the cadherin receptor-ligand pair DCHS1 and FAT4 disrupt cerebral cortical development. *Nat Genet.* 2013;45:1300–1308.
613. Kang HS, Beak JY, Kim YS, et al. Glis3 is associated with primary cilia and Wt1/TAZ and implicated in polycystic kidney disease. *Mol Cell Biol.* 2009;29:2556–2569.
614. Senee V, Chelala C, Duchatelet S, et al. Mutations in GLIS3 are responsible for a rare syndrome with neonatal diabetes mellitus and congenital hypothyroidism. *Nat Genet.* 2006;38:682–687.
615. Cano-Gauci DF, Song HH, Yang H, et al. Glycan-3-deficient mice exhibit developmental overgrowth and some of the abnormalities typical of Simpson-Golabi-Behmel syndrome. *J Cell Biol.* 1999;146:255–264.
616. Grisaru S, Rosenblum ND. Glycans and the biology of renal malformations. *Pediatr Nephrol.* 2001;16:302–306.
617. Grisaru S, Cano-Gauci D, Tee J, et al. Glycan-3 modulates BMP- and FGF-mediated effects during renal branching morphogenesis. *Dev Biol.* 2001;231:31–46.
618. Murcia NS, Richards WG, Yoder BK, et al. The Oak Ridge Polycystic Kidney (orpk) disease gene is required for left-right axis determination. *Development.* 2000;127:2347–2355.
619. Moyer JH, Lee-Tischler MJ, Kwon HY, et al. Candidate gene associated with a mutation causing recessive polycystic kidney disease in mice. *Science.* 1994;264:1329–1333.

620. Gong X, Guo X, Huang R, et al. Expression of ILK in renal stroma is essential for multiple aspects of renal development. *Am J Physiol Renal Physiol*. 2018.
621. Mochizuki T, Tsuchiya K, Yokoyama T. Molecular cloning of a gene for inversion of embryo turning (inv) with cystic kidney. *Nephrol Dial Transplant*. 2002;17(suppl 9):68–70.
622. Mochizuki T, Saijoh Y, Tsuchiya K, et al. Cloning of inv, a gene that controls left/right asymmetry and kidney development. *Nature*. 1998;395:177–181.
623. Lin F, Hiesberger T, Cordes K, et al. Kidney-specific inactivation of the KIF3A subunit of kinesin-II inhibits renal ciliogenesis and produces polycystic kidney disease. *Proc Natl Acad Sci U S A*. 2003;100:5286–5291.
624. Moriguchi T, Hamada M, Morito N, et al. MafB is essential for renal development and F4/80 expression in macrophages. *Mol Cell Biol*. 2006;26:5715–5727.
625. Wang PW, Eisenbart JD, Cordes SP, et al. Human KRML (MAFB): cDNA cloning, genomic structure, and evaluation as a candidate tumor suppressor gene in myeloid leukemias. *Genomics*. 1999;59:275–281.
626. Kyttala M, Tallila J, Salonen R, et al. MKS1, encoding a component of the flagellar apparatus basal body proteome, is mutated in Meckel syndrome. *Nat Genet*. 2006;38:155–157.
627. Lu W, Peissel B, Babakhanloo H, et al. Perinatal lethality with kidney and pancreas defects in mice with a targeted Pkd1 mutation. *Nat Genet*. 1997;17:179–181.
628. Hossain Z, Ali SM, Ko HL, et al. Glomerulocystic kidney disease in mice with a targeted inactivation of Wwtr1. *Proc Natl Acad Sci U S A*. 2007;104:1631–1636.
629. Makita R, Uchijima Y, Nishiyama K, et al. Multiple renal cysts, urinary concentration defects, and pulmonary emphysematous changes in mice lacking TAZ. *Am J Physiol Renal Physiol*. 2008;294:F542–F553.
630. Rankin EB, Tomaszewski JE, Haase VH. Renal cyst development in mice with conditional inactivation of the von Hippel-Lindau tumor suppressor. *Cancer Res*. 2006;66:2576–2583.
631. Condac E, Silasi-Mansat R, Kosanke S, et al. Polycystic disease caused by deficiency in xylosyltransferase 2, an initiating enzyme of glycosaminoglycan biosynthesis. *Proc Natl Acad Sci U S A*. 2007;104:9416–9421.
632. Rasouly HM, Kumar S, Chan S, et al. Loss of Zeb2 in mesenchyme-derived nephrons causes primary glomerulocystic disease. *Kidney Int*. 2016;90:1262–1273.
633. Oliverio MI, Madsen K, Best CF, et al. Renal growth and development in mice lacking AT1A receptors for angiotensin II. *Am J Physiol*. 1998;274:F43–F50.
634. Toyama K, Morisaki H, Cheng J, et al. Proteinuria in AMPD2-deficient mice. *Genes Cells*. 2012;17:28–38.
635. Auguste D, Maier M, Baldwin C, et al. Disease-causing mutations of RhoGDIalpha induce Rac1 hyperactivation in podocytes. *Small GTPases*. 2016;7:107–121.
636. Sachs N, Kreft M, van den Bergh Weerman MA, et al. Kidney failure in mice lacking the tetraspanin CD151. *J Cell Biol*. 2006;175:33–39.
637. Karamatic Crew V, Burton N, Kagan A, et al. CD151, the first member of the tetraspanin (TM4) superfamily detected on erythrocytes, is essential for the correct assembly of human basement membranes in kidney and skin. *Blood*. 2004;104:2217–2223.
638. Weinhold B, Sellmeier M, Schaper W, et al. Deficits in sialylation impair podocyte maturation. *J Am Soc Nephrol*. 2012;23:1319–1328.
639. Miner JH, Sanes JR. Molecular and functional defects in kidneys of mice lacking collagen alpha 3(IV): implications for Alport syndrome. *J Cell Biol*. 1996;135:1403–1413.
640. Cosgrove D, Meehan DT, Grunkemeyer JA, et al. Collagen COL4A3 knockout: a mouse model for autosomal Alport syndrome. *Genes Dev*. 1996;10:2981–2992.
641. Lu W, Phillips CL, Killen PD, et al. Insertional mutation of the collagen genes Col4a3 and Col4a4 in a mouse model of Alport syndrome. *Genomics*. 1999;61:113–124.
642. Rheault MN, Kren SM, Thielken BK, et al. Mouse model of X-linked Alport syndrome. *J Am Soc Nephrol*. 2004;15:1466–1474.
643. Park E, Ahn YH, Kang HG, et al. COQ6 mutations in children with steroid-resistant focal segmental glomerulosclerosis and sensorineural hearing loss. *Am J Kidney Dis*. 2017;70:139–144.
644. Ebarasi L, Ashraf S, Bierzynska A, et al. Defects of CRB2 cause steroid-resistant nephrotic syndrome. *Am J Hum Genet*. 2015;96:153–161.
645. George B, Fan Q, Dlugos CP, et al. Crk1/2 and CrkL form a hetero-oligomer and functionally complement each other during podocyte morphogenesis. *Kidney Int*. 2014;85:1382–1394.
646. Tachibana K, Hirota S, Iizasa H, et al. The chemokine receptor CXCR4 is essential for vascularization of the gastrointestinal tract. *Nature*. 1998;393:591–594.
647. Soda K, Balkin DM, Ferguson SM, et al. Role of dynamin, synaptosomal-associated protein 25, and endophilin in podocyte foot processes. *J Clin Invest*. 2012;122:4401–4411.
648. Fukusumi Y, Zhang Y, Yamagishi R, et al. Nephrin-binding Ephrin-B1 at the slit diaphragm controls podocyte function through the JNK pathway. *J Am Soc Nephrol*. 2018;29:1462–1474.
649. Gee HY, Sadowski CE, Aggarwal PK, et al. FAT1 mutations cause a glomerulotubular nephropathy. *Nat Commun*. 2016;7:10822.
650. Sun Y, Guo C, Ma P, et al. Kindlin-2 association with Rho GDP-dissociation inhibitor α suppresses Rac1 activation and podocyte injury. *J Am Soc Nephrol*. 2017;28:3545–3562.
651. Motojima M, Kume T, Matsusaka T. Foxc1 and Foxc2 are necessary to maintain glomerular podocytes. *Exp Cell Res*. 2017;352:265–272.
652. Motojima M, Tanimoto S, Ohtsuka M, et al. Characterization of kidney and skeleton phenotypes of mice double heterozygous for Foxc1 and Foxc2. *Cells Tissues Organs*. 2016;201:380–389.
653. Yu CC, Yen TS, Lowell CA, et al. Lupus-like kidney disease in mice deficient in the Src family tyrosine kinases Lyn and Fyn. *Curr Biol*. 2001;11:34–38.
654. Moriguchi T, Yu L, Otsuki A, et al. Gata3 hypomorphic mutant mice rescued with a yeast artificial chromosome transgene suffer a glomerular mesangial cell defect. *Mol Cell Biol*. 2016;36:2272–2281.
655. Lachmann P, Hickmann L, Steglich A, et al. Interference with Gsalpha-Coupled receptor signaling in renin-producing cells leads to renal endothelial damage. *J Am Soc Nephrol*. 2017;28:3479–3489.
656. Chen L, Kim SM, Oppermann M, et al. Regulation of renin in mice with Cre recombinase-mediated deletion of G protein Gsalpha in juxtaglomerular cells. *Am J Physiol Renal Physiol*. 2007;292:F27–F37.
657. Wharram BL, Goyal M, Gillespie PJ, et al. Altered podocyte structure in GLEPP1 (Ptpro)-deficient mice associated with hypertension and low glomerular filtration rate. *J Clin Invest*. 2000;106:1281–1290.
658. Welsh GI, Hale IJ, Eremina V, et al. Insulin signaling to the glomerular podocyte is critical for normal kidney function. *Cell Metab*. 2010;12:329–340.
659. Viquez OM, Yazlovitskaya EM, Tu T, et al. Integrin alpha6 maintains the structural integrity of the kidney collecting system. *Matrix Biol*. 2017;57–58:244–257.
660. Jarad G, Cunningham J, Shaw AS, et al. Proteinuria precedes podocyte abnormalities in Lamb2^{-/-} mice, implicating the glomerular basement membrane as an albumin barrier. *J Clin Invest*. 2006;116:2272–2279.
661. Burghardt T, Kastner J, Suleiman H, et al. LMX1B is essential for the maintenance of differentiated podocytes in adult kidneys. *J Am Soc Nephrol*. 2013;24:1830–1848.
662. Rohr C, Prestel J, Heidet L, et al. The LIM-homeodomain transcription factor Lmx1b plays a crucial role in podocytes. *J Clin Invest*. 2002;109:1073–1082.
663. Miner JH, Morello R, Andrews KL, et al. Transcriptional induction of slit diaphragm genes by Lmx1b is required in podocyte differentiation. *J Clin Invest*. 2002;109:1065–1072.
664. Bierzynska A, Soderquest K, Dean P, et al. MAGI2 mutations cause congenital nephrotic syndrome. *J Am Soc Nephrol*. 2017;28:1614–1621.
665. Balbas MD, Burgess MR, Murali R, et al. MAGI-2 scaffold protein is critical for kidney barrier function. *Proc Natl Acad Sci U S A*. 2014;111:14876–14881.
666. Ihara K, Asanuma K, Fukuda T, et al. MAGI-2 is critical for the formation and maintenance of the glomerular filtration barrier in mouse kidney. *Am J Pathol*. 2014;184:2699–2708.
667. Weide T, Vollenbroker B, Schulze U, et al. Palsl haploinsufficiency results in proteinuria and cyst formation. *J Am Soc Nephrol*. 2017;28:2093–2107.
668. Weiher H, Noda T, Gray DA, et al. Transgenic mouse model of kidney disease: insertional inactivation of ubiquitously expressed gene leads to nephrotic syndrome. *Cell*. 1990;62:425–434.
669. Cina DP, Onay T, Paltoo A, et al. Inhibition of MTOR disrupts autophagic flux in podocytes. *J Am Soc Nephrol*. 2012;23:412–420.
670. Sanna-Cherchi S, Burgess KE, Nees SN, et al. Exome sequencing identified MYO1E and NEIL1 as candidate genes for human autosomal recessive steroid-resistant nephrotic syndrome. *Kidney Int*. 2011;80:389–396.
671. Mele C, Iatropoulos P, Donadelli R, et al. MYO1E mutations and childhood familial focal segmental glomerulosclerosis. *N Engl J Med*. 2011;365:295–306.

37.e14 SECTION I – NORMAL STRUCTURE AND FUNCTION

672. Lebel SP, Chen Y, Gingras D, et al. Morphofunctional studies of the glomerular wall in mice lacking entactin-1. *J Histochem Cytochem*. 2003;51:1467–1478.
673. Surendran K, Boyle S, Barak H, et al. The contribution of Notch1 to nephron segmentation in the developing kidney is revealed in a sensitized Notch2 background and can be augmented by reducing Mint dosage. *Dev Biol*. 2009.
674. Roselli S, Heidet L, Sich M, et al. Early glomerular filtration defect and severe renal disease in podocin-deficient mice. *Mol Cell Biol*. 2004;24:550–560.
675. Zimmerman SE, Hiremath C, Tsunezumi J, et al. Nephronectin regulates mesangial cell adhesion and behavior in glomeruli. *J Am Soc Nephrol*. 2018;29:1128–1140.
676. Bechtel W, Helmstädter M, Balica J, et al. The class III phosphatidylinositol 3-kinase PIK3C3/VPS34 regulates endocytosis and autophagosome-autolysosome formation in podocytes. *Autophagy*. 2013;9.
677. Bechtel W, Helmstädter M, Balica J, et al. Vps34 deficiency reveals the importance of endocytosis for podocyte homeostasis. *J Am Soc Nephrol*. 2013;24:727–743.
678. Doyonnas R, Kershaw DB, Duhme C, et al. Anuria, omphalocele, and perinatal lethality in mice lacking the CD34-related protein podocalyxin. *J Exp Med*. 2001;194:13–27.
679. Kang HG, Lee M, Lee KB, et al. Loss of podocalyxin causes a novel syndromic type of congenital nephrotic syndrome. *Exp Mol Med*. 2017;49:e414.
680. Ozaltin F, Ibsirlioglu T, Taskiran EZ, et al. Disruption of PTPRO causes childhood-onset nephrotic syndrome. *Am J Hum Genet*. 2011;89:139–147.
681. Giardino L, Armelloni S, Corbelli A, et al. Podocyte glutamatergic signaling contributes to the function of the glomerular filtration barrier. *J Am Soc Nephrol*. 2009;20:1929–1940.
682. Fan X, Li Q, Pisarek-Horowitz A, et al. Inhibitory effects of Robo2 on nephrin: a crosstalk between positive and negative signals regulating podocyte structure. *Cell Rep*. 2012;2:52–61.
683. Ly JP, Onay T, Sison K, et al. The Sweet Pee model for Sglt2 mutation. *J Am Soc Nephrol*. 2011;22:113–123.
684. Takahashi S, Tomioka M, Hiromura K, et al. SIRPalpha signaling regulates podocyte structure and function. *Am J Physiol Renal Physiol*. 2013;305:F861–F870.
685. Huang J, Arsenault M, Kann M, et al. The transcription factor Sry-related HMG box-4 (SOX4) is required for normal renal development in vivo. *Dev Dyn*. 2013;242:790–799.
686. Fukusumi Y, Wakamatsu A, Takashima N, et al. SV2B is essential for the integrity of the glomerular filtration barrier. *Lab Invest*. 2015;95:534–545.
687. Itoh M, Nakadate K, Horibata Y, et al. The structural and functional organization of the podocyte filtration slits is regulated by Tjp1/ZO-1. *PLoS ONE*. 2014;9:e106621.
688. Gigante M, Caridi G, Montemurno E, et al. TRPC6 mutations in children with steroid-resistant nephrotic syndrome and atypical phenotype. *Clin J Am Soc Nephrol*. 2011;6:1626–1634.
689. Krall P, Canales CP, Kairath P, et al. Podocyte-specific overexpression of wild type or mutant trpc6 in mice is sufficient to cause glomerular disease. *PLoS ONE*. 2010;5:e12859.
690. Eckel J, Lavin PJ, Finch EA, et al. TRPC6 enhances angiotensin II-induced albuminuria. *J Am Soc Nephrol*. 2011;22:526–535.
691. Kistler AD, Singh G, Altintas MM, et al. Transient receptor potential channel 6 (TRPC6) protects podocytes during complement-mediated glomerular disease. *J Biol Chem*. 2013;288:36598–36609.
692. Eremina V, Jefferson JA, Kowalewska J, et al. VEGF inhibition and renal thrombotic microangiopathy. *N Engl J Med*. 2008;358:1129–1136.
693. Schell C, Baumhakl L, Salou S, et al. N-wasp is required for stabilization of podocyte foot processes. *J Am Soc Nephrol*. 2013;24:713–721.
694. Roker LA, Nemri K, Yu J. Wnt7b signaling from the ureteric bud epithelium regulates medullary capillary development. *J Am Soc Nephrol*. 2017;28:259.
695. Nagy II, Xu Q, Naillat F, et al. Impairment of Wnt11 function leads to kidney tubular abnormalities and secondary glomerular cystogenesis. *BMC Dev Biol*. 2016;16:30.
696. Naray-Fejes-Toth A, Fejes-Toth G. Novel mouse strain with Cre recombinase in 11beta-hydroxysteroid dehydrogenase-2-expressing cells. *Am J Physiol Renal Physiol*. 2007;292:F486–F494.
697. Nelson RD, Stricklett P, Gustafson C, et al. Expression of an AQP2 Cre recombinase transgene in kidney and male reproductive system of transgenic mice. *Am J Physiol*. 1998;275:C216–C226.
698. Raphael KL, Strait KA, Stricklett PK, et al. Inactivation of Pkd1 in principal cells causes a more severe cystic kidney disease than in intercalated cells. *Kidney Int*. 2009;75:626–633.
699. Miller RL, Lucero OM, Riemondy KA, et al. The V-ATPase B1-subunit promoter drives expression of Cre recombinase in intercalated cells of the kidney. *Kidney Int*. 2009;75:435–439.
700. Oxburgh L, Chu GC, Michael SK, et al. TGFbeta superfamily signals are required for morphogenesis of the kidney mesenchyme progenitor population. *Development*. 2004;131:4593–4605.
701. Shao X, Johnson JE, Richardson JA, et al. A minimal Ksp-cadherin promoter linked to a green fluorescent protein reporter gene exhibits tissue-specific expression in the developing kidney and genitourinary tract. *J Am Soc Nephrol*. 2002;13:1824–1836.
702. Shao X, Somlo S, Igarashi P. Epithelial-specific Cre/lox recombination in the developing kidney and genitourinary tract. *J Am Soc Nephrol*. 2002;13:1837–1846.
703. Boyle S, Misfeldt A, Chandler KJ, et al. Fate mapping using Cited1-CreERT2 mice demonstrates that the cap mesenchyme contains self-renewing progenitor cells and gives rise exclusively to nephronic epithelia. *Dev Biol*. 2008;313:234–245.
704. Gorski JA, Talley T, Qiu M, et al. Cortical excitatory neurons and glia, but not GABAergic neurons, are produced in the Emx1-expressing lineage. *J Neurosci*. 2002;22:6309–6314.
705. Humphreys BD, Lin SL, Kobayashi A, et al. Fate tracing reveals the pericyte and not epithelial origin of myofibroblasts in kidney fibrosis. *Am J Pathol*. 2010;176:85–97.
706. Cebran C, Asai N, D'Agati V, et al. The number of fetal nephron progenitor cells limits ureteric branching and adult nephron endowment. *Cell Rep*. 2014;7:127–137.
707. Sepulveda AR, Huang SL, Lebovitz RM, et al. A 346-base pair region of the mouse gamma-glutamyl transpeptidase type II promoter contains sufficient cis-acting elements for kidney-restricted expression in transgenic mice. *J Biol Chem*. 1997;272:11959–11967.
708. Lowe LA, Yamada S, Kuehn MR, HoxB6-Cre transgenic mice express Cre recombinase in extra-embryonic mesoderm, in lateral plate and limb mesoderm and at the midbrain/hindbrain junction. *Genesis*. 2000;26:118–120.
709. Lavoie JL, Lake-Bruse KD, Sigmund CD. Increased blood pressure in transgenic mice expressing both human renin and angiotensinogen in the renal proximal tubule. *Am J Physiol Renal Physiol*. 2004;286:F965–F971.
710. Li H, Zhou X, Davis DR, et al. An androgen-inducible proximal tubule-specific Cre recombinase transgenic model. *Am J Physiol Renal Physiol*. 2008;294:F1481–F1486.
711. Moeller MJ, Kovari IA, Holzman LB. Evaluation of a new tool for exploring podocyte biology: mouse Nphs1 5' flanking region drives LacZ expression in podocytes. *J Am Soc Nephrol*. 2000;11:2306–2314.
712. Wong MA, Cui S, Quaggin SE. Identification and characterization of a glomerular-specific promoter from the human nephrin gene. *Am J Physiol Renal Physiol*. 2000;279:F1027–F1032.
713. Moeller MJ, Sanden SK, Soofi A, et al. Two gene fragments that direct podocyte-specific expression in transgenic mice. *J Am Soc Nephrol*. 2002;13:1561–1567.
714. Grieshammer U, Agarwal P, Martin GR. A Cre transgene active in developing endodermal organs, heart, limb, and extra-ocular muscle. *Genesis*. 2008;46:69–73.
715. Mugford JW, Sipila P, Kobayashi A, et al. Hoxd11 specifies a program of metanephric kidney development within the intermediate mesoderm of the mouse embryo. *Dev Biol*. 2008;319:396–405.
716. Lan Y, Wang Q, Ovitt CE, et al. A unique mouse strain expressing Cre recombinase for tissue-specific analysis of gene function in palate and kidney development. *Genesis*. 2007;45:618–624.
717. Ohyama T, Groves AK. Generation of Pax2-Cre mice by modification of a Pax2 bacterial artificial chromosome. *Genesis*. 2004;38:195–199.
718. Engleka KA, Gitler AD, Zhang M, et al. Insertion of Cre into the Pax3 locus creates a new allele of Splotch and identifies unexpected Pax3 derivatives. *Dev Biol*. 2005;280:396–406.
719. Li J, Chen F, Epstein JA. Neural crest expression of Cre recombinase directed by the proximal Pax3 promoter in transgenic mice. *Genesis*. 2000;26:162–164.
720. Traykova-Brauch M, Schonig K, Greiner O, et al. An efficient and versatile system for acute and chronic modulation of renal tubular function in transgenic mice. *Nat Med*. 2008;14:979–984.
721. Espana-Agusti J, Zou X, Wong K, et al. Generation and characterisation of a Pax8-CreERT2 transgenic line and a Slc22a6-CreERT2

- knock-in line for inducible and specific genetic manipulation of renal tubular epithelial cells. *PLoS ONE*. 2016;11:e0148055.
722. Claxton S, Kostourou V, Jadeja S, et al. Efficient, inducible Cre-recombinase activation in vascular endothelium. *Genesis*. 2008;46:74–80.
723. Lakhe-Reddy S, Li V, Arnold TD, et al. Mesangial cell $\alpha v\beta 3$ -integrin regulates glomerular capillary integrity and repair. *Am J Physiol Renal Physiol*. 2014;306:F1400–F1409.
724. Truman LA, Bentley KL, Smith EC, et al. ProxTom lymphatic vessel reporter mice reveal Prox1 expression in the adrenal medulla, megakaryocytes, and platelets. *Am J Pathol*. 2012;180:1715–1725.
725. Srinivasan RS, Dillard ME, Lagutin OV, et al. Lineage tracing demonstrates the venous origin of the mammalian lymphatic vasculature. *Genes Dev*. 2007;21:2422–2432.
726. Srinivasan RS, Geng X, Yang Y, et al. The nuclear hormone receptor Coup-TFII is required for the initiation and early maintenance of Prox1 expression in lymphatic endothelial cells. *Genes Dev*. 2010;24:696–707.
727. Luo W, Enomoto H, Rice FL, et al. Molecular identification of rapidly adapting mechanoreceptors and their developmental dependence on ret signaling. *Neuron*. 2009;64:841–856.
728. Inoue S, Inoue M, Fujimura S, et al. A mouse line expressing Sall1-driven inducible Cre recombinase in the kidney mesenchyme. *Genesis*. 2010;48:207–212.
729. Rubera I, Poujeol C, Bertin G, et al. Specific cre/lox recombination in the mouse proximal tubule. *J Am Soc Nephrol*. 2004;15:2050–2056.
730. Kartopawiro J, Bower NI, Karnezis T, et al. Arap3 is dysregulated in a mouse model of hypotrichosis-lymphedema-telangiectasia and regulates lymphatic vascular development. *Hum Mol Genet*. 2014;23:1286–1297.
731. Davies JA, Little MH, Aronow B, et al. Access and use of the GUDMAP database of genitourinary development. *Methods Mol Biol*. 2012;886:185–201.
732. Harding SD, Armit C, Armstrong J, et al. The GUDMAP database—an online resource for genitourinary research. *Development*. 2011;138:2845–2853.
733. Sakata K, Ohmura M, Araki K, et al. Generation and analysis of serine protease inhibitor kazal type 3-cre driver mice. *Exp Anim*. 2014;63:45–53.
734. Wang Y, Tripathi P, Guo Q, et al. Cre/lox recombination in the lower urinary tract. *Genesis*. 2009;47:409–413.
735. Kisanuki YY, Hammer RE, Miyazaki J, et al. Tie2-Cre transgenic mice: a new model for endothelial cell-lineage analysis in vivo. *Dev Biol*. 2001;230:230–242.
736. Koni PA, Joshi SK, Temann UA, et al. Conditional vascular cell adhesion molecule 1 deletion in mice: impaired lymphocyte migration to bone marrow. *J Exp Med*. 2001;193:741–754.
737. Braren R, Hu H, Kim YH, et al. Endothelial FAK is essential for vascular network stability, cell survival, and lamellipodial formation. *J Cell Biol*. 2006;172:151–162.
738. Gustafsson E, Brakebusch C, Hietanen K, et al. Tie-1-directed expression of Cre recombinase in endothelial cells of embryoid bodies and transgenic mice. *J Cell Sci*. 2001;114:671–676.
739. Zhu X, Cheng J, Gao J, et al. Isolation of mouse THP gene promoter and demonstration of its kidney-specific activity in transgenic mice. *Am J Physiol Renal Physiol*. 2002;282:F608–F617.
740. Shan J, Jokela T, Peltoketo H, et al. Generation of an allele to inactivate Wnt4 gene function conditionally in the mouse. *Genesis*. 2009;47:782–788.
741. Barak H, Boyle SC. Organ culture and immunostaining of mouse embryonic kidneys. *Cold Spring Harb Protoc*. 2011;2011:pdb prot5558.

BOARD REVIEW QUESTIONS

1. Which of the following class of drugs is not recommended for antihypertensive treatment during pregnancy and why? Which aspect of renal development is prominently affected by these contraindicated medications?

- a. Adrenergic blockers
- b. Calcium channel blockers
- c. ACE inhibitors and angiotensin receptor blockers (ARBs)

Answer: c

Rationale: ACE inhibitors/ARBs are teratogens, causing multiorgan congenital malformations (not limited to the genitourinary tract) and fetal death. Angiotensin is important in the normal development of collecting ducts, and its inhibition causes atrophy of the renal papillae and pelvis.

2. Fetal vitamin A status is proposed as a factor contributing to variability of kidney size and nephron endowment across populations. Which of the following is not true about the effect of vitamin A on renal development?

- a. Vitamin A modulates the pattern of ureteric branching
- b. Vitamin A regulates epithelial transformation of the metanephric mesenchyme
- c. Vitamin A promotes the conversion of the interstitial stroma into nephrons
- d. Vitamin A deficiency can cause paucity in nephrons (oligonephronia)

Answer: c

Rationale: Vitamin A is required for the patterned branching of the ureteric bud (UB) and the epithelialization of the

metanephric mesenchyme (MM) into nephrons. Defective renal branching and nephrogenesis due to vitamin A deficiency can contribute to asymptomatic renal hypoplasia. The interstitial stroma is important for both the synthesis of renal retinoic acid (active vitamin A) and express vitamin A receptors, allowing the stroma to signal to both the UB and the MM to induce their differentiation. The stromal cells are distinct from the precursors of nephrons.

3. A patient presenting with recurring urinary tract infection was shown to have duplex kidneys by radiography. Which developmental anomaly is less likely to be the cause?

- a. Expanded zone of glial cell-derived neurotrophic factor (GDNF) expression in the metanephric mesenchyme
- b. Cystic dilatation of renal tubules
- c. Ureteric bud inappropriately induced
- d. Misexpression of Ret receptor along the wolffian duct

Answer: b

Rationale: The collecting ducts, the renal calyces, and the ureter are all derivatives of the ureteric bud (UB). The UB is normally induced on a single site on each wolffian duct. Inappropriate emergence of the UB along the wolffian duct, either through abnormal expansion of GDNF expression in the presumptive metanephric mesenchyme or the misplaced expression of Ret along the wolffian duct, can lead to ectopic UBs and duplicated collecting duct systems with attendant errors in ureter-bladder connections, thus causing urinary obstruction and reflux.

Anatomy of the Kidney

Jill W. Verlander | William L. Clapp

CHAPTER OUTLINE

| | |
|-------------------------------------|----------------------------------|
| GROSS FEATURES, 38 | COLLECTING DUCT, 65 |
| THE NEPHRON, 39 | PAPILLARY SURFACE EPITHELIUM, 73 |
| JUXTAGLOMERULAR APPARATUS, 50 | INTERSTITIUM, 73 |
| PROXIMAL TUBULE, 52 | LYMPHATICS, 75 |
| THIN LIMBS OF THE LOOP OF HENLE, 57 | INNERVATION, 77 |
| DISTAL TUBULE, 59 | |

The structure of the kidney, including the ultrastructure of individual cell types, their axial distribution, and arrangement within the kidney, is essential to normal renal function. In this chapter, we describe normal mammalian renal structure, including gross anatomy, histology, and ultrastructure.

GROSS FEATURES

Normal mammalian kidneys are paired and retroperitoneal. In the human, the kidneys are located approximately between the twelfth thoracic and third lumbar vertebrae on opposite sides of the vertebral column. The right kidney is usually slightly more caudal in position than the left. Each kidney normally weighs between 125 to 170 g in adult males and 115 to 155 g in adult females, and measures approximately 11 to 12 cm long, 5.0 to 7.5 cm wide, and 2.5 to 3.0 cm thick. By magnetic resonance imaging, the mean kidney lengths are 12.4 ± 0.9 cm for men and 11.6 ± 1.1 cm for women, and the mean kidney volumes are 202 ± 36 mL for men and 154 ± 33 mL for women.¹ Located on the medial or concave surface of each kidney is the hilum, an indentation where the renal pelvis, the renal artery and vein, the lymphatics, and a nerve plexus pass into the sinus of the kidney. A thin tough fibrous capsule covers the surface of the kidney.

In humans and most mammals, each kidney is normally supplied by a single renal artery, although one or more accessory renal arteries may be present. The renal artery enters the hilum and usually divides into an anterior and a posterior branch. Three segmental or lobar arteries arise from the anterior branch and supply the upper, middle, and lower thirds of the anterior surface of the kidney (Fig. 2.1). The posterior branch supplies more than half of the posterior surface and occasionally gives rise to a small apical segmental branch. However, the apical segmental or lobar branch arises most commonly from the anterior division. No collateral circulation exists between individual segmental or lobar arteries or their subdivisions. The kidneys often receive aberrant arteries from the superior mesenteric, suprarenal,

testicular, or ovarian arteries. True accessory arteries that arise from the abdominal aorta usually supply the lower pole of the kidney. The arterial and venous circulations in the kidney are described in detail in Chapter 3.

On the cut surface of a bisected human kidney, two main regions are visible, a granular outer region, the cortex, and a striated inner region, the medulla (Fig. 2.2). In humans, the medulla is composed of renal pyramids, conical tissue masses with the base of each pyramid at the corticomedullary boundary, and the apex extending toward the renal pelvis, forming a papilla. On the tip of each papilla is the area cribrosa (Fig. 2.3), where the distal ends of collecting ducts (ducts of Bellini) open into the renal pelvis. A single renal pyramid and its surrounding cortex comprise a renal lobe. In contrast to the human kidney, the kidney of the rat and many other laboratory animals has a single renal pyramid with its overlying cortex and is therefore termed “unipapillary.” Otherwise, these kidneys resemble the human kidney in their gross appearance. In humans, the renal cortex is about 1 cm in thickness, forms a cap over the base of each renal pyramid, and extends downward between the individual pyramids to form the columns of Bertin (see Figs. 2.2 and 2.4). From the base of the renal pyramid, at the corticomedullary junction, the “medullary rays” extend into the cortex. The medullary rays are formed by the cortical collecting ducts, the straight segments of the proximal tubules, and the cortical thick ascending limbs (TALs) of loop of Henle, aligned together. These straight segments are interposed among the convoluted tubules and appear to radiate from the medulla into the cortex, hence the name.

The renal pelvis represents the expanded portion of the upper urinary tract. In humans, transitional epithelium or urothelium, composed of multiple cell layers, lines the pelvis and ureter. In rodents, cuboidal epithelium lines the renal pelvis and also covers the urinary surface of the papilla. Two and sometimes three extensions of the renal pelvis, the major calyces, reach outward from the upper dilated part of the pelvis, which further divides into several minor calyces. These receive the urine discharged at the area cribrosa of each renal

pyramid. In unipapillary kidneys, the papilla is directly surrounded by the renal pelvis. The ureters originate from the distal renal pelvis at the ureteropelvic junction and discharge into the fundus of the urinary bladder. In adult humans, the ureters are approximately 28 to 34 cm long and have a mean diameter of 1.8 mm, with a maximum of 3 mm considered normal.² The walls of the calyces, pelvis, and ureters contain smooth muscle-related cells and interstitial cells, which serve a pacemaker function to propel the urine to the bladder.

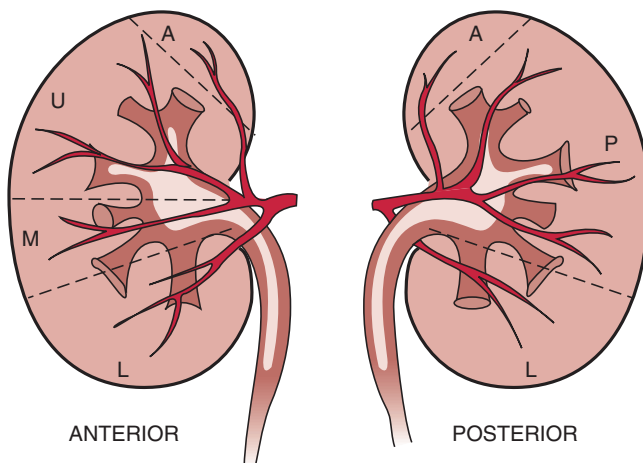


Fig. 2.1 Diagram of the vascular supply of the human kidney. The anterior half of the kidney can be divided into upper (U), middle (M), and lower (L) segments, each supplied by a segmental branch of the anterior division of the renal artery. A small apical segment (A) is usually supplied by a division from the anterior segmental branch. The posterior half of the kidney is divided into apical (A), posterior (P), and lower (L) segments, each supplied by branches of the posterior division of the renal artery. (Modified from Graves FT. The anatomy of the intrarenal arteries and its application to segmental resection of the kidney. *Br J Surg.* 1954;42:132–139.)

THE NEPHRON

The nephron is the functional unit of the kidney, composed of the renal corpuscle (the term renal or Malpighian corpuscle comprises the glomerulus and Bowman's capsule) and the associated renal tubules from the proximal tubule through the connecting segment (CNT) (Fig. 2.5). Although the average nephron number in adult humans is approximately 900,000 to 1 million per kidney, numbers for individual human kidneys range from approximately 200,000 to more than 2.5 million,^{3–6} contrasting with the approximately 30,000 nephrons in each adult rat kidney.^{7–9} The origin of the nephron is the metanephric blastema. Although there has not been universal agreement on the origin of the connecting tubule, it is now generally believed also to derive from the metanephric

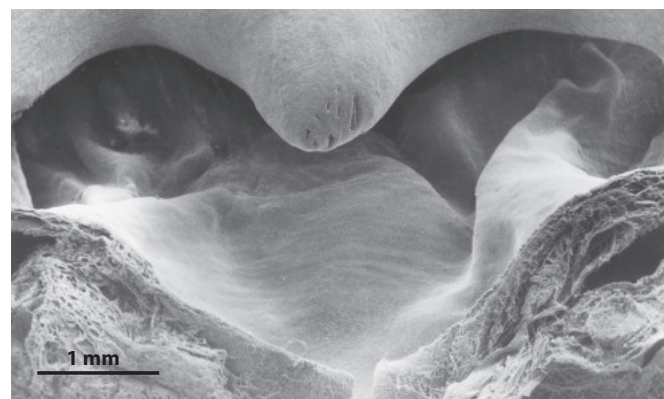


Fig. 2.3 Scanning electron micrograph of papilla from a rat kidney (upper center), illustrating the area cribrosa formed by slit-like openings where the ducts of Bellini terminate. The renal pelvis (below) surrounds the papilla.

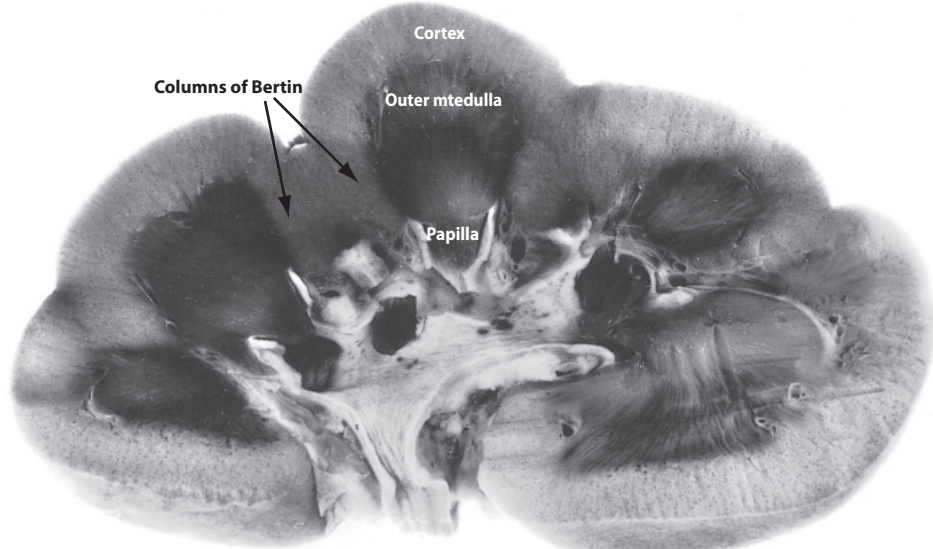


Fig. 2.2 Bisected kidney from a 4-year-old child demonstrating the difference in appearance between the light-staining cortex and the dark-staining outer medulla. The inner medulla and papillae are less dense than the outer medulla. The columns of Bertin can be seen extending downward to separate the papillae.

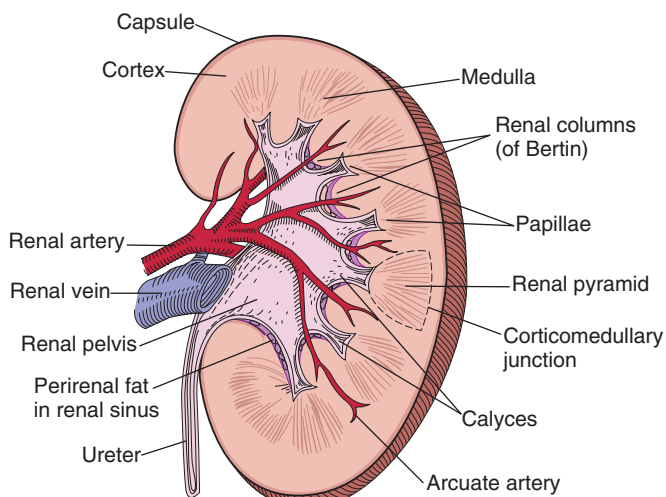


Fig. 2.4 Diagram of the cut surface of a bisected kidney, depicting important anatomic structures.

blastema.¹⁰ The collecting duct system, which includes the initial collecting tubule (ICT), the cortical collecting duct (CCD), the outer medullary collecting duct (OMCD), and the inner medullary collecting duct (IMCD), is not considered part of the nephron because it has a different embryonic origin, the ureteric bud, multiple nephrons merge into the system, and the collecting duct was formerly considered simply a conduit for the tubule fluid. Thus, the collecting duct classically has not been included as a component of an individual functional unit. Nonetheless, the collecting ducts make critical contributions to renal function and the components of the nephron and the collecting duct system are functionally interrelated.

The various tubule segments are composed of structurally distinct epithelial cells along a basement membrane that faces the interstitium on the blood side of the cell. A tubule lumen is formed at the apical side of the cell, which contains the glomerular filtrate that is modified by transport processes to ultimately produce urine. With the exception of intercalated cells and the IMCD cell in the terminal portion of the IMCD, all epithelial cells in the renal tubules and glomeruli contain a single cilium that extends into the tubule lumen or Bowman's space. Many epithelial cells of the renal tubules exhibit significant structural alterations in response to physiologic stimuli, such as changes in cell size, the complexity of the plasma membrane compartments, the abundance of cytoplasmic vesicles, and the abundance and appearance of lysosomes and multivesicular bodies. As such, the specific descriptions of epithelial cell ultrastructure that follow are based on observations of the cells under basal conditions, with added examples of structural alterations induced by changes in diet or physiologic stimuli.

Individual nephrons are classified as superficial, midcortical, and juxtamedullary, based on the position of the glomerulus in the cortex. These typically have differences in the length of loop of Henle and are subject to variations in blood supply under different physiologic states. The loop of Henle contains the straight portion of the proximal tubule (pars recta), descending and ascending thin limb segments, and the straight portion of the distal tubule (TAL, or pars recta) (see

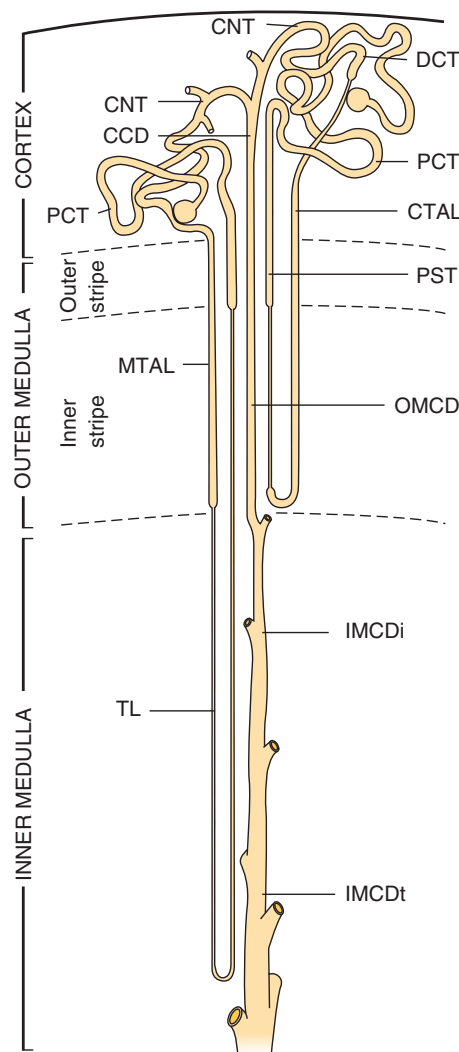


Fig. 2.5 Diagram illustrating superficial and juxtamedullary nephron. CCD, Cortical collecting duct; CNT, connecting tubule; CTAL, cortical thick ascending limb; DCT, distal convoluted tubule; IMCDi, initial inner medullary collecting duct; IMCDt, terminal inner medullary collecting duct; MTAL, medullary thick ascending limb; OMCD, outer medullary collecting duct; PCT, proximal convoluted tubule; PST, proximal straight tubule; TL, thin limb of loop of Henle. (Modified from Madsen KM, Tisher CC. Structural-functional relationship along the distal nephron. *Am J Physiol*. 1986;250:F1–F15.)

Fig. 2.5). The length of the loop of Henle is generally related to the position of its parent glomerulus in the cortex. Most nephrons originating from superficial and midcortical locations have shorter loops of Henle that bend within the inner stripe of the outer medulla close to the inner medulla; these nephrons have no, or very short, ascending thin limbs, as the hairpin turn connects descending thin limb to TAL. A few species, including humans, also possess cortical nephrons with extremely short loops that never enter the medulla but turn back within the cortex.¹¹ Juxtamedullary nephrons have long loops of Henle with long descending and ascending thin limb segments that extend into the inner medulla. Many variations exist, however, between the two basic types of nephrons, depending on their relative positions in the cortex. The ratio of long- and short-loop nephrons varies

among species. Humans and rodents have more short-looped than long-looped nephrons.^{12–16} Renal tubules that are located on the surface of the renal cortex, where they are accessible for micropuncture experiments, belong almost exclusively to superficial, hence short-looped, nephrons.

The medulla is divided into inner and outer regions; the outer medulla is subdivided into inner and outer stripes (Figs. 2.5 and 2.6). These distinctions are based on the populations of specific renal tubule segments. The inner medulla is easily distinguished from the outer medulla by the absence of TALs. There is a distinct border between the two regions, visible in histologic sections, where the thin ascending limbs make an abrupt transition to TALs (Fig. 2.6). The inner medulla contains both descending and ascending thin limbs and collecting ducts, but no TALs. In the outer medulla, the inner and outer stripes are easily distinguished by the presence of proximal tubules in the outer stripe and their absence in the inner stripe; the border is marked by the abrupt transition from proximal straight tubules (PSTs) to descending thin limbs (Fig. 2.6). Thus, the inner stripe contains TALs, descending thin limbs, and collecting ducts, but no proximal tubules. The outer stripe contains the terminal portion of PSTs, TALs, and collecting ducts. By contrast, the renal cortex contains the glomeruli, both convoluted and PSTs, TALs, distal convoluted tubules (DCTs), CNTs, and collecting ducts, but not thin limbs of loop of Henle.

GLOMERULUS

The nephron begins with the glomerulus, which is composed of a capillary network lined by a thin layer of endothelial cells, a central region of mesangial cells with surrounding matrix material, and the visceral epithelial cells (podocytes) overlying the capillaries (Figs. 2.7–2.10). The parietal layer of Bowman's capsule with its basement membrane encases the glomerulus. Bowman's space, or the urinary space, is the cavity between the visceral and parietal epithelia. Although “renal corpuscle” is strictly the correct terminology to refer to the glomerulus and Bowman's capsule, glomerulus is used throughout this chapter because of its common use. At the vascular pole, where the afferent and efferent arterioles enter and exit the glomerulus, the visceral epithelium is continuous with the parietal epithelium. The parietal epithelium transitions to proximal tubule epithelium at or near the urinary pole. The average diameter of a glomerulus is approximately 200 µm in the human kidney and 120 µm in the rat kidney. However, the size and number of glomeruli vary significantly with age, gender, birth weight, and renal health. The average glomerular volume is 0.6 to 1 million µm³ in rats^{7,8} and 3 to 7 million µm³ in humans,^{3,4,6} although individual glomerular volume within single human kidneys can vary as much as eightfold.⁵ Rat juxtamedullary glomeruli are larger than superficial glomeruli; this is not the case in the human kidney.¹⁷

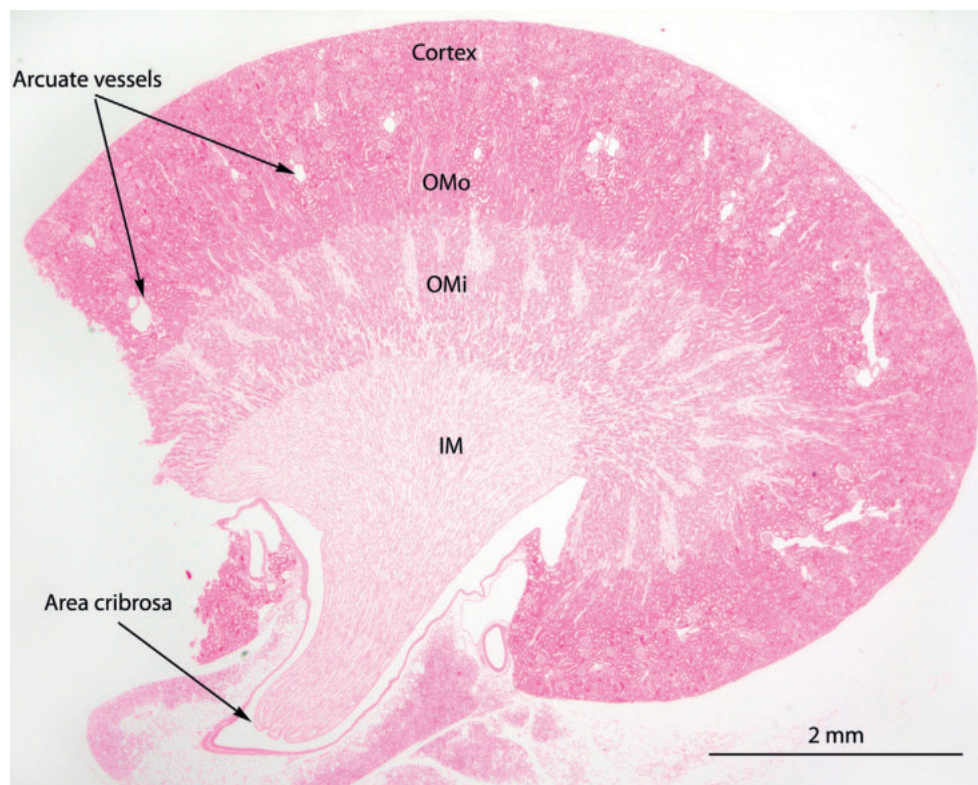


Fig. 2.6 Light micrograph of a sagittal section of normal mouse kidney. The renal cortex is the region between the arcuate vessels and the renal capsule. The borders between the outer stripe of the outer medulla (OMo), inner stripe or the outer medulla (OMi), and inner medulla (IM) are easily distinguished by the changes in the staining intensity. The OMo, which contains proximal tubules, has a similar staining intensity as the cortex. OMi by comparison, has paler staining due to the absence of proximal tubules. IM stains even more weakly due to the absence of thick ascending limbs in this region. The tip of the papilla, identified by the area cribrosa, extends into the proximal ureter in mouse kidneys. Hematoxylin and eosin stain.

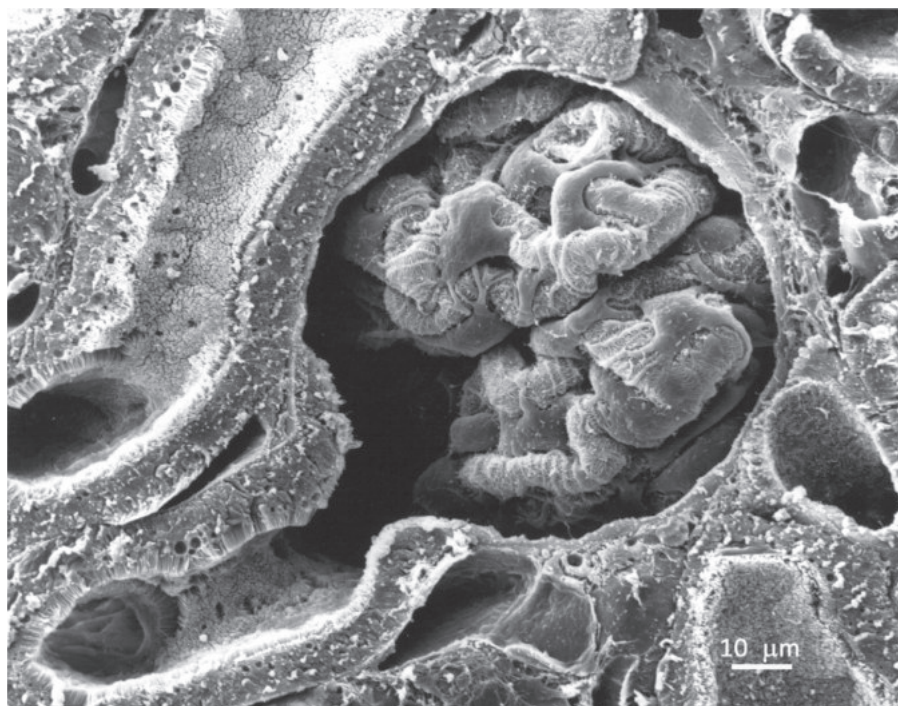


Fig. 2.7 Scanning electron micrograph of a rat glomerulus. The glomerular tuft is encased by Bowman's capsule. Podocytes, with their interdigitating foot processes, cover the capillaries. The glomerular filtrate drains into the proximal tubule at the urinary pole. (From Sands JM, Verlander JW. Functional anatomy of the kidney. In: McQueen C, ed. *Comprehensive Toxicology*, 3rd ed. St. Louis: Elsevier; 2017.)

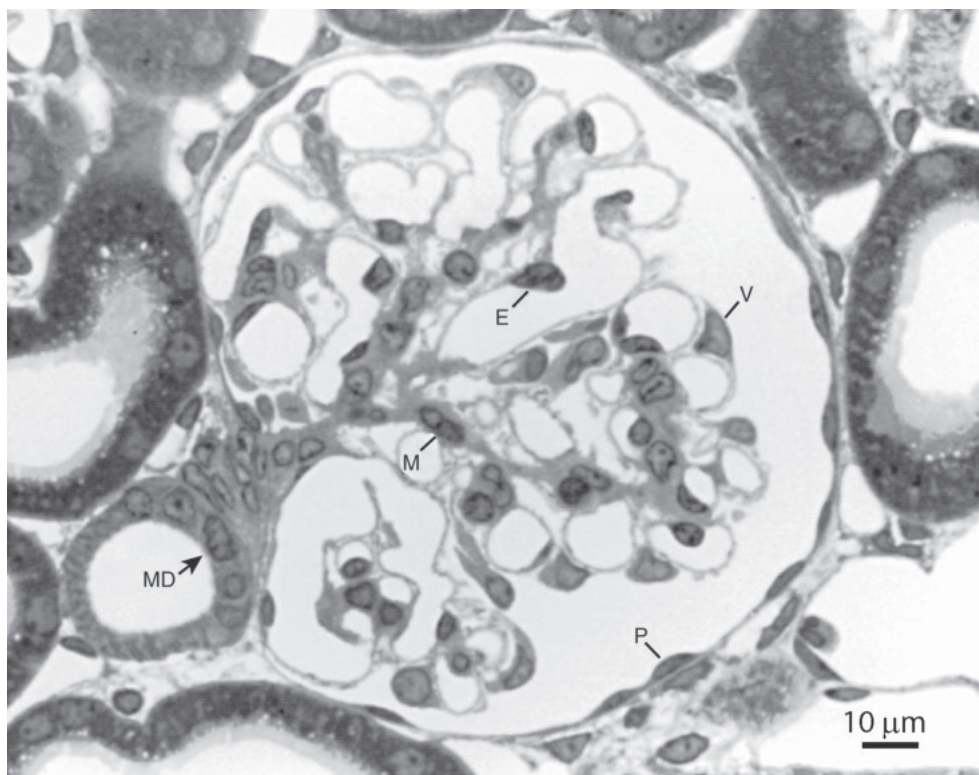


Fig. 2.8 Light micrograph of a normal glomerulus from a rat, demonstrating the four major cellular components: endothelial cell (E), mesangial cell (M), parietal epithelial cell (P), and visceral epithelial cell or podocyte (V). The macula densa (MD) is located in the thick ascending limb at the vascular pole.

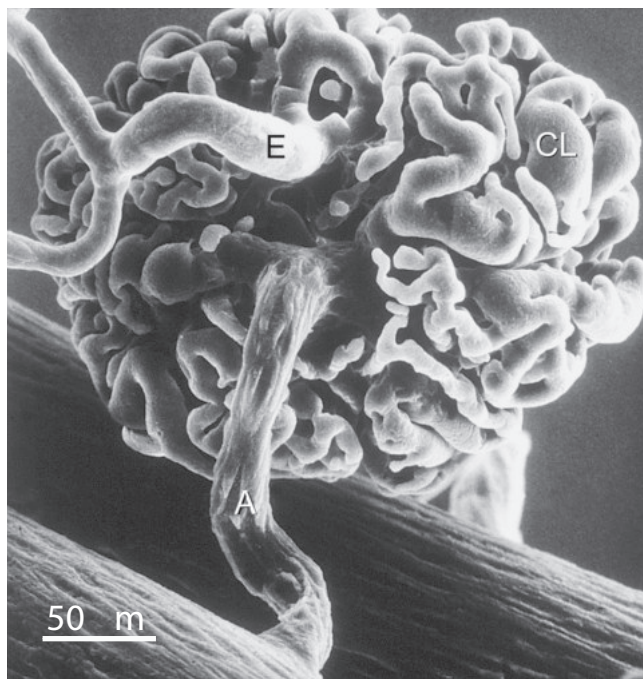


Fig. 2.9 Scanning electron micrograph of a cast of a glomerulus with its many capillary loops (*CL*) and adjacent renal vessels. The afferent arteriole (*A*) takes its origin from an interlobular artery at lower left. The efferent arteriole (*E*) branches to form the peritubular capillary plexus (*upper left*). (Courtesy Waykin Nopanitaya, PhD.)

The main function of the glomerulus is filtration of the plasma. The layers of the glomerular capillary wall, the fenestrated capillary endothelium, the glomerular basement membrane (GBM), and the filtration slit diaphragm between the foot processes of the visceral epithelial cells form the filtration barrier between the blood and the urinary space (Fig. 2.11). To cross the capillary wall, a molecule must pass sequentially through the fenestrated endothelium, the GBM, and the filtration slit diaphragm. Although the glomerular capillary wall allows passage of small molecules, the prevailing view is that it normally restricts the passage of cells and larger molecules, such as albumin, due to its size- and charge-selective properties.¹⁸

ENDOTHELIAL CELLS

The glomerular capillaries are lined by a thin fenestrated endothelium (Figs. 2.11 and 2.12). These endothelial cells form the initial barrier to the passage of blood constituents from the capillary lumen to Bowman's space. Under normal conditions, the formed elements of the blood, including erythrocytes, leukocytes, and platelets, do not gain access to the subendothelial space.

The endothelial cell nucleus lies adjacent to the mesangium, with the remainder of the cell irregularly attenuated around the capillary lumen (see Fig. 2.10). The endothelium contains pores or fenestrae that range from 70 to 100 nm in diameter in human (see Figs. 2.11 and 2.12).¹⁹ Nonfenestrated,

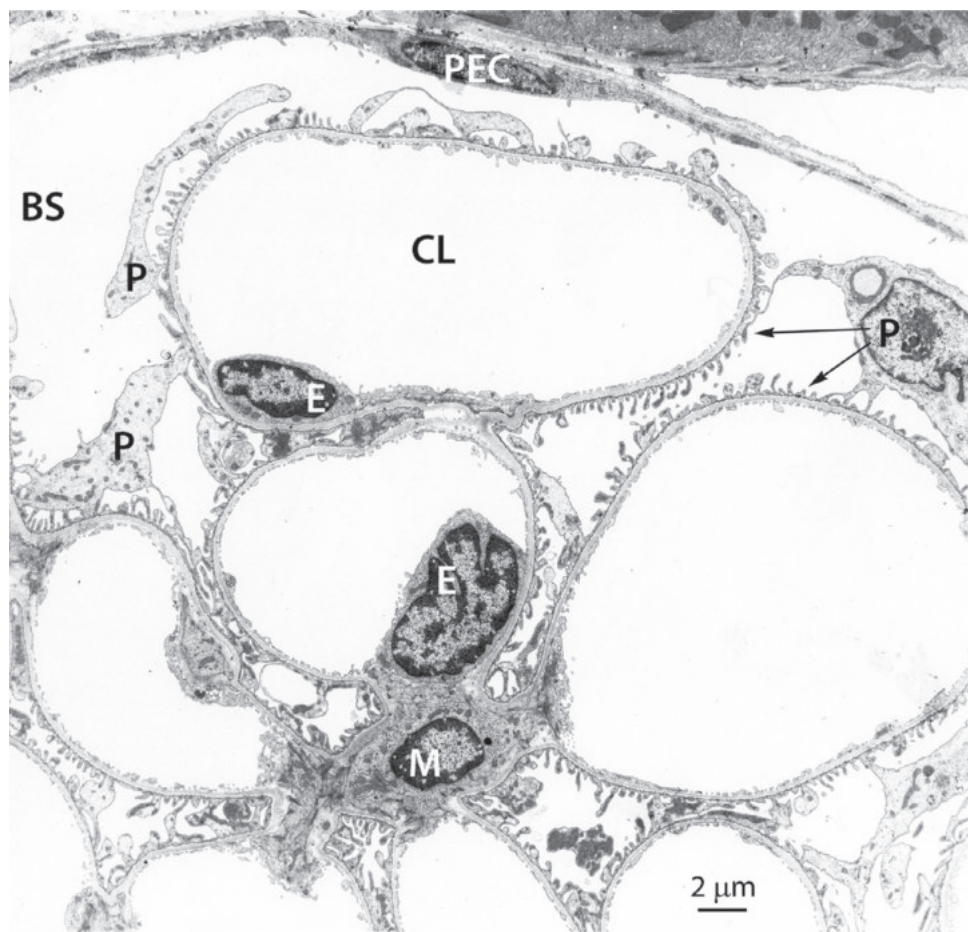


Fig. 2.10 Transmission electron micrograph of a normal rat glomerulus. The capillary loops are lined by fenestrated endothelial cells (*E*), facing the capillary lumen (*CL*). Mesangial cells (*M*) lie beneath the endothelial cells, among the capillary loops. Podocytes (*P*) and their extensive, interdigitating primary and secondary foot processes (arrows), cover the surface of the capillaries, facing the glomerular filtrate in Bowman's space (*BS*). Parietal epithelial cells (*PEC*) line Bowman's capsule facing Bowman's space.

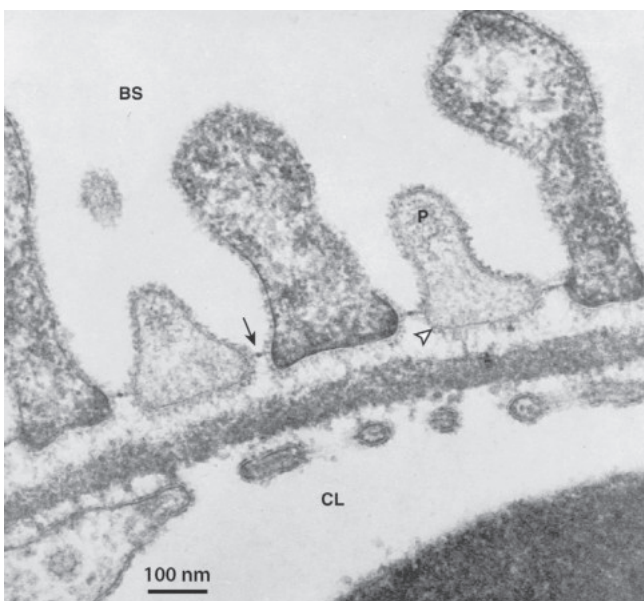


Fig. 2.11 Transmission electron micrograph of normal rat glomerular capillary wall fixed in a 1% glutaraldehyde solution containing tannic acid. Note the relationship among the three layers of the glomerular basement membrane and the presence of the pedicels (*P*) embedded in the lamina rara externa (arrowhead). The filtration slit diaphragm with the central dense spot (thin arrow) is especially evident between the individual pedicels. The fenestrated endothelial lining of the capillary loop is shown below the basement membrane. A portion of an erythrocyte is located in the extreme lower right corner. *BS*, Bowman's space; *CL*, capillary lumen.

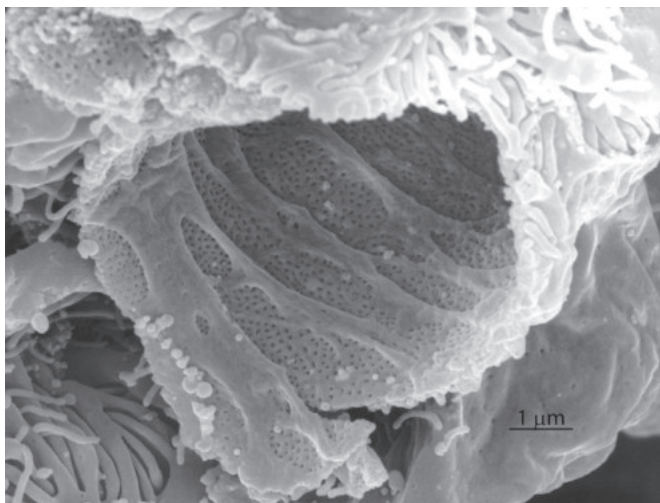


Fig. 2.12 Scanning electron micrograph of a glomerular capillary from the kidney of a normal rat. Numerous endothelial pores, or fenestrae, are present in the endothelial cells lining the capillary lumen. The ridgelike structures are localized thickenings of the endothelial cells. Interdigitating foot processes of the podocytes cover the urinary side of the capillaries.

ridgelike structures termed “cytostacks” are found near the cell borders. An extensive network of intermediate filaments and microtubules is present in the endothelial cells, and microfilaments surround the fenestrae.²⁰ Most studies indicate adult glomerular endothelial cells lack diaphragms across the fenestrae, whereas diaphragmed fenestrae are

present in the embryo, where they may compensate for the functional immaturity of the embryonic glomerular filtration barrier.²¹ The glomerular endothelium is covered by a glycocalyx layer, the visualization of which requires special methods such as electron microscopy with cationic dyes or lipid particles.^{22–24} The glycocalyx also fills the endothelial fenestrae forming “sieve plugs,” the exact function of which is unknown.²⁵ The glycocalyx consists of membrane-bound proteoglycans (syndecan and glypcan) with attached glycosaminoglycans (GAGs), secreted glycoproteins (perlecan and versican), and secreted GAGs (hyaluronan), which provide a negative charge.²⁶

Classic ultrastructural studies demonstrated that endogenous albumin is largely confined to the glomerular capillary lumen and does not pass through the endothelium.²⁷ In recent years, more studies have addressed the potential role of the glomerular endothelium, and particularly its glycocalyx, in filtration. Studies in rats showed that eluting molecular components of the glomerular endothelial glycocalyx with hypertonic sodium chloride induced a 12-fold increase in proteinuria.²⁸ Injection of hyaluronidase, a hyaluronan-degrading enzyme, in mice led to disruption of the glomerular endothelial glycocalyx and leakage of albumin across the endothelium.²⁹ Using isolated human and rodent glomeruli, enzymatic disruption of the glomerular endothelial glycocalyx resulted in increased glomerular albumin permeability.³⁰ Thus, experimental evidence supports that the glomerular endothelial glycocalyx is an important component of the filtration barrier.

Signaling between glomerular cells is critical for the development and maintenance of the filtration barrier.³¹ The surfaces of glomerular endothelial cells express receptors for the vascular endothelial growth factor (VEGF) family.³² VEGF is synthesized by podocytes (glomerular visceral epithelial cells) and is an important regulator of microvascular permeability.^{32,33} VEGF increases endothelial cell permeability and induces the formation of endothelial fenestrations.^{34,35} VEGF-A is the best characterized podocyte growth factor, and its principal receptor is VEGFR2, expressed on endothelial cells. Podocyte-specific alterations of VEGF-A have demonstrated that it is required for normal differentiation of glomerular endothelial cells.^{36,37} Moreover, drug inhibition of VEGF-A in patients or podocyte-specific deletion of VEGF-A in adult mice results in severe glomerular endothelial injury and thrombotic microangiopathy.³⁸ Thus, VEGF produced by podocytes plays a critical role in the differentiation and maintenance of glomerular endothelial cells and is an important regulator of endothelial cell permeability.

Several other cell-cell communication pathways exist between glomerular cells. For example, angiopoietin-TIE signaling regulates endothelial homeostasis in an intricate manner.³¹ Angiopoietin-1 (ANGPT1) produced in podocytes binds to endothelial-expressed tyrosine kinase receptor TIE2, the phosphorylation of which promotes endothelial survival. In contrast, angiopoietin-2 secreted by endothelial cells is an antagonist of ANGPT1-mediated TIE2 activation in endothelial cells.

GLOMERULAR BASEMENT MEMBRANE

By transmission electron microscopy, the GBM is composed of a central dense layer, the lamina densa, and two thinner,

more electron-lucent layers, the lamina rara externa and the lamina rara interna (see Fig. 2.11). The latter two layers measure approximately 20 to 40 nm in thickness.¹⁹ Although in the rat the width of the GBM has been found to be 132 nm,³⁹ the width of the human GBM has consistently been reported to be more than 300 nm^{40,41} with a slightly thicker basement membrane in men (373 nm) than in women (326 nm).⁴² Compared with other basement membranes, the GBM is thicker, likely at least in part from fusion of endothelial and epithelial basement membranes during development.⁴³ Mass spectrometry-based proteomic analysis has revealed at least 212 proteins in the normal human glomerular extracellular matrix; however, like other basement membranes in the body, the GBM is composed primarily of type IV collagen, laminin, nidogen (entactin), and heparan sulfate proteoglycans (HSPGs).^{44–49}

Type IV collagen consists of six chains, α_1 (IV) through α_6 (IV). Three α (IV) chains self-associate intracellularly to form triple helical molecules called protomers. Three types of promoters are formed: $\alpha_1\alpha_2\alpha_1$, $\alpha_3\alpha_4\alpha_5$, and $\alpha_5\alpha_6\alpha_5$. Upon secretion into the extracellular space, the protomers self-associate via their amino- and carboxy-terminal domains to form polymerized networks. Three sets of collagen IV networks form: $\alpha_1\alpha_2\alpha_1$ (IV)- $\alpha_1\alpha_2\alpha_1$ (IV), $\alpha_3\alpha_4\alpha_5$ (IV)- $\alpha_3\alpha_4\alpha_5$ (IV), and $\alpha_1\alpha_2\alpha_1$ (IV)- $\alpha_5\alpha_6\alpha_5$ (IV). The networks undergo specific extracellular modifications to form an elaborate scaffold that tethers other molecules, serve as a cell-signaling interface, and provide support for adjacent cells.⁵⁰ Halogens facilitate the assembly of the collagen IV scaffold. For example, extracellular chloride ions activate a molecular switch that enables individual promoter carboxy domains to oligomerize,⁵¹ and ionic bromide is essential for enzymatic cross-linking to stabilize the protomer–protomer connections.⁵² The $\alpha_3\alpha_4\alpha_5$ (IV)- $\alpha_3\alpha_4\alpha_5$ (IV) network predominates in the GBM, whereas the $\alpha_1\alpha_2\alpha_1$ (IV)- $\alpha_5\alpha_6\alpha_5$ (IV) network is in Bowman's capsule. Whereas $\alpha_1\alpha_2\alpha_1$ (IV) protomers are synthesized from both endothelial cells and podocytes, $\alpha_3\alpha_4\alpha_5$ (IV) protomers are secreted only by podocytes.⁵³ Mutations in the genes encoding α_3 , α_4 , and α_5 (IV) chains cause Alport syndrome, and autoantibodies against the carboxy terminal α_3 (IV) chain are responsible for anti-GBM disease.⁵⁴

Laminins (LMs) are large heterotrimeric glycoproteins composed of three chains; α , β , and γ . The major laminin in the adult GBM is LM-521 (containing the α_5 , β_2 , and γ_1 chains). Both glomerular endothelial cells and podocytes synthesize laminin α_5 and β_2 .⁵⁵ Mutations of laminin β_2 result in a congenital nephrotic syndrome called Pierson syndrome in humans.⁵⁶

Nidogens, also known as entactins, are glycoproteins. Nidogen-1 binds to both collagen IV and laminin but does not appear essential for GBM formation.⁵⁷ HSPGs consist of a core protein linked to sulfated GAG side chains. Agrin, perlecan, and type XVIII collagen are HSPGs found in the GBM.⁵⁸ Agrin is the major HSPG in the GBM, whereas perlecan and type XVIII collagen are found mainly in the mesangium.

Subdiffraction resolution stochastic optical reconstruction microscopy has provided a precise view of the nanoscale organization of these molecular networks within the GBM.⁵⁹ The $\alpha_3\alpha_4\alpha_5$ (IV) network localizes to the center of the GBM, whereas the $\alpha_1\alpha_2\alpha_1$ (IV) network maps near the endothelial

side of the GBM. Laminin-521 is situated in two layers near the endothelial and podocyte sides of the GBM and also in the central portion of the GBM. Agrin localizes in two layers along the endothelial and podocyte surfaces of the GBM, with more detected near the podocytes.

The contribution of the GBM to the glomerular filtration barrier has been studied for decades.^{60,61} Ultrastructural tracer studies provided evidence to suggest that the GBM constitutes both a size-selective and a charge-selective barrier.^{62–64} Additional studies revealed a lattice of anionic sites with a spacing between them of approximately 60 nm (Fig. 2.13) throughout the lamina rara interna and lamina rara externa.^{65,66} The anionic sites in the GBM consist of heparan sulfate GAG side chains of the proteoglycans rich in heparan sulfate.^{67,68} Removal of the heparan sulfate side chains by enzymatic digestion resulted in an increase in the in vitro permeability of the GBM to ferritin⁶⁹ and to bovine serum albumin,⁷⁰ suggesting that HSPGs play a role in establishing the permeability properties of the GBM to plasma proteins (see Fig. 2.13). However, in vivo studies have addressed the role of proteoglycans and charge selectivity in the GBM. Overexpression of heparanase in transgenic mice led to a fivefold reduction in GAG-associated sites in the GBM but no proteinuria.⁷¹ Moreover, podocyte-specific deletion of agrin alone or in combination with deletion of perlecan heparan sulfate side chains in mice resulted in a dramatic reduction in GBM anionic sites but did not alter the filtration barrier to albumin or a negatively charged tracer.^{72,73} Thus, more recent data suggest the role of GBM anionic charge, at least that contributed by proteoglycans, is minimal in the function of the glomerular filtration barrier.

Nevertheless, a variety of genetic findings in humans and studies in mice indicate that an intact GBM serves a barrier function to protein permeability. The absence of an intact $\alpha_3\alpha_4\alpha_5$ (IV) network in the GBM of Alport syndrome eventually results in proteinuria. In humans and animal models of Alport syndrome, there is a compensatory increase in the $\alpha_1\alpha_2\alpha_1$ (IV) network, laminin α_5 chain, and ectopic laminin isoforms (α_1 , α_2 , and β_1 chains) in the defective GBM.^{74,75} These secondary changes alter cell matrix signaling, are accompanied by characteristic splitting and “basket-weave” lamellation of the GBM, and produce proteinuria.

Strong evidence for a specific role of the GBM in the filtration barrier is the presence of laminin β_2 mutations in humans or mice resulting in massive proteinuria.^{76,77} Laminin- β_2 -deficient ($Lamb2^{-/-}$) mice develop severe proteinuria and ectopic laminin chains ($\alpha_1, \alpha_2, \alpha_3, \beta_3$, and γ_2) that accumulate in the GBM, but this ectopic deposition fails to compensate for the absence of laminin β_2 .⁷⁸ Importantly, the albuminuria in the mice precedes podocyte foot process effacement and filtration slit diaphragm abnormalities, indicating the GBM has an essential role in the filtration barrier. Remarkably, injection of recombinant human LM-521 accumulates in the correct orientation in the GBM and delays the onset of proteinuria in $Lamb2^{-/-}$ mice, which lack LM-521.⁷⁹

PODOCYTES

Podocytes (visceral epithelial cells) are the largest cells in the glomerulus and are positioned on the outside of the glomerular capillary wall (see Figs. 2.7, 2.10–2.12, and 2.14). Mature podocytes are terminally differentiated and generally

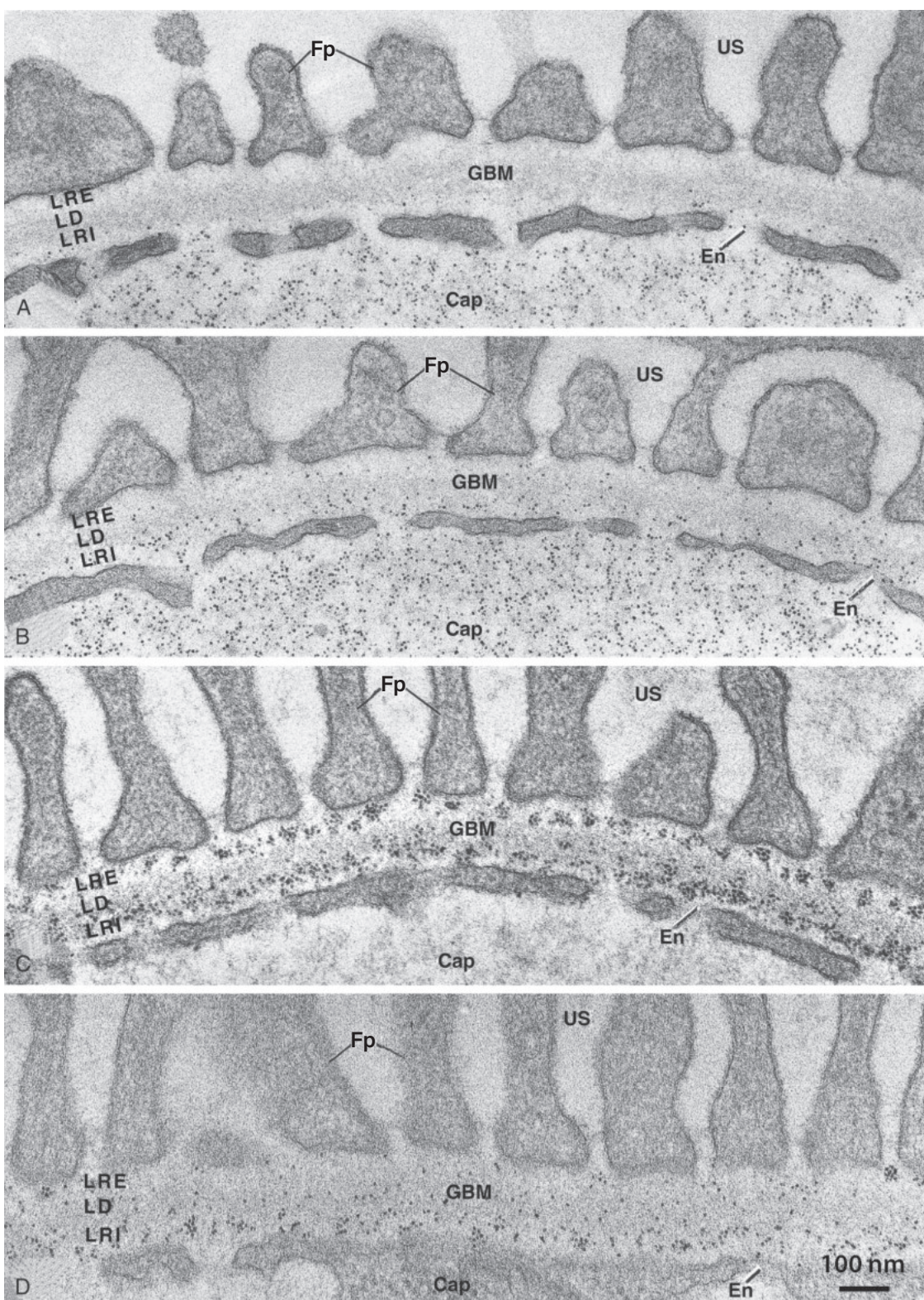


Fig. 2.13 Transmission electron micrographs of the glomerular filtration barrier in normal rats perfused with native anionic ferritin (A) or cationic ferritin (C) and in rats treated with heparitinase before perfusion with anionic (B) or cationic ferritin (D). In normal animals, anionic ferritin is present in the capillary (Cap) but does not enter the glomerular basement membrane (GBM), as shown in (A). In contrast, cationic ferritin binds to the negatively charged sites in the lamina rara interna (LRI) and lamina rara externa (LRE) of the GBM (see C). After treatment with heparitinase, both anionic (B) and cationic (D) ferritin penetrate into the GBM, but there is no labeling of negatively charged sites by cationic ferritin. En, Endothelial fenestrae; Fp, foot processes; LD, lamina densa; US, urinary space. (Modified from Kanwar YS. Biophysiology of glomerular filtration and proteinuria. *Lab Invest*. 1984;51:7-21.)

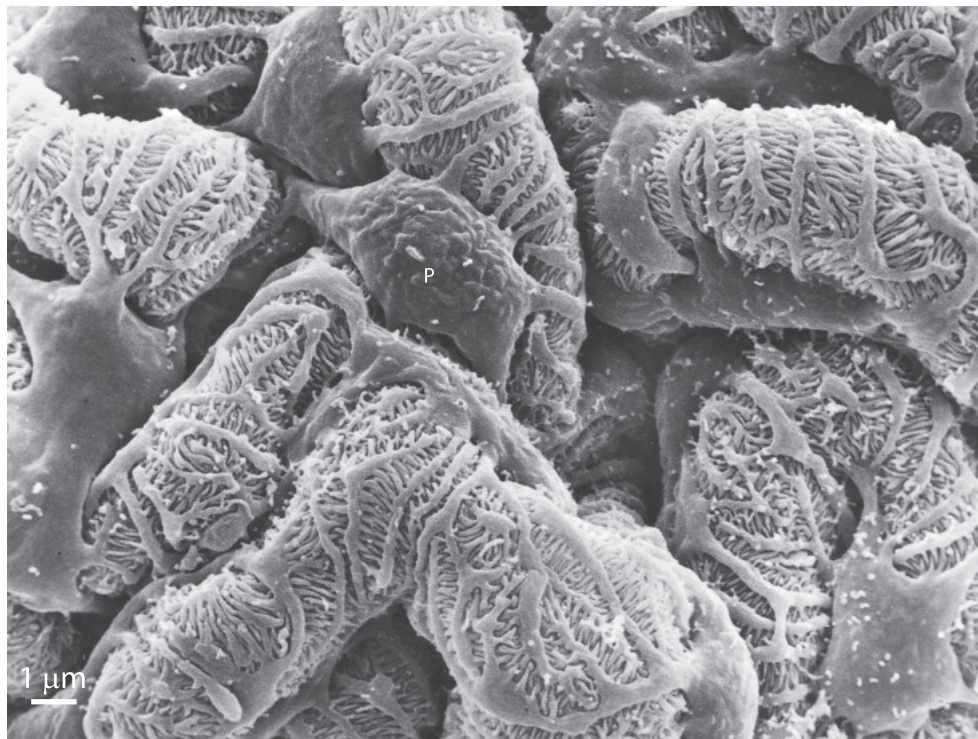


Fig. 2.14 Scanning electron micrograph of a glomerulus from the kidney of a normal rat. The visceral epithelial cells, or podocytes (P), extend multiple processes outward from the main cell body to wrap around individual capillary loops. Immediately adjacent pedicels, or foot processes, arise from different podocytes.

do not replicate. They have a prominent cell body containing nuclei, endoplasmic reticulum, Golgi apparatus, and an endocytic–lysosomal system. The cell bodies give rise to long cytoplasmic primary processes that branch into secondary and tertiary processes, surround the capillaries, and finally divide into foot processes. The foot processes come into direct contact with the lamina rara externa of the GBM (see Figs. 2.11 and 2.13). By scanning electron microscopy (SEM), it is apparent that adjacent foot processes are derived from different podocytes (Fig. 2.14). The gap between adjacent foot processes is bridged by a thin structure called the “filtration slit diaphragm.” Advanced techniques, including serial block-face SEM (SBF-SEM) and focused ion beam SEM (FIB-SEM), show that foot processes emerge directly from the podocyte cell body as well as the elongated cytoplasmic processes.^{80,81} These studies reveal tortuous ridgelike prominences along the basal surface of the cell body and the cytoplasmic processes, from which the proximal portions of the foot processes emerge.

A series of studies using three-dimensional (3D) electron microscopic reconstruction and SBF-SEM have supported the existence of a subpodocyte space (SPS) under the podocyte cell body and a narrow interpodocyte space, which interconnects the SPS with the peripheral Bowman’s space.^{82,83} Whether these spaces act as a resistance pathway across the filtration barrier remains to be determined.

Podocytes have an elaborate cytoskeleton that underlies their shape, stability, adhesion, and response to stress.⁸⁴ Large numbers of microtubules and intermediate filaments (vimentin) are present in the cell body and primary processes,⁸⁵ whereas actin filaments are especially abundant in the foot

processes.⁸⁶ Ultrastructural studies have demonstrated two distinct actin filament networks in foot processes of rat podocytes.^{87,88} “Actin bundles,” containing α -actinin and synaptopodin, extend along the longitudinal axis of the foot processes above the level of the slit diaphragm. The cortical actin network, containing cortactin, lies between the actin bundle and the plasma membrane. In glomerular diseases associated with proteinuria, the podocyte cytoskeleton is disrupted, slit diaphragms are lost, and the interdigitating foot processes are replaced by broad regions of podocyte processes covering the GBM.⁸⁹ This “foot process effacement” is often accompanied by aggregated filaments appearing as a cytoplasmic mat juxtaposed to the GBM.

Actin fibers are composed of bundles of actin filaments. Both contractile and noncontractile actin fibers are present in most cells, and the former (actin stress fibers) are characterized by periodic alternating bands of α -actinin and myosin.⁹⁰ Studies using superresolution microscopic methods have revealed a detailed model of the podocyte actin cytoskeleton in both mice and humans.⁹¹ Actin fibers in the center of the foot process contain α -actinin and synaptopodin but lack myosin IIA, whereas actin fibers in the podocyte cell body and primary processes contain myosin IIA but lack synaptopodin. These findings suggest the actin fibers in the foot process are noncontractile, whereas the actin fibers in the cell body and primary processes are contractile. In podocyte injury models with foot process effacement and proteinuria, myosin IIA translocates to cytoplasm adjacent to the GBM, forming sarcomere-like structures with alternating synaptopodin and α -actinin staining. Thus, podocytes contain distinct actin filament networks that appear to provide

tensional integrity (tensegrity) and can redistribute in response to injury.⁹²

Foot processes contain two structures, focal adhesions (FAs) and filtration slit diaphragms (SDs), that interact with and control the actin cytoskeleton.⁹³ FAs anchor the base of the foot processes to the GBM. They consist of transmembrane protein complexes through which the actin cytoskeleton is regulated by extracellular signaling.⁹⁴ Cell adhesions rich in integrins and their interacting proteins are known as the “integrin adhesome.”⁹⁵ FAs are a form of integrin adhesome and, at the foot process–GBM interface, consist of $\alpha 3\beta 1$ integrin and various adaptor proteins, kinases, and phosphatases and guanosine triphosphatases (GTPases). The $\alpha 3\beta 1$ integrin interconnects laminin in the GBM with the talin, paxillin, and vinculin adaptor cytoplasmic complex, which link to the actin cytoskeleton. Mutations of the integrin $\alpha 3$ subunit in humans are associated with massive proteinuria.⁹⁶ Podocyte adhesion to the GBM is supported by the interaction of integrin $\alpha 3\beta 1$ with the tetraspanin protein CD151, the absence of which leads to severe proteinuria.⁹⁷ FA kinase and integrin-linked kinase localize to FAs and mediate signaling with the actin cytoskeleton.

The Rho family of small GTPases, including RhoA, Rac1, and Cdc42, regulate actin cytoskeleton dynamics.⁹⁸ Activation of podocyte RhoA and Rac1 in transgenic mice leads to proteinuria and podocyte foot process effacement.^{99–102} In contrast, podocyte deletion of C4dc42 results in proteinuria and foot process effacement.^{103,104} Rho GTPases cycle between an active GTP-bound form and an inactive guanosine diphosphate (GDP)-bound form.¹⁰⁵ Rho GTPases are inactivated by GTPase-activating proteins (GAPs), which increase GTP hydrolysis or by guanine nucleotide dissociation inhibitors (GDIs), which sequester their inactive GDP-bound form in the cytoplasm. Mutations in the genes that encode Arhgap24, a GAP, and Arhgdia, a GDI, result in Rac1 activation and proteinuria in humans.^{106,107} Moreover, mutations in Kank2 (kidney ankyrin repeat-containing protein), an *Arhgdia*-interacting protein that localizes to FAs, leads to RhoA activation and proteinuria.¹⁰⁸ Dynamin is a large GTPase that has a role in clathrin-mediated endocytosis but also directly binds actin filaments and promotes actin polymerization.¹⁰⁹ Dynamin regulates FA maturation in podocytes in vitro, and its conditional deletion in mouse podocytes results in foot process effacement and severe proteinuria.^{110,111} These studies suggest dynamin serves as a molecular link between endocytosis and actin remodeling in podocytes. Thus, an intricate physiologic balance of the various GTPases is required for normal podocyte homeostasis.

The filtration SD is the second structure that controls the actin cytoskeleton. It appears as a thin line on electron microscopy (see Fig. 2.11) and bridges the 30–40 nm space (called the filtration slit) between adjacent foot processes. A central dot within the SD may occasionally be seen on ultrastructural cross-sections, and it appears as a continuous central filament on sections parallel to the plane of the GBM (see Fig. 2.15). Based on these observations, Rodewald and Karnovsky proposed a porous zipper-like model for the SD.¹¹² In this model, there are regularly spaced cross-bridges that extend from the membranes of two adjacent foot processes to a linear central filament that runs equidistant and parallel to the cell membranes. The cross-bridge structures measuring 7 × 14 nm are separated by pores measuring 4 × 40 nm. Advanced

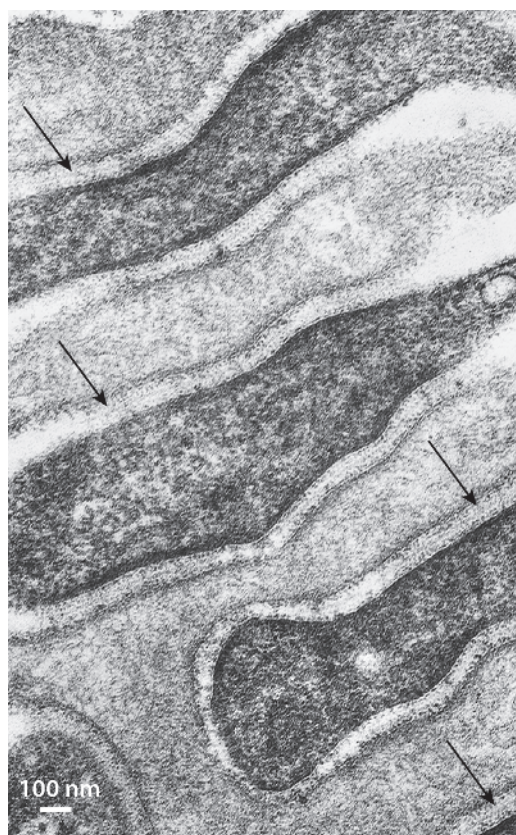


Fig. 2.15 Electron micrograph showing the epithelial foot processes of normal rat glomerulus preserved in a 1% glutaraldehyde solution containing tannic acid. In several areas, the slit diaphragm has been sectioned parallel to the plane of the basement membrane, revealing a highly organized substructure. The thin central filament corresponding to the central dot observed on cross-section (see Fig. 2.11) is indicated by the arrows.

microscopy techniques have provided alternative models and insights into the SD structure. Based on a freeze-etching replica ultrastructural method, it was proposed the SD has a sheetlike rather than a zipper-like substructure.¹¹³ Electron microscope tomography showed the SD to consist of a network of winding cross strands, 30–35 nm in length, which merge centrally into a longitudinal density.¹¹⁴ Although this study generally concurred with the zipper-like model, the pores surrounding the strands appeared more irregular than originally proposed. In contrast, an investigation using enhanced SEM revealed variable-shape pores in the center of the SD and no central filament.¹¹⁵ This finding is more consistent with the SD as a heteroporous structure rather than the zipper-like model. High-resolution helium-ion SEM studies demonstrate the SD with cross-bridging filaments and surrounding pores forming a ladderlike structure in the middle of the filtration slit, also without a distinct central midline, thus generally supporting the heteroporous model.^{116,117} The complexity of the SD is further illustrated by cryo-EM tomographic studies showing distinct cross-bridging strands are composed of different molecules.¹¹⁸ Bridging shorter strands in the lower part of the SD closest to the GBM consist of the nephrin-related protein, Neph1, whereas longer strands in the top part of the SD toward the apical side contain nephrin. This study supports

the existence of a layered bipartite molecular assembly within the SD.

Our understanding of the podocyte role and its SD in the filtration barrier was accelerated with identification of the protein nephrin, encoded by *NPHS1*, the gene mutated in congenital nephrotic syndrome of the Finnish type.¹¹⁹ Nephrin normally localizes to the SD, and its absence in the human congenital syndrome or in transgenic mice leads to loss of the SD, foot process effacement, and massive proteinuria. The SD area or domain of the podocyte includes the SD itself and the adjacent foot process membrane and cytoplasm. An expanding number of proteins localize to the SD domain, where they interact with nephrin and other partners, forming a multiprotein complex. Mutations in over 30 genes, many of which localize to the SD domain and the podocyte actin cytoskeleton, cause human nephrotic syndrome.¹²⁰ For example, mutations or deficiencies of genes encoding SD domain proteins, such as podocin, CD2-associated protein, phospholipase C ϵ 1, and transient receptor potential cation channel type 6, result in SD loss, foot process effacement, and proteinuria. Thus, there is convincing genetic evidence for the essential role of the SD, likely as a size-selective element, in the filtration barrier.

In addition to functioning as a critical structural barrier in filtration, the SD also functions as a signaling hub to regulate actin dynamics.¹²¹ Although the signaling pathways are incompletely understood, nephrin plays a central role. For example, phosphorylation of tyrosine residues within the intracellular domain of nephrin by Fyn kinase results in the recruitment of actin adaptor proteins such as Nck proteins (Nck1 and Nck2), which, in turn, induce actin polymerization.^{122,123} Moreover, Nck protein binding to Fyn promotes increased phosphorylation of nephrin.¹²⁴ Downstream of its interaction with nephrin, Nck directly binds to and activates the neuronal Wiskott-Aldrich syndrome protein (N-WASP), an actin nucleation protein. N-WASP binds and activates the ubiquitously expressed Arp2/3 multiprotein complex, which induces actin polymerization.^{125,126} The importance of this signaling pathway is highlighted by studies showing that intact nephrin phosphorylation and the presence of podocyte Nck and N-WASP proteins are required for an intact filtration barrier of foot processes and stabilization of foot processes.^{127–129} There is also increasing evidence that the phosphorylation state of nephrin plays a role in its endocytic trafficking within the podocyte and is important for turnover and maintenance of the SD.¹³⁰

MESANGIAL CELLS

The mesangial cells and their surrounding matrix constitute the mesangium, which provides a scaffold for the surrounding glomerular capillaries.^{19,131,132} The mesangium is separated from the capillary lumens by the endothelium and is surrounded by the GBM between capillary loops (see Figs. 2.8 and 2.10). Thus, the mesangium directly abuts both the endothelium and the GBM. The points where the GBM no longer encircles the capillary and starts to surround the mesangium are called the “mesangial angles.” Three-dimensional reconstruction studies reveal continuity of the entire mesangium as a continuous arborizing structure within the glomerulus.¹³³ Mesangial cells are located within the central axial region of the mesangium and are irregular in shape with a dense nucleus. They have

elongated cytoplasmic processes that extend toward the endothelium and the adjacent GBM (paramesangial GBM). At the endothelial interface, the fingerlike mesangial cell processes may extend a short distance into the space between the endothelium and GBM. In certain forms of glomerular injury, the mesangial processes may insinuate between the endothelium and GBM for a noticeable distance along the peripheral capillary wall (mesangial interposition). In addition to the usual complement of organelles, mesangial cells possess an extensive array of microfilaments containing actin, myosin, and α -actinin.¹³⁴ The mesangial processes, containing bundles of microfilaments, appear to bridge the gap in the GBM encircling the capillary, adhere to endothelial cells, and interconnect opposing mesangial angles of the GBM. This cell–matrix interconnection is believed to prevent capillary wall distention secondary to elevation of the intracapillary hydraulic pressure.^{134–136}

Several studies have elucidated molecules that mediate the interactions between mesangial cells and other glomerular cells and also the GBM.¹³⁷ Afadin, an F-actin binding protein, localizes to cell contacts between mesangial and endothelial cells, also colocalizes with β -catenin, and may play a role in mesangial cell migration.¹³⁸ Integrin $\alpha 3\beta 1$ and Lu/BCAM are mesangial receptors that mediate adhesion of mesangial cells to the laminin $\alpha 5$ chain in the GBM.¹³⁹ An actin cross-linking protein, EPLIN, is highly expressed in mesangial cell processes at the mesangial angles, where they attach to the GBM.¹⁴⁰ Nephronectin, a protein within the GBM, binds to its receptor a8b1 integrin, produced by mesangial cells to form a GBM–mesangial adhesion at the lateral base (near the mesangial angles) of the capillary loops.¹⁴¹

The mesangium is continuous with the extraglomerular mesangium, a component of the juxtaglomerular apparatus (JGA). The intraglomerular and extraglomerular cells are similar, and gap junctions exist between them.¹⁴² Cells of renin lineage within the extraglomerular mesangium have been shown to migrate and repopulate the mesangium after glomerular injury.¹⁴³

As proposed by Schlondorff,¹⁴⁴ the mesangial cell may have some specialized features of pericytes and possesses many of the functional properties of smooth muscle cells. In addition to providing structural support for the glomerular capillary loops, the mesangial cell has contractile properties and is thought to play a role in the regulation of glomerular filtration.¹⁴⁴ The local generation of autacoids, such as prostaglandin E₂, by the mesangial cell may provide a counterregulatory mechanism to oppose the effect of vasoconstrictors.

Mesangial cells exhibit phagocytic properties and participate in the clearance of macromolecules from the mesangium,^{144,145} as evidenced by the uptake of tracers such as ferritin,¹³¹ colloidal carbon,¹⁴⁶ and aggregated proteins.¹⁴⁷ Mesangial cells are also involved in the generation and metabolism of the extracellular mesangial matrix.^{144,148} Because of both their distinct anatomic localization and their production of various vasoactive substances (e.g., nitric oxide), growth factors (e.g., VEGF, platelet-derived growth factor [PDGF], transforming growth factor [TGF]), and cytokines and chemokines (interleukins, chemokine [C-X-C motif] ligand 1, chemokine [C-C motif] ligand [CCLs]), mesangial cells are also perfectly suited to mediate an extensive crosstalk to both endothelial cells and podocytes to control and maintain glomerular function.¹⁴⁹ The PDGF-B isoform, the main ligand for the

receptor PDGFR- β , is a potent mitogen for mesangial cell proliferation, and genetic deletion of PDGF-B and PDGFR- β results in an absence of mesangial cells and mesangium.¹⁵⁰ As such, the mesangial cells also importantly contribute to a number of glomerular diseases, including IgA nephropathy and diabetic nephropathy.

The mesangial cell is surrounded by a matrix that is similar to but not identical with the GBM; the mesangial matrix is more coarsely fibrillar and slightly less electron dense. The presence of abundant thin microfibrils, best observed with tannic acid staining, likely explains the fibrillary character of the mesangial matrix.¹⁵¹ Fibrillin-1 is the major protein of the microfibrils, but other associated proteins include microfibril-associated glycoproteins 1 and 2 and latent TGF-binding protein-1.^{152,153} Fibrillin-1 and $\alpha 8$ integrin colocalize in the mesangium and appear to interact to regulate mesangial adhesion.¹⁵⁴

The mesangial matrix also contains fibronectin, type IV collagen $\alpha 1$ and $\alpha 2$ chains (not type IV $\alpha 3$, $\alpha 4$, or $\alpha 5$ chains, which are present in the GBM), type V collagen, various laminin isoforms (not laminin-521, which is present in the GBM), and the proteoglycan perlecan (not the proteoglycan agrin, which is present in the GBM). For example, laminin $\alpha 1$ is present in the mesangial matrix (not the GBM), and studies suggest it regulates mesangial cell homeostasis and matrix deposition by inhibiting TGF- β /Smad pathway signaling.¹⁵⁵ Several cell surface receptors of the β -integrin family have been identified on the mesangial cells, including $\alpha 1\beta 1$, $\alpha 3\beta 1$, and the fibronectin receptor, $\alpha 5\beta 1$.^{156–158} These integrins mediate attachment of the mesangial cells to specific molecules in the extracellular mesangial matrix and link the matrix to the cytoskeleton. The attachment to the mesangial matrix is important for cell anchorage, contraction, and migration; ligand–integrin binding also serves as a signal transduction mechanism that regulates the production of extracellular matrix as well as the synthesis of various vasoactive mediators, growth factors, and cytokines.^{148,159}

PARIETAL EPITHELIAL CELLS

The parietal epithelium, which lines the inner aspect of Bowman's capsule, consists of flat squamous-like cells known as PECs (parietal epithelial cells) (Fig. 2.10).¹⁹ At the urinary pole, there is an abrupt transition from the PECs to the taller cuboidal cells of the proximal tubule, which has a well-developed brush border (Fig. 2.16). The PECs are 0.1 to 0.3 μm in height, except at the nucleus, where they increase to 2.0 to 3.5 μm . Each cell has a long cilium, and organelles are generally sparse but include small mitochondria, numerous vesicles of 40 to 90 nm in diameter, and the Golgi apparatus. Large vacuoles and multivesicular bodies are rare. PECs express Pax-2 and claudin-1. The thickness of the basement membrane of Bowman's capsule varies from 1200 to 1500 nm.¹⁹ The basement membrane often has a lamellated appearance and increases in thickness with disease processes. At both the vascular pole and the urinary pole, the thickness of Bowman's capsule decreases markedly. In contrast to the GBM, the basement membrane of the capsule contains the $\alpha 6$ chain of type IV collagen, which is part of the $\alpha 1\alpha 2\alpha 1$ (IV)- $\alpha 5\alpha 6\alpha 5$ (IV) protomer network.

PECs function as a permeability barrier for the urinary filtrate. In experimental glomerulonephritis, this barrier is

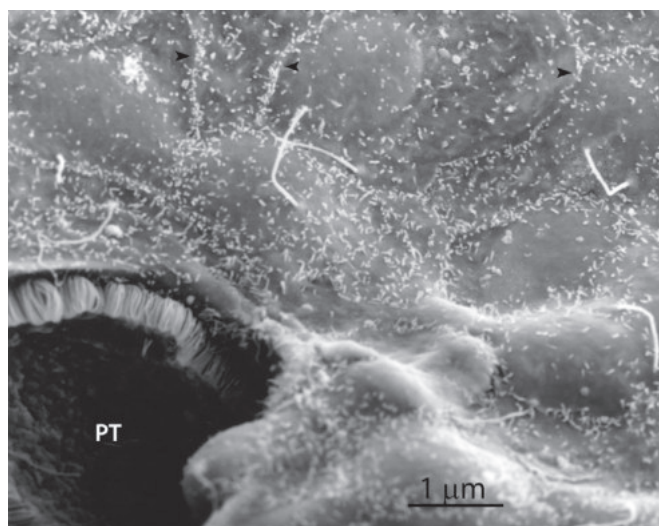


Fig. 2.16 Scanning electron micrograph showing the surface of the parietal epithelial cells adjacent to the early proximal tubule (PT) at the urinary pole. Parietal epithelial cells have single cilia, and their lateral cell margins are accentuated by short microvilli (arrowheads).

compromised, and macromolecules can leak into the space between the PECs and the basement membrane of Bowman's capsule and subsequently into the periglomerular space.¹⁶⁰ Several investigations suggest different populations of PECs exist.¹⁶¹ Cells located at the glomerular vascular pole interposed between the PECs and podocytes have been called “peripolar cells.”¹⁶² By electron microscopy, these cells have prominent cytoplasmic granules, and display an immunophenotype between PECs and podocytes and are currently called “transitional cells.”^{163,164} Their function is unknown. Other cells lining Bowman's capsule near the vascular pole expressing podocyte markers and forming interdigitating foot processes are called “parietal podocytes” (or “ectopic podocytes”).^{163,165} In glomerular disease, PECs may transform into cuboidal cells with enlarged nuclei and express CD44.¹⁶⁶ These “activated PECs” demonstrate proliferation, migration, and matrix deposition and play a role in diseases such as focal segmental glomerulosclerosis.

Several studies have addressed the role of PECs as possible progenitor cells to renew podocytes.¹⁶⁷ These various investigations using different experimental mouse models of podocyte depletion and genetic labeling methods have shown that PECs may serve as podocyte progenitor cells, transdifferentiating into podocytes, which repopulate the glomerular tuft.^{164,168–170} In some studies of experimental glomerular injury, a subpopulation of podocytes actually migrates to Bowman's capsule and expresses PEC markers.^{171–173} An understanding of these bidirectional differentiation pathways involving PECs and podocytes awaits further investigations.

JUXTAGLOMERULAR APPARATUS

The JGA is located at the vascular pole of the glomerulus, where the TAL of loop of Henle comes into contact with its parent glomerulus. It represents a major structural component

of the renin–angiotensin system and contributes to the regulation of glomerular arteriolar resistance and glomerular filtration.¹⁷⁴

The JGA has vascular and tubular components. The vascular components are the terminal portion of the afferent arteriole, the initial portion of the efferent arteriole, and the extraglomerular mesangium. The tubular component is the macula densa, located in the terminal portion of the TAL that lies between the afferent and efferent arterioles, in contact with the extraglomerular mesangium.^{175–177} The extraglomerular mesangium, also called the polar cushion (polkissen) or the lacis, is bounded by the macula densa, the specialized regions of the afferent and efferent glomerular arterioles at their junction with the glomerular tuft, and the mesangial cells of the glomerular tuft (the intraglomerular mesangial cells). Specialized cell types of the JGA include the juxtaglomerular granular cells, the agranular extraglomerular mesangial cells, and the epithelial cells that make up the macula densa.

JUXTAGLOMERULAR GRANULAR CELLS

The juxtaglomerular granular cells are located primarily in the walls of the afferent and, less commonly, the efferent arterioles.^{176–179} They exhibit features of both smooth muscle

cells and secretory epithelial cells and therefore have been called epithelioid or myoepithelial cells.¹⁷⁶ They contain myofilaments in the cytoplasm, a well-developed endoplasmic reticulum, and small “proteogranules” with a crystalline substructure in the Golgi complex.^{176,180} The signature feature of juxtaglomerular cells is the numerous electron-dense, membrane-bound granules of variable size and shape (Fig. 2.17),¹⁷⁹ which contain the aspartyl protease renin.^{179,181} In addition to renin granules, lipofuscin-like granules are common in juxtaglomerular cells in the human kidney, as well as in extraglomerular mesangial cells.^{178,180}

In addition to renin, the juxtaglomerular granular cells express angiotensin II, which localizes in the same granules as renin¹⁷⁹ and has highest activity in the afferent arteriole.¹⁸² Like lysosomes, renin-containing granules have an acid pH and contain lysosomal enzymes, including acid phosphatases and cathepsin B, and have the capacity to take up and degrade internalized material.^{142,179,183} During kidney development, renin expression is present in the intrarenal arteries, but by adulthood in normal conditions, renin granules are largely found only in juxtaglomerular granular cells in the distal afferent arteriole.¹⁸⁴ Nonetheless, in adults, renin expression may again extend into more proximal arterial portions in some conditions, such as extravascular volume depletion, hypotension, and hemorrhage.^{185–187}

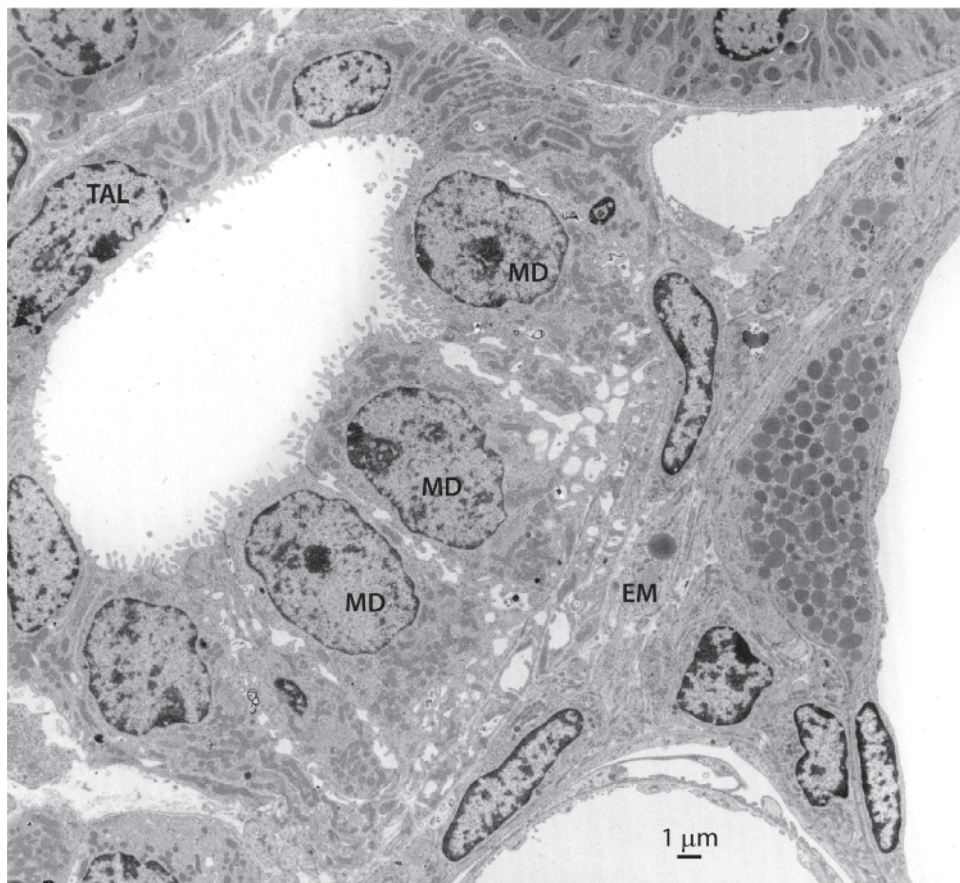


Fig. 2.17 Transmission electron micrograph of juxtaglomerular apparatus from a rabbit kidney, illustrating macula densa (MD), extraglomerular mesangium (EM), and a portion of an arteriole (on the right), containing numerous electron-dense granules. Macula densa cells are significantly taller and narrower than the adjacent thick ascending limb (TAL) cells.

EXTRAGLOMERULAR MESANGIUM

Located between the afferent and efferent arterioles in close contact with the macula densa (see Fig. 2.17), the extraglomerular mesangium is continuous with the intraglomerular mesangium and is composed of cells that are similar in ultrastructure to the mesangial cells.^{176,177} The extraglomerular mesangial cells possess long, thin cytoplasmic processes separated by basement membrane material. Although not typical, extraglomerular mesangial cells occasionally contain renin granules. The extraglomerular mesangial cells are in contact with the afferent and efferent arterioles and the macula densa, and gap junctions are commonly observed between the various cells of the vascular portion of the JGA.^{142,188} Gap junctions, formed at least in part from connexin 40,¹⁸⁹ exist between extraglomerular and intraglomerular mesangial cells, enabling signaling to be conveyed from the macula densa through the extraglomerular mesangium to the glomerulus.^{142,190} Moreover, there is evidence that altered gap junction structure and function may eliminate the tubuloglomerular feedback response.^{190,191}

MACULA DENSA

The macula densa is a specialized region in the TAL adjacent to the hilum of the parent glomerulus (see Figs. 2.8 and 2.17). Macula densa cells are morphologically distinct from the surrounding cells of the TAL. They are columnar cells with large, apically placed nuclei, although there are considerable species differences in the height of macula densa cells. Compared with TAL cells, macula densa cells have relatively little cytoplasm, few basolateral plasma membrane infoldings, and lower mitochondrial density; mitochondria are small and either scattered (rat) or basal to the nucleus (human), and rarely enclosed within basolateral plasma membrane infoldings. The Golgi apparatus is lateral to and beneath the cell nucleus and other cell organelles, including lysosomes, autophagic vacuoles, ribosomes, and smooth and rough endoplasmic reticulum, and also is located principally beneath the cell nucleus. Basal cytoplasmic extensions contact the vascular elements, and at these points, the macula densa basement membrane is fused with basement membrane of the vascular elements.^{175,176} Macula densa cells lack the lateral cell processes and interdigitations that are characteristic of the TAL, and the width of the lateral intercellular spaces varies with the physiologic state of the animal.¹⁹²

PROXIMAL TUBULE

The proximal tubule consists of the proximal convoluted tubule (PCT, pars convoluta), which originates at the glomerular urinary pole and is located in the cortical labyrinth, and the PST, pars recta, which is distal to the PCT and located in the medullary ray in the cortex and extending through the outer stripe of the outer medulla (see Fig. 2.5). The proximal tubule length varies among species, measured at ~10 mm in rabbits,¹⁹³ ~8 mm in rats, 4 to 5 mm in mice,¹⁵ and ~14 mm in humans.¹⁹⁴ The volume density of proximal tubules in the cortex is greater in males than females in rats and mice^{195,196}; in mice, proximal tubules account for ~60% of the cortical volume in males and only ~40% in females.¹⁹⁵

These structural differences correlate with sexual dimorphism in proximal tubule transporter expression.¹⁹⁷

In the rat¹⁹⁸ and the rhesus monkey,¹⁹⁹ three morphologically distinct segments—S1, S2, and S3—have been identified based on their ultrastructural characteristics^{198,200,201} (Figs. 2.18–2.20). The S1 segment is the initial portion of the proximal tubule; it begins at the glomerulus (see Figs. 2.7 and 2.16) and constitutes approximately two-thirds of the PCT in rat. The S2 segment contains the distal third of the PCT and the initial portion of the PST. The S3 segment is the remainder of the PST, located in the deep inner cortex and the outer stripe of the outer medulla.

Ultrastructurally, S1 cells have a tall brush border, a well-developed vacuolar–lysosomal system, and extensive lateral plasma membrane invaginations and lateral cell processes, which extend from the apical to the basal surface and interdigitate with processes from adjacent cells. Elongated mitochondria are located in the lateral cell processes near the plasma membrane. The ultrastructure of S2 cells is similar, except the brush border is shorter, the basolateral invaginations are less prominent, and the mitochondria are smaller. Numerous small processes, termed “micropedici” (little feet), are located close to the base of the cell. The endocytic compartment is less prominent than in the S1 segment, with the number and size of the lysosomes varying among species and between males and females, being more abundant and larger in males.^{193,198}

In rat kidney, where the S1, S2, and S3 designations were first described, S3 cells are characterized by a long brush border; few lateral cell processes and invaginations; small, randomly distributed mitochondria; and small and sparse endocytic vacuoles and lysosomes.¹⁹⁸ Peroxisomes are present throughout the proximal tubule, although they are more abundant in the straight portion of S2 and in S3 compared with S1.¹⁹⁸

The S1, S2, and S3 designations were originally defined based on ultrastructural characteristics in the rat kidney, and due to variations in the ultrastructure among species, these terms are only properly applied to particular species. For example, the late PST has a relatively short brush border in humans¹⁹⁴ and large endocytic vacuoles and numerous small lysosomes in rabbits.¹⁹³ In rabbits, the S2 segment represents a transition between the S1 and S3 segments.^{202,203} A morphometric study in mice found no structural segmentation in the cortical segments of the proximal tubule¹⁵; however, variations in the length of the brush border are evident among mouse proximal tubule profiles in the cortex, and the PST in the outer stripe of the outer medulla typically has a longer brush border compared with most cortical segments. Furthermore, the mouse proximal tubule exhibits clear axial heterogeneity in expression of certain proteins, such as the electrogenic sodium bicarbonate cotransporter splice variant 1-A (NBCe1-A), which is abundant in the basolateral plasma membrane in the PCT and early PST in the cortex, but undetectable in the PST in the outer medulla²⁰⁴ and the basolateral glutamine transporter, SN1 (SNAT3), which is confined to the PST in the outer medulla and medullary ray under basal conditions, but not detectable in PCT.^{205,206} In the nondiseased human kidney, only the PCT and the PST have been positively identified and described.¹⁹⁴ Thus, the terms PCT and PST will be used hereafter unless the S1–S3 terminology is specifically intended.

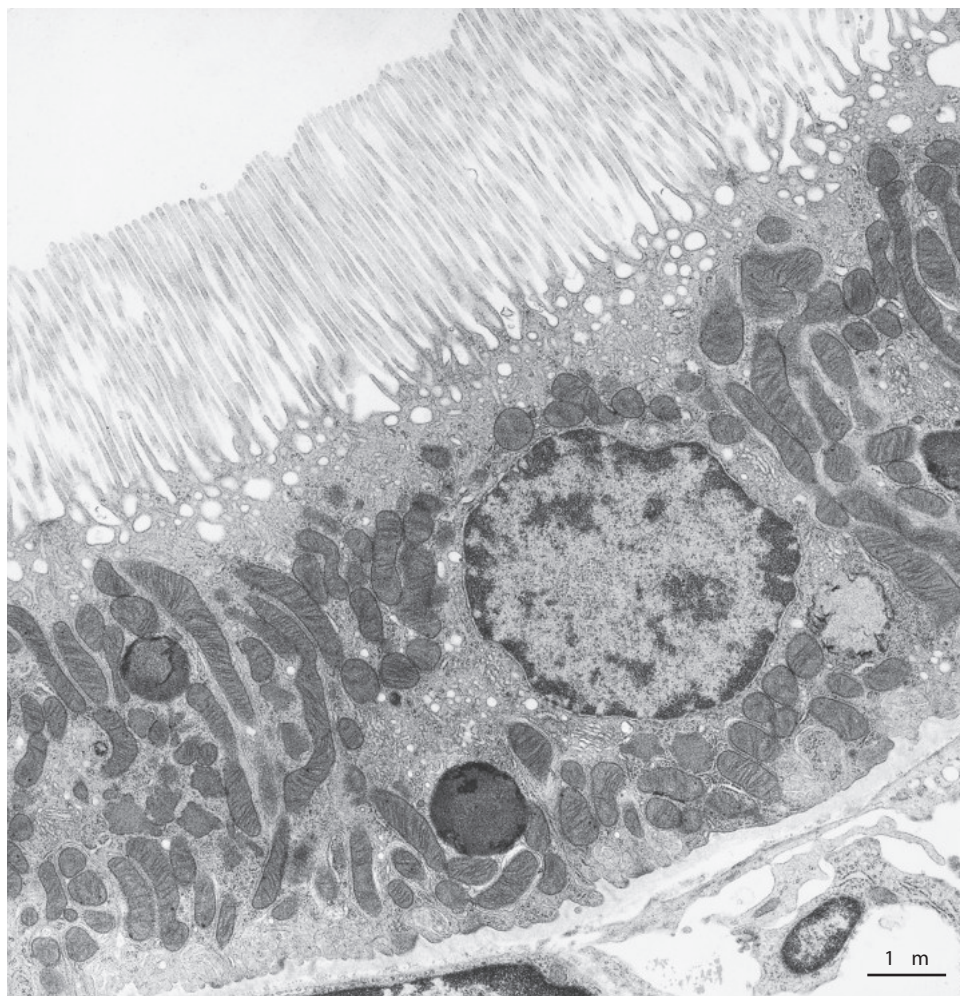


Fig. 2.18 Transmission electron micrograph of the S1 segment of a rat proximal tubule. The cells are characterized by a tall brush border, a prominent endocytic–lysosomal apparatus, and extensive invaginations of the basolateral plasma membrane with numerous long mitochondria aligned among the basolateral plasma membrane infoldings.

PROXIMAL CONVOLUTED TUBULE

Cells of the PCT are structurally complex.^{202,207,208} Large primary ridges extend laterally from the apical to the basal surfaces of the cells. Large lateral processes, often containing mitochondria, extend outward from the primary ridges and interdigitate with similar processes in adjacent cells (Fig. 2.21). Near the luminal surfaces of the cells, smaller lateral processes extend from the primary ridges to interdigitate with those of adjacent cells. Small basal villi that do not contain mitochondria are found along the basal cell surfaces (Figs. 2.18, 2.19, 2.21, and 2.22). These extensive interdigitations result in a complex extracellular compartment, the basolateral intercellular space (Figs. 2.21–2.23), which is separated from the tubule lumen (apical cell surface) by the tight junctions (zonula occludens).²⁰⁹ Proximal tubule tight junctions express specific claudin proteins, which confer specific ion permeabilities and likely contribute to the high rates of paracellular sodium and water transport.^{210–212} Below the tight junction lies the belt-like intermediate junction, the zonula adherens,²⁰⁹ followed by several desmosomes distributed randomly at variable distances beneath the intermediate junction. In mammalian and invertebrate renal proximal tubules, gap

junctions are present in small numbers²¹³ and can provide a pathway for the movement of ions between cells and for cell–cell communication via a family of proteins known as connexins.²¹⁴ The lateral intercellular space of each PCT cell is open at the basement membrane, which separates the cell from the peritubular interstitium and capillaries. The thickness of the basement membrane gradually decreases along the proximal tubule. For example, in the rhesus monkey, the basement membrane thickness is approximately 250 nm, 145 nm, and 70 nm in the S1, S2, and S3 segments, respectively.¹⁹⁹

The lateral cell processes of PCT cells combined with extensive invaginations of the plasma membrane increase both the intercellular space and surface area of the basolateral plasma membrane. In rabbits, the area of the lateral surface equals that of the luminal surface and amounts to 2.9 mm² per mm of tubule.²¹⁵ Elongated mitochondria are located in the lateral cell processes near the plasma membrane (see Figs. 2.18 and 2.23), where sodium–potassium adenosine triphosphatase (Na⁺-K⁺-ATPase) resides.^{216,217} Although mitochondria often appear rod-shaped in two-dimensional images, many mitochondria are branched and connected with one another.²¹⁸ A system of smooth membranes, the

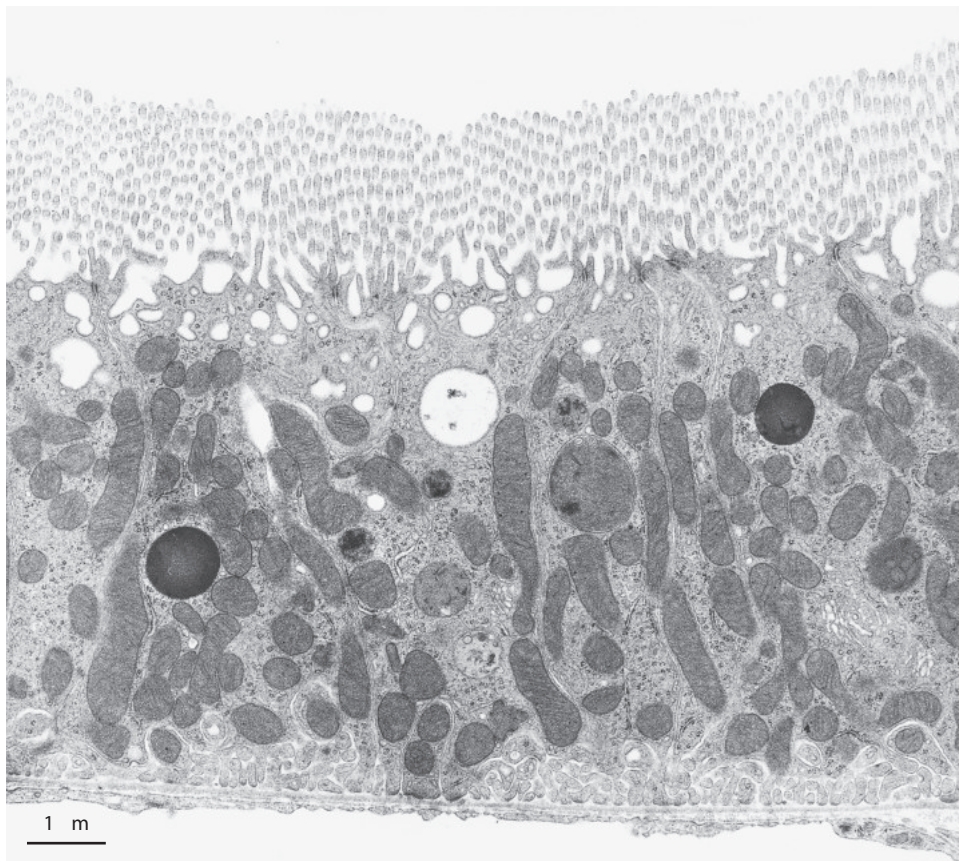


Fig. 2.19 Transmission electron micrograph of the S2 segment of a rat proximal tubule. The brush border is shorter than in the S1 segment. Mitochondria are numerous and generally aligned with the basolateral plasma membrane infoldings. There are numerous small lateral processes at the base of the cell.

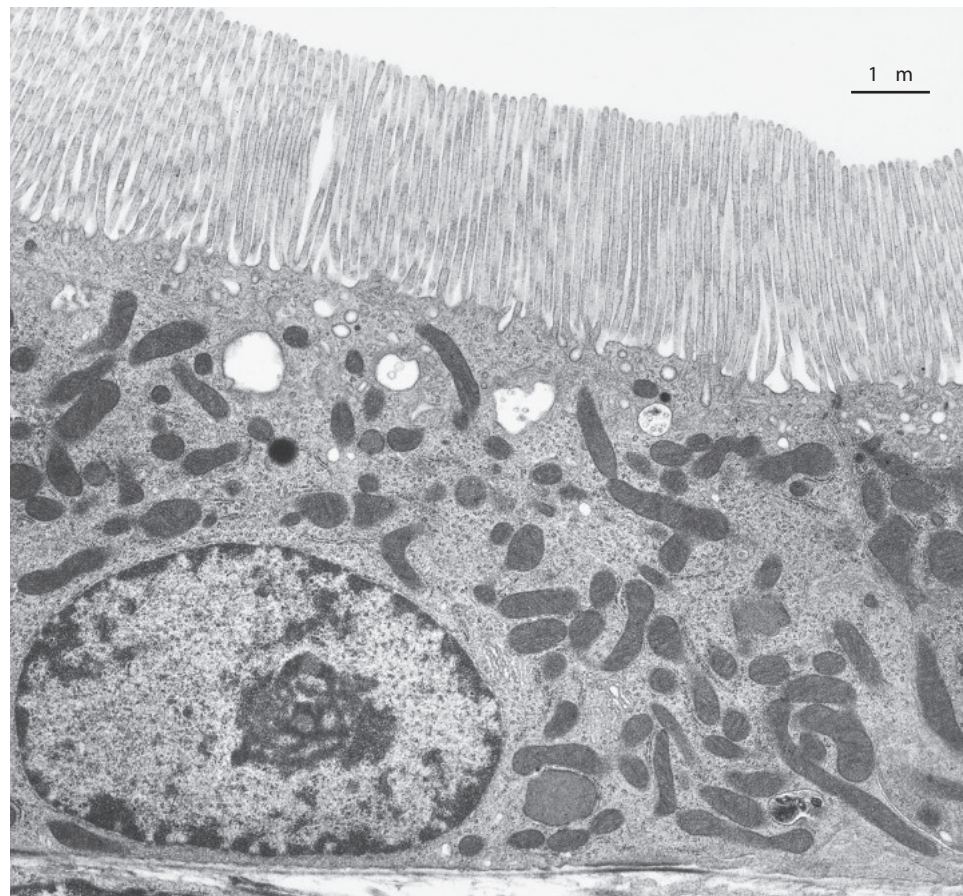


Fig. 2.20 Transmission electron micrograph of the S3 segment of a rat proximal tubule. The brush border is tall, but the endocytic-lysosomal apparatus is less prominent than in the S1 and S2 segments. Basolateral invaginations are sparse, and mitochondria are scattered randomly throughout the cytoplasm.

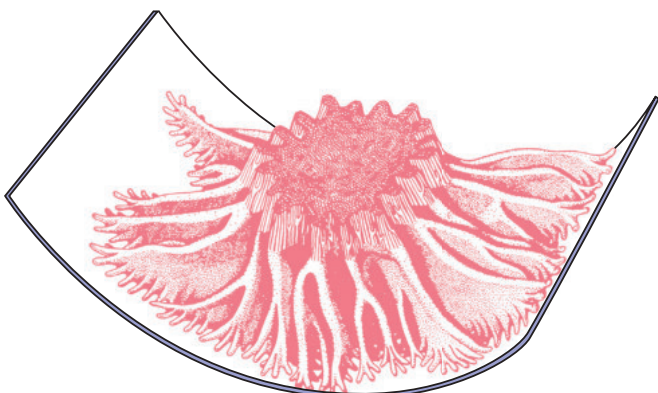


Fig. 2.21 Schematic drawing illustrating the three-dimensional configuration of the proximal convoluted tubule cell. (From Welling LW, Welling DJ. Shape of epithelial cells and intercellular channels in the rabbit proximal nephron. *Kidney Int.* 1976;9:385–394.)

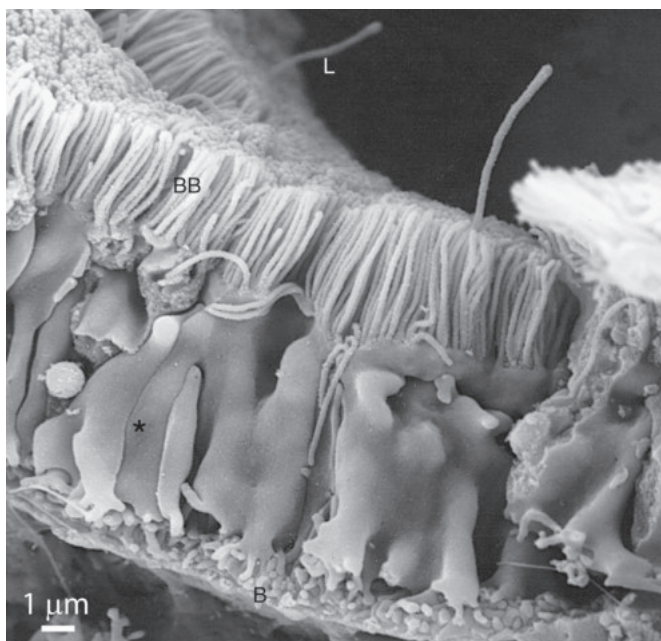


Fig. 2.22 Scanning electron micrograph of rat proximal convoluted tubule, illustrating the lush brush border (BB), primary cilia extending into the lumen, prominent lateral cell processes, and multiple small basal processes (B), called micropedici. (Modified from Verlander JW. Solute reabsorption. In Cunningham's Veterinary Physiology, 6th ed. St Louis: Elsevier; In press.)

paramembranous cisternal system, which may be in continuity with the smooth endoplasmic reticulum, is often observed between the plasma membrane and mitochondria. PCT cells contain large quantities of smooth and rough endoplasmic reticulum, and free ribosomes are abundant. A well-developed Golgi apparatus, composed of smooth-surfaced sacs or cisternae, coated vesicles, uncoated vesicles, and larger vacuoles, is located above and lateral to the nucleus. In addition, an extensive system of microtubules is located throughout the cytoplasm of proximal tubule cells.

PCT cells have lush luminal brush borders formed by densely packed, fingerlike projections of the apical plasma

membranes, the microvilli. The brush border greatly increases the apical cell surface,²¹⁵ increasing the absorptive surface facing the luminal fluid. Each microvillus contains 6 to 10 actin filaments of approximately 6 nm in diameter that extend variable distances into the cell body. A network of filaments containing myosin and spectrin,²¹⁹ the terminal web, is located in the apical cytoplasm just beneath and perpendicular to the microvilli.²²⁰ Each PCT cell has a well-developed endocytic–lysosomal apparatus that is involved in the reabsorption of macromolecules from the ultrafiltrate and their degradation.^{221,222} The endocytic compartment includes an extensive system of coated pits, small coated vesicles, apical dense tubules, and larger endocytic vacuoles without a cytoplasmic coat (Fig. 2.24). The coated pits are invaginations of the apical plasma membrane at the base of the microvilli and contain clathrin,²¹⁹ megalin,^{223–225} and cubilin,²²⁵ proteins that are involved in receptor-mediated endocytosis. The cytoplasmic coat of the small vesicles is similar in ultrastructure to the coat that is present on the cytoplasmic side of the coated pits.

PCT cells contain numerous lysosomes of variable size, shape, and ultrastructural appearance (Fig. 2.25).^{221,226} Lysosomes are membrane-bound, heterogeneous organelles that contain proteases, lipases, glycosidases, and acid hydrolases, including acid phosphatases. Lysosomes degrade material absorbed by endocytosis (heterophagocytosis) and often contain electron-dense deposits that are believed to represent reabsorbed substances such as proteins (see Figs. 2.19 and 2.25). Lysosomes also participate in the normal turnover of intracellular constituents by autophagocytosis, and autophagic vacuoles containing fragments of cell organelles are often seen in PCT cells.²²⁶ Lysosomes containing nondigestible substances are called residual bodies; these can empty their contents into the tubule lumen by exocytosis. Multivesicular bodies (MVBs), which are part of the vacuolar–lysosomal system, are often observed in the cytoplasm of PCT cells. MVBs were originally thought to be involved in membrane retrieval and/or membrane disposal, but later studies suggest that MVBs may provide an exit route for plasma membrane vesicles formed by endocytosis and could function as a signaling mechanism to downstream nephron segments.^{227,228} The extensive vacuolar–lysosomal system of proximal tubule cells plays an important role in the reabsorption and degradation of albumin and low-molecular-weight plasma proteins from the glomerular filtrate.^{221,229,230} Under normal conditions, the vacuolar–lysosomal system is most prominent in the PCT, but in proteinuric states, large vacuoles and extensive lysosomes can be observed in the PST as well.^{193,198}

PROXIMAL STRAIGHT TUBULE

In the rat, the proximal straight tubule (PST, pars recta) includes the terminal portion of the S2 segment, located in the medullary ray, and the entire S3 segment. PST morphology varies considerably among species. For example, the rat S3 brush border measures up to 4 μm long, whereas in the rabbit and human PST, the brush border is relatively short. The S3 epithelium is simpler than both the S1 and S2 segments.^{198,202} Basolateral plasma membrane invaginations are virtually absent, mitochondria are small and randomly scattered throughout the cytoplasm, and intercellular spaces



Fig. 2.23 Transmission electron micrograph of the proximal convoluted tubule from a normal human kidney. The mitochondria (*M*) are elongated and tortuous, occasionally doubling back on themselves. The endocytic apparatus, composed of apical vacuoles (*AV*), apical vesicles (*V*), and apical dense tubules (*arrows*), is well developed. *G*, Golgi apparatus; *IS*, intercellular space; *L*, lysosome; *Mv*, microvilli forming the brush border; *TL*, tubule lumen.

are smaller and less complex (Figs. 2.20 and 2.26). These morphologic characteristics are in agreement with studies demonstrating that Na^+/K^+ -ATPase activity is significantly less in the PST compared to PCT.²³¹ In contrast to PCT cells, the vacuolar–lysosomal system is less prominent in rat S3 cells, although in both rabbits and humans, many small lysosomes containing electron-dense membranelike material are present in the late PST.^{193,194,232} Peroxisomes are common in the PST (Fig. 2.27). In contrast to lysosomes, peroxisomes are irregular in shape, are surrounded by a 6.5-nm-thick membrane, and do not contain acid hydrolases.²²⁶ Peroxisomes within the PST vary considerably in appearance among species. In the rat, small, circular profiles are visible by transmission electron microscopy just inside the limiting membrane, and rod-shaped

structures often project outward from the organelle. In addition, a small nucleoid is often present in peroxisomes in the PST. Peroxisomes contain abundant catalase, which is involved in the degradation of hydrogen peroxide, and various oxidative enzymes, including l- α -hydroxy-acid oxidase and D-amino acid oxidase.^{233,234}

The proximal tubule plays a major role in the reabsorption of Na^+ , HCO_3^- , Cl^- , K^+ , Ca^{2+} , PO_4^{3-} , water, and organic solutes such as vitamins, glucose, and amino acids; secretion of protons, ammonia, and organic anions; and uptake of filtered peptides and proteins. The ultrastructural features of proximal tubule cells aid in these transport processes, most notably the high surface density of both the apical and basolateral plasma membrane compartments, the high mitochondrial



Fig. 2.24 Transmission electron micrograph of the apical region of a human proximal tubule, illustrating the endocytic apparatus, including coated pits (Cp), coated vesicles (Cv), apical dense tubules (Dat), and endosomes (E).

density in early proximal tubule segments, and the abundant endocytic vesicles and lysosomal system. Proximal tubule cells alter transport capacity in some instances by redistribution of specific transporters located in the brush border. For example, the apical sodium–hydrogen exchanger, NHE3, is rapidly redistributed between the brush border microvilli and the base of the microvilli in models that alter proximal tubule sodium uptake,^{235,236} whereas parathyroid hormone stimulates redistribution of the sodium phosphate transporter, NaPi-2, from the microvilli to endosomes.²³⁶ Changes in the hydraulic and oncotic pressures across the tubule and capillary wall cause significant ultrastructural changes in the proximal tubule, especially in the configuration of the lateral intercellular spaces.^{237,238}

THIN LIMBS OF THE LOOP OF HENLE

The thin limbs of the loop of Henle connect the proximal and distal tubules of the nephron. The thin limbs arise

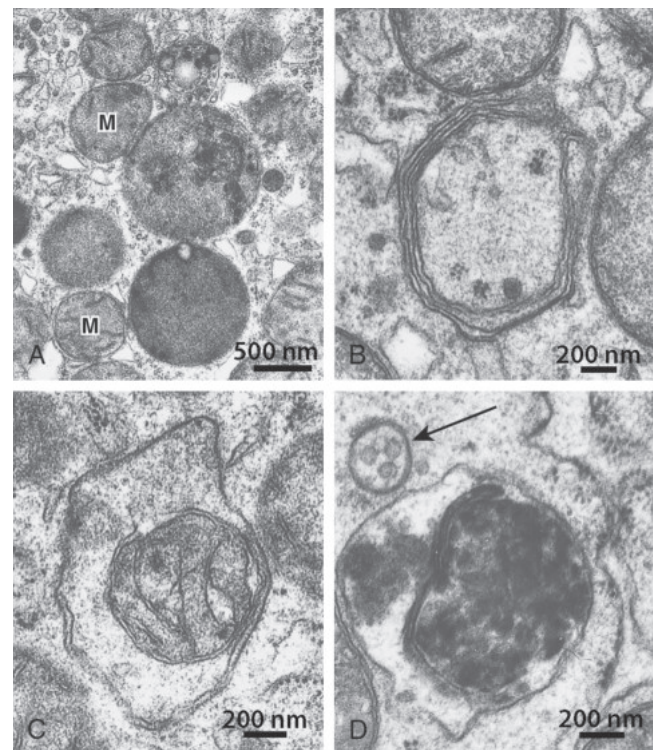


Fig. 2.25 Transmission electron micrographs illustrating the appearance of different types of lysosomes from human proximal tubules. (A) Lysosomes. Several mitochondria (M) are also shown. (B) Early stage of formation of an autophagic vacuole. (C) Fully formed autolyso- some containing a mitochondrion undergoing digestion. (D) Autolyso- some containing a microbody undergoing digestion. A multivesicular body (arrow) is also shown. (From Tisher CC, Bulger RE, Trump BF. Human renal ultrastructure. I: Proximal tubule of healthy individuals. *Lab Invest*. 1966;15:1357–1394.)

abruptly from the distal end of the PST, descend a variable distance, make a hairpin turn, and ascend to the abrupt transition to the TAL. The transition from the proximal tubule to the descending thin limb (Figs. 2.5, 2.6, 2.28, and 2.29) defines the boundary between the outer and inner stripes of the outer medulla, and the transition from the thin ascending limb to the thick ascending limb defines the boundary between the outer and inner medulla (see Figs. 2.5 and 2.6). Short-looped nephrons, which originate from superficial and midcortical glomeruli, have a short descending thin limb that transitions to the TAL at the hairpin turn near the border of the outer and inner medulla. Long-looped nephrons, which originate from juxamedullary glomeruli, have long descending and ascending thin limbs connected by a hairpin turn located at variable depths in the inner medulla. Nephrons arising in the extreme outer cortex have only short cortical loops that do not extend into the medulla. Although these features are generally consistent among mammalian species, detailed studies of the organization of the renal medulla in several laboratory animals, including 3D reconstruction studies, have described variations among species in the length and ultrastructure of the thin-limb segments.^{13,239}

There are four types of thin-limb epithelia, types I through IV, based on ultrastructural characteristics^{240–244} (Fig. 2.30).

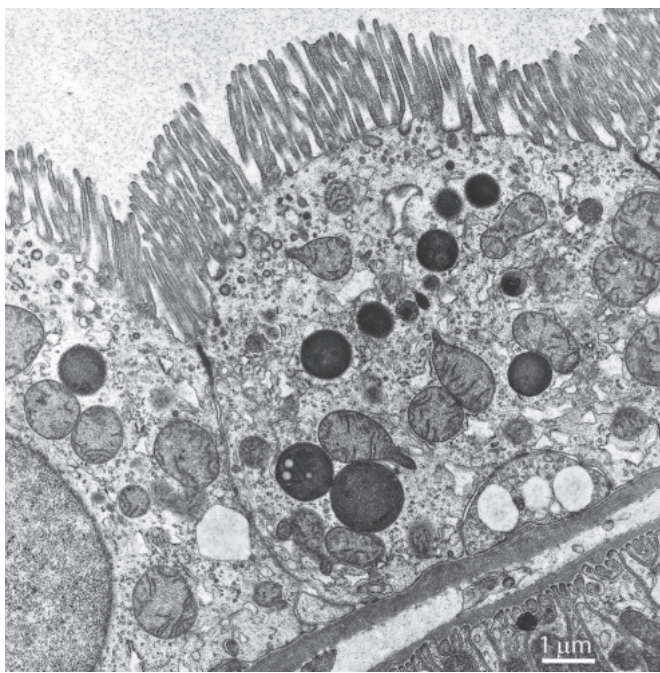


Fig. 2.26 Low-magnification transmission electron micrograph of a segment of the proximal straight tubule from a human kidney. The microvilli on the convex apical cell surface are not as long as those in the rat proximal straight tubule. The lysosomes are extremely electron dense. The clear, single membrane-limited structures at the base of the cell to the right represent lipid droplets. (Courtesy R.E. Bulger, PhD.)

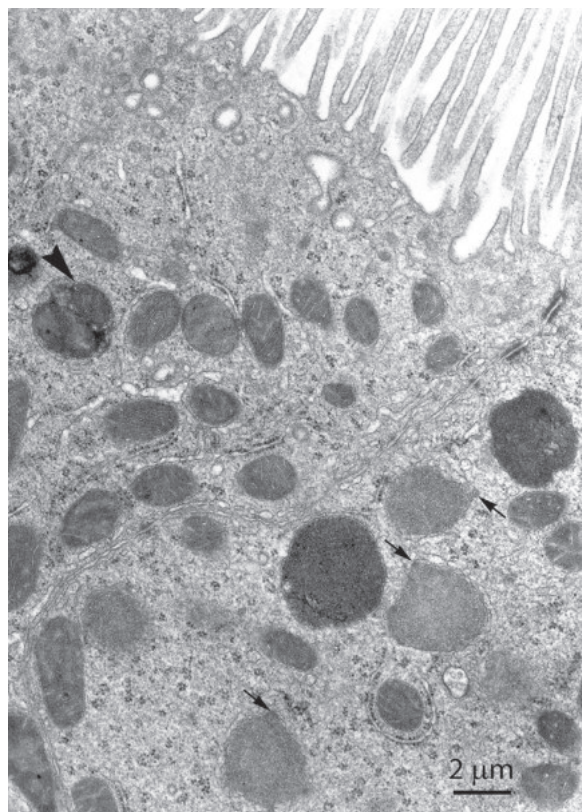


Fig. 2.27 Transmission electron micrograph of the rat proximal straight tubule, S3 segment. Endocytic vesicles, lysosomes, and autophagic vacuoles (arrowhead) are less abundant than in S1 and S2 segments. However, peroxisomes are abundant and identified by their irregular, angular shape and small, circular protuberances along the edges (arrows).

Type I epithelium is found exclusively in the descending thin limb of short-looped nephrons. It is extremely thin, and both the apical and basolateral plasma membranes are relatively smooth, with few apical microplications and few basolateral infoldings. Lateral interdigitations and cellular organelles are sparse. Tight junctions are intermediate in depth with several junctional strands, characteristics of a tight epithelium.^{245–247}

The descending thin limb of long-looped nephrons contains type II epithelium in the outer medulla and type III epithelium in the inner medulla. Type II epithelium is taller than type I epithelium and exhibits considerable species differences. In the rat,²⁴⁸ mouse,²⁴⁰ *Psammomys obesus*,²⁴⁴ and hamster,²⁴² the type II epithelium has extensive lateral and basal interdigitations (Fig. 2.31). The tight junctions are extremely shallow and contain a single junctional strand, characteristics of a “leaky” epithelium. Short, blunt microvilli cover the luminal surface. Cell organelles, including mitochondria, are more prominent than in other segments of the thin limb. In the rabbit the type II epithelium is less complex,²⁰² lateral interdigitations are less prominent, and tight junctions are deeper.²⁴⁷

Compared with type II epithelium, type III epithelium is thinner and simpler in structure. The cells do not interdigitate, the tight junctions are intermediate in depth, and there are fewer luminal surface microplications (Figs. 2.30 and 2.32). Type IV epithelium forms the bends of the long loops and the entire ascending thin limb. Type IV epithelium (Figs. 2.30 and 2.32) is generally low and flat and has relatively few organelles. It has few surface microplications but abundant lateral cell processes and interdigitations.

The tight junctions are shallow, characteristic of a leaky epithelium.

Thin limb segments exhibit specific expression patterns for several transport proteins, including Na^+/K^+ -ATPase, the water channel, aquaporin-1 (AQP1), and the urea transporter, UT-A2. Correlating to its more complex structural features, the rat type II epithelium has significantly greater Na^+/K^+ -ATPase protein expression²⁴⁹ and activity²⁵⁰ compared with other descending thin limb segments. In rabbit, the type II thin limb does not have complex basolateral plasma membrane infoldings and, like all segments of the rabbit thin limb, has very low Na^+/K^+ -ATPase activity.²⁵¹ AQP1^{239,252,253} and the urea transporter, UT-A2,^{254–256} are expressed in specific segmental patterns, exclusively in the descending thin limbs. However, in the Munich-Wistar rat, segments with structural features and immunoreactivity for AQP1 and UT-A2 typical of descending thin limbs are intermingled with segments typical of ascending limbs.²⁵⁷

The 3D arrangement of the inner medulla has been characterized in detailed structural studies, documenting the spatial organization of specific thin limb segments relative to vasa recta and collecting ducts in the medulla, which, along with the specific transport properties of the thin limb segments, is believed to be a necessary element of the urine concentrating mechanism.^{13,258–267}

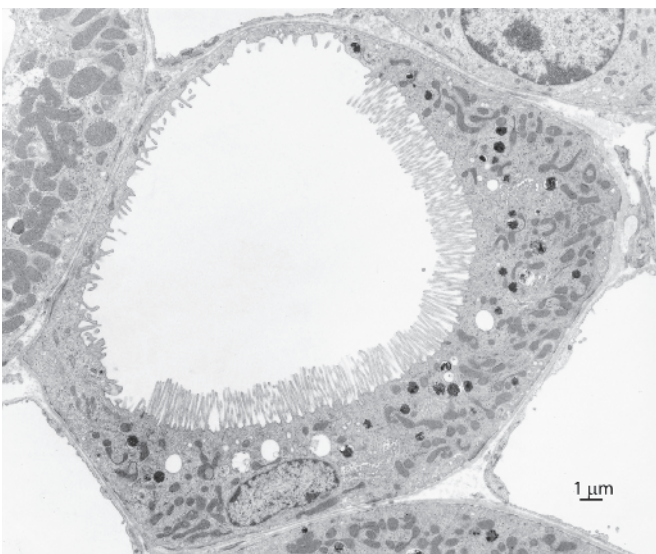


Fig. 2.28 Transmission electron micrograph from rabbit kidney illustrating the abrupt transition from the proximal straight tubule to the descending thin limb of the loop of Henle. (Modified from Madsen KM, Park CH. Lysosome distribution and cathepsin B and L activity along the rabbit proximal tubule. *Am J Physiol*. 1987;253:F1290–F1301.)

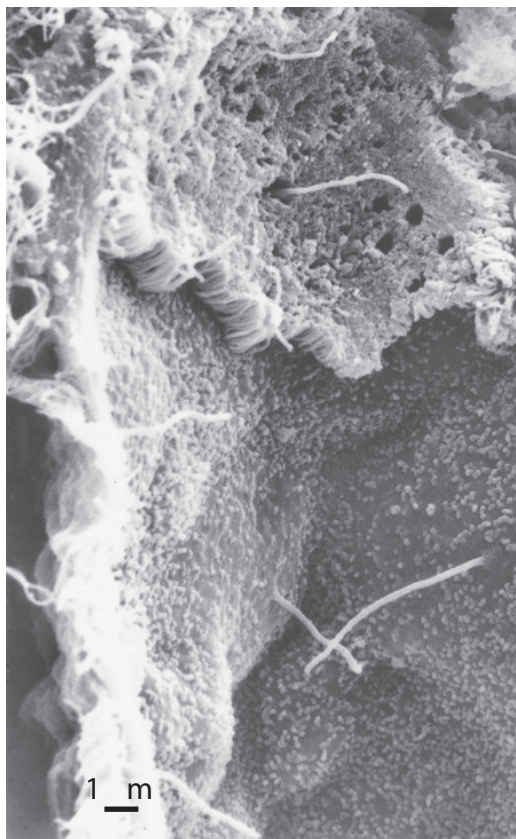


Fig. 2.29 Scanning electron micrograph depicting the abrupt transition from the terminal S3 segment of the rat proximal tubule (top) to the descending thin limb (bottom). Elongated cilia project into the lumen from cells of the proximal tubule and the thin limb.

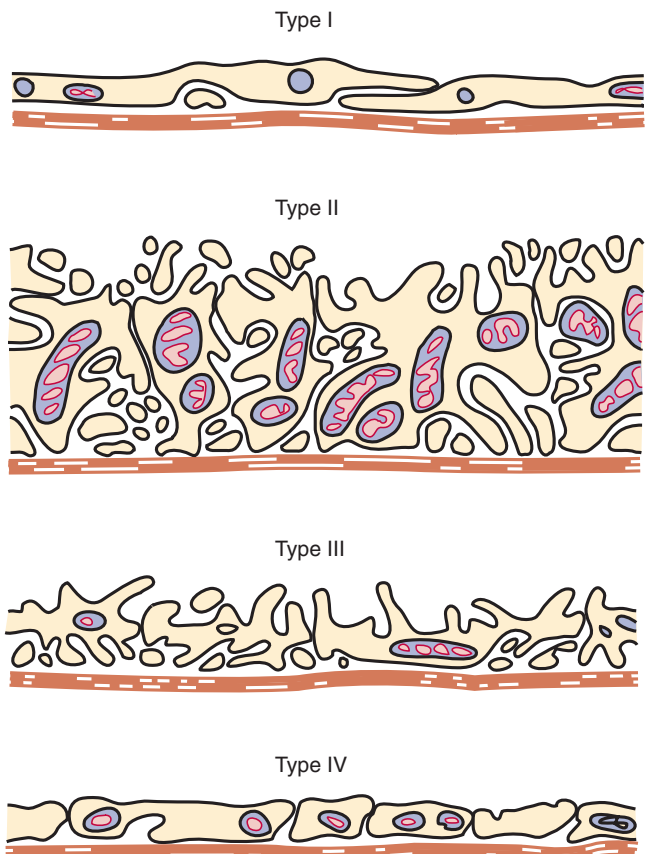


Fig. 2.30 Diagram depicting the appearance of the four types of thin limb segments in a rat kidney. (See text for explanation.)

DISTAL TUBULE

The term “distal tubule” has been used in different ways to encompass different segments of the distal nephron. According to the standard nomenclature of renal anatomists, the “distal tubule” includes the TAL of loop of Henle (pars recta or distal straight tubule), which contains the macula densa and the distal convoluted tubule (pars convoluta).²⁶⁸ However, in micropuncture studies and more common usage, the distal tubule includes the segments from just distal to the macula densa to the first confluence of two tubules. By this definition, the distal tubule may include up to four different epithelial segments, a short portion of TAL, DCT, connecting tubule (CNT), and ICT.^{202,269,270} The lengths of the segments that make up the distal tubule vary among species and rat strains. The length of the tubule from the macula densa to the first tubule junction in the rat is reported to be 2.4–2.5 mm.²⁶⁹ In Sprague-Dawley and Brattleboro rats, DCT accounts for ~75%–77% of distal tubule accessible by micropuncture, whereas in Wistar rats, DCT constitutes only ~48% of the distal tubule, with the remainder being CNT and ICT.²⁶⁹ In studies of microdissected rabbit distal tubule, segments designated as DCT_b, DCT_g, and DCT_l, likely correlating to DCT, CNT, and ICT, measured 0.49 mm, 0.42 mm, and 0.41 mm, respectively.²⁷¹ However, the rabbit DCT was measured at ~1 mm long in structural studies.²⁰²

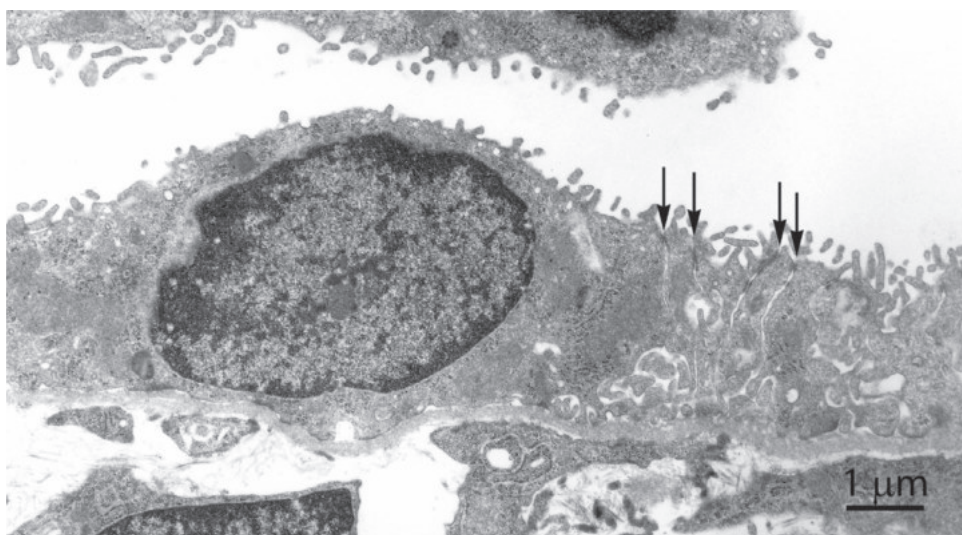


Fig. 2.31 Transmission electron micrograph of type II epithelium of the thin limb of loop of Henle in the inner stripe of the outer medulla of a rat kidney. Compared with other thin limb types, type II epithelium is taller and has more organelles, prominent apical plasma membrane microprojections, and complex basolateral plasma membrane infoldings. The cells have extensive lateral interdigitations attached near the apical surface by short tight junctions (arrows). (Modified from Verlander JW. Normal ultrastructure of the kidney and lower urinary tract. *Toxicol Pathol*. 1998;Jan-Feb;26(1):1–17.)

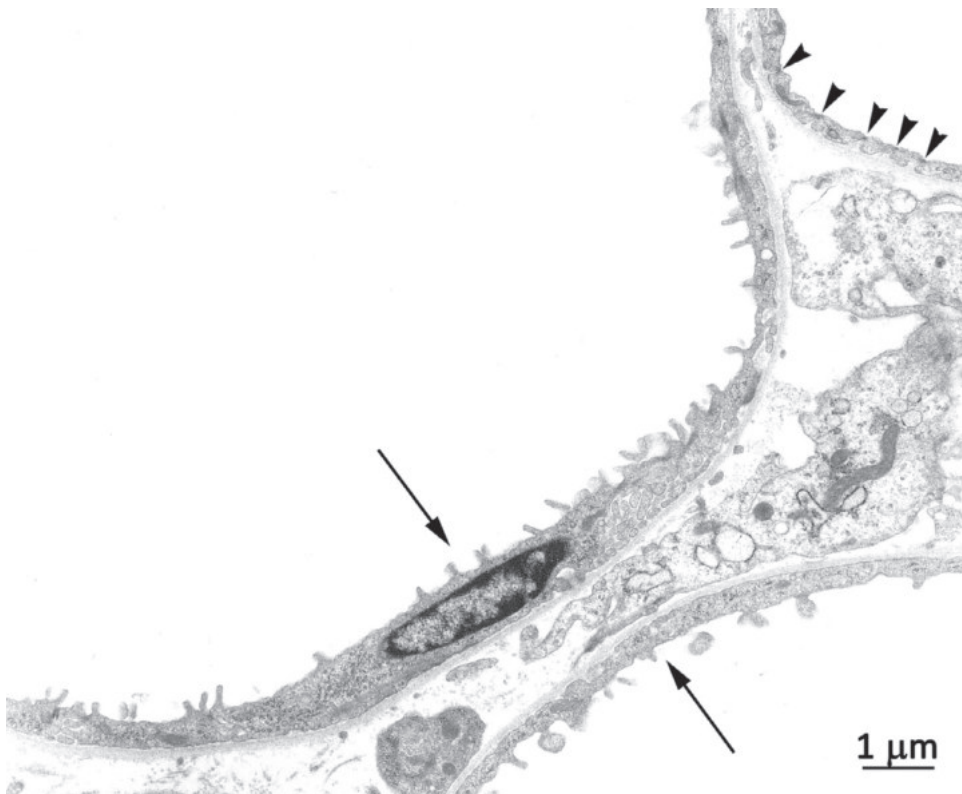


Fig. 2.32 Transmission electron micrograph of thin limbs of the loop of Henle in the initial inner medulla of rat kidney. Type III epithelium (arrows) has prominent apical plasma membrane microprojections. It is a very low, flat epithelium with relatively few basolateral plasma membrane infoldings compared with type II epithelium. A small portion of type IV thin limb epithelium is also visible, which also is very flat but has numerous tight junctions (arrowheads) due to the abundant lateral interdigitations. (From Sands JM, Verlander JW. Functional anatomy of the kidney. In: McQueen C, ed. *Comprehensive toxicology*, 3rd ed. St Louis: Elsevier; 2017.)

THICK ASCENDING LIMB

The TAL arises abruptly from the thin limbs of loop of Henle, spans the inner and outer stripes of the outer medulla, extends through the cortex in the medullary rays, contacts the glomerulus of its own nephron at the macula densa, and extends a short distance beyond the macula densa before the transition to the DCT^{202,270} (see Fig. 2.5). In short-looped nephrons, the transition to the TAL can occur shortly before the hairpin turn, but this is not the case in all species.¹⁵ In the outer medulla, TAL cells are taller in the inner stripe, beginning at ~11 µm and declining to between 7 and 8 µm in height.^{202,270,272} As the tubule ascends toward the cortex, cell height gradually decreases further to ~5 µm in the cortical TAL (cTAL) of the rat.²⁷² In rabbits also, the cTAL is lower than the medullary TAL (mTAL) in height, averaging 4.5 µm but declining to ~2 µm in the terminal part.^{202,273}

TAL cells have extensive infoldings of the basolateral plasma membrane and interdigitations between adjacent cells (Figs. 2.33 and 2.34). The basolateral infoldings often extend from the base to two-thirds or more of the cell height, particularly in the mTAL in the inner stripe. The cell nucleus is centrally located, with little cytoplasm or organelles between the nucleus and either the apical or basal surface. Abundant elongated mitochondria are located in lateral cell processes, generally oriented perpendicularly to the basement membrane, similar to the S1 segment of the proximal tubule, and they contain prominent granules in the matrix. The TAL also has a well-developed Golgi complex; small, subapical cytoplasmic vesicles

and tubulovesicles; multivesicular bodies and lysosomes; and abundant smooth and rough endoplasmic reticulum. The tight junctions are 0.1 to 0.2 µm in depth in the rat²⁰⁹; in rabbit, the length of the tight junctions increases from the mTAL to the cTAL.²⁰² Intermediate junctions are also present, but desmosomes appear to be lacking.

By SEM, the TAL of the rat kidney has two morphologically distinct cells, designated “smooth” and “rough,” distinguished by the appearance of the luminal plasma membrane and lateral cell borders.²⁷⁰ Rough TAL cells have numerous small apical microprojections, whereas the apical surface of smooth TAL cells has few microprojections except along the cell borders (Fig. 2.33); both types have a single, central primary cilium. In the inner stripe of the outer medulla, rough TAL cells generally have prominent lateral processes that interdigitate with neighboring cells, producing an undulating cell border, whereas smooth TAL cells typically have only shallow lateral processes and hence a relatively simple cell border; these differences are not present in the cTAL.²⁷⁰ However, compared with rough TAL cells, smooth TAL cells have a more prominent subapical cytoplasmic vesicle and tubulovesicle compartment. The smooth surface pattern predominates in the mTAL, but as the thick limb ascends, the number of rough TAL cells increases, and luminal microprojections and apical lateral invaginations become more prominent. Consequently, the surface area of the luminal plasma membrane is significantly greater in the cTAL than in the mTAL.²⁷²

The structural characteristics of the TAL, notably the high density of mitochondria interposed between extensive basolateral plasma membrane infoldings, contribute to its important role in active reabsorption of NaCl via the Na⁺, K⁺, 2Cl⁻ cotransporter located in the apical plasma membrane²⁷⁴ driven by abundant basolateral Na⁺-K⁺-ATPase. Within the TAL, axial heterogeneity in the ultrastructural features correlates with Na⁺-K⁺-ATPase activity, with the mTAL in the inner stripe having the greatest basolateral plasma membrane area, mitochondrial density, and Na⁺-K⁺-ATPase activity.^{249,272,275,276} However, functional correlations with the observed axial and cellular structural heterogeneity are limited.²⁷⁷ Some physiologic studies using the isolated perfused tubule technique found that NaCl transport is greater in the medullary segment than in the cortical segment of the TAL,²⁷⁸ consistent with the structural differences, but others did not observe this.^{279,280} Similarly, functional differences between the smooth and rough forms of TAL cells have not been defined. Although cellular heterogeneity in the expression of various transport proteins, including ROMK, H⁺ATPase, and NKCC2, has been observed in the TAL, these variations in protein expression have not yet been correlated with the apical surface patterns described using electron microscopy.²⁷⁷

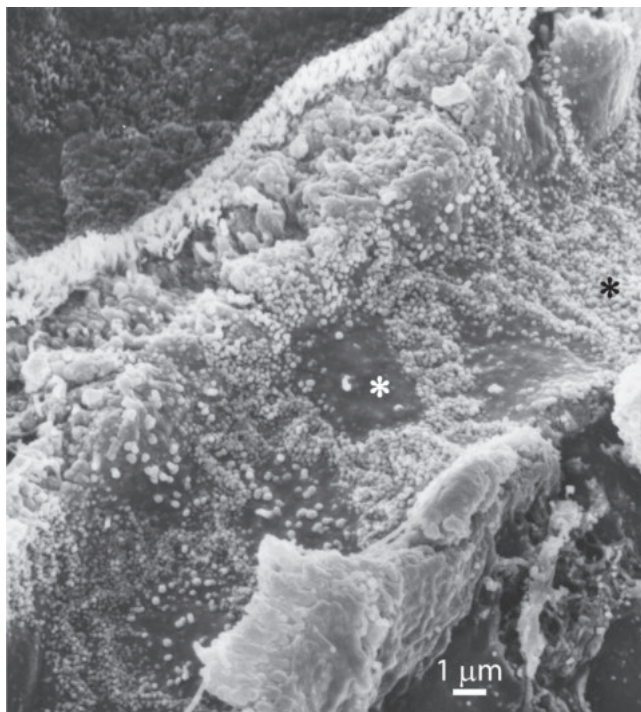


Fig. 2.33 Scanning electron micrograph illustrating the luminal surface of rat medullary thick ascending limb. The white asterisk denotes smooth-surfaced cells; the black asterisk identifies rough-surfaced cells. (Modified from Madsen KM, Verlander, Tisher CC. Relationship between structure and function in distal tubule and collecting duct. *J Electron Microsc Tech*. 1988;9:187–208.)

DISTAL CONVOLUTED TUBULE

The abrupt transition from the TAL to the DCT occurs a short distance distal to the macula densa and is located in the cortical labyrinth (Figs. 2.5 and 2.35). Like TAL cells, DCT cells contain extensive basolateral plasma membrane infoldings and a dense array of long mitochondria aligned with the plasma membrane infoldings perpendicular to the basement membrane (Fig. 2.36). However, DCT cells are significantly taller than TAL cells, and the cell nuclei are

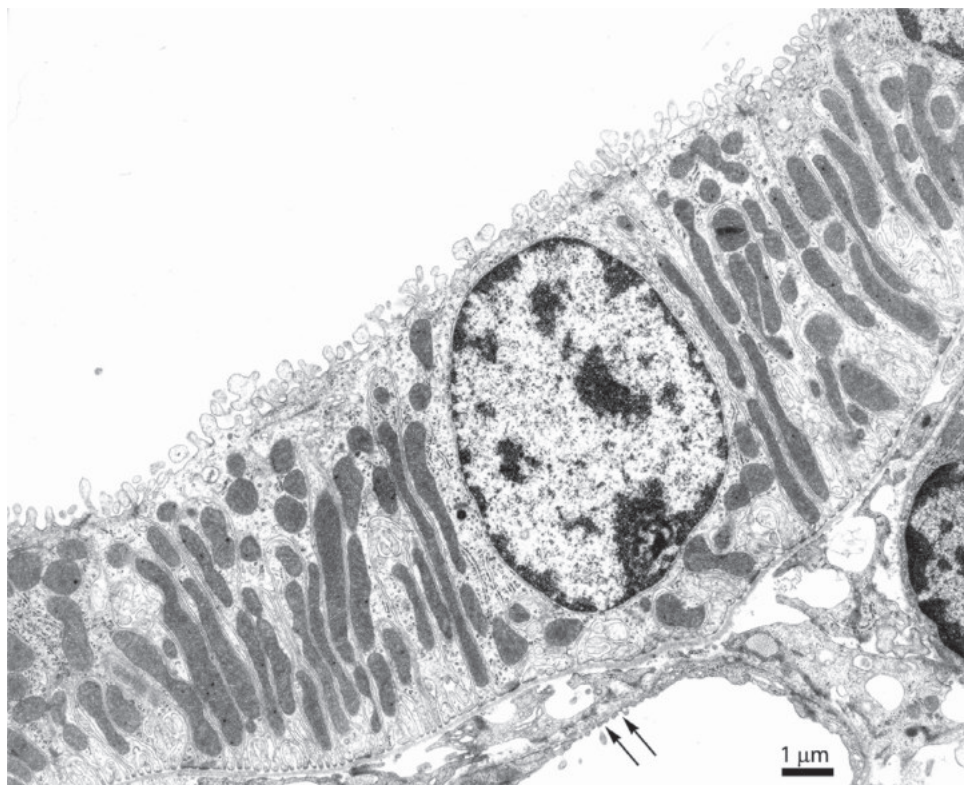


Fig. 2.34 Transmission electron micrograph of cortical thick ascending limb (TAL) in rat kidney. The apical surface has numerous short apical microprojections, typical of the rough TAL cells common in the cortical TAL, and deep, complex invaginations of the basal plasma membrane extend into the apical region of the cell and enclose elongated mitochondrial profiles. There are few organelles and little cytoplasm between the nucleus and the apical and basal aspects of the cell compared with the distal convoluted tubule (see Fig. 2.36). A peritubular capillary with fenestrated endothelium (arrows) is adjacent to the basal side of the TAL cell.

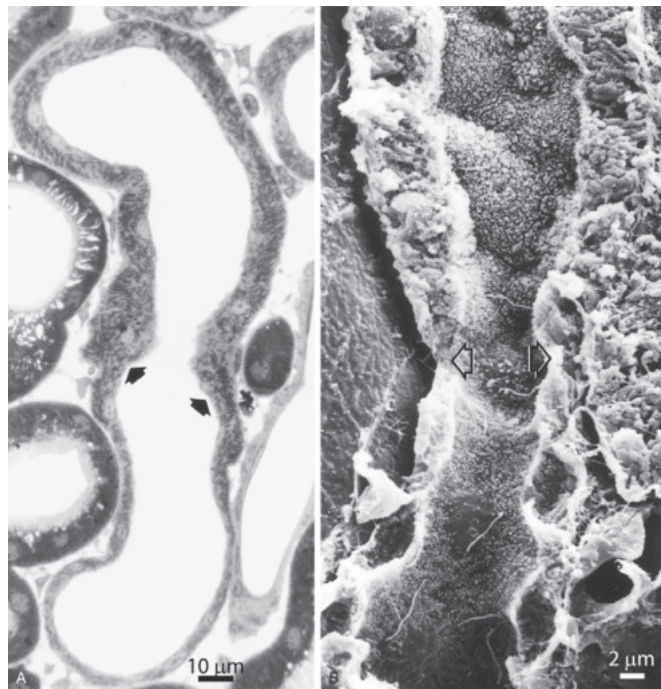


Fig. 2.35 Micrographs depicting the abrupt transition (arrows) from the thick ascending limb of Henle (below) to the distal convoluted tubule (above). (A) Light micrograph of normal rat kidney. (B) Scanning electron micrograph of normal rabbit kidney. (B, Courtesy Ann LeFurgey, PhD.)

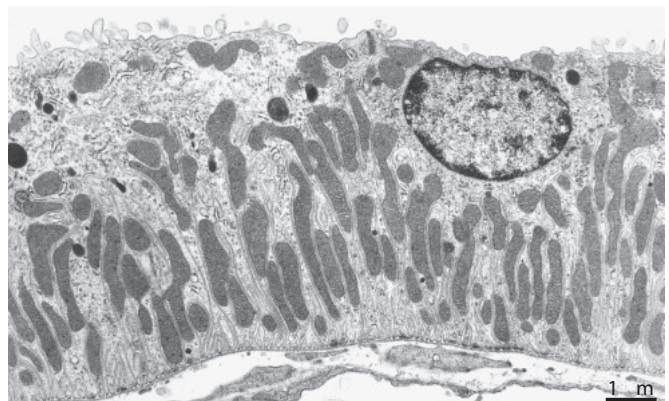


Fig. 2.36 Transmission electron micrograph of rat distal convoluted tubule (DCT). Although the structure of DCT cells is similar to thick ascending limb (TAL) cells in many ways, DCT cells are considerably taller, with numerous basal plasma membrane infoldings and mitochondria interposed between the nucleus and the basement membrane. Compare with the TAL cell in Fig. 2.34.

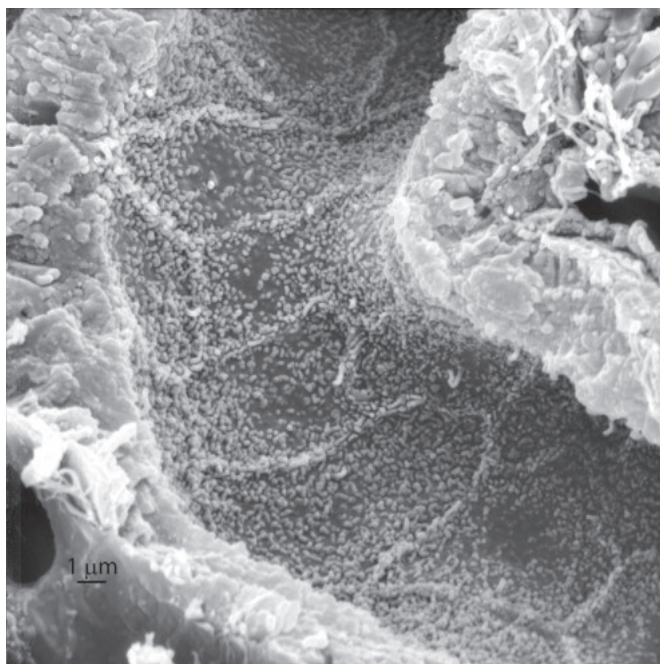


Fig. 2.37 Scanning electron micrograph showing the luminal surface of a distal convoluted tubule from a rat kidney. Short microvilli are prominent, cell borders are accentuated by longer and more abundant microvilli, and the cell borders in the apical region are simple, lacking the interdigitations seen in the thick ascending limb (TAL). (Compare with Fig. 2.33.)

close to the apical plasma membrane with basolateral plasma membrane infoldings and mitochondria interposed between the nucleus and basement membrane. On the luminal surface, DCT cells have a single central cilium and numerous small microprojections, which are more prominent at the lateral cell borders; the lateral borders are simple compared with TAL cells (Fig. 2.37). The junctional complex is composed of a tight junction, which is approximately 0.3 μm in depth, and an intermediate junction.²⁰⁹ The Golgi complex is well-developed, and lysosomes and multivesicular bodies are present but less common than in the proximal tubule. The cells contain numerous small subapical vesicles, microtubules, free ribosomes, and rough and smooth endoplasmic reticulum.

As mentioned previously, in micropuncture studies, the “distal tubule” includes tubule segments from immediately distal to the macula densa to the first junction with another renal tubule, which includes as many as four different types of epithelia (Fig. 2.38). In general, the “early” or “bright” distal tubule corresponds largely to the DCT plus a short segment of TAL, whereas the “late” or “granular” distal tubule corresponds to the connecting tubule and the initial portion of the collecting duct in the cortical labyrinth, the ICT.^{209,281} In several species, the DCT exhibits axial heterogeneity with respect to cell morphology and transporter expression.²⁸² In rabbits, the transition from DCT to CNT is morphologically distinct, but in rats, mice, and humans, the late portion of the DCT shares features of the CNT, including the presence of intercalated cells and several proteins expressed in CNT cells. In fact, two DCT segments, DCT1 and DCT2, have been defined in the rat based on protein expression characteristics. Expression of the apical thiazide-sensitive NaCl

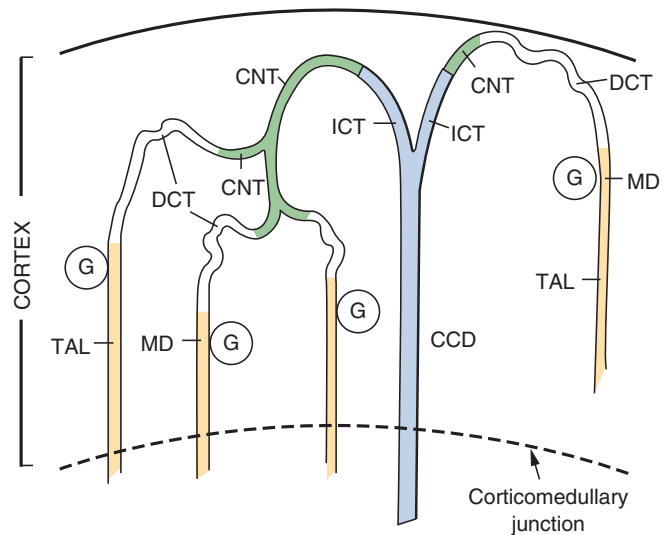


Fig. 2.38 Diagram of the various anatomic arrangements of the distal tubule and cortical collecting duct in superficial and juxtamedullary nephrons. (See text for detailed explanation.) CCD, Cortical collecting duct; CNT, connecting segment; DCT, distal convoluted tubule; G, glomerulus; ICT, initial collecting tubule; MD, macula densa; TAL, ascending thick limb (of Henle).

cotransporter, NCC, is definitive for DCT cells and is present throughout the entire DCT. The initial DCT segment, DCT1, is distinguished from the late segment, DCT2, by the presence in DCT2 of the $\text{Na}^+–\text{Ca}^{2+}$ exchanger (NCX1) and vitamin D-dependent calcium-binding protein, calbindin-D28K,²⁸³ proteins that are also expressed in CNT cells.²⁸⁴ In mice^{285,286} and humans,²⁸⁷ NCX and calbindin-D28K are expressed throughout most of the DCT; thus, DCT1 and DCT2 are not distinguishable, at least not as originally defined. Nonetheless, in rat, mouse, and human, the early DCT is distinct from the late DCT in that the latter portion expresses the epithelial sodium channel (ENaC),²⁸⁶ which is also expressed in CNT cells, and in mice and rats, the late DCT expresses the apical calcium channel TRPV5, which is absent from the early DCT.^{288,289} Furthermore, in rat and mouse, the late portion of the DCT also contains intercalated cells, predominantly the so-called non-A, non-B subtype, which is described in detail in the section on the collecting duct.

The DCT has the highest $\text{Na}^+–\text{K}^+$ -ATPase activity of all nephron segments,^{231,251} which drives ion transport and correlates with the high mitochondrial density and elaborate basolateral plasma membrane infoldings in this segment. The NCC is present in the apical plasma membrane and subapical vesicles.^{290–292} A number of studies have demonstrated structural changes in the DCT in response to physiologic stimuli that alter the transport activity in this segment.^{293–297} For example, treatment with furosemide, an inhibitor of the TAL transporter NKCC2, causes a marked increase in DCT cell size, basolateral plasma membrane area, and cell proliferation, along with increased NCC expression and sodium uptake, suggesting structural adaptations correlating with functional adaptations to conserve sodium when NKCC2 is inhibited and NaCl delivery to the DCT is increased.^{293,298} In animals fed a low-salt diet, NCC is largely expressed in the apical plasma membrane where it mediates

apical NaCl uptake, whereas feeding a high-salt diet or acute induction of hypertension causes redistribution of NCC to the subapical cytoplasmic vesicles.^{299,300} Conversely, angiotensin II administration acutely causes a significant increase in the apical plasma membrane expression of NCC and a reduction in NCC expression in apical cytoplasmic membrane vesicles, whereas treatment with captopril, an angiotensin-converting enzyme inhibitor, has the opposite effect on NCC distribution,³⁰¹ although under these conditions, phosphorylated NCC is found exclusively in the apical plasma membrane and not in cytoplasmic vesicles.³⁰² Similarly, estradiol administration in ovariectomized rats, which increases NCC phosphorylation and activity,³⁰³ causes an increase in apical plasma membrane complexity and apical plasma membrane NCC expression along with depletion of apical cytoplasmic vesicles.³⁰⁴ Thus, structural changes occur in the DCT in response to stimuli that alter NCC transporter expression and functional activity.

CONNECTING SEGMENT

The CNT constitutes the main portion of the “late” or “granular” distal tubule as defined in the micropuncture literature. The CNTs of superficial nephrons continue directly into ICTs, whereas CNTs from midcortical and juxtamedullary nephrons join to form arcades that ascend in the cortex and continue into ICTs (see Fig. 2.38).^{202,271} CNTs are present throughout the cortical labyrinth but are present in higher density surrounding interlobular vessels; the CNT makes contact with the afferent arteriole of its own glomerulus, upstream of the JGA.^{305,306} These contacts enable crosstalk between the CNT and renal vasculature, which regulates renal perfusion in addition to the classic tubuloglomerular feedback mechanism mediated through the JGA.^{307–310}

In the rabbit, the CNT is a well-defined segment composed of two cell types: the CNT cell and the intercalated cell.^{202,297} However in other species, including rats,^{269,281} mice,²⁹⁷ and humans,^{178,311} the transition from DCT to CNT is not structurally distinct. More distally, the rat and mouse CNT clearly differs from the late DCT in the increased frequency of intercalated cells and the structural characteristics of the majority cell type, the CNT cell (Fig. 2.39). The CNT transitions to the ICT, which is located in the cortical labyrinth and connects the CNT to the CCD, which is located in the medullary ray. The ICT is a lower epithelium than the CNT, and like the CCD, is made up of principal cells and intercalated cells (Fig. 2.40). In rabbit kidney, the CNT to ICT transition is distinct. In rat kidney, although there is some intermingling of CNT cells and principal cells in the late portion of the CNT, the CNT and ICT are largely distinguishable by the morphologic characteristics of CNT cells versus principal cells. In mouse, the transition from CNT to ICT is more gradual, and only the early CNT and late ICT are clearly identifiable as such based on cellular morphology.

The CNT contains primarily two cell types: the majority cell type, the CNT cell, which occurs only in this segment, and intercalated cells, which account for approximately 40% of the cells. The CNT cell is tall with an apically located nucleus like the DCT cell, but has a rounder nucleus, more cytoplasm and organelles between the apical plasma membrane and the nucleus, shallower and less uniform basolateral

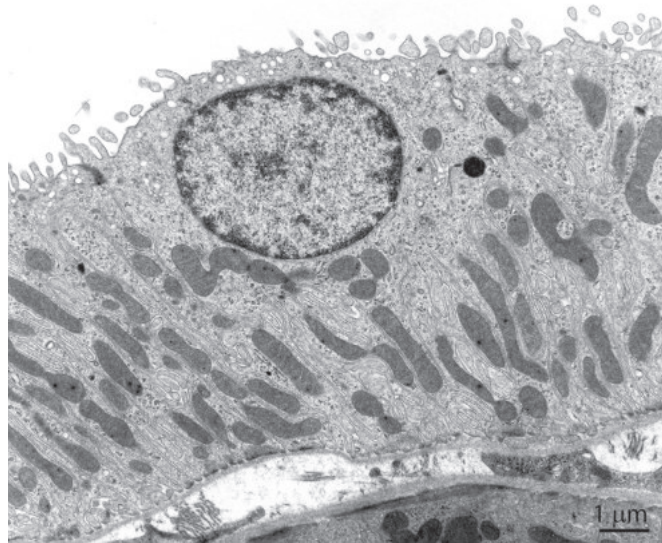


Fig. 2.39 Transmission electron micrograph of rat connecting segment (CNT) cell. The CNT cell has deep basolateral plasma membrane infoldings with numerous mitochondria, but a lower mitochondrial density than distal convoluted tubule (DCT) cells, and the nucleus is typically rounder than DCT cell nuclei. (Compare with Fig. 2.36.)

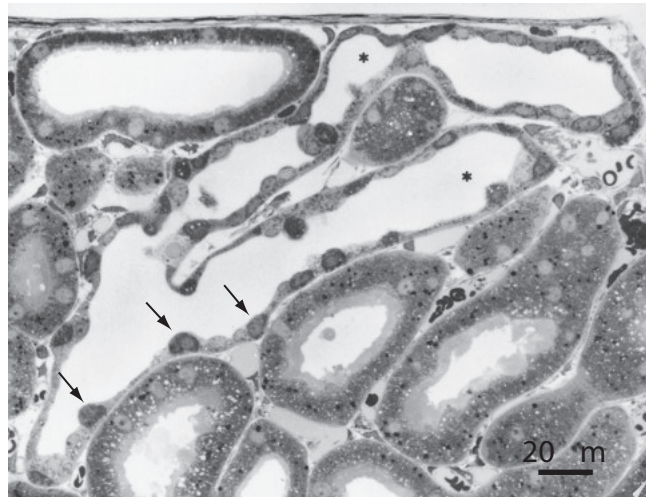


Fig. 2.40 Light micrograph of initial collecting tubules (asterisks) in toluidine blue-stained rat kidney. One tubule lies just beneath the renal capsule (*top of picture*), where it would be easily accessible to micropuncture. Dark staining cells (arrows) are intercalated cells. This segment of the collecting duct corresponds to the so-called late distal tubule as defined in micropuncture studies.

plasma membrane infoldings, and fewer, more randomly arranged mitochondria.³¹²

Three distinct intercalated cell subtypes are present in the CNT, based on not only morphologic characteristics but also distinct patterns of transporter expression: type A, type B, and non A, non B.^{313–316} In rat and mouse CNT, the so-called non A, non B intercalated cell is the most prevalent subtype, followed by type A cells and type B cells.³¹³ The morphologic characteristics and localization of specific ion transporters distinguishing these three intercalated cell subtypes

and their axial distribution are detailed in the following section.

The CNT contributes to regulated reabsorption of sodium, calcium, and water via specific proteins expressed in CNT cells. In addition to basolateral Na^+/K^+ -ATPase, CNT cells and principal cells in the ICT express the ENaC^{282,286,287} and the apical potassium channel, ROMK.³¹⁷ Proteins mediating calcium transport expressed by CNT cells include the basolateral $\text{Na}^+/\text{Ca}^{2+}$ exchanger, NCX1, Ca^{2+} -ATPase, apical TRPV5, and calbindin-D28K.^{292,318–323} In rats, mice, and humans, the CNT, like the collecting duct, expresses the vasopressin-sensitive AQP2,^{287,324,325} although AQP2 appears to be absent from the rabbit CNT.³²⁶

In rat kidney, a small population of cells in the late DCT at the transition to the CNT expresses both the NCC and the $\text{Na}^+/\text{Ca}^{2+}$ exchanger, which have been considered specific for DCT cells and CNT cells, respectively.^{284,318} In rabbit kidney, the CNT is distinct from the DCT in both structure and function, and cells coexpressing NCC and the $\text{Na}^+/\text{Ca}^{2+}$ exchanger are not evident in either segment.²⁹¹ The CNT makes a transition to the ICT, a segment composed of principal cells and intercalated cells located in the cortical labyrinth before joining with the CCD in the medullary ray. Expression of the $\text{Na}^+/\text{Ca}^{2+}$ exchanger is abundant in the basolateral plasma membrane of CNT cells but undetectable in CCD principal cells.²⁸²

Potassium loading in rats stimulates potassium secretion in the CNT and increases the basolateral plasma membrane surface area of CNT cells and principal cells of both the CNT and the ICT³²⁷ where Na^+/K^+ -ATPase resides, as well as the apical expression of the potassium channel, ROMK.³¹⁷ In rabbits, feeding a low-sodium, high-potassium diet induces a similar increase in CNT basolateral plasma membrane.²⁹⁷ These structural changes are consistent with increased basolateral Na^+/K^+ -ATPase expression and activity driving apical potassium secretion.

COLLECTING DUCT

The collecting duct extends from the initial connecting tubule in the cortex to the tip of the papilla. Subsegments of the collecting duct are defined by their location in the kidney: ICT, CCD, OMCD, and IMCD. The CCD is the portion of the collecting duct located in the medullary ray in the cortex and runs parallel with the cortical PST and TAL. The CCD begins at the fusion of the ICT, located in the cortical labyrinth, with the collecting duct in the medullary ray. The OMCD includes a portion in the outer stripe of the outer medulla, OMCD_O, and in the inner stripe, OMCD_I. IMCD subsegments in the rat kidney are designated as IMCD₁, IMCD₂, and IMCD₃, corresponding to the proximal, middle, and distal thirds of the IMCD,^{328,329} or initial IMCD (IMCD_I) and terminal IMCD (IMCD_T). In rats, IMCD_I corresponds to IMCD₁, which is the portion in the base of the inner medulla, whereas IMCD_T corresponds to IMCD₂ and IMCD₃, the papillary portion of the IMCD. The IMCDs terminate as the ducts of Bellini, which open at the tip of the papilla to form the area cibrosa (see Figs. 2.3 and 2.6).

In the ICT, CCD, OMCD, and IMCD_I, there are two major cell types: principal cells and intercalated cells (Fig. 2.41). Principal cells are the majority cell type, normally accounting



Fig. 2.41 Scanning electron micrograph showing the luminal surface of a rat cortical collecting duct. Principal cells have small, stubby apical microprojections, and a single cilium. Two configurations of intercalated cells are present: type A (arrows), with a large luminal surface covered mostly with microplicae, and type B (arrowhead), with a more angular outline and a surface covered mostly with small microvilli. (Modified from Madsen KM, Verlander JW, Tisher CC. Relationship between structure and function in distal tubule and collecting duct. *J Electron Microscop Tech*. 1988;9:187–208.)

for ~60%–65% of cells in the rat and mouse CCD and OMCD^{313,314,330} and ~90% of cells in the rat IMCD.^{328,329} Intercalated cells account for the remainder, with axial heterogeneity in the incidence of the different intercalated cell subtypes. However, the number of intercalated cells is not fixed, even in adult wild-type animals, as several studies have documented increased numbers and percentage of intercalated cells during chronic carbonic anhydrase inhibition,³³¹ chronic potassium depletion,^{332,333} and chronic lithium administration,^{334–337} the latter producing even an atypical distribution of intercalated cell subtypes in mice.³³⁴ The terminal portion of the IMCD is made up of a distinct epithelial cell type, the IMCD cell.

CORTICAL COLLECTING DUCT

The collecting duct in the cortex includes ICT in the cortical labyrinth and the CCD in the medullary ray (see Fig. 2.5). The cells of the ICT are taller than those of the CCD and generally have more complex plasma membrane microprojections and infoldings (Fig. 2.42) and more intense plasma membrane transporter expression, but otherwise these two subsegments are morphologically similar. Nonetheless, because of these subtle differences in ultrastructure, it is important to distinguish between ICT and CCD when quantifying morphologic components or subcellular immunolabeling.

Principal cells account for approximately 60%–65% of cells in the CCD of rabbit,³³⁸ as in rat and mouse.^{313,314,330} The nucleus in principal cells is located close to the apical surface, a feature that helps distinguish principal cells from intercalated cells, which have a central or basal nucleus. By transmission electron microscopy, principal cells have relatively few small cytoplasmic vesicles between the nucleus and the apical plasma membrane, a light-staining cytoplasm, and few apical plasma membrane microprojections. By SEM, these apical microprojections appear as short, stubby microvilli that are less numerous near the single central cilium than at the periphery of the cell (see Fig. 2.41). Principal cells have numerous basal plasma membrane infoldings, without interposition of mitochondria or other organelles (see Fig. 2.42). Lateral cell processes and interdigitations are virtually absent.³³⁹ Cell organelles are relatively sparse: mitochondria are small and scattered randomly in the cytoplasm; there are few lysosomes, autophagic vacuoles, and multivesicular bodies; and the Golgi body, rough and smooth endoplasmic reticulum, and free ribosomes are present but not prominent.

Intercalated cells in the CCD are distinguishable from principal cells by several morphologic features. As mentioned earlier, intercalated cells lack cilia and have a more centrally or basally located nucleus versus the apical nucleus of principal

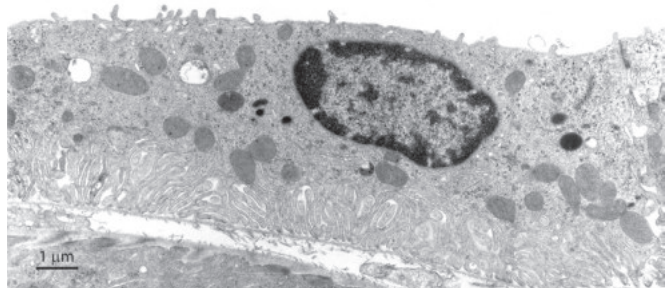


Fig. 2.42 Transmission electron micrograph of a principal cell from the initial collecting tubule (ICT) from normal rat kidney. Principal cells in the ICT are similar to those in the cortical collecting duct, but typically are slightly taller and have more extensive infoldings of the basal plasma membrane.

cells. Under basal conditions, intercalated cells have more abundant apical plasma membrane microprojections, higher mitochondrial density, abundant cytoplasmic vesicles, numerous polyribosomes, and a prominent Golgi apparatus. In the CNT through CCD, intercalated cells in plastic sections stain more intensely with toluidine blue than principal cells, partly due to cytoplasmic staining and partly due to the high mitochondrial density. This characteristic earned them the designation “dark cells,” in early morphologic studies (see Fig. 2.40). By transmission electron microscopy, the electron density of intercalated cell cytoplasm varies with the subtype but generally is somewhat darker than surrounding principal and CNT cells.

In the rat, mouse, and human kidney, three distinct intercalated cell subtypes are present in the CNT, ICT, and CCD. These subtypes are recognizable by ultrastructural features and cell-specific expression and subcellular distribution of various membrane and cytoplasmic proteins. Ultrastructural studies characterized two distinct populations of intercalated cells in the rat CCD, types A and type B, with ~60% of intercalated cells identified as type A and ~40% as type B (Fig. 2.43).³⁴⁰ The existence of a third distinct intercalated cell subtype was recognized later, the so-called non-A, non-B intercalated cell, which occurs almost exclusively in the CNT and ICT (Fig. 2.44).^{313,315,341–344}

By transmission electron microscopy under basal conditions, type A intercalated cells are characterized by moderate apical plasma membrane microprojections, a prominent apical cytoplasmic vesicle compartment, numerous mitochondria, a centrally located nucleus, and moderate basolateral plasma membrane infoldings (see Fig. 2.43). Profiles of the subapical vesicles appear as spherical vesicles and elongated tubulo-vesicles, which occasionally can be seen in contact with, or invaginating from, the apical plasma membrane (Fig. 2.45). Both the apical plasma membrane and the apical cytoplasmic vesicles are relatively electron-dense, in part due to coating of the cytoplasmic surfaces with characteristic club-shaped particles or “studs,” which are also present in the structurally similar OMCD intercalated cells^{340,343–346} and which are associated with the vacuolar proton pump, H⁺-ATPase.³⁴⁷ By SEM, the apical plasma membrane microprojections are mostly in the form of small folds, “microplicae,” rather than microvilli, again similar to OMCD intercalated cells.^{330,340,348}

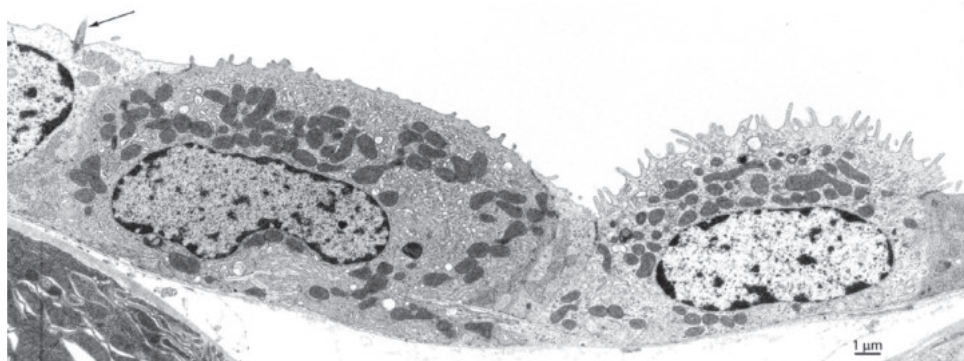


Fig. 2.43 Transmission electron micrograph from rat cortical collecting duct illustrating type A (right) and type B (left) intercalated cells under basal conditions. Note differences in the density of the cytoplasm the location of the nuclei, the distribution of the mitochondria and cytoplasmic vesicles, and the number of apical projections between the two cell types. (Modified from Madsen KM, Verlander JW, Tisher CC. Relationship between structure and function in distal tubule and collecting duct. *J Electron Microsc Tech*. 1988;9:187–208.)

By SEM under basal conditions, type B intercalated cells typically have a smaller, more angular luminal cell outline than type A cells and only sparse microprojections, mostly in the form of short microvilli (see Fig. 2.41).³⁴⁰ By transmission electron microscopy, the type B intercalated cell has a denser cytoplasm and more abundant, frequently clustered mitochondria, and the cell nucleus is typically eccentric, rather than centered (see Fig. 2.43). Numerous vesicles are present throughout the cytoplasm, but the cytoplasmic vesicle membranes are more delicate in appearance and less electron-dense compared with those in type A cells, and few membrane

“studs” are evident. The apical plasma membrane is relatively smooth, with small, short microprojections, and a band of dense cytoplasm without organelles or vesicles typically is present just beneath the apical plasma membrane. The basolateral plasma membrane infoldings are more elaborate than in type A cells, except in regions of cytoplasmic extensions filled with vesicles that frequently contact the basement membrane. In the rat under basal conditions, the surface density of the basolateral plasma membrane in type B intercalated cells is significantly greater, and that of the apical plasma membrane is significantly less than in type A cells.³⁴⁰

The so-called non-A, non-B intercalated cell represents approximately half of the intercalated cells in the mouse CNT and ICT but is less common in the rat.³¹³ This cell was initially dubbed “non-A, non-B” because it exhibited protein expression patterns different from the recognized A and B cell types, but it was unclear whether it was a distinct cell type. It now appears clear that this cell is indeed a distinct cell type that can be characterized and differentiated from A and B cells by specific protein expression patterns, in addition to its structural features (Figs. 2.44 and 2.46).

In rabbit kidney, intercalated cells are generally similar to those of rat and mouse. Early studies described “light” and “dark” forms of intercalated cells, with the dark form predominantly in the cortex and the light form predominantly in the outer medulla, suggesting that “light” and “dark” forms may correspond to type A and type B cells, respectively.²⁰² Four different surface configurations by SEM were described in rabbit collecting duct, based on the presence of microplicae, long and short microvilli, and combinations of these. The precise correlation of the surface configurations to type A and B intercalated cells is not known. However, cells with microplicae were most prevalent in the outer medulla and inner portion of the CCD³⁸⁸; this distribution and similarity to the morphology of type A intercalated cells of rat suggest they are type A cells in rabbit as well.

It is well established that intercalated cells contribute to acid–base homeostasis by transport of protons, bicarbonate,



Fig. 2.44 Transmission electron micrograph of a non-A, non-B intercalated cell in rat kidney. This intercalated cell subtype has a very high mitochondrial density compared with type A and type B intercalated cells, complex basolateral plasma membrane infoldings, and abundant long apical microprojections under basal conditions.

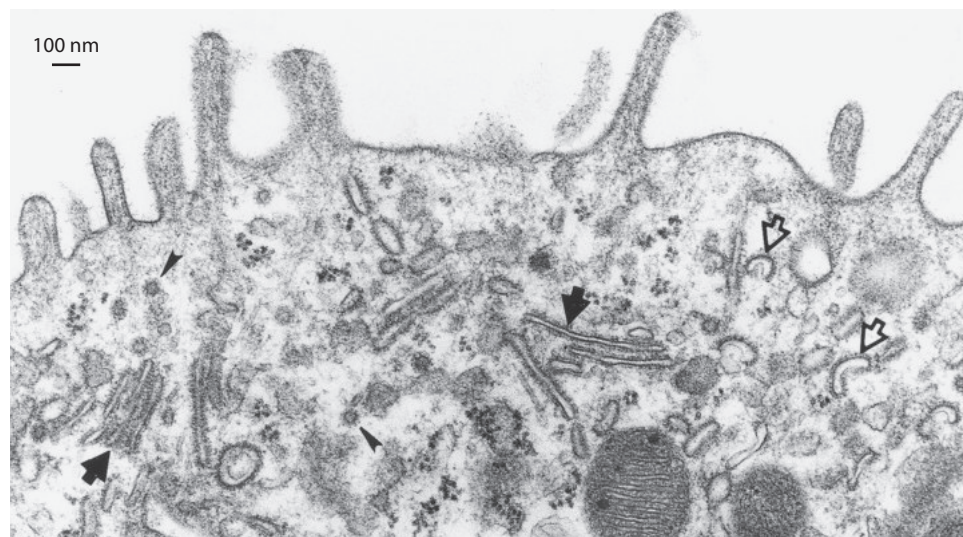


Fig. 2.45 Transmission electron micrograph illustrating the apical region of a type A intercalated cell from a rat kidney. Note the large number of tubulovesicles (solid arrows), invaginated vesicles (open arrows), and small coated vesicles with the appearance of clathrin vesicles (arrowheads).

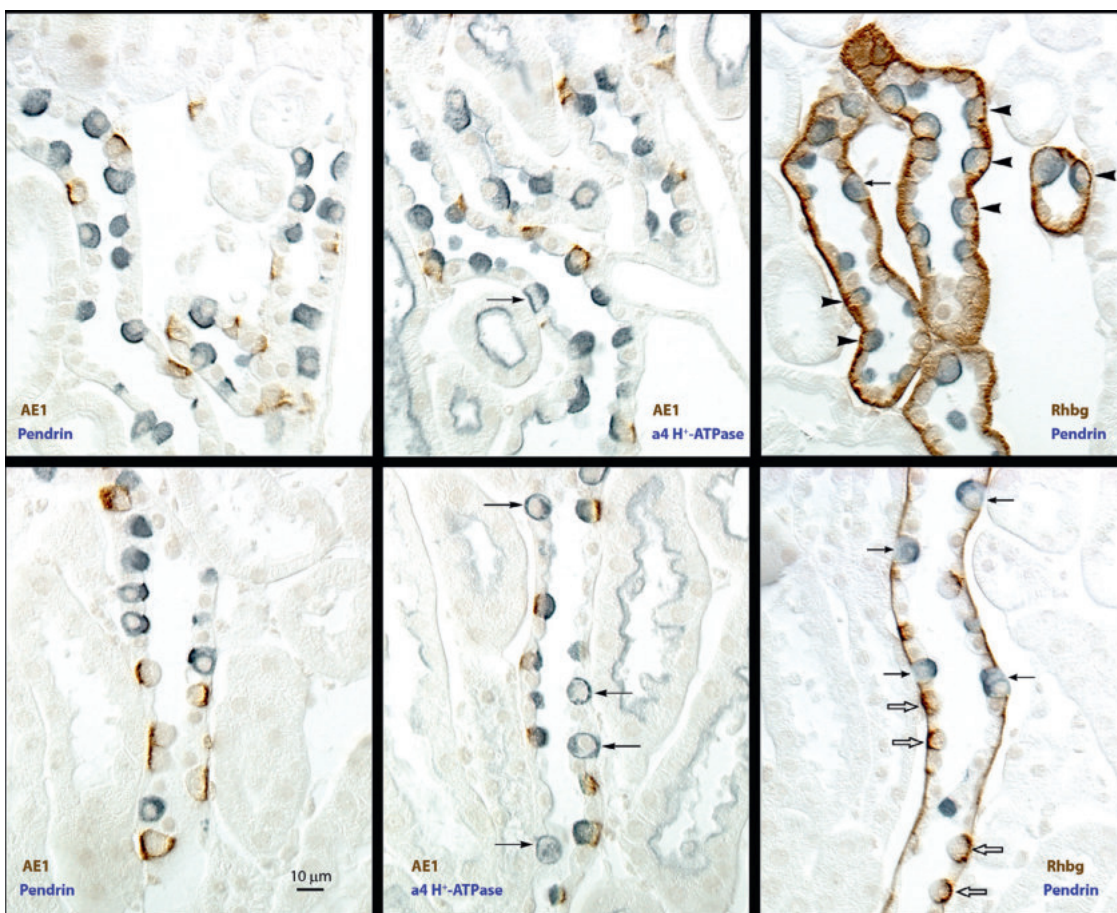


Fig. 2.46 Characteristic immunolabeling of three distinct intercalated cell subtypes in the connecting segment (CNT, top panels) and cortical collecting duct (CCD, bottom panels) by differential interference contrast microscopy (DIC). Type A intercalated cells express the basolateral anion exchanger, AE1, apical H^+ -ATPase, and the basolateral ammonia transporter, Rhbg. Type B intercalated cells express the apical anion exchanger, pendrin, and basolateral H^+ -ATPase, but no AE1 or Rhbg. The third type, the so-called non-A, non-B intercalated cell (or type C intercalated cell), expresses apical pendrin and basolateral Rhbg, but no AE1. Left column: Double labeling for AE1 (brown), which is definitive for type A intercalated cells, and apical pendrin (blue), which is present in type B and non-A, non-B intercalated cells. Pendrin labeling is exclusively in AE1-negative cells. Middle column: Double labeling for AE1 (brown) and the a4 subunit of H^+ -ATPase (blue). Type A intercalated cells (AE1-positive) have apical H^+ -ATPase label. Type B intercalated cells have basolateral H^+ -ATPase label (arrows), as well as diffuse apical label, which correlates with cytoplasmic vesicle labeling shown by immunogold electron microscopy. Type B intercalated cells are uncommon in the connecting segment (CNT), but represent virtually all of the non-A intercalated cells in the cortical collecting duct (CCD). In the CNT, the majority of non-A intercalated cells have apical H^+ -ATPase label but no basolateral label. These are non-A, non-B (type C) intercalated cells. Right column: Double labeling for pendrin (blue) and Rhbg (brown). Type B intercalated cells and non-A, non-B intercalated cells, both pendrin-positive, can be discriminated by basolateral Rhbg expression. Non-A, non-B intercalated cells, which express basolateral Rhbg (arrowheads), are the predominant pendrin-positive cell type in the CNT. Type B intercalated cells do not express detectable Rhbg (arrows) and comprise virtually all of the pendrin-positive cells in the CCD. Rhbg immunolabel is also present in type A intercalated cells (open arrows), CNT cells, and CCD principal cells.

and ammonia. All intercalated cell subtypes express carbonic anhydrase type II (CA II) throughout the cytoplasm, although the different subtypes exhibit varied patterns of expression.^{341,349,350} Type A intercalated cells have the most intense immunolabeling for CA II, with more intense labeling near the apical and basolateral plasma membrane domains. CA II expression in type B intercalated cells is diffuse and relatively weak, whereas the level in non-A, non-B cells is intermediate.³⁴¹

The electrogenic proton pump, H^+ -ATPase, is also strongly expressed in all intercalated cells, but the subcellular distribution determined by immunogold electron microscopy varies among the subtypes.^{314,351–353} In type A intercalated cells, H^+ -ATPase is present in the apical plasma membrane and apical cytoplasmic vesicle membranes. In type B intercalated

cells, H^+ -ATPase is present in the basolateral plasma membrane but not in the apical plasma membrane, and in cytoplasmic vesicles throughout the cell, including subapical vesicles, which likely accounts for cells with “bipolar” H^+ -ATPase immunolabeling, have been observed by light (Fig. 2.46).³¹³ Like A cells, non-A, non-B intercalated cells have H^+ -ATPase in the apical plasma membrane and subapical cytoplasmic vesicles. These distinctions in H^+ -ATPase distribution may not be discernible by light microscopy techniques, depending on the resolution of the method and the characteristics of the anti- H^+ -ATPase antibody used (Fig. 2.46). In rabbits, cells with the subcellular distribution of H^+ -ATPase typical of type A and type B intercalated cells are present in the CNT, ICT, and CCD under basal conditions, the most

prevalent distribution pattern is exclusively in intracytoplasmic vesicles in small intercalated cells with relatively uncomplicated plasma membrane compartments, suggestive of an inactive cell.³⁵³ Intercalated cells in the rabbit CNT and ICT have the typical polarized distribution of H⁺-ATPase seen in rat and mouse intercalated cells.³⁵³

Expression of the Cl⁻/HCO₃⁻ anion exchanger, AE1, is definitive for type A intercalated cells, as it is the only renal epithelial cell that expresses this protein. In rat and mouse kidney, AE1 is almost entirely expressed in the basolateral plasma membrane,^{314,342,354,355} whereas in rabbit kidney under basal conditions, a large portion of AE1 is intracellular in multivesicular bodies and cytoplasmic vesicles, in addition to the basolateral plasma membrane.^{356,357}

In addition to being devoid of AE1, type B and non-A, non-B intercalated cells are distinguished from type A cells by the expression of the apical Cl⁻/HCO₃⁻ exchanger, pendrin (Slc26a4).^{313,315,358–360} In both type B and non-A, non-B intercalated cells, pendrin is present in the apical plasma membrane and subapical cytoplasmic vesicles, although in basal conditions, the subcellular distribution is significantly different; pendrin is predominantly in the apical plasma membrane of non-A, non-B cells but predominantly in subapical vesicles in type B cells, with little apical plasma membrane expression.³¹⁵

The three recognized intercalated cell subtypes also have cell-specific expression of other transporters and enzymes, particularly those involved in ammonia metabolism. Type A and non-A, non-B intercalated cells express the ammonia transporters, Rhbg and Rhcg, and cytoplasmic glutamine synthetase.^{361,362} In both cell types, Rhbg is exclusively in the basolateral plasma membrane, whereas Rhcg is expressed in both the apical and basolateral plasma membranes in type A cells, in the apical plasma membrane in non-A, non-B cells, and in apical cytoplasmic vesicles in both cell types.^{316,353,363–365} In contrast, type B intercalated cells do not express detectable Rhcg, Rhbg, or glutamine synthetase.^{361,362,366}

The pattern of transporter and enzyme expression in intercalated cell subtypes combined with physiologic studies and morphologic studies documenting cell-specific alterations in ultrastructural features and transporter distribution in response to physiologic maneuvers together have established that type A intercalated cells secrete acid, whereas type B intercalated cells secrete bicarbonate, indicating that the existence of these functionally distinct intercalated cells subtypes is responsible for the ability of the CCD to accomplish both net acid secretion and net bicarbonate secretion.^{367,368} Many structural studies have documented intercalated cell subtype-specific changes in ultrastructure and subcellular distribution of ion and ammonia transporters in response to physiologic disturbances.^{340,352,357,369–372} Such studies have demonstrated an increase in apical plasma membrane surface area and diminished apical cytoplasmic vesicles and redistribution of H⁺-ATPase and Rhcg to the apical plasma membrane in type A intercalated cells in models of acidosis^{340,357,369} and increased basolateral plasma membrane surface area along with redistribution of AE1 from intracellular compartments to the basolateral plasma membrane in type A cells of acid-loaded rabbits,³⁵⁷ consistent with activation of acid and ammonia secretion by type A cells during acidosis. In contrast, chloride-depletion metabolic acidosis decreases apical plasma membrane complexity and increases the abundance

of apical cytoplasmic vesicles concomitant with internalization of H⁺-ATPase in type A cells, suggesting inactivation of acid secretion.³⁵² In type B intercalated cells, various models in mice that enhance bicarbonate secretion and chloride uptake increase apical plasma membrane surface area, decrease apical cytoplasmic vesicles, and cause redistribution of pendrin from the cytoplasmic vesicles to the apical plasma membrane.^{370–372} In rats, chloride-depletion metabolic acidosis increases type B intercalated cell size, basolateral plasma membrane complexity, and basolateral plasma membrane H⁺-ATPase expression.³⁵²

Non-A, non-B intercalated cells have the ability to secrete bicarbonate via apical pendrin and to secrete protons via apical H⁺-ATPase, but the net effect of these processes is poorly understood because the anatomy of the CNT, where most non-A, non-B cells reside, makes *in vitro* studies of these specific cells extremely difficult if not impossible. Type B and non-A, non-B intercalated cells appear to have an important role in transcellular chloride reabsorption via coordination of apical pendrin-mediated Cl⁻/HCO₃⁻ exchange and basolateral chloride exit via ClC-K2 channels.^{373,374} In mouse models that increase pendrin activity in type B intercalated cells, described above, non-A, non-B cells typically exhibit increased apical plasma membrane area and pendrin expression as well, although the relative distribution of pendrin between cytoplasmic vesicles and the apical plasma membrane frequently does not change.^{370–372,375}

The functions of type A, acid-secreting, and type B, bicarbonate-secreting, intercalated cells correspond well to their names. Although changes in nomenclature can create confusion initially, because the “non-A, non-B” cell is primarily found in the CNT and is believed to have an important role in chloride transport, designating it as a “type C” intercalated cell would be logical.

In contrast to intercalated cells, principal cells express abundant Na⁺K⁺-ATPase in the basolateral plasma membrane, the ENaC, and the potassium channel, ROMK, in the apical plasma membrane. AQP2 is present in the apical plasma membrane and cytoplasmic vesicles, as well as in the basolateral plasma membrane.^{324,376,377} The ammonia transporters Rhbg and Rhcg are less abundant than in intercalated cells in the basal state but otherwise are expressed in a pattern similar to type A intercalated cells. These transporters enable principal cells to reabsorb sodium and secrete potassium, to reabsorb water when vasopressin is present, and to contribute to ammonia secretion.

Structural correlates in principal cells in cortical segments to changes in the physiologic state are typically not as dramatic as those seen in intercalated cells. In rats and rabbits, feeding a high-potassium diet^{297,327} or treating with aldosterone or the mineralocorticoid analog deoxycorticosterone^{378–380} significantly increases the basolateral plasma membrane surface area of principal cells. Furthermore, models that enhance sodium reabsorption in the CCD cause redistribution and increased apical plasma membrane expression of ENaC subunits.^{381–384} These structural and immunolocalization studies correlate with the roles of principal cells in regulated sodium reabsorption and potassium secretion.

OUTER MEDULLARY COLLECTING DUCT

Like the CCD, the OMCD epithelium is made up of principal cells and intercalated cells. In rat and mouse kidney,

intercalated cells represent 35%–40% of the cells in both the OMCDo and the OMCDi.^{314,330} In rabbit kidney, the percentage of intercalated cells in the OMCD is less, approximately 18%, with the percentage declining axially from the OMCDo to the deep OMCDi.³³⁸ However, some investigators did not observe distinct epithelial cell heterogeneity in the rabbit OMCDi based on morphologic criteria, although the cells varied in mitochondrial content, subapical vesicle abundance, and density of rod-shaped particles in the apical plasma membrane.³⁸⁵

Principal cells of the OMCD are structurally similar to those in the CCD, although they become slightly taller, and the number of organelles and basal infoldings decreases as the collecting duct descends through the outer medulla. Like principal cells in the CCD, those in the OMCDo express apical plasma membrane ENaC and AQP2 and basolateral plasma membrane Na⁺K⁺-ATPase, consistent with their function in sodium and water reabsorption.^{217,377,381,386} The ammonia transporters, Rhbg and Rhcg, are also expressed in a similar pattern as in CCD principal cells, with basolateral Rhbg and apical and basolateral Rhcg, consistent with a role in ammonia secretion.^{361,365}

The majority of intercalated cells of the OMCD are structurally similar to type A intercalated cells of the CCD (Fig. 2.47), although with more prominent apical plasma membrane microprojections and fewer apical cytoplasmic vesicles under basal conditions. They also have similar transporter expression patterns, including H⁺ATPase and Rhcg in the apical plasma membrane and apical cytoplasmic vesicles and AE1, Rhbg, and Rhcg in the basolateral plasma membrane.^{351–354,361} In the OMCDi, the intercalated cells are taller, there are generally fewer apical cytoplasmic tubulovesicles, and the cytoplasm is less electron-dense such that it is similar to that of principal cells. Type B intercalated cells, identified by pendrin expression, are generally absent, but when present are typically

sparse and limited to the OMCDo near the corticomedullary junction. The presence of only the acid-secreting intercalated cell subtype in the OMCD is consistent with this segment's ability to secrete acid and inability to secrete bicarbonate.³⁶⁷

Under basal conditions, intercalated cells in the outer medulla exhibit moderate apical plasma membrane surface microfolds and cytoplasmic tubulovesicles; the cytoplasmic face of the tubulovesicles is coated with electron-dense stud-like particles^{343,344} associated with the vacuolar H⁺-ATPase (see Fig. 2.45).³⁴⁷ After induction of acute respiratory acidosis, metabolic acidosis, or hypokalemia, the apical cytoplasmic tubulovesicles are depleted, and apical plasma membrane microfolds proliferate and protrude into the lumen, producing a marked increase in apical plasma membrane surface area^{330,343,344,387} and an increase in apical plasma membrane exhibiting studs on the cytoplasmic face, visible by transmission electron microscopy.^{343,344} These ultrastructural changes coincide with increased apical plasma membrane expression of H⁺ATPase and Rhcg and decreased expression of these transporters in the apical cytoplasmic vesicle compartment, consistent with enhanced proton and ammonia secretion during these conditions.^{369,388,389} Conversely, during chloride-depletion metabolic acidosis, apical plasma membrane surface area and H⁺ATPase expression decrease, whereas apical cytoplasmic vesicles and H⁺ATPase expression increase, consistent with reduced acid secretion in response to alkalosis.³⁵² Similar responses have been documented in type A intercalated cells in the CCD.^{340,352,357}

In rabbit kidney, additional structural changes are associated with acid-loading involving the redistribution of expression of AE1, the basolateral Cl⁻/HCO₃⁻ exchanger. Under basal conditions, rabbit OMCD intercalated cells contain prominent intracytoplasmic multivesicular bodies that express AE1.³⁵⁶ After acid loading, these multivesicular bodies are reduced in number, and basolateral plasma membrane boundary

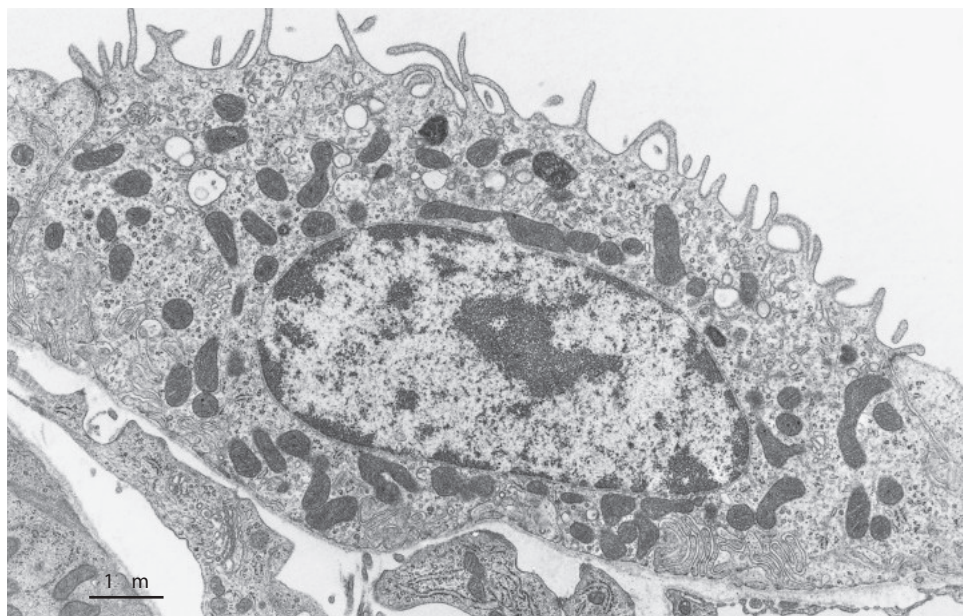


Fig. 2.47 Transmission electron micrograph of an intercalated cell in the outer medullary collecting duct of a normal rat kidney. The cell has a prominent tubulovesicular membrane compartment and many microprojections on the apical surface. (Modified from Madsen KM, Tisher CC. Response of intercalated cells of rat outer medullary collecting duct to chronic metabolic acidosis. *Lab Invest*. 1984;51:268–276.)

length and AE1 expression increase, along with the development of prominent basolateral extensions that give the cells a stellate appearance by light microscopy.³⁵⁷ These findings suggest that in rabbits, acidosis stimulates not only redistribution of proton pumps from the cytoplasmic pool to the apical plasma membrane but also redistribution of intracellular AE1 to the basolateral plasma membrane, thus enabling enhanced proton secretion and bicarbonate reabsorption.

INNER MEDULLARY COLLECTING DUCT

The IMCD extends from the boundary between the outer and inner medulla, defined by the transitions from thin to thick ascending limbs, to the papillary tip. In rat and rabbit, the transition from thin to thick ascending limbs, and thus the beginning of the IMCD, occurs within the renal parenchyma proximal to the papilla, forming the base of the inner medulla. However, in some mice, the TALs arise in the proximal portion of the papilla, in which case the IMCD is entirely contained within the papilla.

The IMCDs fuse successively as they descend in the inner medulla, such that few tubules remain at the papillary tip (Fig. 2.48). Cell height and tubule diameter increase distally, and the most distal portion, the ducts of Bellini, are composed of relatively tall, columnar epithelium. The IMCDt opens on the tip of the papilla at the area cribrosa (see Figs. 2.3 and 2.6). The length of the papilla, the number of collecting duct fusions, and cell height vary among species.^{241,390} In the rabbit, the cell height gradually increases from ~10 µm initially to ~50 µm near the papillary tip, whereas in the rat, the height increases from ~6 µm to ~15 µm at the papillary tip.^{241,391} In the rabbit and rat, the papillary tip is located in the renal pelvis at or near the renal hilum, whereas in the mouse, the papilla extends beyond the hilum, turning and extending a short distance into the ureter.

For ultrastructural characterization in the rat, the inner medulla was subdivided arbitrarily into thirds, and the IMCD

in each region designated accordingly.^{328,329,391} The outer third, IMCD₁, is the portion in the base of the inner medulla. The middle and terminal thirds, IMCD₂ and IMCD₃, are the portions in the proximal and terminal halves of the papilla, respectively. IMCD₁ is similar in ultrastructure to the OMCD_i (Fig. 2.49), although the percentage of intercalated cells is only ~10% in rat IMCD₁.^{328,329} In rabbit, the IMCD_i is essentially composed of only one cell type, similar in ultrastructure to the principal cell in the OMCD_i, with intercalated cells typically representing only 1% or less of cells.^{202,338} Rat IMCD₂ contains a mixture of ciliated cells similar to the principal cells in IMCD₁, a population of nonciliated cells, termed IMCD cells, and only rare intercalated cells (Fig. 2.50).^{328,329} Ciliated cells disappear in the distal IMCD₂, and IMCD₃ is composed entirely of IMCD cells, similar to those in IMCD₂ but taller (Fig. 2.51). In physiologic studies, the rat IMCD segments are often divided into an initial portion, the IMCD_i, corresponding to IMCD₁, and a terminal or papillary portion, the IMCD_t, which includes IMCD₂ and IMCD₃. Such studies in the rat have demonstrated that the structurally defined IMCD segments are also functionally distinct in comparisons of IMCD_i (IMCD₁) to IMCD_t (IMCD₂ and IMCD₃).^{392–394}

The IMCD cell of IMCD₂ and IMCD₃ is structurally distinct from principal cells (compare Figs. 2.52 and 2.49).^{328,391} It is one of the two epithelial cell types in the kidney (the other being intercalated cells) that has no central cilium. The luminal surface is covered with abundant, small, stubby plasma membrane microprojections that are covered with a prominent glycocalyx. Basal plasma membrane infoldings are relatively sparse, whereas lateral plasma membrane infoldings are prominent. Although both the apical and basal plasma membrane surface densities decrease progressively from IMCD₁ to IMCD₃, the absolute area of these membrane compartments does not change. In contrast, the lateral plasma membrane surface density and absolute area progressively increase. IMCD cells typically have a light-staining cytoplasm, few cell organelles, numerous free ribosomes, and many

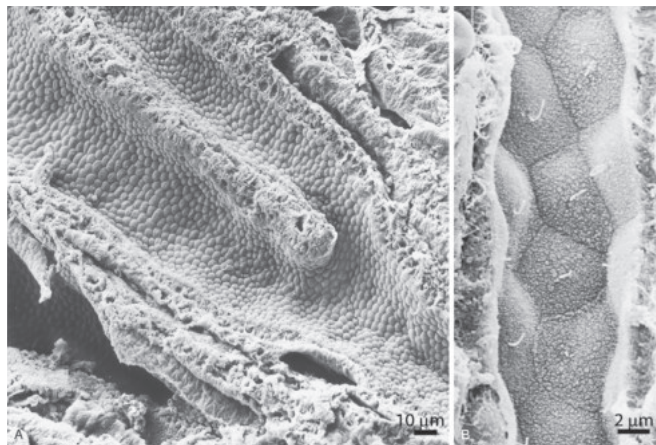


Fig. 2.48 Scanning electron micrographs of the normal papillary collecting duct of a rabbit. (A) The junction between two subdivisions at low magnification. (B) Higher-magnification view illustrating the luminal surfaces of individual cells with prominent microvilli and single cilia. (A, Courtesy Ann LeFurgey, PhD; B, modified from LeFurgey A, Tisher CC. Morphology of rabbit collecting duct. *Am J Anat.* 1979;155:111–124.)



Fig. 2.49 Transmission electron micrograph of a principal cell from the initial portion of the rat inner medullary collecting duct. There are few organelles in the cytoplasm, and apical microprojections are sparse. An interstitial fibroblast (asterisk) with dilated rough endoplasmic reticulum and a thin limb (TL) of loop of Henle are also illustrated.

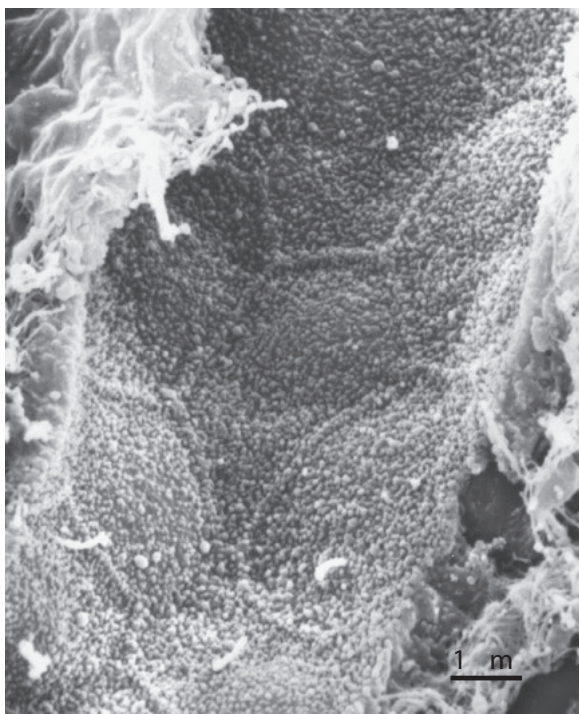


Fig. 2.50 Scanning electron micrograph from the middle portion of the rat inner medullary collecting duct. The luminal surface is covered with small microvilli, and some cells have single cilia, whereas others do not. (Modified from Madsen KM, Clapp WL, Verlander JW. Structure and function of the inner medullary collecting duct. *Kidney Int.* 1988;34:441–454.)

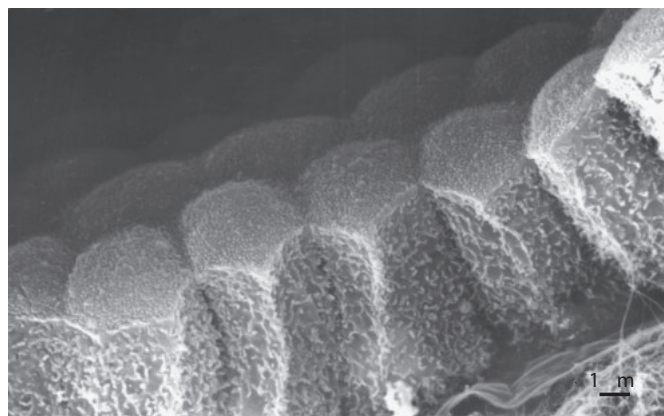


Fig. 2.51 Scanning electron micrograph of the terminal portion of rabbit inner medullary collecting duct. The cells are tall and covered with small microvilli on their luminal surfaces, but lack cilia. Small lateral cell processes project into the lateral intercellular spaces. (Modified from Madsen KM, Clapp WL, Verlander JW. Structure and function of the inner medullary collecting duct. *Kidney Int.* 1988;34:441.)

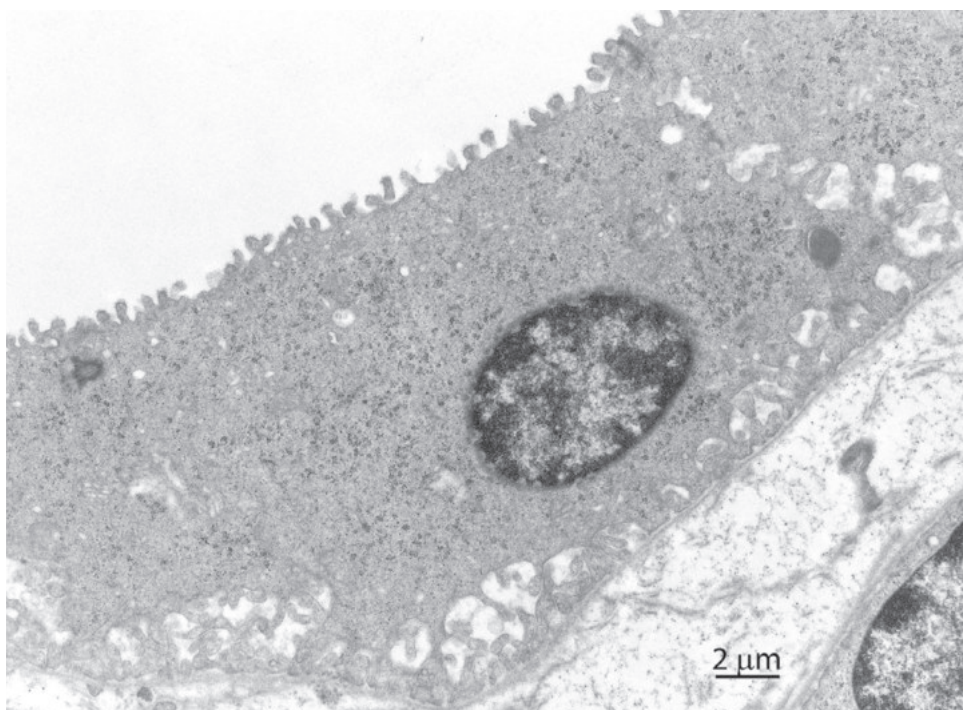


Fig. 2.52 Transmission electron micrograph of rat inner medullary collecting duct (IMCD) cell. IMCD cells are tall, possess few organelles, and have small microprojections on their apical surfaces. Ribosomes are abundant, and small vesicles are scattered throughout the cytoplasm.

small, coated vesicles resembling clathrin-coated vesicles (Fig. 2.52). IMCD cells, particularly those in IMCD₃, contain electron-dense, intracytoplasmic bodies representing lysosomes or lipid inclusions, often located beneath the nucleus.³²⁸

IMCD₁ and OMCDi principal and intercalated cells have similar transporter expression patterns and are believed to be functionally similar. However, IMCD₂ and IMCD₃ (IMCDt) not only have distinct structural features but also are distinct with respect to transporter expression. Notably, IMCD cells, present only in IMCD₂ and IMCD₃, express the urea transporters UT-A1 and UT-A3, whereas principal cells in IMCD₁ do not.³⁹⁵ Although few studies have correlated structural and functional responses in the IMCD, the rat IMCD₁ principal cell responds to chronic low-protein diet with a marked increase in basolateral plasma membrane area and enhanced urea transport, whereas IMCD cells in IMCD₂ show no change in ultrastructure or urea transport.³⁹² Later studies identified a sodium-dependent, active urea transport process present in IMCD₁ but absent in IMCD₂ and IMCD₃.³⁹³ IMCD cells also express AQP2 and regulation of its subcellular distribution occurs in response to vasopressin and water restriction, which stimulate redistribution of AQP2 from intracytoplasmic vesicles to the apical plasma membrane, thus enabling enhanced water uptake.^{377,378,396–398}

PAPILLARY SURFACE EPITHELIUM

The papilla is covered by a simple cuboidal epithelium, aptly named the papillary surface epithelium (PSE). PSE cells typically have a relatively smooth apical surface, numerous cytoplasmic vesicles, few mitochondria, and moderate basolateral infoldings. Multiple immunolocalization studies have detected expression of various transporters and other proteins, including the urea transporter, UT-B1, Na⁺-K⁺-ATPase, H⁺-K⁺-ATPase α_{2c} , NKCC1, and osteopontin.^{399–402} PSE cellular expression of H⁺-K⁺-ATPase α_{2c} is heterogeneous, suggesting heterogeneity in the epithelial cell types.⁴⁰¹ Limited physiologic studies have demonstrated transport activity consistent with the reported protein expression,^{403–405} and the presence of osteopontin supports the concept that PSE has a role in inhibiting urinary crystal deposition.³⁹⁹

INTERSTITIUM

The renal interstitium is composed of the structures interposed between the basement membranes of the renal tubules, glomeruli, and the vascular elements.^{406,407} Included in this space are several types of interstitial cells, extracellular matrix, interstitial fluid, lymphatics, and nerves.^{406–408} The interstitial volume in the rat and rabbit kidney constitutes approximately 13% and 18% of the total kidney volume, respectively.⁴⁰⁹ There is a considerable difference in the abundance of interstitium in the cortex compared with the medulla. In the rat kidney cortex, the peritubular interstitium constitutes 4% to 9% of the tissue volume.^{45,410,411} Interstitial volume increases from 10% to 20% in the outer medulla to approximately 30% to 40% at the papillary tip in both the rat and the rabbit.^{390,412}

The interstitium may be subdivided into different compartments, primarily the peritubular interstitium and the periarterial connective tissue.⁴⁰⁷ Although the glomerular and

extraglomerular mesangium may be considered part of the interstitium, based on their location, the makeup of the cells, and their communication with the peritubular interstitium,⁴⁰⁷ they are a specialized component of the glomerulus and JGA, discussed in a previous section, and are not included here.

The peritubular interstitium includes the interstitial cells, extracellular matrix, and interstitial fluid interposed between the basement membranes of the renal tubules and peritubular capillaries; it is continuous with the connective tissue of the renal capsule.⁴¹¹ The periarterial interstitium is a layer of connective tissue and interstitial cells surrounding the arteries in the renal cortex and may account for half of the cortical interstitial volume.^{407,411} It is most abundant around the interlobular and arcuate arteries and communicates with the peritubular interstitium⁴⁰⁷ and with the connective tissue underlying the epithelium of the renal pelvis.⁴¹¹ The periarterial interstitium is composed of a network of fibroblasts, similar to those in the peritubular interstitium, amid loose connective tissue; embedded in this are lymphatics and nerve fibers. The periarterial interstitium diminishes along the smaller arterioles and ends at the vascular pole of the glomerulus.

Interstitial cells can be classified most simply into two types: fibroblasts and cells of the immune system^{411,413}; these cell types correspond to the earlier designations, type 1 and type 2 interstitial cells.^{408,413–415} Fibroblasts, also known as “stellate” or “sustentacular cells,” are resident cells and are the most abundant cell type in the peritubular interstitium.^{407,411,413,416} In healthy kidney, interstitial fibroblasts are interconnected by intermediate junctions and form a network throughout the renal parenchyma, spanning between the capillaries and renal tubules. Interstitial fibroblasts form a scaffold, maintaining the architecture of the kidney, in part through attachments of their cellular extensions, “attachment plaques” filled with actin fibers, to the basement membranes of the capillaries and tubules and also by synthesis of collagen fibers of the extracellular matrix and microfilaments. The morphology of “quiescent” fibroblasts in the cortical interstitium of healthy kidney is typical of fibroblasts in other tissues, characterized by an elongated cell shape, angular nucleus, long cytoplasmic extensions, and abundant intracellular actin filaments (Fig. 2.53). The larger cytoplasmic extensions are flattened, perforated “leaflike” extensions or longer filiform processes. The cytoplasm contains numerous mitochondria and free ribosomes and prominent rough endoplasmic reticulum with dilated cisterns containing flocculent material. In inflammatory disease, interstitial fibroblasts increase in number, and the morphology of these “activated” fibroblasts differs from the fibroblasts of healthy kidney interstitium. These are termed “myofibroblasts” due to characteristics in common with smooth muscle cells, particularly formation of bundles of myofilaments and increased expression of α -smooth muscle actin. In the deep inner stripe of the outer medulla and the inner medulla, the fibroblast morphology differs from those in the cortex, containing numerous lipid inclusions, such that they have been called “lipid-laden” cells. These cells have relatively few mitochondria, rough endoplasmic reticulum with widely dilated cisterns and frequent contacts with the plasma membrane, and a more prominent cytoskeleton near the plasma membrane and extending into the cytoplasmic extensions, containing α -smooth muscle actin and vimentin filaments.^{411,417}

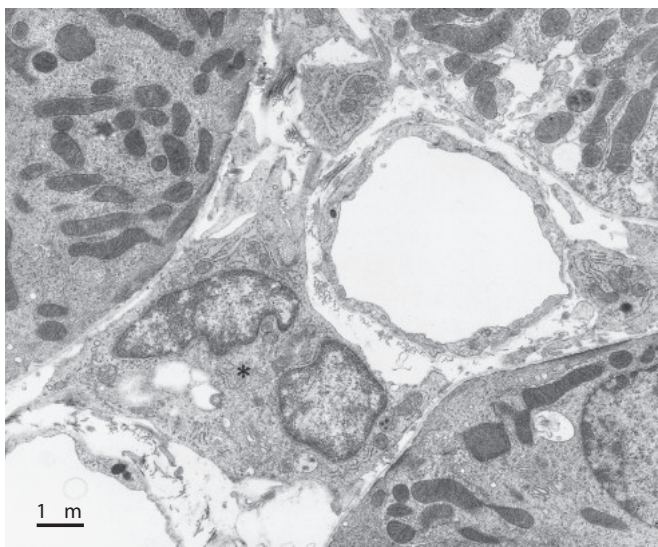


Fig. 2.53 Transmission electron micrograph of cortical interstitial fibroblast (asterisk) from a rat. A peritubular capillary is located at right center.

Pericytes are contractile cells intimately associated with the capillaries in both the renal cortex and medulla and may be considered a component of the renal interstitium.^{407,417–419} These cells correspond to cells previously identified in the medullary interstitium and designated “type 3 interstitial cells.” They are most abundant in the inner stripe of the outer medulla in association with descending vasa recta, but are also present in the renal cortex. Pericytes are attached to or embedded in the basement membrane of capillaries and wrap long cytoplasmic extensions around the vessel. In the renal medulla, they frequently contain lipid inclusions, which are less abundant than in medullary fibroblasts. Multiphoton imaging of pericytes using cell-specific markers recently demonstrated that pericyte density is greatest at branch points of the microvasculature where shear stress is greatest, with the cell bodies downstream of the branch point and cellular extensions reaching upstream, wrapping around the capillaries at the branch point.⁴²⁰ Pericytes proliferate during inflammation and appear to be the progenitors of the interstitial myofibroblasts, leading to increased matrix deposition and fibrosis.⁴²¹

The other major category of cells in the interstitium includes various cells of the immune system.⁴¹¹ Of these, the most common are dendritic cells. Dendritic cells in the kidney have a typical stellate shape, long cytoplasmic extensions, few lysosomes, and abundant mitochondria and rough endoplasmic reticulum. Dendritic cells are distinguished from fibroblasts by the lack of actin filament bundles under the plasma membrane and within cytoplasmic extensions; furthermore, the organelles in dendritic cells are clustered around the nucleus and absent from the cytoplasmic extensions.^{411,413,416} Less commonly found in the interstitium are transitory cells of the immune system, mainly macrophages and lymphocytes. In the healthy kidney, macrophages are mostly located in the periarterial interstitium, but they are not abundant. Lymphocytes are uncommon, and granulocytes are rare.⁴¹¹

The extracellular matrix of the interstitium consists of collagen fibrils within a ground substance of sulfated and nonsulfated GAGs and interstitial fluid.^{407,408} Collagen fibrils of types I, III, V, VI, VII, and XV have been identified in the extracellular matrix^{407,418,422,423} as well as fibronectin and laminin.^{407,422}

CORTICAL INTERSTITIUM

In the renal cortex, the peritubular interstitium is compartmentalized into a wide interstitial space, between two or more adjacent renal tubules, and a narrow or slit-like interstitial space between the basement membrane of a single tubule and the adjacent peritubular capillary.^{415,424} Approximately two-thirds of the total peritubular capillary wall faces the narrow compartment, and this portion of the vessel wall is fenestrated.⁴¹⁰

Fibroblasts and dendritic cells constitute the majority of interstitial cells in the peritubular interstitium, are distributed homogeneously, and are in close proximity to each other.⁴¹¹ The cell types can be discriminated by light microscopy by immunolabeling, as the cortical fibroblasts express the enzyme, ecto-5'-nucleotidase (5'NT), whereas dendritic cells express MHC class II.⁴¹¹ Under basal conditions, 5'NT expression in cortical fibroblasts is strongest in the cortical labyrinth in the deep inner cortex.^{411,425} As 5'NT mediates production of extracellular adenosine, a signaling molecule implicated in control of renal vascular resistance, cortical interstitial fibroblasts may contribute to regulation of renal hemodynamics.^{406,416} Peritubular interstitial fibroblasts and/or pericytes in the deep inner cortex are also the renal source of erythropoietin,^{417,426} and perivascular interstitial cells associated with the afferent arteriole can be recruited to produce renin during salt and volume depletion, renal hypoperfusion, or inhibition of the renin–angiotensin–aldosterone system.⁴¹⁷

MEDULLARY INTERSTITIUM

As in the cortex, fibroblasts and dendritic cells constitute the vast majority of interstitial cells in the healthy renal medulla.^{411,413,427} As described earlier, the fibroblasts of the medullary interstitium differ most notably from the cortical fibroblasts in the abundance of intracytoplasmic lipid inclusions, with an average diameter of 0.4 to 0.5 μm; the lipid droplets are homogeneous in density and have no limiting membrane (Figs. 2.54 and 2.55).^{415,424,427,428} Only occasional cortical fibroblasts contain lipid droplets; the incidence of these “lipid-laden” fibroblasts increases in the inner stripe of the outer medulla and they are present throughout the inner medulla.⁴¹¹ Unlike the fibroblasts of the cortex, medullary interstitial fibroblasts do not express erythropoietin messenger RNA or 5'NT.^{425,426}

Medullary interstitial fibroblasts form a ladderlike structure between the loops of Henle and vasa recta, arranged in columns along the corticomedullary axis and oriented perpendicular to the adjacent tubules and vessels (see Fig. 2.54). The elongated cell processes are in close contact with the thin limbs of Henle and the vasa recta, but direct contact with collecting ducts is rarely observed. Often, a single cell is in contact with several vessels and thin limbs.⁴²⁴ The long cytoplasmic processes from different cells are often connected by specialized cell junctions that vary in both size and shape

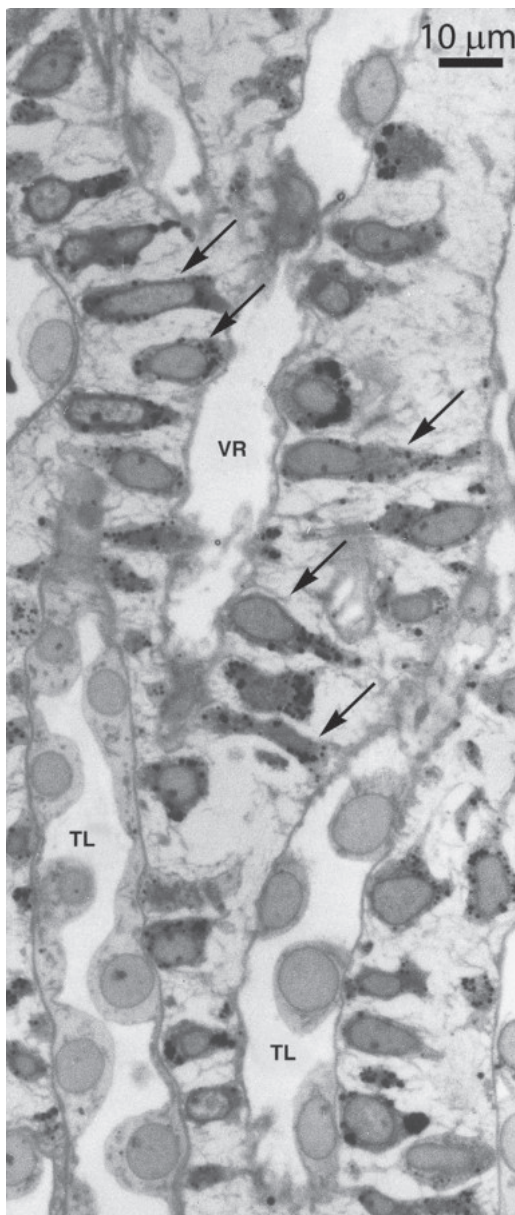


Fig. 2.54 Light micrograph of the renal medullary interstitium from a normal rat. The lipid-laden interstitial fibroblasts bridge the interstitial space between adjacent thin limbs of Henle (TL) and vasa recta (VR).

and contain elements of tight junctions, intermediate junctions, and gap junctions.^{429,430} The cells likely provide structural support in the medulla because of their special arrangement perpendicular to the tubules and vessels. The close relationship between medullary interstitial fibroblasts and the thin limbs and capillaries also suggests a possible interaction with these structures. Three-dimensional reconstructions of the inner medulla have demonstrated arrangements of ascending thin limbs, ascending vasa recta, and collecting ducts to form interstitial nodal spaces or microdomains, which are abundant in rodent kidney but relatively infrequent in human inner medulla.^{12,265,431} The interstitial nodal spaces align in stacks along the corticomedullary axis and are believed to be divided by the interstitial fibroblasts.^{12,431,432} Peritubular interstitial



Fig. 2.55 Higher-magnification electron micrograph illustrating the relationship between the electron-dense lipid droplets, which almost fill the medullary interstitial fibroblasts, and the granular endoplasmic reticulum (arrows). Wisps of basement membrane–like material adjacent to the surfaces of the cells are contiguous with the basement membranes of the adjacent tubules (*lower right*).

fibroblasts in the medulla express cyclooxygenase-2 and are a major site of prostaglandin synthesis, with the major product being PGE₂.^{417,433}

Dendritic cells are also present in the medullary interstitium and can be identified at the light microscopic level by immunoreactivity for MHC II. However, their prevalence varies among the regions of the medulla. They are most abundant in the inner stripe of the outer medulla, frequently aligned with collecting ducts. They are less abundant in the upper third of the inner medulla, and disappear in the distal portions of the inner medulla in the healthy kidney.⁴¹¹

LYMPHATICS

The renal lymphatic circulation includes capsular, subcapsular, and intrarenal components.^{434,435} The subcapsular component consists of a network of lymphatics in the space between the renal capsule and the renal parenchyma. The intrarenal component includes lymphatic capillaries and channels that coalesce and drain via bundles of lymphatic vessels at the hilum of the kidney. Subcapsular lymphatics may drain directly to the lymphatics at the hilum or may communicate with intrarenal lymphatic vessels. Intrarenal

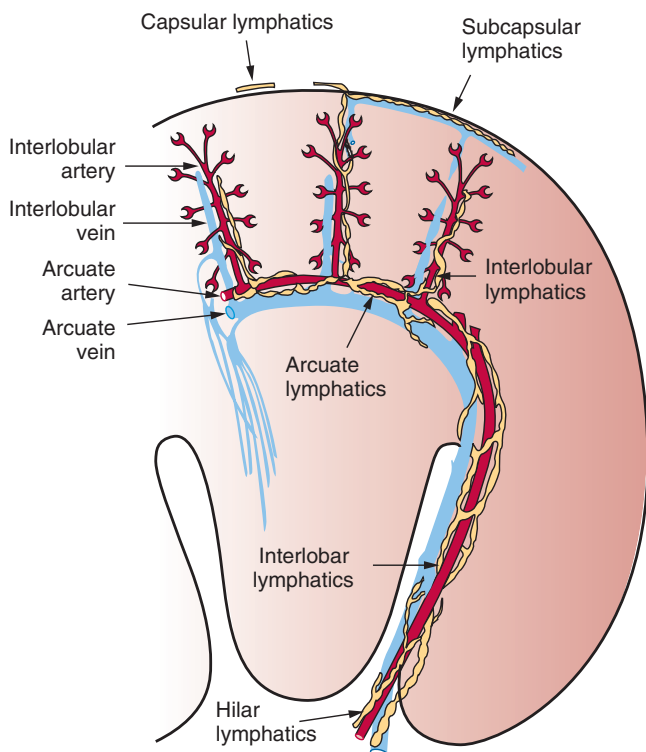


Fig. 2.56 Diagram of the lymphatic circulation in the mammalian kidney. (Modified from Kriz W, Dieterich HJ. The lymphatic system of the kidney in some mammals. Light and electron microscopic investigations. *Z Anat Entwicklungsgesch.* 1970;131:111–147.)

lymphatics neighboring the interlobular blood vessels drain into the arcuate lymphatic vessels near the corticomedullary junction, which drain through interlobar lymphatics to hilar lymphatic vessels (Fig. 2.56).⁴³⁶

Communications between the capsular lymphatics and intrarenal lymphatics have been described in some animals, such that the lymphatic vessels of the renal capsule drain into subcapsular lymphatic channels, providing continuous lymphatic drainage from the renal capsule, through the cortex, and into the hilar region (Fig. 2.57). In dog kidney, “communicating” and “perforating” lymphatic channels that transverse the renal capsule have been described.⁴³⁷ In these studies, a small number of communicating lymphatic channels were found, usually associated with an interlobular artery and vein; these lymphatics penetrated the capsule and appeared to represent a connection between the hilar and capsular systems. The perforating lymphatic channel penetrated the capsule alone or in association with a small vein; these channels appeared to represent a primary pathway for lymph drainage from the superficial cortex.

The intrarenal lymphatics represent a small fraction of the renal tissue, with the lymphatic volume density in the cortex ranging from 0.02%–0.37%, depending on the species.^{438,439} In normal human, rat, mouse, and pig kidney, the majority of lymphatic capillaries in the renal parenchyma cluster in the adventitia around the interlobular and arcuate arteries (Fig. 2.58),^{434,436,440} and in the mouse, they also extend along the afferent arteriole.⁴⁴⁰ In most animal species, lymphatic capillaries are rarely found among renal tubules and glomeruli, but in the horse and dog, lymphatics are abundant

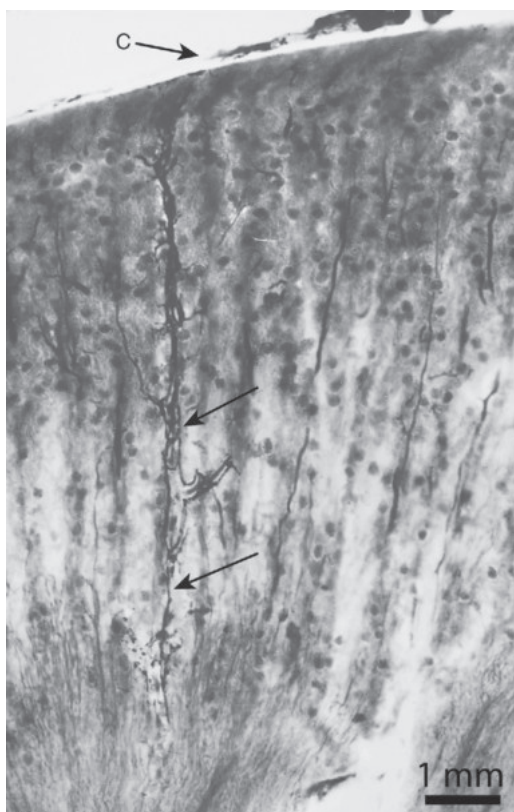


Fig. 2.57 Light micrograph of a sagittal section through the cortex and outer medulla of a dog kidney. A capsular lymphatic (C) was injected with India ink. Intrarenal lymphatics (arrows) follow the distribution of the interlobular arteries in the cortex. (Modified from Bell RD, Keyl MJ, Shrader FR, et al. Renal lymphatics: the internal distribution. *Nephron.* 1968;5:454–463.)

around glomeruli,⁴³⁴ and in dog kidney, small lymphatics are found in proximity to proximal and distal tubules.^{438,441} Studies of normal human kidney using immunolabeling to detect lymphatics found lymphatic capillaries most commonly in the adventitia surrounding interlobular and arcuate vessels, as in other species^{442,443}; lymphatic capillaries among renal tubules were rare in one study⁴⁴³ and in another were described as interspersed among renal tubules in the cortex, though they were less common than vascular capillaries and were sporadic near glomeruli.⁴⁴² Lymphatics are rarely found in the medulla of healthy kidneys, a finding that is consistent among species.^{440,442,444,445}

Lymphatic capillaries, including the interlobular lymphatics, are composed of a layer of lymphatic endothelial cells, but unlike capillaries of the vascular system, they lack a basement membrane and fenestrations.^{436,445} Lymphatic capillary endothelial cells are anchored by filaments attached to basal cytoplasmic projections.^{435,445} The interlobar and hilar lymphatic channels are *collecting* lymphatic vessels and contain numerous valves,^{434,436} semilunar projections in the lumen of the lymphatic vessels that limit backflow of lymph. Collecting lymphatics also are distinguished from lymphatic capillaries by the presence of a continuous basement membrane and pericytes around the interstitial face of the lymphatic.⁴⁴⁵

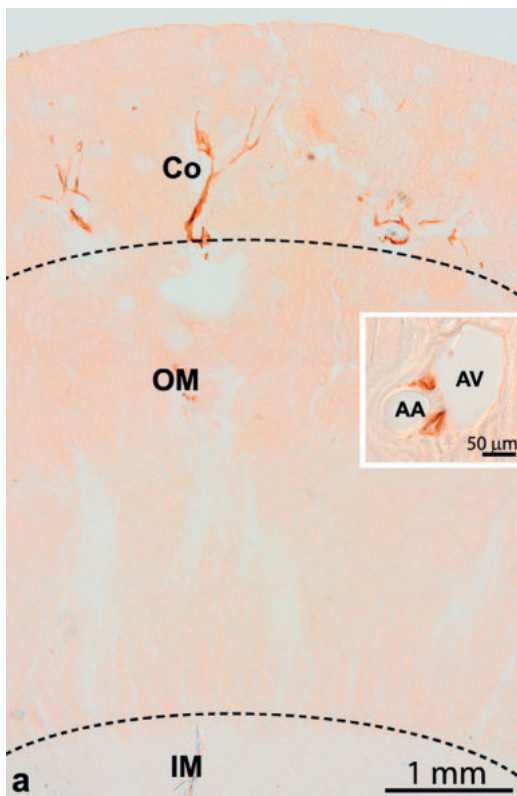


Fig. 2.58 Light micrograph of 50- μm -thick section of adult mouse kidney labeled for lymphatic endothelium-specific hyaluronan receptor LYVE-1, which marks lymphatic endothelial cells almost exclusively. The lymphatics are largely clustered around the arcuate and interlobular vessels. Co, Cortex; OM, outer medulla; IM, inner medulla; AA, arcuate artery; AV, arcuate vein (Modified from Lee HW, Qin YX, Kim YM, et al. Expression of lymphatic endothelium-specific hyaluronan receptor LYVE-1 in the developing mouse kidney. *Cell Tissue Res.* 2011;343:429–444.)

The majority of efferent renal hilar lymphatics drain to regional lymph nodes. The right kidney lymphatics drain into the paracaval, precaval, interaortocaval, and retrocaval nodes, and the left kidney lymphatics drain into the preaortic, paraaortic, and retroaortic nodes. In addition, posterior efferent renal lymphatic vessels may communicate directly with the thoracic duct.^{446–448} Finally, in some rat and primate species, lymphovenous drainage has been detected, with direct connections between the lymphatic system and the renal veins or the vena cava near the renal veins. These multiple and variable drainage patterns may have important clinical implications in the pathogenesis, staging, and diagnosis of renal cell carcinoma metastases.^{449,450}

Until relatively recently, identification of the intrarenal lymphatics relied on structural studies using lymphatic injections, microradiography, and electron microscopy. These laborious techniques limited the examination of the effects of physiologic and pathologic processes on the lymphatic system. However, the discovery of specific proteins expressed by lymphatic endothelial cells has enabled immunodetection of these cells (Fig. 2.58). The various markers used to detect intrarenal lymphatic endothelial cells include the hyaluronate receptor, LYVE-1; the lymphatic transcription factor, Prox-1; vascular endothelial growth factor receptor 3; the integral membrane glycoprotein, podoplanin; and the sialoglycopro-

tein, D2-40.^{435,440,451} Lymphatic endothelial cells also express AQP1.^{253,452} Using immunolabeling for lymphatic endothelial cell markers, several studies have reported proliferation of intrarenal lymphatics in the renal parenchyma in forms of hypertension,⁴⁵³ tubulointerstitial nephritis,⁴⁴³ transplant rejection,^{454,455} ureteral obstruction,⁴⁵⁶ and diabetic nephropathy⁴⁵⁷ and in the tissue surrounding renal cell carcinomas.⁴⁴² The role of lymphangiogenesis in these nephropathies is not well understood. It has been implicated in the pathogenesis of renal inflammation,⁴³⁵ but some studies suggest it may be beneficial and limit renal injury, at least in some conditions.^{453,456}

INNERVATION

The sympathetic innervation of the kidney arises from the intermediolateral column of the spinal cord between T6 and L2,⁴⁵⁸ although some report a narrower range, between T9 and T13.⁴⁵⁹ Neurons from the brain project to this region of the spinal cord primarily from the raphe nucleus and rostral ventrolateral medulla in the vasomotor center of the brain, the pontine A5 noradrenergic cell group, and the paraventricular nucleus in the hypothalamus;^{460,461} these areas in the brain determine the sympathetic signaling to the kidney.⁴⁵⁹ The sympathetic preganglionic fibers exit the spinal cord between T11 and L3 or L4 and connect with postganglionic fibers in both paravertebral and prevertebral ganglia, the latter including the aorticorenal, splanchnic, celiac, and mesenteric ganglia, and in the renal plexus^{459,462–464} and postganglionic fibers arising from different ganglia appear to innervate different regions of the kidney.⁴⁶⁴ There is considerable variation among species and among individuals in the spinal cord segment that supplies the preganglionic fibers and in the ganglia where the postganglionic fibers to the kidney originate.^{459,460}

The postganglionic fibers form the extrinsic nerves to the kidney, which contain both unmyelinated and myelinated fibers. The vast majority of renal nerve fibers in rat and mouse are unmyelinated, 96%–98% in the rat,^{465,466} and 99.5% unmyelinated fibers in the mouse.⁴⁶⁷ The diameter of the renal nerves differs considerably between these species, measuring ~98 μm in diameter in the rat⁴⁶⁶ and ~35 μm in diameter in the mouse,⁴⁶⁷ due to a greater number of fibers in the rat extrinsic renal nerves rather than a significant difference in the diameter of unmyelinated nerve fibers between species.^{466,467} Nerve fibers in the rabbit renal cortex fall into two groups based on fiber diameters,^{468,469} but morphometric studies of rat and mouse extrinsic renal nerves have not consistently found this pattern.⁴⁵⁹ Although a bimodal distribution of unmyelinated nerve fiber diameter was found in the renal nerve of Sprague-Dawley rats,⁴⁶⁵ in Wistar rats⁴⁶⁶ and C57BL/6J mice,⁴⁶⁷ the average diameter of unmyelinated fibers ranged between 0.5 and 0.7 μm in a unimodal size distribution.

The renal nerves enter the kidney at the hilum and run with the renal arteries into the kidney, where they continue along the arterial circulation as it subdivides, lying within the perivascular interstitium and penetrating the vessel walls to innervate vascular smooth muscle cells in interlobar, arcuate, and interlobular arteries and in afferent and efferent arterioles, including juxtaglomerular cells.^{176,458,459,470–473}

Nerve endings are in contact with approximately one-third of the cells of the efferent arteriole and somewhat less of the afferent arteriole,⁴⁷⁴ and synapses between autonomic nerve endings and granular and agranular cells of the JGA are visible by transmission electron microscopy.⁴⁷⁵ Consistent with these observations, renin secretion is modulated by renal sympathetic nerve activity.^{462,476} Neuroeffector junctions at the macula densa are infrequent in comparison to the afferent and efferent arterioles.⁴⁷⁴

Single nerve fibers penetrate the cortical and juxtamedullary renal parenchyma and parts of the medulla.^{213,459,477–479} Unmyelinated nerve fibers accompanying the efferent arterioles of juxtamedullary glomeruli extend with the vasculature to the level of the inner stripe of the outer medulla.⁴⁸⁰ Sympathetic nerve terminals make contact with the basement membranes of the tubule epithelial cells at nerve varicosities containing dense-cored vesicles, which contain norepinephrine^{213,470,479} and tyrosine hydroxylase, the rate-limiting enzyme in norepinephrine production.⁴⁶² Although neuroeffector junctions are present on all renal tubule types, the density of nerve varicosities varies among the renal tubules; the TAL has the highest density, followed by the DCT, the proximal tubule, and the collecting duct.²¹³

The majority of the renal innervation is efferent. However, afferent nerves are also present, principally innervating the renal pelvis, but also the interlobar, arcuate, and interlobular arteries, and afferent arterioles.^{458,470,481–483} Approximately 75%–80% of afferent renal nerves are unmyelinated.^{458,484,485} Unlike efferent nerve fibers, which express tyrosine hydroxylase, afferent nerve fibers express calcitonin gene-related peptide, and thus, efferent and afferent fibers can be discriminated using immunolocalization for these enzymes.^{470,483,486}

ACKNOWLEDGMENTS

Portions of this chapter are adapted from the chapters written previously by Kirsten M. Madsen, Soren Nielsen, and C. Craig Tisher (8th edition), Søren Nielsen, Tae-Hwan Kwon, Robert A. Fenton, and Jeppe Praetorius (9th edition), and Robert A. Fenton and Jeppe Praetorius (10th edition).

The authors are grateful for the support and encouragement of our families, for our mentors in our early careers, particularly Dr. C. Craig Tisher and Dr. Kirsten Madsen, and for our collaborators and colleagues. The work of our laboratories over the years was only possible due to the dedication of many talented microscopists, particularly Dr. Sharon W. Matthews, Chao Chen, Wendy Wilber, and Fred Kopp, and the support of the National Institutes of Health, American Heart Association, and Gatorade Research Fund.

 Complete reference list available at ExpertConsult.com.

KEY REFERENCES

5. Bertram JF, Douglas-Denton RN, Diouf B, et al. Human nephron number: implications for health and disease. *Pediatr Nephrol*. 2011;26(9):1529–1533. doi:10.1007/s00467-011-1843-8. [doi].
11. Christensen EI, Wagner CA, Kaissling B. Uriniferous tubule: structural and functional organization. *Compr Physiol*. 2012;2(2):805–861. doi:10.1002/cphy.c100073. [doi].
22. Dane MJ, van den Berg BM, Lee DH, et al. A microscopic view on the renal endothelial glycocalyx. *Am J Physiol Renal Physiol*. 2015;308(9):F956–F966. doi:10.1152/ajprenal.00532.2014. [doi].
31. Bartlett CS, Jeansson M, Quaggia SE. Vascular growth factors and glomerular disease. *Annu Rev Physiol*. 2016;78:437–461. doi:10.1146/annurev-physiol-021115-105412. [doi].
49. Miner JH. The glomerular basement membrane. *Exp Cell Res*. 2012;318(9):973–978. doi:10.1016/j.yexcr.2012.02.031. [doi].
53. Abramson DR, Hudson BG, Stroganova L, et al. Cellular origins of type IV collagen networks in developing glomeruli. *J Am Soc Nephrol*. 2009;20(7):1471–1479. doi:10.1681/ASN.2008101086. [doi].
59. Suleiman H, Zhang L, Roth R, et al. Nanoscale protein architecture of the kidney glomerular basement membrane. *Elife*. 2013;2:e01149. doi:10.7554/elife.01149. [doi].
78. Jarad G, Cunningham J, Shaw AS, et al. Proteinuria precedes podocyte abnormalities in *Lamb2*-/- mice, implicating the glomerular basement membrane as an albumin barrier. *J Clin Invest*. 2006;116(8):2272–2279. doi:10.1172/JCI28414. [doi].
80. Ichimura K, Miyazaki N, Sadayama S, et al. Three-dimensional architecture of podocytes revealed by block-face scanning electron microscopy. *Sci Rep*. 2015;5:8993. doi:10.1038/srep08993. [doi].
81. Burghardt T, Hochapfel F, Salecker B, et al. Advanced electron microscopic techniques provide a deeper insight into the peculiar features of podocytes. *Am J Physiol Renal Physiol*. 2015;309(12):F1082–F1089. doi:10.1152/ajprenal.00338.2015. [doi].
84. Schell C, Huber TB. The evolving complexity of the podocyte cytoskeleton. *J Am Soc Nephrol*. 2017;28(11):3166–3174. doi:10.1681/ASN.2017020143. [doi].
91. Suleiman HY, Roth R, Jain S, et al. Injury-induced actin cytoskeleton reorganization in podocytes revealed by super-resolution microscopy. *JCI Insight*. 2017;2(16):doi:10.1172/jci.insight.94137. [doi].
116. Rice WL, Van Hoek AN, Paunescu TG, et al. High resolution helium ion scanning microscopy of the rat kidney. *PLoS ONE*. 2013;8(3):e57051. doi:10.1371/journal.pone.0057051. [doi].
117. Tsui K, Paunescu TG, Suleiman H, et al. Re-characterization of the glomerulopathy in CD2AP deficient mice by high-resolution helium ion scanning microscopy. *Sci Rep*. 2017;7(1):8321–017-08304-3. doi:10.1038/s41598-017-08304-3. [doi].
118. Grahammer F, Wigge C, Schell C, et al. A flexible, multilayered protein scaffold maintains the slit in between glomerular podocytes. *JCI Insight*. 2016;1(9). doi:10.1172/jci.insight.86177 [pii].
121. New LA, Martin CE, Jones N. Advances in slit diaphragm signaling. *Curr Opin Nephrol Hypertens*. 2014;23(4):420–430. doi:10.1097/MNH.000000000000018. mnh.0000447018.28852.b6. [doi].
149. Schlondorff D, Banas B. The mesangial cell revisited: no cell is an island. *J Am Soc Nephrol*. 2009;20(6):1179–1187. doi:10.1681/ASN.2008050549. [doi].
161. Shankland SJ, Smeets B, Pippin JW, et al. The emergence of the glomerular parietal epithelial cell. *Nat Rev Nephrol*. 2014;10(3):158–173. doi:10.1038/nrneph.2014.1. [doi].
167. Shankland SJ, Freedman BS, Pippin JW. Can podocytes be regenerated in adults? *Curr Opin Nephrol Hypertens*. 2017;26(3):154–164. doi:10.1097/MNH.0000000000000311. [doi].
179. Hackenthal E, Paul M, Ganten D, et al. Morphology, physiology, and molecular biology of renin secretion. *Physiol Rev*. 1990;70(4):1067–1116. doi:10.1152/physrev.1990.70.4.1067. [doi].
198. Maunsbach AB. Observations on the segmentation of the proximal tubule in the rat kidney. comparison of results from phase contrast, fluorescence and electron microscopy. *J Ultrastruct Res*. 1966;16(3):239–258.
202. Kaissling B, Kriz W. Structural analysis of the rabbit kidney. *Adv Anat Embryol Cell Biol*. 1979;56:1–123.
236. Yang LE, Maunsbach AB, Leong PK, et al. Differential traffic of proximal tubule Na⁺ transporters during hypertension or PTH: NHE3 to base of microvilli vs. NaPi2 to endosomes. *Am J Physiol Renal Physiol*. 2004;287(5):F896–F906. doi:10.1152/ajprenal.00160.2004. [doi].
259. Christensen EI, Grann B, Kristoffersen IB, et al. Three-dimensional reconstruction of the rat nephron. *Am J Physiol Renal Physiol*. 2014;306(6):F664–F671. doi:10.1152/ajprenal.00522.2013. [doi].
265. Wei G, Rosen S, Dantzler WH, et al. Architecture of the human renal inner medulla and functional implications. *Am J Physiol Renal Physiol*. 2015;309(7):F627–F637. doi:10.1152/ajprenal.00236.2015. [doi].
266. Pannabecker TL. Structure and function of the thin limbs of the loop of henle. *Compr Physiol*. 2012;2(3):2063–2086. doi:10.1002/cphy.c110019. [doi].
268. Kriz W, Bankir L. A standard nomenclature for structure of the kidney. the renal commission of the international union of physiological sciences(IUPS). *Anat Embryol (Berl)*. 1988;178(2):N1–N8.

269. Woodhall PB, Tisher CC. Response of the distal tubule and cortical collecting duct to vasopressin in the rat. *J Clin Invest.* 1973; 52(12):3095–3108. doi:10.1172/JCI107509. [doi].
285. Campean V, Kricke J, Ellison D, et al. Localization of thiazide-sensitive Na(+)-Cl(-) cotransport and associated gene products in mouse DCT. *Am J Physiol Renal Physiol.* 2001;281(6):F1028–F1035. doi:10.1152/ajprenal.0148.2001. [doi].
305. Dorup J, Morsing P, Rasch R. Tubule-tubule and tubule-arteriole contacts in rat kidney distal nephrons. A morphologic study based on computer-assisted three-dimensional reconstructions. *Lab Invest.* 1992;67(6):761–769.
306. Ren Y, Garvin JL, Liu R, et al. Crosstalk between the connecting tubule and the afferent arteriole regulates renal microcirculation. *Kidney Int.* 2007;71(11):1116–1121. doi: S0085-2538(15)52273-4 [pii].
314. Teng-umnuay P, Verlander JW, Yuan W, et al. Identification of distinct subpopulations of intercalated cells in the mouse collecting duct. *J Am Soc Nephrol.* 1996;7(2):260–274.
328. Clapp WL, Madsen KM, Verlander JW, et al. Morphologic heterogeneity along the rat inner medullary collecting duct. *Lab Invest.* 1989;60(2):219–230.
340. Verlander JW, Madsen KM, Tisher CC. Effect of acute respiratory acidosis on two populations of intercalated cells in rat cortical collecting duct. *Am J Physiol.* 1987;253(6 Pt 2):F1142–F1156.
344. Madsen KM, Tisher CC. Response of intercalated cells of rat outer medullary collecting duct to chronic metabolic acidosis. *Lab Invest.* 1984;51(3):268–276.
357. Verlander JW, Madsen KM, Cannon JK, et al. Activation of acid-secreting intercalated cells in rabbit collecting duct with ammonium chloride loading. *Am J Physiol.* 1994;266(4 Pt 2):F633–F645.
369. Seshadri RM, Klein JD, Smith T, et al. Changes in subcellular distribution of the ammonia transporter, Rhcg, in response to chronic metabolic acidosis. *Am J Physiol Renal Physiol.* 2006;290(6):F1443–F1452. doi: 00459.2005 [pii].
371. Verlander JW, Kim YH, Shin W, et al. Dietary Cl(-) restriction upregulates pendrin expression within the apical plasma membrane of type B intercalated cells. *Am J Physiol Renal Physiol.* 2006;291(4):F833–F839. doi: 00474.2005 [pii].
380. Kaissling B, Le Hir M. Distal tubular segments of the rabbit kidney after adaptation to altered Na- and K-intake. I. structural changes. *Cell Tissue Res.* 1982;224(3):469–492.
387. Elger M, Bankir L, Kriz W. Morphometric analysis of kidney hypertrophy in rats after chronic potassium depletion. *Am J Physiol.* 1992;262(4 Pt 2):F656–F667. doi:10.1152/ajprenal.1992.262.4.F656. [doi].
389. Brown D, Paunescu TG, Breton S, et al. Regulation of the V-ATPase in kidney epithelial cells: dual role in acid-base homeostasis and vesicle trafficking. *J Exp Biol.* 2009;212(Pt 11):1762–1772. doi:10.1242/jeb.028803. [doi].
407. Lemley KV, Kriz W. Anatomy of the renal interstitium. *Kidney Int.* 1991;39(3):370–381. doi: S0085-2538(15)57139-1 [pii].
411. Kaissling B, Hegyi I, Loeffing J, et al. Morphology of interstitial cells in the healthy kidney. *Anat Embryol (Berl).* 1996;193(4):303–318.
419. Takahashi-Iwanaga H. The three-dimensional cytoarchitecture of the interstitial tissue in the rat kidney. *Cell Tissue Res.* 1991;264(2): 269–281.
426. Bachmann S, Le Hir M, Eckardt KU. Co-localization of erythropoietin mRNA and ecto-5'-nucleotidase immunoreactivity in peritubular cells of rat renal cortex indicates that fibroblasts produce erythropoietin. *J Histochem Cytochem.* 1993;41(3):335–341. doi:10.1177/41.3.8429197. [doi].
432. Gilbert RL, Pannabecker TL. Architecture of interstitial nodal spaces in the rodent renal inner medulla. *Am J Physiol Renal Physiol.* 2013;305(5):F745–F752. doi:10.1152/ajprenal.00239.2013. [doi].
435. Yazdani S, Navis G, Hillebrands JL, et al. Lymphangiogenesis in renal diseases: passive bystander or active participant? *Expert Rev Mol Med.* 2014;16:e15. doi:10.1017/erm.2014.18. [doi].
442. Ishikawa Y, Akasaka Y, Kiguchi H, et al. The human renal lymphatics under normal and pathological conditions. *Histopathology.* 2006;49(3):265–273. doi: HIS2478 [pii].
467. Fazan VP, Ma X, Chapleau MW, et al. Qualitative and quantitative morphology of renal nerves in C57BL/6j mice. *Anat Rec.* 2002;268(4):399–404. doi:10.1002/ar.10174. [doi].
470. Barajas L, Liu L, Powers K. Anatomy of the renal innervation: intrarenal aspects and ganglia of origin. *Can J Physiol Pharmacol.* 1992;70(5):735–749.

REFERENCES

1. Cheong B, Muthupillai R, Rubin MF, et al. Normal values for renal length and volume as measured by magnetic resonance imaging. *Clin J Am Soc Nephrol.* 2007;2(1):38–45. doi: CJN.00930306 [pii].
2. Zelenko N, Coll D, Rosenfeld AT, et al. Normal ureter size on unenhanced helical CT. *AJR Am J Roentgenol.* 2004;182(4):1039–1041. doi:10.2214/ajr.182.4.1821039. [doi].
3. Hughson M, Farris AB 3rd, Douglas-Denton R, et al. Glomerular number and size in autopsy kidneys: the relationship to birth weight. *Kidney Int.* 2003;63(6):2113–2122. doi: S0085-2538(15)49128-8 [pii].
4. Keller G, Zimmer G, Mall G, et al. Nephron number in patients with primary hypertension. *N Engl J Med.* 2003;348(2):101–108. doi:10.1056/NEJMoa020549. [doi].
5. Bertram JF, Douglas-Denton RN, Diouf B, et al. Human nephron number: implications for health and disease. *Pediatr Nephrol.* 2011;26(9):1529–1533. doi:10.1007/s00467-011-1843-8. [doi].
6. Nyengaard JR, Bendtsen TF. Glomerular number and size in relation to age, kidney weight, and body surface in normal man. *Anat Rec.* 1992;232(2):194–201. doi:10.1002/ar.1092320205. [doi].
7. Bertram JF, Soosaipillai MC, Ricardo SD, et al. Total numbers of glomeruli and individual glomerular cell types in the normal rat kidney. *Cell Tissue Res.* 1992;270(1):37–45.
8. Nyengaard JR. The quantitative development of glomerular capillaries in rats with special reference to unbiased stereological estimates of their number and sizes. *Microvasc Res.* 1993;45(3):243–261. S0026-2862(83)71022-8 [pii].
9. Baines AD, de Rouffignac C. Functional heterogeneity of nephrons. II. filtration rates, intraluminal flow velocities and fractional water reabsorption. *Pflugers Arch.* 1969;308(3):260–276.
10. Georgas K, Rumballe B, Valerius M, et al. Analysis of early nephron patterning reveals a role for distal RV proliferation in fusion to the ureteric tip via a cap mesenchyme-derived connecting segment. *Dev Biol.* 2009;332:273–286.
11. Christensen EI, Wagner CA, Kaissling B. Uriniferous tubule: structural and functional organization. *Compr Physiol.* 2012;2(2):805–861. doi:10.1002/cphy.c100073. [doi].
12. Pannabecker TL, Dantzer WH. Three-dimensional architecture of inner medullary vasa recta. *Am J Physiol Renal Physiol.* 2006;290(6):F1355–F1366. doi: 00481.2005 [pii].
13. Pannabecker TL, Dantzer WH. Three-dimensional architecture of collecting ducts, loops of Henle, and blood vessels in the renal papilla. *Am J Physiol Renal Physiol.* 2007;293(3):F696–F704. 00231.2007 [pii].
14. Pannabecker TL. Loop of Henle interaction with interstitial nodal spaces in the renal inner medulla. *Am J Physiol Renal Physiol.* 2008;295(6):F1744–F1751. doi:10.1152/ajprenal.90483.2008. [doi].
15. Zhai XY, Birn H, Jensen KB, et al. Digital three-dimensional reconstruction and ultrastructure of the mouse proximal tubule. *J Am Soc Nephrol.* 2003;14(3):611–619.
16. Zhai XY, Thomsen JS, Birn H, et al. Three-dimensional reconstruction of the mouse nephron. *J Am Soc Nephrol.* 2006;17(1):77–88. doi: ASN.2005080796 [pii].
17. Samuel T, Hoy WE, Douglas-Denton R, et al. Determinants of glomerular volume in different cortical zones of the human kidney. *J Am Soc Nephrol.* 2005;16(10):3102–3109. doi: ASN.2005010123 [pii].
18. Brenner BM, Bohrer MP, Baylis C, et al. Determinants of glomerular permselectivity: insights derived from observations in vivo. *Kidney Int.* 1977;12(4):229–237. doi: S0085-2538(15)31799-3 [pii].
19. Jorgensen F. *The Ultrastructure of the Normal Human Glomerulus.* Copenhagen: Ejnar Munksgaard; 1966.
20. Vasmant D, Maurice M, Feldmann G. Cytoskeleton ultrastructure of podocytes and glomerular endothelial cells in man and in the rat. *Anat Rec.* 1984;210(1):17–24. doi:10.1002/ar.1092100104. [doi].
21. Ichimura K, Stan RV, Kurihara H, et al. Glomerular endothelial cells form diaphragms during development and pathologic conditions. *J Am Soc Nephrol.* 2008;19(8):1463–1471. doi:10.1681/ASN.2007101138. [doi].
22. Dane MJ, van den Berg BM, Lee DH, et al. A microscopic view on the renal endothelial glycocalyx. *Am J Physiol Renal Physiol.* 2015;308(9):F956–F966. doi:10.1152/ajprenal.00532.2014. [doi].
23. Hjalmarsson C, Johansson BR, Haraldsson B. Electron microscopic evaluation of the endothelial surface layer of glomerular capillaries. *Microvasc Res.* 2004;67(1):9–17. doi: S0026286203000992 [pii].
24. Hegermann J, Lunsdorf H, Ochs M, et al. Visualization of the glomerular endothelial glycocalyx by electron microscopy using cationic colloidal thorium dioxide. *Histochem Cell Biol.* 2016;145(1):41–51. doi:10.1007/s00418-015-1378-3. [doi].
25. Rostgaard J, Qvortrup K. Sieve plugs in fenestrae of glomerular capillaries as site of the filtration barrier? *Cells Tissues Organs.* 2002;170(2–3):132–138. doi: cto/70132 [pii].
26. Satchell S. The role of the glomerular endothelium in albumin handling. *Nat Rev Nephrol.* 2013;9(12):717–725. doi:10.1038/nrneph.2013.197. [doi].
27. Ryan GB, Karnovsky MJ. Distribution of endogenous albumin in the rat glomerulus: role of hemodynamic factors in glomerular barrier function. *Kidney Int.* 1976;9(1):36–45. doi: S0085-2538(15)31553-2.
28. Friden V, Oveland E, Tenstad O, et al. The glomerular endothelial cell coat is essential for glomerular filtration. *Kidney Int.* 2011;79(12):1322–1330. doi:10.1038/ki.2011.58. [doi].
29. Dane MJ, van den Berg BM, Avramut MC, et al. Glomerular endothelial surface layer acts as a barrier against albumin filtration. *Am J Pathol.* 2013;182(5):1532–1540. doi:10.1016/j.ajpath.2013.01.049. [doi].
30. Desideri S, Onions K, Qiu Y. A novel assay provides sensitive measurement of physiologically relevant changes in albumin permeability in isolated human and rodent glomeruli. *Kidney Int.* 2018;93(5):1087–1097. doi: 10.1016/j.kint.2017.12.003.
31. Bartlett CS, Jeansson M, Quaggin SE. Vascular growth factors and glomerular disease. *Annu Rev Physiol.* 2016;78:437–461. doi:10.1146/annurev-physiol-021115-105412. [doi].
32. Simon M, Grone HJ, Johnsen O, et al. Expression of vascular endothelial growth factor and its receptors in human renal ontogenesis and in adult kidney. *Am J Physiol.* 1995;268(2 Pt 2):F240–F250. doi:10.1152/ajppre.1995.268.2.F240. [doi].
33. Brown LF, Berse B, Tognazzi K, et al. Vascular permeability factor mRNA and protein expression in human kidney. *Kidney Int.* 1992;42(6):1457–1461. doi: S0085-2538(15)57870-8 [pii].
34. Esser S, Wolburg K, Wolburg H, et al. Vascular endothelial growth factor induces endothelial fenestrations in vitro. *J Cell Biol.* 1998;140(4):947–959.
35. Roberts WG, Palade GE. Increased microvascular permeability and endothelial fenestration induced by vascular endothelial growth factor. *J Cell Sci.* 1995;108(Pt 6):2369–2379.
36. Eremina V, Sood M, Haigh J, et al. Glomerular-specific alterations of VEGF-A expression lead to distinct congenital and acquired renal diseases. *J Clin Invest.* 2003;111(5):707–716. doi:10.1172/JCI17423. [doi].
37. Ballermann BJ. Glomerular endothelial cell differentiation. *Kidney Int.* 2005;67(5):1668–1671. doi: S0085-2538(15)50640-6 [pii].
38. Eremina V, Jefferson JA, Kowalewska J, et al. VEGF inhibition and renal thrombotic microangiopathy. *N Engl J Med.* 2008;358(11):1129–1136. doi:10.1056/NEJMoa0707330. [doi].
39. Rasch R. Prevention of diabetic glomerulopathy in streptozotocin diabetic rats by insulin treatment. *Diabetologia.* 1979;16(5):319–324.
40. Jorgensen F, Bentzon MW. The ultrastructure of the normal human glomerulus. thickness of glomerular basement membrane. *Lab Invest.* 1968;18(1):42–48.
41. Osterby R. Morphometric studies of the peripheral glomerular basement membrane in early juvenile diabetes. I. development of initial basement membrane thickening. *Diabetologia.* 1972;8(2):84–92.
42. Steffes MW, Barbosa J, Basgen JM, et al. Quantitative glomerular morphology of the normal human kidney. *Lab Invest.* 1983;49(1):82–86.
43. Abrahamson DR. Structure and development of the glomerular capillary wall and basement membrane. *Am J Physiol.* 1987;253(5 Pt 2):F783–F794. doi:10.1152/ajprenal.1987.253.5.F783. [doi].
44. Courtoy PJ, Timpl R, Farquhar MG. Comparative distribution of laminin, type IV collagen, and fibronectin in the rat glomerulus. *J Histochem Cytochem.* 1982;30(9):874–886. doi:10.1177/30.9.7130672. [doi].
45. Courtoy PJ, Kanwar YS, Hynes RO, et al. Fibronectin localization in the rat glomerulus. *J Cell Biol.* 1980;87(3 Pt 1):691–696.
46. Dean DC, Barr JF, Freytag JW, et al. Isolation of type IV procollagen-like polypeptides from glomerular basement membrane. characterization of pro-alpha 1(IV). *J Biol Chem.* 1983;258(1):590–596.
47. Miner JH. Renal basement membrane components. *Kidney Int.* 1999;56(6):2016–2024. doi: S0085-2538(15)46538-X [pii].
48. Lennon R, Byron A, Humphries JD, et al. Global analysis reveals the complexity of the human glomerular extracellular matrix.

- J Am Soc Nephrol.* 2014;25(5):939–951. doi:10.1681/ASN.2013030233. [doi].
49. Miner JH. The glomerular basement membrane. *Exp Cell Res.* 2012;318(9):973–978. doi:10.1016/j.yexcr.2012.02.031. [doi].
 50. Fidler AL, Boudko SP, Rokas A, et al. The triple helix of collagens—an ancient protein structure that enabled animal multicellularity and tissue evolution. *J Cell Sci.* 2018;131(7). doi:10.1242/jcs.203950. [pii].
 51. Cummings CF, Pedchenko V, Brown KL, et al. Extracellular chloride signals collagen IV network assembly during basement membrane formation. *J Cell Biol.* 2016;213(4):479–494. doi:10.1083/jcb.201510065. [doi].
 52. McCall AS, Cummings CF, Bhave G, et al. Bromine is an essential trace element for assembly of collagen IV scaffolds in tissue development and architecture. *Cell.* 2014;157(6):1380–1392. doi:10.1016/j.cell.2014.05.009. [doi].
 53. Abrahamson DR, Hudson BG, Stroganova L, et al. Cellular origins of type IV collagen networks in developing glomeruli. *J Am Soc Nephrol.* 2009;20(7):1471–1479. doi:10.1681/ASN.2008101086. [doi].
 54. Hudson BG. The molecular basis of Goodpasture and Alport syndromes: beacons for the discovery of the collagen IV family. *J Am Soc Nephrol.* 2004;15(10):2514–2527. doi: 10/2514 [pii].
 55. St John PL, Abrahamson DR. Glomerular endothelial cells and podocytes jointly synthesize laminin-1 and -11 chains. *Kidney Int.* 2001;60(3):1037–1046. doi: S0085-2538(15)47958-X [pii].
 56. Zenker M, Aigner T, Wendler O, et al. Human laminin beta2 deficiency causes congenital nephrosis with mesangial sclerosis and distinct eye abnormalities. *Hum Mol Genet.* 2004;13(21):2625–2632. doi:10.1093/hmg/ddh284. [doi].
 57. Murshed M, Smyth N, Miosge N, et al. The absence of nidogen 1 does not affect murine basement membrane formation. *Mol Cell Biol.* 2000;20(18):7007–7012.
 58. McCarthy KJ, Wassenhove-McCarthy DJ. The glomerular basement membrane as a model system to study the bioactivity of heparan sulfate glycosaminoglycans. *Microsc Microanal.* 2012;18(1):3–21. doi:10.1017/S1431927611012682. [doi].
 59. Suleiman H, Zhang L, Roth R, et al. Nanoscale protein architecture of the kidney glomerular basement membrane. *Elife.* 2013;2:e01149. doi:10.7554/elife.01149. [doi].
 60. Farquhar MG. Editorial: the primary glomerular filtration barrier—basement membrane or epithelial slits? *Kidney Int.* 1975;8(4):197–211. doi: S0085-2538(15)31511-8 [pii].
 61. Kanwar YS. Continuum of historical controversies regarding the structural-functional relationship of the glomerular ultrafiltration unit. *Am J Physiol Renal Physiol.* 2015;308(5):F420–F424. doi:10.1152/ajprenal.00640.2014. [doi].
 62. Caulfield JP, Farquhar MG. The permeability of glomerular capillaries to graded dextrans. identification of the basement membrane as the primary filtration barrier. *J Cell Biol.* 1974;63(3):883–903.
 63. Rennke HG, Patel Y, Venkatachalam MA. Glomerular filtration of proteins: clearance of anionic, neutral, and cationic horseradish peroxidase in the rat. *Kidney Int.* 1978;13(4):278–288. doi: S0085-2538(15)31878-0 [pii].
 64. Rennke HG, Venkatachalam MA. Glomerular permeability: in vivo tracer studies with polyanionic and polycationic ferritins. *Kidney Int.* 1977;11(1):44–53. doi: S0085-2538(15)31700-2 [pii].
 65. Caulfield JP, Farquhar MG. Distribution of anionic sites in glomerular basement membranes: their possible role in filtration and attachment. *Proc Natl Acad Sci U S A.* 1976;73(5):1646–1650.
 66. Kanwar YS, Farquhar MG. Anionic sites in the glomerular basement membrane. in vivo and in vitro localization to the laminae rarae by cationic probes. *J Cell Biol.* 1979;81(1):137–153.
 67. Kanwar YS, Farquhar MG. Presence of heparan sulfate in the glomerular basement membrane. *Proc Natl Acad Sci U S A.* 1979;76(3):1303–1307.
 68. Kanwar YS, Farquhar MG. Isolation of glycosaminoglycans (heparan sulfate) from glomerular basement membranes. *Proc Natl Acad Sci U S A.* 1979;76(9):4493–4497.
 69. Kanwar YS, Linker A, Farquhar MG. Increased permeability of the glomerular basement membrane to ferritin after removal of glycosaminoglycans (heparan sulfate) by enzyme digestion. *J Cell Biol.* 1980;86(2):688–693.
 70. Rosenzweig LJ, Kanwar YS. Removal of sulfated (heparan sulfate) or nonsulfated (hyaluronic acid) glycosaminoglycans results in increased permeability of the glomerular basement membrane to 125I-bovine serum albumin. *Lab Invest.* 1982;47(2):177–184.
 71. van den Hoven MJ, Wijnhoven TJ, Li JP, et al. Reduction of anionic sites in the glomerular basement membrane by heparanase does not lead to proteinuria. *Kidney Int.* 2008;73(3):278–287. doi: S0085-2538(15)52994-3 [pii].
 72. Goldberg S, Harvey SJ, Cunningham J, et al. Glomerular filtration is normal in the absence of both agrin and perlecan-heparan sulfate from the glomerular basement membrane. *Nephrol Dial Transplant.* 2009;24(7):2044–2051. doi:10.1093/ndt/gfn758. [doi].
 73. Harvey SJ, Jarad G, Cunningham J, et al. Disruption of glomerular basement membrane charge through podocyte-specific mutation of agrin does not alter glomerular permselectivity. *Am J Pathol.* 2007;171(1):139–152. doi: S0002-9440(10)61950-5 [pii].
 74. Kashian CE, Kim Y, Lees GE, et al. Abnormal glomerular basement membrane laminins in murine, canine, and human alport syndrome: aberrant laminin alpha2 deposition is species independent. *J Am Soc Nephrol.* 2001;12(2):252–260.
 75. Abrahamson DR, Isom K, Roach E, et al. Laminin compensation in collagen alpha3(IV) knockout (Alport) glomeruli contributes to permeability defects. *J Am Soc Nephrol.* 2007;18(9):2465–2472. doi: ASN.2007030328 [pii].
 76. Matejas V, Hinkes B, Alkandari F, et al. Mutations in the human laminin beta2 (LAMB2) gene and the associated phenotypic spectrum. *Hum Mutat.* 2010;31(9):992–1002. doi:10.1002/humu.21304. [doi].
 77. Noakes PG, Miner JH, Gautam M, et al. The renal glomerulus of mice lacking s-laminin/laminin beta 2: nephrosis despite molecular compensation by laminin beta 1. *Nat Genet.* 1995;10(4):400–406. doi:10.1038/ng0895-400. [doi].
 78. Jarad G, Cunningham J, Shaw AS, et al. Proteinuria precedes podocyte abnormalities in Lamb2-/- mice, implicating the glomerular basement membrane as an albumin barrier. *J Clin Invest.* 2006;116(8):2272–2279. doi:10.1172/JCI28414. [doi].
 79. Lin MH, Miller JB, Kikkawa Y, et al. Laminin-521 protein therapy for glomerular basement membrane and podocyte abnormalities in a model of Pierson syndrome. *J Am Soc Nephrol.* 2018. doi: ASN.2017060690 [pii].
 80. Ichimura K, Miyazaki N, Sadayama S, et al. Three-dimensional architecture of podocytes revealed by block-face scanning electron microscopy. *Sci Rep.* 2015;5:8993. doi:10.1038/srep08993. [doi].
 81. Burghardt T, Hochapfel F, Salecker B, et al. Advanced electron microscopic techniques provide a deeper insight into the peculiar features of podocytes. *Am J Physiol Renal Physiol.* 2015;309(12):F1082–F1089. doi:10.1152/ajprenal.00338.2015. [doi].
 82. Neal CR, Crook H, Bell E, et al. Three-dimensional reconstruction of glomeruli by electron microscopy reveals a distinct restrictive urinary subpodocyte space. *J Am Soc Nephrol.* 2005;16(5):1223–1235. doi: ASN.2004100822 [pii].
 83. Arkill KP, Qvortrup K, Starborg T, et al. Resolution of the three dimensional structure of components of the glomerular filtration barrier. *BMC Nephrol.* 2014;15:24. doi:10.1186/1471-2369-15-24. [doi].
 84. Schell C, Huber TB. The evolving complexity of the podocyte cytoskeleton. *J Am Soc Nephrol.* 2017;28(11):3166–3174. doi:10.1681/ASN.2017020143. [doi].
 85. Drenckhahn D, Franke RP. Ultrastructural organization of contractile and cytoskeletal proteins in glomerular podocytes of chicken, rat, and man. *Lab Invest.* 1988;59(5):673–682.
 86. Andrews PM, Bates SB. Filamentous actin bundles in the kidney. *Anat Rec.* 1984;210(1):1–9. doi:10.1002/ar.1092100102. [doi].
 87. Ichimura K, Kurihara H, Sakai T. Actin filament organization of foot processes in rat podocytes. *J Histochem Cytochem.* 2003;51(12):1589–1600. doi:10.1177/002215540305101203. [doi].
 88. Ichimura K, Kurihara H, Sakai T. Actin filament organization of foot processes in vertebrate glomerular podocytes. *Cell Tissue Res.* 2007;329(3):541–557. doi:10.1007/s00441-007-0440-4. [doi].
 89. Kriz W, Shirato I, Nagata M, et al. The podocyte's response to stress: the enigma of foot process effacement. *Am J Physiol Renal Physiol.* 2013;304(4):F333–F347. doi:10.1152/ajprenal.00478.2012. [doi].
 90. Pellegrin S, Mellor H. Actin stress fibres. *J Cell Sci.* 2007;120(Pt 20):3491–3499. doi: 120/20/3491 [pii].
 91. Suleiman HY, Roth R, Jain S, et al. Injury-induced actin cytoskeleton reorganization in podocytes revealed by super-resolution microscopy. *JCI Insight.* 2017;2(16). doi:10.1172/jci.insight.94137. [doi].
 92. Stamenovic D, Ingber DE. Tensegrity-guided self assembly: from molecules to living cells. *Soft Matter.* 2009;5:1137–1145.

93. Perico L, Conti S, Benigni A, et al. Podocyte-actin dynamics in health and disease. *Nat Rev Nephrol.* 2016;12(11):692–710. doi:10.1038/nrmp.2016.127. [doi].
94. Sever S, Schiffer M. Actin dynamics at focal adhesions: a common endpoint and putative therapeutic target for proteinuric kidney diseases. *Kidney Int.* 2018. doi: S0085-2538(18)30170-4 [pii].
95. Horton ER, Humphries JD, James J, et al. The integrin adhesion network at a glance. *J Cell Sci.* 2016;129(22):4159–4163. doi: jcs.192054 [pii].
96. Has C, Sparta G, Kiritsi D, et al. Integrin alpha3 mutations with kidney, lung, and skin disease. *N Engl J Med.* 2012;366(16):1508–1514. doi:10.1056/NEJMoa1110813. [doi].
97. Sachs N, Claessen N, Aten J, et al. Blood pressure influences end-stage renal disease of cd151 knockout mice. *J Clin Invest.* 2012;122(1):348–358. doi:10.1172/JCI58878. [doi].
98. Mouawad F, Tsui H, Takano T. Role of rho-GTPases and their regulatory proteins in glomerular podocyte function. *Can J Physiol Pharmacol.* 2013;91(10):773–782. doi:10.1139/cjpp-2013-0135. [doi].
99. Zhu L, Jiang R, Aoudjit L, et al. Activation of RhoA in podocytes induces focal segmental glomerulosclerosis. *J Am Soc Nephrol.* 2011;22(9):1621–1630. doi:10.1681/ASN.2010111146. [doi].
100. Wang L, Ellis MJ, Gomez JA, et al. Mechanisms of the proteinuria induced by rho GTPases. *Kidney Int.* 2012;81(11):1075–1085. doi:10.1038/ki.2011.472. [doi].
101. Yu H, Suleiman H, Kim AH, et al. Rac1 activation in podocytes induces rapid foot process effacement and proteinuria. *Mol Cell Biol.* 2013;33(23):4755–4764. doi:10.1128/MCB.00730-13. [doi].
102. Robins R, Baldwin C, Aoudjit L, et al. Rac1 activation in podocytes induces the spectrum of nephrotic syndrome. *Kidney Int.* 2017;92(2):349–364. doi: S0085-2538(17)30200-4 [pii].
103. Scott RP, Hawley SP, Ruston J, et al. Podocyte-specific loss of cdc42 leads to congenital nephropathy. *J Am Soc Nephrol.* 2012;23(7):1149–1154. doi:10.1681/ASN.2011121206. [doi].
104. Blattner SM, Hodgin JB, Nishio M, et al. Divergent functions of the rho GTPases rac1 and cdc42 in podocyte injury. *Kidney Int.* 2013;84(5):920–930. doi:10.1038/ki.2013.175. [doi].
105. Hodge RG, Ridley AJ. Regulating rho GTPases and their regulators. *Nat Rev Mol Cell Biol.* 2016;17(8):496–510. doi:10.1038/nrm.2016.67. [doi].
106. Akilesh S, Suleiman H, Yu H, et al. Arhgap24 inactivates rac1 in mouse podocytes, and a mutant form is associated with familial focal segmental glomerulosclerosis. *J Clin Invest.* 2011;121(10):4127–4137. doi:10.1172/JCI46458. [doi].
107. Gee HY, Saisawat P, Ashraf S, et al. ARHGDIA mutations cause nephrotic syndrome via defective RHO GTPase signaling. *J Clin Invest.* 2013;123(8):3243–3253. doi:10.1172/JCI69134. [doi].
108. Gee HY, Zhang F, Ashraf S, et al. KANK deficiency leads to podocyte dysfunction and nephrotic syndrome. *J Clin Invest.* 2015;125(6):2375–2384. doi:10.1172/JCI79504. [doi].
109. Schiffer M, Teng B, Gu C, et al. Pharmacological targeting of actin-dependent dynamin oligomerization ameliorates chronic kidney disease in diverse animal models. *Nat Med.* 2015;21(6):601–609. doi:10.1038/nm.3843. [doi].
110. Gu C, Lee HW, Garbarcauskas G, et al. Dynamin autonomously regulates podocyte focal adhesion maturation. *J Am Soc Nephrol.* 2017;28(2):446–451. doi:10.1681/ASN.2016010008. [doi].
111. Soda K, Balkin DM, Ferguson SM, et al. Role of dynamin, synaptotagmin, and endophilin in podocyte foot processes. *J Clin Invest.* 2012;122(12):4401–4411. doi:10.1172/JCI65289. [doi].
112. Rodewald R, Karnovsky MJ. Porous substructure of the glomerular slit diaphragm in the rat and mouse. *J Cell Biol.* 1974;60(2):423–433.
113. Hora K, Ohno S, Oguchi H, et al. Three-dimensional study of glomerular slit diaphragm by the quick-freezing and deep-etching replica method. *Eur J Cell Biol.* 1990;53(2):402–406.
114. Wartiovaara J, Ofverstedt LG, Khoshnoodi J, et al. Nephrin strands contribute to a porous slit diaphragm scaffold as revealed by electron tomography. *J Clin Invest.* 2004;114(10):1475–1483. doi:10.1172/JCI22562. [doi].
115. Gagliardini E, Conti S, Benigni A, et al. Imaging of the porous ultrastructure of the glomerular epithelial filtration slit. *J Am Soc Nephrol.* 2010;21(12):2081–2089. doi:10.1681/ASN.2010020199. [doi].
116. Rice WL, Van Hoek AN, Paunescu TG, et al. High resolution helium ion scanning microscopy of the rat kidney. *PLoS ONE.* 2013;8(3):e57051. doi:10.1371/journal.pone.0057051. [doi].
117. Tsuji K, Paunescu TG, Suleiman H, et al. Re-characterization of the glomerulopathy in CD2AP deficient mice by high-resolution helium ion scanning microscopy. *Sci Rep.* 2017;7(1):8321. doi:10.1038/s41598-017-08304-3. [doi].
118. Grahammer F, Wigge C, Schell C, et al. A flexible, multilayered protein scaffold maintains the slit in between glomerular podocytes. *JCI Insight.* 2016;1(9). doi:10.1172/jci.insight.86177. [pii].
119. Kestila M, Lenkkeri U, Mannikko M, et al. Positionally cloned gene for a novel glomerular protein—nephrin—is mutated in congenital nephrotic syndrome. *Mol Cell.* 1998;1(4):575–582. doi: S1097-2765(00)80057-X [pii].
120. Lovric S, Ashraf S, Tan W, et al. Genetic testing in steroid-resistant nephrotic syndrome: when and how? *Nephrol Dial Transplant.* 2016;31(11):1802–1813. doi: gfv355 [pii].
121. New LA, Martin CE, Jones N. Advances in slit diaphragm signaling. *Curr Opin Nephrol Hypertens.* 2014;23(4):420–430. doi:10.1097/01.mnh.0000447018.28852.b6. [doi].
122. Jones N, Blasutig IM, Eremina V, et al. Nck adaptor proteins link nephrin to the actin cytoskeleton of kidney podocytes. *Nature.* 2006;440(7085):818–823. doi: nature04662 [pii].
123. Verma R, Kovari I, Soofi A, et al. Nephrin ectodomain engagement results in src kinase activation, nephrin phosphorylation, nck recruitment, and actin polymerization. *J Clin Invest.* 2006;116(5):1346–1359. doi:10.1172/JCI27414. [doi].
124. New LA, Keyvani Chahri A, Jones N. Direct regulation of nephrin tyrosine phosphorylation by nck adaptor proteins. *J Biol Chem.* 2013;288(3):1500–1510. doi:10.1074/jbc.M112.439463. [doi].
125. Okrut J, Prakash S, Wu Q, et al. Allosteric N-WASP activation by an inter-SH3 domain linker in nck. *Proc Natl Acad Sci U S A.* 2015;112(47):E6436–E6445. doi:10.1073/pnas.1510876112. [doi].
126. Molinie N, Gautreau A. The Arp2/3 regulatory system and its deregulation in cancer. *Physiol Rev.* 2018;98(1):215–238. doi:10.1152/physrev.00006.2017. [doi].
127. New LA, Martin CE, Scott RP, et al. Nephrin tyrosine phosphorylation is required to stabilize and restore podocyte foot process architecture. *J Am Soc Nephrol.* 2016;27(8):2422–2435. doi:10.1681/ASN.2015091048. [doi].
128. Jones N, New LA, Fortino MA, et al. Nck proteins maintain the adult glomerular filtration barrier. *J Am Soc Nephrol.* 2009;20(7):1533–1543. doi:10.1681/ASN.2009010056. [doi].
129. Schell C, Baumhakl L, Salou S, et al. N-wasp is required for stabilization of podocyte foot processes. *J Am Soc Nephrol.* 2013;24(5):713–721. doi:10.1681/ASN.2012080844. [doi].
130. Martin CE, Petersen KA, Aoudjit L, et al. ShcA adaptor protein promotes nephrin endocytosis and is upregulated in proteinuric nephropathies. *J Am Soc Nephrol.* 2018;29(1):92–103. doi:10.1681/ASN.2017030285. [doi].
131. Farquhar MG, Palade GE. Functional evidence for the existence of a third cell type in the renal glomerulus: phagocytosis of filtration residues by a distinctive “third” cell. *J Cell Biol.* 1962;13(1):55–87.
132. Latta H, Maunsbach AB, Madden SC. The centrolobular region of the renal glomerulus studied by electron microscopy. *J Ultrastruct Res.* 1960;4:455–472.
133. Inkyo-Hayasaka K, Sakai T, Kobayashi N, et al. Three-dimensional analysis of the whole mesangium in the rat. *Kidney Int.* 1996;50(2):672–683. doi: S0085-2538(15)59658-0 [pii].
134. Drenckhahn D, Schnittler H, Nobiling R, et al. Ultrastructural organization of contractile proteins in rat glomerular mesangial cells. *Am J Pathol.* 1990;137(6):1343–1351.
135. Sakai T, Kriz W. The structural relationship between mesangial cells and basement membrane of the renal glomerulus. *Anat Embryol (Berl).* 1987;176(3):373–386.
136. Kriz W, Elger M, Mundel P, et al. Structure-stabilizing forces in the glomerular tuft. *J Am Soc Nephrol.* 1995;5(10):1731–1739.
137. Kurihara H, Sakai T. Cell biology of mesangial cells: the third cell that maintains the glomerular capillary. *Anat Sci Int.* 2017;92(2):173–186. doi:10.1007/s12565-016-0334-1. [doi].
138. Tsurumi H, Kurihara H, Miura K, et al. Afadin is localized at cell-cell contact sites in mesangial cells and regulates migratory polarity. *Lab Invest.* 2016;96(1):49–59. doi:10.1038/labinvest.2015.133. [doi].
139. Kikkawa Y, Virtanen I, Miner JH. Mesangial cells organize the glomerular capillaries by adhering to the G domain of laminin alpha5 in the glomerular basement membrane. *J Cell Biol.* 2003;161(1):187–196. doi:10.1083/jcb.200211121. [doi].

140. Tsurumi H, Harita Y, Kurihara H, et al. Epithelial protein lost in neoplasm modulates platelet-derived growth factor-mediated adhesion and motility of mesangial cells. *Kidney Int.* 2014;86(3):548–557. doi:10.1038/ki.2014.85. [doi].
141. Zimmerman SE, Hiremath C, Tsunezumi J, et al. Nephronectin regulates mesangial cell adhesion and behavior in glomeruli. *J Am Soc Nephrol.* 2018;29(4):1128–1140. doi:10.1681/ASN.2017070752. [doi].
142. Taugner R, Schiller A, Kaissling B, et al. Gap junctional coupling between the JGA and the glomerular tuft. *Cell Tissue Res.* 1978;186(2):279–285.
143. Starke C, Betz H, Hickmann L, et al. Renin lineage cells repopulate the glomerular mesangium after injury. *J Am Soc Nephrol.* 2015;26(1):48–54. doi:10.1681/ASN.2014030265. [doi].
144. Schlondorff D. The glomerular mesangial cell: an expanding role for a specialized pericyte. *FASEB J.* 1987;1(4):272–281.
145. Michael AF, Keane WF, Raji L, et al. The glomerular mesangium. *Kidney Int.* 1980;17(2):141–154. doi: S0085-2538(15)32230-4 [pii].
146. Elema JD, Hoyer JR, Vernier RL. The glomerular mesangium: uptake and transport of intravenously injected colloidal carbon in rats. *Kidney Int.* 1976;9(5):395–406. doi: S0085-2538(15)31596-9 [pii].
147. Mauer SM, Fish AJ, Blau EB, et al. The glomerular mesangium. I. kinetic studies of macromolecular uptake in normal and nephrotic rats. *J Clin Invest.* 1972;51(5):1092–1101. doi:10.1172/JCI106901. [doi].
148. Rupprecht HD, Schocklmann HO, Sterzel RB. Cell-matrix interactions in the glomerular mesangium. *Kidney Int.* 1996;49(6):1575–1582. doi: S0085-2538(15)59522-7 [pii].
149. Schlondorff D, Banas B. The mesangial cell revisited: no cell is an island. *J Am Soc Nephrol.* 2009;20(6):1179–1187. doi:10.1681/ASN.2008050549. [doi].
150. Floege J, Eitner F, Alpers CE. A new look at platelet-derived growth factor in renal disease. *J Am Soc Nephrol.* 2008;19(1):12–23. doi: ASN.2007050532 [pii].
151. Mundel P, Elger M, Sakai T, et al. Microfibrils are a major component of the mesangial matrix in the glomerulus of the rat kidney. *Cell Tissue Res.* 1988;254(1):183–187.
152. Sterzel RB, Hartner A, Schlotter-Schrehardt U, et al. Elastic fiber proteins in the glomerular mesangium in vivo and in cell culture. *Kidney Int.* 2000;58(4):1588–1602. doi: S0085-2538(15)47257-6 [pii].
153. Schaefer L, Mihalik D, Babelova A, et al. Regulation of fibrillin-1 by biglycan and decorin is important for tissue preservation in the kidney during pressure-induced injury. *Am J Pathol.* 2004;165(2):383–396. doi: S0002-9440(10)63305-6 [pii].
154. Marek I, Volkert G, Hilgers KF, et al. Fibrillin-1 and alpha8 integrin are co-expressed in the glomerulus and interact to convey adhesion of mesangial cells. *Cell Adh Migr.* 2014;8(4):389–395. doi:10.4161/cam.28988. [doi].
155. Ning L, Kurihara H, de Vega S, et al. Laminin alpha1 regulates age-related mesangial cell proliferation and mesangial matrix accumulation through the TGF-beta pathway. *Am J Pathol.* 2014;184(6):1683–1694. doi:10.1016/j.ajpath.2014.02.006. [doi].
156. Kerjaschki D, Ojha PP, Susanu M, et al. A beta 1-integrin receptor for fibronectin in human kidney glomeruli. *Am J Pathol.* 1989;134(2):481–489.
157. Cosio FG, Sedmak DD, Nahman NS Jr. Cellular receptors for matrix proteins in normal human kidney and human mesangial cells. *Kidney Int.* 1990;38(5):886–895. doi: S0085-2538(15)57032-4 [pii].
158. Petermann A, Fees H, Grenz H, et al. Polymerase chain reaction and focal contact formation indicate integrin expression in mesangial cells. *Kidney Int.* 1993;44(5):997–1005. doi: S0085-2538(15)58222-7 [pii].
159. Abboud HE. Mesangial cell biology. *Exp Cell Res.* 2012;318(9):979–985. doi:10.1016/j.yexcr.2012.02.025. [doi].
160. Ohse T, Chang AM, Pippin JW, et al. A new function for parietal epithelial cells: A second glomerular barrier. *Am J Physiol Renal Physiol.* 2009;297(6):F1566–F1574. doi:10.1152/ajprenal.00214.2009. [doi].
161. Shankland SJ, Smeets B, Pippin JW, et al. The emergence of the glomerular parietal epithelial cell. *Nat Rev Nephrol.* 2014;10(3):158–173. doi:10.1038/nrneph.2014.1. [doi].
162. Alcorn D, Ryan GB. The glomerular peripolar cell. *Kidney Int Suppl.* 1993;42:S35–S39.
163. Bariety J, Mandet C, Hill GS, et al. Parietal podocytes in normal human glomeruli. *J Am Soc Nephrol.* 2006;17(10):2770–2780. doi: ASN.2006040325 [pii].
164. Appel D, Kershaw DB, Smeets B, et al. Recruitment of podocytes from glomerular parietal epithelial cells. *J Am Soc Nephrol.* 2009;20(2):333–343. doi:10.1681/ASN.2008070795. [doi].
165. Gibson IW, Downie I, Downie TT, et al. The parietal podocyte: a study of the vascular pole of the human glomerulus. *Kidney Int.* 1992;41(1):211–214. doi: S0085-2538(15)57450-4 [pii].
166. Smeets B, Stucker F, Wetzels J, et al. Detection of activated parietal epithelial cells on the glomerular tuft distinguishes early focal segmental glomerulosclerosis from minimal change disease. *Am J Pathol.* 2014;184(12):3239–3248. doi:10.1016/j.ajpath.2014.08.007. [doi].
167. Shankland SJ, Freedman BS, Pippin JW. Can podocytes be regenerated in adults? *Curr Opin Nephrol Hypertens.* 2017;26(3):154–164. doi:10.1097/MNH.0000000000000311. [doi].
168. Berger K, Schulze K, Boor P, et al. The regenerative potential of parietal epithelial cells in adult mice. *J Am Soc Nephrol.* 2014;25(4):693–705. doi:10.1681/ASN.2013050481. [doi].
169. Wanner N, Hartleben B, Herbach N, et al. Unraveling the role of podocyte turnover in glomerular aging and injury. *J Am Soc Nephrol.* 2014;25(4):707–716. doi:10.1681/ASN.2013050452. [doi].
170. Lasagni L, Angelotti ML, Ronconi E, et al. Podocyte regeneration driven by renal progenitors determines glomerular disease remission and can be pharmacologically enhanced. *Stem Cell Reports.* 2015;5(2):248–263. doi:10.1016/j.stemcr.2015.07.003. [doi].
171. Hackl MJ, Burford JL, Villanueva K, et al. Tracking the fate of glomerular epithelial cells in vivo using serial multiphoton imaging in new mouse models with fluorescent lineage tags. *Nat Med.* 2013;19(12):1661–1666. doi:10.1038/nm.3405. [doi].
172. Schulze K, Berger K, Boor P, et al. Origin of parietal podocytes in atubular glomeruli mapped by lineage tracing. *J Am Soc Nephrol.* 2014;25(1):129–141. doi:10.1681/ASN.2013040376. [doi].
173. Kaverina NV, Eng DG, Schneide RR, et al. Partial podocyte replenishment in experimental FSGS derives from nonpodocyte sources. *Am J Physiol Renal Physiol.* 2016;310(11):F1397–F1413. doi:10.1152/ajprenal.00369.2015. [doi].
174. Schnermann J, Briggs JP. Tubular control of renin synthesis and secretion. *Pflugers Arch.* 2013;465(1):39–51. doi:10.1007/s00424-012-1115-x. [doi].
175. Barajas L. The ultrastructure of the juxtaglomerular apparatus as disclosed by three-dimensional reconstructions from serial sections. the anatomical relationship between the tubular and vascular components. *J Ultrastruct Res.* 1970;33(1):116–147.
176. Barajas L. Anatomy of the juxtaglomerular apparatus. *Am J Physiol.* 1979;237(5):F333–F343. doi:10.1152/ajprenal.1979.237.5.F333. [doi].
177. Barajas L, Salido E. Pathology of the juxtaglomerular apparatus. In: Tisher CC, Brenner BM, eds. *Renal Pathology With Clinical and Functional Correlations.* 2nd ed. Philadelphia: J.B. Lippincott; 1994:948–978.
178. Tisher CC, Bulger RE, Trump BF. Human renal ultrastructure. 3. The distal tubule in healthy individuals. *Lab Invest.* 1968;18(6):655–668.
179. Hackenthal E, Paul M, Ganter D, et al. Morphology, physiology, and molecular biology of renin secretion. *Physiol Rev.* 1990;70(4):1067–1116. doi:10.1152/physrev.1990.70.4.1067. [doi].
180. Biava CG, West M. Fine structure of normal human juxtaglomerular cells. II. specific and nonspecific cytoplasmic granules. *Am J Pathol.* 1966;49(5):955–979.
181. Kurtz A. Renin release: sites, mechanisms, and control. *Annu Rev Physiol.* 2011;73:377–399. doi:10.1146/annurev-physiol-012110-142238. [doi].
182. Celio MR, Inagami T. Angiotensin II immunoreactivity coexists with renin in the juxtaglomerular granular cells of the kidney. *Proc Natl Acad Sci U S A.* 1981;78(6):3897–3900.
183. Friis UG, Madsen K, Stubbe J, et al. Regulation of renin secretion by renal juxtaglomerular cells. *Pflugers Arch.* 2013;465(1):25–37. doi:10.1007/s00424-012-1126-7. [doi].
184. Sauter A, Machura K, Neubauer B, et al. Development of renin expression in the mouse kidney. *Kidney Int.* 2008;73(1):43–51. doi: S0085-2538(15)52818-4 [pii].
185. Gomez RA, Chevalier RL, Everett AD, et al. Recruitment of renin gene-expressing cells in adult rat kidneys. *Am J Physiol.* 1990;259(4 Pt 2):F660–F665. doi:10.1152/ajprenal.1990.259.4.F660. [doi].

186. Sequeira Lopez ML, Pentz ES, Nomasa T, et al. Renin cells are precursors for multiple cell types that switch to the renin phenotype when homeostasis is threatened. *Dev Cell.* 2004;6(5):719–728. doi: S1534-5807(04)00134-0 [pii].
187. Gomez RA, Lopez ML. Plasticity of renin cells in the kidney vasculature. *Curr Hypertens Rep.* 2017;19(2):14. doi:10.1007/s11906-017-0711-8. [doi].
188. Pricam C, Humbert F, Perrelet A, et al. Gap junctions in mesangial and lacis cells. *J Cell Biol.* 1974;63(1):349–354.
189. Wagner C, Kurtz A. Distribution and functional relevance of connexins in renin-producing cells. *Pflugers Arch.* 2013;465(1):71–77. doi:10.1007/s00424-012-1134-7. [doi].
190. Yao J, Oite T, Kitamura M. Gap junctional intercellular communication in the juxtaglomerular apparatus. *Am J Physiol Renal Physiol.* 2009;296(5):F939–F946. doi:10.1152/ajprenal.90612.2008. [doi].
191. Ren Y, Carretero OA, Garvin JL. Role of mesangial cells and gap junctions in tubuloglomerular feedback. *Kidney Int.* 2002;62(2):525–531. doi: S0085-2538(15)48579-5 [pii].
192. Kaissling B, Kriz W. Variability of intercellular spaces between macula densa cells: a transmission electron microscopic study in rabbits and rats. *Kidney Int Suppl.* 1982;12:S9–S17.
193. Madsen KM, Park CH. Lysosome distribution and cathepsin B and L activity along the rabbit proximal tubule. *Am J Physiol.* 1987;253(6 Pt 2):F1290–F1301. doi:10.1152/ajprenal.1987.253.6.F1290. [doi].
194. Tisher CC, Bulger RE, Trump BF. Human renal ultrastructure. I. proximal tubule of healthy individuals. *Lab Invest.* 1966;15(8):1357–1394.
195. Harris AN, Lee HW, Osis G, et al. Differences in renal ammonia metabolism in male and female kidney. *Am J Physiol Renal Physiol.* 2018;doi:10.1152/ajprenal.00084.2018. [doi].
196. Oudar O, Elger M, Bankir L, et al. Differences in rat kidney morphology between males, females and testosterone-treated females. *Ren Physiol Biochem.* 1991;14(3):92–102.
197. Veiras LC, Girardi ACC, Curry J, et al. Sexual dimorphic pattern of renal transporters and electrolyte homeostasis. *J Am Soc Nephrol.* 2017;28(12):3504–3517. doi:10.1681/ASN.2017030295. [doi].
198. Maunsbach AB. Observations on the segmentation of the proximal tubule in the rat kidney. comparison of results from phase contrast, fluorescence and electron microscopy. *J Ultrastruct Res.* 1966;16(3):239–258.
199. Tisher CC, Rosen S, Osborne GB. Ultrastructure of the proximal tubule of the rhesus monkey kidney. *Am J Pathol.* 1969;56(3):469–517.
200. Faarup P, Holstein-Rathlou NH, Norgaard T, et al. Functionally induced changes in water transport in the proximal tubule segment of rat kidneys. *Int J Nephrol Renovasc Dis.* 2011;4:73–84. doi:10.2147/IJNRD.S15459. [doi].
201. Dorup J, Maunsbach AB. Three-dimensional organization and segmental ultrastructure of rat proximal tubules. *Exp Nephrol.* 1997;5(4):305–317.
202. Kaissling B, Kriz W. Structural analysis of the rabbit kidney. *Adv Anat Embryol Cell Biol.* 1979;56:1–123.
203. Woodhall PB, Tisher CC, Simonton CA, et al. Relationship between para-aminohippurate secretion and cellular morphology in rabbit proximal tubules. *J Clin Invest.* 1978;61(5):1320–1329. doi:10.1172/JCII109049. [doi].
204. Lee HW, Osis G, Harris AN, et al. NBCe1-a regulates proximal tubule ammonia metabolism under basal conditions and in response to metabolic acidosis. *J Am Soc Nephrol.* 2018;29(4):1182–1197. doi:10.1681/ASN.2017080935. [doi].
205. Lee HW, Osis G, Handlogten ME, et al. Proximal tubule-specific glutamine synthetase deletion alters basal and acidosis-stimulated ammonia metabolism. *Am J Physiol Renal Physiol.* 2016;310(11):F1229–F1242. doi:10.1152/ajprenal.00547.2015. [doi].
206. Moret C, Dave MH, Schulz N, et al. Regulation of renal amino acid transporters during metabolic acidosis. *Am J Physiol Renal Physiol.* 2007;292(2):F555–F566. doi: 00113.2006 [pii].
207. Welling LW, Welling DJ. Shape of epithelial cells and intercellular channels in the rabbit proximal nephron. *Kidney Int.* 1976;9(5):385–394. doi: S0085-2538(15)31595-7 [pii].
208. Welling LW, Welling DJ. Relationship between structure and function in renal proximal tubule. *J Electron Microsc Tech.* 1988;9(2):171–185. doi:10.1002/jemt.1060090205. [doi].
209. Farquhar MG, Palade GE. Junctional complexes in various epithelia. *J Cell Biol.* 1963;17:375–412.
210. Rosenthal R, Milatz S, Krug SM, et al. Claudin-2, a component of the tight junction, forms a paracellular water channel. *J Cell Sci.* 2010;123(Pt 11):1913–1921. doi:10.1242/jcs.060665. [doi].
211. Muto S, Hata M, Taniguchi J, et al. Claudin-2-deficient mice are defective in the leaky and cation-selective paracellular permeability properties of renal proximal tubules. *Proc Natl Acad Sci U S A.* 2010;107(17):8011–8016. doi:10.1073/pnas.0912901107. [doi].
212. Denker BM, Sabath E. The biology of epithelial cell tight junctions in the kidney. *J Am Soc Nephrol.* 2011;22(4):622–625. doi:10.1681/ASN.2010090922. [doi].
213. Barajas L, Powers K, Wang P. Innervation of the renal cortical tubules: a quantitative study. *Am J Physiol.* 1984;247(1 Pt 2):F50–F60. doi:10.1152/ajprenal.1984.247.1.F50. [doi].
214. Hanner F, Sorensen CM, Holstein-Rathlou NH, et al. Connexins and the kidney. *Am J Physiol Regul Integr Comp Physiol.* 2010;298(5):R1143–R1155. doi:10.1152/ajpregu.00808.2009. [doi].
215. Welling LW, Welling DJ. Surface areas of brush border and lateral cell walls in the rabbit proximal nephron. *Kidney Int.* 1975;8(6):343–348. doi: S0085-2538(15)31533-7 [pii].
216. Ernst SA. Transport ATPase cytochemistry: ultrastructural localization of potassium-dependent and potassium-independent phosphatase activities in rat kidney cortex. *J Cell Biol.* 1975;66(3):586–608.
217. Kashgarian M, Biemesderfer D, Caplan M, et al. Monoclonal antibody to na,K-ATPase: immunocytochemical localization along nephron segments. *Kidney Int.* 1985;28(6):899–913. doi: S0085-2538(15)33564-X [pii].
218. Bergeron M, Guerette D, Forget J, et al. Three-dimensional characteristics of the mitochondria of the rat nephron. *Kidney Int.* 1980;17(2):175–185. doi: S0085-2538(15)32233-X [pii].
219. Rodman JS, Mooseker M, Farquhar MG. Cytoskeletal proteins of the rat kidney proximal tubule brush border. *Eur J Cell Biol.* 1986;42(2):319–327.
220. Coudrier E, Kerjaschki D, Louvard D. Cytoskeleton organization and submembranous interactions in intestinal and renal brush borders. *Kidney Int.* 1988;34(3):309–320. doi: S0085-2538(15)34356-8 [pii].
221. Christensen EI, Nielsen S. Structural and functional features of protein handling in the kidney proximal tubule. *Semin Nephrol.* 1991;11(4):414–439. doi: 0270-9295(91)90062-O [pii].
222. Birn H, Christensen EI, Nielsen S. Kinetics of endocytosis in renal proximal tubule studied with ruthenium red as membrane marker. *Am J Physiol.* 1993;264(2 Pt 2):F239–F250. doi:10.1152/ajprenal.1993.264.2.F239. [doi].
223. Kerjaschki D, Farquhar MG. The pathogenic antigen of heymann nephritis is a membrane glycoprotein of the renal proximal tubule brush border. *Proc Natl Acad Sci U S A.* 1982;79(18):5557–5561.
224. Kerjaschki D, Noronha-Blob L, Sacktor B, et al. Microdomains of distinctive glycoprotein composition in the kidney proximal tubule brush border. *J Cell Biol.* 1984;98(4):1505–1513.
225. Christensen EI, Birn H, Storm T, et al. Endocytic receptors in the renal proximal tubule. *Physiology (Bethesda).* 2012;27(4):223–236. doi:10.1152/physiol.00022.2012. [doi].
226. Maunsbach AB. Observations on the ultrastructure and acid phosphatase activity of the cytoplasmic bodies in rat kidney proximal tubule cells. with a comment on their classification. *J Ultrastruct Res.* 1966;16(3):197–238.
227. Street JM, Birkhoff W, Menzies RI, et al. Exosomal transmission of functional aquaporin 2 in kidney cortical collecting duct cells. *J Physiol.* 2011;589(Pt 24):6119–6127. doi:10.1113/jphysiol.2011.220277. [doi].
228. Ludwig AK, Giebel B. Exosomes: small vesicles participating in intercellular communication. *Int J Biochem Cell Biol.* 2012;44(1):11–15. doi:10.1016/j.biocel.2011.10.005. [doi].
229. Maunsbach AB. Absorption of I-125-labeled homologous albumin by rat kidney proximal tubule cells. A study of microperfused single proximal tubules by electron microscopic autoradiography and histochemistry. *J Ultrastruct Res.* 1966;15(3):197–241.
230. Maack T, Johnson V, Kau ST, et al. Renal filtration, transport, and metabolism of low-molecular-weight proteins: a review. *Kidney Int.* 1979;16(3):251–270. doi: S0085-2538(15)32142-6 [pii].
231. Katz AI, Doucet A, Morel F. Na-K-ATPase activity along the rabbit, rat, and mouse nephron. *Am J Physiol.* 1979;237(2):F114–F120. doi:10.1152/ajprenal.1979.237.2.F114. [doi].
232. Clapp WL, Park CH, Madsen KM, et al. Axial heterogeneity in the handling of albumin by the rabbit proximal tubule. *Lab Invest.* 1988;58(5):549–558.
233. Ohno S. Peroxisomes of the kidney. *Int Rev Cytol.* 1985;95:131–162.
234. Angermuller S, Leupold C, Zaar K, et al. Electron microscopic cytochemical localization of alpha-hydroxyacid oxidase in rat kidney

- cortex. Heterogeneous staining of peroxisomes. *Histochemistry*. 1986;85(5):411–418.
235. Riquier-Brisson AD, Leong PK, Pihakaski-Maunsbach K, et al. Angiotensin II stimulates trafficking of NHE3, NaPi2, and associated proteins into the proximal tubule microvilli. *Am J Physiol Renal Physiol*. 2010;298(1):F177–F186. doi:10.1152/ajprenal.00464.2009. [doi].
236. Yang LE, Maunsbach AB, Leong PK, et al. Differential traffic of proximal tubule Na⁺ transporters during hypertension or PTH: NHE3 to base of microvilli vs. NaPi2 to endosomes. *Am J Physiol Renal Physiol*. 2004;287(5):F896–F906. doi:10.1152/ajprenal.00160.2004. [doi].
237. Tripathi S, Boulaep EL, Maunsbach AB. Isolated perfused *ambystoma* proximal tubule: hydrodynamics modulates ultrastructure. *Am J Physiol*. 1987;252(6 Pt 2):F1129–F1147. doi:10.1152/ajprenal.1987.252.6.F1129. [doi].
238. Maunsbach AB, Tripathi S, Boulaep EL. Ultrastructural changes in isolated perfused proximal tubules during osmotic water flow. *Am J Physiol*. 1987;253(6 Pt 2):F1091–F1104.
239. Zhai XY, Fenton RA, Andreasen A, et al. Aquaporin-1 is not expressed in descending thin limbs of short-loop nephrons. *J Am Soc Nephrol*. 2007;18(11):2937–2944. doi: ASN.2007010056 [pii].
240. Dieterich HJ, Barrett JM, Kriz W, Bulhoff JP. The ultrastructure of the thin loop limbs of the mouse kidney. *Anat Embryol (Berl)*. 1975;147(1):1–18.
241. Jamison R, Kriz W. *Urinary Concentrating Mechanism: Structure and Function*. New York: Oxford University Press; 1982.
242. Bachmann S, Kriz W. Histotopography and ultrastructure of the thin limbs of the loop of henle in the hamster. *Cell Tissue Res*. 1982;225(1):111–127.
243. Barrett JM, Kriz W, Kaissling B, et al. The ultrastructure of the nephrons of the desert rodent (*Psammomys obesus*) kidney. I. Thin limb of henle of short-looped nephrons. *Am J Anat*. 1978;151(4):487–497. doi:10.1002/aja.1001510404. [doi].
244. Barrett JM, Kriz W, Kaissling B, et al. The ultrastructure of the nephrons of the desert rodent (*psammomys obesus*) kidney. II. Thin limbs of Henle of long-looped nephrons. *Am J Anat*. 1978;151(4):499–514. doi:10.1002/aja.1001510405. [doi].
245. Kriz W, Schiller A, Taugner R. Freeze-fracture studies on the thin limbs of Henle's loop in *psammomys obesus*. *Am J Anat*. 1981;162(1):23–33. doi:10.1002/aja.1001620103. [doi].
246. Schwartz MM, Karnovsky MJ, Venkatachalam MA. Regional membrane specialization in the thin limbs of Henle's loops as seen by freeze-fracture electron microscopy. *Kidney Int*. 1979;16(5): 577–589.
247. Schiller A, Taugner R, Kriz W. The thin limbs of Henle's loop in the rabbit. A freeze fracture study. *Cell Tissue Res*. 1980;207(2): 249–265.
248. Schwartz MM, Venkatachalam MA. Structural differences in thin limbs of Henle: physiological implications. *Kidney Int*. 1974;6(4):193–208. doi: S0085-2538(15)31371-5 [pii].
249. Ernst SA, Schreiber JH. Ultrastructural localization of Na⁺,K⁺-ATPase in rat and rabbit kidney medulla. *J Cell Biol*. 1981;91(3 Pt 1):803–813.
250. Terada Y, Knepper MA. Na⁺,K⁺-ATPase activities in renal tubule segments of rat inner medulla. *Am J Physiol*. 1989;256(2 Pt 2):F218–F223. doi:10.1152/ajprenal.1989.256.2.F218. [doi].
251. Garg LC, Knepper MA, Burg MB. Mineralocorticoid effects on na-K-ATPase in individual nephron segments. *Am J Physiol*. 1981;240(6):F536–F544. doi:10.1152/ajprenal.1981.240.6.F536. [doi].
252. Maunsbach AB, Marples D, Chin E, et al. Aquaporin-1 water channel expression in human kidney. *J Am Soc Nephrol*. 1997;8(1):1–14.
253. Nielsen S, Pallone T, Smith BL, et al. Aquaporin-1 water channels in short and long loop descending thin limbs and in descending vasa recta in rat kidney. *Am J Physiol*. 1995;268(6 Pt 2):F1023–F1037.
254. Wade JB, Lee AJ, Liu J, et al. UT-a2: a 55-kda urea transporter in thin descending limb whose abundance is regulated by vasopressin. *Am J Physiol Renal Physiol*. 2000;278(1):F52–F62. doi:10.1152/ajprenal.2000.278.1.F52. [doi].
255. Kim WY, Lee HW, Han KH, et al. Descending thin limb of the intermediate loop expresses both aquaporin 1 and urea transporter A2 in the mouse kidney. *Histochem Cell Biol*. 2016;146(1):1–12. doi:10.1007/s00418-016-1434-7. [doi].
256. Kim YH, Kim DU, Han KH, et al. Expression of urea transporters in the developing rat kidney. *Am J Physiol Renal Physiol*. 2002;282(3):F530–F540. doi:10.1152/ajprenal.00246.2001. [doi].
257. Pannabecker TL, Dahlmann A, Brokl OH, et al. Mixed descending-and ascending-type thin limbs of Henle's loop in mammalian renal inner medulla. *Am J Physiol Renal Physiol*. 2000;278(2):F202–F208. doi:10.1152/ajprenal.2000.278.2.F202. [doi].
258. Dantzler WH, Layton AT, Layton HE, et al. Urine-concentrating mechanism in the inner medulla: function of the thin limbs of the loops of Henle. *Clin J Am Soc Nephrol*. 2014;9(10):1781–1789. doi:10.2215/CJN.08750812. [doi].
259. Christensen EI, Grann B, Kristoffersen IB, et al. Three-dimensional reconstruction of the rat nephron. *Am J Physiol Renal Physiol*. 2014;306(6):F664–F671. doi:10.1152/ajprenal.00522.2013. [doi].
260. Pannabecker TL, Dantzler WH. Three-dimensional lateral and vertical relationships of inner medullary loops of Henle and collecting ducts. *Am J Physiol Renal Physiol*. 2004;287(4):F767–F774. doi:10.1152/ajprenal.00122.2004. [doi].
261. Pannabecker TL, Abbott DE, Dantzler WH. Three-dimensional functional reconstruction of inner medullary thin limbs of Henle's loop. *Am J Physiol Renal Physiol*. 2004;286(1):F38–F45. doi:10.1152/ajprenal.00285.2003. [doi].
262. Ren H, Gu L, Andreasen A, et al. Spatial organization of the vascular bundle and the interbundle region: three-dimensional reconstruction at the inner stripe of the outer medulla in the mouse kidney. *Am J Physiol Renal Physiol*. 2014;306(3):F321–F326. doi:10.1152/ajprenal.00429.2013. [doi].
263. Pannabecker TL, Dantzler WH, Layton HE, et al. Role of three-dimensional architecture in the urine concentrating mechanism of the rat renal inner medulla. *Am J Physiol Renal Physiol*. 2008;295(5):F1271–F1285. doi:10.1152/ajprenal.90252.2008. [doi].
264. Pannabecker TL, Henderson CS, Dantzler WH. Quantitative analysis of functional reconstructions reveals lateral and axial zonation in the renal inner medulla. *Am J Physiol Renal Physiol*. 2008;294(6):F1306–F1314. doi:10.1152/ajprenal.00068.2008. [doi].
265. Wei G, Rosen S, Dantzler WH, et al. Architecture of the human renal inner medulla and functional implications. *Am J Physiol Renal Physiol*. 2015;309(7):F627–F637. doi:10.1152/ajprenal.00236.2015. [doi].
266. Pannabecker TL. Structure and function of the thin limbs of the loop of Henle. *Compr Physiol*. 2012;2(3):2063–2086. doi:10.1002/cphy.c110019. [doi].
267. Pannabecker TL, Layton AT. Targeted delivery of solutes and oxygen in the renal medulla: role of microvessel architecture. *Am J Physiol Renal Physiol*. 2014;307(6):F649–F655. doi:10.1152/ajprenal.00276.2014. [doi].
268. Kriz W, Bankir L. A standard nomenclature for structure of the kidney. the renal commission of the international union of physiological sciences (IUPS). *Anat Embryol (Berl)*. 1988;178(2):N1–N8.
269. Woodhall PB, Tisher CC. Response of the distal tubule and cortical collecting duct to vasopressin in the rat. *J Clin Invest*. 1973;52(12):3095–3108. doi:10.1172/JCI107509. [doi].
270. Allen F, Tisher CC. Morphology of the ascending thick limb of Henle. *Kidney Int*. 1976;9(1):8–22. doi: S0085-2538(15)31550-7 [pii].
271. Morel F, Chabardes D, Imbert M. Functional segmentation of the rabbit distal tubule by microdetermination of hormone-dependent adenylate cyclase activity. *Kidney Int*. 1976;9(3):264–277. doi: S0085-2538(15)31576-3 [pii].
272. Kone BC, Madsen KM, Tisher CC. Ultrastructure of the thick ascending limb of Henle in the rat kidney. *Am J Anat*. 1984;171(2):217–226. doi:10.1002/aja.1001710207. [doi].
273. Welling LW, Welling DJ, Hill JJ. Shape of cells and intercellular channels in rabbit thick ascending limb of Henle. *Kidney Int*. 1978;13(2):144–151. doi: S0085-2538(15)31858-5 [pii].
274. Kaplan MR, Plotkin MD, Lee WS, et al. Apical localization of the Na-K-Cl cotransporter, rBSC1, on rat thick ascending limbs. *Kidney Int*. 1996;49(1):40–47. doi: S0085-2538(15)59336-8 [pii].
275. Rocha AS, Kokko JP. Sodium chloride and water transport in the medullary thick ascending limb of Henle. Evidence for active chloride transport. *J Clin Invest*. 1973;52(3):612–623. doi:10.1172/JCI107223. [doi].
276. Garg LC, Mackie S, Tisher CC. Effect of low potassium-diet on Na-K-ATPase in rat nephron segments. *Pflugers Arch*. 1982;394(2):113–117.
277. Dimke H, Schnermann J. Axial and cellular heterogeneity in electrolyte transport pathways along the thick ascending limb. *Acta Physiol (Oxf)*. 2018;223(1):e13057. doi:10.1111/apha.13057. [doi].
278. Stokes JB. Effect of prostaglandin E2 on chloride transport across the rabbit thick ascending limb of Henle. Selective inhibitions of the

- medullary portion. *J Clin Invest.* 1979;64(2):495–502. doi:10.1172/JCI109487. [doi].
279. Sasaki S, Imai M. Effects of vasopressin on water and NaCl transport across the in vitro perfused medullary thick ascending limb of henle's loop of mouse, rat, and rabbit kidneys. *Pflugers Arch.* 1980;383(3):215–221.
 280. Burg MB, Green N. Function of the thick ascending limb of Henle's loop. *Am J Physiol.* 1973;224(3):659–668. doi:10.1152/ajplegacy.1973.224.3.659. [doi].
 281. Crayen ML, Thoenes W. Architecture and cell structures in the distal nephron of the rat kidney. *Cytobiologie.* 1978;17(1):197–211.
 282. Loffing J, Kaissling B. Sodium and calcium transport pathways along the mammalian distal nephron: from rabbit to human. *Am J Physiol Renal Physiol.* 2003;284(4):F628–F643. doi:10.1152/ajprenal.00217.2002. [doi].
 283. Bachmann S, Bostanjoglo M, Schmitt R, et al. Sodium transport-related proteins in the mammalian distal nephron—distribution, ontogeny and functional aspects. *Anat Embryol (Berl).* 1999;200(5):447–468.
 284. Bostanjoglo M, Reeves WB, Reilly RF, et al. 11Beta-hydroxysteroid dehydrogenase, mineralocorticoid receptor, and thiazide-sensitive na-cl cotransporter expression by distal tubules. *J Am Soc Nephrol.* 1998;9(8):1347–1358.
 285. Campean V, Kricke J, Ellison D, et al. Localization of thiazide-sensitive Na(+)–Cl(–) cotransport and associated gene products in mouse DCT. *Am J Physiol Renal Physiol.* 2001;281(6):F1028–F1035. doi:10.1152/ajprenal.0148.2001. [doi].
 286. Loffing J, Loffing-Cueni D, Valderrabano V, et al. Distribution of transcellular calcium and sodium transport pathways along mouse distal nephron. *Am J Physiol Renal Physiol.* 2001;281(6):F1021–F1027. doi:10.1152/ajprenal.0085.2001. [doi].
 287. Biner HL, Arpin-Bott MP, Loffing J, et al. Human cortical distal nephron: distribution of electrolyte and water transport pathways. *J Am Soc Nephrol.* 2002;13(4):836–847.
 288. Hofmeister MV, Fenton RA, Praetorius J. Fluorescence isolation of mouse late distal convoluted tubules and connecting tubules: effects of vasopressin and vitamin D3 on Ca2+ signaling. *Am J Physiol Renal Physiol.* 2009;296(1):F194–F203. doi:10.1152/ajprenal.90495.2008. [doi].
 289. Loffing J, Vallon V, Loffing-Cueni D, et al. Altered renal distal tubule structure and renal Na(+) and Ca(2+) handling in a mouse model for gitelman's syndrome. *J Am Soc Nephrol.* 2004;15(9):2276–2288. doi:10.1097/01.ASN.0000138234.18569.63. [doi].
 290. Plotkin MD, Kaplan MR, Verlander JW, et al. Localization of the thiazide sensitive Na-Cl cotransporter, rTSC1 in the rat kidney. *Kidney Int.* 1996;50(1):174–183. doi: S0085-2538(15)59594-X [pii].
 291. Bachmann S, Velazquez H, Obermuller N, et al. Expression of the thiazide-sensitive Na-Cl cotransporter by rabbit distal convoluted tubule cells. *J Clin Invest.* 1995;96(5):2510–2514. doi:10.1172/JCI118311. [doi].
 292. Obermuller N, Bernstein P, Velazquez H, et al. Expression of the thiazide-sensitive Na-Cl cotransporter in rat and human kidney. *Am J Physiol.* 1995;269(6 Pt 2):F900–F910. doi:10.1152/ajprenal.1995.269.6.F900. [doi].
 293. Kaissling B, Bachmann S, Kriz W. Structural adaptation of the distal convoluted tubule to prolonged furosemide treatment. *Am J Physiol.* 1985;248(3 Pt 2):F374–F381. doi:10.1152/ajprenal.1985.248.3.F374. [doi].
 294. Kaissling B, Stanton BA. Adaptation of distal tubule and collecting duct to increased sodium delivery. I. Ultrastructure. *Am J Physiol.* 1988;255(6 Pt 2):F1256–F1268. doi:10.1152/ajprenal.1988.255.6.F1256. [doi].
 295. Stanton BA, Kaissling B. Adaptation of distal tubule and collecting duct to increased Na delivery. II. Na+ and K+ transport. *Am J Physiol.* 1988;255(6 Pt 2):F1269–F1275. doi:10.1152/ajprenal.1988.255.6.F1269. [doi].
 296. Ellison DH, Velazquez H, Wright FS. Adaptation of the distal convoluted tubule of the rat. Structural and functional effects of dietary salt intake and chronic diuretic infusion. *J Clin Invest.* 1989;83(1):113–126. doi:10.1172/JCI113847. [doi].
 297. Kaissling B. Structural aspects of adaptive changes in renal electrolyte excretion. *Am J Physiol.* 1982;243(3):F211–F226. doi:10.1152/ajprenal.1982.243.3.F211. [doi].
 298. Abdallah JG, Schrier RW, Edelstein C, et al. Loop diuretic infusion increases thiazide-sensitive Na(+)–Cl(–)-cotransporter abundance: role of aldosterone. *J Am Soc Nephrol.* 2001;12(7):1335–1341.
 299. Lee DH, Riquier AD, Yang LE, et al. Acute hypertension provokes acute trafficking of distal tubule Na-Cl cotransporter (NCC) to subapical cytoplasmic vesicles. *Am J Physiol Renal Physiol.* 2009;296(4):F810–F818. doi:10.1152/ajprenal.90606.2008. [doi].
 300. Sandberg MB, Maunsbach AB, McDonough AA. Redistribution of distal tubule Na+-Cl- cotransporter (NCC) in response to a high-salt diet. *Am J Physiol Renal Physiol.* 2006;291(2):F503–F508. doi: 00482.2005 [pii].
 301. Sandberg MB, Riquier AD, Pihakaski-Maunsbach K, et al. ANG II provokes acute trafficking of distal tubule Na+-Cl(-) cotransporter to apical membrane. *Am J Physiol Renal Physiol.* 2007;293(3):F662–F669. doi: 00064.2007 [pii].
 302. Lee DH, Maunsbach AB, Riquier-Brison AD, et al. Effects of ACE inhibition and ANG II stimulation on renal Na-Cl cotransporter distribution, phosphorylation, and membrane complex properties. *Am J Physiol Cell Physiol.* 2013;304(2):C147–C163. doi:10.1152/ajpcell.00287.2012. [doi].
 303. Rojas-Vega L, Reyes-Castro LA, Ramirez V, et al. Ovarian hormones and prolactin increase renal NaCl cotransporter phosphorylation. *Am J Physiol Renal Physiol.* 2015;308(8):F799–F808. doi:10.1152/ajprenal.00447.2014. [doi].
 304. Verlander JW, Tran TM, Zhang L, et al. Estradiol enhances thiazide-sensitive NaCl cotransporter density in the apical plasma membrane of the distal convoluted tubule in ovariectomized rats. *J Clin Invest.* 1998;101(8):1661–1669. doi:10.1172/JCI601. [doi].
 305. Dorup J, Morsing P, Rasch R. Tubule-tubule and tubule-arteriole contacts in rat kidney distal nephrons. A morphologic study based on computer-assisted three-dimensional reconstructions. *Lab Invest.* 1992;67(6):761–769.
 306. Ren Y, Garvin JL, Liu R, et al. Crosstalk between the connecting tubule and the afferent arteriole regulates renal microcirculation. *Kidney Int.* 2007;71(11):1116–1121. doi: S0085-2538(15)52273-4 [pii].
 307. Ren Y, D'Ambrosio MA, Garvin JL, et al. Angiotensin II enhances connecting tubule glomerular feedback. *Hypertension.* 2010;56(4):636–642. doi:10.1161/HYPERTENSIONAHA.110.153692. [doi].
 308. Wang H, Garvin JL, D'Ambrosio MA, et al. Connecting tubule glomerular feedback antagonizes tubuloglomerular feedback in vivo. *Am J Physiol Renal Physiol.* 2010;299(6):F1374–F1378. doi:10.1152/ajprenal.00403.2010. [doi].
 309. Wang H, D'Ambrosio MA, Garvin JL, et al. Connecting tubule glomerular feedback in hypertension. *Hypertension.* 2013;62(4):738–745. doi:10.1161/HYPERTENSIONAHA.113.01846. [doi].
 310. Ren Y, Garvin JL, Liu R, et al. Cross-talk between arterioles and tubules in the kidney. *Pediatr Nephrol.* 2009;24(1):31–35. doi:10.1007/s00467-008-0852-8. [doi].
 311. Myers CE, Bulger RE, Tisher CC, et al. Human ultrastructure. IV. Collecting duct of healthy individuals. *Lab Invest.* 1966;15(12):1921–1950.
 312. Welling LW, Evan AP, Welling DJ, et al. Morphometric comparison of rabbit cortical connecting tubules and collecting ducts. *Kidney Int.* 1983;23(2):358–367. doi: S0085-2538(15)32897-0 [pii].
 313. Kim J, Kim YH, Cha JH, et al. Intercalated cell subtypes in connecting tubule and cortical collecting duct of rat and mouse. *J Am Soc Nephrol.* 1999;10(1):1–12.
 314. Teng-umnuay P, Verlander JW, Yuan W, et al. Identification of distinct subpopulations of intercalated cells in the mouse collecting duct. *J Am Soc Nephrol.* 1996;7(2):260–274.
 315. Wall SM, Hassell KA, Royaux IE, et al. Localization of pendrin in mouse kidney. *Am J Physiol Renal Physiol.* 2003;284(1):F229–F241. doi:10.1152/ajprenal.00147.2002. [doi].
 316. Han KH, Croker BP, Clapp WL, et al. Expression of the ammonia transporter, Rh C glycoprotein, in normal and neoplastic human kidney. *J Am Soc Nephrol.* 2006;17(10):2670–2679. doi: ASN.2006020160 [pii].
 317. Wade JB, Fang L, Coleman RA, et al. Differential regulation of ROMK (Kir1.1) in distal nephron segments by dietary potassium. *Am J Physiol Renal Physiol.* 2011;300(6):F1385–F1393. doi:10.1152/ajprenal.00592.2010. [doi].
 318. Reilly RF, Shugrue CA, Lattanzi D, et al. Immunolocalization of the Na+/Ca2+ exchanger in rabbit kidney. *Am J Physiol.* 1993;265(2 Pt 2):F327–F332. doi:10.1152/ajprenal.1993.265.2.F327. [doi].
 319. Borke JL, Minami J, Verma AK, et al. Co-localization of erythrocyte Ca++Mg++ ATPase and vitamin D-dependent 28-kDa-calcium binding protein. *Kidney Int.* 1988;34(2):262–267. doi: S0085-2538(15)34347-7 [pii].

320. Borke JL, Caride A, Verma AK, et al. Plasma membrane calcium pump and 28-kDa calcium binding protein in cells of rat kidney distal tubules. *Am J Physiol*. 1989;257(5 Pt 2):F842–F849. doi:10.1152/ajprenal.1989.257.5.F842. [doi].
321. Roth J, Brown D, Norman AW, et al. Localization of the vitamin D-dependent calcium-binding protein in mammalian kidney. *Am J Physiol*. 1982;243(3):F243–F252. doi:10.1152/ajprenal.1982.243.3.F243. [doi].
322. Boros S, Bindels RJ, Hoenderop JG. Active Ca(2+) reabsorption in the connecting tubule. *Pflugers Arch.* 2009;458(1):99–109. doi:10.1007/s00424-008-0602-6. [doi].
323. Yang CW, Kim J, Kim YH, et al. Inhibition of calbindin D28K expression by cyclosporin A in rat kidney: the possible pathogenesis of cyclosporin A-induced hypercalcaturia. *J Am Soc Nephrol*. 1998;9(8):1416–1426.
324. Coleman RA, Wu DC, Liu J, et al. Expression of aquaporins in the renal connecting tubule. *Am J Physiol Renal Physiol*. 2000;279(5):F874–F883. doi:10.1152/ajprenal.2000.279.5.F874. [doi].
325. Kortenoeven ML, Pedersen NB, Miller RL, et al. Genetic ablation of aquaporin-2 in the mouse connecting tubules results in defective renal water handling. *J Physiol*. 2013;591(8):2205–2219. doi:10.1113/jphysiol.2012.250852. [doi].
326. Loffing J, Loffing-Cueni D, Macher A, et al. Localization of epithelial sodium channel and aquaporin-2 in rabbit kidney cortex. *Am J Physiol Renal Physiol*. 2000;278(4):F530–F539. doi:10.1152/ajprenal.2000.278.4.F530. [doi].
327. Stanton BA, Biemesderfer D, Wade JB, et al. Structural and functional study of the rat distal nephron: effects of potassium adaptation and depletion. *Kidney Int*. 1981;19(1):36–48. doi: S0085-2538(15)32429-7 [pii].
328. Clapp WL, Madsen KM, Verlander JW, et al. Morphologic heterogeneity along the rat inner medullary collecting duct. *Lab Invest*. 1989;60(2):219–230.
329. Clapp WL, Madsen KM, Verlander JW, et al. Intercalated cells of the rat inner medullary collecting duct. *Kidney Int*. 1987;31(5):1080–1087. doi: S0085-2538(15)33981-8 [pii].
330. Hansen GP, Tisher CC, Robinson RR. Response of the collecting duct to disturbances of acid-base and potassium balance. *Kidney Int*. 1980;17(3):326–337. doi: S0085-2538(15)32250-X [pii].
331. Bagnis C, Marshansky V, Breton S, et al. Remodeling of the cellular profile of collecting ducts by chronic carbonic anhydrase inhibition. *Am J Physiol Renal Physiol*. 2001;280(3):F437–F448. doi:10.1152/ajprenal.2001.280.3.F437. [doi].
332. Kim WY, Nam SA, Choi A, et al. Aquaporin 2-labeled cells differentiate to intercalated cells in response to potassium depletion. *Histochem Cell Biol*. 2016;145(1):17–24. doi:10.1007/s00418-015-1372-9. [doi].
333. Park EY, Kim WY, Kim YM, et al. Proposed mechanism in the change of cellular composition in the outer medullary collecting duct during potassium homeostasis. *Histol Histopathol*. 2012;27(12):1559–1577. doi:10.14670/HH-27.1559. [doi].
334. Himmel NJ, Wang Y, Rodriguez DA, et al. Chronic lithium treatment induces novel patterns of pendrin localization and expression. *Am J Physiol Renal Physiol*. 2018;doi:10.1152/ajprenal.00065.2018. [doi].
335. Treciccone F, Capasso G, Nielsen S, et al. Evaluation of cellular plasticity in the collecting duct during recovery from lithium-induced nephrogenic diabetes insipidus. *Am J Physiol Renal Physiol*. 2013;305(6):F919–F929. doi:10.1152/ajprenal.00152.2012. [doi].
336. Christensen BM, Marples D, Kim YH, et al. Changes in cellular composition of kidney collecting duct cells in rats with lithium-induced NDI. *Am J Physiol Cell Physiol*. 2004;286(4):C952–C964. doi:10.1152/ajpcell.00266.2003. [doi].
337. Christensen BM, Kim YH, Kwon TH, et al. Lithium treatment induces a marked proliferation of primarily principal cells in rat kidney inner medullary collecting duct. *Am J Physiol Renal Physiol*. 2006;291(1):F39–F48. doi: 00383.2005 [pii].
338. LeFurgey A, Tisher CC. Morphology of rabbit collecting duct. *Am J Anat*. 1979;155(1):111–124. doi:10.1002/aja.1001550108. [doi].
339. Welling LW, Evan AP, Welling DJ. Shape of cells and extracellular channels in rabbit cortical collecting ducts. *Kidney Int*. 1981;20(2):211–222. doi: S0085-2538(15)32540-0 [pii].
340. Verlander JW, Madsen KM, Tisher CC. Effect of acute respiratory acidosis on two populations of intercalated cells in rat cortical collecting duct. *Am J Physiol*. 1987;253(6 Pt 2):F1142–F1156.
341. Kim J, Tisher CC, Linser PJ, et al. Ultrastructural localization of carbonic anhydrase II in subpopulations of intercalated cells of the rat kidney. *J Am Soc Nephrol*. 1990;1(3):245–256.
342. Alper SL, Natale J, Gluck S, et al. Subtypes of intercalated cells in rat kidney collecting duct defined by antibodies against erythroid band 3 and renal vacuolar H+-ATPase. *Proc Natl Acad Sci U S A*. 1989;86(14):5429–5433.
343. Madsen KM, Tisher CC. Cellular response to acute respiratory acidosis in rat medullary collecting duct. *Am J Physiol*. 1983;245(6):F670–F679.
344. Madsen KM, Tisher CC. Response of intercalated cells of rat outer medullary collecting duct to chronic metabolic acidosis. *Lab Invest*. 1984;51(3):268–276.
345. Humbert F, Pricam C, Perrelet A, et al. Specific plasma membrane differentiations in the cells of the kidney collecting tubule. *J Ultrastruct Res*. 1975;52(1):13–20.
346. Stetson DL, Wade JB, Giebisch G. Morphologic alterations in the rat medullary collecting duct following potassium depletion. *Kidney Int*. 1980;17(1):45–56. doi: S0085-2538(15)32226-2 [pii].
347. Brown D, Gluck S, Hartwig J. Structure of the novel membrane-coating material in proton-secreting epithelial cells and identification as an H+-ATPase. *J Cell Biol*. 1987;105(4):1637–1648.
348. Madsen KM, Verlander JW, Tisher CC. Relationship between structure and function in distal tubule and collecting duct. *J Electron Microsc Tech*. 1988;9(2):187–208. doi:10.1002/jemt.1060090206. [doi].
349. Holthofer H, Schulte BA, Pasternack G, et al. Immunocytochemical characterization of carbonic anhydrase-rich cells in the rat kidney collecting duct. *Lab Invest*. 1987;57(2):150–156.
350. Lonnerholm G, Ridderstrale Y. Intracellular distribution of carbonic anhydrase in the rat kidney. *Kidney Int*. 1980;17(2):162–174. doi: S0085-2538(15)32232-8 [pii].
351. Brown D, Hirsch S, Gluck S, et al. ATPase in opposite plasma membrane domains in kidney epithelial cell subpopulations. *Nature*. 1988;331(6157):622–624. doi:10.1038/331622a0. [doi].
352. Verlander JW, Madsen KM, Galla JH, et al. Response of intercalated cells to chloride depletion metabolic alkalosis. *Am J Physiol*. 1992;262(2 Pt 2):F309–F319.
353. Verlander JW, Madsen KM, Stone DK, et al. Ultrastructural localization of H+-ATPase in rabbit cortical collecting duct. *J Am Soc Nephrol*. 1994;4(8):1546–1557.
354. Verlander JW, Madsen KM, Low PS, et al. Immunocytochemical localization of band 3 protein in the rat collecting duct. *Am J Physiol*. 1988;255(1 Pt 2):F115–F125.
355. Drenckhahn D, Schluter K, Allen DP, et al. Colocalization of band 3 with ankyrin and spectrin at the basal membrane of intercalated cells in the rat kidney. *Science*. 1985;230(4731):1287–1289.
356. Madsen KM, Kim J, Tisher CC. Intracellular band 3 immunostaining in type a intercalated cells of rabbit kidney. *Am J Physiol*. 1992;262(6 Pt 2):F1015–F1022.
357. Verlander JW, Madsen KM, Cannon JK, et al. Activation of acid-secreting intercalated cells in rabbit collecting duct with ammonium chloride loading. *Am J Physiol*. 1994;266(4 Pt 2):F633–F645.
358. Royaux IE, Wall SM, Karniski LP, et al. Pendrin, encoded by the pendred syndrome gene, resides in the apical region of renal intercalated cells and mediates bicarbonate secretion. *Proc Natl Acad Sci U S A*. 2001;98(7):4221–4226. doi:10.1073/pnas.071516798. [doi].
359. Kim YH, Kwon TH, Frische S, et al. Immunocytochemical localization of pendrin in intercalated cell subtypes in rat and mouse kidney. *Am J Physiol Renal Physiol*. 2002;283(4):F744–F754. doi:10.1152/ajprenal.00037.2002. [doi].
360. Chen L, Lee JW, Chou CL, et al. Transcriptomes of major renal collecting duct cell types in mouse identified by single-cell RNA-seq. *Proc Natl Acad Sci U S A*. 2017;114(46):E9989–E9998. doi:10.1073/pnas.1710964114. [doi].
361. Weiner ID, Verlander JW. Ammonia transport in the kidney by rhesus glycoproteins. *Am J Physiol Renal Physiol*. 2014;306(10):F1107–F1120. doi:10.1152/ajprenal.00013.2014. [doi].
362. Verlander JW, Chu D, Lee HW, et al. Expression of glutamine synthetase in the mouse kidney: localization in multiple epithelial cell types and differential regulation by hypokalemia. *Am J Physiol Renal Physiol*. 2013;305(5):F701–F713. doi:10.1152/ajprenal.00030.2013. [doi].
363. Han KH, Lee HW, Handlogten ME, et al. Expression of the ammonia transporter family member, Rh B glycoprotein, in the human kidney. *Am J Physiol Renal Physiol*. 2013;304(7):F972–F981. doi:10.1152/ajprenal.00550.2012. [doi].
364. Kim HY, Verlander JW, Bishop JM, et al. Basolateral expression of the ammonia transporter family member Rh C glycoprotein in the

- mouse kidney. *Am J Physiol Renal Physiol.* 2009;296(3):F543–F555. doi:10.1152/ajprenal.90637.2008. [doi].
365. Seshadri RM, Klein JD, Kozlowski S, et al. Renal expression of the ammonia transporters, Rhbg and Rhcg, in response to chronic metabolic acidosis. *Am J Physiol Renal Physiol.* 2006;290(2):F397–F408. doi: 00162.2005 [pii].
366. Verlander JW, Miller RT, Frank AE, et al. Localization of the ammonium transporter proteins RhBG and RhCG in mouse kidney. *Am J Physiol Renal Physiol.* 2003;284(2):F323–F337. doi:10.1152/ajprenal.00050.2002. [doi].
367. Atkins JL, Burg MB. Bicarbonate transport by isolated perfused rat collecting ducts. *Am J Physiol.* 1985;249(4 Pt 2):F485–F489. doi:10.1152/ajprenal.1985.249.4.F485. [doi].
368. McKinney TD, Burg MB. Bicarbonate transport by rabbit cortical collecting tubules. effect of acid and alkali loads in vivo on transport in vitro. *J Clin Invest.* 1977;60(3):766–768. doi:10.1172/JCI108830. [doi].
369. Seshadri RM, Klein JD, Smith T, et al. Changes in subcellular distribution of the ammonia transporter, Rhcg, in response to chronic metabolic acidosis. *Am J Physiol Renal Physiol.* 2006;290(6):F1443–F1452. doi: 00459.2005 [pii].
370. Verlander JW, Hassell KA, Royaux IE, et al. Deoxycorticosterone upregulates PDS (Slc26a4) in mouse kidney: role of pendrin in mineralocorticoid-induced hypertension. *Hypertension.* 2003;42(3): 356–362. doi:10.1161/01.HYP.0000088321.67254.B7. [doi].
371. Verlander JW, Kim YH, Shin W, et al. Dietary Cl(-) restriction upregulates pendrin expression within the apical plasma membrane of type B intercalated cells. *Am J Physiol Renal Physiol.* 2006;291(4):F833–F839. doi: 00474.2005 [pii].
372. Verlander JW, Hong S, Pech V, et al. Angiotensin II acts through the angiotensin Ia receptor to upregulate pendrin. *Am J Physiol Renal Physiol.* 2011;301(6):F1314–F1325. doi:10.1152/ajprenal.00114.2011. [doi].
373. Wall SM. The role of pendrin in blood pressure regulation. *Am J Physiol Renal Physiol.* 2016;310(3):F193–F203. doi:10.1152/ajprenal.00400.2015. [doi].
374. Wall SM, Weinstein AM. Cortical distal nephron Cl(-) transport in volume homeostasis and blood pressure regulation. *Am J Physiol Renal Physiol.* 2013;305(4):F427–f438. doi:10.1152/ajprenal.00022.2013. [doi].
375. Wall SM, Kim YH, Stanley L, et al. NaCl restriction upregulates renal slc26a4 through subcellular redistribution: role in Cl- conservation. *Hypertension.* 2004;44(6):982–987. doi: 01.HYP.0000145863.96091.89 [pii].
376. Kishore BK, Mandon B, Oza NB, et al. Rat renal arcade segment expresses vasopressin-regulated water channel and vasopressin V2 receptor. *J Clin Invest.* 1996;97(12):2763–2771. doi:10.1172/JCI118731. [doi].
377. Nielsen S, DiGiovanni SR, Christensen EI, et al. Cellular and subcellular immunolocalization of vasopressin-regulated water channel in rat kidney. *Proc Natl Acad Sci U S A.* 1993;90(24):11663–11667.
378. Wade JB, O’Neil RG, Pryor JL, Boulpaep EL. Modulation of cell membrane area in renal collecting tubules by corticosteroid hormones. *J Cell Biol.* 1979;81(2):439–445.
379. Stanton B, Janzen A, Klein-Robbenhaar G, et al. Ultrastructure of rat initial collecting tubule. effect of adrenal corticosteroid treatment. *J Clin Invest.* 1985;75(4):1327–1334. doi:10.1172/JCI11833. [doi].
380. Kaispling B, Le Hir M. Distal tubular segments of the rabbit kidney after adaptation to altered na- and K-intake. I. structural changes. *Cell Tissue Res.* 1982;224(3):469–492.
381. Hager H, Kwon TH, Vinnikova AK, et al. Immunocytochemical and immunoelectron microscopic localization of alpha-, beta-, and gamma-ENaC in rat kidney. *Am J Physiol Renal Physiol.* 2001; 280(6):F1093–f1106. doi:10.1152/ajprenal.2001.280.6.F1093. [doi].
382. Masilamani S, Kim GH, Mitchell C, et al. Aldosterone-mediated regulation of ENaC alpha, beta, and gamma subunit proteins in rat kidney. *J Clin Invest.* 1999;104(7):R19–R23. doi:10.1172/JCI7840. [doi].
383. Beutler KT, Masilamani S, Turban S, et al. Long-term regulation of ENaC expression in kidney by angiotensin II. *Hypertension.* 2003;41(5):1143–1150. doi:10.1161/01.HYP.0000066129.12106.E2. [doi].
384. Pech V, Wall SM, Nanami M, et al. Pendrin gene ablation alters ENaC subcellular distribution and open probability. *Am J Physiol Renal Physiol.* 2015;309(2):F154–F163. doi:10.1152/ajprenal.00564.2014. [doi].
385. Ridderstrale Y, Kashgarian M, Koeppen B, et al. Morphological heterogeneity of the rabbit collecting duct. *Kidney Int.* 1988;34(5): 655–670. doi: S0085-2538(15)34403-3 [pii].
386. Duc C, Farman N, Canessa CM, et al. Cell-specific expression of epithelial sodium channel alpha, beta, and gamma subunits in aldosterone-responsive epithelia from the rat: localization by in situ hybridization and immunocytochemistry. *J Cell Biol.* 1994;127(6 Pt 2):1907–1921.
387. Elger M, Bankir L, Kriz W. Morphometric analysis of kidney hypertrophy in rats after chronic potassium depletion. *Am J Physiol.* 1992;262(4 Pt 2):F656–F667. doi:10.1152/ajprenal.1992.262.4.F656. [doi].
388. Bastani B, Purcell H, Hemken P, et al. Expression and distribution of renal vacuolar proton-translocating adenosine triphosphatase in response to chronic acid and alkali loads in the rat. *J Clin Invest.* 1991;88(1):126–136. doi:10.1172/JCI115268. [doi].
389. Brown D, Paunescu TG, Breton S, et al. Regulation of the V-ATPase in kidney epithelial cells: dual role in acid-base homeostasis and vesicle trafficking. *J Exp Biol.* 2009;212(Pt 11):1762–1772. doi:10.1242/jeb.028803. [doi].
390. Knepper MA, Danielson RA, Saidel GM, et al. Quantitative analysis of renal medullary anatomy in rats and rabbits. *Kidney Int.* 1977;12(5):313–323. doi: S0085-2538(15)31810-X [pii].
391. Madsen KM, Clapp WL, Verlander JW. Structure and function of the inner medullary collecting duct. *Kidney Int.* 1988;34(4):441–454. doi: S0085-2538(15)34374-X [pii].
392. Isozaki T, Verlander JW, Sands JM. Low protein diet alters urea transport and cell structure in rat initial inner medullary collecting duct. *J Clin Invest.* 1993;92(5):2448–2457. doi:10.1172/JCI116852. [doi].
393. Kato A, Sands JM. Active sodium-urea counter-transport is inducible in the basolateral membrane of rat renal initial inner medullary collecting ducts. *J Clin Invest.* 1998;102(5):1008–1015. doi:10.1172/JCI3588. [doi].
394. Sands JM, Nonoguchi H, Knepper MA. Vasopressin effects on urea and h2o transport in inner medullary collecting duct sub-segments. *Am J Physiol.* 1987;253(5 Pt 2):F823–F832. doi:10.1152/ajprenal.1987.253.5.F823. [doi].
395. Jung JV, Madsen KM, Han KH, et al. Expression of urea transporters in potassium-depleted mouse kidney. *Am J Physiol Renal Physiol.* 2003;285(6):F1210–F1224. doi:10.1152/ajprenal.00111.2003. [doi].
396. DiGiovanni SR, Nielsen S, Christensen EI, et al. Regulation of collecting duct water channel expression by vasopressin in Brattleboro rat. *Proc Natl Acad Sci U S A.* 1994;91(19):8984–8988.
397. Wade JB, Nielsen S, Coleman RA, et al. Long-term regulation of collecting duct water permeability: freeze-fracture analysis of isolated perfused tubules. *Am J Physiol.* 1994;266(5 Pt 2):F723–F730. doi:10.1152/ajprenal.1994.266.5.F723. [doi].
398. Marples D, Knepper MA, Christensen EI, et al. Redistribution of aquaporin-2 water channels induced by vasopressin in rat kidney inner medullary collecting duct. *Am J Physiol.* 1995;269(3 Pt 1): C655–C664. doi:10.1152/ajpcell.1995.269.3.C655. [doi].
399. Madsen KM, Zhang L, Abu Shamat AR, et al. Ultrastructural localization of osteopontin in the kidney: induction by lipopolysaccharide. *J Am Soc Nephrol.* 1997;8(7):1043–1053.
400. Lucien N, Bruneval P, Lasbennes F, et al. UT-b1 urea transporter is expressed along the urinary and gastrointestinal tracts of the mouse. *Am J Physiol Regul Integr Comp Physiol.* 2005;288(4):R1046–R1056. doi: 00286.2004 [pii].
401. Verlander JW, Moudy RM, Campbell WG, et al. Immunohistochemical localizations of H-K-ATPase alpha(2c)-subunit in rabbit kidney. *Am J Physiol Renal Physiol.* 2001;281(2):F357–F365. doi:10.1152/ajprenal.2001.281.2.F357. [doi].
402. Ahn KY, Madsen KM, Tisher CC, et al. Differential expression and cellular distribution of mRNAs encoding alpha- and beta-isoforms of na(+)-K(+) -ATPase in rat kidney. *Am J Physiol.* 1993;265(6 Pt 2):F792–F801. doi:10.1152/ajprenal.1993.265.6.F792. [doi].
403. Sands JM, Knepper MA, Spring KR. Na-K-Cl cotransport in apical membrane of rabbit renal papillary surface epithelium. *Am J Physiol.* 1986;251(3 Pt 2):F475–F484. doi:10.1152/ajprenal.1986.251.3.F475. [doi].
404. Sands JM, Knepper MA. Urea permeability of mammalian inner medullary collecting duct system and papillary surface epithelium. *J Clin Invest.* 1987;79(1):138–147. doi:10.1172/JCI112774. [doi].

405. Chandhoke PS, Packer RK, Knepper MA. Apical acidification by rabbit papillary surface epithelium. *Am J Physiol.* 1990;258(4 Pt 2):F893–F899. doi:10.1152/ajprenal.1990.258.4.F893. [doi].
406. Zeisberg M, Kalluri R. Physiology of the renal interstitium. *Clin J Am Soc Nephrol.* 2015;10(10):1831–1840. doi:10.2215/CJN.00640114. [doi].
407. Lemley KV, Kriz W. Anatomy of the renal interstitium. *Kidney Int.* 1991;39(3):370–381. doi: S0085-2538(15)57139-1 [pii].
408. Bohman S. The ultrastructure of the renal medulla and the interstitial cells. In: Mandal A, ed. *The Renal Papilla and Hypertension*. New York: Plenum; 1980:7.
409. Wolgast M, Larson M, Nygren K. Functional characteristics of the renal interstitium. *Am J Physiol.* 1981;241(2):F105–F111. doi:10.1152/ajprenal.1981.241.2.F105. [doi].
410. Pedersen J, Persson AE, Maunsbach AB. Ultrastructure and quantitative characterization of the cortical interstitium in the rat kidney. In: Maunsbach AB, Olsen T, Christensen EI, eds. *Functional Ultrastructure of the Kidney*. London: Academic Press; 1980:443.
411. Kaissling B, Hegyi I, Loeffing J, et al. Morphology of interstitial cells in the healthy kidney. *Anat Embryol (Berl).* 1996;193(4):303–318.
412. Pfaller W. *Structure Function Correlation on Rat Kidney. Quantitative Correlation of Structure and Function in the Normal and Injured Rat Kidney*. Berlin: Springer-Verlag; 1982.
413. Kaissling B, Le Hir M. Characterization and distribution of interstitial cell types in the renal cortex of rats. *Kidney Int.* 1994;45(3):709–720. doi: S0085-2538(15)58404-4 [pii].
414. Sundelin B, Bohman SO. Postnatal development of the interstitial tissue of the rat kidney. *Anat Embryol (Berl).* 1990;182(4):307–317.
415. Bulger RE, Nagle RB. Ultrastructure of the interstitium in the rabbit kidney. *Am J Anat.* 1973;136(2):183–203. doi:10.1002/aja.1001360206. [doi].
416. Kaissling B, Le Hir M. The renal cortical interstitium: morphological and functional aspects. *Histochem Cell Biol.* 2008;130(2):247–262. doi:10.1007/s00418-008-0452-5. [doi].
417. Kurtz A. Endocrine functions of the renal interstitium. *Pflugers Arch.* 2017;469(7–8):869–876. doi:10.1007/s00424-017-2008-9. [doi].
418. Humphreys BD. Mechanisms of renal fibrosis. *Annu Rev Physiol.* 2018;80:309–326. doi:10.1146/annurev-physiol-022516-034227. [doi].
419. Takahashi-Iwanaga H. The three-dimensional cytoarchitecture of the interstitial tissue in the rat kidney. *Cell Tissue Res.* 1991;264(2):269–281.
420. Lemos DR, Marsh G, Huang A, et al. Maintenance of vascular integrity by pericytes is essential for normal kidney function. *Am J Physiol Renal Physiol.* 2016;311(6):F1230–F1242. doi:10.1152/ajprenal.00030.2016. [doi].
421. Humphreys BD, Lin SL, Kobayashi A, et al. Fate tracing reveals the pericyte and not epithelial origin of myofibroblasts in kidney fibrosis. *Am J Pathol.* 2010;176(1):85–97. doi:10.2353/ajpath.2010.090517. [doi].
422. Mounier F, Foidart JM, Gubler MC. Distribution of extracellular matrix glycoproteins during normal development of human kidney. an immunohistochemical study. *Lab Invest.* 1986;54(4):394–401.
423. Martinez-Hernandez A, Gay S, Miller EJ. Ultrastructural localization of type V collagen in rat kidney. *J Cell Biol.* 1982;92(2):343–349.
424. Bohman SO. The ultrastructure of the rat renal medulla as observed after improved fixation methods. *J Ultrastruct Res.* 1974;47(3):329–360.
425. Le Hir M, Kaissling B. Distribution of 5'-nucleotidase in the renal interstitium of the rat. *Cell Tissue Res.* 1989;258(1):177–182.
426. Bachmann S, Le Hir M, Eckardt KU. Co-localization of erythropoietin mRNA and ecto-5'-nucleotidase immunoreactivity in peritubular cells of rat renal cortex indicates that fibroblasts produce erythropoietin. *J Histochem Cytochem.* 1993;41(3):335–341. doi:10.1177/41.3.8429197. [doi].
427. Bohman SO, Jensen PK. The interstitial cells in the renal medulla of rat, rabbit, and gerbil in different states of diuresis. *Cell Tissue Res.* 1978;189(1):1–18.
428. Bohman SO, Jensen PK. Morphometric studies on the lipid droplets of the interstitial cells of the renal medulla in different states of diuresis. *J Ultrastruct Res.* 1976;55(2):182–192.
429. Schiller A, Taugner R. Junctions between interstitial cells of the renal medulla: a freeze-fracture study. *Cell Tissue Res.* 1979;203(2):231–240.
430. Majack RA, Larsen WJ. The bicellular and reflexive membrane junctions of renomedullary interstitial cells: functional implications of reflexive gap junctions. *Am J Anat.* 1980;157(2):181–189. doi:10.1002/aja.1001570206. [doi].
431. Layton AT, Gilbert RL, Pannabecker TL. Isolated interstitial nodal spaces may facilitate preferential solute and fluid mixing in the rat renal inner medulla. *Am J Physiol Renal Physiol.* 2012;302(7):F830–F839. doi:10.1152/ajprenal.00539.2011. [doi].
432. Gilbert RL, Pannabecker TL. Architecture of interstitial nodal spaces in the rodent renal inner medulla. *Am J Physiol Renal Physiol.* 2013;305(5):F745–F752. doi:10.1152/ajprenal.00239.2013. [doi].
433. Zusman RM, Keiser HR. Prostaglandin biosynthesis by rabbit renomedullary interstitial cells in tissue culture. Stimulation by angiotensin II, bradykinin, and arginine vasopressin. *J Clin Invest.* 1977;60(1):215–223. doi:10.1172/JCI108758. [doi].
434. Bell RD, Keyl MJ, Shrader FR, et al. Renal lymphatics: the internal distribution. *Nephron.* 1968;5(6):454–463. doi:10.1159/000179655. [doi].
435. Yazdani S, Navis G, Hillebrands JL, et al. Lymphangiogenesis in renal diseases: passive bystander or active participant? *Expert Rev Mol Med.* 2014;16:e15. doi:10.1017/erm.2014.18. [doi].
436. Kriz W, Dieterich HJ. The lymphatic system of the kidney in some mammals. Light and electron microscopic investigations. *Z Anat Entwicklungs gesch.* 1970;131(2):111–147.
437. Holmes MJ, O'Morchoe PJ, O'Morchoe CC. Morphology of the intrarenal lymphatic system. capsular and hilar communications. *Am J Anat.* 1977;149(3):333–351. doi:10.1002/aja.1001490303. [doi].
438. Albertine KH, O'Morchoe CC. Distribution and density of the canine renal cortical lymphatic system. *Kidney Int.* 1979;16(4):470–480. doi: S0085-2538(15)32166-9 [pii].
439. Niiri GK, Jarosz HM, O'Morchoe PJ, O'Morchoe CC. The renal cortical lymphatic system in the rat, hamster, and rabbit. *Am J Anat.* 1986;177(1):21–34. doi:10.1002/aja.1001770104. [doi].
440. Lee HW, Qin YX, Kim YM, et al. Expression of lymphatic endothelium-specific hyaluronan receptor LVVE-1 in the developing mouse kidney. *Cell Tissue Res.* 2011;343(2):429–444. doi:10.1007/s00441-010-1098-x. [doi].
441. Nordquist RE, Bell RD, Sinclair RJ, et al. The distribution and ultrastructural morphology of lymphatic vessels in the canine renal cortex. *Lymphology.* 1973;6(1):13–19.
442. Ishikawa Y, Akasaka Y, Kiguchi H, et al. The human renal lymphatics under normal and pathological conditions. *Histopathology.* 2006;49(3):265–273. doi: HIS2478 [pii].
443. Sakamoto I, Ito Y, Mizuno M, et al. Lymphatic vessels develop during tubulointerstitial fibrosis. *Kidney Int.* 2009;75(8):828–838. doi:10.1038/ki.2008.661. [doi].
444. Albertine KH, O'Morchoe CC. An integrated light and electron microscopic study on the existence of intramedullary lymphatics in the dog kidney. *Lymphology.* 1980;13(2):100–106.
445. Tamabe M, Shimizu A, Masuda Y, et al. Development of lymphatic vasculature and morphological characterization in rat kidney. *Clin Exp Nephrol.* 2012;16(6):833–842. doi:10.1007/s10157-012-0637-z. [doi].
446. Assouad J, Riquet M, Berna P, et al. Intrapulmonary lymph node metastasis and renal cell carcinoma. *Eur J Cardiothorac Surg.* 2007;31(1):132–134. doi: S1010-7940(06)00989-4 [pii].
447. Assouad J, Riquet M, Foucault C, et al. Renal lymphatic drainage and thoracic duct connections: implications for cancer spread. *Lymphology.* 2006;39(1):26–32.
448. Parker A. Studies on the main posterior lymph channels of the abdomen and their connections with the lymphatics of the genito-urinary system. *Am J Anat.* 1935;56:409–443.
449. Karmali RJ, Suami H, Wood CG, et al. Lymphatic drainage in renal cell carcinoma: back to the basics. *BJU Int.* 2014;114(6):806–817. doi:10.1111/bju.12814. [doi].
450. Capitanio U, Leibovich BC. The rationale and the role of lymph node dissection in renal cell carcinoma. *World J Urol.* 2017;35(4):497–506. doi:10.1007/s00345-016-1886-3. [doi].
451. van Goor H, Leuvenink HG. The goddess of the waters. *Kidney Int.* 2009;75(8):767–769. doi:10.1038/ki.2009.45. [doi].
452. Kim J, Kim WY, Han KH, et al. Developmental expression of aquaporin 1 in the rat renal vasculature. *Am J Physiol.* 1999;276(4 Pt 2):F498–F509.
453. Lopez Gelston CA, Balasubramanian D, Abouelkheir GR, et al. Enhancing renal lymphatic expansion prevents hypertension in mice. *Circ Res.* 2018. doi: CIRCRESAHA.118.312765 [pii].
454. Kerjaschki D, Huttary N, Raab I, et al. Lymphatic endothelial progenitor cells contribute to de novo lymphangiogenesis in human renal transplants. *Nat Med.* 2006;12(2):230–234. doi: nml340 [pii].

455. Kerjaschki D, Regele HM, Moosberger I, et al. Lymphatic neoangiogenesis in human kidney transplants is associated with immunologically active lymphocytic infiltrates. *J Am Soc Nephrol.* 2004;15(3):603–612.
456. Hasegawa S, Nakano T, Torisu K, et al. Vascular endothelial growth factor-C ameliorates renal interstitial fibrosis through lymphangiogenesis in mouse unilateral ureteral obstruction. *Lab Invest.* 2017;97(12):1439–1452. doi:10.1038/labinvest.2017.77. [doi].
457. Uchiyama T, Takata S, Ishikawa H, et al. Altered dynamics in the renal lymphatic circulation of type 1 and type 2 diabetic mice. *Acta Histochem Cytochem.* 2013;46(2):97–104. doi:10.1267/ahc.13006. [doi].
458. Osborn JW, Foss JD. Renal nerves and long-term control of arterial pressure. *Compr Physiol.* 2017;7(2):263–320. doi:10.1002/cphy.c150047. [doi].
459. Johns EJ, Kopp UC, DiBona GF. Neural control of renal function. *Compr Physiol.* 2011;1(2):731–767. doi:10.1002/cphy.c100043. [doi].
460. DiBona GF, Kopp UC. Neural control of renal function. *Physiol Rev.* 1997;77(1):75–197. doi:10.1152/physrev.1997.77.1.75. [doi].
461. Nishi EE, Bergamaschi CT, Campos RR. The crosstalk between the kidney and the central nervous system: the role of renal nerves in blood pressure regulation. *Exp Physiol.* 2015;100(5):479–484. doi:10.1113/expphysiol.2014.079889. [doi].
462. Burnstock G, Loesch A. Sympathetic innervation of the kidney in health and disease: emphasis on the role of purinergic cotransmission. *Auton Neurosci.* 2017;204:4–16. doi: S1566-0702(16)30055-8 [pii].
463. Maeda S, Kuwahara-Otani S, Tanaka K, et al. Origin of efferent fibers of the renal plexus in the rat autonomic nervous system. *J Vet Med Sci.* 2014;76(5):763–765. doi: DN/JST:JSTAGE/jvms/13-0617 [pii].
464. Maeda S, Fujihira M, Minato Y, et al. Differential distribution of renal nerves in the sympathetic ganglia of the rat. *Anat Rec (Hoboken).* 2017;300(12):2263–2272. doi:10.1002/ar.23680. [doi].
465. DiBona GF, Sawin LL, Jones SY. Differentiated sympathetic neural control of the kidney. *Am J Physiol.* 1996;271(1 Pt 2):R84–R90. doi:10.1152/ajpregu.1996.271.1.R84. [doi].
466. Sato KL, do Carmo JM, Fazan VP. Ultrastructural anatomy of the renal nerves in rats. *Brain Res.* 2006;1119(1):94–100. doi: S0006-8993(06)02439-5 [pii].
467. Fazan VP, Ma X, Chapleau MW, et al. Qualitative and quantitative morphology of renal nerves in C57BL/6j mice. *Anat Rec.* 2002;268(4):399–404. doi:10.1002/ar.10174. [doi].
468. Denton KM, Luff SE, Shweta A, et al. Differential neural control of glomerular ultrafiltration. *Clin Exp Pharmacol Physiol.* 2004;31(5–6):380–386. doi:10.1111/j.1440-1681.2004.04002.x. [doi].
469. Luff SE, Hengstberger SG, McLachlan EM, et al. Distribution of sympathetic neuroeffector junctions in the juxtaglomerular region of the rabbit kidney. *J Auton Nerv Syst.* 1992;40(3):239–253. doi: 0165-1838(92)90206-V [pii].
470. Barajas L, Liu L, Powers K. Anatomy of the renal innervation: intrarenal aspects and ganglia of origin. *Can J Physiol Pharmacol.* 1992;70(5):735–749.
471. Barajas L, Wang P, Powers K, et al. Identification of renal neuroeffector junctions by electron microscopy of reembedded light microscopic autoradiograms of semithin sections. *J Ultrastruct Res.* 1981;77(3):379–385.
472. Ditting T, Tiegs G, Veelken R. Autonomous innervation in renal inflammatory disease-innocent bystander or active modulator? *J Mol Med.* 2009;87(9):865–870. doi:10.1007/s00109-009-0498-4. [doi].
473. Luff SE, Hengstberger SG, McLachlan EM, et al. Two types of sympathetic axon innervating the juxtaglomerular arterioles of the rabbit and rat kidney differ structurally from those supplying other arteries. *J Neurocytol.* 1991;20(10):781–795.
474. Barajas L, Muller J. The innervation of the juxtaglomerular apparatus and surrounding tubules: a quantitative analysis by serial section electron microscopy. *J Ultrastruct Res.* 1973;43(1):107–132.
475. Barajas L. The innervation of the juxtaglomerular apparatus. An electron microscopic study of the innervation of the glomerular arterioles. *Lab Invest.* 1964;13:916–929.
476. Kopp UC, DiBona GF. Neural regulation of renin secretion. *Semin Nephrol.* 1993;13(6):543–551.
477. Barajas L, Powers K, Wang P. Innervation of the late distal nephron: an autoradiographic and ultrastructural study. *J Ultrastruct Res.* 1985;92(3):146–157.
478. Barajas L, Powers KV. Innervation of the thick ascending limb of henle. *Am J Physiol.* 1988;255(2 Pt 2):F340–F348. doi:10.1152/ajpren.1988.255.2.F340. [doi].
479. Muller J, Barajas L. Electron microscopic and histochemical evidence for a tubular innervation in the renal cortex of the monkey. *J Ultrastruct Res.* 1972;41(5):533–549.
480. Newstead J, Munkaci I. Electron microscopic observations on the juxtamедullary efferent arterioles and arteriolae rectae in kidneys of rats. *Z Zellforsch Mikrosk Anat.* 1969;97(4):465–490.
481. Ferguson M, Bell C. Ultrastructural localization and characterization of sensory nerves in the rat kidney. *J Comp Neurol.* 1988;274(1):9–16. doi:10.1002/cne.902740103. [doi].
482. Marfurt CF, Echtenkamp SF. Sensory innervation of the rat kidney and ureter as revealed by the anterograde transport of wheat germ agglutinin-horseradish peroxidase (WGA-HRP) from dorsal root ganglia. *J Comp Neurol.* 1991;311(3):389–404. doi:10.1002/cne.903110309. [doi].
483. Sakakura K, Ladich E, Cheng Q, et al. Anatomic assessment of sympathetic peri-arterial renal nerves in man. *J Am Coll Cardiol.* 2014;64(7):635–643. doi:10.1016/j.jacc.2014.03.059. [doi].
484. Knuepfer MM, Schramm LP. The conduction velocities and spinal projections of single renal afferent fibers in the rat. *Brain Res.* 1987;435(1–2):167–173. doi: 0006-8993(87)91598-8 [pii].
485. Nijima A. Observation on the localization of mechanoreceptors in the kidney and afferent nerve fibres in the renal nerves in the rabbit. *J Physiol.* 1975;245(1):81–90.
486. Ferguson M, Ryan GB, Bell C. Localization of sympathetic and sensory neurons innervating the rat kidney. *J Auton Nerv Syst.* 1986;16(4):279–288. doi: 0165-1838(86)90034-2 [pii].

BOARD REVIEW QUESTIONS

1. Structural features of the podocyte (visceral epithelial cell) that contribute to an intact filtration barrier and prevent proteinuria include:
 - a. The interdigitating foot processes, with focal adhesions to the glomerular basement membrane (GBM), and the filtration slit diaphragm.
 - b. The prominent endocytic apparatus, which removes glomerular basement membrane anionic proteins and increases permeability.
 - c. The prominent secretory apparatus, which increases glomerular basement membrane cationic sites and decreases permeability.
 - d. The fenestrated primary and secondary foot processes.
 - e. Gap junctions with intraglomerular mesangial cells, which mediate signaling to regulate contraction of the podocyte actin cytoskeleton.

Answer: a

2. The anatomical structure enabling classic tubuloglomerular feedback, the juxtaglomerular apparatus, is made up of which structures?
 - a. The glomerular capillary tuft, the extraglomerular mesangium, and the afferent and efferent arterioles.
 - b. The glomerular capillary tuft, Bowman's capsule, and the afferent and efferent arterioles.
 - c. The afferent and efferent arterioles, the extraglomerular mesangium, and the macula densa in the thick ascending limb of Henle.
 - d. The afferent and efferent arterioles, the extraglomerular mesangium, and the macula densa in the distal convoluted tubule.
 - e. The juxtaglomerular mesangial cells, the afferent arteriole, and the peripolar cells of the glomerular tuft.

Answer: c

3. High rates of reabsorption of filtered substances is enabled by which structural features of the proximal convoluted tubule?
 - a. The highest mitochondrial density of any tubule in the kidney, which provides energy for active transport.

- b. The very high density of integral membrane transport proteins in the relatively simple apical and basal plasma membrane compartments.
- c. The presence of renin-secreting cells, which stimulate proximal tubule solute reabsorption when glomerular filtration rate increases.
- d. The apical brush border and complex basolateral plasma membrane infoldings, which contain abundant integral membrane transport proteins, and the prominent endocytic apparatus, which enables receptor-mediated endocytosis of filtered peptides and proteins.
- e. Its alignment with vasa recta, which enhances removal of reabsorbed solutes via the countercurrent mechanism.

Answer: d

4. The distal convoluted tubule, which is the site of the thiazide-sensitive NaCl cotransporter (NCC), responds to treatment with a loop diuretic, such as furosemide, with:
 - a. Atrophy of the epithelial cells
 - b. Hypertrophy of the epithelial cells
 - c. Epithelial cell death
 - d. Transformation into thick ascending limb cells
 - e. Hyperplasia of intercalated cells

Answer: b

5. The cortical collecting duct (CCD) is able to generate either net acid or net bicarbonate secretion in response to physiologic needs because:
 - a. Vasopressin stimulates the insertion of AQP2 channels into the apical plasma membrane of principal cells.
 - b. Aldosterone increases the abundance of the epithelial Na channel, ENaC, in the principal cell apical plasma membrane.
 - c. The majority cell type, principal cells, can either secrete or reabsorb bicarbonate.
 - d. The CCD contains Type A intercalated cells, which can either secrete or reabsorb bicarbonate.
 - e. The CCD contains two specific intercalated cell subtypes; Type A, which secretes protons and ammonia, and Type B, which secretes bicarbonate.

Answer: e

The Renal Circulations and Glomerular Filtration

Luis Gabriel Navar | David A. Maddox | Karen A. Munger

CHAPTER OUTLINE

INTRODUCTION, 81

RENAL BLOOD FLOW AND GLOMERULAR FILTRATION RATE, 82

PARACRINE AND ENDOCRINE FACTORS REGULATING RENAL HEMODYNAMICS AND GLOMERULAR FILTRATION RATE, 95

NEURAL REGULATION OF RENAL CIRCULATION, 112

GLOMERULAR HEMODYNAMICS IN THE AGING KIDNEY, 112

KEY POINTS

- Renal blood flow and GFR increase with protein intake in men and women and, at any given level of protein intake, GFR is greater in younger (20–50 years of age) than in older subjects (55–88 years of age) and greater in men than in women, even when factored for body surface area.
- The decline in hydraulic pressure between the renal artery and glomerular capillaries is greatest along the afferent arteriole, whereas 70% of the decline in postglomerular hydraulic pressure occurs at the efferent arteriole. The last 50 to 150 μm of the afferent arteriole and the first early part of the efferent arteriole (first 50–150 μm) provide most of the preglomerular and postglomerular resistances.
- Glomerular capillary blood pressure, P_{GC} , declines only slightly within the capillary network, thus maintaining the transcapillary hydraulic pressure gradient ($\Delta P = P_{GC}$ minus Bowman's space pressure, P_{BS}) at a relatively constant rate. However, glomerular capillary protein oncotic pressure (π_{GC}) rises along the length of the glomerular capillaries as protein-free fluid is filtered into Bowman's space, thus reducing the net filtration pressure, with π_{G} reaching and becoming equal to ΔP in some cases such as hydropenia.
- The barrier to the filtration of fluid and macromolecules includes the glycocalyx lining the endothelial cells, the fenestrations of the endothelial layer of the glomerular capillaries, the layers of the glomerular basement membrane, the filtration slits between the podocytes surrounding the capillaries, and the filtration slit diaphragm extending along the filtration slits to connect adjacent foot processes. Breakdown or injury in any of the restrictive barriers may lead to increased passage of albumin and other proteins.
- The high resistance of the afferent and efferent arterioles leads to a large drop in vascular hydraulic pressure prior to the peritubular capillaries so that peritubular capillary pressure is much lower than glomerular capillary pressure (15–20 mm Hg). The oncotic pressure of fluid entering the peritubular capillaries is elevated because of the filtration of protein-free fluid out of the glomerular capillaries. The net balance between the transcapillary oncotic and hydraulic pressure gradients thus favors entry of the fluid reabsorbed by the tubules into the peritubular capillaries.
- The finding that both renal blood flow and GFR are autoregulated indicates that the principal resistance change due to autoregulatory adjustments is primarily localized to the preglomerular vasculature. The autoregulation mechanisms provide a powerful mechanism to maintain the intrarenal hemodynamic environment in balance with the metabolically determined tubular transport function.

KEY POINTS—cont'd

- The myogenic and tubuloglomerular feedback mechanisms are primarily responsible for the autoregulatory responses. The myogenic mechanism refers to the ability of arterial smooth muscle to contract and relax in response to increases and decreases in vascular wall tension. The tubuloglomerular feedback mechanism provides signals from the macula densa to the afferent arteriole. Paracrine mediators include ATP, adenosine, nitric oxide and arachidonic acid metabolites.
- Overall renal hemodynamic function is regulated by complex interactions between extrinsic and intrinsic mechanisms, including the sympathetic nervous system, circulating vasoactive factors, endothelial nitric oxide, intrarenal angiotensin II, arachidonic acid metabolites, purinergic factors and other paracrine systems, which exert direct effects and modulate the sensitivity of the tubuloglomerular feedback mechanism.

INTRODUCTION

The kidneys are unique in having three distinct microvascular networks identified as the glomerular capillary microcirculation, the cortical peritubular capillary microcirculation, and the unique medullary microcirculation, which nourishes the medullary tissues and maintains the interstitial environment. Each of these circulations has specialized functions that allow filtration of a large volume of fluid at the glomerular capillaries, the consequent reabsorption of most of the filtrate back into the circulation, and the establishment of a medullary environment having a high interstitial osmolality. These renal circulations not only provide the renal cells and tissues with oxygen and nutrients, but also maintain and regulate the hemodynamic environment to achieve their designated functions. Under resting conditions, blood flow to the kidneys represents approximately 20% of cardiac output in humans, even though these organs constitute less than 1% of body mass. This renal blood flow (RBF), approximately 400 mL/100 g of tissue per minute, is significantly greater than that observed in other vascular beds considered to be well perfused, such as the heart, liver, and brain.^{1,2} From this enormous blood flow (1.0–1.2 L/min), approximately 20% of the plasma flow is filtered and becomes the glomerular filtrate, but only a small volume of urine, about 1%, is formed from that filtrate. Although the metabolic energy requirements of tubular transport processes are relatively high, the renal arteriovenous O₂ difference reveals that blood flow far exceeds that needed for metabolic demands. In fact, the high blood flow is essential to provide the appropriate hemodynamic environments necessary for the filtration at the glomeruli and the reabsorption into the postglomerular capillaries.^{3,4}

In Chapter 2, the gross anatomy of the kidney and arrangement of tubular segments are described in detail. In this chapter, we consider the intrarenal organization of the discrete microcirculatory networks, as shown in Fig. 3.1. We will also consider the differences in regional blood flows and how the structure of the microcirculation contributes to the regulation of the intrarenal hemodynamic environment, thus maintaining appropriate levels of RBF and glomerular filtration rate (GFR).

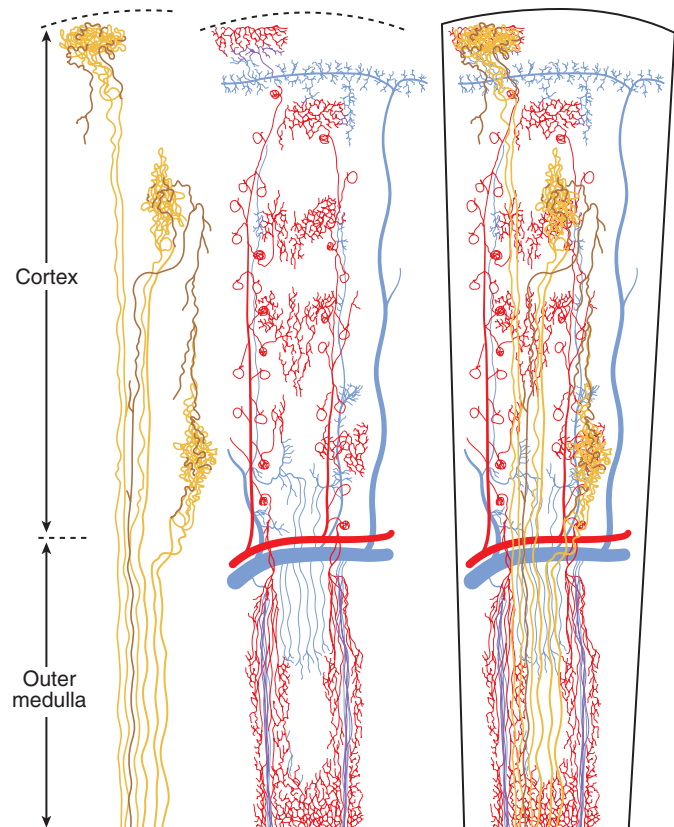


Fig. 3.1 Renal vasculature and tubule organization. Left, Three nephrons are shown without accompanying vascular structures. Vascular structures are shown in the *central portion* of the figure. Right, Vascular and tubular structures are superimposed. Configurations of tubular segments were generalized from patterns found by silicone rubber injections. For clarity, more distal parts of the nephron are shown in deeper colors. Arterial components of the vascular system are shown in *red*, venous components in *blue*. Only representative venous connections are shown. (From Beeuwkes R III, Bonventre JV. Tubular organization and vascular tubular relations in the dog kidney. *Am J Physiol*. 1975;229:695–713.)

RENAL BLOOD FLOW AND GLOMERULAR FILTRATION RATE

Historically, GFR and renal plasma flow (RPF) have been estimated using the clearance of inulin for the determination of GFR and of *p*-aminohippuric acid (PAH) for the determinations of RPF, from which RBF can be calculated using RPF and hematocrit.⁵ Whereas inulin is only filtered across the glomerulus and actively secreted by the tubules. This results in the renal extraction of 80% to 90% of PAH from the blood. PAH is not completely extracted from the blood because of flow through regions of the kidney, in particular the medulla, that do not perfuse proximal tubule segments, where secretion occurs, and limitations of the secretory process of PAH in cortical regions, along with the presence of a few periglomerular shunts (Fig. 3.2). Thus, PAH clearance is an approximation often termed “effective” or “estimated” renal plasma flow (ERPF) and provides an estimate of RPF without the need for a renal venous blood sample.⁵ However, this estimate of RPF is much less accurate in renal disease because extraction is further reduced by damage to proximal tubule segments or rarefaction of the peritubular capillaries involved in PAH secretion.⁶ Values taken from a composite of studies in normal human subjects⁵ are shown in Table 3.1. As indicated in the data presented, RBF and GFR are lower in women than in men, even when corrected for body surface area. Values for normal subjects vary considerably in different studies, as reflected in Fig. 3.3, which shows more recently obtained data on ERPF and GFR in adult humans from various studies that were not corrected for body surface area. The data also reveal marked differences in GFR and ERPF between obese and lean subjects. These differences are likely the result of increased food intake and, hence, increased protein consumption.⁷ Indeed, as shown in Fig. 3.4, GFR increases with protein intake in men and women and, at any given level of protein intake, GFR is higher in young people (20–50 years of age; mean, 31 years) than in older subjects (55–88 years of age; mean, 70 years). Improved methods of RBF

Table 3.1 Renal Blood Flow, Renal Plasma Flow, Glomerular Filtration Rates and Filtration Fractions in Healthy Men and Women^a

| Subject(s) | RBF, mL/min | RPF, mL/min | GFR, mL/min | Filtration Fraction |
|------------|----------------|----------------|----------------|------------------------|
| Men | 1166 | 655 | 127 | 0.193 |
| Women | 940 | 600 | 118 | 0.197 |
| Combined | 1165 | 634 | 123 | .197 |

^aData for RPF based on clearances of Diodrast as well as *p*-aminohippuric acid (PAH) and for GFR based on clearance of inulin. Clearances are corrected to 1.73 m² and suggest lower normalized RBF, RPF, and GFR values in women. GFR, glomerular filtration rate; RBF, renal blood flow; RPF, renal plasma flow.

Data from Smith HW. *The kidney: Structure and function in health and disease*. New York: Oxford University Press; 1951:544–545.

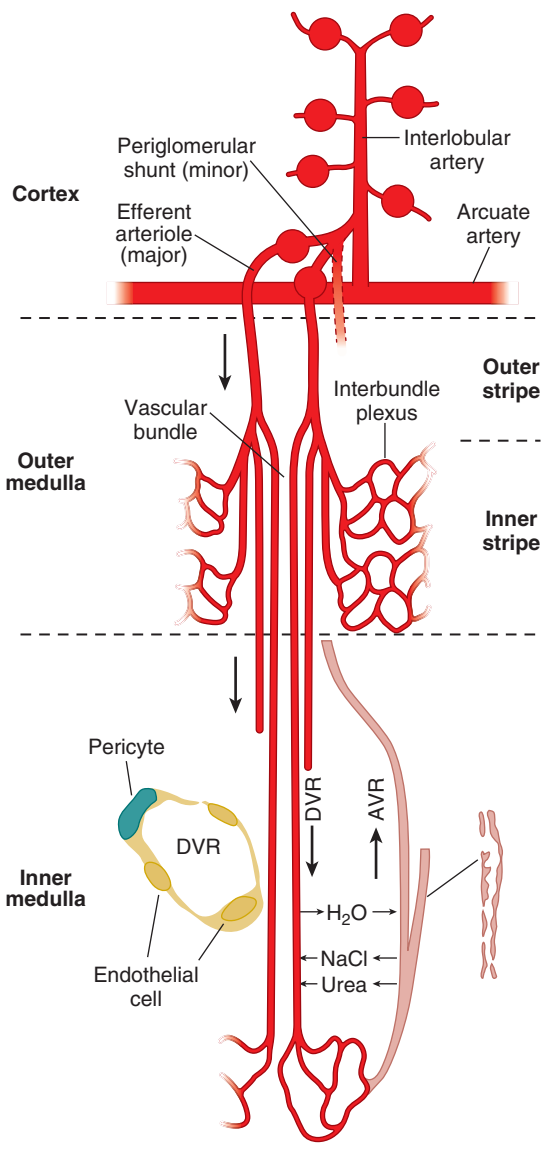


Fig. 3.2 The medullary microcirculation. In the cortex, interlobular arteries arise from the arcuate artery and ascend toward the cortical surface. Cortical and juxtamedullary afferent arterioles leading to glomeruli branch from the interlobular artery. Most of the blood flow reaches the medulla through juxtamedullary efferent arterioles; however, a small fraction may also arise from periglomerular shunt pathways. In the outer medulla, juxtamedullary efferent arterioles in the outer stripe give rise to descending vasa recta (DVR), which coalesce to form vascular bundles in the inner stripe. DVR on the periphery of vascular bundles give rise to the interbundle capillary plexus that surrounds nephron segments—thick ascending limb, collecting duct, long looped thin descending limbs (not shown). DVR in the center continue across the inner-outer medullary junction to perfuse the inner medulla. Vascular bundles disappear in the inner medulla, and vasa recta become dispersed with nephron segments. Ascending vasa recta (AVR) that arise from the sparse capillary plexus of the inner medulla return to the cortex by passing through outer medullary vascular bundles. Inset, DVR have a continuous endothelium. (From Pallone TL, Zhang Z, Rhinehart K. Physiology of the renal medullary microcirculation. Am J Physiol. 2003;284:F253–F266, 2003.)

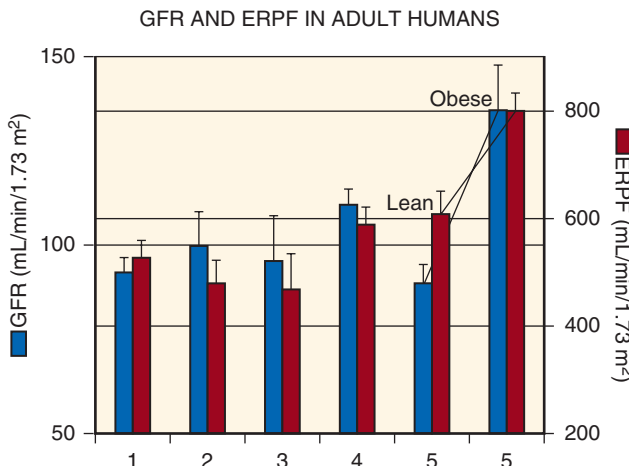


Fig. 3.3 Typical values for glomerular filtration rate (GFR) and estimated renal plasma flow (ERPF) from five studies in adults. Values from men and women were pooled. Numbers under each set of bars refer to the following studies: 1, Giordano and DeFronzo⁵¹⁷; 2, Winetz et al.⁵¹⁸; 3, Hostetter⁵¹⁹; 4, Deen et al.⁵²⁰; 5, Chagnac et al.⁵²¹. For studies 1 through 3 and 5, values were obtained after approximately 12 hours of fasting; subjects in study 4 were allowed food ad lib. For study 5, values from lean subjects (average body mass index [BMI] = 22) were compared with those from obese nondiabetic individuals (BMI >38) after a 10-hour fast but are not corrected for body surface area.

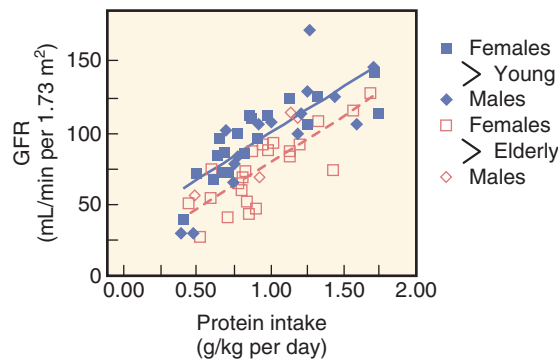


Fig. 3.4 Relationship between protein intake and glomerular filtration rate (GFR). Data from younger (mean age, 31 years; range, 20–50 years) and older (mean age, 70 years; range, 55–88 years) healthy humans. Closed symbols, younger subjects; open symbols, older subjects; squares, women; diamonds, men. (From Lew SQ, Bosch P. Effect of diet on creatinine clearance in young and elderly healthy subjects and in patients with renal disease. *J Am Soc Nephrol*. 1991;2:856–865.)

measurement include laser Doppler flowmetry, video microscopy, and imaging techniques such as positron emission tomography (PET), high-speed computed tomography (CT), and magnetic resonance imaging (MRI).^{6,8–12} These methods have been especially useful in determining changes in regional blood flow.

MAJOR ARTERIES AND VEINS

Blood supply to each kidney is provided by a renal artery that branches directly from the abdominal aorta. The renal artery typically branches into multiple segmental vessels at

a point just before entry into the renal parenchyma and continues to branch in a nonanastomotic manner to supply the glomeruli prior to entering the postglomerular microcirculation (see Fig. 3.1).³ Therefore, complete obstruction of an arterial segmental vessel results in ischemia and infarction of the tissue in its area of distribution. Ligation of individual segmental arteries has frequently been performed in experimental studies to reduce renal mass and produce the remnant kidney model of chronic renal failure.^{13,14} Morphologic studies in this model have revealed the presence of ischemic zones adjacent to the totally infarcted areas. These regions contain viable glomeruli that appear shrunken and crowded together, demonstrating that some portions of the renal cortex may have partial dual perfusion.¹⁵ The anatomic distribution just described is most common; however, other patterns may occur.^{16,17} Secondary renal arteries found in 20% to 30% of normal individuals may result from division of the renal artery at the aorta. These vessels, which most often supply the lower pole,¹⁸ may be the sole arterial supply of some part of the kidney.¹⁹

Within the renal sinus of the human kidney, division of the segmental arteries gives rise to the interlobar arteries. These vessels, in turn, give rise to the arcuate arteries, whose several divisions lie at the border between the cortex and medulla. The interlobular arteries branch from the arcuate arteries more or less sharply, usually as a common trunk that divides two to five times as it extends toward the kidney surface^{20,21} (see Fig. 3.1). Afferent arterioles leading to glomeruli arise from the interlobular arteries (see Figs. 3.1 and 3.2). Glomeruli are classified according to their position within the cortex as superficial (i.e., near the kidney surface), midcortical, or juxtamedullary, near the corticomedullary border (see Fig. 3.1). The capillary network of each glomerulus originates from the afferent arteriole as it enters into a manifold-like chamber. The glomerular capillaries coalesce into an efferent chamber leading to an efferent arteriole that delivers blood to the postglomerular capillary circulation, forming both the cortical peritubular capillaries and complex medullary capillaries. The arrangement of the medullary microcirculation plays an important role in the process of concentration of urine.

Venous drainage of the peritubular capillaries from the superficial cortex is via superficial cortical veins.^{20,22} In the middle and inner cortices, venous drainage is achieved mainly by the interlobular veins. The dense peritubular capillary network surrounding the interlobular vessels drains directly into the interlobular veins through multiple connections, whereas the less dense, long-meshed network of the medullary rays appears to anastomose with the interlobular network and thus drains laterally (see Fig. 3.1). The medullary circulation also shows two different types of drainage. The outer medullary networks typically extend into the medullary rays before joining interlobular veins, whereas the long vascular bundles of the inner medulla (vasa recta) converge abruptly and join the arcuate veins.

OXYGEN CONSUMPTION

Because of the unique juxtaposition of the arteriolar and venular network, much of the abundant oxygen supply to the kidneys diffuses from the arterioles to the venules.²³ The shunting of oxygen, coupled with the very high rate of oxygen

consumption ($\sim 4 \mu\text{mol}/\text{min/g}$), leaves the oxygen tension (pO_2) in the cortex much lower than what would be predicted from the pO_2 in renal venous blood. Tissue pO_2 values in the cortex border on hypoxia, varying from 40 to 45 mm Hg in the outer and mid cortices and even lower (30 mm Hg) in the deep cortex.^{13,24,25} As shown in Fig. 3.5, the countercurrent arrangement between the descending and ascending vasa recta permits further shunting of oxygen, leaving pO_2 values in the medullary tissues of 20 mm Hg or lower toward the papillary tip.^{23,25–27}

About 75% of the oxygen consumption by the kidneys provides the energy required by the Na^+/K^+ -ATPase, which is the major active transport system of the tubules. Changes in oxygen consumption rate vary proportionally with the changes in net Na transport by the tubules. Reduced tissue oxygen levels occur in hypertension, which can compromise renal function.^{24,28} The shunting of oxygen from arterioles to venules suggests that diffusible gas molecules that are formed in the kidney, including CO_2 , NO, and hydrogen sulfide (H_2S), may also undergo shunting, but from venules

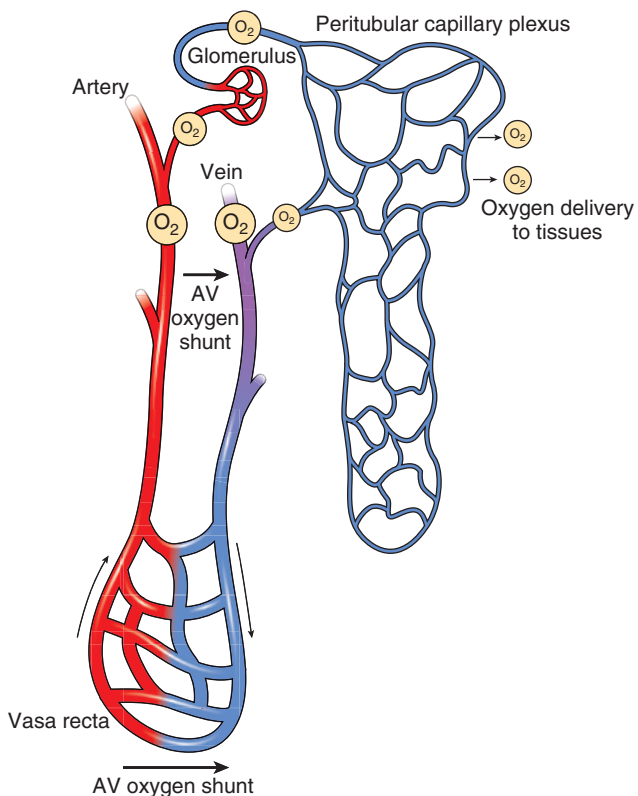


Fig. 3.5 The arterial to venous (AV) oxygen shunt. Oxygen is delivered by red blood cells in the artery. Red blood cells release oxygen in the capillaries, which diffuses into the interstitium to reach target cells. Blood with low oxygen tension passes into the vein. The juxtaposition of the arteries and veins present in the kidney facilitates oxygen diffusion from the artery to the vein. Oxygen tensions in the capillaries are relatively low when red blood cells reach the peritubular capillary plexus, which indicate that the kidney is inefficient in extracting oxygen. The relative oxygen tensions are represented by the size of the circles surrounding O_2 . (From Mimura I, Nangaku M. The suffocating kidney: tubulointerstitial hypoxia in end-stage renal disease. *Nat Rev Nephrol*. 2010;6:667–678.)

to arterioles, thus making it more difficult to wash out unwanted substances such as CO_2 but also accentuating intrarenal retention of protective molecules such as nitric oxide (NO; see Fig. 3.5).²⁹

HYDRAULIC PRESSURE PROFILE AND VASCULAR RESISTANCES

The decline in hydraulic pressure between the systemic vasculature and the end of the interlobular artery in both the superficial and juxtamedullary microvasculatures can be as much as 25 mm Hg at normal perfusion pressures, with most of that pressure drop occurring along the interlobular arteries (Fig. 3.6). Based on studies of the vasculature of juxtamedullary nephrons, most of the preglomerular pressure drop between the arcuate artery and the glomerulus occurs along the afferent arteriole.^{30,31} Approximately 70% of the postglomerular hydraulic pressure drop occurs along the efferent arterioles. The very late portion of the afferent arteriole (last 50–150 μm) and the early portion of the efferent arteriole (first 50–150 μm) provide the major fraction of the total preglomerular and postglomerular resistance (see Fig. 3.6).^{30,31} Multiphoton imaging studies have indicated the presence of an intraglomerular precapillary sphincter at the terminal end of afferent arterioles (Fig. 3.7).^{32,33} Collectively, the total resistance (R_t) consists of two major sites, the afferent (R_a) and efferent (R_e) arterioles and a minor contribution

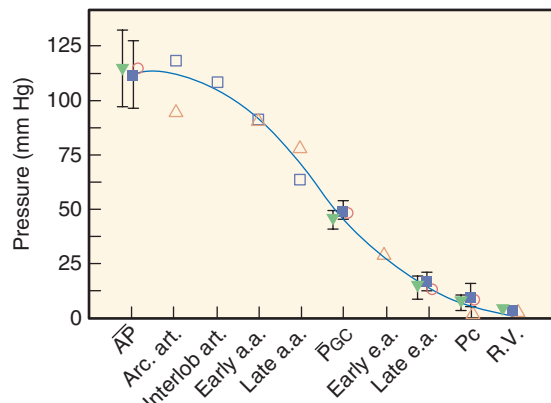


Fig. 3.6 Hydraulic pressure profile in the kidney. Filled squares and triangles denote values (mean ± 2 standard deviation) obtained from euvolemic and hydropenic Munich-Wistar rats. Values from studies in the squirrel monkey⁷⁸ are shown as open diamonds. Open inverted triangles and open squares are from studies in the Sprague Dawley rat in juxtamedullary nephrons perfused with whole blood. These nephrons are located inside the cortical surface opposed to the pelvic lining and arcuate veins, in which entire pressure profiles can be obtained from the interlobular artery (Interlob Art), the proximal (Early a.a.) and distal (Late a.a.) portions of the afferent arteriole, the glomerular capillaries (PGC), the proximal (Early e.a.) and late (Late e.a.) segments of the efferent arteriole, the peritubular capillaries (PC), and the renal vein (R.V.). AP, Arterial pressure; Arc. art., arcuate artery; P_{GC}, glomerular capillary pressure. (Modified from Maddox DA, Brenner BM. Glomerular ultrafiltration. In *Brenner and Rector's The Kidney*, 7th Edition. Philadelphia: W.B. Saunders Company; 2004, pp 353–412; Casellas D, Navar LG. In vitro perfusion of juxtamedullary nephrons in rats. *Am J Physiol*. 1984;246:F349–F358; Imig JD, Roman RJ. Nitric oxide modulates vascular tone in preglomerular arterioles. *Hypertension*. 1992;19(6 Pt 2):770–774.)

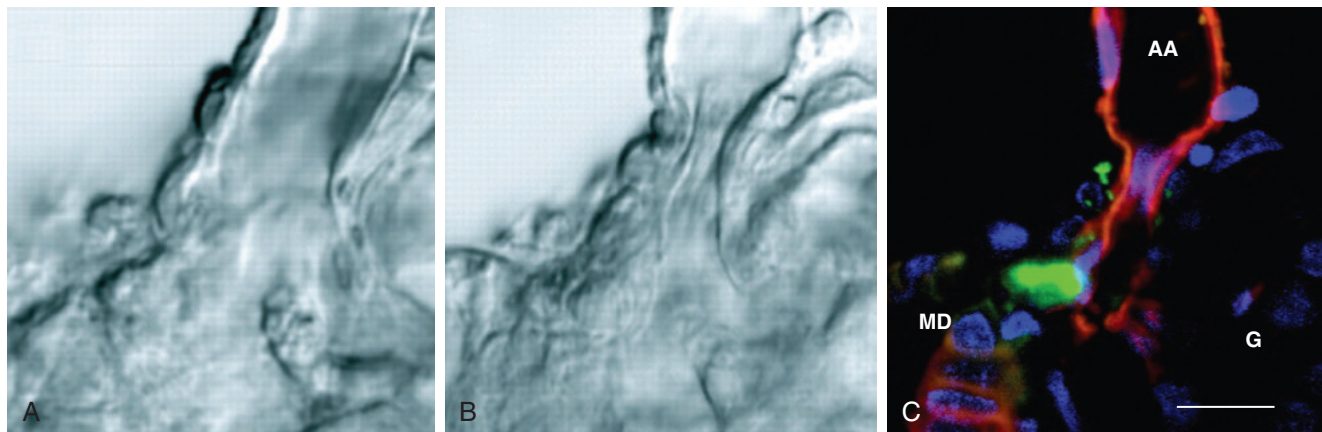


Fig. 3.7 Constriction of the terminal afferent arteriole (AA) via an intraglomerular precapillary sphincter in response to elevations in distal tubular NaCl content. (A, B) Transmitted light differential interference contrast (DIC) images. (A) Control, with NaCl concentration at the macula densa at 10 mM. (B) NaCl concentration is increased to 60 mM, resulting in an almost complete closure of the AA. (C) Fluorescence image of the same preparation as shown in B. Vascular endothelium and tubular epithelium are labeled with R18 (red), renin granules with quinacrine (green), and cell nuclei with Hoechst 33342 (blue). Note that renin-positive granular cells constitute the sphincter, demonstrating contractile responses in glomerular cells. G;Glomerulus; MD, macula densa. Scale bar = 10 μ m. (From Peti-Peterdi J. Multiphoton imaging of renal tissues in vitro. *Am J Physiol Renal Physiol.* 2005;288:F1079–F1083.)

from the outflowing venules and veins (R_v). Accordingly, the following relationships describe the intrarenal cortical vascular resistances:

$$R_T = R_a + R_e + R_v \quad (1)$$

$$R_a = (AP - P_{GC})/RBF \quad (2)$$

$$R_e = (P_{GC} - P_c)/EABF \quad (3)$$

where EABF = RBF – GFR

$$R_v = (P_c - P_v)/RBF \quad (4)$$

where AP = arterial pressure; P_{GC} = glomerular capillary pressure; P_c = peritubular capillary pressure; P_v = renal vein pressure; and EABF = efferent arteriolar blood flow.

INTRARENAL BLOOD FLOW DISTRIBUTION

The cortex accounts for filtration at the glomeruli and most of the reabsorption from proximal and distal nephron cortical tubules, whereas the medulla reabsorbs less than 20% of the total reabsorbate, in keeping with its primary function to maintain a hypertonic interstitial gradient when needed to excrete a concentrated urine. Blood flow to these regions is differentially regulated in response to the differing functions and demands of these two kidney regions.³⁴ Approximately 80% of the RBF perfuses the cortex and is under the control of numerous intrinsic paracrine vasoactive factors, as well as extrinsic humoral and neural influences. Vasoconstrictors, including angiotensin II (Ang II), endothelin, purinergic agents, and norepinephrine, as well as vasodilators, including bradykinin and nitric oxide, interact to regulate cortical blood flow and medullary blood flow.^{34,35} There can be extensive redistribution of blood flow in the kidney under various conditions that may be important in physiologic and pathophysiological conditions.³⁶

Structural differences in vascular components of the cortex and the medulla may account for differences in RBF—namely, the organization of the afferent and efferent arterioles of the cortical and juxtamedullary glomeruli. The cortical

afferent arterioles have larger internal diameters than the efferent arterioles, whereas juxtapamedullary afferent and efferent arterioles are larger than the outer cortical arterioles, and efferent arterioles of juxtapamedullary nephrons are more muscular compared with the cortical arterioles.^{34,37} In addition, the cortical peritubular capillaries, derived from efferent arterioles of cortical glomeruli, are about half the diameter of the medullary vasa recta derived from efferent arterioles of the juxtapamedullary glomeruli (Fig. 3.8).³⁴ These features may partially explain the differential control of medullary and cortical blood flows.

VASCULAR-TUBULE RELATIONS

Cortical vascular-tubule relations have been described extensively (see Figs. 3.1 and 3.2).^{20,38,39} The efferent peritubular capillary network and the tubules arising from each glomerulus in the outermost region of the cortex are tightly associated, but this relationship becomes dissociated in deeper regions of the cortex. This close association does not mean that each vessel adjacent to a given tubule necessarily arises from the same glomerulus. Although superficial nephron segments and peritubular capillaries arising from the same glomerulus are closely associated, each postglomerular efferent arteriole may serve segments of more than one nephron.⁴⁰ However, the loops of Henle of all nephrons, as they descend into the medullary ray, are supplied by postglomerular blood vessels emerging from midcortical and deep nephrons, with some of the branches from deep nephrons descending into the medullary ray, termed the *vasa recta* (see Figs. 3.1 and 3.2). The dissociation between individual tubules and the corresponding postglomerular capillary network is most apparent in the inner cortex. The convoluted tubule segments of these nephrons lie above the glomeruli surrounded by the dense network close to the interlobular vessels or by capillary networks arising from other inner cortical glomeruli. With regard to efferent vessel patterns and vascular-tubule relationships,^{39,41} there is a close association between the initial portions of peritubular capillaries and early and late proximal tubule segments of the same glomerulus.⁴²⁻⁴⁴

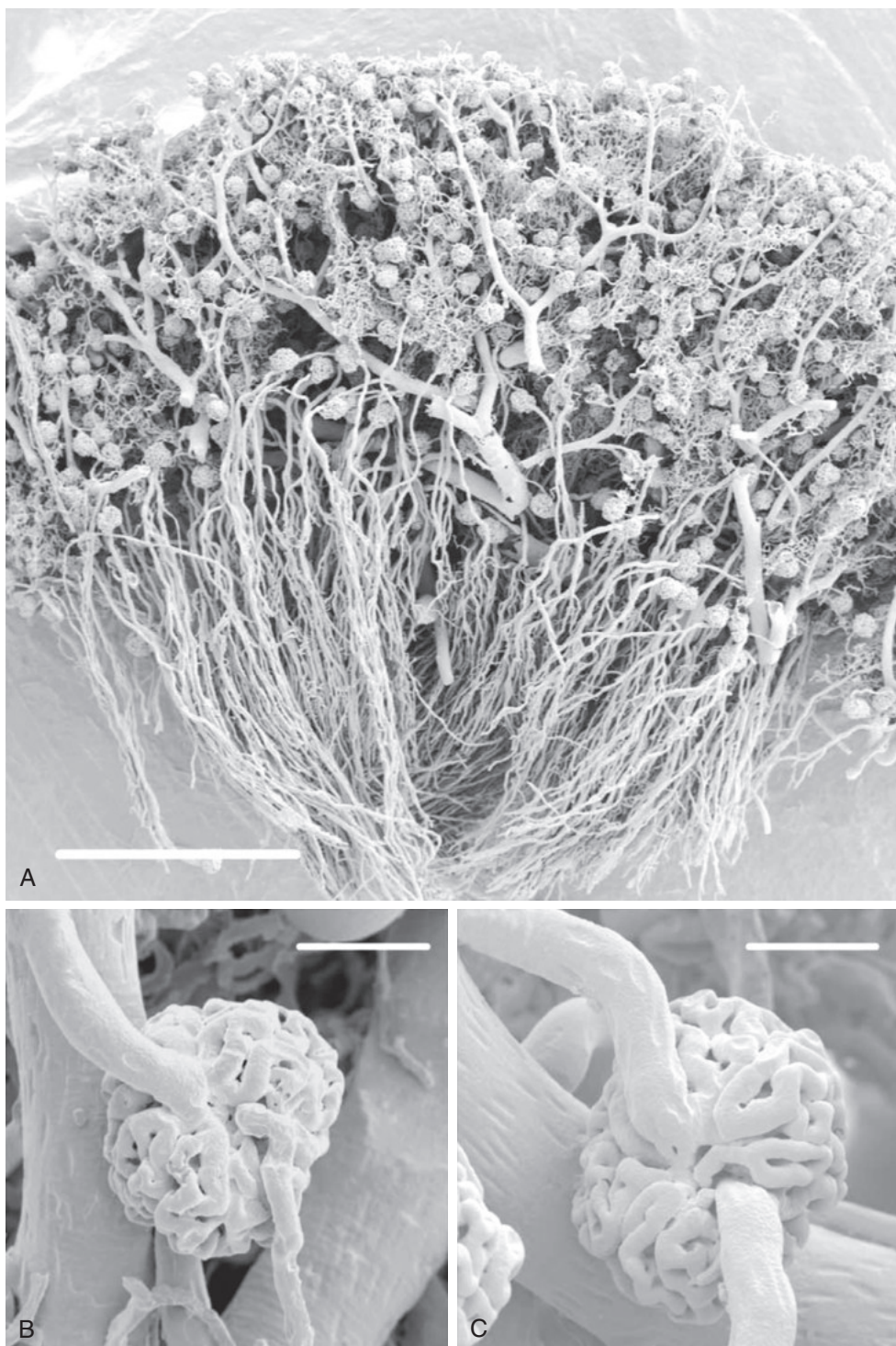


Fig. 3.8 A, Resin casts of renal glomeruli of a rabbit, depicting both cortical and medullary glomeruli. For Panel A, the scale bar represents 1 mm. B, Cortical glomerulus showing afferent (upper vessel) and efferent arterioles and the capillary tuft (scale bar = 60 μ m). C, A juxtapamedullary glomerulus showing afferent (upper vessel) and efferent arterioles and the capillary tuft (scale bar 60 = μ m). Note that the juxtapamedullary arterioles are larger in diameter than the cortical glomerular arterioles, particularly the efferent arterioles. (From Evans RG, Eppel GA, Anderson WP, Denton KM: Mechanisms underlying the differential control of blood flow in the renal medulla and cortex. *J Hypertens*. 2004;22:1439–1451.)

STRUCTURAL AND FUNCTIONAL ASPECTS OF THE GLOMERULAR MICROCIRCULATION

Some of the structural relationships of the glomerular microcirculation are seen in Fig. 3.8, which shows a scanning

electron micrograph of a resin-filled cast of a kidney. The afferent arteriole branching from the interlobular artery, the many loops of the glomerular capillaries, and the efferent arteriole as it emerges from the glomerular tuft can be seen in B and C. An ultrastructural analysis of the vascular pole of

the renal glomerulus has revealed differences in the structure and branching patterns of the afferent and efferent arterioles as these vessels enter and exit the tuft.⁴⁵ Afferent arterioles lose their internal elastic layer and smooth muscle cell layer prior to entering the glomerular tuft. Smooth muscle cells are replaced by renin-positive, myosin-negative granular cells that are in close contact with the extraglomerular mesangium (Fig. 3.9).^{32,46} On entering Bowman's space, afferent arterioles

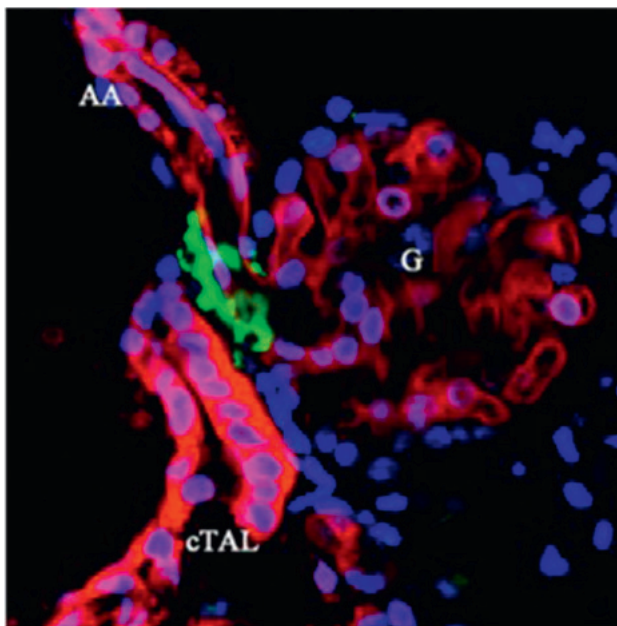


Fig. 3.9 Multicolor labeling of the in vitro microperfused juxtaglomerular apparatus with attached glomerulus. Cell membranes of tubular epithelium (cortical thick ascending limb, [cTAL] containing the macula densa), vascular endothelium of the afferent arteriole (AA), and glomerulus (G) are labeled with R18 (red), renin granules with quinacrine (green), and cell nuclei with Hoechst 33342 (blue). (From Petri-Peterdi J. Multiphoton imaging of renal tissues in vitro. *Am J Physiol Renal Physiol.* 2005;288:F1079–F1083.)

undergo a transition into a vascular chamber that has a manifold-like structure distributing primary branches along the surface of the glomerular tuft, which branch further into the individual glomerular capillaries.^{45,47}

The primary branches have wide lumens and immediately acquire features of glomerular capillaries, including a fenestrated endothelium, characteristic glomerular basement membrane, and epithelial foot processes. In human glomeruli, however, these primary branches serve as conduit vessels that branch into the filtering capillaries (Fig. 3.10).⁴⁷ In contrast, the efferent arteriole originates deep within the tuft, from the convergence of capillaries into multiple lobules that exit into an efferent vascular chamber, which narrows into an efferent arteriole. Additional tributaries join the efferent arteriole as it travels toward the vascular pole. The structure of the capillary wall begins to change, even before the vessels coalesce to form the efferent arteriole, losing fenestrae progressively until a smooth epithelial lining is formed. At the arteriole's terminal portion within the tuft, endothelial cells may bulge into the lumen, reducing its internal diameter.⁴⁵ Efferent arterioles acquire a smooth muscle cell layer, which is observed distal to the entry point of the final glomerular capillary. The efferent arteriole is also in close contact with the glomerular mesangium as it forms inside the tuft and with the extraglomerular mesangium as it exits the tuft. This precise and close anatomic relationship between the afferent and efferent arterioles and mesangium with the macula densa cells of the ascending loop of Henle provides the structural basis for the presence of an intraglomerular signaling system, known as the “tubuloglomerular feedback mechanism,” which participates in the regulation of blood flow and GFR.^{32,45,48}

The appearance of the vascular pathways within the glomerulus may change under different physiologic conditions. The glomerular mesangium (Fig. 3.11) has been shown to contain contractile elements^{45,49} and to exhibit contractile activity when exposed to Ang II.⁵⁰ Mesangial cells, which possess AT1 receptors for Ang II, undergo contraction when exposed to this peptide in vitro.⁵¹ Three-dimensional

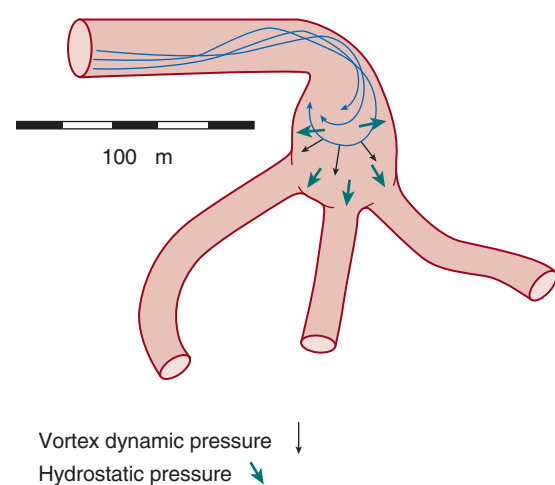
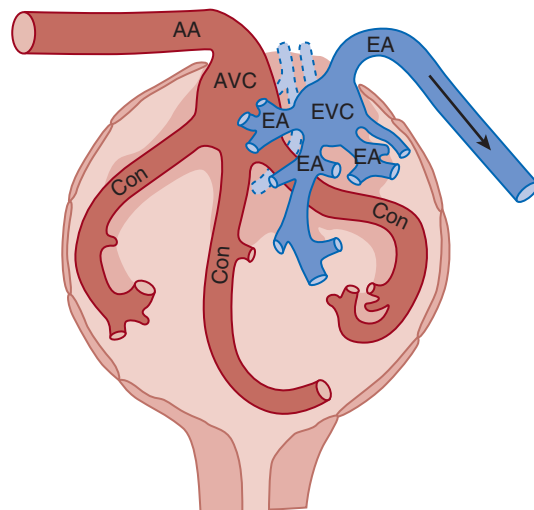


Fig. 3.10 Structure of the human glomerulus. Note the sharp turn made by the afferent arteriole (AA) as it enters the afferent vascular chamber (AVC), which flows into the conduit afferent capillaries (Con). Efferent first-order vessels (E1) and the efferent vascular chamber (EVC) transition into the efferent arteriole (EA). Right, Distribution of hydraulic forces in the AVC. (From Neal CR, Arkell K, Bell JS, et al. Novel hemodynamic structures in the human glomerulus. *Am J Physiol Renal Physiol.* 2018;315(5):F1370–F1384; color figures courtesy Dr. Christopher Neal.)

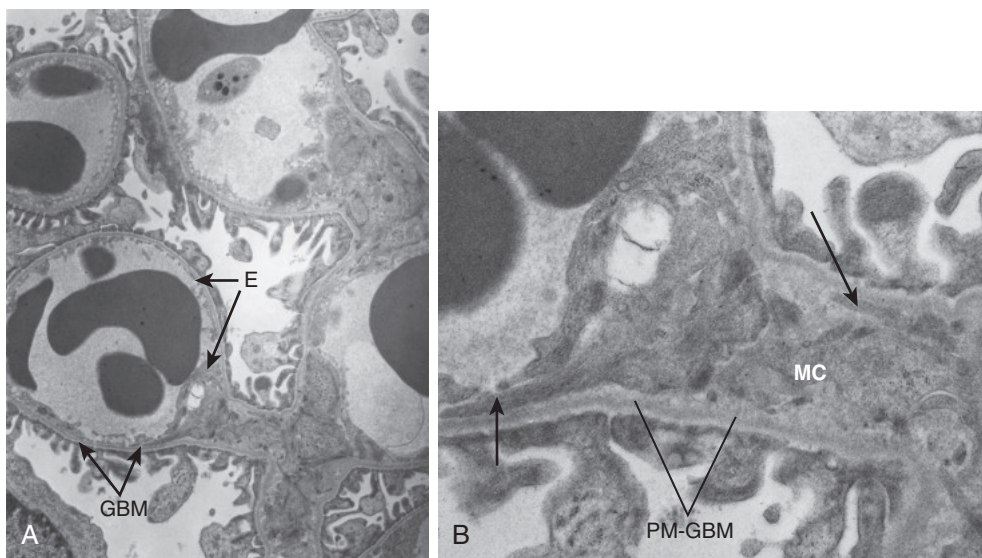


Fig. 3.11 Electron micrographs of glomerular capillaries of a Munich-Wistar rat. (A) Overview of several capillaries ($\approx \times 14,500$). Most of the glomerular capillary endothelium (E) is in contact with the glomerular basement membrane (GBM), with only a small portion in contact with the mesangium (M). At its outer aspect, the GBM is covered by podocyte foot processes. There is no basement membrane separating the endothelium from the mesangium at their interface. (B) Mesangial cell (MC) extends outward to meet the glomerular capillary ($\approx \times 42,000$). Kriz and co-workers have suggested that such cylinder-like stalks appear to be contractile filament bundles (short arrow) that attach to the perimesangial glomerular basement membranes (PM-GBM) and extend to the GBM at the mesangial angles (long arrow). For this preparation the nephron was perfusion-fixed by micropuncture with 1.25% glutaraldehyde through Bowman's space, thereby yielding the fixation of glomerular structures, as well as the red cells in the capillaries. (Modified from Kriz W, Elger M, Mundel P, Lemley KV. Structure-stabilizing forces in the glomerular tuft. *J Am Soc Nephrol*. 1995;5(10):1731–1739; Kriz W, Kaissling B. *Structural organization of the mammalian kidney*. Third Edition ed: Lippincott, Williams & Wilkins; 2000; Drenckhahn D, Schnittler H, Nobiling R, Kriz W. Ultrastructural organization of contractile proteins in rat glomerular mesangial cells. *Am J Pathol*. 1990;137(6):1343–1351.)

reconstruction of the entire mesangium in the rat has suggested that approximately 15% of capillary loops may be entirely enclosed within armlike extensions of mesangial cells that are anchored to the extracellular matrix.⁵² Contraction of these cells might alter local blood flow and filtration rate, as well as the intraglomerular distribution of blood flow and total filtration surface area. Many hormones and other vasoactive substances capable of altering glomerular filtration may bring about this adjustment, in part by altering the state of contraction of mesangial cells.

DETERMINANTS OF GLOMERULAR FILTRATION

A critical function of the mechanisms regulating renal hemodynamics is to maintain the blood flow and pressure profile within the glomerular tufts at levels such that the filtration rate allows optimum function of reabsorptive and secretory processes by the tubular network. The exquisite differential regulation of the preglomerular (afferent) and postglomerular (efferent) resistances exert fine control of the intraglomerular hemodynamic environment and thus the GFR. This nesting of the glomerular capillary system between the afferent and efferent arterioles allows for precise regulation of the intraglomerular forces governing filtration. These forces, coupled with the unique restrictive molecular permeability of the glomerular capillary structure, lead to the formation of a nearly protein-free filtrate, from the glomerular capillaries into Bowman's space, as the first step in the process of urine formation.

PERMEABILITY OF THE GLOMERULAR FILTRATION BARRIER

In addition to the unique role of the glomerular capillary wall and surrounding glomerular epithelial cells in regulating fluid movement from the glomerular capillary into Bowman's space, these structures also regulate the movement of macromolecules. Molecules the size of inulin or smaller are normally able to cross the glomerular capillary wall without restriction. However, the transglomerular permeation of molecules of increasing size becomes limited, so that molecules the size of albumin or larger are almost completely prevented from crossing into Bowman's space.

As shown in Fig. 3.12, the composite filtration barrier includes the glycocalyx lining the endothelial cells, the fenestrations of the endothelial layer of the glomerular capillaries, the three layers of the glomerular basement membrane, the filtration slits between adjacent foot processes of the visceral epithelial cells (podocytes) that surround the capillaries, and the filtration slit diaphragm that extends along the filtration slits and connects adjacent foot processes to form the ultimate barrier to filtration⁵³ (see Fig. 3.12). This complex barrier has a high permeability to small molecules such as water, electrolytes, amino acids, glucose, and other endogenous or exogenous compounds with molecular radii smaller than 20 Å. This allows these compounds to be freely filtered from the blood into Bowman's space while virtually excluding molecules larger than around 50 Å.^{54–61} In studies using fractional clearances of neutral

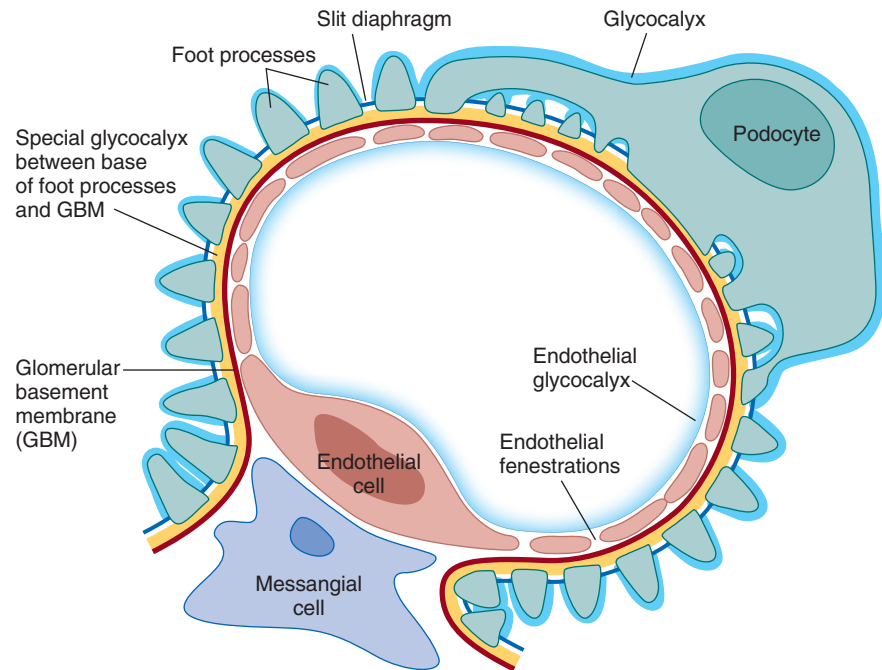


Fig. 3.12 Schematic drawing of a glomerular capillary. The elements considered as part of the glomerular filtration barrier include the following: endothelial glycocalyx, fenestrated endothelium, basement membrane, specialized glycocalyx between the foot processes and basement membrane, and podocyte and slit diaphragm. (From Schlöndorff D, Wyatt CM, Campbell KN. Revisiting the determinants of glomerular filtration barrier: what goes round must come round, *Kidney Int.* 2017;92:533–536.)

dextran, comparable size selectivity⁶² was observed in rats,⁶³ dogs,⁶⁴ and humans.⁶⁵ As recently emphasized,⁵³ there has been considerable controversy regarding the component primarily responsible for the exclusion of macromolecules from the filtrate. The size selectivity of the glomerular filtration barrier is determined largely by a combination of the slit diaphragms between podocyte foot processes and the glomerular basement membrane (GBM). Although there is some controversy regarding glomerular charge selectivity, there is good evidence for a role of charge in restricting the transmural movement of negatively charged macromolecules such as albumin at the level of the GBM, which contains negatively charged heparan sulfate proteoglycans, as well as laminin, type IV collagen, and nidogen.^{66,67}

Other studies have now demonstrated the presence of a fine meshwork of glycosaminoglycans covering the luminal endothelial layer and bridging the endothelial fenestrations so that the endothelial layer is now considered the initial coarse barrier for macromolecular exclusion.⁶⁸ Further studies using negatively charged gold nanoparticles have confirmed that the lamina densa of the basement membrane serves as an exclusion barrier for molecules the size of immunoglobulin G (IgG) and albumin. Small particles permeated into the lamina densa and accumulated upstream, covering the base of the foot processes.⁶⁹

HYDRAULIC AND ONCOTIC FORCES IN THE GLOMERULAR CAPILLARIES AND BOWMAN'S SPACE

The process of filtration of fluid at any given point of the glomerular capillary is governed by the net balance among the transcapillary hydraulic pressure gradient (ΔP), the transcapillary colloid osmotic pressure gradient ($\Delta\pi$), and

the hydraulic conductivity of the filtration barrier per surface area unit (L_p), coupled with the surface area (S_f). The product of L_p and S_f is called the “filtration coefficient” (K_f). Fluid flow (J_v) at any given point in the capillary is determined by the Starling equation:

$$J_v = L_p [(P_{GC} - P_{BS}) - (\pi_{GC} - \pi_{BS})] \quad (5)$$

where P_{GC} and P_{BS} are the hydraulic pressures in the glomerular capillaries and Bowman's space, respectively, and π_{GC} and π_{BS} are the corresponding colloid osmotic pressures at any given point. Because the protein concentration of the fluid in Bowman's space is very low, π_{BS} approaches zero and can be disregarded. The total GFR of fluid for a single nephron (SNGFR) is equal to the product of the surface area for filtration (S_f) and the hydraulic conductivity (L_p), defined as the filtration coefficient (K_f) and the values of the right-hand terms in Eq. 5 averaged along the length of the glomerular capillaries yielding the expression:

$$SNGFR = L_p S_f [(P_{GC} - P_{BS}) - (\pi_{GC})] \text{ or } SNGFR = K_f (\Delta P - \pi_{GC}) \quad (6)$$

Thus,

$$SNGFR = K_f \times P_{UF} \quad (7)$$

where P_{UF} = the mean filtration pressure, the difference between the mean transcapillary hydraulic and colloid osmotic pressure gradients, ΔP and π_{GC} , respectively.

It is important to emphasize the difference between L_p , the hydraulic conductivity, and the macromolecular permeability. These are regulated differently and are not closely coupled. Based on known ultrastructural detail and the hydrodynamic properties of the individual components of

the filtration barrier, mathematical modeling suggests that only around 2% of the total hydraulic resistance is accounted for by the fenestrated capillary endothelium, whereas the basement membrane accounts for nearly 50%.^{66,69,70} The remaining hydraulic resistance resides in the diaphragm of the filtration slits, which are complex structures containing numerous proteins, including nephrin and podocin.^{66,70–72} Disruption of these slit diaphragm proteins leads to substantial proteinuria.⁷² A reduction in the frequency of intact filtration slits is an important factor in the deterioration of filtration in some disease states.^{66,73} In the case of macromolecule permeability, mathematical modeling efforts contend that the sieving efficiency of the layers of the glomerular filtration barrier are interdependent. Moreover, whereas hydraulic resistances are additive, macromolecule sieving coefficients are multiplicative; thus, a small change in the macromolecule permeability of one layer can significantly change the overall permeability of the filtration barrier.^{62,66}

Because surface glomeruli are not present in most experimental animals, indirect approaches to measure glomerular pressure have been used in many experimental studies to evaluate the responses of glomerular pressure. The stop-flow technique has been used by many investigators to estimate P_{GC} .^{2,35,74,75} When fluid movement in the early proximal tubule

is blocked, intratubular pressure upstream from the block increases until net filtration at the glomerulus ceases.⁷⁶ At that point, the sum of this hydrostatic pressure in the early proximal tubule plus the systemic colloid oncotic pressure is equal to the pressure in the glomerular capillaries (P_{GCSF}). The stop-flow technique has been used in different strains of rats, as well as in dogs and mice, with the P_{GCSF} averaging 55 to 60 mm Hg in the dog and about 50 mm Hg in the rat.^{4,55} Glomerular capillary pressures calculated using this stop-flow have been compared with values obtained by direct micropuncture of glomerular capillaries in a number of studies; these indicate that P_{GCSF} , measured at normal APs, provides a close estimate of P_{GC} measured directly.^{35,55,74,75}

Direct measurements of glomerular capillary hydraulic pressure in vertebrates (P_{GC}) became possible when it was discovered that a mutant strain of the Munich-Wistar rat had surface glomeruli that allowed direct puncture of glomerular capillaries.⁷⁷ Subsequent studies have confirmed the original observations, demonstrating that values for P_{GC} in surface glomeruli average 43 to 49 mm Hg in this strain of rats (Fig. 3.13), and similar values were found in the squirrel monkey, which also has some superficial glomeruli.⁷⁸ Because the glomerular capillaries are nested between the afferent and efferent arterioles, P_{GC} is nearly constant along the length

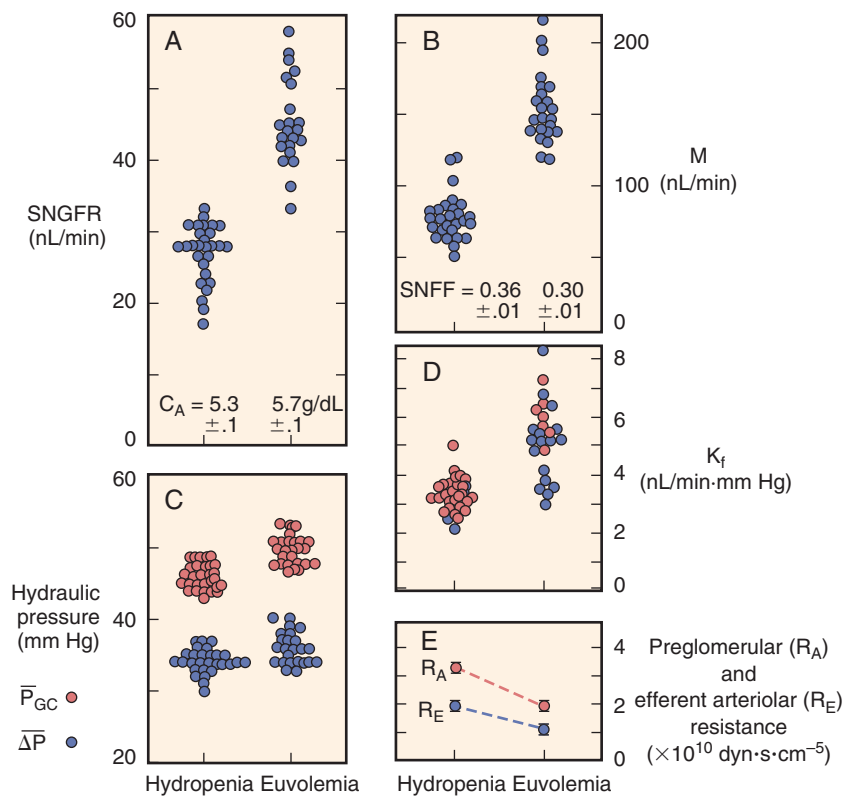


Fig. 3.13 Glomerular filtration in the Munich-Wistar rat. (A–E) Each point represents the mean value reported for studies in hydropenic and euvolemic rats provided food and water ad lib until the time of study. Data from euvolemic rats are thought to be representative of nonanesthesia conditions. Only data from studies using male or a mix of male and female rats are shown. Values of the ultrafiltration coefficient, K_f (red circles in D), denote minimum values because the animals were in filtration pressure equilibrium. Blue circles represent unique values of K_f calculated under conditions of filtration pressure disequilibrium ($\pi_e/\Delta P \leq 0.95$). C_A , Concentration in the afferent arteriole; ΔP , pressure gradient; P_{GC} , pressure in the glomerular capillaries; Q_A , glomerular plasma flow rate; SNFF, single-nephron filtration fraction; SNGFR, single-nephron glomerular filtration. (From Maddox DA, Brenner BM. Glomerular ultrafiltration. In: Brenner BM, ed. *The kidney*. 7th ed. Philadelphia: Saunders; 2004:353–412; Maddox DA, Deen WM, Brenner BM. *Handbook of physiology: Section 8; Renal physiology* Vol 1. New York: Oxford University Press; 1992, pp. 545–638.)

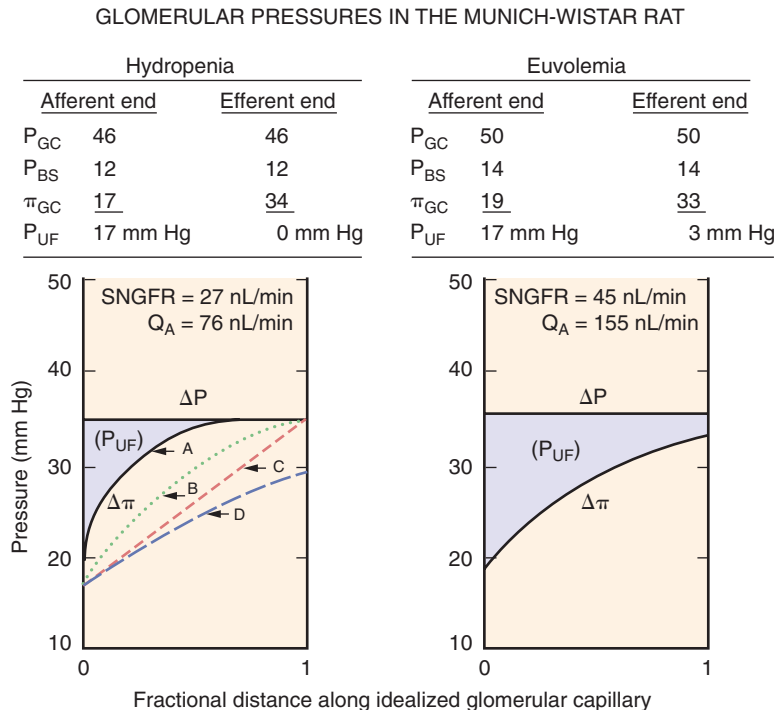


Fig. 3.14 Hydraulic and colloid osmotic pressure profiles along idealized glomerular capillaries in hydropenic and euvoemic rats. Values shown are mean values derived from the studies shown in Fig. 3.13. The transcapillary hydraulic pressure gradient, ΔP , is equal to $P_{GC} - P_T$, and the transcapillary colloid osmotic pressure gradient, $\Delta\pi$, is equal to $\pi_{GC} - \pi_{BS}$, where P_{GC} and P_{BS} are the hydraulic pressures in the glomerular capillary and Bowman's space, respectively, and π_{GC} and π_{BS} are the corresponding colloid osmotic pressures. Because the value of π_{BS} is negligible, $\Delta\pi$ essentially equals π_{GC} . P_{UF} . Left, Lines A and B represent two of the many possible profiles under conditions of filtration pressure equilibrium; line D represents disequilibrium and line C represents the hypothetical linear $\Delta\pi$ profile. Right, Pressure profile after correction for surgical induced loss of plasma volume depicts a small positive ΔP at the efferent level indicative of disequilibrium conditions. Q_A , Glomerular plasma flow; SNGFR, single-nephron glomerular filtration rate.

of the capillary bed, resulting in a transcapillary hydraulic pressure gradient that averages 34 mm Hg in hydropenic Munich-Wistar rats (see Fig. 3.13). Coupling these hydraulic pressure measurements with determinations of systemic plasma protein concentration and efferent arteriolar protein concentrations of superficial nephrons has permitted an opportunity to determine the hydraulic and oncotic pressures that govern glomerular filtration at the beginning and end of the capillary network.

The early direct measurements of P_{GC} made in hydropenic rats were under conditions of surgically induced reductions in plasma volume and GFR. Subsequent studies, in which plasma volume was restored to a euvoemic state, equal to that of the awake animal,⁷⁰ by infusion of iso-oncotic plasma, yielded SNGFR values substantially higher than in hydropenic rats. This is primarily as a consequence of increases in glomerular plasma flow (Q_A) associated with a fall in preglomerular (R_A) and efferent arteriolar (R_E) resistance values (see Fig. 3.13), indicating that the early studies in hydropenic rats were performed under conditions of elevated activity of the sympathetic nervous system. Collectively, the experimental studies in Munich-Wistar rats (see Fig. 3.13) and several other strains of rats studied under euvoemic conditions have indicated that glomerular pressure in rats is in the range of 50 mm Hg, leading to higher transglomerular capillary pressures.

Glomerular capillary hydraulic and oncotic pressure profiles for rats under hydropenic and euvoemic conditions are shown in Fig. 3.14, using the mean values determined from the studies shown in Fig. 3.13. In hydropenic animals, by the time the blood reaches the efferent end of the glomerular capillaries, plasma oncotic pressure (π_E) rises to a value that, on average, equals ΔP . As a consequence, the net local filtration pressure, P_{UF} ($P_{GC} - [P_T + \pi_{GC}]$), is reduced from approximately 17 mm Hg at the afferent end of the glomerular capillary network to essentially zero by the efferent end (referred to as “filtration pressure equilibrium”). The value of ΔP is nearly constant along the glomerular capillaries, and the decline in P_{UF} along the capillary network is due to a rise in π_{GC} (see Fig. 3.14). An exact profile of the $\Delta\pi$ curve cannot be ascertained under conditions of filtration pressure equilibrium, and hence only maximum estimates of P_{UF} and minimum estimates of K_f can be obtained by assuming a linear rise in the $\Delta\pi$ curve. To obtain accurate measurements of the $\Delta\pi$ curve, Deen and colleagues plasma-expanded rats to increase plasma flow to obtain filtration pressure disequilibrium (Fig. 3.14, curve D), permitting an exact determination of P_{UF} and hence K_f .⁸⁰ Filtration pressure disequilibrium is present in about 60% of the studies in the euvoemic Munich-Wistar rat (see Fig. 3.13) and in most of the studies in Sprague-Dawley rats and in dogs,^{4,74,75,81} permitting exact determinations of P_{UF} along the entire length of the glomerular

capillaries and hence an accurate K_f reflecting the total surface area.

DETERMINATION OF THE FILTRATION COEFFICIENT

As shown in Eq. 7, SNGFR equals the filtration coefficient (K_f) times the net driving force for filtration averaged over the length of the glomerular capillaries (P_{UF}). The values of K_f from many studies in euvolemic Munich-Wistar rats studied under conditions of filtration pressure disequilibrium (see Fig. 3.13) averaged $5.0 \pm 0.3 \text{ nL}/(\text{min} \cdot \text{mm Hg})$. These are values similar to those found in other rat strains and in dogs ($3\text{--}5 \text{ nL}/[\text{min} \cdot \text{mm Hg}]$).^{4,55,74,75} Because this value remains essentially unchanged over a twofold range of changes in Q_A , the data suggest that changes in Q_A per se do not affect K_f .⁸⁰

In the rat, total capillary basement membrane surface area per glomerulus (A_s) has been determined to be around 0.003 cm^2 in superficial nephrons and 0.004 cm^2 in deep nephrons.⁸² A large portion of the capillary surface area faces the mesangium and, as a consequence, only the peripheral area of the capillaries surrounded by podocytes participates in filtration. This peripheral area available for filtration (A_p) is only about half that of A_s ($\sim 0.0016\text{--}0.0018; 0.0019\text{--}0.0022 \text{ cm}^2$ in the superficial and deep glomeruli, respectively).⁸² Using a value of K_f of around $5 \text{ nL}/\text{min mm Hg}$, as determined by micropuncture techniques, with these estimates of A_p , yields a hydraulic conductivity (L_p) of 45 to $48 \text{ nL}/(\text{sec} \cdot \text{mm Hg} \cdot \text{cm}^2)$. These estimates of k for the rat glomerulus are all one or two orders in magnitude higher than those reported for capillary networks in mesentery, skeletal muscle, omentum or peritubular capillaries of the kidney,^{55,83} thus supporting the premise of very high glomerular hydraulic permeability of the glomerular capillaries.

DETERMINANTS OF GLOMERULAR FILTRATION COEFFICIENT IN HUMAN SUBJECTS

Hydraulic pressure in the glomerular capillaries of human kidneys cannot be measured using micropuncture of glomerular capillaries or measurements of stop-flow pressures in proximal tubules or free-flow pressures in Bowman's space. From determinations of plasma protein concentrations, and thus the afferent arteriolar oncotic pressure together with the whole-kidney filtration fraction, efferent arteriolar oncotic pressure can be calculated, generally yielding values around 37 mm Hg . In addition, peritubular capillary pressure has been estimated from intrarenal venous pressure measurements, yielding estimates of proximal tubule hydraulic pressure of 20 to 25 mm Hg .^{84,85} Coupled with an efferent oncotic pressure of 37 mm Hg , this indicates that the minimal value for glomerular capillary pressure in humans is in the range of 57 to 62 mm Hg . Glomerular volumes and diameters of human kidneys are larger than in the experimental species, suggesting that the single-nephron K_f is greater than in the experimental animals. It is thought that in humans, filtration pressure disequilibrium is normally present, and GFR exhibits less plasma flow dependency than in rats.² The molecular sieving approach has been used as an alternative noninvasive means for the evaluation of the hydraulic conductivity characteristics and filtration coefficient in studies of glomerular dynamics in humans. By using uncharged macromolecules with varying molecular radii, which are partially restricted, the sieving coefficients for molecules of different sizes can

be obtained.^{63,86,87} Combining the sieving data with mathematical models, estimated data for K_f values can be derived. Values for single-nephron K_f in normal human subjects have varied from 3.6 to $9.4 \text{ nL}/\text{min mm Hg}$, with an average value of about 6 to $7 \text{ nL}/\text{min mm Hg}$.^{2,4,75,88,89}

SELECTIVE ALTERATIONS IN THE PRIMARY DETERMINANTS OF GLOMERULAR FILTRATION

The four primary determinants of filtration are Q_A , ΔP , K_f , and π_{A_e} , and alterations in each of these will affect the GFR. The degree to which such alterations will modify SNGFR has been examined by mathematical modeling⁸⁰ and compared with values obtained experimentally (see Arendshorst and Navar,² Navar et al.,⁴ and Lowenstein et al.⁸⁴).

Glomerular Plasma Flow (Q_A)

Because protein is normally excluded from the glomerular filtrate, the total amount of protein entering the glomerular capillary network from the afferent arteriole is maintained, leading to progressively increasing protein concentration as the plasma traverses the glomerular capillaries to the efferent arteriole. Thus, there is a substantial increase in the plasma colloid osmotic pressure (π_g) in the glomerular capillaries as the plasma traverses from the inlet to the outlet. This increase in π_g counteracts the net hydraulic filtration pressure and may completely offset the ΔP , so that $\pi_g = \Delta P$ if equilibrium is reached before the plasma reaches the efferent arteriole, preventing further net filtration of fluid into Bowman's space. Under this condition of filtration pressure equilibrium, where $\Delta P = \pi_{E_e}$, SNGFR will vary directly with changes in Q_A as a greater filtering surface area is recruited. Once Q_A increases enough to produce disequilibrium, π_E becomes less than ΔP , and the SNGFR will no longer vary linearly with Q_A .⁹⁰ However, there is still an effect of increases in plasma flow to increase GFR, although to a lesser extent, because the filtration fraction will decrease and there will be a lesser overall increase in π_g . As shown in Fig. 3.15, increases in plasma flow are associated with increases in GFR in a number of studies in rats, dogs, nonhuman primates, and humans.

Transcapillary Hydraulic Pressure Difference (ΔP)

Mathematical modeling indicates that isolated changes in the glomerular transcapillary hydraulic pressure gradient exert strong effects on SNGFR.^{2,4,80} In particular, when ΔP exceeds the colloid osmotic pressure at the efferent end of the glomerular capillary, filtration occurs throughout the glomerular capillary network, and SNGFR increases as ΔP increases. The relationship between SNGFR and ΔP is nonlinear, however, because the rise in SNGFR at any given fixed value of Q_A results in a concurrent increase in $\Delta\pi$. Because net effective filtration pressure is a small fraction of P_{GC} , small isolated changes in P_{GC} can cause large percentile changes in net filtration pressure.

Glomerular Capillary Filtration Coefficient (K_f)

Glomerular damage from a variety of kidney diseases and various hormonal and pharmacologic influences can result in alterations in the glomerular filtration coefficient (K_f) due to reductions in surface area available for filtration and/or to reductions in the hydraulic conductivity because of thickening of the basement membrane or other derangements.

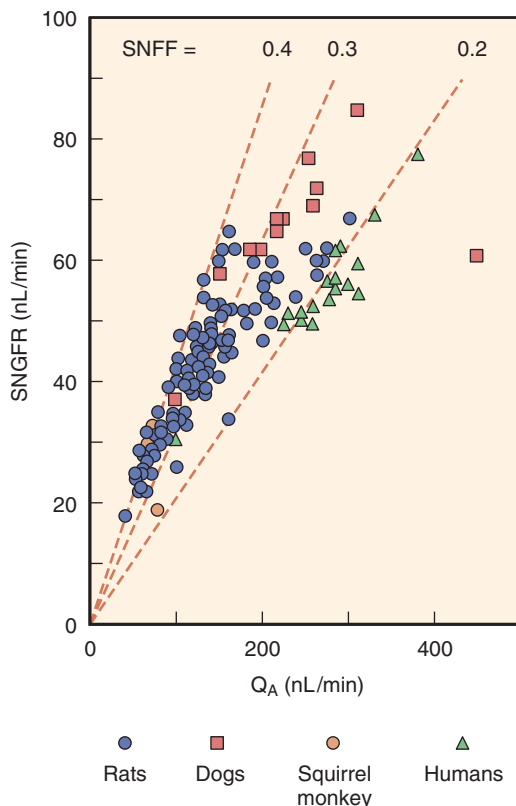


Fig. 3.15 Association between single-nephron glomerular filtration rate (SNGFR) and glomerular plasma flow (Q_A); data are from rats, dogs, squirrel monkeys, and humans. The values for SNGFR and Q_A for humans were calculated by dividing the whole-kidney GFR and renal plasma flow by the estimated total number of nephrons/kidney (1 million). Each point represents the mean value for a given study. SNFF, Single-nephron filtration fraction. (Data from Maddox DA, Brenner BM. Glomerular ultrafiltration. In: Brenner BM, ed. *The kidney*. 7th ed. Philadelphia: Saunders; 2004:353–412; Maddox DA, Deen WM, Brenner BM. *Handbook of physiology: Section 8: Renal physiology Vol 1*. New York: Oxford University Press; 1992.)

Hydraulic conductivity of the glomerular basement membrane demonstrates an inverse relationship to ΔP , indicating that K_f may be directly influenced by ΔP .⁹¹ K_f is also affected by the plasma protein concentration.^{81,92} Under conditions of filtration pressure equilibrium, reductions in K_f do not affect SNGFR until K_f is reduced enough to produce filtration pressure disequilibrium. However, increases in K_f above normal will increase SNGFR until equilibrium conditions occur.^{80,83} When plasma flow is high, and disequilibrium exists, there is a more direct relationship between K_f and SNGFR.^{80,83}

Colloid Osmotic Pressure (π_A)

SNGFR and the single-nephron filtration fraction (SNFF) are each theoretically predicted to vary reciprocally as a function of π_A .⁸⁰ If Q_A , ΔP , and K_f are held constant, reductions in π_A are predicted to increase P_{UF} , leading to an increase in SNGFR. An increase in π_A should produce a decrease in SNGFR until π_A equals ΔP (normally, ~35 mm Hg), at which point filtration stops. In contrast to theoretic predictions, experimentally induced reductions in π_A do not lead to a rise in SNGFR because there are changes in P_{BS} and K_f so that a reduction in π_A results in a reduction in K_f , thereby

offsetting variations in P_{UF} that occur with changes in π_A .⁸³ Studies in isolated glomeruli have indicated that extremely low concentrations of albumin produce an increase in K_f , whereas extremely high concentrations of albumin result in a decrease in K_f .⁸³ However, *in vivo* studies have shown that increases in plasma π will increase K_f in both rats⁹² and dogs.⁸¹ These divergent results of the effects of protein concentration or π_A on K_f can be partially explained by the results from studies of isolated glomerular basement membranes, which have shown a biphasic relationship between albumin concentration and hydraulic permeability.⁹¹ There were lower values of hydraulic permeability at an albumin concentration of 4 g/dL than at either 0 or 8 g/dL.

POSTGLOMERULAR CIRCULATION

PERITUBULAR CAPILLARY DYNAMICS

The same Starling forces that control fluid movement across all capillary beds govern the rate of fluid movement across the peritubular capillary walls of the renal cortex. Owing to the high resistance of the afferent and efferent arterioles, a large drop in hydraulic pressure occurs prior to the peritubular capillaries so that peritubular capillary pressure is 15 to 20 mm Hg. In addition, because protein-free fluid is filtered out of the glomerular capillaries and into Bowman's space, the plasma proteins become concentrated, yielding an elevated oncotic pressure of blood flowing into the peritubular capillaries. As a consequence, the balance between the transcapillary oncotic and hydraulic pressure gradients favors movement of the tubular reabsorbate into the capillaries. However, variations in these forces have significant effects on net proximal reabsorption.^{35,54,93} The absolute amount of movement resulting from this driving force also depends on the peritubular capillary surface area available for fluid uptake and the hydraulic conductivity of the peritubular capillary wall. Values for the hydraulic conductivity of the peritubular capillaries are not as great as those for the glomerular capillaries, but this difference is offset by the much greater total surface area of the peritubular capillary network.

The peritubular capillary surface contains fenestrations that are bridged by a thin diaphragm and glycocalyx that is negatively charged.^{3,94} Beneath the fenestrae of the endothelial cells lies a thin basement membrane that surrounds the capillary. The peritubular capillaries are closely opposed to cortical tubules (Fig. 3.16), so that the extracellular space between the tubules and capillaries constitutes only about 5% of the cortical volume.⁹⁵ The tubular epithelial cells are surrounded by the tubular basement membrane, which is distinct from and wider than the capillary basement membrane (see Fig. 3.16). Numerous microfibrils connect the tubular and capillary basement membranes, a feature that may help limit expansion of the interstitium and maintain close contact between tubular epithelial cells and the peritubular capillaries during periods of high fluid flux.⁹⁶ Thus, the pathway for fluid reabsorption from the tubular lumen to the peritubular capillary is composed, in series, from the epithelial cell, lateral spaces, tubular basement membrane, a narrow interstitial region containing microfibrils, the capillary basement membrane, and the thin membrane bridging the endothelial fenestrae.⁹⁶

Like the endothelial cells, the basement membrane of the peritubular capillaries possesses anionic sites.^{94,97} The

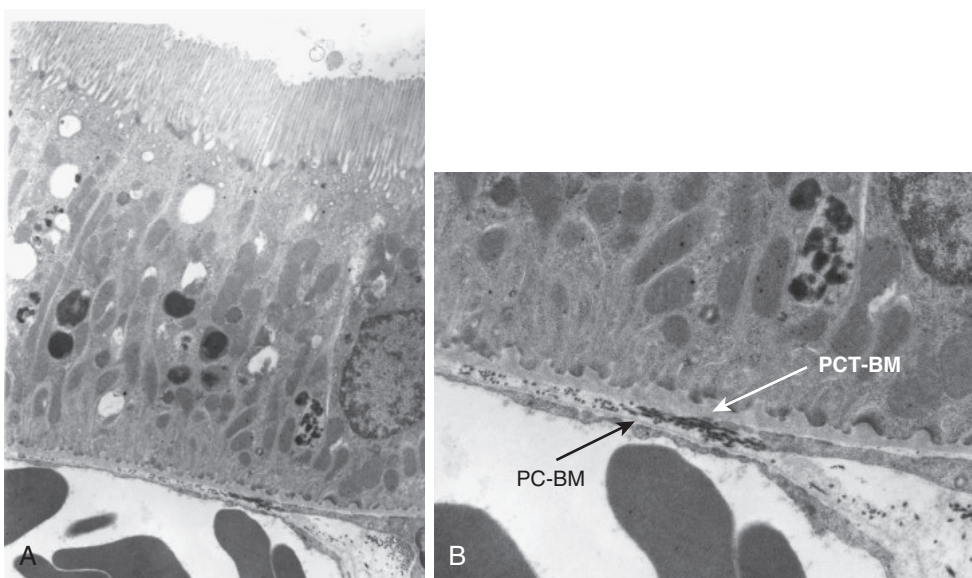


Fig. 3.16 Apposition of peritubular capillaries with basolateral tubular membranes. Shown are electron micrographs of a proximal tubule of a Munich-Wistar rat. The tubule was perfusion-fixed with 1.25% glutaraldehyde, thereby also fixing red cells in adjacent capillaries. (A) The apposition of the basolateral surface of the tubular cells with the adjacent peritubular capillaries is close, leaving little interstitial space where the two come in contact (magnification $\approx 13,000$). (B) The proximal tubule basement membrane (PCT-BM) is relatively thick in comparison with the peritubular capillary basement membrane (PC-BM; magnification $\approx 25,000$). (Courtesy D. Maddox.)

electronegative charge density of the peritubular capillary basement membrane is significantly greater than that observed in the unfenestrated capillaries of skeletal muscle and similar to that observed in the glomerular capillary bed. These anionic sites in the peritubular capillaries compensate for the greater permeability of fenestrated capillaries, allowing free exchange of water and small molecules while restricting anionic plasma proteins to the circulation. The renal peritubular capillaries are reported to be more permeable to both small and large molecules than are other beds,⁹⁸ but this may be an artifact of the experimental conditions used. Indeed, other studies have indicated that the permeability of the peritubular vessels to dextrans and albumin is extremely low.^{97,99}

MEDULLARY MICROCIRCULATION

Similar to cortical peritubular vessels, the functional role of the medullary peritubular vasculature is to supply the metabolic needs of nearby tissues, but this unique vasculature is also responsible for the uptake and removal of water extracted from collecting ducts during the process of urine concentration. Because the urinary concentration process requires the development and maintenance of a hypertonic interstitium, the countercurrent arrangement of vasa recta plays a vital role in maintaining the medullary solute gradient through passive countercurrent exchange.

Medullary blood flow constitutes only about 10% to 15% of total RBF^{3,6,100,101} and is derived entirely from efferent arterioles of the juxamedullary nephrons (see Figs. 3.1 and 3.2).^{22,37,102–105} Depending on the species and the method of evaluation, from 7% to 18% of glomeruli give rise to efferent arterioles that supply the medulla.^{22,106} Efferent arterioles of juxamedullary nephrons are larger in diameter, possess thicker endothelium, and have more prominent smooth muscle layers than efferent arterioles originating from superficial glomeruli.^{34,107}

Despite the fact that medullary flow is less than 20% of the cortical flow, it is still relatively high compared with other tissues per gram of tissue; outer medullary flow exceeds that of liver, and inner medullary flow is comparable to that of resting muscle or brain.¹⁰⁸ The high efficiency of countercurrent mechanisms in this area permits the existence and maintenance of the inner medullary solute concentration gradients in the presence of such large flows. The descending vasa recta have a continuous endothelium, in which water moves across water channels, and urea moves through endothelial carriers.^{109,110} The ascending vasa recta are fenestrated, with a high hydraulic conductivity, and water movement is governed by transcapillary hydraulic and oncotic pressure gradients.¹¹⁰ Medullary blood flow is highest under conditions of water diuresis and declines during antidiuresis.¹⁰⁰ A direct vasoconstrictive effect of vasopressin on the medullary microcirculation contributes to this decrease during antidiuresis.¹¹¹ Vasodilatory factors act to preserve medullary blood flow and prevent ischemia. Acetylcholine,¹¹² vasodilator prostaglandins,¹¹³ kinins,¹¹⁴ adenosine,¹¹⁵ atrial peptides,¹¹⁶ bradykinin,⁹ and nitric oxide¹¹⁷ increase medullary RBF. In contrast to their vasoconstrictor effects in the renal cortex, Ang II^{118–121} and endothelin¹¹⁸ increase medullary blood flow, effects mediated in part by vasodilatory prostaglandins,^{119,120} whereas vasopressin decreases medullary blood flow.^{111,122} Alterations in medullary blood flow may be a key determinant of medullary fluid tonicity and, thereby, of solute transport in the loops of Henle and the control of sodium excretion and blood pressure.¹²³ During hemorrhage, there is primarily cortical ischemia, with maintained blood flow through the medulla.¹²⁴

The precise location of the boundary between the renal cortex and medulla is difficult to discern because the medullary rays of the cortex merge imperceptibly with the medulla. In general, the arcuate arteries or sites at which

the interlobular arteries branch into arcuate arteries mark this boundary. When considering the medullary circulation, most studies have focused on its relation to the countercurrent mechanism, as facilitated by the parallel array of descending and ascending vasa recta. This configuration is characteristic of the inner medulla, but the medulla also contains an outer zone consisting of two morphologically distinct regions, the outer and inner stripes of the outer medulla (see Fig. 3.2). The boundary between the outer medulla and inner medulla is defined by the beginning of the thick ascending limbs of Henle (see Fig. 3.1). In addition to the thick ascending limbs, the outer medulla contains descending straight segments of proximal tubules (pars recta), descending thin limbs, and collecting ducts. The nephron segments of the inner stripe of the outer medulla include thick ascending limbs, thin descending limbs, and collecting ducts. Each of these morphologically distinct medullary regions is supplied and drained by a specific vascular system.

Both the outer and inner stripes contain two distinct circulatory regions—the vascular bundles, formed by the coalescence of the descending and ascending vasa recta, and the interbundle capillary plexus. Vascular bundles of the descending and ascending vasa recta arise from the efferent arterioles of juxamedullary glomeruli and descend through the outer stripe of the outer medulla to supply the inner stripe of the outer medulla and inner medulla (see Fig. 3.2). Within the outer stripe, nutrient flow is provided by the ascending vasa recta rising from the inner stripe. This notion is supported by the large area of contact between the ascending vasa recta and descending proximal straight tubules within this zone.^{103,106,125}

The outer medulla includes the metabolically active thick ascending limbs. Nutrients and O₂ to this energy-demanding tissue in the inner stripe are delivered by a dense capillary plexus arising from a few descending vasa recta at the periphery of the bundles. Of the 10% to 15% of total RBF directed to the medulla, the largest portion perfuses this inner stripe capillary plexus. The descending vasa recta possess a contractile layer composed of smooth muscle cells in the early segments that evolve into pericytes by the more distal portions of the vessels. These pericytes contain smooth muscle α -actin, suggesting that they serve as contractile elements and participate in the regulation of medullary blood flow,¹²⁶ as well as in vascular-tubular crosstalk.¹²⁷ Each of these vessels also displays a continuous endothelium that persists until the hairpin turn is reached, and the vessels divide to form the medullary capillaries. In contrast, ascending vasa recta, like true capillaries, lack a contractile layer and are characterized by a highly fenestrated endothelium.^{128,129} The smooth muscle cells of the descending vasa recta are replaced by pericytes surrounding the endothelium, with subsequent loss of the pericytes and transformation into medullary capillaries accompanied by endothelial fenestrations.^{102,125}

The rich capillary network of the inner stripe drains into numerous veins, which, for the most part, do not join the vascular bundles but ascend directly to the outer stripe. These veins subsequently rise to the cortical-medullary junction and join with cortical veins at the level of the inner cortex.¹³⁰ A few veins may extend within the medullary rays to regions near the kidney surface.^{20,104,130} Thus, the capillary network of the inner stripe makes no contact with the vessels draining the inner medulla.

The inner medulla contains the thin descending and thin ascending limbs of Henle, together with collecting ducts (see Fig. 3.2). Within this region, the straight, unbranching vasa recta descend in bundles, with individual vessels leaving at every level to divide into a simple capillary network characterized by elongated links (see Figs. 3.1 and 3.2).^{102,106,130} These capillaries converge to form the venous vasa recta. Within the inner medulla, the descending and ascending vascular pathways remain in close apposition, although distinct vascular regions can no longer be clearly discerned. The venous vasa recta rise toward the outer medulla in parallel with the supply vessels to join the vascular bundles. Within the outer stripe of the outer medulla, the vascular bundles spread out and traverse the outer stripe as wide tortuous channels that lie in close apposition to the tubules, eventually emptying into arcuate or deep interlobular veins.¹⁰⁶ The venous pathways in the bundles are both larger and more numerous than the arterial vessels, suggesting lower flow velocities in the ascending (venous) than in the descending (arterial) vessels.¹³¹ The close apposition of the arterial and venous pathways in the vascular bundles is important for maintaining the hypertonicity of the inner medulla.

The mechanism of urine concentration requires coordinated function of the vascular and tubular components of the medulla. In species capable of marked concentrating ability, medullary vascular-tubular relationships show a high degree of organization favoring particular exchange processes by the juxtaposition of specific tubular segments and blood vessels.^{130,132} In addition to anatomic proximity, the absolute magnitude of these exchanges is greatly influenced by the permeability characteristics of the structures involved, which may vary significantly among species.¹³³

PARACRINE AND ENDOCRINE FACTORS REGULATING RENAL HEMODYNAMICS AND GLOMERULAR FILTRATION RATE

EXTRINSIC AND INTRINSIC REGULATION OF THE RENAL MICROCIRCULATIONS

A variety of hormonal, neural, and paracrine factors exert regulating influences on RBF and GFR.^{35,55,83} Renal blood vessels from the arcuate arteries and interlobular arteries to the afferent and efferent arterioles are influenced to a greater or lesser extent by these intrinsic and extrinsic influences. As a result, the vascular tones of preglomerular and postglomerular resistance vessels are regulated to control RBF, glomerular hydraulic pressure, and the transcapillary hydraulic pressure gradient. The glomerular mesangium is the site of action and production of many such substances. Vasoactive compounds may elicit acute alterations in K_f by changing the effective surface area for filtration through contraction of mesangial cells, causing shunting of blood to fewer capillary loops.^{35,134,135} In addition, contraction of glomerular epithelial cells (podocytes), which contain filamentous actin molecules, may decrease the size of the filtration slit pores, thereby altering hydraulic conductivity of the filtration pathway and reducing K_f.¹³⁶ Various growth factors influence chronic changes in renal hemodynamics by promoting mesangial cell proliferation and expansion of the extracellular matrix,

leading to obliteration of capillary loops and a reduction in the filtration coefficient.

Our understanding of afferent and efferent arteriolar vascular responses to neural, paracrine hormonal, and vasoactive substances have, to a large extent, come from micro-puncture studies of glomerular hemodynamics. Various other methods have been used to examine the effects of vasoactive substances on the preglomerular and postglomerular vasculature.^{35,55,83,137–144} The results using these different techniques have provided important insights into the vasoactive properties of the preglomerular and postglomerular vasculature that control renal hemodynamics and glomerular filtration rate.

The renal vasculature and glomerular mesangium respond to numerous endogenous hormones and vasoactive peptides, such as Ang II, by vasoconstriction, reductions in RBF and GFR, and reductions in the glomerular capillary filtration coefficient. Among the vasoconstrictors are Ang II, norepinephrine, leukotrienes C4 and D4, platelet-activating factor (PAF), adenosine 5'-triphosphate (ATP), endothelin, vasopressin, serotonin, and epidermal growth factor.^{35,55,83} Similarly, vasodilatory substances, such as NO and prostaglandin E2 (PGE2), and PGI2, histamine, bradykinin, acetylcholine, insulin, insulin-like growth factor, calcitonin gene-related peptide, cyclic adenosine monophosphate, and relaxin can increase RBF and GFR.^{35,55,83} However, in addition to having their own direct effects on RBF and GFR, a number of these complex vasoactive systems, such as the renin-angiotensin-aldosterone system (RAAS) and arachidonic acid metabolites, produce both vasoconstriction and vasodilator effects and can also stimulate production and release of other factors thus, masking their primary effect. Furthermore, vasoconstrictor agents such as Ang II may result in a feedback stimulation of vasodilatory compensatory factors yielding a complex interactive balance regulating renal hemodynamics.

INTRINSIC MECHANISMS: RENAL AUTOREGULATION

Renal autoregulation refers to the intrinsic ability of the kidney to respond to a perturbation that elicits a vasoactive response, which alters renal vascular resistance in the direction that maintains RBF and GFR. Changes in perfusion pressure are the manipulation most commonly used to demonstrate autoregulatory efficiency. Although the efficiency with which blood flow is maintained differs from organ to organ (being most efficient in brain and kidney), all organs and tissues exhibit autoregulation. As shown in Fig. 3.17, the kidney autoregulates renal blood flow over a wide range of renal perfusion pressures. Autoregulation of blood flow in response to changes in perfusion pressure requires parallel changes in resistance.

The finding that both RBF and GFR are autoregulated with a high efficiency indicates that the principal resistance change due to autoregulatory adjustments is localized to the preglomerular vasculature. Studies of single-nephron function of superficial nephrons have demonstrated that SNGFR also exhibits efficient autoregulation, as long as the tubular fluid collections do not block flow to the macula densa. Furthermore, direct measurements of glomerular pressures in the Munich-Wistar rat, which has glomeruli on the renal cortical surface that is accessible to micropuncture, have demonstrated autoregulation of glomerular pressure in response to variations in renal arterial perfusion pressure. Fig. 3.18 summarizes the effects of graded reductions in renal perfusion pressure

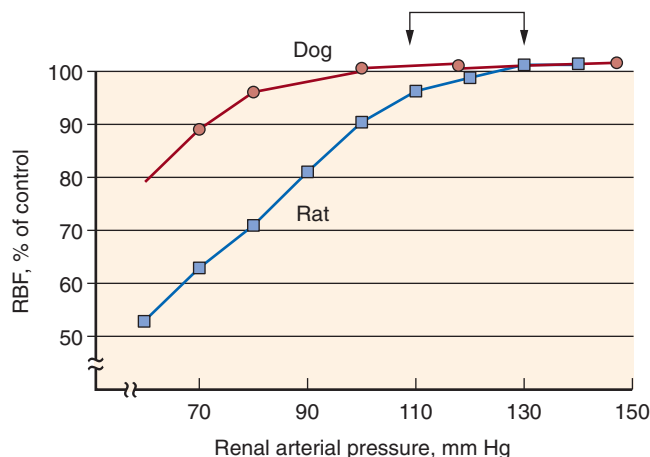


Fig. 3.17 Autoregulatory response of total renal blood flow (RBF) to changes in renal perfusion pressure in the dog and rat. In general, the normal anesthetized dog exhibits greater autoregulatory capability to maintain RBF and glomerular filtration rate to lower arterial pressures than the rat. (From Navar LG, Bell PD, Burke TJ: Role of a macula densa feedback mechanism as a mediator of renal autoregulation. *Kidney Int*. 1982;22:S157–S164.)

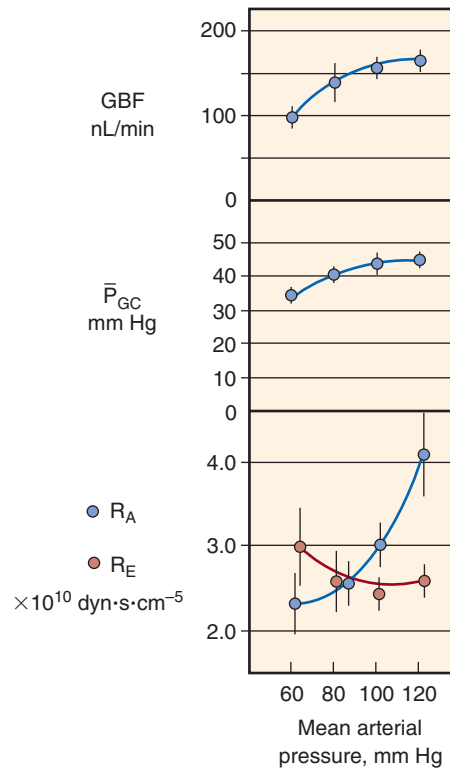


Fig. 3.18 Glomerular dynamics in response to reductions of renal arterial pressure in the normal hydropenic rat. As can be seen, glomerular blood flow (GBF) and glomerular capillary hydraulic pressure (P_{GC}) remained relatively constant as blood pressure was lowered from ≈ 120 to ≈ 80 mm Hg over the range of perfusion pressure examined, primarily as a result of reductions in afferent arteriolar resistance (R_A). Efferent arteriolar resistance (R_E) was relatively constant but increased slightly at lower pressures. (Modified from Robertson CR, Deen WM, Troy JL, Brenner BM: Dynamics of glomerular ultrafiltration in the rat. III: hemodynamics and autoregulation. *Am J Physiol*. 1972;223:1191, 1972.)

on P_{GC} and preglomerular (R_A) and efferent arteriolar (R_E) resistance.¹⁴⁵ Graded reductions in renal perfusion pressure from 120 to 80 mm Hg result in only a modest decline in glomerular capillary blood flow, whereas a further reduction in perfusion pressure to 60 mm Hg leads to a more pronounced decline (see Fig. 3.18).

Autoregulation of glomerular capillary blood flow and P_{GC} as perfusion pressure decreased from 120 to 80 mm Hg is the result primarily of a pronounced decrease in R_A , with little or no change in R_E . Over the range of renal perfusion pressures from 120 to 60 mm Hg, R_E tended to increase slightly at the lower perfusion pressure. Under conditions of modest plasma volume expansion, R_A declines while R_E increases slightly as renal perfusion pressure is lowered so that P_{GC} and ΔP are virtually unchanged over the entire range of renal perfusion pressures.¹⁴⁵ The mean glomerular transcapillary hydraulic pressure difference (ΔP) exhibits almost perfect autoregulation over the entire range of perfusion pressures.¹⁴⁵ These results indicate that autoregulation of GFR is the consequence of the autoregulation of glomerular blood flow and glomerular capillary pressure. Similar results have been obtained in other rat strains and in dogs, where proximal and distal tubular pressures and peritubular capillary pressure also demonstrated autoregulation.¹⁴⁶

Although more controversial, autoregulation also occurs in the medullary circulation,^{147–149} an effect that may be influenced by the volume status of the animal.¹⁴⁸ In the split hydronephrotic rat kidney preparation,¹⁵⁰ reductions in perfusion pressure from 120 to 95 mm Hg elicited dilation of all preglomerular vessels, including the arcuate and interlobular arteries. The large preglomerular arterioles, including the interlobular arteries, contribute to the constancy of outer cortical blood flow in the upper autoregulatory range.¹⁵¹ These responses notwithstanding, most evidence has indicated that the major preglomerular resistance components are the afferent arterioles.^{33,152–154} Direct observations of perfused juxtamedullary nephrons have revealed parallel reductions in the luminal diameters of arcuate, interlobular, and afferent arterioles in response to elevations in perfusion pressure. However, because quantitatively similar reductions in vessel diameter produce much greater elevations in resistance in smaller than in larger vessels, the predominant effect of these changes is an increase in afferent arteriolar resistance.^{30,152}

Under conditions of substantial plasma volume expansion, medullary blood flow autoregulation efficiency is diminished, whereas cortical blood flow autoregulatory responses are maintained. This loss of medullary blood flow autoregulation is thought to contribute to the exaggerated pressure natriuresis during plasma volume expansion.^{36,155}

Cellular Mechanisms Involved in Renal Autoregulation

Autoregulation of the afferent arteriole and interlobular artery is blocked by administration of L-type calcium channel blockers, inhibition of mechanosensitive cation channels, and a calcium-free perfusate.^{156–159} Thus, the autoregulatory response involves gating of mechanosensitive channels, which produces membrane depolarization and activation of voltage-dependent calcium channels and leads to an increase in intracellular calcium concentration and vasoconstriction.^{156,160,161} Indeed, calcium channel blockade almost completely blocks the autoregulation of RBF.^{162,163} Intrinsic

metabolites of the cytochrome P450 epoxygenase pathway attenuate the autoregulatory capacity of the afferent arteriole, whereas metabolites of the cytochrome P450 hydroxylase pathway enhance autoregulatory responsiveness.¹⁶⁴

Inhibition of nitric oxide (NO) does not prevent autoregulation of GFR and RBF, but values for RBF are reduced at any given renal perfusion pressure as compared with control values.^{165–168} In the isolated, perfused, juxtamedullary afferent arteriole, the initial vasodilatation observed when pressure was increased was of shorter duration when endogenous NO formation was blocked, but the autoregulatory response was unaffected.¹⁶¹ Cortical and juxtamedullary preglomerular vessels in the split hydronephrotic kidney also autoregulate in the presence of NO inhibition.¹⁶⁹ Thus, the evidence indicates that NO is not essential for the manifestation of renal autoregulation, although it does greatly influence the plateau of the autoregulatory response. Furthermore, NO plays a role in tubuloglomerular feedback, as will be discussed.^{35,170}

Myogenic and Tubuloglomerular Feedback Mechanisms

There is general consensus that both myogenic and tubuloglomerular feedback mechanisms contribute to autoregulatory responses. The myogenic mechanism refers to the ability of arterial smooth muscle to contract and relax in response to increases and decreases in vascular wall tension.^{153,156,171,172} Thus, an increase in perfusion pressure, which initially distends the vascular wall, is followed by contraction of a resistance vessel, resulting in a recovery of blood flow from an initial elevation to a value comparable to the control level. Evidence that the renal vasculature is intrinsically responsive to changes in the transmural hydraulic pressure difference and exhibits myogenic responses has been obtained in isolated afferent arterioles. Myogenic control of renal vascular resistance has been estimated to contribute up to 50% of the total autoregulatory response.^{153,173}

Autoregulation of renal blood flow is observed, even when tubuloglomerular feedback is inhibited by furosemide, suggesting an important role for a myogenic mechanism.¹⁷⁴ This myogenic mechanism of autoregulation occurs very rapidly, reaching a full response in 3 to 10 seconds.^{174,175} Autoregulation occurs in all the preglomerular resistance vessels of the *in vitro*, blood-perfused, juxtamedullary nephron preparation.^{152,153,164,175–177} Of note, the afferent arterioles in this preparation constricted in response to rapid increases in perfusion pressure, even when flow to the macula densa was prevented by resection of the papilla, indicating a myogenic response.¹⁷⁵ Isolated perfused rabbit afferent arterioles respond to step increases of intraluminal pressure with a decrease in luminal diameter.¹⁴³ In contrast, efferent arteriolar segments showed vasodilation when submitted to the same procedure, probably reflecting simple passive physical properties.

Autoregulation is also observed in the afferent arteriole and arcuate and interlobular arteries of the nonfiltering hydronephrotic kidney preparation but, again, the efferent arteriole does not autoregulate in this model.^{156,158,159,169,178} However, it should be noted that efferent arteriolar resistance *in vivo* may increase in response to prolonged reductions in AP.^{145,179} This may result from increased activity of the intrarenal renin-angiotensin system (RAS). These data may

also explain why autoregulation of GFR is more efficient than autoregulation of RBF.

The autoregulatory threshold can be reset in response to a variety of perturbations. Autoregulation in the afferent arteriole is attenuated in diabetic kidneys and may contribute to the hyperfiltration seen early in this disease.¹⁷⁸ Autoregulation is partially restored by insulin treatment and/or by inhibition of endogenous prostaglandin production.¹⁷⁸ Autoregulation in the remnant kidney is markedly attenuated 24 hours after the reduction in renal mass but is restored by cyclooxygenase inhibition, suggesting that release of vasodilatory prostaglandins may be involved in the initial response to increased SNGFR in the remaining nephrons after an acute partial nephrectomy.¹⁸⁰ Much higher pressures than normal are required to evoke a vasoconstrictor response in the afferent arteriole during the development of spontaneous hypertension.¹⁸¹ Both the afferent arterioles and the interlobular arteries of Dahl salt-sensitive hypertensive rats exhibit reduced myogenic responsiveness to increases in perfusion pressure when fed a high-salt diet.¹⁸² Thus, alterations in autoregulatory responses of the renal vasculature occur in a variety of disease states and may influence the kidney's ability to alter excretory responses to increased plasma volume expansion.

During development of the nephron, the tubule develops a segment that descends from the cortex into the medulla, but the connection with the originating glomerulus remains throughout the developmental process and provides the structural basis for the regulatory mechanism known as “tubuloglomerular feedback” (TGF; Fig. 3.19). A specialized nephron segment macula densa, at the end of the thick ascending limb of the loop of Henle, has distinct morphologic characteristics, including the presence of a primary cilium.¹⁸³ Macula densa cells are adjacent to the cells of the glomerulus and connect with the extraglomerular mesangium and afferent and efferent arterioles of the glomerulus (see Fig. 3.19). This anatomic arrangement of macula densa cells, extraglomerular mesangial cells, arteriolar smooth muscle cells, and renin-secreting cells of the afferent arteriole is known as the “juxtaglomerular apparatus” (JGA).¹⁸⁴

The JGA is ideally suited to serve as a feedback system whereby a physicochemical stimulus in the tubular fluid activates the macula densa cells, which in turn transmit signals to the arterioles to alter the degree of contraction, thus regulating afferent arteriolar resistance. Changes in the volume flow and composition of the fluid flowing past the macula densa elicit rapid alterations in afferent arteriolar resistance and glomerular filtration, with increases in delivery of fluid resulting in decreases in SNGFR and P_{GC} of the same nephron.^{35,185,186} The TGF system senses delivery of fluid to the macula densa and “feeds back” signals to control filtration rate, thus providing a powerful feedback mechanism to regulate the pressures and flows that govern GFR in response to acute perturbations in delivery of fluid to the macula densa. The TGF mechanism is thus another important mechanism that helps explain the very high efficiency of autoregulation of RBF and GFR. Increased RBF or glomerular capillary pressure leads to increased GFR and, therefore, greater delivery of volume and solute to the distal tubule. Increased distal delivery is sensed by the macula densa, which activates effector mechanisms that increase preglomerular resistance, reducing RBF, glomerular pressure, and GFR.⁴⁸

Increased perfusion of the late proximal tubule into the distal tubule causes a reduction in glomerular blood flow, glomerular pressure, and GFR.¹⁸⁷ Furthermore, experimental maneuvers that decrease distal tubule fluid flow induce afferent arteriolar vasodilation and interfere with the normal autoregulatory response.^{35,170,188} In addition, perfusion with furosemide-containing solutions into the macula densa segment abrogate the normal constrictor response of afferent arterioles to increased perfusion pressure,¹⁸⁹ presumably by blocking the $\text{Na}^+/\text{K}^+/\text{2Cl}^-$ transporter on the luminal membrane of the macula densa cells.^{153,190} These studies have suggested that the autoregulatory response in juxtaglomerular nephrons is also highly dependent on the TGF mechanism. Moreover, deletion of the A_1 adenosine receptor gene in mice to block TGF results in less efficient autoregulation, again indicating the role for TGF in the autoregulatory response.¹⁹¹

To examine the role of TGF in autoregulation, investigators have studied spontaneous oscillations in proximal tubule pressure and RBF and the response of the renal circulation to high-frequency oscillations in tubule flow or renal perfusion pressure.¹⁹² Oscillations in tubule pressure have been observed in anesthetized rats at a rate of about three cycles/min that are sensitive to small changes in delivery of fluid to the macula densa.¹⁹³ These spontaneous oscillations are eliminated by loop diuretics.¹⁹⁴ To examine this hypothesis,¹⁹² sinusoidal oscillations were induced in distal tubule flow in rats at a frequency similar to that of the spontaneous fluctuations in tubule pressure. Varying distal delivery at this rate caused parallel fluctuations in stop-flow pressure (an index of glomerular capillary pressure), probably mediated by alterations in afferent resistance, again consistent with dynamic regulation of glomerular blood flow by the TGF system. To investigate the role of this system in autoregulation,¹⁹⁵ the effects of sinusoidal variations in AP at varying frequencies on renal blood flow were examined. Two separate components of autoregulation were identified, one operating at about the same frequency as the spontaneous fluctuations in tubule pressure, the TGF component, and one operating at a much higher frequency consistent with spontaneous fluctuations in vascular smooth muscle tone by the myogenic component.¹⁹⁶ These data have suggested that slow pressure changes elicit a predominant TGF response, whereas the rapid response reflects the myogenic mechanism.

The TGF mechanism stabilizes delivery of volume and solute to the distal nephron. Under normal conditions, flow-related changes in the tubular fluid composition at the macula densa are sensed, and signals are transmitted to the afferent arterioles to regulate the filtered load. Early distal tubular fluid is hypotonic (~120 mOsm/kg H₂O), and its composition is closely coupled to fluid flow along the ascending loop of Henle, so that increases in flow cause increases in tubular fluid osmolality and NaCl concentration at the macula densa, which lead to vasoconstriction of the afferent arteriole. At the cellular level, increases in tubular fluid osmolality elicit increases in cytosolic [Ca²⁺] in macula densa cells, which result in release of a vasoconstrictive factor from these cells.¹⁹⁷ As depicted in Fig. 3.20, suggested mediators of TGF include purinergic compounds, such as adenosine and ATP, and one or more of the eicosanoids, such as prostaglandin E2 (PGE2) or 20-hydroxyeicosatetraenoic acid (20-HETE). The factor mediating TGF responses vasoconstricts

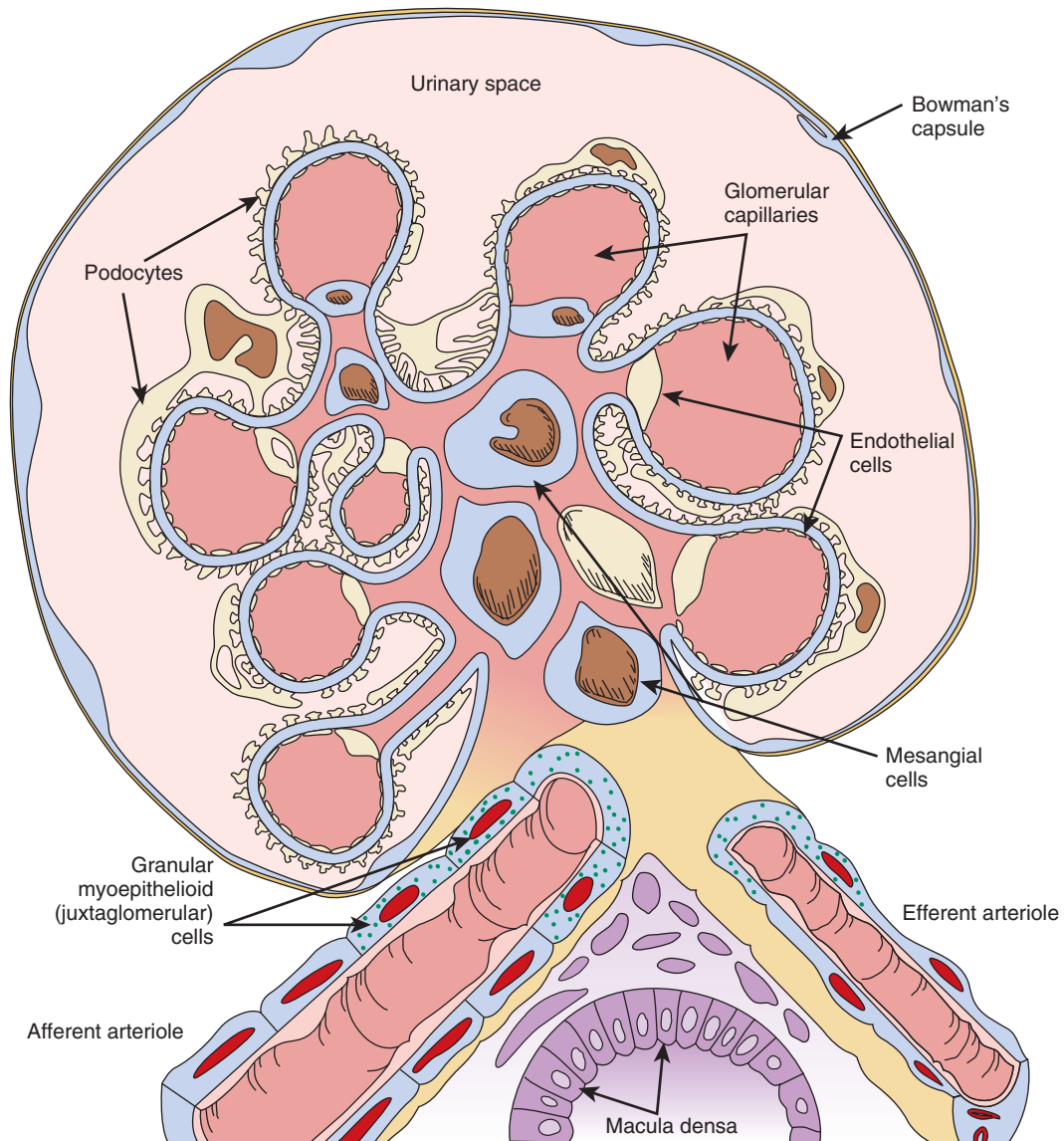


Fig. 3.19. Schematic drawing of a cross-section of a glomerulus, vascular pole, and macula densa cells forming the juxtaglomerular apparatus. As the afferent arteriole enters the glomerular tuft (large vessel, lower left), it breaks into a capillary network, and blood leaves the glomerular tuft via the efferent arteriole (large vessel, lower right). The glomerular capillaries have a fenestrated endothelium. The capillary network and mesangium located between the capillaries are bound together by a common basement membrane (blue line between the podocytes and capillaries). The basement membrane is absent between the capillary lumen and mesangial cells. The outer side of the basement membrane is surrounded by interdigitating visceral epithelial cells known as podocytes. Kriz and coworkers¹⁸⁴ have pointed out that the glomerular mesangium is continuous with the extraglomerular mesangium (consisting of extraglomerular mesangial cells and matrix) at the vascular pole. The extraglomerular mesangium, along with the macula densa cells of the distal tubule and the afferent arteriole, form the juxtaglomerular apparatus. (Courtesy D.A. Maddox.)

afferent arteriolar vessels through the opening of voltage-gated Ca^{2+} channels in vascular smooth muscle cells.³⁵

The sensitivity of the TGF mechanism can be modulated by many agents and circumstances. TGF sensitivity is diminished during volume expansion, thus allowing a greater delivery of fluid and electrolytes to the distal nephron for any given level of GFR. Reductions in TGF sensitivity allow correction of volume expansion. In contrast, contraction of extracellular fluid and blood volume is associated with an enhanced sensitivity of the TGF mechanism, which together with an augmented proximal reabsorption helps conserve fluid and electrolytes. A major regulator of TGF sensitivity

is Ang II. In states of low Ang II activity (e.g., extracellular volume expansion, salt loading), the TGF mechanism is less responsive, whereas feedback sensitivity is enhanced during conditions of high Ang II activity, such as occurs during dehydration, hypotension, or hypovolemia.

The interactions between the myogenic mechanism and the TGF are complex and not simply additive. Contributions from other systems add additional complexity. For example, glomerulotubular balance, whereby proximal tubule reabsorption increases as GFR rises, blunts the effects of alterations in GFR on distal delivery. In addition, the persistence of some autoregulatory behavior in nonfiltering kidneys¹⁹⁸ and

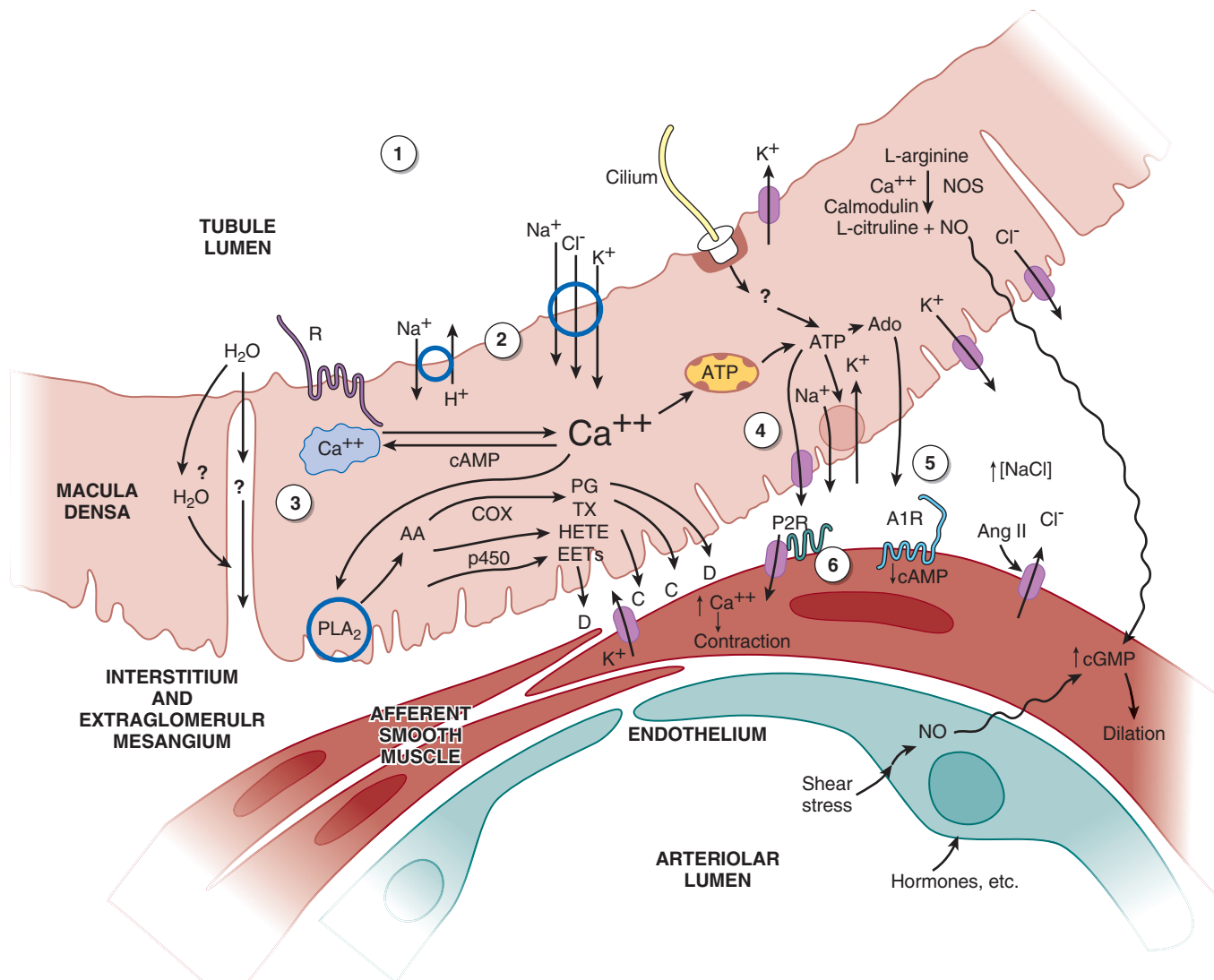


Fig. 3.20 Proposed macula densa tubuloglomerular feedback (TGF) signaling mechanisms. Numbers in circles refer to the following sequence of events: 1, Flow-dependent changes in tubular fluid composition, including Na^+ , Cl^- , osmolality, signals from intratubular paracrine agents, and cilia disturbance; 2, membrane activation step, including membrane depolarization, enhanced Na^+ , Cl^- , K^+ uptake, or other sensing mechanism; 3, transmission from membrane to intracellular signal mobilization; 4, formation and release of TGF mediators, including ATP and adenosine (Ado), arachidonic acid (AA) metabolites, and nitric oxide (NO); 5, receptor activation by released agents, membrane depolarization, and activation of Ca^{2+} channels in vascular smooth muscle cells; 6, afferent arteriolar vasoconstriction partially countered by NO-stimulated increases in cGMP and other released mediators—local angiotensin II (Ang II) and neuronal nitric oxide synthase (nNOS) activity modulate the response. ATP, Adenosine triphosphate; A1R, adenosine A1 receptor; C, constriction; cGMP, cyclic guanosine monophosphate; COX, cyclooxygenase; D, dilation; EET, epoxyeicosatrienoic acid; HETE, hydroxyeicosatetraenoic acid; P2R, P2 purinergic receptors; p450, cytochrome P 450; PG, prostaglandins; PLA₂, phospholipase A2; TX, thromboxanes. (Modified from Navar LG, Bell PD, Burke TJ: Role of a macula densa feedback mechanism as a mediator of renal autoregulation. *Kidney Int*. 1982;22:S157–S164.)

in isolated blood vessels has suggested that the delivery of filtrate to the distal tubule is not absolutely required for constancy of blood flow. Nevertheless, the myogenic and TGF mechanisms are not mutually exclusive, and various models of renal autoregulation incorporate both systems.^{172,199} Because the myogenic and TGF responses share the same effector site, the afferent arteriole, interactions between these two systems are unavoidable, and each response is capable of modulating the other. The prevailing view is that these two mechanisms act in concert to accomplish the same end, a stabilization of renal function when blood pressure is altered.^{35,173,200} Furthermore, the time constraints are different;

the myogenic component of autoregulation requires less than 10 seconds for completion and normally follows first-order kinetics without rate-sensitive components.¹⁷³ The response time for the tubuloglomerular feedback may occur as rapidly as 5 seconds,¹⁵⁴ although others have suggested that it takes 30 to 60 seconds and shows spontaneous oscillations at 0.025 to 0.033 Hz.¹⁷³ The myogenic and tubuloglomerular feedback mechanisms account for most of the autoregulatory responses, but additional systems have been suggested.¹⁷³ Furthermore, the nature of their interaction may be complex, with the TGF primarily influencing the sensitivity of the myogenic mechanism.³⁵

Mechanisms of Tubuloglomerular Feedback

Control of Renal Blood Flow and Glomerular Filtration Rate

There appear to be several factors that have been identified as tubular signals for TGF.²⁰¹ Changes in delivery of Na^+ , Cl^- , and K^+ are thought to be sensed by the macula densa through the $\text{Na}^+/\text{K}^+/\text{2Cl}^-$ cotransporter on the luminal cell membrane of the macula densa cells.²⁰² Alterations in Na^+ , K^+ , and Cl^- reabsorption result in inverse changes in SNGFR and renal vascular resistance, primarily due to changes in preglomerular resistance. For example, when salt concentration increases at the macula densa, the feedback mechanism increases afferent arteriolar resistance, thus decreasing glomerular pressure and SNGFR. Agents such as furosemide that interfere with the $\text{Na}^+/\text{K}^+/\text{2Cl}^-$ cotransporter in the macula densa cells¹⁹⁰ inhibit the feedback response.²⁰³

Additional studies have been performed in which macula densa segments were perfused with solutions that contained minimal concentrations of essential ions needed to maintain the integrity of the $\text{Na}^+/\text{K}^+/\text{2Cl}^-$ cotransporter, with the remaining solute being deficient in Na^+ (choline chloride) or deficient in Cl^- (Na isocyanate). These solutions clearly elicited normal TGF responses.²⁰⁴ Furthermore, orthograde perfusion with nonelectrolyte solutes also elicited TGF responses.^{35,205} Collectively, these results indicate that the integrity of the $\text{Na}^+/\text{K}^+/\text{2Cl}^-$ cotransporter must be maintained for the sensing mechanism to function normally. However, the actual sensing mechanism may be activated by changes in total solute concentration. Furthermore, studies evaluating the possible role of the primary cilium in macula densa cells have suggested that flow-dependent signals may stimulate the cilium and alter the magnitude of the TGF response.^{183,206}

Another area of uncertainty involves the intracellular signaling cascade to generate a vasoactive agent that is secreted. Some studies have suggested that the luminal signal activates release of Ca^{2+} from the intracellular stores that then lead to the formation of ATP, which is secreted and plays a central role in mediating the signal from the luminal cell membrane of the macula densa. This is illustrated in Fig. 3.20, which is derived from based on several sources.^{35,186} According to this scheme, increased delivery of solute to the macula densa results in concentration-dependent increases in solute uptake by the $\text{Na}^+/\text{K}^+/\text{2Cl}^-$ cotransporter and may separately generate a signal to initiate the cascade. This, in turn, stimulates mitochondrial activity in the macula densa cells, leading to the formation of ATP. Macula densa cells respond to an increase in luminal $[\text{NaCl}]$ or total solute concentration by releasing ATP at the basolateral cell membrane through ATP-permeable, large-conductance anion channels, possibly providing a communication link between macula densa cells and adjacent mesangial cells via purinoceptors receptors on the latter.²⁰⁷ The ATP can exert direct actions on the vascular smooth muscle cells and is also metabolized further, with ultimate degradation to the metabolites, adenosine diphosphate (ADP) and adenosine monophosphate (AMP). Activity of cytosolic 5'-nucleotidase or endo-5'-nucleotidase bound to the cell membrane results in the formation of adenosine.¹⁸⁶ In addition to the ATP metabolites, the macula densa cells also produce arachidonic acid metabolites, including PGE₂ and PGI₂, and nitric oxide and reactive oxygen species. Thus, there are several vasoactive substances that are secreted and may alter afferent arteriolar vascular tone. Although ATP

and adenosine are formed in macula densa cells or in the adjacent interstitium, ATP interacts with purinergic (P2) receptors on the extraglomerular mesangial and vascular cells, resulting in an increase in $[\text{Ca}^{2+}]_i$.²⁰⁸ The increase in $[\text{Ca}^{2+}]_i$ may occur, in part, via basolateral membrane depolarization through receptor operated channels, followed by a further increase in Ca^{2+} entry into the cells via voltage-gated Ca^{2+} channels.²⁰⁹ As indicated in Fig. 3.20, gap junctions then transmit the calcium transient to the adjacent afferent arteriole, or ATP can exert similar effects directly on vascular smooth muscle cells, thus leading to vasoconstriction. Some of the ATP elicited by macula densa cells is metabolized to adenosine, which also can directly constrict the afferent arteriole through activation of purinergic P1 receptors.²¹⁰

Although there is general consensus that ATP is secreted by macula densa cells, some investigators have suggested that the ATP metabolite, adenosine, is primarily responsible for mediating tubuloglomerular feedback. Intraluminal administration of an adenosine A1 receptor agonist enhances the TGF response.²¹¹ In addition, TGF is attenuated in adenosine A1 receptor-deficient mice.^{212,213} Blocking adenosine A1 receptors, or inhibition of adenosine synthesis via inhibition of 5'-nucleotidase, reduces TGF efficiency.²¹⁴ Addition of adenosine to the afferent arteriole causes vasoconstriction via activation of the adenosine A1 receptor, and addition of an A1 receptor antagonist blocks both the effects of adenosine and of high macula densa $[\text{NaCl}]$.²¹⁵ These results are consistent with the hypothesis that adenosine is also a mediator of TGF responses invoking an effect of Na^+/K^+ -ATPase activity and leading to increased adenosine synthesis.²¹⁵ However, adenosine also activates adenosine A2 receptors, which cause afferent arteriolar dilation and apparently abrogate the actions of A1 receptors.^{216,217}

Efferent arterioles also respond to adenosine but they vasodilate in response to an increase in NaCl concentration at the macula densa or to direct application due to actions of the adenosine A2 receptors, which antagonize the effects of A1 receptors.^{217,218} The changes in efferent arteriolar resistance tend to be in an opposite direction to that of the afferent arterioles, which vasoconstrict in response to increased NaCl at the macula densa.^{215,219} The net result, however, is decreased glomerular blood flow, decreased glomerular hydraulic pressure, and a reduction in SNGFR.

There are many additional paracrine agents produced and secreted by macula densa cells, as shown in Fig. 3.20. These include metabolites of the arachidonic acid cascade, including prostaglandins PGE₂ and PGI₂, and other products of the cyclooxygenase pathway, products of the cytochrome P450 pathway, including epoxigenases and the cytochrome P450 4A HETEs.^{35,164,220} Another very important regulating paracrine regulator is NO, which exerts vasodilatory responses when released by the macula densa cells. Under normal circumstances, when the NaCl concentration of tubular fluid is increased, there are increases in ATP release coupled with reductions in PGE₂ formation until the ATP release reaches a plateau, and the PGE₂ release is markedly reduced. With further increases in $[\text{NaCl}]$, NO release is augmented to counteract the effects of increased ATP.³⁵

In addition to the paracrine factors released by macula densa cells, there are also many modulatory agents that influence the sensitivity of TGF responses. Ang II is one of the more important factors. TGF is blunted by Ang II

antagonists and Ang II synthesis inhibitors, and TGF is markedly reduced in knockout mice lacking the AT1A Ang II receptors or angiotensin-converting enzyme (ACE).^{221,222} Furthermore, systemic infusion of Ang II in ACE knockout mice restores TGF.^{221,223–228} Ang II also enhances TGF via activation of AT1 receptors on the luminal membrane of the macula densa.²²⁹ Acute inhibition of the AT1 receptor in normal mice reduces TGF responses and reduces autoregulatory efficiency.²²⁴ Several studies have shown the interactions between adenosine and Ang in the TGF mechanism. In these studies, adenosine A₁ receptor antagonist administration results in decreased afferent arteriolar resistance and increased transcapillary hydraulic pressure differences (ΔP), whereas pretreatment with an angiotensin AT1 receptor antagonist prevented these changes.²³⁰ Although it is known that Ang II is not the primary regulator of TGF, these results indicate that Ang II plays a prominent role in modulating tubuloglomerular feedback sensitivity, and that this response is mediated through the AT1 receptor.

Neuronal NO synthase (nNOS or NOS I) is present in macula densa cells.²³¹ NO derived from nNOS in the macula densa provides a vasodilatory influence on tubuloglomerular feedback, decreasing the amount of vasoconstriction of the afferent arteriole that otherwise would occur.^{231,232} Increased distal sodium chloride delivery to the macula densa stimulates nNOS activity and also increases activity of the inducible form of cyclooxygenase (COX-2), which forms PGE2 and counteracts TGF-mediated constriction of the afferent arteriole.^{231,232} Macula densa cell pH increases in response to increased luminal sodium concentration and may be related to the stimulation of nNOS.²³³ Inhibition of macula densa guanylate cyclase increases the TGF response to high luminal [NaCl], further indicating the importance of NO in modulating TGF.²¹⁹ In an isolated perfused JGA preparation, microperfusion of the macula densa with an inhibitor of NO production led to constriction of the adjacent afferent arteriole.²³⁴ When the macula densa was perfused with a solution low in Na concentration, however, the response was blocked, indicating that Na reabsorption is required.²³⁴ Microperfuson of the macula densa with the precursor of NO, L-arginine, blunts TGF responses, especially in salt-depleted animals.^{235–237} These results indicate that NO released from macula densa cells or endothelial cells causes afferent arteriolar vasodilation acutely or may blunt TGF responses. An increase in NO production may also inhibit renin release by increasing cyclic guanosine monophosphate (cGMP) in the granular cells of the afferent arteriole,²³⁸ thereby accentuating its vasodilatory effects. When NO production was chronically blocked in knockout mice lacking nNOS, TGF in response to acute perturbations in distal sodium delivery was normal.²²⁵ However, the presence of intact nNOS in the JGA is required for sodium chloride-dependent renin secretion.²²⁵ The TGF system, which elicits vasoconstriction and a reduction in SNGFR in response to acute increases in sodium and solute delivery to the macula densa, appears to activate a vasodilatory response secondarily via NO release.²³⁹ Stimulation of NO production in response to increased distal salt delivery under conditions of volume expansion would be advantageous by resetting TGF and limiting TGF-mediated vasoconstrictor responses.

The dynamics of the TGF mechanism can be temporally divided into two or more responses with different time

constants. The initial rapid response occurs within a few seconds and elicits a rapid vasoconstriction and decrease in GFR and P_{GC} when sodium delivery to the macula densa cells is acutely increased. A second vasoconstrictor response occurs in seconds to minutes and changes the slope of the response to a slower time constant. This may be due to modulation of the initial response by some of the modulating agents mentioned. The rapid TGF system prevents large changes in GFR under conditions such as spontaneous fluctuations in blood pressure, thereby maintaining tight control of distal sodium delivery in the short term. Over the long term, renin secretion, controlled by the JGA in accordance with the requirements for sodium balance and the TGF system, resets to a new sodium delivery rate.²²⁵ In the uninephrectomized rat with sustained elevations of the GFR, the TGF system appears to be reset.²⁴⁰

Connecting Tubule Glomerular Feedback Mechanism

There is also growing interest in a second feedback loop that links the connecting tubule, which has been shown to be in apposition to its own glomerulus and in close contact with the afferent arteriole.²⁴¹ In vitro perfusion of the connecting tubule has shown that increases in luminal NaCl elicit vasodilation of preconstricted afferent arterioles.²⁴² This action is opposite to the effect of macula densa TGF signaling, in which increases in NaCl cause vasoconstriction, raising the question of how these two opposing systems interact. Additional studies demonstrating that the addition of amiloride to the perfusion solution prevents the action of increased luminal Na⁺, have suggested that the epithelial sodium channel mediates the connecting TGF (CTGF).²⁴² The afferent vasodilator effect of increased E_{NaC} activity appears to be mediated by PGE2 acting on an EP4 receptor on the afferent arteriole.²⁴³ An additional role of epoxyeicosatrienoic acid (EET) has also been suggested.²⁴⁴ Furthermore, the presence of Ang II in the luminal fluid enhances the afferent arteriolar vasodilator effect caused by increases in luminal Na⁺ concentration.²⁴⁵ This CTGF mechanism is thought to mediate resetting of the macula densa TGF mechanism by partially reducing its sensitivity.²⁴⁶ A modulating role of CTGF has been observed in experimental hypertension,²⁴⁷ during high salt intake,²⁴⁸ and in the renal vasodilatory response that occurs in the remaining kidney after unilateral nephrectomy.²⁴⁹

ENDOTHELIAL FACTORS AND GASEOUS TRANSMITTERS CONTROLLING RENAL HEMODYNAMICS AND GLOMERULAR FILTRATION RATE

A particularly intriguing and growing area of research involves the paracrine interactions between endothelial cells and the underlying smooth muscle cells. As shown in Fig. 3.21, endothelial cells respond to various physical and chemical stimuli, including pressure, flow, shear stress, and circumferential strain, as well as vasoactive factors normally present in the blood. Under normal conditions, an increase in shear stress may activate endothelial cells to produce NO and the prostaglandins PGE2 and PGI2, which help adjust vascular tone to accommodate the increased load. However, during conditions of tissue injury or inflammation, the endothelial cells may also be stimulated to produce endothelin, thromboxane,

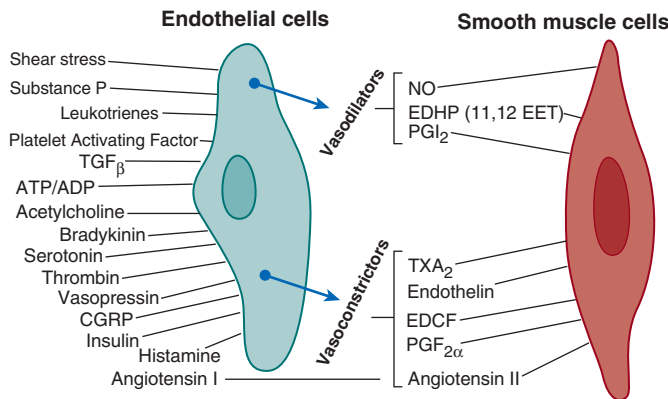


Fig. 3.21 Interaction of endothelial cells with smooth muscle or mesangial cells. As indicated in the text, several agents interact with endothelial cells to produce the vasodilator nitric oxide (NO). Others yield vasoconstriction (see text and other sources). Angiotensin-converting enzyme converts angiotensin I to the potent vasoconstrictor angiotensin II. ATP-ADP, Adenosine triphosphate—adenosine diphosphate; CGRP, calcitonin gene-related peptide; EDCF, endothelial-derived constricting factor; EDHP, endothelial-derived hyperpolarizing factor; EET, epoxyeicosatrienoic acid; PGF_{2α}, prostaglandin F_{2α}; PGl₂, prostaglandin I₂; TGF_β, transforming growth factor beta; TXA₂, thromboxane A₂. (Modified from Arendshorst W, Navar LG. Renal circulation and glomerular hemodynamics. In: Schrier RW, Coffman TM, Falk RJ, Molitoris BA, Neilson EG, eds. *Schrier's diseases of the kidney*. Philadelphia: Lippincott Williams & Wilkins; 2013:74–131; Navar LG, Arendshorst WJ, Pallone TL, Inscho EW, Imig JD, Bell PD. The renal microcirculation. In: Tuma RF, Duran WN, Ley K, eds. *Handbook of physiology: Microcirculation*. Vol 2: Academic Press; 2008:550–683; Maddox DA, Deen WL, and Brenner BM. Glomerular Filtration; *Handbook of Physiology: Section 8 Renal Physiology*. American Physiological Society, New York: Oxford University Press; 1992, 545–638; Maddox DA, Brenner BM. Glomerular ultrafiltration. In: Brenner BM, ed. *The kidney*. 7th ed. Philadelphia: Saunders; 2004:353–412.)

certain growth and profibrotic factors that elicit vasoconstriction, and/or additional paracrine factors associated with tissue injury and fibrosis. Several of these factors associated with regulation of the renal microcirculation are gaseous physiologic transmitters, called “gasotransmitters,” which have been identified over the last 2 decades. NO is the first such gasotransmitter discovered, but carbon monoxide (CO) and hydrogen sulfide (H₂S) have also been shown to influence the renal microcirculation.

Nitric Oxide and Nitric Oxide Synthases

In 1980, Furchtgott and Zawadzki²⁵⁰ demonstrated that the vasodilatory action of acetylcholine requires the presence of an intact endothelium. Acetylcholine binds to receptors on endothelial cells, leading to the formation and release of an “endothelial-derived relaxing factor,” now known to be NO.^{251,252} Many cell types, including the endothelium, produce NO from the amino acid L-arginine^{35,83,253} by a family of nitric oxide synthases (NOSs) that are present in many cell types, including vascular endothelial cells, macrophages, neurons, glomerular mesangial cells, macula densa, and renal tubular cells.^{35,254–256} Three main NOS isoforms have been isolated. Neuronal NOS, also termed “NOS I” or “nNOS,” and endothelial NOS, also called “NOS III” or “eNOS,” are constitutively present in the kidney. A third NOS, iNOS or NOS II, is inducible, is expressed after transcriptional induction, and

remains active for prolonged periods.^{35,83} All three isoforms of NOS are found in the kidney. The arcuate and interlobular arteries, as well as the afferent and efferent arterioles, all produce NO, which regulates basal vascular tone, as indicated by the constriction that occurs in response to inhibition of endogenous NO production.^{35,83}

Once released by the endothelium, NO diffuses into adjacent and downstream vascular smooth muscle cells,²⁵⁷ where it stimulates the activity of soluble guanylate cyclase and increases cGMP formation.^{83,258–263} cGMP reduces calcium influx, intracellular calcium release, and intracellular calcium concentration. This occurs, in part, through a cGMP-dependent protein kinase (PKG)-mediated phosphorylation of targets, which include inositol trisphosphate (IP₃) receptors, calcium channels, and phospholipase A2,²⁶⁴ thereby reducing the amount of free calcium available for contraction, hence promoting relaxation.²⁶⁵

In addition to stimulation by acetylcholine, NO formation in the vascular endothelium increases in response to bradykinin,^{262,266–269} thrombin,²⁷⁰ platelet-activating factor,²⁷¹ endothelin,²⁷² and calcitonin gene-related peptide.^{267,273–276} Elevation of blood flow through vessels with intact endothelium or across cultured endothelial cells results in increased shear stress and increased NO release. Both the pulse frequency and pulse pressure modulate flow-induced NO release.^{259,266,268,277–281} Elevated perfusion pressure and shear stress also increase NO release from afferent arterioles.²⁸²

NO plays a major role in modulation of renal hemodynamics, regulation of medullary perfusion, modulation of the sensitivity of the TGF mechanism, inhibition of tubular sodium reabsorption, modulation of renal sympathetic neural activity, and mediation of pressure natriuresis.^{35,283–287} NO dominates integrated renal hyperemic responses to acetylcholine and bradykinin, and renal endothelium-dependent vasodilation is diminished in diabetes due to impaired NO function.²⁸⁸ Pressure natriuresis in experimental models using stepwise increases of both renal perfusion pressure and medullary blood flow involve increased NO release, which can exert direct tubular effects to promote sodium and water excretion.^{289,290} Tubular epithelial cells are capable of releasing NO but, during increased medullary flow, the vasa recta may be a primary source of the NO, as suggested by the fact that flow-dependent increases of NO also occur, even during microperfusion of isolated outer medullary vasa recta.²⁹¹

There are important interactions among NO, Ang II, and renal nerves in the control of renal function and blood pressure.²⁹² Nonselective NOS inhibition using competitive inhibitors of NO results in decreases in RPF, increases in mean arterial blood pressure (AP), and generally a reduction in GFR.^{165,293,294} These effects are largely prevented by the simultaneous administration of excess L-arginine, the NOS substrate.²⁹³ Selective inhibition of neuronal NOS (nNOS or type I NOS), which is found in the thick ascending limb of the loop of Henle, the macula densa, and efferent arterioles,^{256,285} decreases GFR without affecting blood pressure or RBF.²⁹⁵ Because eNOS is found in the endothelium of renal blood vessels, including both the afferent and efferent arterioles and glomerular capillary endothelial cells,²⁵⁶ differences in the effects of generalized NOS inhibition versus specific inhibition of nNOS on NO formation and RBF appear to be related to the distinct distribution of eNOS versus nNOS in the kidney. Both acute and chronic inhibition of

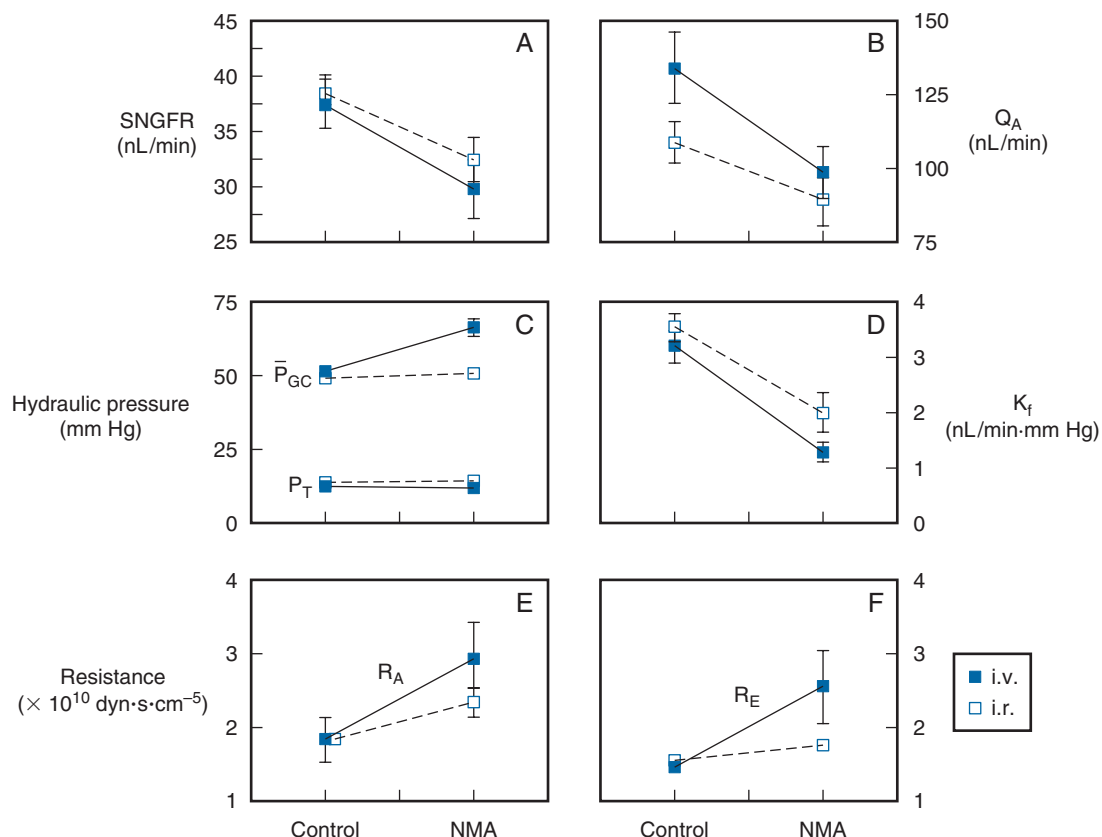


Fig. 3.22 (A–F) Role of nitric oxide in the control of glomerular filtration dynamics. Studies were performed in euvolemic Munich-Wistar rats receiving intravenous pressor doses of the nonselective nitric oxide synthase (NOS) blocker, *N*-monomethyl-L-arginine (NMA; i.v., filled squares) or nonpressor doses of NMA at the origin of the renal artery (i.r., open squares). K_f , Filtration coefficient; P_{GC} , pressure in the glomerular capillaries; P_T , pressure in the tubules; Q_A , glomerular plasma flow rate; R_A , preglomerular arteriolar resistance; R_E , efferent arteriolar resistance; SNGFR, single-nephron glomerular filtration rate. (Data [mean \pm SE] obtained from Deng A, Baylis C: Locally produced NO controls preglomerular resistance and filtration coefficient. *Am J Physiol.* 1993;264:F212–F215.)

NO production result in systemic and glomerular capillary hypertension, an increase in preglomerular (R_A) and efferent arteriolar (R_E) resistance, a decrease in K_f , and decreases in both single-nephron plasma flow and GFR.^{296–300}

As shown in Fig. 3.22, acute administration of pressor doses of a blocker of NO production results in a decline in SNGFR, Q_A , and K_f and increases in both preglomerular and efferent arteriolar resistances. Administration of nonpressor doses of the inhibitor of NO formation through the renal artery yielded an increase in preglomerular resistance and a decrease in SNGFR and K_f but no effect on efferent resistance.²⁹⁷ These studies suggest that the cortical afferent, but not efferent, arterioles are under tonic control by NO. However, others have found that the renal artery, arcuate and interlobular arteries, and afferent and efferent arterioles all produce NO and constrict in response to inhibition of endogenous NO production.^{144,169,234,257,301–304} In agreement with this finding, investigators^{31,302} have reported that NO dilates both efferent and afferent arterioles in perfused juxamedullary nephrons. Interestingly, the modulatory influence of nNOS on afferent arteriolar tone is dependent on the maintenance of distal tubular fluid, indicative of a critical interaction with the TGF mechanism.³⁰⁴

Controversy exists regarding the role of the RAS in the genesis of the increase in vascular resistance that follows

blockade of NOS. Studies of in vitro perfused nephrons³⁰² and of anesthetized rats in vivo³⁰⁵ suggest that the increase in renal vascular resistance that follows NOS blockade is blunted when Ang II formation or receptor binding is blocked. NO inhibits renin release, whereas acute Ang II infusion increases cortical NOS activity and protein expression, and chronic Ang II infusion increases mRNA levels for eNOS and nNOS.^{305,306} Ang II increases NO production in isolated perfused afferent arterioles via activation of the AT1 Ang II receptors.³⁰⁷ In contrast, nonselective NOS inhibition increases renal oxygen consumption, independently of Ang II.³⁰⁸ Additionally, inhibition of NOS in conscious rats had similar effects on renal hemodynamics in the intact and Ang II-blocked state.³⁰⁹ This suggests that the vasoconstrictor response to NOS blockade is not mediated by Ang II. Further studies³¹⁰ have shown that when the Ang II levels are acutely raised by the infusion of Ang II, acute NO blockade amplifies the renal vasoconstrictor actions of Ang II. An observation in agreement with this finding is that intrarenal inhibition of NO enhances Ang II-induced afferent, but not efferent, arteriolar vasoconstriction.^{144,311} In the juxtaglomerular nephron, however, blockade of nNOS enhanced efferent but not afferent arteriolar responsiveness to Ang II.³⁰⁴ These data suggest that NO modulates the vasoconstrictor effects of Ang II on glomerular arterioles in vivo, perhaps blunting

Ang II's vasoconstrictor response in the afferent arteriole, with some results showing similar responses on the efferent arteriole.

Effects of Heme Oxygenase and Carbon Monoxide on Renal Function

Heme is degraded by heme oxygenase (HO) enzymes (HO-1 and HO-2) producing carbon monoxide (CO), biliverdin, and bilirubin and by the release of free iron.^{2,35,312–315} Induction of HO-1 with hemin in anesthetized rats resulted in significant increases in RBF and GFR, a lower renal vascular resistance, and an increase in sodium excretion in untreated control rats without affecting blood pressure. Furthermore, auto-regulatory responses to acute Ang II infusion were blunted, and these studies suggested a vasodilatory influence of HO-1 induction and hence CO production.³¹³ When a heme oxygenase inhibitor was administered either alone or to rats receiving an NOS inhibitor—N(ω)-nitro-L-arginine methyl ester (L-NAME)—for 4 days, blockade of HO in control rats decreased CO, HO-1 levels, urine volume, and sodium excretion, but did not affect AP, RBF, or GFR. In rats undergoing NOS inhibition with L-NAME, blockade of HO decreased endogenous CO and renal HO-1 levels, urine volume, and sodium excretion, but again had no effect on AP, RBF, or GFR. An increase in plasma renin activity was observed in untreated rats but not in L-NAME-treated rats, indicating that the effects on urine volume and sodium excretion are associated, even when NO was inhibited. This suggests that inhibition of HO promotes water and sodium excretion by a direct tubular action, independently of renal hemodynamics or the NO system.³¹⁴

Inhibition of renal medullary HO activity and CO production decreases medullary blood flow and sodium excretion; the abundance of both the HO-1 and HO-2 isoforms of HO are higher in the inner medulla and lower in the cortex.³¹⁶ Inhibition of HO significantly reduces renal medullary cGMP concentrations when infused into the renal medullary interstitial space. These results suggest that both HO-1 and HO-2 are highly expressed in the renal medulla that HO, and its products play a key role in maintaining the constancy of blood flow to the renal medulla; cGMP may mediate the vasodilator effect of HO and CO in the renal medullary circulation.³¹⁶ In anesthetized rats, increases in renal perfusion pressure were found to increase CO concentrations in the renal medulla. An HO inhibitor reduced HO activity and pressure-dependent increases in CO in the medulla and blunted pressure natriuresis.³¹⁷ In conscious rats fed a normal-sodium diet, chronic infusion of an HO inhibitor into the renal medulla increased mean AP. When rats were placed on a high-salt diet, inhibition of HO activity caused a further increase in AP. Thus, renal medullary HO activity plays a key role in the control of arterial blood pressure and the control of pressure natriuresis.³¹⁷

Using a CO-releasing molecule (CORM-A1), Ryan and coworkers demonstrated that increases in CO in the mouse increase RBF, with comparable results obtained from infusion of the vasodilator acetylcholine.³¹⁸ Pretreatment with an inhibitor of guanylate cyclase to block acetylcholine reduced the increase in RBF by CORM-A1. In isolated vasoconstricted renal interlobular arteries, CORM-A1-induced vasodilation was attenuated with the guanylate cyclase inhibitor, as observed in vivo. Inhibition of calcium-activated potassium

channels (K_{Ca}) with iberiotoxin completely blocked CORM-A1 vasodilation. Thus, CO released from CORM-A1 increases RBF and decreases vascular resistance by activating guanylate cyclase and opening K_{Ca} channels.³¹⁸

The vascular effects of HO may be related to CO synthesis and are affected by NO release linked to the HO-CO system. Administration of a CO donor into the renal artery of rats increased RBF, GFR, urinary cGMP excretion, and blood carboxyhemoglobin levels.³¹⁹ Inhibition of HO induced acute renal failure, with decreases in RBF, GFR, and cGMP excretion. These effects were nearly eliminated by the addition of a CO donor, which also decreased renal cortical NO concentration, urinary excretion of nitrates and nitrites, and urinary cGMP excretion and increased blood carboxyhemoglobin levels. Inhibition of renal HO resulted in acute renal failure, characterized by a large drop (~77%) in RBF and GFR (~93%). Supplementing HO inhibition with CO donor administration reversed the effects of HO inhibition on RBF and GFR, suggesting that the deleterious effects of HO on RBF and GFR were caused by the inhibition of CO. HO inhibition also decreased cortical NO concentration and increased urinary nitrate and/or nitrite excretion of the HO-CO system, whereas a CO donor increased renal NO levels and decreased nitrate and nitrite excretion. These results have suggested that changes in NO release contribute to the renal effects of the HO-CO system.³¹⁹

Administration of heme decreases vascular resistance and increases RBF and sodium excretion, excretion of 6-keto-PGF 1α , and the concentration of CO in renal cortical microdialysate. Pretreatment with an inhibitor of HO blunted heme-induced renal vasodilation and increased RBF. Pretreatment with sodium meclofenamate blunted the renal vasodilatory effect of heme, suggesting that heme-induced renal vasodilation is cyclooxygenase-dependent, yielding increased synthesis of PGI 2 .

Hydrogen Sulfide

A growing body of evidence has shown that H $_2$ S, an endogenous bioactive gas synthesized in nearly all organs, plays an important role in the regulation of kidney function. H $_2$ S generation by kidney cells is reduced in acute and chronic disease states, and H $_2$ S donors ameliorate injury³²⁰ but, under some conditions, H $_2$ S may lead to kidney injury.³²¹ H $_2$ S is produced by cystathione beta-synthase (CBS) and cystathione gamma-lyase (CGL) by the transsulfuration of homocysteine.^{322,323} Incubation of renal tissue homogenates with L-cysteine as a substrate yields H $_2$ S. This response was prevented by inhibitors of both CBS and CGL in combination, whereas either inhibitor alone induced only a small decrease in H $_2$ S.³²²

H $_2$ S plays a role in renal hemodynamics, as shown by the effects of intrarenal infusion of a donor of H $_2$ S (NaHS), which increased renal blood flow and GFR, as well as urinary sodium and potassium excretion. Infusion of L-cysteine also increases endogenous H $_2$ S production.³²² Simultaneous infusion of both an inhibitor of CBS and CGL to decrease H $_2$ S production decreased GFR and sodium and potassium excretion, but either inhibitor alone did not affect these renal functions.³²² H $_2$ S causes endothelium-dependent/cytochrome P450-dependent vasodilation and vascular smooth muscle hyperpolarization of small arterial vessels, increasing ryanodine-mediated Ca $^{2+}$ release through the activation of

large conductance calcium activated potassium channels, causing membrane hyperpolarization and vasodilation.³²⁴ The involvement of cGMP-dependent protein kinase-I in H₂S-induced vasorelaxation was shown in preconstricted aortic rings, with or without intact endothelium.³²⁵ Treatment of the aortic rings with NaHS (an H₂S donor) indicated that a cGMP-dependent protein kinase (PKG) is activated by H₂S. Incubation with a PKG-1 inhibitor blocked NaHS-stimulated vasodilation.³²⁵ NaHS-induced vasorelaxation was reduced by removal of the endothelium and by inhibitors of either NO or cGMP production.³²⁶ H₂S also relaxes smooth muscle by activating ATP-sensitive potassium channels.³²⁷

Increases in TGF-β1 are associated with the development of tubulointerstitial fibrosis and glomerular sclerosis in other renal diseases and are mediated, at least in part, by Ang II. Ang II- and transforming growth factor beta 1 (TGF-β1)-induced renal tubular epithelial-mesenchymal transition (EMT) plays a pivotal role leading to renal sclerosis. One study has demonstrated that Ang II stimulates EMT in renal tubular epithelial cells by increasing the level of α-smooth actin and decreasing E-cadherin.³²⁸ This effect was blocked by a TGF-β receptor kinase inhibitor. Ang II stimulated TGF-β activation and exogenous TGF-β1-induced EMT. The H₂S donor NaHS blocked the promotion of EMT by Ang II and TGF-β1 and reduced TGF-β activity. H₂S cleaves the disulfide bond in dimeric active TGF-β1, promoting the formation of inactive TGF-β1 monomer.³²⁸ These results have suggested the potential to treat sclerosis in the kidney (both glomerular sclerosis and tubulointerstitial fibrosis), as well as other diseases associated with fibrosis and TGF-β1 (e.g., pulmonary fibrosis) by stimulating H₂S or using another means to form the inactive TGF-β1 monomer.

REACTIVE OXYGEN SPECIES

Reactive oxygen species (ROS) are products of a one-electron reduction of dioxygen (oxygen gas, O₂) to form the anionic form of O₂, superoxide, O₂⁻. Superoxide is generated by the catalytic actions of oxidative enzymes, such as nicotinamide adenine dinucleotide (NADH)/reduced NADPH oxidase (NOX) and cytochrome oxidase.^{2,35} Superoxide is toxic and organisms creating O₂⁻ have developed isoforms of superoxide dismutase (SOD), which catalyzes the conversion of superoxide to hydrogen peroxide (H₂O₂). Other enzymes degrade H₂O₂, protecting against the deleterious actions of this ROS.^{2,35} ROS are produced in the kidney by endothelial cells, epithelial cells, vascular smooth muscle cells, mesangial cells, podocytes, and other cell types and have effects on the kidney vasculature.³²⁹

Normally, oxidative and antioxidative enzymes in the kidney yield a balanced production of NO and the superoxide anion. ROS are formed in the arteries, arterioles, glomeruli, and juxtaglomerular apparatus and other nephron segments, and the oxidases NOX 1, 2, and 4, NOS, and COX are also found in the kidney.^{2,35} In the renal vasculature, NOX 1 and NOX 2 produce O₂⁻, whereas NOX 4 in epithelial cells produces H₂O₂. Superoxide dismutase converts superoxide to H₂O₂; catalase and glutathione peroxidase degrade H₂O₂.

Stimulants of O₂⁻ production include Ang II,^{330–332} endothelin,³³³ norepinephrine,² TGF-β1,³³⁴ and stretch of vascular walls by increased intravascular pressure.^{335,336} Ang II activates NADPH oxidases in afferent arterioles to form O₂⁻, leading to calcium release from intracellular stores by activation of

the inositol triphosphate receptor (IP3R).³³⁰ Superoxide also enhances calcium entry pathways into afferent arterioles through L-type channels by membrane depolarization.³³⁷ NOX2 NADPH oxidase is activated by Ang II, promoting the generation of ROS, which scavenge NO and cause subsequent NO-deficiency.³³¹ O₂⁻ and H₂O₂ activate different signaling pathways in vascular smooth muscle cells linked to discrete membrane channels, with opposite effects on membrane potential and voltage-operated Ca²⁺ channels, and therefore have opposite effects on myogenic contractions.³³⁵

Increased perfusion pressure and Ang II increase O₂⁻ production and increase myogenic responses in arterioles of superoxide gene-deleted mice compared with controls.³³⁸ In the macula densa of blood-perfused juxamedullary nephrons, O₂⁻ was undetectable in control normotensive mice, but was markedly elevated in Ang II-induced hypertensive animals. NO was found in the macula densa of control mice but was undetectable in the macula densa of hypertensive animals.³³⁹ These data suggest that under normal conditions, NO generated in the macula densa reduces tubuloglomerular feedback sensitivity, but in Ang II-induced hypertension, the TGF response is augmented by O₂⁻ generated by the macula densa.³³⁹ Increased perfusion pressure causes vascular O₂⁻ production from NADPH oxidase, enhancing myogenic contractions independently of NO, whereas H₂O₂ impairs pressure-induced contractions but is not involved in the normal myogenic response.³⁴⁰

In the remnant kidney model, COX-2 is induced, leading to activation of thromboxane prostanoid receptors (TP-Rs), which enhance ET-1, ROS generation, and contractions.³³³ Compared with controls, diabetic mouse afferent arterioles also have increased production of O₂⁻ and H₂O₂ and enhanced responses to ET-1. These responses are accompanied by reduced protein expression and activities for catalase and superoxide dismutase-2. ET-1 further increases O₂⁻, whereas H₂O₂ is unchanged by ET-1. Increased ROS in diabetes (notably H₂O₂) contributes to the enhanced arteriolar responses to ET-1.³⁴¹ TGF-β1, a growth factor involved in glomerular and tubular injury in diabetes, blocks autoregulation of afferent arterioles, an effect prevented with an ROS scavenger or an NADPH oxidase inhibitor. In smooth muscle cells, TGF-β1 stimulated ROS formation that was inhibited by NADPH oxidase inhibitors.³³⁴

In afferent arterioles from rats with spontaneous hypertension, pressure-induced increases in ROS were four times greater in SHR than in WKY rats. Both a scavenger of O₂⁻ and an NOX2-based (NADPH oxidase) inhibitor attenuated pressure-induced constriction in SHR vessels but not in WKY. Thus, NOX2-derived O₂⁻ may contribute to an enhanced myogenic response in SHR afferent arterioles.³⁴² Of note, arterioles from rats with ischemia-reperfusion injury had a 38% increase in H₂O₂, which could act to buffer the effect of Ang II and be a protective mechanism.³⁴³

Endothelin

Endothelin is a potent vasoconstrictor agent derived primarily from vascular endothelial cells.³⁴⁴ There are three distinct genes for endothelin, each encoding distinct 21-amino acid isopeptides, ET-1, ET-2, and ET-3.^{344–346} Proteolytic cleavage of a 212-amino acid preproendothelin by furin yields a 38- to 40-amino acid proendothelin, which in turn is cleaved by endothelin-converting enzyme to yield endothelin

peptides.^{347,348} ET-1, the primary endothelin produced in the kidney, is formed in arcuate arteries and veins, interlobular arteries, afferent and efferent arterioles, glomerular capillary endothelial cells, glomerular epithelial cells, and glomerular mesangial cells.^{349–360} ET-1 acts in an autocrine or paracrine fashion, or both,³⁶¹ to alter a variety of biologic processes in these cells. Endothelins are potent vasoconstrictors, and the renal vasculature is highly sensitive to these agents.³⁶² Once released from endothelial cells, endothelins bind to specific receptors on vascular smooth muscle, the ET_A receptors that bind both ET-1 and ET-2.^{361,363–366} ET_B receptors are expressed in the glomerulus on mesangial cells and podocytes and have equal affinity for ET-1, ET-2, and ET-3.^{365,366} There are two subtypes of ET_B receptors, the ET_{B1} linked to vasodilation and the ET_{B2} linked to vasoconstriction.³⁶⁷ An endothelin-specific protease modulates endothelin levels in the kidney.^{368–370}

Endothelin production is stimulated by physical factors, including shear stress and vascular stretch.^{371,372} A variety of hormones, growth factors, and vasoactive peptides increase endothelin production, including TGF-β, platelet-derived growth factor, tumor necrosis factor-α, Ang II, arginine vasopressin, insulin, bradykinin, thromboxane A2, and thrombin.^{349,353,355,359,373–376} Endothelin production is inhibited by atrial and brain natriuretic peptides acting through a cGMP-dependent process^{368,377} and by factors that increase intracellular cAMP and protein kinase A activation, such as β-adrenergic agonists.³⁵⁵ ATP-binding renal purinergic (P2) receptors may regulate ET-1 production.³⁷⁸

Intravenous infusion of ET-1 induces a marked, prolonged pressor response^{344,379} accompanied by increases in preglomerular and efferent arteriolar resistances and a decrease in RBF and GFR, without changes in fractional Na excretion.³⁷⁹ As shown in Fig. 3.23, infusion of subpressor doses of ET-1 decreases SNGFR, Q_A, and whole-kidney RBF and GFR,^{380–384} accompanied by increases in preglomerular and postglomerular resistances and filtration fraction.^{380,382,385} Vasoconstriction of afferent and efferent arterioles by endothelin has been confirmed in the split hydronephrotic rat kidney preparation^{386,387} and in isolated perfused arterioles.^{301,388,389} Endothelin also causes mesangial cell contraction.^{346,390} The vasoconstrictor effects of the endothelins can be modulated by several factors,^{364,391} including NO,^{301,392} bradykinin,³⁹³ prostaglandin E2,³⁹⁴ and prostacyclin.^{394,395} The endothelin pathways demonstrate significant sexual dimorphisms that may affect the progression of renal disease and treatment choices.³⁹⁶

The ET_A and ET_B receptors have been cloned and characterized.^{366,397,398} ET_A receptors are abundant on vascular smooth muscle, have a high affinity for ET-1, and play a prominent role in the pressor response to endothelin.³⁹⁹ ET_B receptors are present on endothelial cells, where they may mediate NO release and relaxation.³⁹⁸ Both ET_A and ET_B receptors are expressed in the media of interlobular arteries and afferent and efferent arterioles. Only ET_A receptors are present on vascular smooth muscle cells of interlobar and arcuate arteries.⁴⁰⁰ There is strong labeling of ET_B receptors on peritubular and glomerular capillaries, as well as the vasa

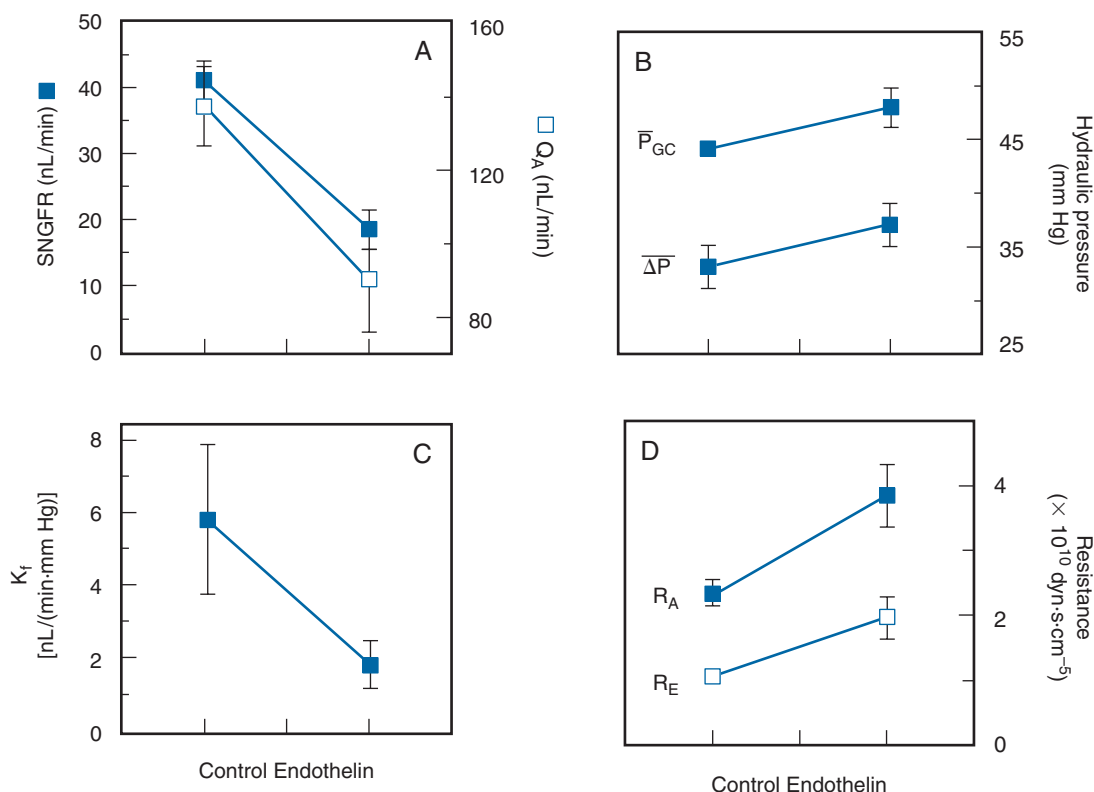


Fig. 3.23 (A–D) Effects of intravenous administration of endothelin (subpressor dose) on glomerular dynamics. K_f, Filtration coefficient; ΔP, mean transcapillary pressure gradient; P_{GC}, mean glomerular capillary pressure; Q_A, single-nephron glomerular plasma flow; R_A, afferent arteriolar resistance; R_E, efferent arteriolar resistance; SNGFR, single-nephron glomerular filtration rate. (Data [mean ± SE] obtained in Munich-Wistar rats from Badr KF, et al. Mesangial cell, glomerular and renal vascular responses to endothelin in the rat kidney. Elucidation of signal transduction pathways. *J Clin Invest.* 1989;83(1):336–342.)

recta endothelium.⁴⁰⁰ ET_A receptors are evident on glomerular mesangial cells and pericytes of descending vasa recta bundles.⁴⁰⁰ Endogenous endothelin may actually dilate the afferent arteriole and lower K_f via ET_B receptors.⁴⁰¹

ET_A receptor antagonists may be useful for patients with diabetic nephropathy.⁴⁰² These ET_A receptor antagonists have been shown to reduce albuminuria in diabetic nephropathy, although the albuminuria returns on cessation of the drug. It has been used alone and in conjunction with renin-angiotensin blockade.^{403,404} However, ET_A receptor antagonists have been associated with edema and heart failure, so patients already manifesting these conditions should be excluded from this type of medication.⁴⁰⁵

Endothelin stimulates the production of vasodilatory prostaglandins,^{383,392,395,406,407} yielding a feedback loop to dampen the vasoconstrictor effects of endothelin. ET-1, ET-2, and ET-3 also stimulate NO production in the arterioles and glomerular mesangium via activation of the ET_B receptor.^{270,272,301,392,408} Resistance in the renal and systemic vasculature is markedly increased during inhibition of NO production. There is a dynamic interrelationship between NO and endothelin effects, so that ET_A blockade or inhibition of endothelin-converting enzyme leads to increased renal resistance caused by NO inhibition.^{409,410} The vasoconstrictive effects of Ang II may be mediated, in part, by stimulation of ET-1 production, which acts on ET_A receptors to produce vasoconstriction.^{373,376} Chronic administration of Ang II reduces renal blood flow, an effect reduced by a mixed ET_A-ET_B receptor antagonist, suggesting that endothelin contributes to the renal vasoconstrictive effects of Ang II.³⁷³

Blood flow through the renal medulla is influenced by ET-1 as well as by Ang II, norepinephrine, nitric oxide, and vasodilatory prostaglandins. Medullary vasodilation measured by laser Doppler techniques was seen to occur at low doses of endothelin when cortical blood flow was decreased.⁴¹¹ An ET_A receptor antagonist blocked cortical vasoconstriction by ET-1 but failed to prevent medullary dilation. The endothelin-induced medullary vasodilation was blocked by an ET_{A/B} receptor antagonist and was mimicked by an ET_B receptor agonist. Inhibition of NO completely blocked the endothelin-induced vasodilation of medullary blood flow, and inhibition of prostaglandins attenuated the response. These results have indicated that endothelin causes cortical vasoconstriction mediated by ET_A receptors, whereas activation of ET_B receptors causes medullary vasodilation mediated by the release of NO.⁴¹¹

Medullary blood flow occurs through vasa recta capillaries, and most regions of the vasa recta are covered by pericytes capable of vasoconstriction. The role of these pericytes in controlling blood flow through the vasa recta has been examined with confocal microscopy and pericyte-mediated vasoconstriction and vasodilation were visualized. Ang II, endothelin, and norepinephrine all caused vasoconstriction at pericyte locations.⁴¹² These effects were attenuated by an NO donor and enhanced with inhibitors of NO production or inhibition of prostaglandin release by nonselective cyclooxygenase inhibition with indomethacin. Because of the narrow diameter of the vasa recta (normally, ~10 µm), constriction of pericytes can cause impairment of the movement of red cells and hence blood flow through the medulla. These results suggest an important role for pericytes in the control of the medullary circulation.⁴¹²

ROLE OF THE RENIN-ANGIOTENSIN-ALDOSTERONE SYSTEM IN THE CONTROL OF RENAL BLOOD FLOW AND GLOMERULAR FILTRATION RATE

The RAS exerts major autocrine, paracrine, and endocrine functions regulating RBF and GFR. As presented in detail in several recent reviews,^{2,35,55,83} renin is a proteolytic enzyme synthesized, stored, and released from the kidney, and also synthesized in the liver. In the kidney, it is synthesized and secreted primarily by the granulated epithelioid cells of the JGA adjacent to the terminal portion of the afferent arteriole; renin is also formed in the proximal tubules and in the principal cells of the connecting tubule and collecting duct.^{2,35,413–415} Renin release from the kidneys is stimulated by a decrease in sodium intake, a reduction in extracellular fluid volume and blood volume, a decrease in arterial blood pressure, and increased sympathetic nerve activity.⁴¹⁶ Renin cleaves a decapeptide, angiotensin I (Ang I) from angiotensinogen, a glycoprotein formed in the proximal tubules of the kidney⁴¹⁵ and the liver. Circulating angiotensinogen is present in the α₂-globulin fraction of plasma. Subsequent conversion of Ang I by angiotensin-converting enzyme (ACE), identical to kininase II, yields the octapeptide Ang II. ACE is present in many tissues, including lung. In the kidney, it is bound to the luminal sides of endothelial cells of blood vessels and tubular cells, including the brush border of the proximal tubule. All components needed for the production and degradation (the latter by angiotensinase A) of Ang II are present in the immediate region of the juxtaglomerular region of the nephron, allowing direct local regulation of glomerular blood flow and filtration rate.^{35,55}

Ang II is a potent vasoconstrictor, and numerous studies have demonstrated that preglomerular vessels, including the arcuate arteries, interlobular arteries, and afferent arterioles, as well as the postglomerular efferent arterioles, constrict in response to exogenous and endogenous Ang II.^{144,174,303,389,417,418}

Some studies have indicated that efferent arterioles have a greater sensitivity to Ang II, whereas others have shown similar effects on both afferent and efferent arterioles.^{35,144,303,389,418} Fig. 3.24 shows the effects of Ang II on diameters in these vessels. As shown in Fig. 3.24, both L-type and T-type Ca⁺⁺ channels are involved in the afferent arteriolar responses to Ang II while the T-type Ca⁺⁺ channels are predominate at the efferent arterioles.^{522,523} In addition to constricting vascular smooth muscle cells, Ang II increases myocardial contractility, stimulates aldosterone release, increases salt appetite and thirst, and helps regulate sodium transport by the kidney tubules and intestine.⁴¹⁹ The overall effect of Ang II is to minimize renal fluid and sodium losses and maintain extracellular fluid volume (ECFV) and arterial blood pressure.⁴¹⁶

There are two major classes of Ang II receptors, AT1 and AT2, but the hypertensinogenic and vasoconstrictive actions of Ang II are primarily due to the AT1 receptor, which is widely distributed throughout all segments of the renal microvasculature in the cortical and medullary circulatory beds and are also present in the glomeruli, including mesangial cells, glomerular capillary endothelial cells, and podocytes.^{35,83,420} In rodents, afferent arterioles have both AT1a and AT1b receptors, whereas efferent arterioles have only AT1a receptors.^{420,421} AT1 receptors are also present in the proximal and distal tubules, loop of Henle and macula densa

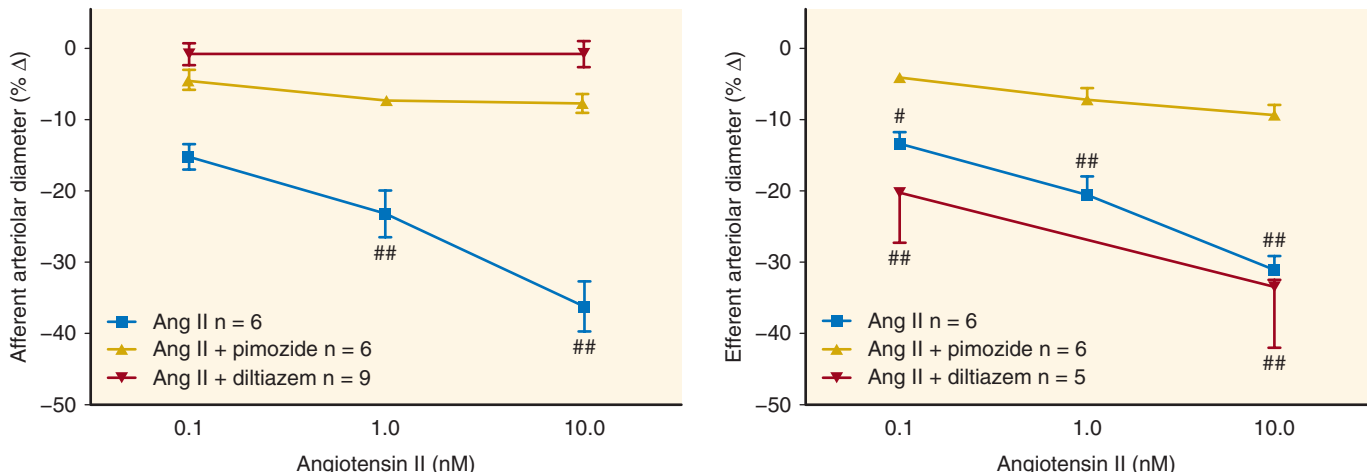


Fig. 3.24 Role of L- and T-type Ca^{2+} channels in angiotensin II (Ang II)-mediated afferent and efferent arteriolar vasoconstriction. Ang II constricts both afferent and efferent arterioles. The vasoconstrictor effects of Ang II on afferent arterioles are blocked by both L-type and T-type Ca^{2+} channel blockers. In contrast, the efferent vasoconstrictor effects of Ang II are not blocked by L-type Ca^{2+} channel blockers, but are blocked by T-type Ca^{2+} channel blockers.^{35,522,523} (From Carmines PK, Navar LG. Disparate effects of Ca channel blockade on afferent and efferent arteriolar responses to Ang II. *Am J Physiol Renal Physiol.* 1989;256(6 Pt 2):F1015–F1020; Feng MG, Navar LG. Angiotensin II-mediated constriction of afferent and efferent arterioles involves T-type Ca^{2+} channel activation. *Am J Nephrol.* 2004;24(6):641–648.)

cells, cortical and medullary collecting ducts, glomerular podocytes, and mesangial cells.⁴¹⁹

The vasoconstrictor effects of Ang II are blunted by the endogenous production of vasodilators including NO, cyclooxygenase, and cytochrome P450 epoxigenase metabolites in the afferent but not the efferent arterioles.^{140,144,303,311,422–425} Ang II-simulated release of NO in the afferent arterioles occurs through activation of the AT1 receptors.^{307,426} Ang II increases the production of prostaglandins (both PGE2 and PGI2) in afferent arteriolar smooth muscle cells, and PGE2, PGI2, and cAMP all blunt Ang II-induced calcium entry into these cells,⁴²³ potentially explaining, at least in part, the different effects of Ang II on vasoconstriction of the afferent and efferent arterioles.^{422,423} In contrast to effects on the afferent arteriole, PGE2 had no effect on Ang II-induced vasoconstriction of the efferent arteriole.¹⁴⁰ The effects of PGE2 on Ang II-induced vasoconstriction of the afferent arteriole are concentration-dependent, with low concentrations acting as a vasodilator via interaction with prostaglandin EP4 receptors and high concentrations of PGE2 acting on prostaglandin EP3 receptors to restore the Ang II effects in that segment.¹⁴⁰ Ang II infusion alone produces decreases in renal blood flow, with lesser effects on GFR resulting in an increase in filtration fraction.³⁵ However, when combined with cyclooxygenase inhibition, Ang II causes marked reductions in SNGFR and Q_A , suggesting an important role for endogenous vasodilatory prostaglandins in ameliorating the vasoconstrictor effects of Ang II.⁴²⁷ Because Ang II increases renal production of vasodilatory prostaglandins, this serves as a feedback loop to modulate the vasoconstrictor effects on Ang II under chronic conditions when the RAAS is stimulated.⁸³

Ang II decreases K_f ⁴²⁷ and contracts mesangial cells.⁴²⁸ One possible cause for the changes in K_f is that contraction of the mesangial cells reduces effective filtration area by blocking flow through some glomerular capillaries, but no direct evidence has been obtained to support this hypothesis. Alternatively, Ang II might decrease hydraulic conductivity,

rather than or as well as reducing the surface area available for filtration, thereby reducing K_f .⁴²⁹ Glomerular epithelial cells possess both AT1 and AT2 receptors and respond to Ang II by increasing cAMP production, suggesting a possible role for these cells in reducing K_f .⁴³⁰ Alterations in epithelial structure or the size of the filtration slits, however, have not been detected following infusion of Ang II at a dose sufficient to decrease GFR and K_f .⁴³¹

The vasoconstrictive effect of Ang II on glomerular mesangial cells is markedly reduced by NO. Release of NO from endothelial cells stimulated by bradykinin increases cGMP production in co-incubated mesangial cells. Comparable results were obtained when mesangial cells were incubated with NO alone.²⁶² Ang II alone caused constriction of the mesangial cells, but this effect was largely eliminated when the cells were co-incubated with both Ang II and NO. These studies suggest that local NO production from endothelial cells can modify the effects of Ang II on glomerular mesangial cells.²⁶² Glomerular epithelial cells contain Ang II receptors and, together with mesangial cells, may play an important role in Ang II-mediated control of the glomerular filtration barrier.⁴³⁰

Blockade of the AT1 receptors caused a dose-dependent dilation when Ang II was added to the lumen or bath of isolated afferent arterioles preconstricted by norepinephrine. This effect was blocked by pretreatment with an AT2 receptor antagonist, suggesting that activation of the AT2 causes vasodilation of afferent arterioles. Disruption of the endothelium or simultaneous inhibition of the cytochrome P450 pathway also abolished the vasodilation by Ang II. Thus, activation of AT2 receptors may cause endothelium-dependent vasodilation via a cytochrome P450 pathway, counteracting the vasoconstrictor effects of Ang II at AT1 receptors.^{432,433}

As indicated, Ang II produces prohypertensive and renal vasoconstrictor effects via the activation of AT1 receptors, whereas activation of AT2 receptors results in modest vasodilation.^{35,433} Several metabolic fragments of the octapeptide

Ang II, once believed to be inactive, have now been shown to have physiologic effects on the kidney, often opposing the actions of Ang II. The related peptide, Ang 1-7, has been shown to induce vasodilation of preconstricted renal arterioles.⁴³⁴ These effects of Ang 1-7 occur independently of binding to AT1 or AT2 receptors and appear to involve activation of the G protein–coupled Mas receptor,⁴³⁵ which has been shown to be expressed on the afferent arteriole.⁴³⁶ In addition, an isoform of ACE, known as “ACE2,”^{437,438} is involved in the formation of Ang 1-7.⁴³⁹ Ang 1-7, ACE2, and the Mas receptor have all been detected in the kidney. The balance between opposing actions of the vasoconstrictor peptide, Ang II, and the vasodilator peptide, Ang 1-7, may be influenced by the ratio of ACE to ACE2 and AT1 to Mas receptor content in specific vascular regions (and tubular segments) of the kidney. Cardiovascular and renal diseases may involve an imbalance of these peptides, enzymes, or receptors.⁴³⁶

Additional mechanisms involved in Ang II-induced hypertension have been proposed. The principal cells of the connecting tubule and collecting duct express prorenin receptors and produce renin, which, coupled with delivery of angiotensinogen from the proximal tubule,⁴¹⁴ allows for the local formation of Ang I.^{2,413,433} Luminal ACE in the collecting duct is then available to produce Ang II, which in turn can increase sodium reabsorption by enhancing activity of ENaC and other transporters in the collecting duct, an effect that may be important in the progression of diabetes and Ang II-induced hypertension.^{413,414,433,440}

ROLE OF ANGIOTENSIN II IN GLOMERULAR AND TISSUE INJURY

Chronic renal failure is characterized by a progressive decline in renal function, with glomerular and tubular injury and systemic hypertension. An important demonstration of an elevation of glomerular hydraulic pressure in kidney disease was in a model of nephrotoxic serum nephritis (NSN),⁴⁴¹ where Ang II is thought to have a key role in the renal complications that develop. Intravenous infusion of Ang II increases P_{GC} and ΔP in rats with reduced renal mass.⁴⁴² In the remnant kidney model of renal failure, inhibition of Ang II production by an ACE inhibitor lowered P_{GC} and ΔP toward normal and prevented proteinuria and glomerular injury.⁴⁴³ Over the last 30 years, the efficacy of blockade of the RAAS with ACE inhibitors and/or Ang II type 1 receptor antagonists (angiotensin receptor blockers [ARBs]) in limiting or slowing the progression of some types of kidney disease has been established.⁴⁴⁴ ACE inhibitors and ARBs also are effective in the treatment of spontaneous glomerulosclerosis associated with aging.^{445,446} Both ACE inhibitors and ARBs prevented hypertension, limited proteinuria, and ameliorated sclerosis in several experimental models of glomerulonephritis.⁴⁴⁷ In one study, ACE inhibition was suggested to promote regeneration of new renal tissue.⁴⁴⁸ Similarly, in the remnant kidney model of renal disease, there is evidence that chronic treatment with an ACE inhibitor causes reversal of renal injury.⁴⁴⁹

Accumulation of extracellular matrix proteins, including collagen and fibronectin, leads to glomerular and tubular injury.⁴⁵⁰ Enhanced production of TGF-β1 in the remnant kidney increases matrix formation by stimulating the production of TGF-β1. Administration of a neutralizing antibody or an Ang II receptor antagonist reduces plasma TGF-β1 levels and

blood pressure toward normal.⁴⁵¹ ACE inhibition in the obese Zucker rat has significantly reduced proteinuria compared with untreated obese animals, downregulated expression of nephrin, and decreased expression of TGB-β1, collagen IV, and fibronectin.⁴⁵² Similarly, in an animal model of myocardial infarction (MI), rats with MI had significant renal injury, and treatment by ACE inhibition exerted beneficial effects.⁴⁵³

Ang II induces upregulation and activation of a transcription factor called “sterol-responsive element-binding protein” (SREBP-1), leading to upregulation of TGF-β1 and increased production of matrix collagen and fibronectin.⁴⁵⁰ An ARB prevented the increase in TGF-β1 formation and the induction of SREBP-1. Inhibition of SREBP-1 prevented Ang II-induced glomerular upregulation of TGF-β1 and matrix synthesis, demonstrating a significant role of the transcription factor in glomerular injury and indicating that TGF-β1 plays a role in the stimulation of matrix production.⁴⁵⁰ SREBP-1 upregulation is observed in diabetic kidneys; SREBP-1 is activated by high glucose levels and mediates profibrogenic responses in primary rat mesangial cells.⁴⁵⁴ In these cells, high glucose levels activated SREBP-1, which binds to the TGF-β1 promoter, resulting in TGF-β1 upregulation.⁴⁵⁴

Treatment with an ARB in rats with NSN protected against interstitial inflammation, tubular degeneration, and segmental glomerulosclerosis.⁴⁵⁵ NSN rats were treated with pirfenidone (an antifibrotic, antiinflammatory compound first used to treat pulmonary fibrosis) or with pirfenidone plus an ARB. Pirfenidone alone yielded a decrease in proteinuria and the ARB a slightly greater decrease; the two together had additive effects on proteinuria, interstitial inflammation, tubular degeneration, and segmental glomerulosclerosis.⁴⁵⁵ Transgenic mice overexpressing active renin from the liver develop progressive pulmonary fibrosis, much like that seen in humans with pulmonary fibrosis. There was increased extracellular matrix deposition of fibronectin and collagens and increased production of TGF-β1 and connective tissue growth factor (CTGF).⁴⁵⁶ Two weeks of treatment with a renin inhibitor or an ARB reduced production of TGF-β1 and CTGF and decreased deposition of matrix proteins.

ARACHIDONIC ACID METABOLITES REGULATING RENAL BLOOD FLOW AND GLOMERULAR FILTRATION RATE

The processing of the essential polyunsaturated fatty acid, linoleic acid, in the liver yields the polyunsaturated fatty acid arachidonic acid, which is stored in membrane phospholipids. Biologically active eicosanoids, C20 metabolites of arachidonic acid, are produced by three primary enzymatic pathways, including the following: cyclooxygenase-generating prostaglandins (PGs) and thromboxanes (TBXs); lipoxygenase (OX) yielding leukotrienes (LTs) and HETEs; and cytochrome P450 pathways synthesizing HETEs and EETs. Arachidonic acid (AA) is released from cell membranes, predominantly by phospholipase A2 (PLA2).^{457–461} These eicosanoids regulate the renal microcirculation, in part by activating G protein–coupled receptors in the endothelium and vascular smooth muscles.^{458,462}

Prostaglandins

Following the interaction of various hormones and vasoactive substances with their membrane receptors, PLA2 is activated, resulting in the release of AA from the cell membranes. This

allows the enzymatic action of cyclooxygenase to process AA into prostaglandins—PGG2 and subsequently PGH2. PGH2 is then converted into a number of biologically active prostaglandins, including PGE2, prostacyclin (PGI2), PGF α , PGE1, PGD2, and thromboxane (TxA2). Prostaglandins play important roles in healthy and diseased kidneys.^{93,463–466} PGE2 receptors are the most abundant prostaglandin receptors in the kidney. The effects of PGE2 on the kidneys depend on the location of the receptor subtype and interaction with other active compounds. PGE2 activates at least four receptors, EP1 to EP4. Prostaglandin EP1 receptor activation results in contractile effects in smooth muscle through the Gq alpha protein linkage, whereas EP2 and EP4 are relaxant via the Gs alpha subunit. EP3 is an inhibitory receptor (Gi alpha), decreasing cAMP, which causes vasoconstriction.^{35,463,464}

In the kidneys, PGE1, PGI2, and PGE2 are vasodilator prostaglandins that generally increase renal plasma flow yet produce little or no increase in GFR and SNGFR, in part due to a decline in K_r.^{93,464–466} TxA2 generally results in contraction of the glomerular mesangial cells via the Gq alpha subunit. During blockade of endogenous prostaglandin production, infusion of PGE2 or PGI2 decreases SNGFR and Q_A, accompanied by an increase in renal vascular resistance (particularly R_E), increases in P_{GC} and ΔP, and a decline in K_r.⁴⁶⁷ Additional blockade of Ang II receptors during cyclooxygenase inhibition results in vasodilation in response to PGE2 or PGI2, resulting in a return of SNGFR and Q_A equal to or more than control values, a fall in P_{GC} below control values, and a return of K_r to normal.⁴⁶⁷ Thus, the renal vasoconstriction induced by exogenous PGE2 or PGI2 appears to be mediated by induction of renin and Ang II production.

Vasodilation at the whole-kidney level resulting from PGI2 infusion during cyclooxygenase and Ang II inhibition has not always been observed.⁴⁶⁸ Topical application (but not luminal) of PGE2 to the afferent arteriole increased the vasoconstrictive effect of Ang II and norepinephrine, whereas PGI2 only attenuated norepinephrine-induced vasoconstriction.⁴⁶⁹ PGE2 also constricted interlobular arteries but neither prostaglandin produced vasodilation of vessels preconstricted by Ang II.⁴⁶⁹ Indomethacin alone induced vasoconstriction of preglomerular and postglomerular resistance vessels of superficial and juxamedullary nephrons, indicating that vasodilatory prostaglandins normally modulate endogenous vasoconstrictors.⁴⁷⁰ However, there appears to be gender-dependent differences in mechanisms, because indomethacin treatment results in net renal vasodilation in female rats.⁴⁷¹ The combination of cyclooxygenase inhibition with an ACE inhibitor caused vasodilation of preglomerular but not postglomerular vessels of the cortical nephrons due to the effects of continued NO production in the preglomerular vessels.⁴⁷⁰ Additionally, the PGE2 EP3 receptor regulates COX-2 through a negative feedback loop in the thick ascending limb of the loop of Henle.⁴⁷² These data, taken together, indicate that differences in the response to vasoactive prostaglandins between superficial and deep nephrons may be due to prostaglandin receptor subtypes and cyclooxygenase activity.

Leukotrienes and Lipoxins

Leukotrienes are a class of lipid products formed from AA via the lipoxygenase pathway. Leukotrienes that affect glomerular

filtration and renal blood flow are leukotriene C4 (LTC4), leukotriene D4 (LTD4), and leukotriene B4 (LTB4). LTC4 and LTD4 are potent vasoconstrictors,⁴⁷³ whereas LTB4 produces moderate renal vasodilation and an increase in RBF, with no change in GFR in the normal rat.⁴⁷⁴ Intravenous infusion of LTC4 increases renal vascular resistance, leading to a decrease in RBF and GFR, as well as a decrease in plasma volume and cardiac output.^{475,476} The decline in RBF is diminished by saralasin, an Ang II receptor antagonist, and indomethacin, an inhibitor of cyclooxygenase, indicating the involvement of Ang II and cyclooxygenase products in the response to LTC4, as well as a direct effect of LTC4 on the renal resistance vessels.⁴⁷⁵ Similarly, LTD4 decreased K_r, but increased renal vascular resistance, particularly, R_E, a fall in Q_A and SNGFR, and a rise in P_{GC} and ΔP during blockade of Ang II and control of renal perfusion pressure, demonstrating a direct effect of this leukotriene on renal hemodynamics.⁴⁷⁷ Leukotrienes often mediate drug-associated nephrotoxicity in some models of kidney disease.⁴⁷⁸

Inflammatory injury also activates the 5-, 12-, and 15-lipoxygenase pathways in neutrophils and platelets to form acyclic eicosanoids called lipoxins (LXs), of which there are two main types, LXA4 and LXB4.⁴⁷⁹ LXB4 and 7-cis-11-trans-LXA4 produce renal vasoconstriction.^{478,480} By contrast, intrarenal infusion of LXA4 induces a reduction in preglomerular resistance (R_A) without affecting R_E, thereby resulting in an increase in P_{GC} and ΔP.⁴⁷⁷ The specific vasodilation of the preglomerular vessels by LXA4 was blocked by cyclooxygenase inhibition, indicating that vasodilatory prostaglandins are responsible for this effect.^{477,480} Unique to this compound, LXA4 produced vasodilation while simultaneously causing a reduction in K_r.⁴⁸⁰ Because P_{GC}, ΔP, and Q_A were increased, SNGFR also increased.⁴⁷⁷ Furthermore, transfection of rat kidney with the 15-lipoxygenase gene suppressed inflammation and preserved function in experimental glomerulonephritis.⁴⁸¹ The lipoxins have also been used to treat acute renal failure in mice.^{482,483}

Cytochrome P450

A rapidly growing field of study is that of eicosanoids formed through the cytochrome P 450 (CYP450) monooxygenase pathway. AA is metabolized via the CYP450 enzymes to other active metabolites, including EETs, dihydroxyeicosatetraenoic acids (DiHETEs), and HETEs, which act locally in a paracrine manner.³⁵ Early researchers demonstrated the role of one metabolite, 20-HETE, involved in regulating renal hemodynamics through direct actions, as well as exerting modulatory actions on the TGF mechanism.⁴⁶⁰ In addition to its vascular effects, 20-HETE inhibits sodium transport in the proximal tubule and the thick ascending loop of Henle. 20-HETE elicits an enhancement of myogenic tone and vasoconstricts afferent arterioles, which may be partially mediated through the augmentation of the TGF mechanism.⁴⁸⁴ Blockade of 20-HETE formation attenuated vascular responses to Ang II, endothelin, norepinephrine, NO, and CO.^{222,484} NO inhibits the production of 20-HETE, which contributes to the vasodilatory effect of NO.^{222,460,463,485–487}

In contrast to the contractile responses of 20-HETE, some of the EETs mentioned also formed via the CYP450 pathway are potent vasodilators.^{35,488} EETs are formed locally and serve as both autocrine and paracrine factors. EETs are endothelium-derived hyperpolarizing factors that elicit potent

vasodilation of the afferent arteriole.⁴⁸⁸ These actions are mediated in part by activating large conductance potassium channels.

NEURAL REGULATION OF RENAL CIRCULATION

The renal vasculature, including the afferent and efferent arterioles, macula densa cells of the distal tubule, and glomerular mesangium are richly innervated.^{83,489} Innervation primarily includes renal efferent sympathetic adrenergic nerves^{489,490} and renal afferent sensory fibers containing peptides, including calcitonin gene-related peptide (CGRP) and substance P.^{83,489} Sympathetic efferent nerves are found in all segments of the vascular tree, from the main renal artery to the afferent arteriole (including the renin-containing juxtaglomerular cells) and efferent arteriole.^{489,490} They play an important role in the regulation of renal hemodynamics, sodium transport, and renin secretion.⁴⁹¹ Afferent nerves containing CGRP and substance P are localized primarily in the main renal artery and interlobar arteries, with some innervation also observed in the arcuate artery, interlobular artery, afferent arteriole, and juxtaglomerular apparatus.^{489,490} Peptidergic nerve fibers immunoreactive for neuropeptide Y (NPY), neuropeptid Y, neuropeptid F, vasoactive intestinal polypeptide, and somatostatin are also found in the kidney.⁵⁵ Neuronal NOS-immunoreactive neurons have been identified in the kidney.⁴⁸⁹ The NOS-containing neuronal stromata are seen in the wall of the renal pelvis, at the renal hilus close to the renal artery, along the interlobar arteries, the arcuate arteries, and extending to the afferent arteriole, supporting their role in the control of RBF.⁴⁸⁹ They are also present in nerve bundles that have vasomotor and sensory fibers, suggesting that they modulate renal neural function.⁴⁸⁹

In micropuncture studies of the effects of renal nerve stimulation (RNS), RNS alone increased R_A and R_E , resulting in a decrease in plasma flow and SNGFR, without any effect on K_f .⁴⁹² When prostaglandin production was inhibited by indomethacin, however, the same level of RNS produced even greater increases in R_A and R_E , accompanied by very large declines in plasma flow and SNGFR and decreases in K_f , P_{GC} , and ΔP .⁴⁹² When saralasin was administered as a competitive inhibitor of endogenous Ang II in conjunction with indomethacin, RNS had no effect on K_f , but both R_A and R_E were still increased, and ΔP was slightly reduced.⁴⁹² The release of norepinephrine by RNS enhances Ang II production and results in arteriolar vasoconstriction and reductions in K_f . The increase in Ang II production may then enhance vasodilator prostaglandin production,^{492,493} which partially ameliorates the constriction.

Continued vasoconstriction by RNS during the blockade of endogenous prostaglandins and Ang II has indicated that norepinephrine has vasoconstrictive properties by itself. The findings that norepinephrine causes constriction of preglomerular vessels support the direct effects of norepinephrine on renal microvessels.⁴²² Inhibition of NOS results in a decline in SNGFR in normal rats but not in rats with surgical renal denervation, suggesting that NO normally modulates the effects of renal adrenergic activity.⁴⁹⁴ However, this modulation does not appear to be related to the sympathetic modulation of renin secretion.⁴⁹⁵ Under conditions of renal injury and

inflammation, the effects of increased renal nerve activity are exacerbated.⁴⁹⁶ The actions of increased sympathetic activity to decrease renal cortical perfusion are attenuated by temporally mediated reductions in ROS.⁴⁹⁷

Renal denervation in animals undergoing acute water deprivation (48-hour duration) or with congestive heart failure produces increases in SNGFR, plasma flow, and K_f .⁴⁹⁸ This indicates that the natural activity of the renal nerves in these settings plays an important role in the constriction of the arterioles and reductions in K_f that were observed with water deprivation and in congestive heart failure.⁴⁹⁸ The vasoconstrictive effects of the renal nerves in both settings were mediated in part by a stimulatory effect on Ang II release, together with direct vasoconstrictive effects on the preglomerular and postglomerular blood vessels.⁴⁹⁸ These studies have demonstrated the important role of the renal nerves in pathophysiological settings.

Clinical trials have focused on whether catheter-based renal artery denervation reduces blood pressure in patients with resistant hypertension. Some studies have demonstrated sustained reduction in blood pressure in patients who underwent renal denervation; however, the blood pressure response did not differ from the sham-treated patients at 6 months after treatment.⁴⁹⁹ More recent clinical trials using improved catheters have provided more promising long-term effects.⁵⁰⁰

GLOMERULAR HEMODYNAMICS IN THE AGING KIDNEY

Aging is commonly associated with the progressive development of chronic renal disease characterized by global glomerulosclerosis, tubular atrophy, interstitial fibrosis, and arteriosclerosis. Over 75 years ago, Davies and Shock demonstrated that beyond 40 to 50 years of age, inulin clearance in humans declined approximately 8 mL/min/1.73 m² in each subsequent decade of age.⁵⁰¹ In healthy adult living kidney donors, the prevalence of glomerulosclerosis, followed by local tubular atrophy and interstitial fibrosis, was found to increase progressively from 2.7% for patients aged 18 to 29 years to 73% for patients aged 70 to 77 years.⁵⁰² Despite these changes, the age-related decline in GFR was not fully explained by these age-related histologic changes.^{502,503} Fig. 3.25 shows the declines in GFR beyond the ages of 40 to 50 years.^{83,504–506} Kidney disease associated with aging is generally accompanied by declines in GFR, RPF, and RBF associated with an increase in filtration fraction. In one study, the calculated filtration coefficient, K_f , was lower in older than in younger subjects (4.9 ± 1.7 nL/[min-mm Hg] in older subjects vs 7.0 ± 2.9 nL/[min-mm Hg] in younger subjects).⁵⁰⁷ However, age-related declines in GFR and RBF do not necessarily occur in everyone.^{502,506,508} As shown in Fig. 3.25, associated with the decline in GFR and RBF is the fact that systolic blood pressure increases with age,^{507,509} which may contribute to a further decline in renal function. Nevertheless, in disease-free older individuals, GFR is generally adequate to sustain quality of life (see Fig. 3.25).

Factors likely involved in the decline in renal function associated with aging include eating high-protein meals, which may lead to episodes of hyperfiltration and glomerular capillary hypertension, development of diabetes, with associated

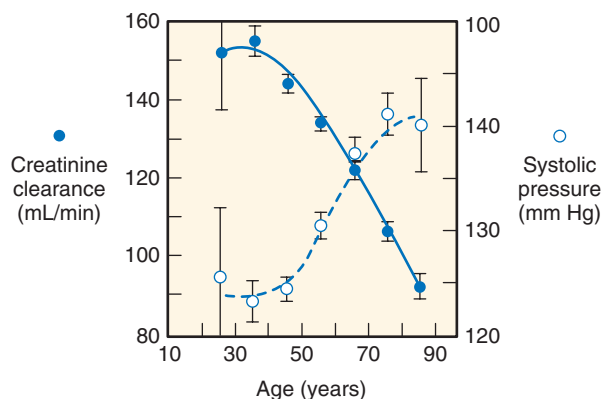


Fig. 3.25 Correlation of aging with systolic blood pressure and creatinine clearance (C_c) in normal adults. (From Lindeman R, Tobin J, Shock N. Association between blood pressure and the rate of decline in renal function with age. *Kidney Int.* 1984;26: 861–868.)

advanced glycosylated end products, obesity, oxidative stress due to chronic exposure to oxygen free radicals, dyslipidemia, excessive exposure to some drugs that reduce renal function, infections, atherosclerotic disease, male gender, genetic and racial differences, and environmental factors.^{506,510–512} Sclerotic glomeruli seen with aging are smaller than functional glomeruli, leading to a decline in average glomerular size. With the progressive loss of filtering glomeruli, unaffected glomeruli undergo compensatory hypertrophy, which helps preserve GFR.⁵⁰² As has been shown in studies of the rat, following removal of 50% to 80% of total renal mass, the remaining nephrons undergo compensatory hypertrophy and increases in SNGFR and glomerular capillary hydraulic pressures.^{14,513,514} In the aging human, progressive loss of functioning nephrons and hypertrophy of remaining filtering units would also result in glomerular capillary hypertension and damage to these remaining nephrons. Because these alterations use renal reserve capacity, there is a reduced capability of the renal vasculature in older individuals to respond to amino acid infusion, so that there is only an increase in GFR and filtration fraction and RPF remains unchanged.^{508,515} In contrast, the vasoconstrictive response to Ang II is identical in younger and older people.⁵¹⁶ These data suggest that there is a blunted renal vasodilatory response but a vasoconstrictive response is maintained in older subjects, indicating that the aged kidney has used reserve capacity and is in a state of compensatory renal vasodilation to compensate for the chronic glomerular injury and loss of functional glomeruli.⁵¹⁵

Complete reference list available at ExpertConsult.com.

KEY REFERENCES

2. Arendshorst W, Navar LG. Renal circulation and glomerular hemodynamics. In: Schrier RW, Coffman TM, Falk RJ, et al, eds. *Schrier's Diseases of the Kidney*. Philadelphia: Lippincott Williams & Wilkins; 2013:74–131.
4. Navar LG, Bell PD, Evan AP. The regulation of glomerular filtration rate in mammalian kidneys. In: Andreoli TE, Hoffman J, Fanestil D, et al, eds. *Physiology of Membrane Disorders*. New York: Plenum Medical Book Co.; 1986:637–667.
5. Smith HW. *The Kidney: Structure and Function in Health and Disease*. Vol 4. New York: Oxford University Press; 1951.
25. Evans RG, Harrop GK, Ngo JP, et al. Basal renal O₂ consumption and the efficiency of O₂ utilization for Na⁺ reabsorption. *Am J Physiol Renal Physiol.* 2014;306(5):F551–F560.
26. Mimura I, Nangaku M. The suffocating kidney: tubulointerstitial hypoxia in end-stage renal disease. *Nat Rev Nephrol.* 2010;6(11): 667–678.
35. Navar LG, Arendshorst WJ, Pallone TL, et al. The renal microcirculation. In: Tuma RF, Duran WN, Ley K, eds. *Handbook of Physiology: Microcirculation*. Vol 2. Academic Press; 2008:550–683.
41. Beeuwkes R 3rd. The vascular organization of the kidney. *Annu Rev Physiol.* 1980;42:531–542.
47. Neal CR, Arkill K, Bell JS, et al. Novel haemodynamic structures in the human glomerulus. *Am J Physiol Renal Physiol.* 2018;315:F1370–F1384.
60. Lawrence MG, Altenburg MK, Sanford R, et al. Permeation of macromolecules into the renal glomerular basement membrane and capture by the tubules. *Proc Natl Acad Sci USA.* 2017;114(11): 2958–2963.
62. Haraldsson B, Nystrom J, Deen WM. Properties of the glomerular barrier and mechanisms of proteinuria. *Physiol Rev.* 2008;88(2): 451–487.
67. Suh JH, Miner JH. The glomerular basement membrane as a barrier to albumin. *Nat Rev Nephrol.* 2013;9(8):470–477.
74. Arendshorst WJ, Gottschalk CW. Glomerular ultrafiltration dynamics: historical perspective. *Am J Physiol Renal Physiol.* 1985;248(2 Pt 2): F163–F174.
75. Oken DE. An analysis of glomerular dynamics in rat, dog, and man. *Kidney Int.* 1982;22(2):136–145.
89. Lenihan CR, Busque S, Derby G, et al. Longitudinal study of living kidney donor glomerular dynamics after nephrectomy. *J Clin Invest.* 2015;125(3):1311–1318.
102. Pallone TL, Zhang Z, Rhinehart K. Physiology of the renal medullary microcirculation. *Am J Physiol Renal Physiol.* 2003;284(2):F253–F266.
127. Peppiatt-Wildman CM. The evolving role of renal pericytes. *Curr Opin Nephrol Hypertens.* 2013;22(1):10–16.
132. Pannabecker TL, Dantzler WH. Three-dimensional architecture of inner medullary vasa recta. *Am J Physiol Renal Physiol.* 2006; 290(6):F1355–F1366.
154. Peti-Peterdi J, Morishima S, Bell PD, et al. Two-photon excitation fluorescence imaging of the living juxtaglomerular apparatus. *Am J Physiol Renal Physiol.* 2002;283(1):F197–F201.
163. Griffin KA, Hacioglu R, Abu-Amara I, et al. Effects of calcium channel blockers on “dynamic” and “steady-state step” renal autoregulation. *Am J Physiol Renal Physiol.* 2004;286(6):F1136–F1143.
191. Hashimoto S, Huang Y, Briggs J, et al. Reduced autoregulatory effectiveness in adenosine 1 receptor-deficient mice. *Am J Physiol Renal Physiol.* 2006;290(4):F888–F891.
200. Loutzenhiser R, Griffin K, Williamson G, et al. Renal autoregulation: new perspectives regarding the protective and regulatory roles of the underlying mechanisms. *Am J Physiol Regul Integr Comp Physiol.* 2006;290(5):R1153–R1167.
202. Schnermann J, Briggs JP. Tubuloglomerular feedback: mechanistic insights from gene-manipulated mice. *Kidney Int.* 2008;74(4):418–426.
217. Feng MG, Navar LG. Afferent arteriolar vasodilator effect of adenosine predominantly involves adenosine A2B receptor activation. *Am J Physiol Renal Physiol.* 2010;299:F310–F315.
220. Fan F, Roman RJ. Effect of cytochrome P450 metabolites of arachidonic acid in nephrology. *J Am Soc Nephrol.* 2017;28(10): 2845–2855.
222. Schnermann J. Concurrent activation of multiple vasoactive signaling pathways in vasoconstriction caused by tubuloglomerular feedback: a quantitative assessment. *Annu Rev Physiol.* 2015;77:301–322.
239. Kovacs G, Komlosi P, Fuson A, et al. Neuronal nitric oxide synthase: its role and regulation in macula densa cells. *J Am Soc Nephrol.* 2003;14(10):2475–2483.
313. Botros FT, Dobrowolski L, Navar LG. Renal heme oxygenase-1 induction with hemin augments renal hemodynamics, renal autoregulation, and excretory function. *Int J Hypertens.* 2012;2012:189512.
320. Kasinath BS, Feliers D, Lee HJ. Hydrogen sulfide as a regulatory factor in kidney health and disease. *Biochem Pharmacol.* 2018;149:29–41.
330. Fellner SK, Arendshorst WJ. Angiotensin II, reactive oxygen species, and Ca²⁺ signaling in afferent arterioles. *Am J Physiol Renal Physiol.* 2005;289(5):F1012–F1019.
336. Li L, Lai EY, Luo Z, et al. Superoxide and hydrogen peroxide counterregulate myogenic contractions in renal afferent arterioles from a mouse model of chronic kidney disease. *Kidney Int.* 2017;92(3):625–633.

337. Vogel PA, Yang X, Moss NG, et al. Superoxide enhances Ca²⁺ entry through L-type channels in the renal afferent arteriole. *Hypertension*. 2015;66(2):374–381.
339. Song J, Lu Y, Lai EY, et al. Oxidative status in the macula densa modulates tubuloglomerular feedback responsiveness in angiotensin II-induced hypertension. *Acta Physiol (Oxf)*. 2015;213(1):249–258.
341. Zhang S, Huang Q, Wang Q, et al. Enhanced renal afferent arteriolar reactive oxygen species and contractility to endothelin-1 are associated with canonical wnt signaling in diabetic mice. *Kidney Blood Press Res*. 2018;43(3):860–871.
370. De Miguel C, Speed JS, Kasztan M, et al. Endothelin-1 and the kidney: new perspectives and recent findings. *Curr Opin Nephrol Hypertens*. 2016;25(1):35–41.
378. Gohar EY, Kasztan M, Pollock DM. Interplay between renal endothelin and purinergic signaling systems. *Am J Physiol Renal Physiol*. 2017;313(3):F666–F668.
413. Prieto MC, Gonzalez AA, Navar LG. Evolving concepts on regulation and function of renin in distal nephron. *Pflugers Arch*. 2013;465(1):121–132.
414. Ramkumar N, Kohan DE. Role of collecting duct renin in blood pressure regulation. *Am J Physiol Regul Integr Comp Physiol*. 2013;305(2):R92–R94.
420. Navar LG. Intrarenal renin-angiotensin system in regulation of glomerular function. *Curr Opin Nephrol Hypertens*. 2014;23(1):38–45.
440. Gonzalez AA, Lara LS, Prieto MC. Role of Collecting Duct Renin in the Pathogenesis of Hypertension. *Curr Hypertens Rep*. 2017;19(8):62.
450. Wang TN, Chen X, Li R, et al. SREBP-1 mediates angiotensin II-induced TGF-beta1 upregulation and glomerular fibrosis. *J Am Soc Nephrol*. 2015;26(8):1839–1854.
457. Navar LG, Inscho EW, Majid SA, et al. Paracrine regulation of the renal microcirculation. *Physiol Rev*. 1996;76(2):425–536.
464. Carlstrom M, Wilcox CS, Arendshorst WJ. Renal autoregulation in health and disease. *Physiol Rev*. 2015;95(2):405–511.
472. Vio CP, Quiroz-Munoz M, Cuevas CA, et al. Prostaglandin E2 EP3 receptor regulates cyclooxygenase-2 expression in the kidney. *Am J Physiol Renal Physiol*. 2012;303(3):F449–F457.
478. Rubinstein M, Dvash E. Leukotrienes and kidney diseases. *Curr Opin Nephrol Hypertens*. 2018;27(1):42–48.
483. Chandrasekharan JA, Sharma-Walia N. Lipoxins: nature's way to resolve inflammation. *J Inflamm Res*. 2015;8:181–192.
484. Roman RJ, Fan F. 20-HETE: hypertension and beyond. *Hypertension*. 2018;72(1):12–18.
488. Imig JD. Epoxycicosatrienoic acids, hypertension, and kidney injury. *Hypertension*. 2015;65(3):476–482.
499. Bhatt DL, Kandzari DE, O'Neill WW, et al. A controlled trial of renal denervation for resistant hypertension. *N Engl J Med*. 2014;370(15):1393–1401.
502. Glasscock RJ, Rule AD. The implications of anatomical and functional changes of the aging kidney: with an emphasis on the glomeruli. *Kidney Int*. 2012;82(3):270–277.
505. Maddox DA, Alavi FK, Zawada ET Jr. The kidney and aging. In: Massry SG, Glasscock RJ, eds. *Textbook of Nephrology*. Baltimore: Lippincott Williams & Wilkins; 2001:1094–1105.

REFERENCES

1. Stein JH, Fadem SZ. The renal circulation. *JAMA*. 1978;239(13):1308–1312.
2. Arendshorst W, Navar LG. Renal circulation and glomerular hemodynamics. In: Schrier RW, Coffman TM, Falk RJ, et al, eds. *Schrier's Diseases of the Kidney*. Philadelphia: Lippincott Williams & Wilkins; 2013:74–131.
3. Navar LG, Evan AP, Rosivall L. Microcirculation of the kidneys. In: Mortillaro N, ed. *The Physiology and Pharmacology of the Microcirculation*. New York: Academic Press; 1983:397–488.
4. Navar LG, Bell PD, Evan AP. The regulation of glomerular filtration rate in mammalian kidneys. In: Andreoli TE, Hoffman J, Fanestil D, et al, eds. *Physiology of Membrane Disorders*. New York: Plenum Medical Book Co.; 1986:637–667.
5. Smith HW. *The Kidney: Structure and Function in Health and Disease*. Vol 4. New York: Oxford University Press; 1951.
6. Dworkin LD, Brenner BM. *The Kidney*. 7th ed. Philadelphia: Saunders; 2004.
7. Maddox DA, Alavi FK, Santella RN, et al. Prevention of obesity-linked renal disease: age-dependent effects of dietary food restriction. *Kidney Int*. 2002;62(1):208–219.
8. Kost CK Jr, Li P, Williams DS, et al. Renal vascular responses to angiotensin II in conscious spontaneously hypertensive and normotensive rats. *J Cardiovasc Pharmacol*. 1998;31(6):854–861.
9. Matsuda H, Hayashi K, Arakawa K, et al. Zonal heterogeneity in action of angiotensin-converting enzyme inhibitor on renal microcirculation: role of intrarenal bradykinin. *J Am Soc Nephrol*. 1999;10(11):2272–2282.
10. Sommer G, Corrigan G, Fredrickson J, et al. Renal blood flow: measurement *in vivo* with rapid spiral MR imaging. *Radiology*. 1998;208(3):729–734.
11. Sommer G, Noorbehesht B, Pelc N, et al. Normal renal blood flow measurement using phase-contrast cine magnetic resonance imaging. *Invest Radiol*. 1992;27(6):465–470.
12. Krier JD, Ritman EL, Bajzer Z, et al. Noninvasive measurement of concurrent single-kidney perfusion, glomerular filtration, and tubular function. *Am J Physiol Renal Physiol*. 2001;281(4):F630–F638.
13. Deng A, Tang T, Singh P, et al. Regulation of oxygen utilization by angiotensin II in chronic kidney disease. *Kidney Int*. 2009;75(2):197–204.
14. Maddox DA, Horn JF, Famiano FC, et al. Load dependence of proximal tubular fluid and bicarbonate reabsorption in the remnant kidney of the Munich-Wistar rat. *J Clin Invest*. 1986;77(5):1639–1649.
15. Correa-Rotter R, Hostetter TH, Manivel JC, et al. Renin expression in renal ablation. *Hypertension*. 1992;20(4):483–490.
16. Sykes D. The correlation between renal vascularisation and lobulation of the kidney. *Br J Urol*. 1964;36:549–555.
17. Sykes D. The arterial supply of the human kidney with special reference to accessory renal arteries. *Br J Surg*. 1963;50:368–374.
18. Boijssen E. Angiographic studies of the anatomy of single and multiple renal arteries. *Acta Radiol Suppl*. 1959;183:1–135.
19. Graves F. *The Arterial Anatomy of the Kidney*. Williams and Wilkins; 1971.
20. Beeuwkes R 3rd. Efferent vascular patterns and early vascular-tubular relations in the dog kidney. *Am J Physiol*. 1971;221(5):1361–1374.
21. Kosinski H. Variation of the structure and course of the interlobular arteries in human kidney. *Folia Morphol (Warsz)*. 1997;56(4):249–252.
22. Moffat DB, Fourman J. A vascular pattern of the rat kidney. 1963. *J Am Soc Nephrol*. 2001;12(3):624–632.
23. Gardiner BS, Thompson SL, Ngo JP, et al. Diffusive oxygen shunting between vessels in the preglomerular renal vasculature: anatomic observations and computational modeling. *Am J Physiol Renal Physiol*. 2012;303(5):F605–F618.
24. Welch WJ, Baumgartl H, Lubbers D, et al. Nephron pO₂ and renal oxygen usage in the hypertensive rat kidney. *Kidney Int*. 2001;59(1):230–237.
25. Evans RG, Harrop GK, Ngo JP, et al. Basal renal O₂ consumption and the efficiency of O₂ utilization for Na⁺ reabsorption. *Am J Physiol Renal Physiol*. 2014;306(5):F551–F560.
26. Mimura I, Nangaku M. The suffocating kidney: tubulointerstitial hypoxia in end-stage renal disease. *Nat Rev Nephrol*. 2010;6(11):667–678.
27. Evans RG, Gardiner BS, Smith DW, et al. Intrarenal oxygenation: unique challenges and the biophysical basis of homeostasis. *Am J Physiol Renal Physiol*. 2008;295(5):F1259–F1270.
28. Palm F, Onozato M, Welch WJ, et al. Blood pressure, blood flow, and oxygenation in the clipped kidney of chronic 2-kidney, 1-clip rats: effects of tempol and Angiotensin blockade. *Hypertension*. 2010;55(2):298–304.
29. Ngo JP, Ow CP, Gardiner BS, et al. Diffusive shunting of gases and other molecules in the renal vasculature: physiological and evolutionary significance. *Am J Physiol Regul Integr Comp Physiol*. 2016;311(5):R797–R810.
30. Casellas D, Navar LG. In vitro perfusion of juxtamedullary nephrons in rats. *Am J Physiol*. 1984;246:F349–F358.
31. Imig JD, Roman RJ. Nitric oxide modulates vascular tone in preglomerular arterioles. *Hypertension*. 1992;19(6 Pt 2):770–774.
32. Peti-Peterdi J. Multiphoton imaging of renal tissues *in vitro*. *Am J Physiol Renal Physiol*. 2005;288(6):F1079–F1083.
33. Peti-Peterdi J, Toma I, Sipos A, et al. Multiphoton imaging of renal regulatory mechanisms. *Physiology (Bethesda)*. 2009;24:88–96.
34. Evans RG, Eppel GA, Anderson WP, et al. Mechanisms underlying the differential control of blood flow in the renal medulla and cortex. *J Hypertens*. 2004;22(8):1439–1451.
35. Navar LG, Arendshorst WJ, Pallone TL, et al. The renal microcirculation. In: Tuma RF, Duran WN, Ley K, eds. *Handbook of Physiology: Microcirculation*. Vol 2. Academic Press; 2008:550–683.
36. Cowley AW Jr. Renal medullary oxidative stress, pressure-natriuresis, and hypertension. *Hypertension*. 2008;52(5):777–786.
37. Pallone TL, Robertson CR, Jamison RL. Renal medullary microcirculation. *Physiol Rev*. 1990;70(3):885–920.
38. Beeuwkes R 3rd, Bonventre JV. The organization and vascular perfusion of canine renal tubules. *Physiologist*. 1973;16:264.
39. Beeuwkes R 3rd, Bonventre JV. Tubular organization and vascular-tubular relations in the dog kidney. *Am J Physiol*. 1975;229(3):695–713.
40. Briggs JP, Wright FS. Feedback control of glomerular filtration rate: site of the effector mechanism. *Am J Physiol*. 1979;236(1):F40–F47.
41. Beeuwkes R 3rd. The vascular organization of the kidney. *Annu Rev Physiol*. 1980;42:531–542.
42. Steinhausen M. Further information on the cortical countercurrent system in rat kidney. *Yale J Biol Med*. 1972;45(3–4):451–456.
43. Steinhausen M, Eisenbach GM, Galaske R. Countercurrent system in the renal cortex of rats. *Science*. 1970;167(925):1631–1633.
44. Weinstein SW, Szajewicz J. Superficial nephron tubular-vascular relationships in the rat kidney. *Am J Physiol*. 1978;234(3):F207–F214.
45. Elger M, Sakai T, Kriz W. The vascular pole of the renal glomerulus of rat. *Adv Anat Embryol Cell Biol*. 1998;139:1–98.
46. Rosivall L, Peti-Peterdi J. Heterogeneity of the afferent arteriole—correlations between morphology and function. *Nephrol Dial Transplant*. 2006;21(10):2703–2707.
47. Neal CR, Arkill K, Bell JS, et al. Novel haemodynamic structures in the human glomerulus. *Am J Physiol Renal Physiol*. 2018;315:F1370–F1384.
48. Navar LG, Bell PD. Romancing the macula densa at UAB. *Kidney Int*. 2004;66(91):S34–S40.
49. Kriz W, Elger M, Mundel P, et al. Structure-stabilizing forces in the glomerular tuft. *J Am Soc Nephrol*. 1995;5(10):1731–1739.
50. Sraer JD, Adida C, Peraldi MN, et al. Species-specific properties of the glomerular mesangium. *J Am Soc Nephrol*. 1993;3(7):1342–1350.
51. Feng Z, Wei C, Chen X, et al. Essential role of Ca²⁺ release channels in angiotensin II-induced Ca²⁺ oscillations and mesangial cell contraction. *Kidney Int*. 2006;70(1):130–138.
52. Inkyo-Hayasaka K, Sakai T, Kobayashi N, et al. Three-dimensional analysis of the whole mesangium in the rat. *Kidney Int*. 1996;50(2):672–683.
53. Schlendorff D, Wyatt CM, Campbell KN. Revisiting the determinants of the glomerular filtration barrier: what goes round must come round. *Kidney Int*. 2017;92(3):533–536.
54. Brenner BM, Troy JL. Postglomerular vascular protein concentration: evidence for a causal role in governing fluid reabsorption and glomerulotubular balance by the renal proximal tubule. *J Clin Invest*. 1971;50(2):336–349.
55. Maddox DA, Deen WM, Brenner BM. *Handbook of Physiology: Section 8: Renal Physiology*. Vol 1. New York: Oxford University Press; 1992.
56. Oliver JD 3rd, Anderson S, Troy JL, et al. Determination of glomerular size-selectivity in the normal rat with Ficoll. *J Am Soc Nephrol*. 1992;3(2):214–228.
57. Scandling JD, Myers BD. Glomerular size-selectivity and microalbuminuria in early diabetic glomerular disease. *Kidney Int*. 1992;41(4):840–846.

114.e2 SECTION I – NORMAL STRUCTURE AND FUNCTION

58. Walker AM, Bott PA, Oliver JJ, et al. The collection and analysis of fluid from single nephrons of the mammalian kidney. *Am J Physiol.* 1941;134:580–595.
59. Wearn JT, Richards AN. Observations on the composition of glomerular urine, with particular reference to the problem of reabsorption in the renal tubule. *Am J Physiol.* 1924;71:209–227.
60. Lawrence MG, Altenburg MK, Sanford R, et al. Permeation of macromolecules into the renal glomerular basement membrane and capture by the tubules. *Proc Natl Acad Sci USA.* 2017;114(11):2958–2963.
61. Bohrer MP, Baylis C, Humes HD, et al. Permselectivity of the glomerular capillary wall. Facilitated filtration of circulating polycations. *J Clin Invest.* 1978;61(1):72–78.
62. Haraldsson B, Nystrom J, Deen WM. Properties of the glomerular barrier and mechanisms of proteinuria. *Physiol Rev.* 2008;88(2):451–487.
63. Chang RL, Ueki IF, Troy JL, et al. Permselectivity of the glomerular capillary wall to macromolecules. II. Experimental studies in rats using neutral dextran. *Biophys J.* 1975;15(9):887–906.
64. Whiteside C, Silverman M. Determination of glomerular permselectivity to neutral dextrans in the dog. *Am J Physiol.* 1983;245(4):F485–F495.
65. Guasch A, Deen WM, Myers BD. Charge selectivity of the glomerular filtration barrier in healthy and nephrotic humans. *J Clin Invest.* 1993;92(5):2274–2282.
66. Deen WM, Lazzara MJ, Myers BD. Structural determinants of glomerular permeability. *Am J Physiol Renal Physiol.* 2001;281(4):F579–F596.
67. Suh JH, Miner JH. The glomerular basement membrane as a barrier to albumin. *Nat Rev Nephrol.* 2013;9(8):470–477.
68. Salmon AH, Satchell SC. Endothelial glycocalyx dysfunction in disease: albuminuria and increased microvascular permeability. *J Pathol.* 2012;226(4):562–574.
69. Deen WM. What determines glomerular capillary permeability? *J Clin Invest.* 2004;114(10):1412–1414.
70. Drumond MC, Deen WM. Structural determinants of glomerular hydraulic permeability. *Am J Physiol.* 1994;266(1 Pt 2):F1–F12.
71. Garg P, Rabelink T. Glomerular proteinuria: a complex interplay between unique players. *Adv Chronic Kidney Dis.* 2011;18(4):233–242.
72. Liu G, Kaw B, Kurfis J, et al. Neph1 and nephrin interaction in the slit diaphragm is an important determinant of glomerular permeability. *J Clin Invest.* 2003;112(2):209–221.
73. Drumond MC, Kristal B, Myers BD, et al. Structural basis for reduced glomerular filtration capacity in nephrotic humans. *J Clin Invest.* 1994;94(3):1187–1195.
74. Arendshorst WJ, Gottschalk CW. Glomerular ultrafiltration dynamics: historical perspective. *Am J Physiol Renal Physiol.* 1985;248(2 Pt 2):F163–F174.
75. Oken DE. An analysis of glomerular dynamics in rat, dog, and man. *Kidney Int.* 1982;22(2):136–145.
76. Gertz KH, Mangos JA, Braun G, et al. Pressure in the glomerular capillaries of the rat kidney and its relation to arterial blood pressure. *Pflugers Arch Gesamte Physiol Menschen Tiere.* 1966;288(4):369–374.
77. Brenner BM, Troy JL, Daugherty TM. The dynamics of glomerular ultrafiltration in the rat. *J Clin Invest.* 1971;50(8):1776–1780.
78. Maddox DA, Deen WM, Brenner BM. Dynamics of glomerular ultrafiltration: VI. Studies in the primate. *Kidney Int.* 1974;5:271–278.
79. Maddox DA, Price DC, Rector FC Jr. Effect of surgery on plasma volume and salt and water excretion in rats. *Am J Physiol.* 1977;233:F600–F606.
80. Deen WM, Robertson CR, Brenner BM. A model of glomerular ultrafiltration in the rat. *Am J Physiol.* 1972;223(5):1178–1183.
81. Thomas CE, Bell PD, Navar LG. Glomerular filtration dynamics in the dog during elevated plasma colloid osmotic pressure. *Kidney Int.* 1979;15:502–512.
82. Pinnick RV, Savin VJ. Filtration by superficial and deep glomeruli of normovolemic and volume-depleted rats. *Am J Physiol.* 1986;250:F86–F91.
83. Maddox DA, Brenner BM. Glomerular ultrafiltration. In: Brenner BM, ed. *The Kidney.* 7th ed. Philadelphia: Saunders; 2004:353–412.
84. Lowenstein J, Beranbaum ER, Chasis H, et al. Intrarenal pressure and exaggerated natriuresis in essential hypertension. *Clin Sci.* 1970;38(3):359–374.
85. Willassen Y, Ofstad J. Renal sodium excretion and the peritubular capillary physical factors in essential hypertension. *Hypertension.* 1980;2(6):771–779.
86. Lambert PP, Verniory A, Gassee JP, et al. Sieving equations and effective glomerular filtration pressure. *Kidney Int.* 1972;2(3):131–146.
87. Andersen S, Blouch K, Bialek J, et al. Glomerular permselectivity in early stages of overt diabetic nephropathy. *Kidney Int.* 2000; 58(5):2129–2137.
88. Tan JC, Busque S, Workeneh B, et al. Effects of aging on glomerular function and number in living kidney donors. *Kidney Int.* 2010;78(7):686–692.
89. Lenihan CR, Busque S, Derby G, et al. Longitudinal study of living kidney donor glomerular dynamics after nephrectomy. *J Clin Invest.* 2015;125(3):1311–1318.
90. Brenner BM, Troy JL, Daugherty TM, et al. Dynamics of glomerular ultrafiltration in the rat. II. Plasma-flow dependence of GFR. *Am J Physiol.* 1972;223(5):1184–1190.
91. Daniels BS, Hauser EB, Deen WM, et al. Glomerular basement membrane: in vitro studies of water and protein permeability. *Am J Physiol.* 1992;262(6 Pt 2):F919–F926.
92. Blantz RC, Rector FC Jr, Seldin DW. Effect of hyperoncotic albumin expansion upon glomerular ultrafiltration in the rat. *Kidney Int.* 1974;6(4):209–221.
93. Baylis C, Deen WM, Myers BD, et al. Effects of some vasodilator drugs on transcapillary fluid exchange in renal cortex. *Am J Physiol.* 1976;230(4):1148–1158.
94. Charonis AS, Wissig SL. Anionic sites in basement membranes. Differences in their electrostatic properties in continuous and fenestrated capillaries. *Microvasc Res.* 1983;25(3):265–285.
95. Kriz W, Napiwotzky P. Structural and functional aspects of the renal interstitium. *Contrib Nephrol.* 1979;16:104–108.
96. Aukland K, Bogusky RT, Renkin EM. Renal cortical interstitium and fluid absorption by peritubular capillaries. *Am J Physiol.* 1994;266(2 Pt 2):F175–F184.
97. Whiteside C, Silverman M. Postglomerular capillary solute flux restricted by shape and charge in the dog. *Am J Physiol.* 1987;253(3 Pt 2):F500–F512.
98. Venkatachalam MA, Karnovsky MJ. Extravascular protein in the kidney. An ultrastructural study of its relation to renal peritubular capillary permeability using protein tracers. *Lab Invest.* 1972;27(5):435–444.
99. Deen WM, Ueki IF, Brenner BM. Permeability of renal peritubular capillaries to neutral dextrans dextran and endogenous albumin. *Am J Physiol.* 1976;231(2):283–291.
100. Zimmerhackl B, Robertson CR, Jamison RL. The microcirculation of the renal medulla. *Circ Res.* 1985;57(5):657–667.
101. Rosivall L, Posch E, Simon G, et al. Intrarenal distribution of renal blood flow in the rat. *Acta Physiol Acad Sci Hung.* 1979;53(4):389–397.
102. Pallone TL, Zhang Z, Rhinehart K. Physiology of the renal medullary microcirculation. *Am J Physiol Renal Physiol.* 2003;284(2):F253–F266.
103. Edwards JG. Efferent arterioles of glomeruli in the juxtamedullary zone of the human kidney. *Anat Rec.* 1956;125(3):521–529.
104. Fourman J. Structural aspects of the kidney. *J Endocrinol.* 1971; 50(3):iv–v.
105. Kriz W, Koepsell H. The structural organization of the mouse kidney. *Z Anat Entwicklungsgesch.* 1974;144(2):137–163.
106. Kriz W. Structural organization of renal medullary circulation. *Nephron.* 1982;31(4):290–295.
107. Dieterich HJ. [Structure of blood vessels in the kidney]. *Norm Pathol Anat (Stuttgart).* 1978;35:1–108.
108. Inoue M, Maeda M, Takao S. Regional differentiation of blood flow responses to microinjection of sodium nitroprusside into the nucleus tractus solitarius of anesthetized rats. *J Auton Nerv Syst.* 1997;63(3):172–178.
109. Lim SW, Han KH, Jung JY, et al. Ultrastructural localization of UTA and UT-B in rat kidneys with different hydration status. *Am J Physiol Regul Integr Comp Physiol.* 2006;290(2):R479–R492.
110. Edwards A, Silldorff EP, Pallone TL. The renal medullary microcirculation. *Front Biosci.* 2000;5:E36–E52.
111. Zimmerhackl B, Robertson CR, Jamison RL. Effect of arginine vasopressin on renal medullary blood flow. A videomicroscopic study in the rat. *J Clin Invest.* 1985;76(2):770–778.
112. Fadem SZ, Hernandez-Llamas G, Patak RV, et al. Studies on the mechanism of sodium excretion during drug-induced vasodilatation in the dog. *J Clin Invest.* 1982;69(3):604–610.
113. Ganguli M, Tobian L, Ferris T, et al. Acute prostaglandin reduction with indomethacin and chronic prostaglandin reduction with an essential fatty acid deficient diet both decrease plasma flow to the renal papilla in the rat. *Prostaglandins.* 1989;38(1):3–19.

114. Nafz B, Berger K, Rosler C, et al. Kinins modulate the sodium-dependent autoregulation of renal medullary blood flow. *Cardiovasc Res.* 1998;40(3):573–579.
115. Zou AP, Nithipatikom K, Li PL, et al. Role of renal medullary adenosine in the control of blood flow and sodium excretion. *Am J Physiol.* 1999;276(3 Pt 2):R790–R798.
116. Dunn BR, Ichikawa I, Pfeffer JM, et al. Renal and systemic hemodynamic effects of synthetic atrial natriuretic peptide in the anesthetized rat. *Circ Res.* 1986;59(3):237–246.
117. Pallone TL, Mattson DL. Role of nitric oxide in regulation of the renal medulla in normal and hypertensive kidneys. *Curr Opin Nephrol Hypertens.* 2002;11(1):93–98.
118. Oliver JJ, Rajapakse NW, Evans RG. Effects of indomethacin on responses of regional kidney perfusion to vasoactive agents in rabbits. *Clin Exp Pharmacol Physiol.* 2002;29(10):873–879.
119. Badzynska B, Grzelecki-Mojzesowicz M, Dobrowolski L, et al. Differential effect of angiotensin II on blood circulation in the renal medulla and cortex of anaesthetised rats. *J Physiol.* 2002;538(Pt 1):159–166.
120. Sarkis A, Liu KL, Lo M, et al. Angiotensin II and renal medullary blood flow in Lyon rats. *Am J Physiol Renal Physiol.* 2003;284(2):F365–F372.
121. Omoro SA, Majid DS, El Dahr SS, et al. Roles of Ang II and bradykinin in the renal regional blood flow responses to ACE inhibition in sodium-depleted dogs. *Am J Physiol Renal Physiol.* 2000;279(2):F289–F293.
122. Kiberd B, Robertson CR, Larson T, et al. Effect of V2-receptor-mediated changes on inner medullary blood flow induced by AVP. *Am J Physiol.* 1987;253(3 Pt 2):F576–F581.
123. Mattson DL. Importance of the renal medullary circulation in the control of sodium excretion and blood pressure. *Am J Physiol Regul Integr Comp Physiol.* 2003;284(1):R13–R27.
124. Daniel PM, Peabody CN, Prichard MM. Cortical ischaemia of the kidney with maintained blood flow through the medulla. *Q J Exp Physiol Cogn Med Sci.* 1952;37(1):11–18.
125. Kriz W, Schnermann J, Koepsell H. The position of short and long loops of Henle in the rat kidney. *Z Anat Entwicklungsgesch.* 1972;138(3):301–319.
126. Park F, Mattson DL, Roberts LA, et al. Evidence for the presence of smooth muscle alpha-actin within pericytes of the renal medulla. *Am J Physiol.* 1997;273(5 Pt 2):R1742–R1748.
127. Peppiatt-Wildman CM. The evolving role of renal pericytes. *Curr Opin Nephrol Hypertens.* 2013;22(1):10–16.
128. Kriz W, Barrett JM, Peter S. The renal vasculature: anatomical-functional aspects. *Int Rev Physiol.* 1976;11:1–21.
129. Schwartz MM, Karnovsky MJ, Vehkatachalam MA. Ultrastructural differences between rat inner medullary descending and ascending vasa recta. *Lab Invest.* 1976;35(2):161–170.
130. Kriz W, Kaissling B. *Structural Organization of the Mammalian Kidney.* 3rd ed. Lippincott Williams & Wilkins; 2000.
131. Marsh DJ, Segel LA. Analysis of countercurrent diffusion exchange in blood vessels of the renal medulla. *Am J Physiol.* 1971;221(3):817–828.
132. Pannabecker TL, Dantzler WH. Three-dimensional architecture of inner medullary vasa recta. *Am J Physiol Renal Physiol.* 2006;290(6):F1355–F1366.
133. Imai M. Functional heterogeneity of the descending limbs of Henle's loop. II. Interspecies differences among rabbits, rats, and hamsters. *Pflugers Arch.* 1984;402(4):393–401.
134. Haley DP, Sarrafian M, Bulger RE, et al. Structural and functional correlates of effects of angiotensin-induced changes in rat glomerulus. *Am J Physiol.* 1987;253(1 Pt 2):F111–F119.
135. Zimmerhackl B, Parekh N, Kücherer H, et al. Influence of systemically applied angiotensin II on the microcirculation of glomerular capillaries in the rat. *Kidney Int.* 1985;27:17–24.
136. Andrews PM, Coffey AK. Cytoplasmic contractile elements in glomerular cells. *Fed Proc.* 1983;42(14):3046–3052.
137. Click RL, Joyner WL, Gilmore JP. Reactivity of glomerular afferent and efferent arterioles in renal hypertension. *Kidney Int.* 1979;15(2):109–115.
138. Steinhausen M, Sterzel RB, Fleming JT, et al. Acute and chronic effects of angiotensin II on the vessels of the split hydronephrotic kidney. *Kidney Int Suppl.* 1987;20:S64–S73.
139. Loutzenhiser R, Bidani A, Chilton L. Renal myogenic response: kinetic attributes and physiological role. *Circ Res.* 2002;90(12):1316–1324.
140. Tang L, Loutzenhiser R, Loutzenhiser R. Biphasic actions of prostaglandin E(2) on the renal afferent arteriole : role of EP(3) and EP(4) receptors. *Circ Res.* 2000;86(6):663–670.
141. Tang L, Parker M, Fei Q, et al. Afferent arteriolar adenosine A2a receptors are coupled to KATP in *in vitro* perfused hydronephrotic rat kidney. *Am J Physiol.* 1999;277(6 Pt 2):F926–F933.
142. Carmines PK, Morrison TK, Navar LG. Angiotensin II effects on microvascular diameters of *in vitro* blood-perfused juxtamedullary nephrons. *Am J Physiol.* 1986;251(4 Pt 2):F610–F618.
143. Edwards RM. Segmental effects of norepinephrine and angiotensin II on isolated renal microvessels. *Am J Physiol.* 1983;244(5):F526–F534.
144. Ito S, Johnson CS, Carretero OA. Modulation of angiotensin II-induced vasoconstriction by endothelium-derived relaxing factor in the isolated microperfused rabbit afferent arteriole. *J Clin Invest.* 1991;87(5):1656–1663.
145. Robertson CR, Deen WM, Troy JL, et al. Dynamics of glomerular ultrafiltration in the rat. III. Hemodynamics and autoregulation. *Am J Physiol.* 1972;223:1191–1200.
146. Navar LG, Bell PD, Burke TJ. Autoregulatory responses of superficial nephrons and their association with sodium excretion during arterial pressure alterations in the dog. *Circ Res.* 1977;41(4):487–496.
147. Eppel GA, Bergstrom G, Anderson WP, et al. Autoregulation of renal medullary blood flow in rabbits. *Am J Physiol Regul Integr Comp Physiol.* 2003;284(1):R233–R244.
148. Pallone TL, Silldorff EP, Turner MR. Intrarenal blood flow: microvascular anatomy and the regulation of medullary perfusion. *Clin Exp Pharmacol Physiol.* 1998;25(6):383–392.
149. Majid DS, Navar LG. Medullary blood flow responses to changes in arterial pressure in canine kidney. *Am J Physiol.* 1996;270(5 Pt 2):F833–F838.
150. Steinhausen M, Blum M, Fleming JT, et al. Visualization of renal autoregulation in the split hydronephrotic kidney of rats. *Kidney Int.* 1989;35(5):1151–1160.
151. Heyeraas KJ, Atukland K. Interlobular arterial resistance: influence of renal arterial pressure and angiotensin II. *Kidney Int.* 1987;31(6):1291–1298.
152. Carmines PK, Inscho EW, Gensure RC. Arterial pressure effects on preglomerular microvasculature of juxtamedullary nephrons. *Am J Physiol.* 1990;258(1 Pt 2):F94–F102.
153. Takenaka T, Harrison-Bernard LM, Inscho EW, et al. Autoregulation of afferent arteriolar blood flow in juxtamedullary nephrons. *Am J Physiol.* 1994;267(5 Pt 2):F879–F887.
154. Peti-Peterdi J, Morishima S, Bell PD, et al. Two-photon excitation fluorescence imaging of the living juxtaglomerular apparatus. *Am J Physiol Renal Physiol.* 2002;283(1):F197–F201.
155. Roman RJ, Cowley AW Jr, Garcia-Estan J, et al. Pressure-diuresis in volume-expanded rats. Cortical and medullary hemodynamics. *Hypertension.* 1988;12(2):168–176.
156. Takenaka T, Suzuki H, Okada H, et al. Mechanosensitive cation channels mediate afferent arteriolar myogenic constriction in the isolated rat kidney. *J Physiol.* 1998;511(Pt 1):245–253.
157. Davis MJ, Hill MA. Signaling mechanisms underlying the vascular myogenic response. *Physiol Rev.* 1999;79(2):387–423.
158. Hayashi K, Epstein M, Loutzenhiser R. Enhanced myogenic responsiveness of renal interlobular arteries in spontaneously hypertensive rats. *Hypertension.* 1992;19(2):153–160.
159. Hayashi K, Epstein M, Loutzenhiser R. Determinants of renal actions of atrial natriuretic peptide. Lack of effect of atrial natriuretic peptide on pressure-induced vasoconstriction. *Circ Res.* 1990;67(1):1–10.
160. Wagner AJ, Holstein-Rathlou NH, Marsh DJ. Endothelial Ca²⁺ in afferent arterioles during myogenic activity. *Am J Physiol.* 1996;270(1 Pt 2):F170–F178.
161. Yip KP, Marsh DJ. [Ca²⁺]i in rat afferent arteriole during constriction measured with confocal fluorescence microscopy. *Am J Physiol.* 1996;271(5 Pt 2):F1004–F1011.
162. Navar LG, Inscho EW, Imig JD, et al. Heterogeneous activation mechanisms in the renal microvasculature. *Kidney Int Suppl.* 1998; 67:S17–S21.
163. Griffin KA, Hacioglu R, Abu-Amarah I, et al. Effects of calcium channel blockers on "dynamic" and "steady-state step" renal autoregulation. *Am J Physiol Renal Physiol.* 2004;286(6):F1136–F1143.
164. Imig JD, Falck JR, Inscho EW. Contribution of cytochrome P450 epoxygenase and hydroxylase pathways to afferent arteriolar auto-regulatory responsiveness. *Br J Pharmacol.* 1999;127(6):1399–1405.
165. Baumann JE, Persson PB, Ehmke H, et al. Role of endothelium-derived relaxing factor in renal autoregulation in conscious dogs. *Am J Physiol.* 1992;263(2 Pt 2):F208–F213.

114.e4 SECTION I – NORMAL STRUCTURE AND FUNCTION

166. Beierwaltes WH, Sigmon DH, Carretero OA. Endothelium modulates renal blood flow but not autoregulation. *Am J Physiol.* 1992;262(6 Pt 2):F943–F949.
167. Majid DS, Inscho EW, Navar LG. P2 purinoceptor saturation by adenosine triphosphate impairs renal autoregulation in dogs. *J Am Soc Nephrol.* 1999;10(3):492–498.
168. Majid DS, Navar LG. Suppression of blood flow autoregulation plateau during nitric oxide blockade in canine kidney. *Am J Physiol.* 1992;262(1 Pt 2):F40–F46.
169. Hoffend J, Cavarape A, Endlich K, et al. Influence of endothelium-derived relaxing factor on renal microvessels and pressure-dependent vasodilation. *Am J Physiol.* 1993;265(2 Pt 2):F285–F292.
170. Navar LG. Integrating multiple paracrine regulators of renal microvascular dynamics. *Am J Physiol.* 1998;274:F433–F444.
171. Bayliss W. On the local reactions of the atrial wall to changes in internal pressure. *J Physiol.* 1902;28:220.
172. Holstein-Rathlou NH, Marsh DJ. A dynamic model of renal blood flow autoregulation. *Bull Math Biol.* 1994;56:411–429.
173. Just A. Mechanisms of renal blood flow autoregulation: dynamics and contributions. *Am J Physiol Regul Integr Comp Physiol.* 2007;292(1):R1–R17.
174. Just A, Ehmke H, Toktomambetova L, et al. Dynamic characteristics and underlying mechanisms of renal blood flow autoregulation in the conscious dog. *Am J Physiol Renal Physiol.* 2001;280(6):F1062–F1071.
175. Walker MI, Harrison-Bernard LM, Cook AK, et al. Dynamic interaction between myogenic and TGF mechanisms in afferent arteriolar blood flow regulation. *Am J Physiol.* 2000;279:F858–F865.
176. Casellas D, Moore LC. Autoregulation of intravascular pressure in preglomerular juxamedullary vessels. *Am J Physiol.* 1993;264: F315–F321.
177. Casellas D, Bouriquet N, Moore LC. Branching patterns and autoregulatory responses of juxamedullary afferent arterioles. *Am J Physiol.* 1997;272(3 Pt 2):F416–F421.
178. Hayashi K, Epstein M, Loutzenhiser R, et al. Impaired myogenic responsiveness of the afferent arteriole in streptozotocin-induced diabetic rats: role of eicosanoid derangements. *J Am Soc Nephrol.* 1992;2(11):1578–1586.
179. Heller J, Horacek V. Autoregulation of superficial nephron function in the alloperfused dog kidney. *Pflugers Arch.* 1979;382(1):99–104.
180. Pelayo JC, Westcott JY. Impaired autoregulation of glomerular capillary hydrostatic pressure in the rat remnant nephron. *J Clin Invest.* 1991;88(1):101–105.
181. Hayashi K, Epstein M, Loutzenhiser R. Pressure-induced vasoconstriction of renal microvessels in normotensive and hypertensive rats. *Circ Res.* 1989;65:1475–1484.
182. Takenaka T, Forster H, De Micheli A, et al. Impaired myogenic responsiveness of renal microvessels in Dahl salt-sensitive rats. *Circ Res.* 1992;71(2):471–480.
183. Cangiotti AM, Lorenzi T, Zingaretti MC, et al. Polarized ends of human macula densa cells: ultrastructural investigation and morphofunctional correlations. *Anat Rec (Hoboken).* 2018;301(5):922–931.
184. Kriz W, Sakai T. Morphological aspects of glomerular function. In: Davison AM, ed. *Nephrology: Proceedings of the Tenth International Congress of Nephrology.* Vol 1988. London: Bailliere-Tindall; 1987:3–23.
185. Schnermann J, Wright FS, Davis JM, et al. Regulation of superficial nephron filtration rate by tubulo-glomerular feedback. *Pflugers Arch.* 1970;318(2):147–175.
186. Vallon V. Tubuloglomerular feedback and the control of glomerular filtration rate. *News Physiol Sci.* 2003;18:169–174.
187. Schnermann J. Localization, mediation and function of the glomerular vascular response to alterations of distal fluid delivery. *Fed Proc.* 1981;40(1):109–115.
188. Navar LG, Bell PD, Burke TJ. Role of a macula densa feedback mechanism as a mediator of renal autoregulation. *Kidney Int Suppl.* 1982;12:S157–S164.
189. Moore LC, Casellas D. Tubuloglomerular feedback dependence of autoregulation in rat juxamedullary afferent arterioles. *Kidney Int.* 1990;37:1402–1408.
190. Schlatte E, Salomonsson M, Persson AE, et al. Macula densa cells sense luminal NaCl concentration via furosemide sensitive Na⁺-2Cl⁻-K⁺-cotransport. *Pflugers Arch.* 1989;414(3):286–290.
191. Hashimoto S, Huang Y, Briggs J, et al. Reduced autoregulatory effectiveness in adenosine 1 receptor-deficient mice. *Am J Physiol Renal Physiol.* 2006;290(4):F888–F891.
192. Holstein-Rathlou NH. Oscillations and chaos in renal blood flow control. *J Am Soc Nephrol.* 1993;4(6):1275–1287.
193. Leyssac PP, Baumbach L. An oscillating intratubular pressure response to alterations in Henle loop flow in the rat kidney. *Acta Physiol Scand.* 1983;117(3):415–419.
194. Leyssac PP, Holstein-Rathlou NH. Effects of various transport inhibitors on oscillating TGF pressure responses in the rat. *Pflugers Arch.* 1986;407(3):285–291.
195. Holstein-Rathlou NH, Wagner AJ, Marsh DJ. Tubuloglomerular feedback dynamics and renal blood flow autoregulation in rats. *Am J Physiol.* 1991;260(1 Pt 2):F53–F68.
196. Flemming B, Arenz N, Seeliger E, et al. Time-dependent autoregulation of renal blood flow in conscious rats. *J Am Soc Nephrol.* 2001;12(11):2253–2262.
197. Bell PD, Navar LG. Cytoplasmic calcium in the mediation of macula densa tubulo-glomerular feedback responses. *Science.* 1982; 215(4533):670–673.
198. Gotshall R, Hess T, Mills T. Efficiency of canine renal blood flow autoregulation in kidneys with or without glomerular filtration. *Blood Vessels.* 1985;22(1):25–31.
199. Aukland K, Oien AH. Renal autoregulation: models combining tubuloglomerular feedback and myogenic response. *Am J Physiol.* 1987;252(4 Pt 2):F768–F783.
200. Loutzenhiser R, Griffin K, Williamson G, et al. Renal autoregulation: new perspectives regarding the protective and regulatory roles of the underlying mechanisms. *Am J Physiol Regul Integr Comp Physiol.* 2006;290(5):R1153–R1167.
201. Singh P, Thomson SC. Renal homeostasis and tubuloglomerular feedback. *Curr Opin Nephrol Hypertens.* 2010;19(1):59–64.
202. Schnermann J, Briggs JP. Tubuloglomerular feedback: mechanistic insights from gene-manipulated mice. *Kidney Int.* 2008;74(4):418–426.
203. Gutsche HU, Brunkhorst R, Muller-Ott K, et al. Effect of diuretics on the tubuloglomerular feedback response. *Can J Physiol Pharmacol.* 1984;62(4):412–417.
204. Bell PD, Navar LG. Relationship between tubulo-glomerular feedback responses and perfusate hypotonicity at constant low chloride concentration. *Kidney Int.* 1982;22:234–239.
205. Bell PD, Navar LG, Plotz DW, et al. Tubuloglomerular feedback responses during perfusion with nonelectrolyte solutions in the rat. *Kidney Int.* 1980;18:460–471.
206. Sipos A, Vargas S, Petri-Peterdi J. Direct demonstration of tubular fluid flow sensing by macula densa cells. *Am J Physiol Renal Physiol.* 2010;299(5):F1087–F1093.
207. Bell PD, Lapointe JY, Sabirov R, et al. Macula densa cell signaling involves ATP release through a maxi anion channel. *Proc Natl Acad Sci USA.* 2003;100(7):4322–4327.
208. Inscho EW, Ohishi K, Cook AK, et al. Calcium activation mechanisms in the renal microvascular response to extracellular ATP. *Am J Physiol.* 1995;268(5 Pt 2):F876–F884.
209. Petri-Peterdi J, Bell PD. Cytosolic [Ca²⁺] signaling pathway in macula densa cells. *Am J Physiol.* 1999;277(3 Pt 2):F472–F476.
210. Hansen PB, Friis UG, Uhrenholt TR, et al. Intracellular signalling pathways in the vasoconstrictor response of mouse afferent arterioles to adenosine. *Acta Physiol (Oxf).* 2007;191(2):89–97.
211. Franco M, Bell PD, Navar LG. Effect of adenosine A1 analogue on tubuloglomerular feedback mechanism. *Am J Physiol.* 1989;257(2 Pt 2):F231–F236.
212. Brown R, Ollerstam A, Johansson B, et al. Abolished tubuloglomerular feedback and increased plasma renin in adenosine A1 receptor-deficient mice. *Am J Physiol Regul Integr Comp Physiol.* 2001;281(5):R1362–R1367.
213. Sun D, Samuelson LC, Yang T, et al. Mediation of tubuloglomerular feedback by adenosine: evidence from mice lacking adenosine 1 receptors. *Proc Natl Acad Sci USA.* 2001;98(17):9983–9988.
214. Thomson S, Bao D, Deng A, et al. Adenosine formed by 5'-nucleotidase mediates tubuloglomerular feedback. *J Clin Invest.* 2000;106(2):289–298.
215. Ren Y, Arima S, Carretero OA, et al. Possible role of adenosine in macula densa control of glomerular hemodynamics. *Kidney Int.* 2002;61(1):169–176.
216. Feng MG, Navar LG. Adenosine A2 receptor activation attenuates afferent arteriolar autoregulation during adenosine receptor saturation in rats. *Hypertension.* 2007;50(4):744–749.
217. Feng MG, Navar LG. Afferent arteriolar vasodilator effect of adenosine predominantly involves adenosine A2B receptor activation. *Am J Physiol Renal Physiol.* 2010;299:F310–F315.
218. Ren Y, Garvin JL, Carretero OA. Efferent arteriole tubuloglomerular feedback in the renal nephron. *Kidney Int.* 2001;59(1):222–229.

219. Ren YL, Garvin JL, Carretero OA. Role of macula densa nitric oxide and cGMP in the regulation of tubuloglomerular feedback. *Kidney Int.* 2000;58:2053–2060.
220. Fan F, Roman RJ. Effect of cytochrome P450 metabolites of arachidonic acid in nephrology. *J Am Soc Nephrol.* 2017;28(10):2845–2855.
221. Schnermann JB, Traynor T, Yang T, et al. Absence of tubuloglomerular feedback responses in AT1A receptor-deficient mice. *Am J Physiol.* 1997;273(2 Pt 2):F315–F320.
222. Schnermann J. Concurrent activation of multiple vasoactive signaling pathways in vasoconstriction caused by tubuloglomerular feedback: a quantitative assessment. *Annu Rev Physiol.* 2015;77:301–322.
223. Traynor T, Yang T, Huang YG, et al. Tubuloglomerular feedback in ACE-deficient mice. *Am J Physiol.* 1999;276(5 Pt 2):F751–F757.
224. Traynor TR, Schnermann J. Renin-angiotensin system dependence of renal hemodynamics in mice. *J Am Soc Nephrol.* 1999;10(suppl 11):S184–S188.
225. Schnermann J, Traynor T, Yang T, et al. Tubuloglomerular feedback: new concepts and developments. *Kidney Int Suppl.* 1998;67:S40–S45.
226. Welch WJ, Wilcox CS. Feedback responses during sequential inhibition of angiotensin and thromboxane. *Am J Physiol.* 1990;258(3 Pt 2):F457–F466.
227. Vallon V. Tubuloglomerular feedback in the kidney: insights from gene-targeted mice. *Pflugers Arch.* 2003;445:470–476.
228. Plot DW, Roy RN. Renin-angiotensin influences on tubuloglomerular feedback activity in the rat. *Kidney Int.* 1982;22(suppl 12):S114–S121.
229. Wang H, Garvin JL, Carretero OA. Angiotensin II enhances tubuloglomerular feedback via luminal AT(1) receptors on the macula densa. *Kidney Int.* 2001;60(5):1851–1857.
230. Munger KA, Jackson EK. Effects of selective A1 receptor blockade on glomerular hemodynamics: involvement of renin-angiotensin system. *Am J Physiol.* 1994;267(5 Pt 2):F783–F790.
231. Wilcox CS, Welch WJ, Murad F, et al. Nitric oxide synthase in macula densa regulates glomerular capillary pressure. *Proc Natl Acad Sci USA.* 1992;89(24):11993–11997.
232. Ichihara A, Imig JD, Inscho EW, et al. Cyclooxygenase-2 participates in tubular flow-dependent afferent arteriolar tone: interaction with neuronal NOS. *Am J Physiol.* 1998;275(4 Pt 2):F605–F612.
233. Liu R, Carretero OA, Ren Y, et al. Increased intracellular pH at the macula densa activates nNOS during tubuloglomerular feedback. *Kidney Int.* 2005;67(5):1837–1843.
234. Ito S, Ren Y. Evidence for the role of nitric oxide in macula densa control of glomerular hemodynamics. *J Clin Invest.* 1993;92(2):1093–1098.
235. Thorup C, Erik A, Persson G. Macula densa derived nitric oxide in regulation of glomerular capillary pressure. *Kidney Int.* 1996;49(2):430–436.
236. Welch WJ, Wilcox CS. Macula densa arginine delivery and uptake in the rat regulates glomerular capillary pressure. Effects of salt intake. *J Clin Invest.* 1997;100(9):2235–2242.
237. Wilcox CS, Welch WJ. Macula densa nitric oxide synthase: expression, regulation, and function. *Kidney Int Suppl.* 1998;67:S53–S57.
238. Vidal MJ, Romero JC, Vanhoufte PM. Endothelium-derived relaxing factor inhibits renin release. *Eur J Pharmacol.* 1988;149(3):401–402.
239. Kovacs G, Komlosi P, Fuson A, et al. Neuronal nitric oxide synthase: its role and regulation in macula densa cells. *J Am Soc Nephrol.* 2003;14(10):2475–2483.
240. Maddox DA, Troy JL, Brenner BM. Autoregulation of filtration rate in the absence of macula densa-glomerulus feedback. *Am J Physiol.* 1974;227(1):123–131.
241. Dorup J, Morsing P, Rasch R. Tubule-tubule and tubule-arteriole contacts in rat kidney distal nephrons. *Lab Invest.* 1992;67:761–769.
242. Ren Y, Garvin JL, Liu R, et al. Crosstalk between the connecting tubule and the afferent arteriole regulates renal microcirculation. *Kidney Int.* 2007;71(11):1116–1121.
243. Ren Y, D'Ambrosio MA, Garvin JL, et al. Prostaglandin E2 mediates connecting tubule glomerular feedback. *Hypertension.* 2013;62(6):1123–1128.
244. Ren Y, D'Ambrosio MA, Garvin JL, et al. Possible mediators of connecting tubule glomerular feedback. *Hypertension.* 2009;53(2):319–323.
245. Ren Y, D'Ambrosio MA, Garvin JL, et al. Angiotensin II enhances connecting tubule glomerular feedback. *Hypertension.* 2010;56:636–642.
246. Wang H, D'Ambrosio MA, Garvin JL, et al. Connecting tubule glomerular feedback mediates acute tubuloglomerular feedback resetting. *Am J Physiol Renal Physiol.* 2012;302(10):F1300–F1304.
247. Wang H, D'Ambrosio MA, Garvin JL, et al. Connecting tubule glomerular feedback in hypertension. *Hypertension.* 2013;62(4):738–745.
248. Wang H, Romero CA, Masjoan Juncos JX, et al. Effect of salt intake on afferent arteriolar dilatation: role of connecting tubule glomerular feedback (CTGF). *Am J Physiol Renal Physiol.* 2017;313(6):F1209–F1215.
249. Monu SR, Ren Y, Masjoan-Juncos JX, et al. Connecting tubule glomerular feedback mediates tubuloglomerular feedback resetting after unilateral nephrectomy. *Am J Physiol Renal Physiol.* 2018;315(4):F806–F811.
250. Furchtgott RF, Zawadzki JV. The obligatory role of endothelial cells in the relaxation of arterial smooth muscle by acetylcholine. *Nature.* 1980;288(5789):373–376.
251. Ignarro LJ, Buga GM, Wood KS, et al. Endothelium-derived relaxing factor produced and released from artery and vein is nitric oxide. *Proc Natl Acad Sci USA.* 1987;84(24):9265–9269.
252. Palmer RM, Ferrige AG, Moncada S. Nitric oxide release accounts for the biological activity of endothelium-derived relaxing factor. *Nature.* 1987;327(6122):524–526.
253. Ignarro LJ. Nitric oxide. A novel signal transduction mechanism for transcellular communication. *Hypertension.* 1990;16(5):477–483.
254. Romero JC, Lahera V, Salom MG, et al. Role of the endothelium-dependent relaxing factor nitric oxide on renal function. *J Am Soc Nephrol.* 1999;2(9):1371–1387.
255. Shultz PJ, Tayeh MA, Marletta MA, et al. Synthesis and action of nitric oxide in rat glomerular mesangial cells. *Am J Physiol.* 1991;261(4 Pt 2):F600–F606.
256. Bachmann S, Bosse HM, Mundel P. Topography of nitric oxide synthesis by localizing constitutive NO synthases in mammalian kidney. *Am J Physiol.* 1995;268(5 Pt 2):F885–F898.
257. Kon V, Harris RC, Ichikawa I. A regulatory role for large vessels in organ circulation. Endothelial cells of the main renal artery modulate intrarenal hemodynamics in the rat. *J Clin Invest.* 1990;85(6):1728–1733.
258. Greenberg SG, He XR, Schnermann JB, et al. Effect of nitric oxide on renin secretion. I. Studies in isolated juxtaglomerular granular cells. *Am J Physiol.* 1995;268(5 Pt 2):F948–F952.
259. Lamontagne D, Pohl U, Busse R. Mechanical deformation of vessel wall and shear stress determine the basal release of endothelium-derived relaxing factor in the intact rabbit coronary vascular bed. *Circ Res.* 1992;70(1):123–130.
260. Murphy ME, Brayden JE. Apamin-sensitive K⁺ channels mediate an endothelium-dependent hyperpolarization in rabbit mesenteric arteries. *J Physiol.* 1995;489(Pt 3):723–734.
261. Radermacher J, Forstermann U, Frolich JC. Endothelium-derived relaxing factor influences renal vascular resistance. *Am J Physiol.* 1990;259(1 Pt 2):F9–F17.
262. Shultz PJ, Schorer AE, Raji L. Effects of endothelium-derived relaxing factor and nitric oxide on rat mesangial cells. *Am J Physiol.* 1990;258(1 Pt 2):F162–F167.
263. Tolins JP, Palmer RM, Moncada S, et al. Role of endothelium-derived relaxing factor in regulation of renal hemodynamic responses. *Am J Physiol.* 1990;258(3 Pt 2):H655–H662.
264. Lucas KA, Pitari GM, Kazerounian S, et al. Guanylyl cyclases and signaling by cyclic GMP. *Pharmacol Rev.* 2000;52(3):375–414.
265. Rapoport RM. Cyclic guanosine monophosphate inhibition of contraction may be mediated through inhibition of phosphatidylinositol hydrolysis in rat aorta. *Circ Res.* 1986;58(3):407–410.
266. Buga GM, Gold ME, Fukuto JM, et al. Shear stress-induced release of nitric oxide from endothelial cells grown on beads. *Hypertension.* 1991;17(2):187–193.
267. Chin JH, Azhar S, Hoffman BB. Inactivation of endothelial derived relaxing factor by oxidized lipoproteins. *J Clin Invest.* 1992;89:10–18.
268. Cooke JP, Rossitch E Jr, Andon NA, et al. Flow activates an endothelial potassium channel to release an endogenous nitrovasodilator. *J Clin Invest.* 1991;88(5):1663–1671.
269. Luckhoff A, Busse R. Calcium influx into endothelial cells and formation of endothelium-derived relaxing factor is controlled by the membrane potential. *Pflugers Arch.* 1990;416(3):305–311.
270. Marsden PA, Brock TA, Ballermann BJ. Glomerular endothelial cells respond to calcium-mobilizing agonists with release of EDRF. *Am J Physiol.* 1990;258(5 Pt 2):F1295–F1303.
271. Handa RK, Strandhoy JW. Nitric oxide mediates the inhibitory action of platelet-activating factor on angiotensin II-induced renal vasoconstriction, in vivo. *J Pharmacol Exp Ther.* 1996;277(3):1486–1491.

272. Edwards RM, Pullen M, Nambi P. Activation of endothelin ETB receptors increases glomerular cGMP via an L-arginine-dependent pathway. *Am J Physiol.* 1992;263(6 Pt 2):F1020–F1025.
273. Fiscus RR, Zhou HL, Wang X, et al. Calcitonin gene-related peptide (CGRP)-induced cyclic AMP, cyclic GMP and vasorelaxant responses in rat thoracic aorta are antagonized by blockers of endothelium-derived relaxant factor (EDRF). *Neuropeptides.* 1991;20(2):133–143.
274. Samuelson UE, Jernbeck J. Calcitonin gene-related peptide relaxes porcine arteries via one endothelium-dependent and one endothelium-independent mechanism. *Acta Physiol Scand.* 1991;141(2):281–282.
275. Gray DW, Marshall I. Nitric oxide synthesis inhibitors attenuate calcitonin gene-related peptide endothelium-dependent vasorelaxation in rat aorta. *Eur J Pharmacol.* 1992;212(1):37–42.
276. Gray DW, Marshall I. Human alpha-calcitonin gene-related peptide stimulates adenylate cyclase and guanylate cyclase and relaxes rat thoracic aorta by releasing nitric oxide. *Br J Pharmacol.* 1992;107(3):691–696.
277. Hutcheson IR, Griffith TM. Release of endothelium-derived relaxing factor is modulated both by frequency and amplitude of pulsatile flow. *Am J Physiol.* 1991;261(1 Pt 2):H257–H262.
278. Koller A, Kaley G. Endothelial regulation of wall shear stress and blood flow in skeletal muscle microcirculation. *Am J Physiol.* 1991;260(3 Pt 2):H862–H868.
279. Nollert MU, Eskin SG, McIntire LV. Shear stress increases inositol trisphosphate levels in human endothelial cells. *Biochem Biophys Res Commun.* 1990;170(1):281–287.
280. O'Neill WC. Flow-mediated NO release from endothelial cells is independent of K⁺ channel activation or intracellular Ca²⁺. *Am J Physiol.* 1995;269(4 Pt 1):C863–C869.
281. Pohl U, Herlan K, Huang A, et al. EDRF-mediated shear-induced dilation opposes myogenic vasoconstriction in small rabbit arteries. *Am J Physiol.* 1991;261(6 Pt 2):H2016–H2023.
282. Pittner J, Wolgast M, Casellas D, et al. Increased shear stress-released NO and decreased endothelial calcium in rat isolated perfused juxtamedullary nephrons. *Kidney Int.* 2005;67(1):227–236.
283. Blantz RC, Deng A, Lortie M, et al. The complex role of nitric oxide in the regulation of glomerular ultrafiltration. *Kidney Int.* 2002;61(3):782–785.
284. Mount PF, Power DA. Nitric oxide in the kidney: functions and regulation of synthesis. *Acta Physiol (Oxf).* 2006;187(4):433–446.
285. Welch WJ, Tojo A, Lee JU, et al. Nitric oxide synthase in the JGA of the SHR: expression and role in tubuloglomerular feedback. *Am J Physiol.* 1999;277(1 Pt 2):F130–F138.
286. Majid DSA, Chin S, Omoro S, et al. Direct assessment of intrarenal nitric oxide (NO) levels during changes in renal arterial pressure (RAP) in anesthetized dogs. *FASEB J.* 1996;10:A40.
287. Navar LG, Majid DSA. Contribution of intrarenal nitric oxide to the mechanism of pressure natriuresis. *J Physiol Biochem.* 1997;53:34.
288. Edgley AJ, Tare M, Evans RG, et al. In vivo regulation of endothelium-dependent vasodilation in the rat renal circulation and the effect of streptozotocin-induced diabetes. *Am J Physiol Regul Integr Comp Physiol.* 2008;295(3):R829–R839.
289. Jin C, Hu C, Polichnowski A, et al. Effects of renal perfusion pressure on renal medullary hydrogen peroxide and nitric oxide production. *Hypertension.* 2009;53(6):1048–1053.
290. Majid DSA, Navar LG. Nitric oxide in the control of renal hemodynamics and excretory function. *Am J Hypertens.* 2001;14:74S–82S.
291. Zhang Z, Pallone TL. Response of descending vasa recta to luminal pressure. *Am J Physiol Renal Physiol.* 2004;287(3):F535–F542.
292. Gabai FB, Blantz RC. Role of nitric oxide in renal hemodynamics. *Semin Nephrol.* 1999;19(3):242–250.
293. Baylis C, Harton P, Engels K. Endothelial derived relaxing factor controls renal hemodynamics in the normal rat kidney. *J Am Soc Nephrol.* 1990;1(6):875–881.
294. Treeck B, Aukland K. Effect of L-NAME on glomerular filtration rate in deep and superficial layers of rat kidneys. *Am J Physiol.* 1997;272(3 Pt 2):F312–F318.
295. Sigmon DH, Beierwaltes WH. Influence of nitric oxide derived from neuronal nitric oxide synthase on glomerular filtration. *Gen Pharmacol.* 2000;34(2):95–100.
296. Baylis C, Mitraka B, Deng A. Chronic blockade of nitric oxide synthesis in the rat produces systemic hypertension and glomerular damage. *J Clin Invest.* 1992;90(1):278–281.
297. Deng A, Baylis C. Locally produced EDRF controls preglomerular resistance and ultrafiltration coefficient. *Am J Physiol.* 1993;264(2 Pt 2):F212–F215.
298. Gonzalez JD, Llinas MT, Nava E, et al. Role of nitric oxide and prostaglandins in the long-term control of renal function. *Hypertension.* 1998;32(1):33–38.
299. Qiu C, Baylis C. Endothelin and angiotensin mediate most glomerular responses to nitric oxide inhibition. *Kidney Int.* 1999;55(6):2390–2396.
300. Zatz R, de Nucci G. Effects of acute nitric oxide inhibition on rat glomerular microcirculation. *Am J Physiol.* 1991;261(2 Pt 2):F360–F363.
301. Ito S, Juncos LA, Nushiro N, et al. Endothelium-derived relaxing factor modulates endothelin action in afferent arterioles. *Hypertension.* 1991;17(6 Pt 2):1052–1056.
302. Ohishi K, Carmines PK, Inscho EW, et al. EDRF-angiotensin II interactions in rat juxamedullary afferent and efferent arterioles. *Am J Physiol.* 1992;263(5 Pt 2):F900–F906.
303. Ito S, Arima S, Ren YL, et al. Endothelium-derived relaxing factor/nitric oxide modulates angiotensin II action in the isolated microperfused rabbit afferent but not efferent arteriole. *J Clin Invest.* 1993;91(5):2012–2019.
304. Ichihara A, Inscho EW, Imig JD, et al. Neuronal nitric oxide synthase modulates rat renal microvascular function. *Am J Physiol Renal Physiol.* 1998;274:F516–F524.
305. Sigmon DH, Carretero OA, Beierwaltes WH. Endothelium-derived relaxing factor regulates renin release in vivo. *Am J Physiol.* 1992;263(2 Pt 2):F256–F261.
306. Moreno C, Lopez A, Llinas MT, et al. Changes in NOS activity and protein expression during acute and prolonged Ang II administration. *Am J Physiol Regul Integr Comp Physiol.* 2002;282(1):R31–R37.
307. Patzak A, Lai EY, Mrowka R, et al. AT1 receptors mediate angiotensin II-induced release of nitric oxide in afferent arterioles. *Kidney Int.* 2004;66(5):1949–1958.
308. Deng A, Miracle CM, Suarez JM, et al. Oxygen consumption in the kidney: effects of nitric oxide synthase isoforms and angiotensin II. *Kidney Int.* 2005;68(2):723–730.
309. Baylis C, Engels K, Samsell L, et al. Renal effects of acute endothelial-derived relaxing factor blockade are not mediated by angiotensin II. *Am J Physiol.* 1993;264(1 Pt 2):F74–F78.
310. Baylis C, Harvey J, Engels K. Acute nitric oxide blockade amplifies the renal vasoconstrictor actions of angiotension II. *J Am Soc Nephrol.* 1994;5(2):211–214.
311. Schnackenberg CG, Wilkins FC, Granger JP. Role of nitric oxide in modulating the vasoconstrictor actions of angiotensin II in preglomerular and postglomerular vessels in dogs. *Hypertension.* 1995;26(6 Pt 2):1024–1029.
312. Stec DE, Vera T, Storm MV, et al. Blood pressure and renal blow flow responses in heme oxygenase-2 knockout mice. *Am J Physiol Regul Integr Comp Physiol.* 2009;297(6):R1822–R1828.
313. Botros FT, Dobrowolski L, Navar LG. Renal heme oxygenase-1 induction with hemin augments renal hemodynamics, renal autoregulation, and excretory function. *Int J Hypertens.* 2012;2012:189512.
314. Jackson KE, Jackson DW, Quadri S, et al. Inhibition of heme oxygenase augments tubular sodium reabsorption. *Am J Physiol Renal Physiol.* 2011;300(4):F941–F946.
315. Abraham NG, Kappas A. Heme oxygenase and the cardiovascular-renal system. *Free Radic Biol Med.* 2005;39(1):1–25.
316. Zou AP, Billington H, Su N, et al. Expression and actions of heme oxygenase in the renal medulla of rats. *Hypertension.* 2000;35(1 Pt 2):342–347.
317. Li N, Yi F, dos Santos EA, et al. Role of renal medullary heme oxygenase in the regulation of pressure natriuresis and arterial blood pressure. *Hypertension.* 2007;49(1):148–154.
318. Ryan MJ, Jernigan NL, Drummond HA, et al. Renal vascular responses to CORM-A1 in the mouse. *Pharmacol Res.* 2006;54(1):24–29.
319. Arregui B, Lopez B, Garcia Salom M, et al. Acute renal hemodynamic effects of dimanganese decacarbonyl and cobalt protoporphyrin. *Kidney Int.* 2004;65(2):564–574.
320. Kasinath BS, Feliers D, Lee HJ. Hydrogen sulfide as a regulatory factor in kidney health and disease. *Biochem Pharmacol.* 2018;149:29–41.
321. Feliers D, Lee HJ, Kasinath BS. Hydrogen sulfide in renal physiology and disease. *Antioxid Redox Signal.* 2016;25(13):720–731.
322. Xia M, Chen L, Muh RW, et al. Production and actions of hydrogen sulfide, a novel gaseous bioactive substance, in the kidneys. *J Pharmacol Exp Ther.* 2009;329(3):1056–1062.

323. Jung KJ, Jang HS, Kim JI, et al. Involvement of hydrogen sulfide and homocysteine transsulfuration pathway in the progression of kidney fibrosis after ureteral obstruction. *Biochim Biophys Acta*. 2013;1832(12):1989–1997.
324. Jackson-Weaver O, Osmond JM, Riddle MA, et al. Hydrogen sulfide dilates rat mesenteric arteries by activating endothelial large-conductance Ca(2)(+)-activated K(+) channels and smooth muscle Ca(2)(+) sparks. *Am J Physiol Heart Circ Physiol*. 2013;304(11):H1446–H1454.
325. Bucci M, Papapetropoulos A, Vellecco V, et al. cGMP-dependent protein kinase contributes to hydrogen sulfide-stimulated vasorelaxation. *PLoS ONE*. 2012;7(12):e53319.
326. Materazzi S, Zagli G, Nassini R, et al. Vasodilator activity of hydrogen sulfide (H₂S) in human mesenteric arteries. *Microvasc Res*. 2017;109:38–44.
327. Li Y, Zang Y, Fu S, et al. H₂S relaxes vas deferens smooth muscle by modulating the large conductance Ca²⁺-activated K⁺ (BKCa) channels via a redox mechanism. *J Sex Med*. 2012;9(11):2806–2813.
328. Huang Y, Zhang Z, Huang Y, et al. Induction of inactive TGF-beta1 monomer formation by hydrogen sulfide contributes to its suppressive effects on Ang II- and TGF-beta1-induced EMT in renal tubular epithelial cells. *Biochem Biophys Res Commun*. 2018;501(2):534–540.
329. Gill PS, Wilcox CS. NADPH oxidases in the kidney. *Antioxid Redox Signal*. 2006;8(9–10):1597–1607.
330. Fellner SK, Arendshorst WJ. Angiotensin II, reactive oxygen species, and Ca²⁺ signaling in afferent arterioles. *Am J Physiol Renal Physiol*. 2005;289(5):F1012–F1019.
331. Carlstrom M, Lai EY, Ma Z, et al. Role of NOX2 in the regulation of afferent arteriole responsiveness. *Am J Physiol Regul Integr Comp Physiol*. 2009;296(1):R72–R79.
332. Lai EY, Solis G, Luo Z, et al. p47(phox) is required for afferent arteriolar contractile responses to angiotensin II and perfusion pressure in mice. *Hypertension*. 2012;59(2):415–420.
333. Wang C, Luo Z, Kohan D, et al. Thromboxane prostanoid receptors enhance contractions, endothelin-1, and oxidative stress in microvessels from mice with chronic kidney disease. *Hypertension*. 2015;65(5):1055–1063.
334. Sharma K, Cook A, Smith M, et al. TGF-beta impairs renal autoregulation via generation of ROS. *Am J Physiol Renal Physiol*. 2005;288(5):F1069–F1077.
335. Li L, Lai EY, Wellstein A, et al. Differential effects of superoxide and hydrogen peroxide on myogenic signaling, membrane potential, and contractions of mouse renal afferent arterioles. *Am J Physiol Renal Physiol*. 2016;310(11):F1197–F1205.
336. Li L, Lai EY, Luo Z, et al. Superoxide and hydrogen peroxide counterregulate myogenic contractions in renal afferent arterioles from a mouse model of chronic kidney disease. *Kidney Int*. 2017;92(3):625–633.
337. Vogel PA, Yang X, Moss NG, et al. Superoxide enhances Ca²⁺ entry through L-type channels in the renal afferent arteriole. *Hypertension*. 2015;66(2):374–381.
338. Li L, Feng D, Luo Z, et al. Remodeling of afferent arterioles from mice with oxidative stress does not account for increased contractility but does limit excessive wall stress. *Hypertension*. 2015;66(3):550–556.
339. Song J, Lu Y, Lai EY, et al. Oxidative status in the macula densa modulates tubuloglomerular feedback responsiveness in angiotensin II-induced hypertension. *Acta Physiol (Oxf)*. 2015;213(1):249–258.
340. Lai EY, Wellstein A, Welch WJ, et al. Superoxide modulates myogenic contractions of mouse afferent arterioles. *Hypertension*. 2011;58(4):650–656.
341. Zhang S, Huang Q, Wang Q, et al. Enhanced renal afferent arteriolar reactive oxygen species and contractility to endothelin-1 are associated with canonical wnt signaling in diabetic mice. *Kidney Blood Press Res*. 2018;43(3):860–871.
342. Ren Y, D'Ambrosio MA, Liu R, et al. Enhanced myogenic response in the afferent arteriole of spontaneously hypertensive rats. *Am J Physiol Heart Circ Physiol*. 2010;298(6):H1769–H1775.
343. Huang Q, Wang Q, Zhang S, et al. Increased hydrogen peroxide impairs angiotensin II contractions of afferent arterioles in mice after renal ischaemia-reperfusion injury. *Acta Physiol (Oxf)*. 2016;218(2):136–145.
344. Yanagisawa M, Kurihara H, Kimura S, et al. A novel potent vasoconstrictor peptide produced by vascular endothelial cells. *Nature*. 1988;332(6163):411–415.
345. Goraca A. New views on the role of endothelin (minireview). *Endocr Regul*. 2002;36(4):161–167.
346. Simonson MS, Dunn MJ. Endothelin-1 stimulates contraction of rat glomerular mesangial cells and potentiates beta-adrenergic-mediated cyclic adenosine monophosphate accumulation. *J Clin Invest*. 1990;85(3):790–797.
347. Barnes K, Brown C, Turner AJ. Endothelin-converting enzyme: ultrastructural localization and its recycling from the cell surface. *Hypertension*. 1998;31(1):3–9.
348. Barnes K, Murphy LJ, Takahashi M, et al. Localization and biochemical characterization of endothelin-converting enzyme. *J Cardiovasc Pharmacol*. 1995;26(suppl 3):S37–S39.
349. Bakris GL, Fairbanks R, Traish AM. Arginine vasopressin stimulates human mesangial cell production of endothelin. *J Clin Invest*. 1991;87(4):1158–1164.
350. Herman WH, Emancipator SN, Rhoten RL, et al. Vascular and glomerular expression of endothelin-1 in normal human kidney. *Am J Physiol*. 1998;275(1 Pt 2):F8–F17.
351. Karet FE, Davenport AP. Localization of endothelin peptides in human kidney. *Kidney Int*. 1996;49(2):382–387.
352. Kasinath BS, Fried TA, Davalath S, et al. Glomerular epithelial cells synthesize endothelin peptides. *Am J Pathol*. 1992;141(2):279–283.
353. Kohan DE. Production of endothelin-1 by rat mesangial cells: regulation by tumor necrosis factor. *J Lab Clin Med*. 1992;119(5):477–484.
354. Marsden PA, Dorfman DM, Collins T, et al. Regulated expression of endothelin 1 in glomerular capillary endothelial cells. *Am J Physiol*. 1991;261(1 Pt 2):F117–F125.
355. Sakamoto H, Sasaki S, Nakamura Y, et al. Regulation of endothelin-1 production in cultured rat mesangial cells. *Kidney Int*. 1992;41(2):350–355.
356. Sakamoto H, Sasaki S, Hirata Y, et al. Production of endothelin-1 by rat cultured mesangial cells. *Biochem Biophys Res Commun*. 1990;169(2):462–468.
357. Ujiie K, Terada Y, Nonoguchi H, et al. Messenger RNA expression and synthesis of endothelin-1 along rat nephron segments. *J Clin Invest*. 1992;90(3):1043–1048.
358. Wilkes BM, Susin M, Mento PF, et al. Localization of endothelin-like immunoreactivity in rat kidneys. *Am J Physiol*. 1991;260(6 Pt 2):F913–F920.
359. Zoja C, Orisio S, Perico N, et al. Constitutive expression of endothelin gene in cultured human mesangial cells and its modulation by transforming growth factor-beta, thrombin, and a thromboxane A2 analogue. *Lab Invest*. 1991;64(1):16–20.
360. Badr KF, Munger KA, Sugiura M, et al. High and low affinity binding sites for endothelin on cultured rat glomerular mesangial cells. *Biochem Biophys Res Commun*. 1989;161(2):776–781.
361. Kohan DE. Endothelins in the normal and diseased kidney. *Am J Kidney Dis*. 1997;29(1):2–26.
362. Madeddu P, Troffia C, Glorioso N, et al. Effect of endothelin on regional hemodynamics and renal function in awake normotensive rats. *J Cardiovasc Pharmacol*. 1989;14(6):818–825.
363. Clozel M, Fischli W. Human cultured endothelial cells do secrete endothelin-1. *J Cardiovasc Pharmacol*. 1989;13(suppl 5):S229–S231.
364. Marsden PA, Danthuluri NR, Brenner BM, et al. Endothelin action on vascular smooth muscle involves inositol triphosphate and calcium mobilization. *Biochem Biophys Res Commun*. 1989;158(1):86–93.
365. Martin ER, Brenner BM, Ballermann BJ. Heterogeneity of cell surface endothelin receptors. *J Biol Chem*. 1990;265(23):14044–14049.
366. Sakurai T, Yanagisawa M, Masaki T. Molecular characterization of endothelin receptors. *Trends Pharmacol Sci*. 1992;13(3):103–108.
367. Pollock DM, Keith TL, Highsmith RF. Endothelin receptors and calcium signaling. *FASEB J*. 1995;9(12):1196–1204.
368. Deng Y, Martin LL, DelGrande D, et al. A soluble protease identified from rat kidney degrades endothelin-1 but not proendothelin-1. *J Biochem*. 1992;112(1):168–172.
369. Maguire JJ, Davenport AP. Endothelin receptors and their antagonists. *Semin Nephrol*. 2015;35(2):125–136.
370. De Miguel C, Speed JS, Kasztan M, et al. Endothelin-1 and the kidney: new perspectives and recent findings. *Curr Opin Nephrol Hypertens*. 2016;25(1):35–41.
371. Katusic ZS, Shepherd JT, Vanhoutte PM. Endothelium-dependent contraction to stretch in canine basilar arteries. *Am J Physiol*. 1987;252(3 Pt 2):H671–H673.
372. Yoshizumi M, Kurihara H, Sugiyama T, et al. Hemodynamic shear stress stimulates endothelin production by cultured endothelial cells. *Biochem Biophys Res Commun*. 1989;161(2):859–864.

373. Herizi A, Jover B, Bouriquet N, et al. Prevention of the cardiovascular and renal effects of angiotensin II by endothelin blockade. *Hypertension*. 1998;31:10–14.
374. Kohno M, Horio T, Ikeda M, et al. Angiotensin II stimulates endothelin-1 secretion in cultured rat mesangial cells. *Kidney Int*. 1992;42(4):860–866.
375. Marsden PA, Brenner BM. Transcriptional regulation of the endothelin-1 gene by TNF-alpha. *Am J Physiol*. 1992;262(4 Pt 1):C854–C861.
376. Rajagopalan S, Laursen JB, Borthayre A, et al. Role for endothelin-1 in angiotensin II-mediated hypertension. *Hypertension*. 1997;30(1 Pt 1):29–34.
377. Munger KA, Sugiura M, Takahashi K, et al. A role for atrial natriuretic peptide in endothelin-induced natriuresis. *J Am Soc Nephrol*. 1991;1(12):1278–1283.
378. Gohar EY, Kasztan M, Pollock DM. Interplay between renal endothelin and purinergic signaling systems. *Am J Physiol Renal Physiol*. 2017;313(3):F666–F668.
379. King AJ, Brenner BM, Anderson S. Endothelin: a potent renal and systemic vasoconstrictor peptide. *Am J Physiol*. 1989;256(6 Pt 2):F1051–F1058.
380. Badr KF, Murray JJ, Breyer MD, et al. Mesangial cell, glomerular and renal vascular responses to endothelin in the rat kidney. Elucidation of signal transduction pathways. *J Clin Invest*. 1989;83(1):336–342.
381. Clavell AL, Stingo AJ, Margulies KB, et al. Role of endothelin receptor subtypes in the in vivo regulation of renal function. *Am J Physiol*. 1995;268(3 Pt 2):F455–F460.
382. Heller J, Kramer HJ, Horacek V. Action of endothelin-1 on glomerular haemodynamics in the dog: lack of direct effects on glomerular ultrafiltration coefficient. *Clin Sci*. 1996;90(5):385–391.
383. Perico N, Dadan J, Gabanelli M, et al. Cyclooxygenase products and atrial natriuretic peptide modulate renal response to endothelin. *J Pharmacol Exp Ther*. 1990;252(3):1213–1220.
384. Stacy DL, Scott JW, Granger JP. Control of renal function during intrarenal infusion of endothelin. *Am J Physiol*. 1990;258(5 Pt 2):F1232–F1236.
385. Kon V, Yoshioka T, Fogo A, et al. Glomerular actions of endothelin in vivo. *J Clin Invest*. 1989;83(5):1762–1767.
386. Fretschner M, Endlich K, Gulbins E, et al. Effects of endothelin on the renal microcirculation of the split hydronephrotic rat kidney. *Ren Physiol Biochem*. 1991;14(3):112–127.
387. Loutzenhiser R, Epstein M, Hayashi K, et al. Direct visualization of effects of endothelin on the renal microvasculature. *Am J Physiol*. 1990;258(1 Pt 2):F61–F68.
388. Edwards RM, Trizna W, Ohlstein EH. Renal microvascular effects of endothelin. *Am J Physiol*. 1990;259(2 Pt 2):F217–F221.
389. Lanese DM, Yuan BH, McMurry IF, et al. Comparative sensitivities of isolated rat renal arterioles to endothelin. *Am J Physiol*. 1992;263(5 Pt 2):F894–F899.
390. Dlugosz JA, Munk S, Zhou X, et al. Endothelin-1-induced mesangial cell contraction involves activation of protein kinase C-alpha, -delta, and -epsilon. *Am J Physiol*. 1998;275(3 Pt 2):F423–F432.
391. Noll G, Wenzel RR, Luscher TF. Endothelin and endothelin antagonists: potential role in cardiovascular and renal disease. *Mol Cell Biochem*. 1996;157(1–2):259–267.
392. Lin H, Smith MJ Jr, Young DB. Roles of prostaglandins and nitric oxide in the effect of endothelin-1 on renal hemodynamics. *Hypertension*. 1996;28(3):372–378.
393. Momose N, Fukuo K, Morimoto S, et al. Captopril inhibits endothelin-1 secretion from endothelial cells through bradykinin. *Hypertension*. 1993;21(6 Pt 2):921–924.
394. Prins BA, Hu RM, Nazario B, et al. Prostaglandin E2 and prostacyclin inhibit the production and secretion of endothelin from cultured endothelial cells. *J Biol Chem*. 1994;269(16):11938–11944.
395. Chou SY, Dahhan A, Porush JG. Renal actions of endothelin: interaction with prostacyclin. *Am J Physiol*. 1990;259(4 Pt 2):F645–F652.
396. Gohar EY, Giachini FR, Pollock DM, et al. Role of the endothelin system in sexual dimorphism in cardiovascular and renal diseases. *Life Sci*. 2016;159:20–29.
397. Arai H, Hori S, Aramori I, et al. Cloning and expression of a cDNA encoding an endothelin receptor. *Nature*. 1990;348(6303):730–732.
398. Sakurai T, Yanagisawa M, Takuwa Y, et al. Cloning of a cDNA encoding a non-isopeptide-selective subtype of the endothelin receptor. *Nature*. 1990;348(6303):732–735.
399. Ihara M, Noguchi K, Saeki T, et al. Biological profiles of highly potent novel endothelin antagonists selective for the ETA receptor. *Life Sci*. 1992;50(4):247–255.
400. Wendel M, Knels L, Kummer W, et al. Distribution of endothelin receptor subtypes ETA and ETB in the rat kidney. *J Histochem Cytochem*. 2006;54(11):1193–1203.
401. Qiu C, Engels K, Baylis C. Endothelin modulates the pressor actions of acute systemic nitric oxide blockade. *J Am Soc Nephrol*. 1995;6(5):1476–1481.
402. Heerspink HJL, Andress DL, Bakris G, et al. Rationale and protocol of the Study Of diabetic Nephropathy with AtRasentan (SONAR) trial: a clinical trial design novel to diabetic nephropathy. *Diabetes Obes Metab*. 2018;20(6):1369–1376.
403. de Zeeuw D, Coll B, Andress D, et al. The endothelin antagonist atrasentan lowers residual albuminuria in patients with type 2 diabetic nephropathy. *J Am Soc Nephrol*. 2014;25(5):1083–1093.
404. Kohan DE, Pritchett Y, Molitch M, et al. Addition of atrasentan to renin-angiotensin system blockade reduces albuminuria in diabetic nephropathy. *J Am Soc Nephrol*. 2011;22(4):763–772.
405. Mann JF, Green D, Jamerson K, et al. Avosentan for overt diabetic nephropathy. *J Am Soc Nephrol*. 2010;21(3):527–535.
406. Oyekan A, Balazy M, McGiff JC. Renal oxygenases: differential contribution to vasoconstriction induced by ET-1 and Ang II. *Am J Physiol*. 1997;273(1 Pt 2):R293–R300.
407. Stier CT Jr, Quillie CP, McGiff JC. Endothelin-3 effects on renal function and prostanoid release in the rat isolated kidney. *J Pharmacol Exp Ther*. 1992;262(1):252–256.
408. Owada A, Tomita K, Terada Y, et al. Endothelin (ET)-3 stimulates cyclic guanosine 3',5'-monophosphate production via ETB receptor by producing nitric oxide in isolated rat glomerulus, and in cultured rat mesangial cells. *J Clin Invest*. 1994;93(2):556–563.
409. Filep JG. Endogenous endothelin modulates blood pressure, plasma volume, and albumin escape after systemic nitric oxide blockade. *Hypertension*. 1997;30(1 Pt 1):22–28.
410. Thompson A, Valeri CR, Lieberthal W. Endothelin receptor A blockade alters hemodynamic response to nitric oxide inhibition in rats. *Am J Physiol*. 1995;269(2 Pt 2):H743–H748.
411. Gurbanov K, Rubinstein I, Hoffman A, et al. Differential regulation of renal regional blood flow by endothelin-1. *Am J Physiol*. 1996;271(6 Pt 2):F1166–F1172.
412. Crawford C, Kennedy-Lydon T, Sprott C, et al. An intact kidney slice model to investigate vasa recta properties and function in situ. *Nephron Physiol*. 2012;120(3):p17–p31.
413. Prieto MC, Gonzalez AA, Navar LG. Evolving concepts on regulation and function of renin in distal nephron. *Pflugers Arch*. 2013;465(1):121–132.
414. Ramkumar N, Kohan DE. Role of collecting duct renin in blood pressure regulation. *Am J Physiol Regul Integr Comp Physiol*. 2013;305(2):R92–R94.
415. Rohrwasser A, Morgan T, Dillon HF, et al. Elements of a paracrine tubular renin-angiotensin system along the entire nephron. *Hypertension*. 1999;34(6):1265–1274.
416. Navar LG. Physiology: hemodynamics, endothelial function, renin-angiotensin-aldosterone system, sympathetic nervous system. *J Am Soc Hypertens*. 2014;8(7):519–524.
417. Denton KM, Anderson WP, Sinniah R. Effects of angiotensin II on regional afferent and efferent arteriole dimensions and the glomerular pole. *Am J Physiol Regul Integr Comp Physiol*. 2000;279(2):R629–R638.
418. Yuan BH, Robinette JB, Conger JD. Effect of angiotensin II and norepinephrine on isolated rat afferent and efferent arterioles. *Am J Physiol*. 1990;258(3 Pt 2):F741–F750.
419. Navar LG, Harrison-Bernard LM, Imig JD, et al. Renal responses to AT1 receptor blockade. *Am J Hypertens*. 2000;13(1 Pt 2):45S–54S.
420. Navar LG. Intrarenal renin-angiotensin system in regulation of glomerular function. *Curr Opin Nephrol Hypertens*. 2014;23(1):38–45.
421. Harrison-Bernard LM, Monjure CJ, Bivona BJ. Efferent arterioles exclusively express the subtype 1A angiotensin receptor: functional insights from genetic mouse models. *Am J Physiol Renal Physiol*. 2006;290(5):F1177–F1186.
422. Juncos LA, Ren Y, Arima S, et al. Angiotensin II action in isolated microperfused rabbit afferent arterioles is modulated by flow. *Kidney Int*. 1996;49(2):374–381.
423. Purdy KE, Arendshorst WJ. Prostaglandins buffer Ang II-mediated increases in cytosolic calcium in preglomerular VSMC. *Am J Physiol*. 1999;277(6 Pt 2):F850–F858.
424. Kohagura K, Endo Y, Ito O, et al. Endogenous nitric oxide and epoxyeicosatrienoic acids modulate angiotensin II-induced

- constriction in the rabbit afferent arteriole. *Acta Physiol Scand.* 2000;168(1):107–112.
425. Patzak A, Kleinmann F, Lai EY, et al. Nitric oxide counteracts angiotensin II induced contraction in efferent arterioles in mice. *Acta Physiol Scand.* 2004;181(4):439–444.
 426. Patzak A, Lai E, Persson PB, et al. Angiotensin II-nitric oxide interaction in glomerular arterioles. *Clin Exp Pharmacol Physiol.* 2005;32(5–6):410–414.
 427. Baylis C, Brenner BM. Modulation by prostaglandin synthesis inhibitors of the action of exogenous angiotensin II on glomerular ultrafiltration in the rat. *Circ Res.* 1978;43(6):889–898.
 428. Takeda K, Meyer-Lehnert H, Kim JK, et al. Effect of angiotensin II on Ca²⁺ kinetics and contraction in cultured rat glomerular mesangial cells. *Am J Physiol.* 1988;254(2 Pt 2):F254–F266.
 429. Wiegmann TB, MacDougall ML, Savin VJ. Glomerular effects of angiotensin II require intrarenal factors. *Am J Physiol.* 1990;258(3 Pt 2):F717–F721.
 430. Sharma M, Sharma R, Greene AS, et al. Documentation of angiotensin II receptors in glomerular epithelial cells. *Am J Physiol.* 1998;274(3 Pt 2):F623–F627.
 431. Pagtalunan ME, Rasch R, Rennke HG, et al. Morphometric analysis of effects of angiotensin II on glomerular structure in rats. *Am J Physiol.* 1995;268(1 Pt 2):F82–F88.
 432. Inishi Y, Okuda T, Arakawa T, et al. Insulin attenuates intracellular calcium responses and cell contraction caused by vasoactive agents. *Kidney Int.* 1994;45(5):1318–1325.
 433. Arima S, Endo Y, Yaoita H, et al. Possible role of P-450 metabolite of arachidonic acid in vasodilator mechanism of angiotensin II type 2 receptor in the isolated microperfused rabbit afferent arteriole. *J Clin Invest.* 1997;100(11):2816–2823.
 434. Ren Y, Garvin JL, Carretero OA. Vasodilator action of angiotensin-(1–7) on isolated rabbit afferent arterioles. *Hypertension.* 2002;39(3):799–802.
 435. Santos RA, Simoes e Silva AC, Maric C, et al. Angiotensin-(1–7) is an endogenous ligand for the G protein-coupled receptor Mas. *Proc Natl Acad Sci USA.* 2003;100(14):8258–8263.
 436. Chappell MC. Emerging evidence for a functional angiotensin-converting enzyme 2-angiotensin-(1–7)-MAS receptor axis: more than regulation of blood pressure? *Hypertension.* 2007;50(4):596–599.
 437. Tipnis SR, Hooper NM, Hyde R, et al. A human homolog of angiotensin-converting enzyme. Cloning and functional expression as a captopril-insensitive carboxypeptidase. *J Biol Chem.* 2000;275(43):33238–33243.
 438. Turner AJ, Tipnis SR, Guy JL, et al. ACEH/ACE2 is a novel mammalian metallocarboxypeptidase and a homologue of angiotensin-converting enzyme insensitive to ACE inhibitors. *Can J Physiol Pharmacol.* 2002;80(4):346–353.
 439. Zisman LS, Meixell GE, Bristow MR, et al. Angiotensin-(1–7) formation in the intact human heart: in vivo dependence on angiotensin II as substrate. *Circulation.* 2003;108(14):1679–1681.
 440. Gonzalez AA, Lara LS, Prieto MC. Role of Collecting Duct Renin in the Pathogenesis of Hypertension. *Curr Hypertens Rep.* 2017;19(8):62.
 441. Maddox DA, Bennett CM, Deen WM, et al. Determinants of glomerular filtration in experimental glomerulonephritis in the rat. *J Clin Invest.* 1975;55(2):305–318.
 442. Myers BD, Deen WM, Brenner B. Effects of norepinephrine and angiotensin II on the determinants of glomerular ultrafiltration and proximal tubule fluid reabsorption in the rat. *Circ Res.* 1975;37:101–110.
 443. Anderson S, Rennke HG, Brenner BM. Therapeutic advantage of converting enzyme inhibitors in arresting progressive renal disease associated with systemic hypertension in the rat. *J Clin Invest.* 1986;77(6):1993–2000.
 444. Ruster C, Wolf G. Renin-angiotensin-aldosterone system and progression of renal disease. *J Am Soc Nephrol.* 2006;17(11):2985–2991.
 445. Remuzzi A, Puntonieri S, Battaglia C, et al. Angiotensin converting enzyme inhibition ameliorates glomerular filtration of macromolecules and water and lessens glomerular injury in the rat. *J Clin Invest.* 1990;85(2):541–549.
 446. Remuzzi A, Malanchini B, Battaglia C, et al. Comparison of the effects of angiotensin-converting enzyme inhibition and angiotensin II receptor blockade on the evolution of spontaneous glomerular injury in male MWF/Ztm rats. *Exp Nephrol.* 1996;4(1):19–25.
 447. Urushihara M, Kinoshita Y, Kondo S, et al. Involvement of the intrarenal renin-angiotensin system in experimental models of glomerulonephritis. *J Biomed Biotechnol.* 2012;2012:601786.
 448. Remuzzi A, Gagliardini E, Sangalli F, et al. ACE inhibition reduces glomerulosclerosis and regenerates glomerular tissue in a model of progressive renal disease. *Kidney Int.* 2006;69(7):1124–1130.
 449. Adamczak M, Gross ML, Amann K, et al. Reversal of glomerular lesions involves coordinated restructuring of glomerular microvasculature. *J Am Soc Nephrol.* 2004;15(12):3063–3072.
 450. Wang TN, Chen X, Li R, et al. SREBP-1 mediates angiotensin II-induced TGF-beta1 upregulation and glomerular fibrosis. *J Am Soc Nephrol.* 2015;26(8):1839–1854.
 451. Lavoie P, Robitaille G, Agharazii M, et al. Neutralization of transforming growth factor-beta attenuates hypertension and prevents renal injury in uremic rats. *J Hypertens.* 2005;23(10):1895–1903.
 452. Sharma R, Sharma M, Reddy S, et al. Chronically increased intrarenal angiotensin II causes nephropathy in an animal model of type 2 diabetes. *Front Biosci.* 2006;11:968–976.
 453. Ichikawa I, Pfeffer JM, Pfeffer MA, et al. Role of angiotensin II in the altered renal function of congestive heart failure. *Circ Res.* 1984;55(5):669–675.
 454. Uttarwar L, Gao B, Ingram AJ, et al. SREBP-1 activation by glucose mediates TGF-beta upregulation in mesangial cells. *Am J Physiol Renal Physiol.* 2012;302(3):F329–F341.
 455. Leh S, Vaagnes O, Margolin SB, et al. Pirfenidone and candesartan ameliorate morphological damage in mild chronic anti-GBM nephritis in rats. *Nephrol Dial Transplant.* 2005;20(1):71–82.
 456. Wang J, Chen L, Chen B, et al. Chronic activation of the renin-angiotensin system induces lung fibrosis. *Sci Rep.* 2015;5:15561.
 457. Navar LG, Inscho EW, Majid SA, et al. Paracrine regulation of the renal microcirculation. *Physiol Rev.* 1996;76(2):425–536.
 458. Imig JD. Eicosanoid regulation of the renal vasculature. *Am J Physiol Renal Physiol.* 2000;279(6):F965–F981.
 459. Hao CM, Breyer MD. Physiologic and pathophysiologic roles of lipid mediators in the kidney. *Kidney Int.* 2007;71(11):1105–1115.
 460. Roman RJ. P-450 metabolites of arachidonic acid in the control of cardiovascular function. *Physiol Rev.* 2002;82(1):131–185.
 461. Smith WL, Marnett LJ, DeWitt DL. Prostaglandin and thromboxane biosynthesis. *Pharmacol Ther.* 1991;49(3):153–179.
 462. Breyer RM, Bagdassarian CK, Myers SA, et al. Prostanoid receptors: subtypes and signaling. *Annu Rev Pharmacol Toxicol.* 2001;41:661–690.
 463. Li Y, Xia W, Zhao F, et al. Prostaglandins in the pathogenesis of kidney diseases. *Oncotarget.* 2018;9(41):26586–26602.
 464. Carlstrom M, Wilcox CS, Arendshorst WJ. Renal autoregulation in health and disease. *Physiol Rev.* 2015;95(2):405–511.
 465. Nielsen CB, Bech JN, Pedersen EB. Effects of prostacyclin on renal haemodynamics, renal tubular function and vasoactive hormones in healthy humans. A placebo-controlled dose-response study. *Br J Clin Pharmacol.* 1997;44(5):471–476.
 466. Villa E, Garcia-Robles R, Haas J, et al. Comparative effect of PGE2 and PGI₂ on renal function. *Hypertension.* 1997;30(3 Pt 2):664–666.
 467. Schor N, Ichikawa I, Brenner B. Mechanisms of action of various hormones and vasoactive substances on glomerular ultrafiltration in the rat. *Kidney Int.* 1981;20:442–451.
 468. Yoshioka T, Yared A, Miyazawa H, et al. In vivo influence of prostaglandin I₂ on systemic and renal circulation in the rat. *Hypertension.* 1985;7(6 Pt 1):867–872.
 469. Inscho EW, Carmines PK, Navar LG. Prostaglandin influences on afferent arteriolar responses to vasoconstrictor agonists. *Am J Physiol.* 1990;259(1 Pt 2):F157–F163.
 470. Endlich K, Forssmann WG, Steinhausen M. Effects of urodilatin in the rat kidney: comparison with ANF and interaction with vasoactive substances. *Kidney Int.* 1995;47(6):1558–1568.
 471. Munger KA, Blantz RC. Cyclooxygenase-dependent mediators of renal hemodynamic function in female rats. *Am J Physiol.* 1990;258(5 Pt 2):F1211–F1217.
 472. Vio CP, Quiroz-Munoz M, Cuevas CA, et al. Prostaglandin E2 EP3 receptor regulates cyclooxygenase-2 expression in the kidney. *Am J Physiol Renal Physiol.* 2012;303(3):F449–F457.
 473. Dahlen SE, Bjork J, Hedqvist P, et al. Leukotrienes promote plasma leakage and leukocyte adhesion in postcapillary venules: in vivo effects with relevance to the acute inflammatory response. *Proc Natl Acad Sci USA.* 1981;78(6):3887–3891.
 474. Yared A, Albrightson-Winslow C, Griswold D, et al. Functional significance of leukotriene B₄ in normal and glomerulonephritic kidneys. *J Am Soc Nephrol.* 1991;2(1):45–56.
 475. Badr KF, Baylis C, Pfeffer JM, et al. Renal and systemic hemodynamic responses to intravenous infusion of leukotriene C₄ in the rat. *Circ Res.* 1984;54(5):492–499.

476. Filep J, Rigter B, Frolich JC. Vascular and renal effects of leukotriene C₄ in conscious rats. *Am J Physiol*. 1985;249(5 Pt 2):F739–F744.
477. Badr KF, Serhan CN, Nicolaou KC, et al. The action of lipoxin-A on glomerular microcirculatory dynamics in the rat. *Biochem Biophys Res Commun*. 1987;145(1):408–414.
478. Rubinstein M, Dvash E. Leukotrienes and kidney diseases. *Curr Opin Nephrol Hypertens*. 2018;27(1):42–48.
479. Serhan CN, Sheppard KA. Lipoxin formation during human neutrophil-platelet interactions. Evidence for the transformation of leukotriene A₄ by platelet 12-lipoxygenase in vitro. *J Clin Invest*. 1990;85(3):772–780.
480. Katoh T, Takahashi K, DeBoer DK, et al. Renal hemodynamic actions of lipoxins in rats: a comparative physiological study. *Am J Physiol*. 1992;263(3 Pt 2):F436–F442.
481. Munger KA, Montero A, Fukunaga M, et al. Transfection of rat kidney with human 15-lipoxygenase suppresses inflammation and preserves function in experimental glomerulonephritis. *Proc Natl Acad Sci USA*. 1999;96(23):13375–13380.
482. Kieran NE, Doran PP, Connolly SB, et al. Modification of the transcriptomic response to renal ischemia/reperfusion injury by lipoxin analog. *Kidney Int*. 2003;64(2):480–492.
483. Chandrasekharan JA, Sharma-Walia N. Lipoxins: nature's way to resolve inflammation. *J Inflamm Res*. 2015;8:181–192.
484. Roman RJ, Fan F. 20-HETE: hypertension and beyond. *Hypertension*. 2018;72(1):12–18.
485. Dordea AC, Vandewijngaert S, Garcia V, et al. Androgen-sensitive hypertension associated with soluble guanylate cyclase-α1/β1 deficiency is mediated by 20-HETE. *Am J Physiol Heart Circ Physiol*. 2016;310(11):H1790–H1800.
486. Tuncat B, Sari AN, Kacan M, et al. NS-398 reverses hypotension in endotoxemic rats: contribution of eicosanoids, NO, and peroxynitrite. *Prostaglandins Other Lipid Mediat*. 2013;104–105:93–108.
487. Tuncat B, Korkmaz B, Cuez T, et al. Contribution of vasoactive eicosanoids and nitric oxide production to the effect of selective cyclooxygenase-2 inhibitor, NS-398, on endotoxin-induced hypotension in rats. *Basic Clin Pharmacol Toxicol*. 2010;107(5):877–882.
488. Imig JD. Epoxyeicosatrienoic acids, hypertension, and kidney injury. *Hypertension*. 2015;65(3):476–482.
489. Liu L, Liu GL, Barajas L. Distribution of nitric oxide synthase-containing ganglionic neuronal somata and postganglionic fibers in the rat kidney. *J Comp Neurol*. 1996;369(1):16–30.
490. Barajas L, Liu L, Powers K. Anatomy of the renal innervation: intrarenal aspects and ganglia of origin. *Can J Physiol Pharmacol*. 1992;70(5):735–749.
491. DiBona GF. Neural control of renal function in health and disease. *Clin Auton Res*. 1994;4:69–74.
492. Pelayo JC, Westcott JY. Renal adrenergic effector mechanisms: glomerular sites for prostaglandin interaction. *Am J Physiol*. 1988;254:F184–F190.
493. Pelayo JC, Ziegler MG, Blantz RC. Angiotensin II in adrenergic-induced alterations in glomerular hemodynamics. *Am J Physiol*. 1984;247:F799–F807.
494. Gabbai FB, Thomson SC, Peterson O, et al. Glomerular and tubular interactions between renal adrenergic activity and nitric oxide. *Am J Physiol*. 1995;268(6 Pt 2):F1004–F1008.
495. Beirwaltes WH. Sympathetic stimulation of renin is independent of direct regulation by renal nitric oxide. *Vascul Pharmacol*. 2003;40:43–49.
496. Abdulla MH, Johns EJ. The innervation of the kidney in renal injury and inflammation: a cause and consequence of deranged cardiovascular control. *Acta Physiol (Oxf)*. 2017;220(4):404–416.
497. Ahmed AF, Rae MG, Johns EJ. Effect of reactive oxygen species and nitric oxide in the neural control of intrarenal haemodynamics in anaesthetized normotensive rats. *Acta Physiol (Oxf)*. 2013;209(2):156–166.
498. Kon V, Yared A, Ichikawa I. Role of sympathetic nerves in mediating hypoperfusion of renal cortical microcirculation in experimental congestive heart failure and acute extracellular volume depletion. *J Clin Invest*. 1985;76:1913–1920.
499. Bhatt DL, Kandzari DE, O'Neill WW, et al. A controlled trial of renal denervation for resistant hypertension. *N Engl J Med*. 2014;370(15):1393–1401.
500. Esler MD. Fine tuning renal denervation. *J Hypertens*. 2018;36(12):2312–2313.
501. Davies DF, Shock NW. Age changes in glomerular filtration rate, effective renal plasma flow, and tubular excretory capacity in adult males. *J Clin Invest*. 1950;29(5):496–507.
502. Glasscock RJ, Rule AD. The implications of anatomical and functional changes of the aging kidney: with an emphasis on the glomeruli. *Kidney Int*. 2012;82(3):270–277.
503. Rule AD, Amer H, Cornell LD, et al. The association between age and nephrosclerosis on renal biopsy among healthy adults. *Ann Intern Med*. 2010;152(9):561–567.
504. Lindeman RD, Tobin J, Shock NW. Longitudinal studies on the rate of decline in renal function with age. *J Am Geriatr Soc*. 1985;33(4):278–285.
505. Maddox DA, Alavi FK, Zawada ET Jr. The kidney and aging. In: Massry SG, Glasscock RJ, eds. *Textbook of Nephrology*. Baltimore: Lippincott Williams & Wilkins; 2001:1094–1105.
506. Elliott MJ, O'Hare AM, Hemmelgarn BR. Care of the Older Adult with Chronic Renal Disease. In: Skorecki K, Chertow GM, Marsden PA, et al, eds. *Brenner and Rector's the Kidney*. Philadelphia: Elsevier; 2016:2586–2601.
507. Hoang K, Tan JC, Derby G, et al. Determinants of glomerular hypofiltration in aging humans. *Kidney Int*. 2003;64(4):1417–1424.
508. Fliser D, Zeier M, Nowack R, et al. Renal functional reserve in healthy elderly subjects. *J Am Soc Nephrol*. 1993;3(7):1371–1377.
509. Lindeman RD, Tobin JD, Shock NW. Association between blood pressure and the rate of decline in renal function with age. *Kidney Int*. 1984;26(6):861–868.
510. Zawada ET Jr, Alavi FK, Santella RN, et al. Influence of dietary macronutrients on glomerular senescence. In: *Current Nephrology*. Vol 20. Mosby Yearbook; 1997:1–47.
511. Baylis C, Corman B. The aging kidney: insights from experimental studies. *J Am Soc Nephrol*. 1998;9(4):699–709.
512. Weinstein JR, Anderson S. The aging kidney: physiological changes. *Adv Chronic Kidney Dis*. 2010;17(4):302–307.
513. Deen WM, Maddox DA, Robertson CR, et al. Dynamics of glomerular ultrafiltration in the rat. VII. Response to reduced renal mass. *Am J Physiol*. 1974;227(3):556–562.
514. Brenner BM. Nephron adaptation to renal injury or ablation. *Am J Physiol*. 1985;249(3 Pt 2):F324–F337.
515. Choudhury D, Palmer B, Levi M. Renal function and dysfunction in aging. In: Seldin DW, Giebisch G, eds. *Seldin and Giebisch's the Kidney, Physiology and Pathophysiology*. Philadelphia: Lippincott Williams & Wilkins; 2000:2571–2595.
516. Baylis C, Fredericks M, Wilson C, et al. Renal vasodilatory response to intravenous glycine in the aging rat kidney. *Am J Kidney Dis*. 1990;15(3):244–251.
517. Giordano M, DeFronzo RA. Acute effect of human recombinant insulin-like growth factor I on renal function in humans. *Nephron*. 1995;71:10–15.
518. Winetz JA, Golbetz HV, Spencer RJ, et al. Glomerular function in advanced human diabetic nephropathy. *Kidney Int*. 1982;21(5):750–756.
519. Hostetter TH. Human renal response to meat meal. *Am J Physiol*. 1986;250(4 Pt 2):F613–F618.
520. Deen WM, Bridges CR, Brenner BM, et al. Heteroporous model of glomerular size selectivity: application to normal and nephrotic humans. *Am J Physiol*. 1985;249(3 Pt 2):F374–F389.
521. Chagnac A, Weinstein T, Korzets A, et al. Glomerular hemodynamics in severe obesity. *Am J Physiol Renal Physiol*. 2000;278(5):F817–F822.
522. Carmines PK, Navar LG. Disparate effects of Ca channel blockade on afferent and efferent arteriolar responses to Ang II. *Am J Physiol Renal Physiol*. 1989;256(6 Pt 2):F1015–F1020.
523. Feng MG, Navar LG. Angiotensin II-mediated constriction of afferent and efferent arterioles involves T-type Ca²⁺ channel activation. *Am J Nephrol*. 2004;24(6):641–648.

BOARD REVIEW QUESTIONS

1. A 21-year old woman runs a marathon and her extracellular fluid volume becomes severely decreased. Immediately following the race, she takes double the prescribed dose of ibuprofen (a non-steroidal anti-inflammatory drug) to alleviate the pain of her aching ankle and knee joints. Which one of the following adverse effects is likely to occur in the renal circulation?
- Increased prostaglandin levels in the kidney.
 - Decreased efferent arteriolar resistance.
 - Increased afferent arteriolar resistance.
 - Increased urinary excretion of salt and water.
 - Increased renal blood flow and GFR.

Answer: c

Rationale: The decreased extracellular fluid volume stimulates increased renal sympathetic activity as well as activation of the renin-angiotensin system. This causes direct renal vasoconstriction of both the afferent and efferent arterioles. This is normally counteracted by vasodilator prostanooids such as prostacyclin and PGE₂ that cause afferent vasodilation. However, NSAID drugs block cyclooxygenase, and therefore prevent afferent vasodilation, leading to impaired renal blood flow and GFR.

2. A 35-year old man is diagnosed with severe hypertension due to bilateral renal artery stenosis. An angiotensin receptor antagonist is administered in order to block the actions of angiotensin II (Ang II) on AT1 receptors. Although blood pressure returns to normal, GFR decreases markedly (by about 50%). In addition to the reduction in blood pressure, which one of the following mechanisms is most responsible for the decrease in GFR?
- Increased bradykinin levels in the kidney.
 - Decreased glomerular ultrafiltration coefficient (K_f).
 - Increased erythropoietin levels in the kidney.
 - Decreased efferent arteriolar resistance.
 - Decreased renin secretion by the juxtaglomerular cells.

Answer: d

Rationale: Bilateral renal artery stenosis reduces renal perfusion pressure beyond the stenosis leading to activation of the renin-angiotensin system and increased systemic and intrarenal Ang II levels. The increased Ang II levels increases afferent and efferent arteriolar resistance but the vasodilator influence of the tubuloglomerular feedback mechanism exerts vasodilator influence on the afferent arterioles, leaving the Ang II influence on the efferent arterioles unopposed. The reduction in blood pressure plus the efferent arteriolar vasodilation due to blockade of the AT₁ receptors cause profound decreases in glomerular pressure and the GFR.

3. Mr. H.I. Stress has not seen a doctor in several years but comes to see you because a screening at a mall showed a blood pressure of 190/100 mmHg. Records from 10 years previously show that he had a plasma creatinine of 1.0 mg/dL and normal blood pressure. The plasma creatinine concentration is now 4 mg/dL. Which one of the following changes in renal function is illustrated in this patient?
- His renal function has been stable.
 - Cannot make conclusions based on data given.
 - He has had a 75% reduction in glomerular function.
 - He has had a 25% reduction in glomerular function.
 - He has had a 50% reduction in GFR.

Answer: c

Rationale: Although not exact, there is a reciprocal relationship between plasma creatinine and GFR such that a 4-fold increase in plasma creatinine concentration reflects reduced glomerular functions to $\frac{1}{4}$ of his original value assuming that the daily production of creatinine has remained unchanged.

4. A 47-year old man is admitted to the intensive care unit because of severe alcohol withdrawal with symptoms and signs of excessive sympathetic stimulation. The effect of this on renal nerve activity would result in which one of the following:
- Decrease in renal blood flow but not GFR.
 - Decrease in both renal blood flow and GFR.
 - Decrease in renal blood flow but increase GFR.
 - Increase in both renal blood flow and GFR due to the increase in arterial pressure.
 - Cause no changes in renal blood flow and GFR because of renal autoregulation.

Answer: b

Rationale: The renal vasculature has abundant sympathetic innervation to all vascular elements. Thus, marked renal sympathetic activity will vasoconstrict both afferent and efferent arterioles causing marked decreases in renal blood flow. Because of the greater amount of preglomerular vascular smooth muscle cells, the preglomerular vasoconstriction will predominate with increased renal sympathetic activity leading to profound decreases in glomerular pressure and thus GFR.

5. A 70-year-old male is seen by his physician for a physical, his first in almost 10 years. He has gained 40 pounds and his BMI has increased from 29 to 34. His HbA1c is now 9.0, up from 6.0 previously. His serum creatinine has gone from 0.8 to 1.8 suggesting some loss of GFR due to type II diabetes and perhaps an age-related decline in renal function. His blood pressure has also increased from 120/80 to 150/90. The physician prescribes an angiotensin converting enzyme (ACE) inhibitor to inhibit the production of angiotensin II (Ang II). Which one of the following responses regarding the effects of Ang II on the kidney is most likely?
- The ACE inhibitor will result in a decrease in renal blood flow and GFR.
 - The reduced intrarenal Ang II will increase sodium reabsorption in the cortical collecting duct.
 - The ACE inhibitor will lead to reductions in intrarenal Ang II allowing maintenance of glomerular capillary hydraulic pressure and GFR.
 - The reduced intrarenal Ang II will decrease production of proliferative factors.
 - The ACE inhibition will increase intrarenal Ang II.

Answer: c

Rationale: Following the conversion of circulating and intrarenal angiotensinogen by renal renin, all components needed to synthesize and degrade Ang II are present in the immediate region of the juxtaglomerular region of the nephron thereby allowing direct local regulation of glomerular blood flow and filtration rate. Both ACE inhibitors and ARBs prevent hypertension, limit proteinuria and ameliorate sclerosis in several experimental models of glomerulonephritis.

Glomerular Cell Biology and Podocytopathies

Catherine Meyer-Schwesinger | Tobias B. Huber

CHAPTER OUTLINE

| | |
|---|--|
| GLOMERULAR CELL ANATOMY AND INJURY RESPONSE PATTERNS, 115 | EFFECTS OF EXISTING THERAPIES ON PODOCYTES, 130 |
| COMMON MECHANISMS OF GLOMERULAR DISEASES, 126 | IDENTIFICATION OF CANDIDATE THERAPEUTIC APPROACHES FOR THE FUTURE, 131 |
| MECHANISMS OF INJURY IN COMMON PODOCYTOPATHIES, 128 | SUMMARY, 131 |

KEY POINTS

- The glomerulus represents a functional and integrated syncytium of four types of glomerular cells, which together ascertain glomerular filtration.
- Together, podocytes and glomerular endothelial cells allow for a size- and charge-selective glomerular filtration due to their specialized three-dimensional structure, extensive glycocalyx coating, and the coordinated synthesis of the unique glomerular basement membrane.
- Mesangial cells provide structural support of the glomerular capillaries, regulate glomerular filtration, and maintain glomerular endothelial health.
- Parietal epithelial cells build the Bowman's capsule to prevent leakage of the primary urine filtrate to the tubulointerstitium, contribute to glomerular scarring, and are thought to constitute a potential reservoir for podocytes in development, maturation, and eventually in adulthood.
- The hallmarks of diseases related to primary podocyte injury of genetic or autoimmune origin are proteinuria (often nephrotic range), foot process effacement, podocyte hypertrophy, and depletion.
- Crosstalk between glomerular cell types attenuates and/or perpetuates glomerular injury.
- Most forms of glomerular injury result from humoral and cellular immunologic mechanisms to which the glomerulus reacts by basic responses such as cellular proliferation, changes in glomerular cell phenotypes, and increased deposition of extracellular matrix.

GLOMERULAR CELL ANATOMY AND INJURY RESPONSE PATTERNS

Loss of protein into the urine (proteinuria), especially albumin (albuminuria), is the hallmark of glomerular disease and an important prognostic marker for a wide variety of kidney diseases, including the numerically and economically increasing challenge of diabetic nephropathy.¹ Albuminuria is also an independent risk factor for cardiovascular mortality.² Therefore, understanding the pathophysiology of albuminuria and therapeutic approaches to its modification has major clinical and health economic significance.

The kidney of a healthy 70-kg adult filters approximately 180 L of plasma per day. Filtration and urine production

takes place in the smallest functional unit of the kidney, called the nephron. The ultimate site of filtration is located at the beginning of the nephron in the renal corpuscle. The renal corpuscle (Fig. 4.1) is composed of the glomerulus, a network (tuft) of capillaries, which is surrounded by parietal epithelial cells (PECs) of Bowman's capsule (BC), and is thereby separated from the tubular system. As described and depicted in detail in Chapter 3, blood enters the glomerulus at the vascular pole through an afferent arteriole of the renal circulation and is drained into an efferent arteriole. The unique resistance of these arterioles generates a high pressure within the capillary convolute of the glomerulus, ultimately driving the ultrafiltration of a primary urinary filtrate through the glomerular filtration barrier into Bowman's space with an effective filtration pressure of approximately 50 mm Hg.³

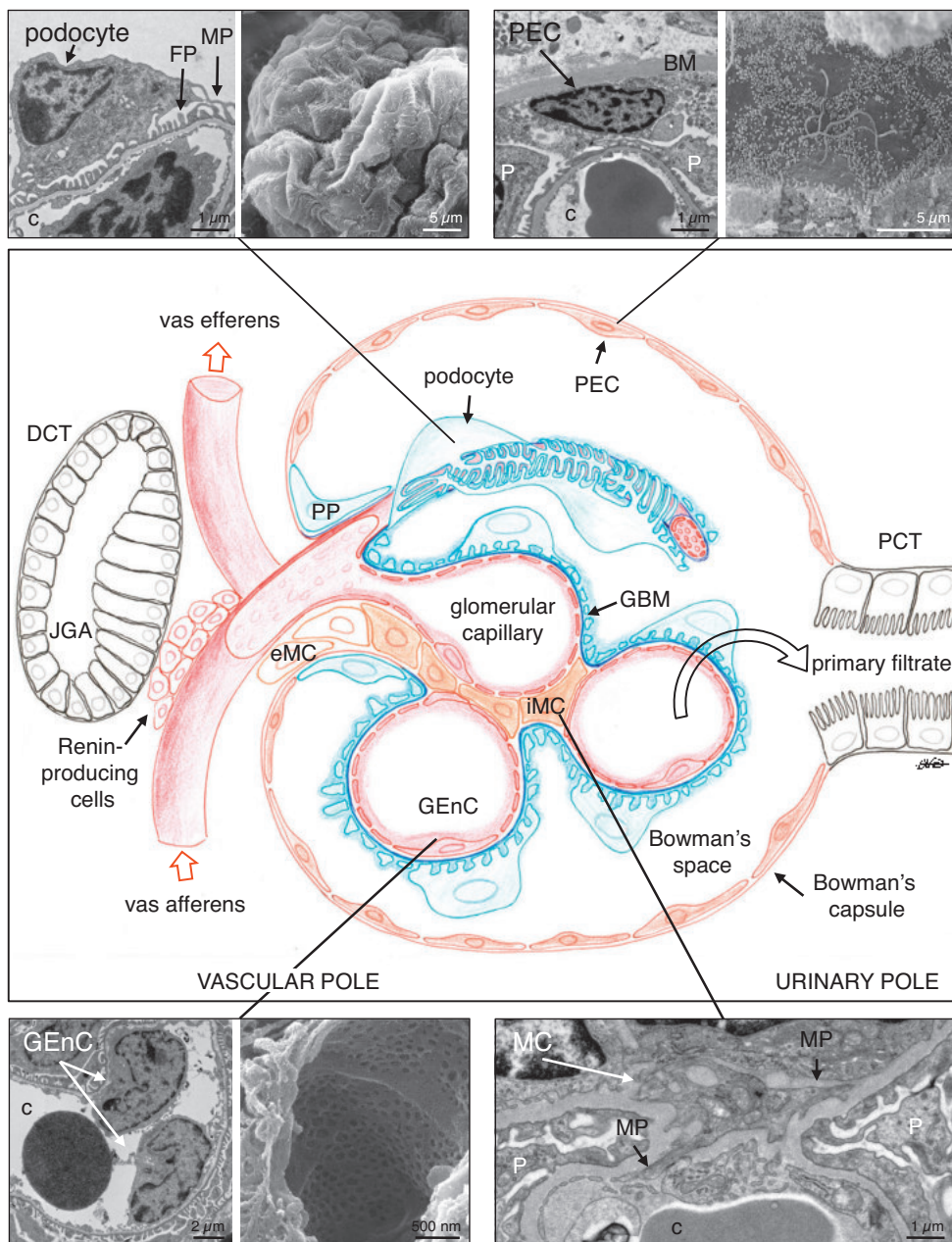


Fig. 4.1 Scheme of the glomerulus depicting the localization of the four resident glomerular cell types. The four types are podocytes, parietal epithelial cells (PEC), glomerular endothelial cells (GEnC), and mesangial cells (MC). Transmission and scanning electron micrographs show the typical ultrastructure of the glomerular cells. BM, Bowman's membrane; c, capillary lumen; DCT, distal convoluted tubule; eMC, extraglomerular mesangial cell; FP, foot process; GBM, glomerular basement membrane; JGA, juxtaglomerular apparatus; iMC, intraglomerular mesangial cell; MP, major process; P, podocyte; PCT, proximal convoluted tubule; PP, parietal podocyte. (All transmission electron microscopy and scanning electron microscope are from Oliver Kretz, Hamburg, Germany.)

Tracer studies point to a charge selectivity favoring the filtration of positively charged solutes.^{4,5} Furthermore, an electrokinetic model of filtration has been proposed. In this model, filtration pressure establishes a streaming potential across the glomerular filtration barrier with Bowman's space being more negatively charged than the endothelial lumen. This might establish a retrograde electrophoretic field that acts opposite to diffusive and convective fluxes and tends to exclude negatively charged macromolecules away from the glomerular filtration barrier in the course of active filtration.⁶ The primary urine exits the renal corpuscle at the urinary

pole to be further processed to final urine in the downstream tubular system. While water and small molecules such as glucose, salt, and amino acids freely pass across the glomerular filtration barrier, a partial impermeability to large molecules, such as albumin, into the primary urine is maintained. The degree of fractional albumin filtration has been a matter of debate, but more recent two-photon *in vivo* imaging studies indicate values for a glomerular sieving coefficient of 0.02–0.04 for albumin filtration into the primary urine, which for the most part is reabsorbed by the proximal tubule.⁷ This partial impermeability to large molecules is achieved by a highly

complex interplay of two types of glomerular cells: the visceral epithelial cells (podocytes) and the glomerular endothelial cells, which ultimately compose the three-layered glomerular filtration barrier (podocyte—the 250–400 nm thick glomerular basement membrane [GBM]—endothelial cell). The GBM is composed of several types of extracellular matrix (ECM) macromolecules (laminin, type IV collagen, the heparan sulfate proteoglycan agrin, and nidogen), which produce an interwoven meshwork thought to impart both size-selective and charge-selective properties.⁸ Finally, intraglomerular mesangial cells (MCs) occupy the space between the glomerular filtration barrier to provide structural support. As specialized pericytes, MCs indirectly participate in filtration by reducing the glomerular surface area by contraction and are also thought to participate in matrix turnover and innate immune function.⁹ Although all glomerular cells form a functional and integrated syncytium, in this chapter each component is described in brief.

Clinical Relevance

The glomerulus is a functional syncytium of four cell types, which interact in physiologic and also pathologic situations, thereby perpetuating and extending the site of glomerular injury.

PODOCYTES

STRUCTURE

Podocytes are highly differentiated, mesenchymal-derived cells.¹⁰ An apicobasal polarity axis allows for podocyte orientation between the urinary space and the GBM.¹¹ Podocytes reside in the urinary space and embrace the glomerular capillaries with their flat cell body, from which they extend long-branching major processes. Major processes give rise to secondary processes (often called foot processes), which interdigitate in a zipper-like fashion with secondary processes of neighboring podocytes¹² (Fig. 4.2). Foot processes attach podocytes to the underlying ECM of the GBM by specific proteins, such as adhesion receptors, including integrins, syndecans, vinculin, talin, and dystroglycan.¹³ Foot processes are interconnected by slit diaphragms, which represent highly sophisticated cell-cell contacts that form an adjustable, nonclogging barrier through which glomerular filtration occurs. Although the term “diaphragm” implicates a thin-layered sieve, recent studies revealed that the slit diaphragm is composed of multiple layers of flexible transmembrane molecules to limit the passage of macromolecules.¹⁴ Structurally, the slit diaphragm combines components of several types of cell-cell junctions, including tight, adhesion, neuronal, and gap junctions. Proteins from tight (ZO-1, JAM4, occludin, and cingulin) and adherens junctions (P-cadherin, FAT1, and the catenin family of proteins) are associated with the immunoglobulin superfamily members nephrin and neph1.¹⁵ Nephrin and neph1 form the core component of the slit diaphragm by a bipartite assembly with neph1 molecules spanning the lower part of the slit close to the GBM and nephrin molecules positioned in the apical side.¹⁴ The stomatin protein family member podocin (NPHS2) helps

anchor nephrin to the plasma membrane and generates a signaling hub in lipid rich membrane compartments, e.g., for the Ca²⁺-permeable transient receptor potential channel (TRPC) 6¹⁶—that might translate mechanical tension to ion channel action and cytoskeletal regulation.¹⁷ On their intracellular C-terminal parts, nephrin and neph1 are associated with several signaling adaptor molecules and scaffold proteins linking the slit diaphragm to the actin cytoskeleton.^{14,18} In general, the podocyte cytoskeleton is highly elaborate. The podocyte cell body and major and secondary processes contain vimentin-rich intermediate filaments that assist in maintaining cell shape and rigidity. Large microtubules form organized structures along major processes. Foot processes contain long actin fiber bundles that run cortically and contiguously to link adjacent podocytes. Actin, α-actinin-4, and myosin form a contractile system in foot processes, which is regulated by the interplay of the actin binding proteins synaptopodin¹⁹ and α-actinin-4 with rho GTPases. This well-orchestrated actin and microtubule cytoskeleton ensures the high plasticity of the podocyte process network.^{20,21} The apical surfaces of podocytes are covered by the surface sialomucin podocalyxin,²² whose highly negative charge functions to keep adjacent foot processes separated, thereby keeping the urinary filtration barrier open.²³

FUNCTION

The main podocyte function is to build, maintain, and regulate the three-layered glomerular filtration barrier.

- 1. The synthesis of the mature GBM** requires the crosstalk of podocytes with endothelial cells.²⁴ Podocytes and endothelial cells both secrete laminin 111 and type IV collagen α1α2α1 in GBM development and the final laminin 521 isoforms after maturation. However, only podocytes secrete type IV collagen α3α4α5 of the fully mature GBM.²⁵
- 2. Podocytes maintain the glomerular filtration barrier** by secreting survival factors such as angiopoietin-1 (Angpt1, which binds to Tie2 on glomerular endothelial cells [GENC] and MCs),²⁶ normosialylated angiopoietin-like-4 (which binds to integrin αVβ5 on GEnC),²⁷ vascular endothelial growth factor A (binds to vascular endothelial growth factor receptor 2 [VEGFR2] on GEnC),²⁸ and stromal derived factor 1 (which binds to CXCR4 on GEnC)²⁹; these factors exert paracrine effects across the filtration barrier on glomerular endothelial and MCs supporting their respective migration, differentiation, and survival.³⁰
- 3. Podocytes stabilize the glomerular filtration barrier** by expressing cell-matrix adhesion receptors such as integrin α3β1, which connects laminin 521 in the GBM through various adaptor proteins to the intracellular actin cytoskeleton or integrins α2β1 and αVβ3, α-dystroglycan, syndecan-4, and type XVII collagen.³¹
- 4. Podocytes regulate glomerular filtration**³² by presumably compressing the GBM through their adhesion to the GBM and the tensile forces of their cytoskeleton, which in turn reduces the permeability to macromolecules.³³ Furthermore, they regulate glomerular filtration through the formation of the slit diaphragm and by sensing the glomerular filtration pressure by a mechanoreceptor complex situated at the slit diaphragm.³⁴

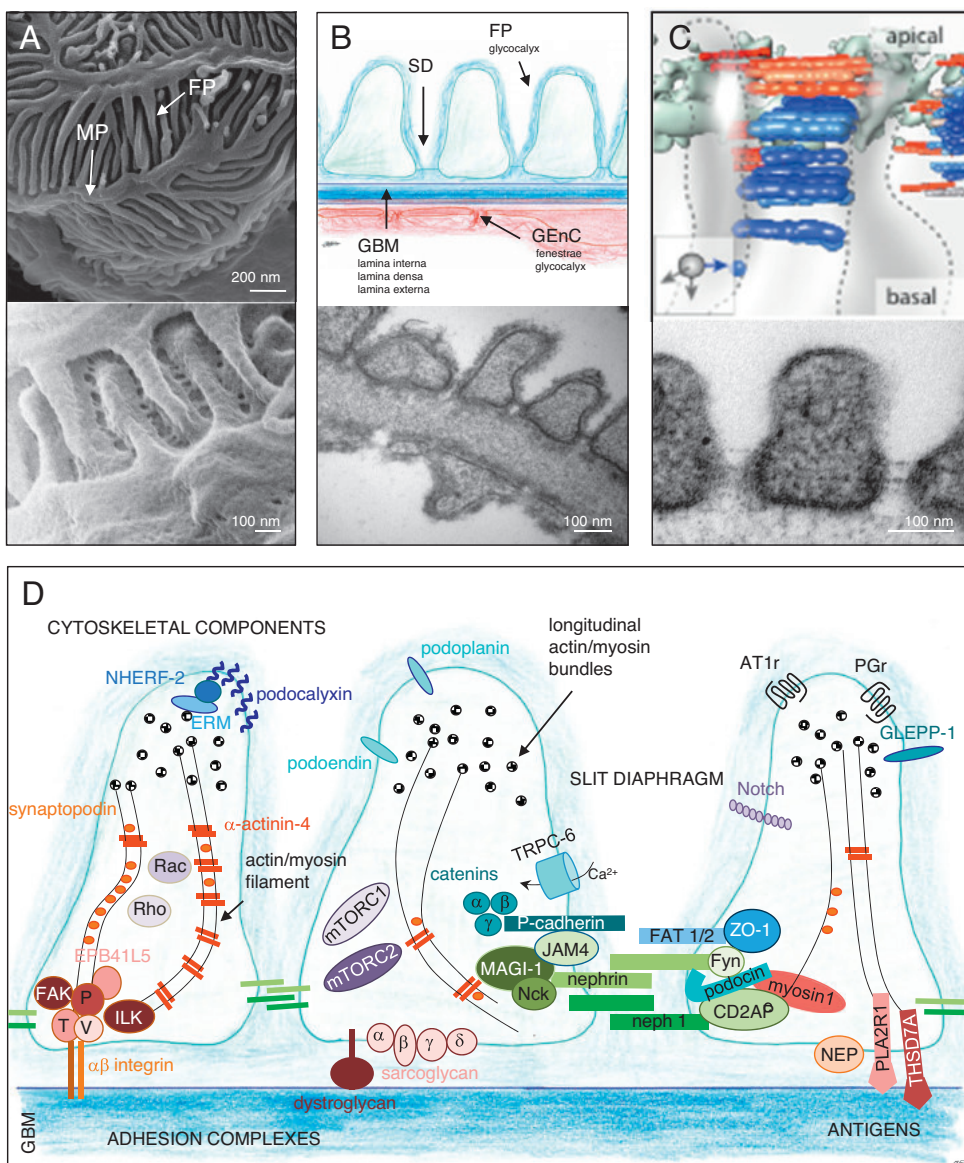


Fig. 4.2 Anatomy of the glomerular filter. (A) Scanning electron microscopy (SEM) of podocyte major processes (MP) and secondary interdigitating foot processes (FP). (B) Scheme and transmission electron microscopy (TEM) of three-layered glomerular filtration barrier consisting of (1) podocyte FPs covered by a glycocalyx, the specialized cell–cell contact called slit diaphragm (SD) connecting the interdigitating foot processes; (2) the three-layered glomerular basement membrane (GBM) consisting of podocyte-derived lamina interna, the podocyte/endothelial cell–derived lamina densa, and the endothelial-derived lamina externa; and (3) the glomerular endothelial cells (GEnC) with the large fenestrae and thick glycocalyx. (C) Scheme of the typical sagittal view of two FPs, showing three layers of ~25 nm long strands that are attributed to nephrin (blue, and 5 IG repeats) and one layer of ~40 nm long strands that represent nephrin (red, and 9 IG repeats). (D) Scheme of podocyte FP proteins constituting the (1) FP cytoskeleton (actin/myosin filaments, the actin binding proteins synaptopodin, α -actinin-4); (2) the podocyte adhesion complex (α 3/ β 1 integrin connecting the GBM to focal adhesions constituted of focal adhesion kinase [FAK], integrin linked kinase [ILK], talin [T], vinculin [V], paxillin [P], FERM domain protein EPB41L5); (3) matrix interacting proteins dystroglycan, sarcoglycan; (4) the slit diaphragm (with the transmembrane proteins nephrin, neph1, FAT1/2, P-cadherin, and the scaffolding protein ZO-1 [zonula occludens 1], the intracellular signaling hub constituted of podocin, TRPC6 [transient receptor potential cation channel, subfamily C, member 6, and the connection to the actin cytoskeleton through CD2AP, CD2-associated protein, the cytoskeletal adaptor protein Nck, the multidomain scaffolding protein MAGI-1 and the junctional cell adhesion protein JAM4]); (5) the negatively-charged sialoprotein podocalyxin (which is connected to the plasma membrane by NHERF-1 = Na⁺/H⁺ exchanger regulatory factor 1 and ERM [ezrin/moesin/radixin proteins]) localizes to the surface of the plasma membrane, as do GLEPP-1 (glomerular epithelial cell membrane protein-tyrosine phosphatase 1), podoplanin, and podoendin; (6) the G-coupled receptors angiotensin receptor 1 (AT1r) and prostaglandin receptor (PGr); (7) the podocyte antigens neutral endopeptidase (NEP); phospholipase A2 receptor 1 (PLA₂R1), and thrombospondin type 1 domain containing 7A (THSD7A) identified in antenatal and adult membranous nephropathy; and (8) intracellular signaling molecules Rho, Rac, mTORC1/2 (mammalian target of rapamycin complex 1 and 2), Notch, and Fyn. ([A, C] All TEM and SEM from mouse glomeruli are from Oliver Kretz, Hamburg, Germany. [B] TEM from mouse glomerulus exhibiting glycocalyx from K. Betteridge, K. Onions, and R. Foster, Bristol, UK. [C] Scheme from Grahammer F, Wigge C, Schell C, et al: A flexible, multilayered protein scaffold maintains the slit in between glomerular podocytes. *JCI Insight* 1, 2016.¹⁴ [D] Drawn by C. Meyer-Schwesinger.)

PODOCYTE PATHOPHYSIOLOGY

Due to their molecular setup and localization, podocytes are permanently targeted by, and required to respond to, various physiologic and pathophysiologic stressors. If exposure is too excessive in time and dosage, this leads to complex adaptive and maladaptive intracellular changes, which then lead to the typical histopathologic sequence of foot process effacement, podocyte hypertrophy, and podocyte detachment from the GBM with loss into the urine (Fig. 4.3). Podocyte dysfunction results in clinical proteinuria and in a variety of glomerular responses, such as disruption of podocyte–endothelial crosstalk and activation of podocyte–parietal cell interactions culminating in glomerulosclerosis.

Over 80 pathways have been described that result in podocyte distress, including circulating factors, cell-surface signaling, metabolism, fibrosis, inflammation, and the actin

cytoskeleton.³⁵ As a general theme, podocyte injury appears to involve reactivation of developmental programs such as those engaged by Notch,³⁶ Wnt,^{37–40} and mTOR pathways.⁴¹ Overactivation, imbalance, and impairment of these central intracellular signaling pathways disrupt normal podocyte energy metabolism⁴² and protein homeostasis,⁴³ thus initiating a mostly irreversible dedifferentiation process.

Podocyte Foot Process Effacement

Podocyte function largely depends on its complex three-dimensional cytoskeletal structure. The identification of over 50 monogenic causes of podocyte disease⁴⁴ has immensely increased our understanding of podocyte function and dysfunction. Regardless of the underlying disease, a characteristic and almost predictable response to podocyte injury is a change in shape, called effacement.⁴⁵ Numerous studies have shown that effacement is an active process, due to

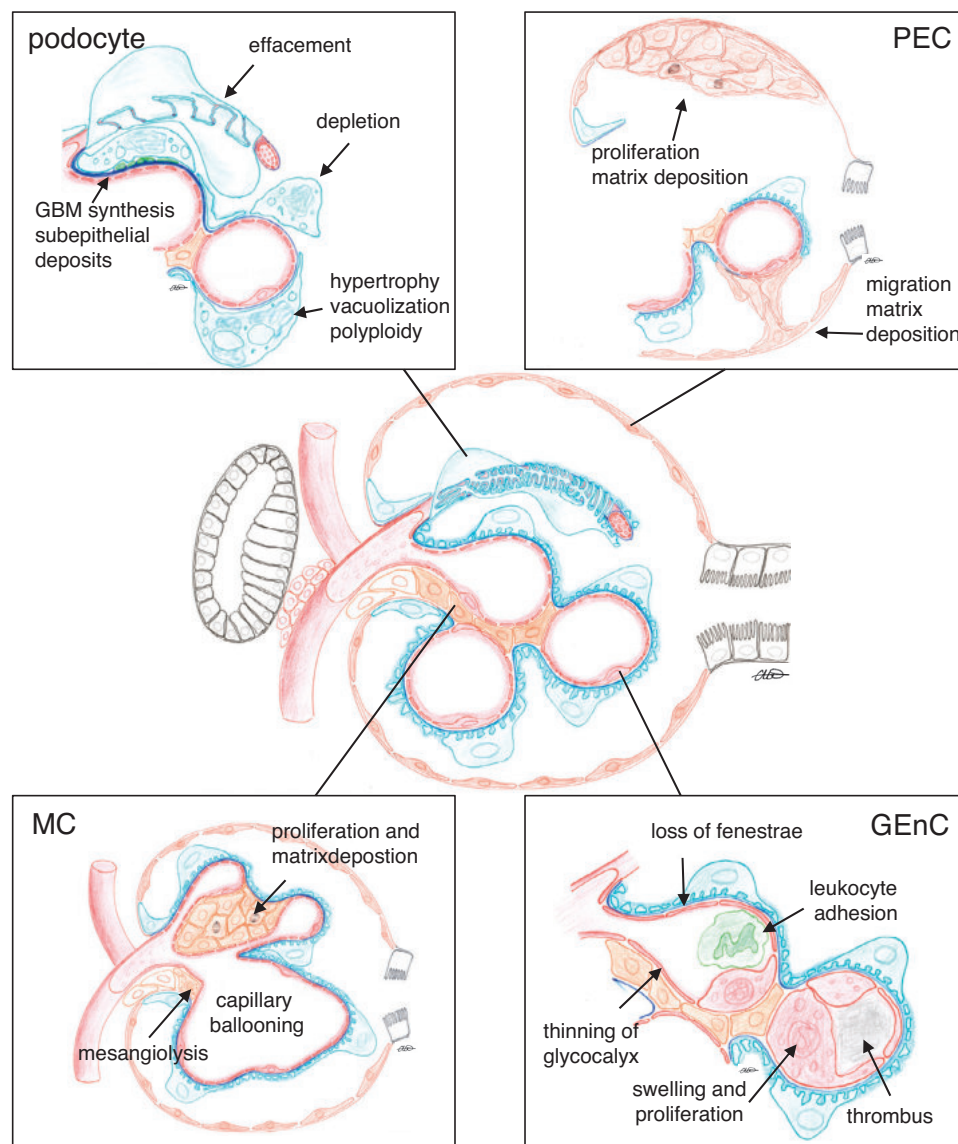


Fig. 4.3 Pathophysiological reaction patterns of glomerular cells. GEnC, Glomerular endothelial cell; MC, mesangial cell; PEC, parietal epithelial cell.

changes in the actin cytoskeleton of the podocyte, which forms the “backbone” of these highly specialized cells.⁴⁶ Further evidence that effacement is an active process is that in some instances it can be reversed, such as in treatment-responsive patients with minimal change disease (MCD). There has been debate as to whether effacement per se causes proteinuria, because proteinuria due to podocyte damage can occur independent of this change in shape. The relationship between podocyte foot process effacement and proteinuria has been questioned,⁴⁷ and it is clear that there is still much to learn about this long-recognized but still poorly understood ultrastructural phenomenon. Confusingly, effacement has also been reported (in the absence of proteinuria) in the protein-malnutrition state kwashiorkor,⁴⁸ suggesting that it may be a feature of hypoalbuminemia rather than of proteinuria per se. However, it is generally accepted that effacement is a manifestation of serious podocyte injury, and that this histologic finding implies changes in either slit diaphragm proteins (i.e., nephrin⁴⁹ and podocin⁵⁰), actin binding and regulating proteins (i.e., α -actinin-4⁵¹ and CD2AP⁵²), podocyte attachment to the GBM (i.e., laminin β 2⁵³ and integrin β 4⁵⁴), nuclear proteins (WT1⁵⁵ and LMX1B⁵⁶), mitochondrial⁵⁷ and lysosomal⁵⁸ components, and/or other events, as genetic studies in humans suggest. Therefore teasing out precisely the biologic role of effacement in the development and maintenance of proteinuria may not be important.

Podocyte Hypertrophy

Podocytes are terminally differentiated epithelial cells and unable to adequately proliferate to cover denuded areas of the GBM in situations of glomerular (GBM) distention (i.e., in case of renal hyperfiltration) or podocyte loss. Despite the virtual absence of podocyte mitosis and regeneration, current knowledge suggests that differentiated podocytes do have at least some capacity to adjust to an altered glomerular architecture by hypertrophy. Therefore hypertrophy can be adaptive in the setting of glomerular development, growth, and numerical minimal podocyte depletion (up to 20%), or can reflect a multifactorial maladaptive response of podocytes due to persistent injury promoting stimuli such as high glucose in diabetic nephropathy or subepithelial deposits in membranous nephropathy.⁵⁹ Recent findings highlight mammalian target of rapamycin (mTOR) and its downstream target, the translational repressor protein 4E-BP1,⁶⁰ as a key regulator of both adaptive and maladaptive podocyte hypertrophy, whereby the timing, extent, and duration of mTOR activation decide whether hypertrophy is adaptive or maladaptive.⁴¹ Inhibition of mTOR by rapamycin in the setting of adaptive hypertrophy results in proteinuria and glomerulosclerosis, whereas inhibition of mTOR in the setting of maladaptive hypertrophy could be therapeutically beneficial.⁶¹ Besides an imbalance of mTOR signaling pathways,^{62,63} podocyte hypertrophy in response to hyperglycemia and stretch have been shown to be also mediated by the cyclin-dependent kinase inhibitor p27Kip1.^{64,65} Hypertrophy in membranous nephropathy seems to originate in part from altered protein degradation and subsequent cytoplasmic accumulation of proteins.⁶⁶

Podocyte Depletion

Many podocyte diseases such as focal segmental glomerulosclerosis (FSGS), membranous nephropathy (MN), and

diabetic kidney disease are accompanied by a progressive decline in overall kidney function, measured clinically by a decrease in glomerular filtration rate. This is largely due to glomerulosclerosis, with or without tubulointerstitial fibrosis. Patterns of glomerulosclerosis histologically include a segmental form (a portion of an individual glomerulus is scarred) and the more extensive global form (the majority of an individual glomerulus scars). Podocyte depletion is a major contributor to the development of age-related glomerulosclerosis in humans and rodents.^{67–70} A decrease in podocyte number is one of the best predictors for a poor outcome in clinical diabetic kidney disease. A loss of 20% of podocytes is tolerated by rats⁷¹ and mice⁷² and is accompanied by MC proliferation and expansion. Segmental glomerulosclerosis ensues when 40% of podocytes are depleted, and global glomerulosclerosis occurs when the podocyte number is below 60% of normal.⁷¹ There has been a long-standing debate on the underlying mechanisms for podocyte depletion, ranging from necrosis, apoptosis, and necroptosis to the detachment of viable cells from the GBM.⁷³ Interestingly, viable podocytes can be isolated from the urine of proteinuric patients, emphasizing the importance of podocyte detachment as a mechanism of podocyte depletion in glomerular diseases.

Studies have suggested that despite a lack of proliferation, podocyte number can be restored following certain therapies such as angiotensin-converting enzyme inhibition.⁷⁴ Despite compelling data, however, it remains unclear whether podocyte regeneration exists in renal aging or in pathophysiologic situations and, if podocyte regeneration exists, from what source of resident progenitor cells the novel podocytes originate.⁷⁵ Possible sources discussed might be progenitor cells derived from glomerular parietal epithelial cells⁷⁶ and/or cells of renin lineage,⁷⁷ although further studies are needed to fully validate these findings.

Podocyte-Related Mechanisms of Proteinuria

Proteinuria is the clinical hallmark of podocyte injury, ensuing from a disruption of their most important biologic function, which is namely to limit the passage of plasma proteins into the urinary space. In general, any kind of injury affecting podocyte function results in proteinuria, either selective as albuminuria (mostly loss of the 60-kDa protein albumin) or nonselective as global proteinuria (loss of a multitude of proteins over 60 kDa of size, including immunoglobulins of 150 kDa) in case of major breakdown of the glomerular filtration barrier. Genetic studies and animal studies have demonstrated that podocyte-dependent proteinuria originates from at least six distinct mechanisms.

Mechanism 1: Alteration of the slit membrane as the size- and charge-selective barrier to proteins through hereditary or acquired defects of one or more structural slit diaphragm proteins, such as nephrin or podocin, leads to increased passage of proteins across this barrier. Either an absolute decrease in slit diaphragm protein levels or a change in their subcellular location is associated with proteinuria. Moreover, given the complex interplay between proteins comprising the slit diaphragm, a change in one slit diaphragm protein often leads to a cascading dysfunction of one or more of the other proteins.⁷⁸

Mechanism 2: Alteration of the podocyte cytoskeletal network either through mutations of structural proteins and

adaptor proteins or through an imbalance of signaling through actin-regulating enzymes and of converging signaling pathways culminate in enhanced or decreased actin polymerization, ultimately leading to proteinuria through a loss of the complex three-dimensional structure and flexibility of the podocyte cytoskeleton.

Mechanism 3: Although no known hereditary mutations of podocalyxin have been described, loss of podocalyxin results in reduced negative surface charge of podocyte processes and proteinuria.²³

Mechanism 4: Podocyte depletion (i.e., through loss of adhesion)⁷⁹ results in denuded GBM areas through which proteins escape.

Mechanism 5: Alteration in GBM composition by podocytes through increased secretion of ECM proteins is typically observed in membranous and diabetic nephropathy. These ECM proteins are laid down along the GBM and eventually lead to the characteristic thickening of the GBM in these diseases.⁸⁰ The altered ECM composition leads to secondary changes (loss) in negative charge to the GBM, thereby enabling increased passage of proteins. In addition, increased production and secretion of reactive oxygen species and metalloproteinases from podocytes leads to degradation of the GBM and proteinuria.

Mechanism 6: Effect on the glomerular endothelial cell whose survival is dependent in part on the VEGFA produced and secreted from podocytes.⁸¹ A decrease in production by podocytes, such as when podocyte number decreases, leads to secondary apoptosis of glomerular endothelial cells, which in turn is accompanied by a decrease in resistance of this layer of the glomerular filtration barrier.

MESANGIAL CELLS

STRUCTURE

MCs are divided into intraglomerular and extraglomerular MCs. MCs are mainly derived from the metanephric mesenchyme⁸² and migrate into the cleft of the comma and S-shaped bodies as well as the maturing glomerulus under the chemotactic control of platelet-derived growth factor B⁸³ and the survival factor VEGF, both secreted from the progenitors of podocytes and GEnC.⁸⁴ In the mature glomerulus, MCs constitute the central stalk and are in continuity with the extraglomerular mesangium and the juxtaglomerular apparatus. Extraglomerular MCs are in close connection to afferent and efferent arteriolar cells by gap junctions, allowing for intercellular communication.⁸⁵ MCs are highly branched with processes extending in all directions. First, MCs have major processes that contain abundant bundles of microfilaments, microtubules, and intermediate filaments.⁸⁶ These major processes contain actin, myosin and α -actinin, and connect MCs with anchoring filaments to the GBM opposite podocyte foot processes and at paramesangial angles, giving them contractile properties.⁸⁷ Second, MCs have abundant microvillus-like projections arising from the cell body or from the major processes. Within the cell body microfilament bundles are less frequent and the perinuclear region is free of microfilaments.⁸⁶ MCs are in direct contact with GEnC without an intervening basement membrane on the capillary lumen side, where the cell membranes of both cell types interdigitate.⁸⁸ MCs do not express highly cell-specific markers; however, they express genes that classify MCs as a

special form of microvascular pericytes.⁸⁹ MCs are positive for vimentin and desmin.

FUNCTION

MCs, together with their matrix, form a functional unit with GEnC and podocytes.⁹

1. MCs are required for the development and for the mechanical (structural) support of glomerular capillary loops.^{90,91} Mechanical support is in part mediated by attachment of MCs to the carboxy-terminus globular domain of laminin $\alpha 5$ in the GBM.⁹²
2. MCs regulate the glomerular capillary flow and ultrafiltration surface and hence the fine-tuning of glomerular filtration by cell contraction at the single nephron level.⁹³ Contraction of MCs is regulated by vasoactive substances⁹⁴ and is dependent on the calcium signaling response and membrane permeability.^{94,95} Relaxation of MCs, on the other hand, is mediated by paracrine factors, hormones, and cyclic adenosine monophosphate (cAMP), with a role for growth factor priming.⁹⁴
3. MCs are responsible for the homeostasis of the mesangial matrix through synthesis and degradation of their own matrix components (type IV collagen $\alpha 1\beta 2$, type V collagen, laminin fibronectin, proteoglycans [heparan and chondroitin sulfate, decorin, and biglycan], entactin, and nidogen).^{83,96–98} The mesangial matrix provides structural support to the glomerulus⁹ and regulates the behavior of MCs, such as growth and proliferation,⁹⁹ partly by binding and sequestering growth factors and thereby influencing their activation and release.⁹ Furthermore, the mesangial matrix signals to MCs in response to mechanical stretch.¹⁰⁰
4. MCs are sources and targets of growth factors, cytokines, and vasoactive agents.⁹ For example, MCs produce transforming growth factor (TGF)-1, VEGF, and CTGF⁹ in response to capillary stretching resulting from glomerular hypertension. MC proliferation, along with eicosanoid and matrix production, is influenced by PDGF-B,¹⁰¹ PDGF-C,¹⁰² fibroblast growth factor (FGF),⁹⁶ hepatocyte growth factor (HGF),⁹⁷ connective growth factor (CTGF),¹⁰³ epidermal growth factor (EGF),¹⁰⁴ and TGF- β .⁹⁸
5. MCs keep the mesangial space free from accumulating macromolecules, which trespass from the capillary lumen through the fenestrated endothelium. For this purpose, MCs phagocytose glomerular basal lamina or immune complexes formed at or delivered to the glomerular capillaries,^{105,106} and aid neutrophils to phagocytose apoptotic cells.¹⁰⁷ Macromolecules are removed by both receptor-dependent and independent mechanisms, depending on the size, charge, concentration, and affinity for MC receptors.^{9,108}
6. MCs are involved in the tubuloglomerular feedback by communicating with vascular smooth muscle cells over gap junctions.¹⁰⁹
7. MCs maintain endothelial health and function by cross communication via the mediators and pathways described above.

PATOPHYSIOLOGY

As of yet, no discrete primary disease of MCs has been described. However, MCs react to changes of the intravascular milieu (soluble factors), immunoglobulin deposition, and

to changes affecting GEnC and podocytes. Glomerular MC injury is commonly associated with mesangial immune deposit formation in IgA nephropathy, lupus nephritis, and Henoch-Schönlein purpura (also designated as IgA vasculitis).¹¹⁰ Even though IgA nephropathy primarily affects the mesangium (mesangioliferative disease), it produces marked hematuria and proteinuria, indicating changes in the permeability of endothelial cells, GBM, and podocytes. The myriad biologic responses of MCs to injury range from mesangiolysis to mesangial hypercellularity, mesangial expansion, and the promotion of glomerular inflammation (see Fig. 4.3). Overall, these biologic responses of MCs to injury are elicited (1) by structural abnormalities of the basement membrane that are either acquired (as in diabetes mellitus) or genetic (as in Alport syndrome); (2) by factors either released from neighboring MCs in an autocrine manner; or (3) from circulating factors affecting MCs in an endocrine manner.

Mesangiolysis is defined as a dissolution or attenuation of mesangial matrix and degeneration of MCs either by apoptosis or lysis without obvious damage to the capillary basement membranes. The matrix swells, loosens, and eventually dissolves; the MCs may show swelling and vacuolization. Mesangiolysis results in a dilation of the glomerular capillary lumina, as the mechanic support of capillaries provided by the anchoring points of MCs to the GBM is lost.¹¹¹ Loss of intraglomerular MCs can be replenished by ingrowth of extraglomerular MCs.¹¹²

Mesangial hypercellularity is characterized by an increase of intraglomerular MC number by hypertrophy, proliferation, and migration⁸² as in IgA nephropathy. In cases where the proliferative insult is limited, mesangial hypercellularity is limited by apoptosis and phagocytosis of these apoptotic cells by adjacent MCs or by infiltrating inflammatory cells.¹¹³

Mesangial expansion is a term characterizing the widening of the intraglomerular mesangium. Mesangial expansion occurs in diabetic nephropathy by excess mesangial matrix production such as fibronectin by MCs¹¹⁴ or by decreased degradation of the mesangial matrix by metalloproteinases.¹¹⁵ Mesangial expansion also occurs through the deposition of immune complexes, light chains, amyloid, fibrils, complement, and worn-out GBM material.¹¹⁶

Promotion of glomerular inflammation: Injured MCs generate reactive oxygen species, proinflammatory activators such as platelet activating factor,¹¹⁷ cytokines (TNF- α , CSF-1 and IL-6), and chemokines,⁹ thus sustaining and perpetuating glomerular inflammation.

GLOMERULAR ENDOTHELIAL CELLS

STRUCTURE

The glomerular microcirculation is unique as unlike other capillary circulations, glomerular capillaries are highly permeable to water and small solutes while maintaining relative impermeability to macromolecules potentially even as small as albumin.¹¹⁸ GEnCs are highly specialized cells that form the continuous inner layer of glomerular capillaries. GEnCs have a particular embryonic origin, with the majority of GEnCs arising by vasculogenesis from mesenchymal precursors in combination with a minority of GEnCs arising from introgresion of existing vessels.^{119,120} In the mature glomerulus, the nucleus of GEnCs bulges into the capillary lumen. The

cytoplasm of GEnCs is 200 nm thin at its slimmest areas and punctuated by numerous fenestrae. The fenestrae of GEnCs are the largest in comparison to the fenestrae of endothelial cells of other organs and represent circular pores of 60 to 80 nm in diameter, which cover 20% of the glomerular endothelial surface.¹²¹ Under special fixation conditions, a diaphragm is visible that spans the fenestrae.¹²² GEnCs are covered by a 200- to 400-nm-thick glycocalyx, which represents a negatively charged gel-like surface structure of proteoglycans with their covalently bound polysaccharide chains named glycosaminoglycans (GAGs), glycoproteins, and glycolipids. The main carbohydrate constituents are heparan sulfate (HS), chondroitin sulfate (CS), and hyaluronan (HA), bound to the HA binding surface proteins such as CD44. The glycocalyx is attached to the GEnC by charge–charge interactions,¹²³ rendering GEnC very sensitive to hemodynamic factors¹¹⁸ such as shear stress.¹²⁴ The glycocalyx covers the fenestrae and the interfenestral domains of GEnC equally¹²⁵; however, the thickness of the glycocalyx differs between fenestrated and nonfenestrated GEnCs.¹²⁶ The GEnC fenestrae are plugged by a high content of HA¹²⁶ and are considered to be a key component of the glomerular permeability barrier. Like other endothelial cells, GEnCs express the specific markers platelet endothelial cell adhesion molecule 1 (PECAM1, CD31), intercellular adhesion molecule 2 (ICAM2), VEGFR2, growth factor receptor Tie2, von Willebrand factor, and vascular endothelial (VE)-cadherin (CD144).¹²⁷

FUNCTION

1. GEnCs are involved in the GBM production together with podocytes but to a lesser extent than podocytes as seen in mice with podocyte-specific type IV collagen $\alpha 5$ chain deletion (Alport model), which exhibit marked thinning and alteration of the GBM.^{128,129}
2. GEnCs contribute to the hydraulic conductivity of the glomerular filtration barrier through GEnC fenestrations,¹³⁰ which are formed in response to VEGF.^{127,131}
3. GEnCs contribute to the size and charge selectivity of the glomerular filtration barrier by the endothelial surface lining composed of the membrane-bound glycocalyx and the loosely bound endothelial cell coat.^{126,132} The glycocalyx adds to size and charge selectivity, most likely by forming a mesh-like structure of negatively charged HSs and the less charged HA,¹³³ as infusion of enzymes that degrade the glycocalyx increases albumin passage through the GEnC.¹³⁴
4. The glycocalyx of GEnC protects against protein leakage, inflammation, and coagulation.¹³⁴ With properties like a hydrogel, the glycocalyx acts as a size barrier to protein. With the high negative charge of polyanions, the glycocalyx electrically repels proteins.^{135–137} GAG-degrading enzymes such as chondroitinase and heparanase alter glomerular permeability.^{138,139} The gel-like, antiadhesive properties of the glycocalyx preclude the interaction of leukocytes with adhesion molecules.

PATHOPHYSIOLOGY

GEnCs are primarily targeted in several forms of vasculitis, in hemolytic uremic syndrome, and in preeclampsia.¹⁴⁰ Even though GEnCs are primarily affected, these conditions are associated with mesangiolysis and proteinuria, indicating endothelium-dependent changes in MCs and podocytes. Injury

of the GEnC induces the release of vasoactive substances and changes the composition of the endothelial glycocalyx and endothelial adhesion molecules, resulting in a net prothrombotic state (see Fig. 4.3).^{141,142} Furthermore, GEnCs hypertrophy, proliferate, go into apoptosis, and detach, further accelerating the thrombosis of glomerular capillaries.¹⁴¹ Experimental models indicate that recovery from glomerular injury is dependent on GEnC angiogenesis.^{143–145} Visualization of GEnC injury remains challenging. Morphologic signs of GEnC injury are swelling of the cell body, thinning of the glycocalyx,^{146,147} loss of fenestrations, and enhanced expression of adhesion markers such as CD34¹⁴⁸ and E-selectin (CD62E), an adhesion receptor for leukocytes. GEnC injury has been demonstrated to arise from an altered crosstalk with podocytes.

Clinical Relevance

Proteinuria is a hallmark of glomerular injury and should usually initiate a workup by a nephrologist to identify eventual underlying genetic, inflammatory, toxic, tumor, and infectious causes.

Endotheliosis: Glomerular capillary endotheliosis describes the swelling of GEnC with the deposition of fibrous material in and beneath GEnC, a condition typically seen in pre-eclamptic glomerular injury. The net result of GEnC swelling and deposition of fibrous material is capillary occlusion.

Changes of glycocalyx and their sequelae because the glycocalyx functions as a molecular scaffold and binds (1) circulating proteins such as growth factors and chemokines; (2) proteins involved in cell attachment, migration, and differentiation; and (3) proteins involved in blood coagulation and inflammation, alterations of the glycocalyx are central to the pathology of GEnC and glomerular injury. GEnC injury induces changes both in the thickness and in the molecular composition of the endothelial glycocalyx. Changes in glycocalyx thickness are mainly due to upregulation of glycocalyx-degrading enzymes such as hyaluronidase, heparanase, and proteinases, thereby shedding glycocalyx fragments into the glomerular circulation. Alteration of glycocalyx composition such as decreased levels of HA or changes in HS sulfation patterns change the antiadhesive and anticoagulative properties of the glycocalyx. In total, loss of glycocalyx thickness and glycocalyx modification result in enhanced permeability of the filtration barrier to proteins, inflammation, and coagulation.¹³⁴

Mediation of the inflammatory reaction: Injured GEnCs release vasoactive substances (nitric oxide and endothelin), which regulate glomerular filtration. Furthermore, GEnCs promote glomerular inflammation by attracting leukocytes by means of shed glycocalyx fragments and by expressing leukocyte adhesion molecules. Upon perturbation of the glycocalyx, these adhesion molecules become unmasked and allow leukocyte interactions with the endothelial surface. HS of the glycocalyx acts as a direct ligand for L-selectin.¹⁴⁹ Upon stimulation with inflammatory stimuli, GEnCs increase the expression of HS domains,¹⁵⁰ which facilitates leukocyte extravasation.¹⁵¹ The endothelium binds chemokines, which

regulate the extravasation of leukocytes upon a chemo attractant gradient.¹⁵² Alterations of glycocalyx composition ensue in enhanced binding of chemokines by way of positive charge interactions.¹⁵³

PARIETAL EPITHELIAL CELLS

PECs are derived from the metanephric mesenchyme and line Bowman's capsule of the renal glomerulus. During the vesicle and comma stages in glomerular development, PECs share a common phenotype with the other epithelial cells of the later glomerulus—namely, podocytes and proximal tubular cells. With the formation of the Bowman's space in the S-shaped body, the phenotypes of PECs, podocytes, and proximal tubular cells diverge. In the mature kidney, PECs are a heterogeneous population of cells as PECs at the urinary pole maintain features of proximal tubular cells and PECs at the vascular pole maintain features of podocytes and are therefore termed parietal podocytes.¹⁵⁴

STRUCTURE

PECs resemble squamous epithelial cells with their small thin cell body ranging in thickness from 0.1 to 0.3 μm and increasing to 2.0 to 3.5 μm at the nucleus. The surface of some PECs is lined by microvilli and cilia in a range from zero to two cilia per cell.¹⁵⁵ They are interconnected by “labyrinth-like” delicate tight junctions located at the apical surface, which consist of claudin-1, -2, -3, K-cadherin (Cdh6), kidney specific cadherin (Cdh16), occludin, and zonula-occludens 1 (ZO-1).¹⁵⁶ PECs have a simple cytoskeleton with filaments at the basal membrane region.¹⁵⁷ They express the intermediate filament protein cytokeratin 8.¹⁵⁸ PECs have the transcriptional prerequisite to express podocyte markers.¹⁵⁹ The expression of podocyte proteins is negatively regulated through protein degradation¹⁵⁹ and by microRNA-193a,¹⁶⁰ which represses Wilms tumor protein 1 (WT1) mRNA levels.¹⁶¹ PECs express the transcription factor Pax2 from the paired box family, which is involved in regulating genes governing proliferation, cell growth, and survival. Furthermore, PECs can be differentiated from podocytes through the expression of EPH receptor A7 belonging to the ephrin receptor subfamily, ladinin (a proposed anchoring filament that is a component of basement membranes), and scinderin (a calcium-dependent protein that regulates cortical actin networks).¹⁶²

FUNCTION

1. PECs at the vascular pole constitute a potential reservoir for podocytes in glomerular development, maturation,^{72,163} and eventually even adulthood.¹⁶⁴
2. PECs presumably form the basement membrane of Bowman's capsule, which consists of laminin-111, laminin-511,^{165,166} type IV collagen α1 α2, and type IV collagen α5 α6^{167,168}; however, this is not definitely proven.
3. PECs prevent the leakage of urine from the urinary space into the periglomerular compartment.¹⁶⁹

PATHOPHYSIOLOGY

To date there is no evidence for glomerular injuries related to primary PEC injury. However, PECs have taken the center stage of attention for their contribution to glomerular diseases such as rapid progressive glomerulonephritis (RPGN) and

FSGS. Activated PECs exhibit a larger cytoplasm and larger rounder nuclei. Further signs of PEC activation are a de novo expression of CD44¹⁷⁰ and the phosphorylation of signaling molecules.^{171,172} The predominant reactions of PECs to glomerular injury are proliferation, migration, and synthesis of a matrix that results in the development of crescents or glomerular tuft scars (see Fig. 4.3). There is an ongoing debate whether PECs serve as an intrinsic fixed progenitor population to replenish podocytes or proximal tubular progenitor cells in glomerular regeneration.¹⁷³ PECs respond to injury with the expression of podocyte markers such as synaptopodin and WT1.^{174,175}

Proliferation and migration: Activation of PECs as in rapid progressive glomerulonephritis (RPGN) results in their proliferation and the formation of extracapillary proliferations, also called cellular glomerular crescents, of which PECs are the major constituents.¹⁷⁶ Crescent formation is not only the result of PEC proliferation but also in part the result of the transdifferentiation of PECs to myofibroblasts,^{170,177} the deposition of matrix, and the infiltration with inflammatory cells. Crescents can occlude the tubular outlet of the glomerulus, resulting in entire nephron degeneration,¹⁷⁸ and are generally associated with a poor prognosis. PEC proliferation is usually associated with glomerular endothelial cell, GBM, or podocyte injury, as leakage of plasma components such as fibrin from the blood circulation is a strong inducer of PEC proliferation.^{179,180} Additionally, PEC depletion initiates PEC proliferation and crescent formation.¹⁸¹ Migration of PECs from Bowman's capsule onto the glomerular tuft is the predominant reaction of PECs in focal segmental glomerulosclerosis (FSGS).¹⁷⁶ In this scenario, PECs are activated and invade the glomerulus at focal areas via adhesions connecting sclerotic capillary areas with Bowman's capsule.¹⁸² PECs are then present in the sclerotic regions^{183,184} and can be visualized by staining for CD44.¹⁸⁵

Matrix deposition: Thickening of Bowman's capsule due to matrix production can be observed in aging glomeruli¹⁸⁶ and glomerular injury. Matrix deposition by PECs is observed in glomerular crescents and in the sclerotic glomerular tuft regions in FSGS. PECs that migrate to the glomerular tuft produce and deposit ECM proteins. The composition of this ECM is related to that of Bowman's capsule¹⁸³ and contains specific heparan sulfate moieties of heparan sulfate proteoglycans.¹⁸⁷

GLOMERULAR CELL CROSSTALK

Podocytes, glomerular endothelial cells, MCs, and PECs with their respective matrix must be considered as a functional unit, in which every cell plays its part in ensuring proper glomerular filtration. As a consequence, 30 years of isolated cell-type-based research is now being replaced by systems biology approaches to integrate the role and contribution of each individual glomerular cell type for the proper glomerular biology and function. Recent advances have demonstrated that glomerular cell crosstalk is the prerequisite for normal glomerular development and health. Furthermore, primary injury of one glomerular cell type affects the other glomerular cell types by crosstalk. Clinical and experimental observations suggest that crosstalk exists between podocytes and GEnC, between GEnC and MCs, between MCs and podocytes, and finally between podocytes and PECs (Fig. 4.4).

PODOCYTES AND GLOMERULAR ENDOTHELIAL CELLS

Podocytes are essential for GEnC development and maintenance, and the first glomerular cell crosstalk to be identified was the cross communication from podocytes to GEnC. Podocytes secrete vascular growth factors, such as VEGFA, which bind to its cognate receptor VEGFR2 on GEnC, a crosstalk crucial for GEnC health⁸¹ and which, if disrupted, results in glomerular injury. A tight control of VEGFA levels is essential for correct glomerular barrier function, and even though other podocyte-specific proteins such as the transcription factor Pod1/Tcf21¹⁸⁸ or the TGF-β activated kinase 1 (Tak1)¹⁸⁹ have been shown to be essential for GEnC development and health, it remains to be established whether this is a direct effect or a consequence of altered VEGFA levels. Podocyte progenitors also express ephrin B2, another vascular growth factor, and by this might contribute to EphB4 receptor expressing GEnC development and health.¹⁹⁰ Angptl is expressed by both podocytes and MCs and binds to the tyrosine-protein kinase receptor (Tie2/Tek) expressed on GEnC. This crosstalk is thought to stabilize the glomerular capillaries, as mice with induced deletion of Angptl at embryonic day 10.5 exhibit dilated capillary loops and disrupted subendothelial GBM structures and reduced MCs, whereas podocytes appear intact.¹⁹¹ Podocytes also secrete the chemokine CXCL12 (SDF1), which binds to its receptor CXCR4 on GEnC, a crosstalk important for the formation of glomerular capillaries.²⁹

Despite their importance in glomerular development and maintenance, some podocyte-derived signals have been shown to perpetuate or attenuate GEnC injury in pathologic settings. Therefore, enhanced circulation of endothelin-1 or enhanced podocyte expression of endothelin-1, which binds in a paracrine way to the endothelin receptor A on GEnC, mediates mitochondrial oxidative stress and dysfunction in adjacent GEnC.^{192,193} Furthermore, endothelin 1 induces podocytes to release the GEnC glycocalyx-degrading enzyme heparanase, contributing to GEnC injury in diabetic nephropathy.¹⁹⁴ Another example for disease-perpetuating crosstalk is the podocyte-specific expression of angiopoietin-2, which results in GEnC apoptosis without affecting podocytes.¹⁹⁵ The CXCL12/CXCR4 crosstalk enhances GEnC injury in diabetic nephropathy¹⁷¹ and in Shiga toxin-associated hemolytic uremic syndrome.¹⁷² A GEnC-protective crosstalk with podocytes was suggested for podocyte-derived angiopoietin-like-4 (Angptl4), which is structurally similar to angiopoietins but does not signal over Tie2. Angptl4 was suggested to protect GEnC from oxidative injury in nephrotic syndrome by binding to αVβ5 integrins.²⁷ A protective reverse signaling from GEnCs to podocytes has been demonstrated for vasohibin secreted from GEnC, which is thought to counteract VEGFA signaling in situations of pathologic elevated VEGFA levels such as in diabetic nephropathy.¹⁹⁶

GLOMERULAR ENDOTHELIAL CELLS AND MESANGIAL CELLS

The fate of MCs and GEnCs is tightly linked. Both communicate directly at the paramesangial areas of glomerular capillaries, where their plasma membranes are in direct contact. Even though MCs secrete a multitude of factors in vitro, which could affect GEnC, only a few MCs secreted factors have been identified that partake in GEnC crosstalk in

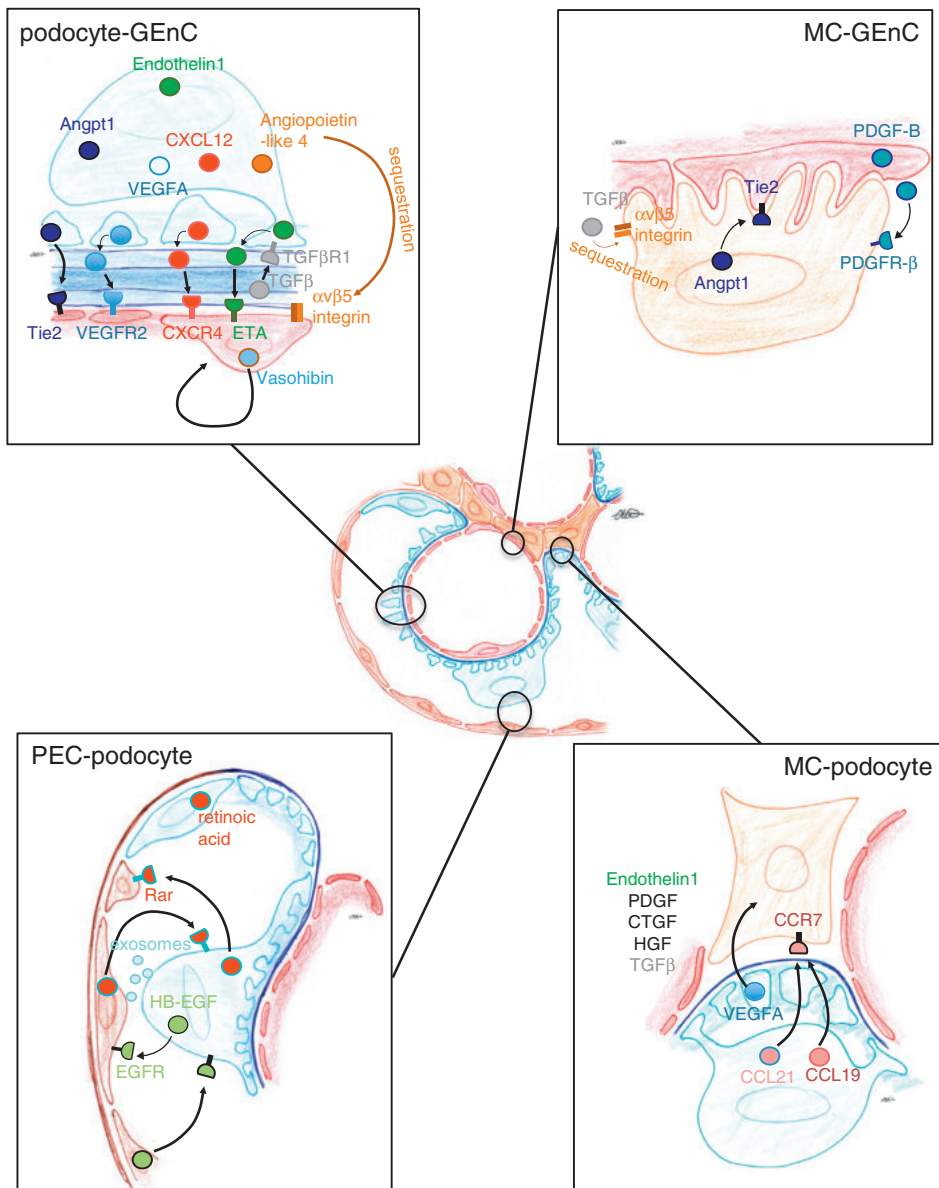


Fig. 4.4 Examples of intra glomerular crosstalk. *Angpt1*, angiopoietin 1; *CTGF*, connective tissue growth factor; *CXCL12*, C-X-C chemokine ligand 12; *CXCR4*, chemokine receptor 4; *EGFR*, epidermal growth factor receptor; *Eta*, endothelin-1 receptor A; *HB-EGF*, heparin-binding epidermal growth factor-like growth factor; *HGF*, hepatocyte growth factor; *PDGF*, platelet-derived growth factor; *PDGF-B*, platelet-derived growth factor B; *PDGFR β* , platelet-derived growth factor receptor β ; *Rar*, retinoic acid receptor; *Tie2*, tyrosine-protein kinase receptor 2; *TGF β* , transforming growth factor β ; *TGF- β R1*, transforming growth factor- β receptor 1; *VEGFA*, vascular endothelial growth factor A; *VEGFR2*, vascular endothelial growth factor receptor 2.

vivo. This is in part a consequence of the lack of glomerular endothelial cell and also of MC-specific gene targeting strategies in vivo, which is a prerequisite for such investigations. Endothelial derived PDGF-B and its receptor PDGFR- β , localized on MCs, have been demonstrated to be of crucial importance for the development and maintenance of glomerular capillaries.⁹ Consequently, injury and loss of GEnCs—for example, due to toxin- or antibody-related GEnC injury—results in decreased PDGF-B levels and MC death (mesangiolysis). MCs maintain endothelial health and function through integrin $\alpha 5\beta 8$ -dependent sequestering of TGF- β , thereby reducing the amount of active TGF- β .¹⁹⁷

Furthermore, like podocytes, MCs synthesize angiopoietin-1, which binds to its receptor Tie2 on GEnC¹⁹¹ to stabilize the vasculature.

PODOCYTES AND MESANGIAL CELLS

It is not clear to date at which sites podocytes communicate with MCs and the in vivo evidence of podocyte–MC crosstalk is scarce. Nonetheless, experimental data and clinical observations in several hereditary forms of nephrotic syndrome due to mutations in podocyte-specific genes¹⁹⁸ suggest that such a communication exists. For example, in glomerular development, mutations in podocyte genes such as the transcription

factor Pod1/tcf21,¹⁹⁹ phospholipase C ϵ ²⁰⁰ laminin α 5,⁹² and Wilms tumor antigen⁵⁵ result in a failure of MCs to migrate into glomeruli. The podocyte-specific deletion of collagen type IV α 3 (Alport mouse) results in enhanced expression of integrin α 1 by MCs,²⁰¹ possibly affecting MCs cell adhesion and cell signaling at the GBM. The chemokines CCL19 and CCL21, generated by podocytes, bind to CCR7 on MCs and are thought to regulate local MC migration and adherence to the GBM.²⁰² Also, a decrease of VEGFA secretion from podocytes results in mesangiolysis,³⁰ supporting the idea of a podocyte-MC crosstalk, which is of relevance in glomerular development. In glomerular injury, experimental data support a communication of podocytes with MCs, although it cannot be excluded that the observed effects on MCs in podocyte injury are not the result from altered PDGF-B levels related to podocyte-dependent GEnC injury. Several signaling pathways might be involved in podocyte-MC crosstalk in the setting of injury, such as endothelin 1, PDGF, CTGF, HGF, and TGF- β .²⁸

PODOCYTES AND PARIELTAL EPITHELIAL CELLS

Under physiologic conditions podocytes and PECs are in close proximity at the vascular pole, where transitional cells called parietal podocytes carry both the characteristics of PECs and podocytes.¹⁵⁴ Another theoretical site of cross communication is across Bowman's space, where the apical membranes of podocytes and PECs can overcome the physical separation given by the primary filtrate and touch. Controlled depletion of PECs results in transient proteinuria with focal podocyte foot process effacement,¹⁸¹ and podocytopenia is associated with PEC hyperplasia,²⁰³ suggesting interdependence of both cells. Communication between PECs and podocytes could also ensue from the uptake of podocyte-derived proteins from the primary urine by PECs.²⁰⁴ Furthermore, podocytes release exosomes to the urine^{205,206} that in turn could affect PECs.

In glomerular injury, podocytes are in close contact to PECs by bridges formed between the capillary tuft and Bowman's capsule²⁰⁷ and in intraglomerular crescents, of which they are both constituents.^{176,208} In glomerulonephritis, mathematical multiscale modeling studies²⁰⁹ and experimental data suggest that podocyte and PEC cross communication might regulate proliferation of both cells and regulate regeneration of podocytes from PECs. Proliferation of both cell types and thereby crescent formation was shown to be dependent of the heparin-binding EGF-like growth factor (HB-EGF), which is de novo expressed by podocytes and PECs in RPGN and the EGF receptor, which is found on both cells.²¹⁰ Lineage tracing experiments suggest that podocyte regeneration in glomerulonephritis occurs from renal progenitor cells located in Bowman's capsule⁷⁶ and that this process can be enhanced by retinoic acid.²¹¹ Therefore, retinoic acid synthesized in glomeruli promotes renal progenitor cells to differentiate toward a podocyte phenotype.²¹²

COMMON MECHANISMS OF GLOMERULAR DISEASES

There appear to be several basic responses of the glomerulus to injury such as cellular proliferation, changes in glomerular cell phenotypes, and increased deposition of extracellular

matrix. Any cause of severe glomerulonephritis (GN) can cause a crescent formation (typical for rapid progressive GN), which is composed of parietal cells,^{181,213} podocytes,²⁰⁸ and inflammatory cells.^{214,215} Most forms of glomerular injury result from immunologic mechanisms,^{216–220} which include both humoral and cellular components. Only little is known about the origin of the etiologic agents that induce the immunologic mechanisms, with the exception of infection-related forms of disease such as beta-hemolytic streptococci in poststreptococcal GN, or hepatitis C and hepatitis B virus in cryoglobulinemic membranoproliferative GN. However, it is likely that drugs, toxins, and other infectious agents induce similar immune responses that result in GN via shared common pathways.

The humoral response is often a T helper cell 2 (Th2) mediated response resulting in B-cell activation, antibody generation and deposition, and complement activation. Immunoglobulin and complement component deposition is found in most human glomerular diseases, suggesting that the humoral response is crucial in the development of glomerular injury, which has been the rationale for the use of therapeutic B-cell depletion in various glomerular diseases. There are three patterns of immunoglobulin deposition in the glomerulus: (1) immune deposits at the GBM and in the subepithelial space (underneath podocytes) are typical for membranous nephropathy and usually do not initiate a strong inflammatory reaction, as the deposits are separated from the circulation by the GBM; (2) immune deposits in the subendothelial space (lupus nephritis and membranoproliferative GN); or (3) in the mesangium (IgA nephropathy and lupus nephritis), on the other hand, initiate multiple inflammatory processes. The final pattern of immunoglobulin deposition is determined by the biologic properties of the immunoglobulins (IgG subtype) deposited, the absolute amount of immunoglobulins deposited, and lastly the mechanisms whereby the deposits are formed. Deposition of the complement-fixing IgG1 or IgG3 subtypes ensues in stronger glomerular injury than deposition of IgA or IgG4, which both poorly activate complement.²²¹ Principally, antibody-antigen binding that takes place within the glomerulus to glomerular self or nonself antigens (termed *in situ* binding) induces stronger complement activation than when preformed immune complexes are deposited in glomeruli. Typical glomerular self-antigens are the phospholipase A2 receptor (PLA₂R1)²²² and thrombospondin type-1 domain-containing 7A (THSD7A)²²³ in membranous nephropathy, or the noncollagenous domain of the α 3 chain of type IV collagen known as the Goodpasture antigen.^{224,225} Nonself antigens localize to glomerular capillaries by mechanisms such as charge affinity for glomerular structures or pure passive trapping in the glomerular sieve in the form of the antigen alone (termed as planted antigens) or as antigen-antibody complexes formed outside the kidney. *In situ* antibody binding to planted nonself antigens is typical in lupus nephritis to DNA nucleosome complexes^{226,227} or in IgA nephropathy to abnormally glycosylated IgA.²²⁸ Glomerular deposition of preformed immune complexes to nonself antigens has been demonstrated in early childhood MN, where immune complexes containing cationic bovine serum albumin are deposited,²²⁹ or in hepatitis C virus-associated membranoproliferative GN where hepatitis C virus-containing cryoglobulins are deposited.²³⁰ There is little experimental evidence that immunoglobulin

binding alone induces significant tissue injury, except for when the antibodies bind to podocyte antigens such as nephrin^{231,232} of the slit membrane or to THSD7A.²³³ Of note, severe inflammation can occur with only little antibody deposited, as in antineutrophil cytoplasmic antibody (ANCA)-associated GN.

The cellular response is a largely T helper cell 1 (Th1)-mediated response characterized by the infiltration of circulating mononuclear cells such as lymphocytes and macrophages into glomeruli and the formation of crescents. Neutrophils are the earliest cells to be found in inflamed glomeruli in human biopsies and are strong inducers of glomerular injury.²³⁴ Animal studies demonstrate that their strongest attractants to inflamed glomeruli are interleukin (IL) 8 and complement factor C5a,²³⁵ bound to the glomerular endothelium via HS proteoglycans.^{150,236} Neutrophils are activated by phagocytosis of immune complex aggregates, which induces them to undergo a respiratory burst with generation of reactive oxygen species such as hydrogen peroxide. Hydrogen peroxide interacts with the neutrophil cationic enzyme myeloperoxidase (MPO) to halogenate the glomerular capillary wall.²³⁷ Furthermore, neutrophils store other cationic enzymes such as proteinase 3 (PR3), elastase, and cathepsin G, which upon release further degrade the glomerular capillary wall. Lastly, neutrophils release extracellular traps, web-like DNA structures expulsed from nuclei with adherent histones, proteases, peptides, and enzymes, which show a modest contribution to glomerular injury in anti-GBM glomerulonephritis,²³⁸ but could be more injurious in ANCA-associated GN and lupus nephritis.²³⁹

Macrophages are typically found in glomerular lesions with crescents and serve as effector cells of both humoral and cell-mediated forms of immune glomerular injury, because their localization to inflamed glomeruli is induced by interactions with immunoglobulins through their Fc receptors and through chemokines, such as CCL5, and CCL2. Similar to neutrophils, macrophages generate direct tissue injury by the release of oxidants and proteases. Additionally, they release tissue factor to induce glomerular fibrin deposition and crescent formation and TGF-β to induce the synthesis of the extracellular matrix, culminating in glomerular sclerosis.²⁴⁰

T cells are rarely found in injured glomeruli except for GNs primarily mediated by macrophages such as crescentic GN. T-cell-mediated glomerular injury is mostly the result from released chemokines and the recruitment of macrophages.²⁴¹ However, ovalbumin-specific CD4+ and CD8+ T cells together can induce glomerular injury in transgenic mice that express the antigen ovalbumin in podocytes.²⁰⁴ Among the known T-cell subtypes, there is strong experimental evidence for the importance of T helper cell 17 (Th17) in crescentic GN.^{242,243} Th17 cells produce and secrete IL-17 A, IL-17F, IL-21, IL-22, which promotes inflammation by directly causing tissue injury and enhancing secretion of proinflammatory cytokines and chemokines by resident cells. This results in augmented infiltration of leukocytes, in particular neutrophils, recruited by CXCL5²⁴⁴ to the affected kidney where they induce further inflammation and injury.²⁴⁵ The kidney-infiltrating Th17 cells are partly recruited from the gut.²⁴⁶

Platelets are present in glomerular lesions in which intracapillary thrombosis is involved, typically observed in thrombotic microangiopathies and antiphospholipid syndrome. Platelets

are important players in the formation of thrombi and in the recruitment of leukocytes to the inflamed glomerulus.²⁴⁷ In addition, they release factors that enhance glomerular permeability to proteins, enhance immune complex deposition,^{248–250} and induce MC proliferation (PDGF)²⁵¹ and MC sclerosis (TGF-β).²⁵²

Dendritic cells (DCs) are restricted to the tubulointerstitium and are absent from glomeruli.²⁵³ However, proteins that pass the glomerular filter are captured by renal DCs or reach the renal lymph nodes by lymphatic drainage²⁵⁴ to induce immune tolerance²⁵⁵ to innocuous proteins, such as food antigens or hormones, or to stimulate infiltrating T cells to produce proinflammatory cytokines.²⁰⁴

The site of glomerular injury, especially when glomerular cell is involved, determines whether the patient has an inflammatory or a noninflammatory injury (Fig. 4.5). Because glomerular endothelial and MCs are in contact with circulating factors such as complement and inflammatory cells, they are prone to react to injury via a principally more dramatic inflammatory response. In contrast, PECs and podocytes are separated by the GBM from the circulation; thus podocyte injury is rarely associated with activation of circulating inflammatory cells. Clinically the distinction between inflammatory and noninflammatory injury is crucial for the adequate diagnosis and management of patients. The clinical characteristics of inflammatory injury are hematuria with dysmorphic erythrocytes with or without red blood cell casts and occasional leukocyturia. Inflammatory injury is accompanied by varying degrees of proteinuria, which ranges from mild to nephrotic range proteinuria and a normal

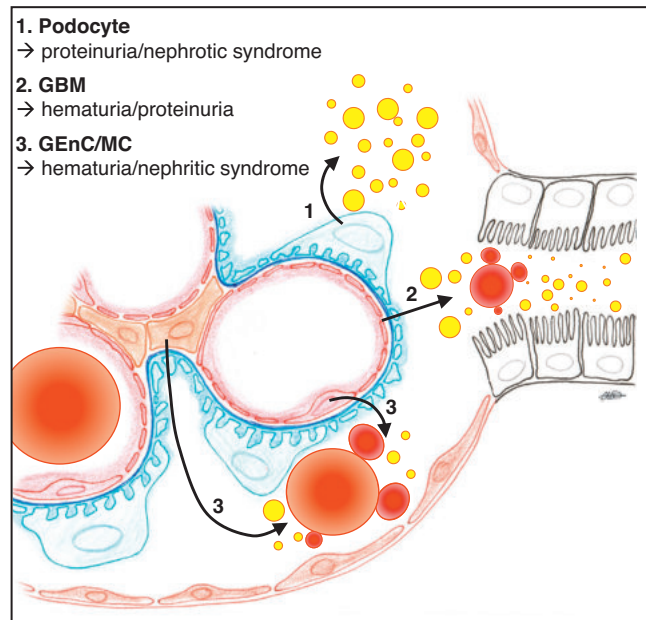


Fig. 4.5 The clinical presentation reflects the localization of glomerular injury. Injury of podocytes results in proteinuria (yellow droplets) eventually leading to the clinical manifestation of nephrotic syndrome. Injury of the glomerular basement membrane (GBM) commonly results in proteinuria and hematuria with dysmorphic erythrocytes. Injury of glomerular endothelial cells (GEnC) and mesangial cells (MC) usually leads to hematuria with dysmorphic erythrocytes and only little proteinuria.

or reduced glomerular filtration rate, depending on the severity of disease. Morphologically, inflammatory injury is characterized by glomerular hypercellularity that results from proliferating resident glomerular (mostly MCs and PECs) and from infiltrating hematopoietic cells (mostly neutrophils and macrophages), phenotype change, and visible structural injury. Glomerular injury arises from the release of inflammatory substances from infiltrating hematopoietic cells and from glomerular cells or from the impairment of protective mediators such as complement factor H²⁵⁶ or complement factor H-related protein 5²⁵⁷ as negative regulators of the complement pathway. The release of inflammatory substances, such as cytokines, growth factors, proteases, products resulting from complement activation (C5a, C5b-9), vasoactive agents, and oxidants,^{217,258,259} initiates thrombosis, necrosis, and crescent formation which, if extensive, leads to the serious clinical condition of rapid progressive glomerulonephritis. Noninflammatory lesions usually involve podocytes and are termed podocytopathies. They are characterized by proteinuria and (if proteinuria is extensive) nephrotic syndrome (a triad consisting of proteinuria over 3.5 g/day, edema, and hypertriglyceridemia) without hematuria.

Clinical Relevance

The site of glomerular injury determines the clinical picture. Whereas involvement of podocytes presents as glomerular injury with proteinuria or nephrotic syndrome, involvement of glomerular endothelial cells, the GBM, and/or MCs typically presents with microhematuria or nephritic syndrome.

MECHANISMS OF INJURY IN COMMON PODOCYTOPATHIES

The most common causes of noninflammatory immune-mediated glomerular injury are minimal change disease (MCD), primary focal segmental glomerulosclerosis (FSGS), and membranous nephropathy (MN). All three entities exhibit a dramatic increase in glomerular permeability with little to significant structural abnormalities by light microscopy in common. These diseases are classified as podocytopathies, as podocytes are thought to be the primary glomerular cell affected in the pathogenesis. In contrast, “nontraditional” podocyte diseases include diabetic kidney disease, human immunodeficiency virus nephropathy, amyloidosis, Fabry disease, membranoproliferative glomerulonephritis, and postinfectious glomerulonephritis. Diabetic nephropathy (covered in detail in Chapter 39) is the numerically and economically most important form of progressive kidney disease worldwide, involving the podocyte, endothelial, and MCs with a perturbation of glomerular cell crosstalk. The inciting causes of each podocyte disease differ, and therefore each disease affects podocytes in different ways; in turn, the response to injury in each disease differs, leading to different histologic and clinical manifestations. Yet, regardless of the inciting causes and their mediators, several common clinical and pathologic responses occur in podocyte injury, as highlighted earlier—namely, hypertrophy, foot process effacement, loss, and proteinuria.

MINIMAL CHANGE DISEASE AND FOCAL SEGMENTAL GLOMERULOSCHLEROSIS

Characteristics of MCD: In MCD the glomerulus is per definition mostly normal by light microscopy with absence of complement or immunoglobulin deposition. In light of the histologic “minimal changes,” pathologic diagnosis is primarily based on electron microscopic evaluations of podocytes, which exhibit foot process effacement, microvillous transformation, and vacuolization. The absence of glomerular sclerosis differentiates MCD from FSGS. MCD typically presents as a steroid-sensitive nephrotic syndrome (SSNS), contrasting with FSGS, which often presents with steroid-resistant nephrotic syndrome (SRNS). Whether steroid-resistant MCD exists as its own disease entity, or whether steroid resistance in histologic MCD represents an early form of FSGS is a matter of debate, considering the high rate of sampling error on renal biopsies, possibly missing present (but rare) glomeruli with sclerosis. It is likely that patients with MCD can progress to FSGS due to a consistent pathologic agent.²⁶⁰

Characteristics of FSGS: FSGS is a generic term for a histologic injury pattern defined by segmental glomerular consolidation into a scar that affects some but not all glomeruli with a wide range of etiologic interpretations. FSGS describes both a disease characterized by a primary podocyte injury (primary FSGS), and a lesion that occurs secondarily in any type of chronic kidney disease (secondary FSGS).²⁶¹ There is abundant evidence that classical FSGS is the consequence of podocyte loss in experimental models,²⁶² which is accompanied by proliferation and migration of PECs to the glomerular tuft (both discussed earlier in the chapter). The underlying causes or mechanisms of FSGS are broadly considered as hereditary/congenital and sporadic/acquired in nature. Primary FSGS presents either with SSNS if triggered by causative circulating agents that increase the permeability of the glomerular filtration barrier (as discussed later) or with SRNS in case of an underlying genetic cause. Secondary FSGS, on the other hand, is associated with nephron loss, drug toxicity, or viral infections and rarely presents with nephrotic syndrome, but is steroid resistant.

PATHOPHYSIOLOGIC CONCEPTS OF MCD AND PRIMARY FSGS

MCD and primary FSGS might represent different histologic patterns of the same disease entity. At least there is a significant overlap in the factors causing these podocytopathies, which are the following:

- Soluble serum factors:** Based on experimental data, soluble serum factors are thought to be causative in MCD and FSGS, as nephrotic plasma has direct cellular effects on cultured podocytes²⁶³ or in single perfused kidneys.²⁶⁴ Many efforts have been undertaken to unravel “the increasing or missing circulating permeability factor” in SSNS and SRNS.²⁶⁵ Roles have been indicated for TNF α ,^{266,267} circulating cardiotrophin-like cytokine factor 1 (member of the IL-6 family), circulating hemopexin,^{268,269} and the soluble urokinase-type plasminogen activator receptor (suPAR)²⁷⁰ in the development of nephrotic syndrome.²⁷¹ These factors, however, need further verification in the context of human disease activity,^{272,273} disease specificity,^{274–276} and therapeutic effects.²⁷⁷

2. Immune dysfunction: Considerable clinical and experimental evidence point toward an immune dysfunction on the T- and B-cell side in MCD. Clinically, MCD is not only very responsive to steroids but also to rituximab,^{278,279} a monoclonal antibody against plasma cell CD20, and a significant association of HLA-DQA1 (a major histocompatibility complex class II) missense coding variants exists.²⁸⁰ Additionally, MCD is associated with Hodgkin disease and with allergies.²⁸¹ On the experimental side, mice develop proteinuria if they receive CD34+ peripheral stem cells from MCD patients²⁸² or following the injection of the supernatant derived from T cells or from peripheral blood mononuclear cells.²⁸³ T- and B-cell dysfunction is further suggested by a different DNA methylation pattern of Th0 cells in MCD patients,²⁸⁴ an altered Th17/regulatory T-cell balance,²⁸⁵ and an upregulation of T-cell-derived IL-13 in patients¹⁶⁰ that can cause proteinuria and foot process effacement in rats.^{286,287} Further pointing toward an immune dysfunction as the origin of nephrotic syndrome is the finding that abatacept, an antibody challenging the CD80 (B7-1)-CTLA-4-axis has been shown to reduce proteinuria in FSGS,²⁸⁸ an effect requiring still further confirmation.²⁸⁹⁻²⁹¹ Recent experimental findings have given rise to the idea of a disease-specific expression of CD80^{288,292} or of the expression of a hyposialylated form of angiopoietin-like-4 by podocytes, which might contribute to glomerular disease.²⁹³⁻²⁹⁵

3. Genetic inheritance: Familial cases are rare in MCD, making genetic causes for MCD unlikely. Nonetheless, whole-exome sequencing in SSNS patients revealed mutations in epithelial membrane protein 2 (EMP2), which is involved in regulating endocytosis and transcytosis,²⁹⁶ shedding new light into possible causes for podocyte disruption in SSNS. There are changes in expression patterns of podocyte-specific transcripts²⁹⁷ and proteins²⁹⁸ in MCD, but it is difficult to determine whether these are cause or effect. There is strong evidence for genetic causes leading to FSGS. Inheritance of genetic causes of primary FSGS may be autosomal dominant or recessive, with a subset of autosomal recessive SRNS presenting as congenital nephrotic syndrome. The biologic functions altered in podocytes by the gene mutations involved in FSGS are broad, ranging from cytoskeletal regulation, slit membrane function, lysosomal function, mitochondrial function, and attachment to the GBM.⁴⁴ In the late 1990s positional cloning of the gene responsible for congenital nephrotic syndrome of the Finnish type led to the identification of the archetypal podocyte-specific protein, nephrin.⁴⁹ This was rapidly followed by the identification of other proteinuric diseases linked to podocyte-specific single-gene disorders, including those affecting podocin,⁵⁰ Wilms tumor 1,²⁹⁹ CD2AP,³⁰⁰ α -actinin-4,⁵¹ TRPC6,³⁰¹ phospholipase C ϵ 1 (PLCE1),²⁰⁰ WW and PDZ domain-containing 2 (MAGI2),³⁰² kidney ankyrin repeat-containing protein (KANK), and others.^{303,304} In each of these conditions it is generally accepted that proteinuria results directly from the disruption of these constitutively expressed genes in the podocyte, leading to FSGS.

It is becoming increasingly clear that monogenic inheritance of abnormalities in podocyte-specific genes is only one aspect of FSGS. Even though the amount of over 50 known mutations of podocyte genes involved in SRNS

is steadily increasing, these mutations are rare and explain less than 30% of patients with hereditary cases and only 20% of patients with sporadic cases of FSGS.⁴⁴ Studies of the increased susceptibility of African Americans to FSGS have implicated variants of another gene expressed in podocytes, apolipoprotein L1 (APOL1).^{305,306} Experimental expression of the APOL1 risk alleles in a podocyte specific manner demonstrated that these were causal for podocyte foot process effacement, proteinuria, and glomerulosclerosis.³⁰⁷ Mechanistically, the risk-variant APOL1 alleles interfere with endosomal trafficking and block autophagic flux, ultimately leading to inflammatory-mediated podocyte death and glomerular scarring.³⁰⁷ A key question for practicing nephrologists is whether podocyte-specific gene mutations or polymorphisms play a role as predisposing factors for the much more common “sporadic” forms of proteinuric disease. In human disease an opportunity to study the very earliest features of FSGS is afforded by studies of FSGS recurrence in transplanted kidneys; changes in podocytes can be seen in reperfusion biopsies and are predictive of full-blown FSGS recurrence.³⁰⁸ Chapter 43 includes an in-depth discussion of inherited glomerular diseases.

4. Altered posttranslational regulation of podocyte proteins: Besides abnormalities in podocyte genes, altered post-translational regulation of podocyte mRNA by small noncoding RNA molecules, termed microRNAs, have been shown to result in FSGS, such as the transcription factor Wilms tumor protein 1 (WT1) by microRNA-193a¹⁶¹ or of Notch1 and p53 by microRNA-30.³⁰⁹

MEMBRANOUS NEPHROPATHY

Membranous nephropathy is an autoimmune disease with the morphologic hallmarks of GBM thickening, granular staining for human IgG and complement components along the glomerular filtration barrier, and subepithelial (subpodocyte) electron-dense deposits by electron microscopy. Although this histologic pattern can arise from the deposition of preformed immune complexes as in lupus nephritis type 5 or from subepithelial antigen trapping in hepatitis B virus and hepatitis C virus-associated secondary forms of MN, primary MN is thought to be the consequence of in situ binding of autoantibodies to podocyte-expressed antigens. The concept that primary MN is an antibody-mediated disease has been supported by the discoveries of autoantibodies to podocyte membrane antigens such as neutral endopeptidase (NEP),³¹⁰ the phospholipase A₂ receptor (PLA₂R1),²⁹² and thrombospondin type 1 domain-containing 7A (THSD7A).²⁹³ PLA₂R1 and THSD7A are targets for a malfunctioning immune system in 70% and 5% of adult cases, respectively, and NEP is important in a small number of neonates with MN caused by alloimmunization due to vertical transfer of antibodies from a genetically NEP-deficient mother.²⁹¹ PLA₂R1 polymorphisms influence the susceptibility to MN, and the association between certain HLA-DQA1 alleles and MN suggests that these HLA class II molecules could facilitate autoimmunity against PLA₂R1.³¹¹ In contrast to PLA₂R1-associated MN, THSD7A-associated MN has a high coincidence of malignancy.^{312,313} The direct pathogenicity of autoantibodies is suggested by the observations that PLA₂R1 or THSD7A

autoantibodies are present in patients with a rapid recurrence of MN in renal transplants,^{223,314,315} the finding that anti-PLA₂R1 antibody levels are associated with disease remission^{316,317} and progression,^{317–319} and the finding that MN can be induced in mice that normally express THSD7A on podocytes^{320,321} by injection of human autoantibodies²³³ or rabbit antibodies to THSD7A.³²² So far there is no proof that PLA₂R1-specific autoantibodies are pathogenic, related to the fact that rodents necessary for such studies normally do not express PLA₂R1 on podocytes. The role of complement in the pathogenesis of human MN remains unclear. First, the deposited IgG in idiopathic MN is typically of the noncomplement fixing IgG4 subtype. Second, in rodent models of MN, clinical and morphologic MN can be induced in the absence of detectable complement deposition,^{233,322} as well as in rodents with genetic deficiency in complement components.^{323,324} On the other hand, C3 and the membrane attack complex C5b9 are usually constituents of the deposits³²⁵; C5b9 inserts into the podocyte membrane and is transported across the cell³²⁶ and excreted into the urine, where high levels of C5b9 can be measured in humans.³²⁷ Experimental studies allow for an injurious as well as a protective function of C5b9. Sublytic C5b9 has been shown to induce podocyte injury by multiple pathways such as the activation of kinases, the induction of endoplasmic reticulum stress, and the production of extracellular matrix.³²⁸ On the other hand, C5b9 enhances the ubiquitin proteasome system,³²⁹ which supports a protective removal of damaged proteins.

EFFECTS OF EXISTING THERAPIES ON PODOCYTES

The basis for therapy of primary nephrotic syndrome (reviewed in Chapter 33) is mostly of a supportive nature, including antihypertensive and antiproteinuric therapy and dietary recommendations.³³⁰ Regrettably, no therapeutic approaches are currently available that specifically target podocytes in disease. However, several therapies have, in addition to their systemic effects, direct biologic actions on podocytes (i.e., pleiotropic actions), and these will be considered in the following sections.

RENIN ANGIOTENSIN SYSTEM BLOCKADE

Blockade of the renin angiotensin system belongs to the standard supportive therapy regimen for primary podocytopathies with proteinuria and remains unchallenged. Systemic and glomerular overactivation of the renin angiotensin system (RAS) through its main effector angiotensin II is central to the pathogenesis of proteinuric glomerular diseases; levels of tissue angiotensin II and the angiotensin subtype 1 receptor are increased in glomeruli³³¹ and podocytes³³² in primary podocytopathies. Activation of RAS is detrimental to glomerular cells including podocytes as it promotes multiple trophic effects, such as apoptosis, ECM protein accumulation, reactive oxygen species production, oxidative stress, alteration in slit diaphragm proteins partly by epigenetic modulation of nephrin promoter methylation,³³³ increased calcium influx through TRPC6 channels,^{334,335} cell cycle inhibition, detachment, and inflammatory cytokine production.^{332,336} Blocking the RAS with angiotensin-converting enzyme inhibitors, angiotensin 1 receptor (AT1R) antagonists, and

mineralocorticoid receptor blockers reduces proteinuria resulting in renoprotection, an effect that is attributed to a reduction in glomerular hydrostatic pressure and an abolishment of the detrimental trophic glomerular effects mentioned earlier.³² For these reasons, inhibition of the renin angiotensin aldosterone system is currently the standard of care for lowering proteinuria.

GLUCOCORTICOIDS

Steroids are immunomodulatory drugs widely used in the treatment of proteinuric diseases, but their modes of action, especially in the noninflammatory forms of nephrotic syndrome such as MCD and primary FSGS, remain completely unknown. Glucocorticoid receptor (GR) expression is ubiquitous; therefore, these drugs could affect any glomerular cell type. It has been shown that GR-induced signaling pathways are functional in murine podocytes, having transcriptional and posttranscriptional effects on podocyte genes.³³⁷ Initial reports in murine³³⁸ and human³³⁹ podocytes showed that dexamethasone had potent biologic effects directly on podocyte structure and function. These include limiting podocyte apoptosis,³⁴⁰ induction of podocyte differentiation by restoring the actin cytoskeleton,³³⁸ increasing levels of the transcription factors Kruppel-like factor 15 (KLF15),³⁴¹ and by preventing the downregulation of protective microRNA-30.³⁰⁹ Specifically, the slit membrane protein nephrin is affected by steroids, as steroids enhance the transport of nephrin from the ER³⁴² and induce the phosphorylation of nephrin,³⁴³ which is reduced in MCD³⁴⁴ and important for the function of nephrin and therefore of the slit membrane.

EVIDENCE FOR DIRECT ACTIONS OF IMMUNOSUPPRESSANTS ON PODOCYTES

The calcineurin inhibitors cyclosporine and tacrolimus are widely used in nephrotic syndrome, either alone or in combination with other therapies. Calcineurin is a Ca²⁺-dependent phosphatase, which dephosphorylates nuclear factor of activated T cells (NFAT), a transcription factor. Dephosphorylation of NFAT initiates its cytoplasmic to nuclear translocation, resulting in an increased transcription of genes such as TRCP6,³⁴⁵ whose gain of function mutations in podocytes induce FSGS.³⁰¹ In accordance, podocyte-expressed NFAT is a strong inducer of glomerulosclerosis in mice.³⁴⁶ Besides their known immunomodulatory effects in T cells, calcineurin inhibitors affect the podocyte cytoskeleton by transcriptional downregulation of the earlier mentioned calcium channel TRPC6,³⁴⁷ and by preventing the degradation of the actin-organizing protein synaptopodin³⁴⁸ in an NFAT-independent manner. Together, these mechanisms appear to result in a stabilization of the podocyte actin cytoskeleton and direct reduction of proteinuria.

The specific anti-B-cell monoclonal antibody rituximab, increasingly thought to be effective in proteinuric diseases even when they are not all obviously immune mediated,³⁴⁹ has been shown to have direct effects on podocytes, including stabilizing their actin cytoskeleton.³⁵⁰ Although monoclonal antibodies are assumed to have very specific binding targets, they can also have “off-target” effects. In this case it seems that rituximab, as well as binding to the CD20 molecule that is its accepted molecular target, also binds to a podocyte protein called sphingomyelin phosphodiesterase acid-like-3b (SMPDL-3b) and this protein stabilizes the actin cytoskeleton.³⁵⁰

IDENTIFICATION OF CANDIDATE THERAPEUTIC APPROACHES FOR THE FUTURE

End-stage renal disease constitutes an enormous burden of morbidity, both to patients who suffer a lifelong chronic disease and to health services that are challenged by high costs arising from dialysis and transplantation. Despite major advances over the past 15 years in unraveling genetic and biologic causes of podocyte dysfunction as the origin of most forms of nephrotic syndrome, glomerular target cell-directed therapies are still in their infancy. Especially in comparison to other specialties in medicine, only a few new drugs have been approved for renal failure in comparison to many new drugs for cancer therapy or for heart diseases. Nonetheless, the separation of monogenic causes of podocyte dysfunction from other causes is now used to stratify those patients in whom immunosuppression can be minimized due to low potential of success. Furthermore, the discovery of the genes involved in hereditary proteinuric disease unraveled critical (and in the future potentially drugable) pathways required for podocyte maintenance, for stabilization of the podocyte actin cytoskeleton and slit diaphragm, and for restoration of metabolic and mitochondrial function.³⁵¹ Several experimental approaches of recent years have aimed at finding podocyte-specific interventions, which stabilize the actin cytoskeletal backbone of podocyte foot processes and by this also of the slit diaphragm.^{352–355} Targeting the metabolic and mitochondrial function in podocytes seems to be another therapeutic option for many forms of podocyte injury. Even though mTOR inhibition is known to induce proteinuria as a typical side effect,^{356,357} inhibition of an overactivated mTOR pathway in the setting of metabolic superfluency, as in diabetic nephropathy, is beneficial for podocyte function and proteinuria.⁶¹ Other examples with therapeutic potential targeting metabolic pathways include lipid lowering (e.g., statins),^{358,359} antidiabetic agents such as thiazolidinediones (TZDs), or glitazones that activate the peroxisome proliferator-activated receptor γ(PPARγ),^{360–363} and manipulation of VEGF levels³⁶⁴ or autophagy.³⁶⁵

SUMMARY

Kidney diseases with glomerular involvement account for the vast majority of end-stage renal diseases. In the past two decades much has been learned about the glomerulus, a functional and integrated syncytium of four types of glomerular cells, which together ascertain glomerular filtration. Podocytes and GEnC comprise the glomerular filtration barrier. Together, both cells allow for a size- and charge-selective glomerular filtration due to their specialized three-dimensional structure, extensive glycocalyx coating, and synthesis of the unique GBM. MCs regulate glomerular filtration by means of contraction and release of vasoactive substances and maintain the health of glomerular endothelial cells. PECs, built Bowman's capsule to prevent leakage of the primary urine to the tubulointerstitium, can contribute to glomerular scarring, and are thought to constitute a potential reservoir for podocytes in development, maturation, and eventually in adulthood. A cell type-specific view of

glomerular physiology and pathophysiology has enhanced our understanding of glomerular cell biology immensely in the past decades. However, the intricate interactions of glomerular cell types are getting more and more center stage attention as clinical and experimental observations demonstrate that the normal functioning of glomerular filtration requires a coordinated interaction of all four cell types and that injury of one glomerular cell type usually affects the others. Several clinical and experimental challenges and opportunities lie ahead. Identification, designing, and delivering glomerular cell specific therapeutic agents is actively being pursued, both to enhance efficacy and to reduce systemic side effects. Noninvasive diagnostic testing is being keenly studied, such as measuring glomerular cell products in the urine, and markers in the serum and urine, which will hopefully translate into clinical practice. The past two decades have witnessed phenomenal advances in understanding glomerular cell biology in health and disease, which hopefully soon translates into better therapeutic options for progressive glomerular and renal kidney disease.

ACKNOWLEDGMENTS

The authors would like to thank Dr. Stuart Shankland and Dr. Peter Mathieson, who contributed to earlier versions of this topic review, and Dr. Pierre Ronco and Dr. William Couser for inspiring our chapter on “common mechanisms of glomerular injury.”

 Complete reference list available at ExpertConsult.com.

KEY REFERENCES

5. Farquhar MG, Wissig SL, Palade GE. Glomerular permeability. I. ferritin transfer across the normal glomerular capillary wall. *J Exp Med*. 1961;113:47–66.
10. Abrahamson DR. Structure and development of the glomerular capillary wall and basement membrane. *Am J Physiol*. 1987;253:F783–F794.
14. Grahammer F, Wigge C, Schell C, et al. A flexible, multilayered protein scaffold maintains the slit in between glomerular podocytes. *JCI Insight*. 2016;1.
16. Huber TB, Schermer B, Muller RU, et al. Podocin and MEC-2 bind cholesterol to regulate the activity of associated ion channels. *Proc Natl Acad Sci USA*. 2006;103:17079–17086.
19. Asanuma K, Yanagida-Asanuma E, Faul C, et al. Synaptopodin orchestrates actin organization and cell motility via regulation of RhoA signalling. *Nat Cell Biol*. 2006;8:485–491.
22. Kerjaschki D, Sharkey DJ, Farquhar MG. Identification and characterization of podocalyxin—the major sialoprotein of the renal glomerular epithelial cell. *J Cell Biol*. 1984;98:1591–1596.
25. Abrahamson DR, Hudson BG, Stroganova L, et al. Cellular origins of type IV collagen networks in developing glomeruli. *J Am Soc Nephrol*. 2009;20:1471–1479.
30. Eremina V, Cui S, Gerber H, et al. Vascular endothelial growth factor signaling in the podocyte-endothelial compartment is required for mesangial cell migration and survival. *J Am Soc Nephrol*. 2006;17:724–735.
49. Kestila M, Lenkkeri U, Mannikko M, et al. Positionally cloned gene for a novel glomerular protein—nephrin—is mutated in congenital nephrotic syndrome. *Mol Cell*. 1998;1:575–582.
50. Boute N, Gribouval O, Roselli S, et al. NPHS2, encoding the glomerular protein podocin, is mutated in autosomal recessive steroid-resistant nephrotic syndrome. *Nat Genet*. 2000;24:349–354.
51. Kaplan JM, Kim SH, North KN, et al. Mutations in ACTN4, encoding alpha-actinin-4, cause familial focal segmental glomerulosclerosis. *Nat Genet*. 2000;24:251–256.
52. Kim JM, Wu H, Green G, et al. CD2-associated protein haploinsufficiency is linked to glomerular disease susceptibility. *Science*. 2003;300:1298–1300.

55. Pelletier J, Bruening W, Kashtan CE, et al. Germline mutations in the Wilms' tumor suppressor gene are associated with abnormal urogenital development in Denys-Drash syndrome. *Cell*. 1991;67:437–447.
57. Diomedi-Camassei F, Di Giandomenico S, Santorelli FM, et al. COQ2 nephropathy: a newly described inherited mitochondrialopathy with primary renal involvement. *J Am Soc Nephrol*. 2007;18:2773–2780.
69. Wiggins JE, Goyal M, Sanden SK, et al. Podocyte hypertrophy, “adaptation,” and “decompensation” associated with glomerular enlargement and glomerulosclerosis in the aging rat: prevention by calorie restriction. *J Am Soc Nephrol*. 2005;16:2953–2966.
72. Wanner N, Hartleben B, Herbach N, et al. Unraveling the role of podocyte turnover in glomerular aging and injury. *J Am Soc Nephrol*. 2014;25:707–716.
81. Eremina V, Sood M, Haigh J, et al. Glomerular-specific alterations of VEGF-a expression lead to distinct congenital and acquired renal diseases. *J Clin Invest*. 2003;111:707–716.
86. Drenckhahn D, Schnittler H, Nobiling R, et al. Ultrastructural organization of contractile proteins in rat glomerular mesangial cells. *Am J Pathol*. 1990;137:1343–1351.
87. Kriz W, Elger M, Lemley K, et al. Structure of the glomerular mesangium: a biomechanical interpretation. *Kidney Int Suppl*. 1990;30:S2–S9.
90. Leveen P, Pekny M, Gebre-Medhin S, et al. Mice deficient for PDGF B show renal, cardiovascular, and hematological abnormalities. *Genes Dev*. 1994;8:1875–1887.
92. Kikkawa Y, Virtanen I, Miner JH. Mesangial cells organize the glomerular capillaries by adhering to the G domain of laminin alpha5 in the glomerular basement membrane. *J Cell Biol*. 2003;161:187–196.
93. Blantz RC, Gabbai FB, Tucker BJ, et al. Role of mesangial cell in glomerular response to volume and angiotensin II. *Am J Physiol*. 1993;264:F158–F165.
101. Ostendorf T, Kunter U, Grone HJ, et al. Specific antagonism of PDGF prevents renal scarring in experimental glomerulonephritis. *J Am Soc Nephrol*. 2001;12:909–918.
130. Deen WM. What determines glomerular capillary permeability? *J Clin Invest*. 2004;114:1412–1414.
135. Chang RL, Deen WM, Robertson CR, et al. Permselectivity of the glomerular capillary wall: III. Restricted transport of polyanions. *Kidney Int*. 1975;8:212–218.
139. Jeansson M, Haraldsson B. Morphological and functional evidence for an important role of the endothelial cell glycocalyx in the glomerular barrier. *Am J Physiol Renal Physiol*. 2006;290:F111–F116.
160. Kietzmann L, Guhr SS, Meyer TN, et al. MicroRNA-193a regulates the transdifferentiation of human parietal epithelial cells toward a podocyte phenotype. *J Am Soc Nephrol*. 2015;26:1389–1401.
161. Gebeschuer CA, Kornauth C, Dong L, et al. Focal segmental glomerulosclerosis is induced by microRNA-193a and its downregulation of WT1. *Nat Med*. 2013;19:481–487.
163. Appel D, Kershaw DB, Smeets B, et al. Recruitment of podocytes from glomerular parietal epithelial cells. *J Am Soc Nephrol*. 2009;20:333–343.
165. Miner JH, Patton BL, Lentz SI, et al. The laminin alpha chains: expression, developmental transitions, and chromosomal locations of alpha1-5, identification of heterotrimeric laminins 8-11, and cloning of a novel alpha3 isoform. *J Cell Biol*. 1997;137:685–701.
185. Smeets B, Stucker F, Wetzel J, et al. Detection of activated parietal epithelial cells on the glomerular tuft distinguishes early focal segmental glomerulosclerosis from minimal change disease. *Am J Pathol*. 2014;184:3239–3248.
204. Heymann F, Meyer-Schwesinger C, Hamilton-Williams EE, et al. Kidney dendritic cell activation is required for progression of renal disease in a mouse model of glomerular injury. *J Clin Invest*. 2009;119:1286–1297.
207. Le Hir M, Keller C, Eschmann V, et al. Podocyte bridges between the tuft and Bowman's capsule: an early event in experimental crescentic glomerulonephritis. *J Am Soc Nephrol*. 2001;12:2060–2071.
212. Lasagni L, Angelotti ML, Ronconi E, et al. Podocyte regeneration driven by renal progenitors determines glomerular disease remission and can be pharmacologically enhanced. *Stem Cell Reports*. 2015;5:248–263.
217. Nangaku M, Couser WG. Mechanisms of immune-deposit formation and the mediation of immune renal injury. *Clin Exp Nephrol*. 2005;9:183–191.
222. Beck LH Jr, Bonegio RG, Lambeau G, et al. M-type phospholipase A2 receptor as target antigen in idiopathic membranous nephropathy. *N Engl J Med*. 2009;361:11–21.
223. Tomas NM, Beck LH Jr, Meyer-Schwesinger C, et al. Thrombospondin type-1 domain-containing 7A in idiopathic membranous nephropathy. *N Engl J Med*. 2014;371:2277–2287.
225. Hudson BG, Tryggvason K, Sundaramoorthy M, et al. Alport's syndrome, Goodpasture's syndrome, and type IV collagen. *N Engl J Med*. 2003;348:2543–2556.
233. Tomas NM, Hoxha E, Reinicke AT, et al. Autoantibodies against thrombospondin type 1 domain-containing 7A induce membranous nephropathy. *J Clin Invest*. 2016;126:2519–2532.
242. Paust HJ, Turner JE, Steinmetz OM, et al. The IL-23/th17 axis contributes to renal injury in experimental glomerulonephritis. *J Am Soc Nephrol*. 2009;20:969–979.
246. Krebs CF, Paust HJ, Krohn S, et al. Autoimmune renal disease is exacerbated by SIP-receptor-1-dependent intestinal th17 cell migration to the kidney. *Immunity*. 2016;45:1078–1092.
270. Wei C, El Hindi S, Li J, et al. Circulating urokinase receptor as a cause of focal segmental glomerulosclerosis. *Nat Med*. 2011;17:952–960.
301. Winn MP, Conlon PJ, Lynn KL, et al. A mutation in the TRPC6 cation channel causes familial focal segmental glomerulosclerosis. *Science*. 2005;308:1801–1804.
310. Debiec H, Guigonis V, Mougenot B, et al. Antenatal membranous glomerulonephritis due to anti-neuronal endopeptidase antibodies. *N Engl J Med*. 2002;346:2053–2060.
313. Hoxha E, Wiech T, Stahl PR, et al. A mechanism for Cancer-associated membranous nephropathy. *N Engl J Med*. 2016;374:1995–1996.
317. Hoxha E, Thiele I, Zahner G, et al. Phospholipase A2 receptor autoantibodies and clinical outcome in patients with primary membranous nephropathy. *J Am Soc Nephrol*. 2014;25:1357–1366.
326. Kerjaschki D, Schulze M, Binder S, et al. Transcellular transport and membrane insertion of the C5b-9 membrane attack complex of complement by glomerular epithelial cells in experimental membranous nephropathy. *J Immunol*. 1989;143:546–552.
348. Faul C, Donnelly M, Merscher-Gomez S, et al. The actin cytoskeleton of kidney podocytes is a direct target of the antiproteinuric effect of cyclosporine A. *Nat Med*. 2008;14:931–938.
350. Fornoni A, Sageshima J, Wei C, et al. Rituximab targets podocytes in recurrent focal segmental glomerulosclerosis. *Sci Transl Med*. 2011;3:85ra46.
355. Schiffer M, Teng B, Gu C, et al. Pharmacological targeting of actin-dependent dynamin oligomerization ameliorates chronic kidney disease in diverse animal models. *Nat Med*. 2015;21:601–609.

REFERENCES

1. Jefferson JA, Shankland SJ, Pichler RH. Proteinuria in diabetic kidney disease: a mechanistic viewpoint. *Kidney Int.* 2008;74:22–36.
2. Gansevoort RT, Correa-Rotter R, Hemmelgarn BR, et al. Chronic kidney disease and cardiovascular risk: epidemiology, mechanisms, and prevention. *Lancet.* 2013;382:339–352.
3. Schmidt RF, Lang F, Heckmann M. *Physiologie des Menschen*. 31. Auflage. Springer, 2011.
4. Farquhar MG, Palade GE. Glomerular permeability. II. Ferritin transfer across the glomerular capillary wall in nephrotic rats. *J Exp Med.* 1961;114:699–716.
5. Farquhar MG, Wissig SL, Palade GE. Glomerular permeability. I. ferritin transfer across the normal glomerular capillary wall. *J Exp Med.* 1961;113:47–66.
6. Moeller MJ, Tenten V. Renal albumin filtration: alternative models to the standard physical barriers. *Nat Rev Nephrol.* 2013;9:266–277.
7. Russo LM, Sandoval RM, McKee M, et al. The normal kidney filters nephrotic levels of albumin retrieved by proximal tubule cells: retrieval is disrupted in nephrotic states. *Kidney Int.* 2007;71:504–513.
8. Suh JH, Miner JH. The glomerular basement membrane as a barrier to albumin. *Nat Rev Nephrol.* 2013;9:470–477.
9. Schlondorff D, Banas B. The mesangial cell revisited: no cell is an island. *J Am Soc Nephrol.* 2009;20:1179–1187.
10. Abrahamson DR. Structure and development of the glomerular capillary wall and basement membrane. *Am J Physiol.* 1987;253:F783–F794.
11. Simons M, Hartleben B, Huber TB. Podocyte polarity signalling. *Curr Opin Nephrol Hypertens.* 2009;18:324–330.
12. Gagliardini E, Conti S, Benigni A, et al. Imaging of the porous ultrastructure of the glomerular epithelial filtration slit. *J Am Soc Nephrol.* 2010;21:2081–2089.
13. Lennon R, Randles MJ, Humphries MJ. The importance of podocyte adhesion for a healthy glomerulus. *Front Endocrinol (Lausanne).* 2014;5:160.
14. Grahammer F, Wigge C, Schell C, et al. A flexible, multilayered protein scaffold maintains the slit in between glomerular podocytes. *JCI Insight.* 2016;1.
15. Grahammer F, Schell C, Huber TB. The podocyte slit diaphragm—from a thin grey line to a complex signalling hub. *Nat Rev Nephrol.* 2013;9:587–598.
16. Huber TB, Schermer B, Muller RU, et al. Podocin and MEC-2 bind cholesterol to regulate the activity of associated ion channels. *Proc Natl Acad Sci U S A.* 2006;103:17079–17086.
17. Wieder N, Greka A. Calcium, TRPC channels, and regulation of the actin cytoskeleton in podocytes: towards a future of targeted therapies. *Pediatr Nephrol.* 2016;31:1047–1054.
18. Greka A, Mundel P. Cell biology and pathology of podocytes. *Annu Rev Physiol.* 2012;74:299–323.
19. Asanuma K, Yanagida-Asanuma E, Faul C, et al. Synaptopodin orchestrates actin organization and cell motility via regulation of RhoA signalling. *Nat Cell Biol.* 2006;8:485–491.
20. Brahler S, Yu H, Suleiman H, et al. Intravital and kidney slice imaging of podocyte membrane dynamics. *J Am Soc Nephrol.* 2016;27:3285–3290.
21. Endlich N, Simon O, Gopferich A, et al. Two-photon microscopy reveals stationary podocytes in living zebrafish larvae. *J Am Soc Nephrol.* 2014;25:681–686.
22. Kerjaschki D, Sharkey DJ, Farquhar MG. Identification and characterization of podocalyxin—the major sialoprotein of the renal glomerular epithelial cell. *J Cell Biol.* 1984;98:1591–1596.
23. Nielsen JS, McNagny KM. The role of podocalyxin in health and disease. *J Am Soc Nephrol.* 2009;20:1669–1676.
24. Byron A, Randles MJ, Humphries JD, et al. Glomerular cell cross-talk influences composition and assembly of extracellular matrix. *J Am Soc Nephrol.* 2014;25:953–966.
25. Abrahamson DR, Hudson BG, Stroganova L, et al. Cellular origins of type IV collagen networks in developing glomeruli. *J Am Soc Nephrol.* 2009;20:1471–1479.
26. Woolf AS, Gnuti L, Long DA. Roles of angiopoietins in kidney development and disease. *J Am Soc Nephrol.* 2009;20:239–244.
27. Clement LC, Mace C, Avila-Casado C, et al. Circulating angiopoietin-like 4 links proteinuria with hypertriglyceridemia in nephrotic syndrome. *Nat Med.* 2014;20:37–46.
28. Dimke H, Maezawa Y, Quaggia SE. Crosstalk in glomerular injury and repair. *Curr Opin Nephrol Hypertens.* 2015;24:231–238.
29. Takabatake Y, Sugiyama T, Kohara H, et al. The CXCL12 (SDF-1)/CXCR4 axis is essential for the development of renal vasculature. *J Am Soc Nephrol.* 2009;20:1714–1723.
30. Eremina V, Cui S, Gerber H, et al. Vascular endothelial growth factor a signaling in the podocyte-endothelial compartment is required for mesangial cell migration and survival. *J Am Soc Nephrol.* 2006;17:724–735.
31. Sachs N, Sonnenberg A. Cell-matrix adhesion of podocytes in physiology and disease. *Nat Rev Nephrol.* 2013;9:200–210.
32. Scott RP, Quaggia SE. Review series: the cell biology of renal filtration. *J Cell Biol.* 2015;209:199–210.
33. Fissell WH, Hofmann CL, Ferrell N, et al. Solute partitioning and filtration by extracellular matrices. *Am J Physiol Renal Physiol.* 2009;297:F1092–F1100.
34. Huber TB, Schermer B, Benzing T. Podocin organizes ion channel-lipid supercomplexes: implications for mechanosensation at the slit diaphragm. *Nephron Exp Nephrol.* 2007;106:e27–e31.
35. Pullen N, Fornoni A. Drug discovery in focal and segmental glomerulosclerosis. *Kidney Int.* 2016;89:1211–1220.
36. Nirajan T, Bielek B, Gruenwald A, et al. The notch pathway in podocytes plays a role in the development of glomerular disease. *Nat Med.* 2008;14:290–298.
37. Wang D, Dai C, Li Y, et al. Canonical Wnt/beta-catenin signaling mediates transforming growth factor-beta1-driven podocyte injury and proteinuria. *Kidney Int.* 2011;80:1159–1169.
38. Kato H, Gruenwald A, Suh JH, et al. Wnt/beta-catenin pathway in podocytes integrates cell adhesion, differentiation, and survival. *J Biol Chem.* 2011;286:26003–26015.
39. Dai C, Stoltz DB, Kiss LP, et al. Wnt/beta-catenin signaling promotes podocyte dysfunction and albuminuria. *J Am Soc Nephrol.* 2009;20:1997–2008.
40. Shkreli M, Sarin KY, Pech MF, et al. Reversible cell-cycle entry in adult kidney podocytes through regulated control of telomerase and wnt signaling. *Nat Med.* 2011;18:111–119.
41. Grahammer F, Wanner N, Huber TB. mTOR controls kidney epithelia in health and disease. *Nephrol Dial Transplant.* 2014;29(suppl 1):i9–i18.
42. Imasawa T, Rossignol R. Podocyte energy metabolism and glomerular diseases. *Int J Biochem Cell Biol.* 2013;45:2109–2118.
43. Beeken M, Lindenmeyer MT, Blattner SM, et al. Alterations in the ubiquitin proteasome system in persistent but not reversible proteinuric diseases. *J Am Soc Nephrol.* 2014;25:2511–2525.
44. Bierzyńska A, Soderquest K, Koziell A. Genes and podocytes—new insights into mechanisms of podocytopathy. *Front Endocrinol (Lausanne).* 2014;5:226.
45. Kriz W, Shirato I, Nagata M, et al. The podocyte's response to stress: the enigma of foot process effacement. *Am J Physiol Renal Physiol.* 2013;304:F333–F347.
46. George B, Holzman LB. Signaling from the podocyte intercellular junction to the actin cytoskeleton. *Semin Nephrol.* 2012;32:307–318.
47. van den Berg JG, van den Bergh Weerman MA, Assmann KJ, et al. Podocyte foot process effacement is not correlated with the level of proteinuria in human glomerulopathies. *Kidney Int.* 2004;66:1901–1906.
48. Golden MH, Brooks SE, Ramdath DD, et al. Effacement of glomerular foot processes in kwashiorkor. *Lancet.* 1990;336:1472–1474.
49. Kestila M, Lenkkeri U, Mannikko M, et al. Positionally cloned gene for a novel glomerular protein—nephrin—is mutated in congenital nephrotic syndrome. *Mol Cell.* 1998;1:575–582.
50. Boute N, Gribouval O, Roselli S, et al. NPHS2, encoding the glomerular protein podocin, is mutated in autosomal recessive steroid-resistant nephrotic syndrome. *Nat Genet.* 2000;24:349–354.
51. Kaplan JM, Kim SH, North KN, et al. Mutations in ACTN4, encoding alpha-actinin-4, cause familial focal segmental glomerulosclerosis. *Nat Genet.* 2000;24:251–256.
52. Kim JM, Wu H, Green G, et al. CD2-associated protein haploinsufficiency is linked to glomerular disease susceptibility. *Science.* 2003;300:1298–1300.
53. Matejas V, Hinkes B, Alkandari F, et al. Mutations in the human laminin beta2 (LAMB2) gene and the associated phenotypic spectrum. *Hum Mutat.* 2010;31:992–1002.
54. Kambham N, Tanji N, Seigle RL, et al. Congenital focal segmental glomerulosclerosis associated with beta4 integrin mutation and epidermolysis bullosa. *Am J Kidney Dis.* 2000;36:190–196.
55. Pelletier J, Bruening W, Kashtan CE, et al. Germline mutations in the Wilms' tumor suppressor gene are associated with

- abnormal urogenital development in Denys-drash syndrome. *Cell*. 1991;67:437–447.
56. Boyer O, Woerner S, Yang F, et al. LMX1B mutations cause hereditary FSGS without extrarenal involvement. *J Am Soc Nephrol*. 2013;24:1216–1222.
 57. Diomedi-Camassei F, Di Giandomenico S, Santorelli FM, et al. COQ2 nephropathy: a newly described inherited mitochondrialopathy with primary renal involvement. *J Am Soc Nephrol*. 2007;18:2773–2780.
 58. Berkovic SF, Dibbens LM, Oshlack A, et al. Array-based gene discovery with three unrelated subjects shows SCARB2/LIMP-2 deficiency causes myoclonus epilepsy and glomerulosclerosis. *Am J Hum Genet*. 2008;82:673–684.
 59. Marshall CB, Shankland SJ. Cell cycle regulatory proteins in podocyte health and disease. *Nephron Exp Nephrol*. 2007;106:e51–e59.
 60. Nishizono R, Kikuchi M, Wang SQ, et al. FSGS as an adaptive response to growth-induced podocyte stress. *J Am Soc Nephrol*. 2017.
 61. Yang Y, Wang J, Qin L, et al. Rapamycin prevents early steps of the development of diabetic nephropathy in rats. *Am J Nephrol*. 2007;27:495–502.
 62. Fogo AB. The targeted podocyte. *J Clin Invest*. 2011;121:2142–2145.
 63. Huber TB, Walz G, Kuehn EW. mTOR and rapamycin in the kidney: signaling and therapeutic implications beyond immunosuppression. *Kidney Int*. 2011;79:502–511.
 64. Petermann AT, Pippin J, Durvasula R, et al. Mechanical stretch induces podocyte hypertrophy in vitro. *Kidney Int*. 2005;67:157–166.
 65. Ruster C, Bondeva T, Franke S, et al. Advanced glycation end-products induce cell cycle arrest and hypertrophy in podocytes. *Nephrol Dial Transplant*. 2008;23:2179–2191.
 66. Lohmann F, Sachs M, Meyer TN, et al. UCH-L1 induces podocyte hypertrophy in membranous nephropathy by protein accumulation. *Biochim Biophys Acta*. 1842:945–958:2014.
 67. Camici M, Carpi A, Cini G, et al. Podocyte dysfunction in aging-related glomerulosclerosis. *Front Biosci*. 2011;3:995–1006.
 68. Wiggins J. Podocytes and glomerular function with aging. *Semin Nephrol*. 2009;29:587–593.
 69. Wiggins JE, Goyal M, Sanden SK, et al. Podocyte hypertrophy, “adaptation,” and “decompensation” associated with glomerular enlargement and glomerulosclerosis in the aging rat: prevention by calorie restriction. *J Am Soc Nephrol*. 2005;16:2953–2966.
 70. Teiken JM, Audette JL, Laturius DI, et al. Podocyte loss in aging OVE26 diabetic mice. *Anatomical record*. 2008;291:114–121.
 71. Wharram BL, Goyal M, Wiggins JE, et al. Podocyte depletion causes glomerulosclerosis: diphtheria toxin-induced podocyte depletion in rats expressing human diphtheria toxin receptor transgene. *J Am Soc Nephrol*. 2005;16:2941–2952.
 72. Wanner N, Hartleben B, Herbach N, et al. Unraveling the role of podocyte turnover in glomerular aging and injury. *J Am Soc Nephrol*. 2014;25:707–716.
 73. Braun F, Becker JU, Brinkkoetter PT. Live or let die: is there any cell death in podocytes? *Semin Nephrol*. 2016;36:208–219.
 74. Benigni A, Morigi M, Rizzo P, et al. Inhibiting angiotensin-converting enzyme promotes renal repair by limiting progenitor cell proliferation and restoring the glomerular architecture. *Am J Pathol*. 2011;179:628–638.
 75. Meyer-Schwesinger C. The role of renal progenitors in renal regeneration. *Nephron*. 2016;132:101–109.
 76. Romagnani P, Lasagni L, Remuzzi G. Renal progenitors: an evolutionary conserved strategy for kidney regeneration. *Nat Rev Nephrol*. 2013;9:137–146.
 77. Pippin JW, Sparks MA, Glenn ST, et al. Cells of renin lineage are progenitors of podocytes and parietal epithelial cells in experimental glomerular disease. *Am J Pathol*. 2013;183:542–557.
 78. Nakatsue T, Koike H, Han GD, et al. Nephrin and podocin dissociate at the onset of proteinuria in experimental membranous nephropathy. *Kidney Int*. 2005;67:2239–2253.
 79. Schell C, Rogg M, Suhm M, et al. The FERM protein EPB41L5 regulates actomyosin contractility and focal adhesion formation to maintain the kidney filtration barrier. *Proc Natl Acad Sci U S A*. 2017;114:E4621–E4630.
 80. Marshall CB. Rethinking glomerular basement membrane thickening in diabetic nephropathy: adaptive or pathogenic? *Am J Physiol Renal Physiol*. 2016;311:F831–F843.
 81. Eremina V, Sood M, Haigh J, et al. Glomerular-specific alterations of VEGF-A expression lead to distinct congenital and acquired renal diseases. *J Clin Invest*. 2003;111:707–716.
 82. Vaughan MR, Quaggin SE. How do mesangial and endothelial cells form the glomerular tuft? *J Am Soc Nephrol*. 2008;19:24–33.
 83. Floege J, Eitner F, Alpers CE. A new look at platelet-derived growth factor in renal disease. *J Am Soc Nephrol*. 2008;19:12–23.
 84. Quaggin SE, Kreidberg JA. Development of the renal glomerulus: good neighbors and good fences. *Development*. 2008;135:609–620.
 85. Barajas L. Cell-specific protein and gene expression in the juxtaglomerular apparatus. *Clin Exp Pharmacol Physiol*. 1997;24:520–526.
 86. Drenckhahn D, Schnittler H, Nobiling R, et al. Ultrastructural organization of contractile proteins in rat glomerular mesangial cells. *Am J Pathol*. 1990;137:1343–1351.
 87. Kriz W, Elger M, Lemley K, et al. Structure of the glomerular mesangium: a biomechanical interpretation. *Kidney Int Suppl*. 1990;30:S2–S9.
 88. Armulik A, Abramsson A, Betsholtz C. Endothelial/pericyte interactions. *Circ Res*. 2005;97:512–523.
 89. Lu Y, Ye Y, Yang Q, et al. Single-cell RNA-sequence analysis of mouse glomerular mesangial cells uncovers mesangial cell essential genes. *Kidney Int*. 2017.
 90. Leeven P, Pekny M, Gebre-Medhin S, et al. Mice deficient for PDGF B show renal, cardiovascular, and hematological abnormalities. *Genes Dev*. 1994;8:1875–1887.
 91. Soriano P. Abnormal kidney development and hematological disorders in PDGF beta-receptor mutant mice. *Genes Dev*. 1994;8:1888–1896.
 92. Kikkawa Y, Virtanen I, Miner JH. Mesangial cells organize the glomerular capillaries by adhering to the G domain of laminin alpha5 in the glomerular basement membrane. *J Cell Biol*. 2003;161:187–196.
 93. Blantz RC, Gabbai FB, Tucker BJ, et al. Role of mesangial cell in glomerular response to volume and angiotensin II. *Am J Physiol*. 1993;264:F158–F165.
 94. Stockard JD, Sansom SC. Glomerular mesangial cells: electrophysiology and regulation of contraction. *Physiol Rev*. 1998;78:723–744.
 95. Meyer TN, Gloy J, Hug MJ, et al. Hydrogen peroxide increases the intracellular calcium activity in rat mesangial cells in primary culture. *Kidney Int*. 1996;49:388–395.
 96. Floege J, Burg M, Hugo C, et al. Endogenous fibroblast growth factor-2 mediates cytotoxicity in experimental mesangioproliferative glomerulonephritis. *J Am Soc Nephrol*. 1998;9:792–801.
 97. Laping NJ, Olson BA, Ho T, et al. Hepatocyte growth factor: a regulator of extracellular matrix genes in mouse mesangial cells. *Biochem Pharmacol*. 2000;59:847–853.
 98. Schnaper HW, Hayashida T, Hubchak SC, et al. TGF-beta signal transduction and mesangial cell fibrogenesis. *Am J Physiol Renal Physiol*. 2003;284:F243–F252.
 99. Ning L, Kurihara H, de Vega S, et al. Laminin alpha1 regulates age-related mesangial cell proliferation and mesangial matrix accumulation through the TGF-beta pathway. *Am J Pathol*. 2014;184:1683–1694.
 100. Bieritz B, Spessotto P, Colombatti A, et al. Role of alpha8 integrin in mesangial cell adhesion, migration, and proliferation. *Kidney Int*. 2003;64:119–127.
 101. Ostendorf T, Kunter U, Grone HJ, et al. Specific antagonism of PDGF prevents renal scarring in experimental glomerulonephritis. *J Am Soc Nephrol*. 2001;12:909–918.
 102. Eitner F, Ostendorf T, Kretzler M, et al. PDGF-C expression in the developing and normal adult human kidney and in glomerular diseases. *J Am Soc Nephrol*. 2003;14:1145–1153.
 103. Crean JK, Furlong F, Finlay D, et al. Connective tissue growth factor [CTGF]/CCN2 stimulates mesangial cell migration through integrated dissolution of focal adhesion complexes and activation of cell polarization. *FASEB J*. 2004;18:1541–1543.
 104. Margolis BL, Bonventre JV, Kremer SG, et al. Epidermal growth factor is synergistic with phorbol esters and vasopressin in stimulating arachidonate release and prostaglandin production in renal glomerular mesangial cells. *Biochem J*. 1988;249:587–592.
 105. Schlondorff D. The glomerular mesangial cell: an expanding role for a specialized pericyte. *FASEB J*. 1987;1:272–281.
 106. Gomez-Guerrero C, Suzuki Y, Egido J. The identification of IgA receptors in human mesangial cells: in the search for “Eldorado.” *Kidney Int*. 2002;62:715–717.
 107. Cortes-Hernandez J, Fossati-Jimack L, Carugati A, et al. Murine glomerular mesangial cell uptake of apoptotic cells is inefficient and involves serum-mediated but complement-independent mechanisms. *Clin Exp Immunol*. 2002;130:459–466.
 108. Schlondorff D. Roles of the mesangium in glomerular function. *Kidney Int*. 1996;49:1583–1585.

109. Ren Y, Carretero OA, Garvin JL. Role of mesangial cells and gap junctions in tubuloglomerular feedback. *Kidney Int.* 2002;62:525–531.
110. Abboud HE. Mesangial cell biology. *Exp Cell Res.* 2012;318:979–985.
111. Morita T, Churg J. Mesangiolysis. *Kidney Int.* 1983;24:1–9.
112. Hugo C, Shankland SJ, Bowen-Pope DF, et al. Extraglomerular origin of the mesangial cell after injury. A new role of the juxtaglomerular apparatus. *J Clin Invest.* 1997;100:786–794.
113. Watson S, Caihier JF, Hughes J, et al. Apoptosis and glomerulonephritis. *Curr Dir Autoimmun.* 2006;9:188–204.
114. Buhl EM, Djudjaj S, Babickova J, et al. The role of PDGF-D in healthy and fibrotic kidneys. *Kidney Int.* 2016;89:848–861.
115. Mason RM, Wahab NA. Extracellular matrix metabolism in diabetic nephropathy. *J Am Soc Nephrol.* 2003;14:1358–1373.
116. Kriz W, Lowen J, Federico G, et al. Accumulation of worn-out GBM material substantially contributes to mesangial matrix expansion in diabetic nephropathy. *Am J Physiol Renal Physiol.* 2017;312:F1101–F1111.
117. Reznichenko A, Korstanje R. The role of platelet-activating factor in mesangial pathophysiology. *Am J Pathol.* 2015;185:888–896.
118. Ryan GB, Karnovsky MJ. Distribution of endogenous albumin in the rat glomerulus: role of hemodynamic factors in glomerular barrier function. *Kidney Int.* 1976;9:36–45.
119. Hyink DP, Tucker DC, St John PL, et al. Endogenous origin of glomerular endothelial and mesangial cells in grafts of embryonic kidneys. *Am J Physiol.* 1996;270:F886–F899.
120. Woolf AS, Loughna S. Origin of glomerular capillaries: is the verdict in? *Exp Nephrol.* 1998;6:17–21.
121. Deen WM, Lazzara MJ, Myers BD. Structural determinants of glomerular permeability. *Am J Physiol Renal Physiol.* 2001;281:F579–F596.
122. Rostgaard J, Qvortrup K. Sieve plugs in fenestrae of glomerular capillaries—site of the filtration barrier? *Cells Tissues Organs.* 2002;170:132–138.
123. Haraldsson B, Nystrom J. The glomerular endothelium: new insights on function and structure. *Curr Opin Nephrol Hypertens.* 2012;21:258–263.
124. Bevan HS, Slater SC, Clarke H, et al. Acute laminar shear stress reversibly increases human glomerular endothelial cell permeability via activation of endothelial nitric oxide synthase. *Am J Physiol Renal Physiol.* 2011;301:F733–F742.
125. Rostgaard J, Qvortrup K. Electron microscopic demonstrations of filamentous molecular sieve plugs in capillary fenestrae. *Microvasc Res.* 1997;53:1–13.
126. Dane MJ, van den Berg BM, Avramut MC, et al. Glomerular endothelial surface layer acts as a barrier against albumin filtration. *Am J Pathol.* 2013;182:1532–1540.
127. Satchell SC, Tasman CH, Singh A, et al. Conditionally immortalized human glomerular endothelial cells expressing fenestrations in response to VEGF. *Kidney Int.* 2006;69:1633–1640.
128. Abrahamson DR. Role of the podocyte (and glomerular endothelium) in building the GBM. *Semin Nephrol.* 2012;32:342–349.
129. Cosgrove D, Meehan DT, Grunkemeyer JA, et al. Collagen COL4a3 knockout: a mouse model for autosomal alport syndrome. *Genes Dev.* 1996;10:2981–2992.
130. Deen WM. What determines glomerular capillary permeability? *J Clin Invest.* 2004;114:1412–1414.
131. Eremina V, Quaggin SE. The role of VEGF-A in glomerular development and function. *Curr Opin Nephrol Hypertens.* 2004;13:9–15.
132. Friden V, Oveland E, Tenstad O, et al. The glomerular endothelial cell coat is essential for glomerular filtration. *Kidney Int.* 2011;79:1322–1330.
133. Henry CB, Duling BR. Permeation of the luminal capillary glycocalyx is determined by hyaluronan. *Am J Physiol.* 1999;277:H508–H514.
134. Dane MJ, van den Berg BM, Lee DH, et al. A microscopic view on the renal endothelial glycocalyx. *Am J Physiol Renal Physiol.* 2015;308:F956–F966.
135. Chang RL, Deen WM, Robertson CR, et al. Permselectivity of the glomerular capillary wall. III. Restricted transport of polyanions. *Kidney Int.* 1975;8:212–218.
136. Chang RL, Ueki IF, Troy JL, et al. Permselectivity of the glomerular capillary wall to macromolecules. II. Experimental studies in rats using neutral dextran. *Biophys J.* 1975;15:887–906.
137. Chang RS, Robertson CR, Deen WM, et al. Permselectivity of the glomerular capillary wall to macromolecules. I. Theoretical considerations. *Biophys J.* 1975;15:861–886.
138. Jeansson M, Haraldsson B. Glomerular size and charge selectivity in the mouse after exposure to glucosaminoglycan-degrading enzymes. *J Am Soc Nephrol.* 2003;14:1756–1765.
139. Jeansson M, Haraldsson B. Morphological and functional evidence for an important role of the endothelial cell glycocalyx in the glomerular barrier. *Am J Physiol Renal Physiol.* 2006;290:F111–F116.
140. Rabelink TJ, de Boer HC, van Zonneveld AJ. Endothelial activation and circulating markers of endothelial activation in kidney disease. *Nat Rev Nephrol.* 2010;6:404–414.
141. Kang DH, Kanellis J, Hugo C, et al. Role of the microvascular endothelium in progressive renal disease. *J Am Soc Nephrol.* 2002;13:806–816.
142. Segal MS, Baylis C, Johnson RJ. Endothelial health and diversity in the kidney. *J Am Soc Nephrol.* 2006;17:323–324.
143. Iruela-Arispe L, Gordon K, Hugo C, et al. Participation of glomerular endothelial cells in the capillary repair of glomerulonephritis. *Am J Pathol.* 1995;147:1715–1727.
144. Masuda Y, Shimizu A, Mori T, et al. Vascular endothelial growth factor enhances glomerular capillary repair and accelerates resolution of experimentally induced glomerulonephritis. *Am J Pathol.* 2001;159:599–608.
145. Shimizu A, Masuda Y, Mori T, et al. Vascular endothelial growth factor resolves glomerular inflammation and accelerates glomerular capillary repair in rat anti-glomerular basement membrane glomerulonephritis. *J Am Soc Nephrol.* 2004;15:2655–2665.
146. Kuwabara A, Satoh M, Tomita N, et al. Deterioration of glomerular endothelial surface layer induced by oxidative stress is implicated in altered permeability of macromolecules in Zucker fatty rats. *Diabetologia.* 2010;53:2056–2065.
147. Jeansson M, Bjorck K, Tenstad O, et al. Adriamycin alters glomerular endothelium to induce proteinuria. *J Am Soc Nephrol.* 2009;20:114–122.
148. Alm-Eldeen A, Tousson E. Deterioration of glomerular endothelial surface layer and the alteration in the renal function after a growth promoter boldenone injection in rabbits. *Hum Exp Toxicol.* 2012;31:465–472.
149. Norgard-Sumnicht KE, Varki NM, Varki A. Calcium-dependent heparin-like ligands for L-selectin in nonlymphoid endothelial cells. *Science.* 1993;261:480–483.
150. Rops AL, van der Vlag J, Lensen JF, et al. Heparan sulfate proteoglycans in glomerular inflammation. *Kidney Int.* 2004;65:768–785.
151. Rops AL, Loeven MA, van Gemst JJ, et al. Modulation of heparan sulfate in the glomerular endothelial glycocalyx decreases leukocyte influx during experimental glomerulonephritis. *Kidney Int.* 2014;86:932–942.
152. Massena S, Christoffersson G, Hjertstrom E, et al. A chemotactic gradient sequestered on endothelial heparan sulfate induces directional intraluminal crawling of neutrophils. *Blood.* 2010;116:1924–1931.
153. Axelsson J, Xu D, Kang BN, et al. Inactivation of heparan sulfate 2-O-sulfotransferase accentuates neutrophil infiltration during acute inflammation in mice. *Blood.* 2012;120:1742–1751.
154. Bariety J, Mandet C, Hill GS, et al. Parietal podocytes in normal human glomeruli. *J Am Soc Nephrol.* 2006;17:2770–2780.
155. Arakawa M, Tokunaga J. A scanning electron microscope study of the human Bowman's epithelium. *Contrib Nephrol.* 1977;6:73–78.
156. Ohse T, Pippin JW, Chang AM, et al. The enigmatic parietal epithelial cell is finally getting noticed: a review. *Kidney Int.* 2009;76:1225–1238.
157. Webber WA, Wong WT. The function of the basal filaments in the parietal layer of Bowman's capsule. *Can J Physiol Pharmacol.* 1973;51:53–60.
158. Dijkman HB, Weening JJ, Smeets B, et al. Proliferating cells in HIV and pamidronate-associated collapsing focal segmental glomerulosclerosis are parietal epithelial cells. *Kidney Int.* 2006;70:338–344.
159. Guhr SS, Sachs M, Wegner A, et al. The expression of podocyte-specific proteins in parietal epithelial cells is regulated by protein degradation. *Kidney Int.* 2013;84:532–544.
160. Kietzmann L, Guhr SS, Meyer TN, et al. MicroRNA-193a regulates the transdifferentiation of human parietal epithelial cells toward a podocyte phenotype. *J Am Soc Nephrol.* 2015;26:1389–1401.
161. Gebeshuber CA, Kornauth C, Dong L, et al. Focal segmental glomerulosclerosis is induced by microRNA-193a and its downregulation of WT1. *Nat Med.* 2013;19:481–487.
162. Kabgani N, Grigoleit T, Schulte K, et al. Primary cultures of glomerular parietal epithelial cells or podocytes with proven origin. *PLoS ONE.* 2012;7:e34907.

163. Appel D, Kershaw DB, Smeets B, et al. Recruitment of podocytes from glomerular parietal epithelial cells. *J Am Soc Nephrol*. 2009;20:333–343.
164. Mazzinghi B, Romagnani P, Lazzeri E. Biologic modulation in renal regeneration. *Expert Opin Biol Ther*. 2016;16:1403–1415.
165. Miner JH, Patton BL, Lentz SI, et al. The laminin alpha chains: expression, developmental transitions, and chromosomal locations of alpha1-5, identification of heterotrimeric laminins 8-11, and cloning of a novel alpha3 isoform. *J Cell Biol*. 1997;137:685–701.
166. Sorokin LM, Pausch F, Durbeej M, et al. Differential expression of five laminin alpha (1-5) chains in developing and adult mouse kidney. *Dev Dyn*. 1997;210:446–462.
167. Kang JS, Wang XP, Miner JH, et al. Loss of alpha3/alpha4(IV) collagen from the glomerular basement membrane induces a strain-dependent isoform switch to alpha5alpha6(IV) collagen associated with longer renal survival in Col4a3-/ alport mice. *J Am Soc Nephrol*. 2006;17:1962–1969.
168. Ninomiya Y, Kagawa M, Iyama K, et al. Differential expression of two basement membrane collagen genes, COL4A6 and COL4A5, demonstrated by immunofluorescence staining using peptide-specific monoclonal antibodies. *J Cell Biol*. 1995;130:1219–1229.
169. Ohse T, Chang AM, Pippin JW, et al. A new function for parietal epithelial cells: a second glomerular barrier. *Am J Physiol Renal Physiol*. 2009;297:F1566–F1574.
170. Smeets B, Uhlig S, Fuss A, et al. Tracing the origin of glomerular extracapillary lesions from parietal epithelial cells. *J Am Soc Nephrol*. 2009;20:2604–2615.
171. Rizzo P, Perico N, Gagliardini E, et al. Nature and mediators of parietal epithelial cell activation in glomerulonephritides of human and rat. *Am J Pathol*. 2013;183:1769–1778.
172. Zhang J, Pippin JW, Kroft RD, et al. Podocyte repopulation by renal progenitor cells following glucocorticoids treatment in experimental FSGS. *Am J Physiol Renal Physiol*. 2013;304:F1375–F1389.
173. Shankland SJ, Smeets B, Pippin JW, et al. The emergence of the glomerular parietal epithelial cell. *Nat Rev Nephrol*. 2014;10:158–173.
174. Ohse T, Vaughan MR, Kopp JB, et al. De novo expression of podocyte proteins in parietal epithelial cells during experimental glomerular disease. *Am J Physiol Renal Physiol*. 2010;298:F702–F711.
175. Zhang J, Hansen KM, Pippin JW, et al. De novo expression of podocyte proteins in parietal epithelial cells in experimental aging nephropathy. *Am J Physiol Renal Physiol*. 2012;302:F571–F580.
176. Moeller MJ, Smeets B. Role of parietal epithelial cells in kidney injury: the case of rapidly progressing glomerulonephritis and focal and segmental glomerulosclerosis. *Nephron Exp Nephrol*. 2014;126:97.
177. Fujigaki Y, Sun DF, Fujimoto T, et al. Mechanisms and kinetics of Bowman's epithelial-myofibroblast transdifferentiation in the formation of glomerular crescents. *Nephron*. 2002;92:203–212.
178. Le Hir M, Besse-Eschmann V. A novel mechanism of nephron loss in a murine model of crescentic glomerulonephritis. *Kidney Int*. 2003;63:591–599.
179. Drew AF, Tucker HL, Liu H, et al. Crescentic glomerulonephritis is diminished in fibrinogen-deficient mice. *Am J Physiol Renal Physiol*. 2001;281:F1157–F1163.
180. Ryu M, Migliorini A, Miosge N, et al. Plasma leakage through glomerular basement membrane ruptures triggers the proliferation of parietal epithelial cells and crescent formation in non-inflammatory glomerular injury. *J Pathol*. 2012;228:482–494.
181. Sicking EM, Fuss A, Uhlig S, et al. Subtotal ablation of parietal epithelial cells induces crescent formation. *J Am Soc Nephrol*. 2012;23:629–640.
182. Dijkman H, Smeets B, van der Laak J, et al. The parietal epithelial cell is crucially involved in human idiopathic focal segmental glomerulosclerosis. *Kidney Int*. 2005;68:1562–1572.
183. Smeets B, Kuppe C, Sicking EM, et al. Parietal epithelial cells participate in the formation of sclerotic lesions in focal segmental glomerulosclerosis. *J Am Soc Nephrol*. 2011;22:1262–1274.
184. Fatima H, Moeller MJ, Smeets B, et al. Parietal epithelial cell activation marker in early recurrence of FSGS in the transplant. *Clin J Am Soc Nephrol*. 2012;7:1852–1858.
185. Smeets B, Stucker F, Wetzels J, et al. Detection of activated parietal epithelial cells on the glomerular tuft distinguishes early focal segmental glomerulosclerosis from minimal change disease. *Am J Pathol*. 2014;184:3239–3248.
186. Roeder SS, Stefanska A, Eng DG, et al. Changes in glomerular parietal epithelial cells in mouse kidneys with advanced age. *Am J Physiol Renal Physiol*. 2015;309:F164–F178.
187. Wijnhoven TJ, Lensen JF, Rops AL, et al. Aberrant heparan sulfate profile in the human diabetic kidney offers new clues for therapeutic glycomimetics. *Am J Kidney Dis*. 2006;48:250–261.
188. Maezawa Y, Onay T, Scott RP, et al. Loss of the podocyte-expressed transcription factor Tcf21/pod1 results in podocyte differentiation defects and FSGS. *J Am Soc Nephrol*. 2014;25:2459–2470.
189. Kim SI, Lee SY, Wang Z, et al. TGF-beta-activated kinase 1 is crucial in podocyte differentiation and glomerular capillary formation. *J Am Soc Nephrol*. 2014;25:1966–1978.
190. Takahashi T, Takahashi K, Gerety S, et al. Temporally compartmentalized expression of ephrin-B2 during renal glomerular development. *J Am Soc Nephrol*. 2001;12:2673–2682.
191. Jeansson M, Gawlik A, Anderson G, et al. Angiopoietin-1 is essential in mouse vasculature during development and in response to injury. *J Clin Invest*. 2011;121:2278–2289.
192. Daehn I, Casalena G, Zhang T, et al. Endothelial mitochondrial oxidative stress determines podocyte depletion in segmental glomerulosclerosis. *J Clin Invest*. 2014;124:1608–1621.
193. Qi H, Casalena G, Shi S, et al. Glomerular endothelial mitochondrial dysfunction is essential and characteristic of diabetic kidney disease susceptibility. *Diabetes*. 2017;66:763–778.
194. Garsen M, Lenoir O, Rops AL, et al. Endothelin-1 induces proteinuria by heparanase-mediated disruption of the glomerular glycocalyx. *J Am Soc Nephrol*. 2016;27:3545–3551.
195. Davis B, Dei Cas A, Long DA, et al. Podocyte-specific expression of angiopoietin-2 causes proteinuria and apoptosis of glomerular endothelia. *J Am Soc Nephrol*. 2007;18:2320–2329.
196. Hinamoto N, Maeshima Y, Yamasaki H, et al. Exacerbation of diabetic renal alterations in mice lacking vasohibin-1. *PLoS ONE*. 2014;9:e107934.
197. Khan S, Lakhe-Reddy S, McCarty JH, et al. Mesangial cell integrin α8 provides glomerular endothelial cell cytoprotection by sequestering TGF-beta and regulating PECAM-1. *Am J Pathol*. 2011;178:609–620.
198. Kaukinen A, Kuusniemi AM, Lautenschlager I, et al. Glomerular endothelium in kidneys with congenital nephrotic syndrome of the finnish type (NPHS1). *Nephrol Dial Transplant*. 2008;23:1224–1232.
199. Quaggin SE, Schwartz L, Cui S, et al. The basic-helix-loop-helix protein pod1 is critically important for kidney and lung organogenesis. *Development*. 1999;126:5771–5783.
200. Hinkes B, Wiggins RC, Gbadegesin R, et al. Positional cloning uncovers mutations in PLCE1 responsible for a nephrotic syndrome variant that may be reversible. *Nat Genet*. 2006;38:1397–1405.
201. Steenhard BM, Vanacore R, Friedman D, et al. Upregulated expression of integrin alpha1 in mesangial cells and integrin alpha3 and vimentin in podocytes of Col4a3-null (Alport) mice. *PLoS ONE*. 2012;7:e50745.
202. Banas B, Wornle M, Berger T, et al. Roles of SLC/CCL21 and CCR7 in human kidney for mesangial proliferation, migration, apoptosis, and tissue homeostasis. *J Immunol*. 2002;168:4301–4307.
203. Suzuki T, Matsusaka T, Nakayama M, et al. Genetic podocyte lineage reveals progressive podocytopenia with parietal cell hyperplasia in a murine model of cellular/collapsing focal segmental glomerulosclerosis. *Am J Pathol*. 2009;174:1675–1682.
204. Heymann F, Meyer-Schweiger C, Hamilton-Williams EE, et al. Kidney dendritic cell activation is required for progression of renal disease in a mouse model of glomerular injury. *J Clin Invest*. 2009;119:1286–1297.
205. Hogan MC, Johnson KL, Zenka RM, et al. Subfractionation, characterization, and in-depth proteomic analysis of glomerular membrane vesicles in human urine. *Kidney Int*. 2014;85:1225–1237.
206. Prunotto M, Farina A, Lane L, et al. Proteomic analysis of podocyte exosome-enriched fraction from normal human urine. *J Proteomics*. 2013;82:193–229.
207. Le Hir M, Keller C, Eschmann V, et al. Podocyte bridges between the tuft and Bowman's capsule: an early event in experimental crescentic glomerulonephritis. *J Am Soc Nephrol*. 2001;12:2060–2071.
208. Moeller MJ, Soofi A, Hartmann I, et al. Podocytes populate cellular crescents in a murine model of inflammatory glomerulonephritis. *J Am Soc Nephrol*. 2004;15:61–67.
209. Tan H, Yi H, Zhao W, et al. Intraglomerular crosstalk elaborately regulates podocyte injury and repair in diabetic patients: insights from a 3D multiscale modeling study. *Oncotarget*. 2016;7:73130–73146.
210. Bollee G, Flamant M, Schordan S, et al. Epidermal growth factor receptor promotes glomerular injury and renal failure in rapidly progressive crescentic glomerulonephritis. *Nat Med*. 2011;17:1242–1250.

211. Peired A, Angelotti ML, Ronconi E, et al. Proteinuria impairs podocyte regeneration by sequestering retinoic acid. *J Am Soc Nephrol*. 2013;24:1756–1768.
212. Lasagni L, Angelotti ML, Ronconi E, et al. Podocyte regeneration driven by renal progenitors determines glomerular disease remission and can be pharmacologically enhanced. *Stem Cell Reports*. 2015;5:248–263.
213. Moeller MJ, Kuppe C. Glomerular disease: the role of parietal epithelial cells in hyperplastic lesions. *Nat Rev Nephrol*. 2014;10:5–6.
214. Barlai J, Bruneval P, Meyrier A, et al. Podocyte involvement in human immune crescentic glomerulonephritis. *Kidney Int*. 2005;68: 1109–1119.
215. Barlai J, Hill GS, Mandet C, et al. Glomerular epithelial-mesenchymal transdifferentiation in pauci-immune crescentic glomerulonephritis. *Nephrol Dial Transplant*. 2003;18:1777–1784.
216. Mathieson PW. Glomerulonephritis. *Semin Immunopathol*. 2007;29: 315–316.
217. Nangaku M, Couser WG. Mechanisms of immune-deposit formation and the mediation of immune renal injury. *Clin Exp Nephrol*. 2005;9:183–191.
218. Tipping PG, Kitching AR. Glomerulonephritis, Th1 and Th2: what's new? *Clin Exp Immunol*. 2005;142:207–215.
219. Puri TS, Quigg RJ. The many effects of complement C3- and C5-binding proteins in renal injury. *Semin Nephrol*. 2007;27:321–337.
220. Kurts C, Panzer U, Anders HJ, et al. The immune system and kidney disease: basic concepts and clinical implications. *Nat Rev Immunol*. 2013;13:738–753.
221. Vivarelli M, Emma F, Pelle T, et al. Genetic homogeneity but IgG subclass-dependent clinical variability of alloimmune membranous nephropathy with anti-neutral endopeptidase antibodies. *Kidney Int*. 2015;87:602–609.
222. Beck LH Jr, Bonegio RG, Lambeau G, et al. M-type phospholipase A2 receptor as target antigen in idiopathic membranous nephropathy. *N Engl J Med*. 2009;361:11–21.
223. Tomas NM, Beck LH Jr, Meyer-Schweisinger C, et al. Thrombospondin type-1 domain-containing 7A in idiopathic membranous nephropathy. *N Engl J Med*. 2014;371:2277–2287.
224. Hudson BG. The molecular basis of Goodpasture and Alport syndromes: beacons for the discovery of the collagen IV family. *J Am Soc Nephrol*. 2004;15:2514–2527.
225. Hudson BG, Tryggvason K, Sundaramoorthy M, et al. Alport's syndrome, Goodpasture's syndrome, and type IV collagen. *N Engl J Med*. 2003;348:2543–2556.
226. Kalaaji M, Fenton KA, Mortensen ES, et al. Glomerular apoptotic nucleosomes are central target structures for nephritogenic antibodies in human SLE nephritis. *Kidney Int*. 2007;71:664–672.
227. O'Flynn J, Flierman R, van der Pol P, et al. Nucleosomes and c1q bound to glomerular endothelial cells serve as targets for autoantibodies and determine complement activation. *Mol Immunol*. 2011;49:75–83.
228. Lai KN, Tang SC, Schena FP, et al. IgA nephropathy. *Nat Rev Dis Primers*. 2016;2:16001.
229. Debier H, Lefeu F, Kemper MJ, et al. Early-childhood membranous nephropathy due to cationic bovine serum albumin. *N Engl J Med*. 2011;364:2101–2110.
230. Stehman-Breen C, Johnson RJ. Hepatitis C virus-associated glomerulonephritis. *Adv Intern Med*. 1998;43:79–97.
231. Kuusniemi AM, Qvist E, Sun Y, et al. Plasma exchange and retransplantation in recurrent nephrosis of patients with congenital nephrotic syndrome of the Finnish type (NPHS1). *Transplantation*. 2007;83:1316–1323.
232. Wang SX, Ahola H, Palmen T, et al. Recurrence of nephrotic syndrome after transplantation in CNF is due to autoantibodies to nephrin. *Exp Nephrol*. 2001;9:327–331.
233. Tomas NM, Hoxha E, Reimicke AT, et al. Autoantibodies against thrombospondin type 1 domain-containing 7A induce membranous nephropathy. *J Clin Invest*. 2016;126:2519–2532.
234. Xiao H, Heeringa P, Liu Z, et al. The role of neutrophils in the induction of glomerulonephritis by anti-myeloperoxidase antibodies. *Am J Pathol*. 2005;167:39–45.
235. Segerer S, Schlondorff D. Role of chemokines for the localization of leukocyte subsets in the kidney. *Semin Nephrol*. 2007;27: 260–274.
236. De Vries AS, Endlich K, Elger M, et al. The role of selectins in glomerular leukocyte recruitment in rat anti-glomerular basement membrane glomerulonephritis. *J Am Soc Nephrol*. 1999;10:2510–2517.
237. Johnson RJ, Couser WG, Chi EY, et al. New mechanism for glomerular injury. Myeloperoxidase-hydrogen peroxide-halide system. *J Clin Invest*. 1987;79:1379–1387.
238. Westhorpe CL, Bayard JE, O'Sullivan KM, et al. In vivo imaging of inflamed glomeruli reveals dynamics of neutrophil extracellular trap formation in glomerular capillaries. *Am J Pathol*. 2017;187:318–331.
239. Soderberg D, Segelmark M. Neutrophil extracellular traps in ANCA-associated vasculitis. *Front Immunol*. 2016;7:256.
240. Han Y, Ma FY, Tesch GH, et al. Role of macrophages in the fibrotic phase of rat crescentic glomerulonephritis. *Am J Physiol Renal Physiol*. 2013;304:F1043–F1053.
241. Ooi JD, Kitching AR, Holdsworth SR. Review: T helper 17 cells: their role in glomerulonephritis. *Nephrology (Carlton)*. 2010;15:513–521.
242. Paust HJ, Turner JE, Steinmetz OM, et al. The IL-23/th17 axis contributes to renal injury in experimental glomerulonephritis. *J Am Soc Nephrol*. 2009;20:969–979.
243. Hunemorder S, Treder J, Ahrens S, et al. TH1 and TH17 cells promote crescent formation in experimental autoimmune glomerulonephritis. *J Pathol*. 2015;237:62–71.
244. Disteldorf EM, Krebs CF, Paust HJ, et al. CXCL5 drives neutrophil recruitment in TH17-mediated GN. *J Am Soc Nephrol*. 2015;26:55–66.
245. Turner JE, Paust HJ, Steinmetz OM, et al. The Th17 immune response in renal inflammation. *Kidney Int*. 2010;77:1070–1075.
246. Krebs CF, Paust HJ, Krohn S, et al. Autoimmune renal disease is exacerbated by SIP-receptor-1-dependent intestinal Th17 cell migration to the kidney. *Immunity*. 2016;45:1078–1092.
247. Devi S, Kuligowski MP, Kwan RY, et al. Platelet recruitment to the inflamed glomerulus occurs via an alphaIIbbeta3/GPVI-dependent pathway. *Am J Pathol*. 2010;177:1131–1142.
248. Perico N, Remuzzi G. Role of platelet-activating factor in renal immune injury and proteinuria. *Am J Nephrol*. 1990;10(suppl 1): 98–104.
249. Barnes JL, Levine SP, Venkatachalam MA. Binding of platelet factor four (PF 4) to glomerular polyanion. *Kidney Int*. 1984;25:759–765.
250. Camussi G, Tetta C, Coda R, et al. Platelet-activating factor-induced loss of glomerular anionic charges. *Kidney Int*. 1984;25:73–81.
251. Johnson RJ, Raines EW, Floege J, et al. Inhibition of mesangial cell proliferation and matrix expansion in glomerulonephritis in the rat by antibody to platelet-derived growth factor. *J Exp Med*. 1992;175:1413–1416.
252. Wang TN, Chen X, Li R, et al. SREBP-1 mediates angiotensin II-induced TGF-beta1 upregulation and glomerular fibrosis. *J Am Soc Nephrol*. 2015;26:1839–1854.
253. Kruger T, Benke D, Eitner F, et al. Identification and functional characterization of dendritic cells in the healthy murine kidney and in experimental glomerulonephritis. *J Am Soc Nephrol*. 2004;15:613–621.
254. Lukacs-Kornek V, Burgdorf S, Diehl L, et al. The kidney-renal lymph node-system contributes to cross-tolerance against innocuous circulating antigen. *J Immunol*. 2008;180:706–715.
255. Gottschalk C, Damuzzo V, Gotto J, et al. Batf3-dependent dendritic cells in the renal lymph node induce tolerance against circulating antigens. *J Am Soc Nephrol*. 2013;24:543–549.
256. Ruseva MM, Vernon KA, Lesher AM, et al. Loss of properdin exacerbates C3 glomerulopathy resulting from factor H deficiency. *J Am Soc Nephrol*. 2013;24:43–52.
257. Gale DP, de Jorge EG, Cook HT, et al. Identification of a mutation in complement factor H-related protein 5 in patients of cyprriot origin with glomerulonephritis. *Lancet*. 2010;376:794–801.
258. Couser WG. Basic and translational concepts of immune-mediated glomerular diseases. *J Am Soc Nephrol*. 2012;23:381–399.
259. Henique C, Papista C, Guyonnet L, et al. Update on crescentic glomerulonephritis. *Semin Immunopathol*. 2014;36:479–490.
260. Ding WY, Koziell A, McCarthy HJ, et al. Initial steroid sensitivity in children with steroid-resistant nephrotic syndrome predicts post-transplant recurrence. *J Am Soc Nephrol*. 2014;25:1342–1348.
261. Fogo AB. Causes and pathogenesis of focal segmental glomerulosclerosis. *Nat Rev Nephrol*. 2015;11:76–87.
262. D'Agati VD. Pathobiology of focal segmental glomerulosclerosis: new developments. *Curr Opin Nephrol Hypertens*. 2012;21:243–250.
263. Coward RJ, Foster RR, Patton D, et al. Nephrotic plasma alters slit diaphragm-dependent signaling and translocates nephrin, podocin, and CD2 associated protein in cultured human podocytes. *J Am Soc Nephrol*. 2005;16:629–637.
264. Cheung PK, Klok PA, Bakker WW. Minimal change-like glomerular alterations induced by a human plasma factor. *Nephron*. 1996;74:586–593.

265. Maas RJ, Deegens JK, Wetzels JF. Permeability factors in idiopathic nephrotic syndrome: historical perspectives and lessons for the future. *Nephrol Dial Transplant*. 2014;29:2207–2216.
266. Bitzan M, Babayeva S, Vasudevan A, et al. TNFalpha pathway blockade ameliorates toxic effects of FSGS plasma on podocyte cytoskeleton and beta3 integrin activation. *Pediatr Nephrol*. 2012;27: 2217–2226.
267. Bakr A, Shokeir M, El-Chenawi F, et al. Tumor necrosis factor-alpha production from mononuclear cells in nephrotic syndrome. *Pediatr Nephrol*. 2003;18:516–520.
268. Bakker WW, van Dael CM, Pierik LJ, et al. Altered activity of plasma hemopexin in patients with minimal change disease in relapse. *Pediatr Nephrol*. 2005;20:1410–1415.
269. Lennon R, Singh A, Welsh GI, et al. Hemopexin induces nephrin-dependent reorganization of the actin cytoskeleton in podocytes. *J Am Soc Nephrol*. 2008;19:2140–2149.
270. Wei C, El Hindi S, Li J, et al. Circulating urokinase receptor as a cause of focal segmental glomerulosclerosis. *Nat Med*. 2011;17: 952–960.
271. Davin JC. The glomerular permeability factors in idiopathic nephrotic syndrome. *Pediatr Nephrol*. 2016;31:207–215.
272. Sinha A, Bajpai J, Saini S, et al. Serum-soluble urokinase receptor levels do not distinguish focal segmental glomerulosclerosis from other causes of nephrotic syndrome in children. *Kidney Int*. 2014;85:649–658.
273. Wada T, Nangaku M, Maruyama S, et al. A multicenter cross-sectional study of circulating soluble urokinase receptor in Japanese patients with glomerular disease. *Kidney Int*. 2014;85:641–648.
274. Cara-Fuentes G, Johnson RJ, Reiser J, et al. CD80 and suPAR in patients with minimal change disease and focal segmental glomerulosclerosis: diagnostic and pathogenic significance: response. *Pediatr Nephrol*. 2014;29:1467–1468.
275. Harita Y, Ishizuka K, Tanego A, et al. Decreased glomerular filtration as the primary factor of elevated circulating suPAR levels in focal segmental glomerulosclerosis. *Pediatr Nephrol*. 2014;29: 1553–1560.
276. Meijers B, Maas RJ, Sprangers B, et al. The soluble urokinase receptor is not a clinical marker for focal segmental glomerulosclerosis. *Kidney Int*. 2014;85:636–640.
277. McCarthy ET, Sharma M, Savin VJ. Circulating permeability factors in idiopathic nephrotic syndrome and focal segmental glomerulosclerosis. *Clin J Am Soc Nephrol*. 2010;5:2115–2121.
278. Iijima K, Sako M, Nozu K, et al. Rituximab for childhood-onset, complicated, frequently relapsing nephrotic syndrome or steroid-dependent nephrotic syndrome: a multicentre, double-blind, randomised, placebo-controlled trial. *Lancet*. 2014;384:1273–1281.
279. Bruchfeld A, Benedek S, Hilderman M, et al. Rituximab for minimal change disease in adults: long-term follow-up. *Nephrol Dial Transplant*. 2014;29:851–856.
280. Gbadegesin RA, Adeyemo A, Webb NJ, et al. HLA-DQ α 1 and PLCG2 are candidate risk loci for childhood-onset steroid-sensitive nephrotic syndrome. *J Am Soc Nephrol*. 2015;26:1701–1710.
281. Shalhoub RJ. Pathogenesis of lipid nephrosis: a disorder of T-cell function. *Lancet*. 1974;2:556–560.
282. Sellier-Leclerc AL, Duval A, Riveron S, et al. A humanized mouse model of idiopathic nephrotic syndrome suggests a pathogenic role for immature cells. *J Am Soc Nephrol*. 2007;18:2732–2739.
283. Maruyama K, Tomizawa S, Shimabukuro N, et al. Effect of supernatants derived from T lymphocyte culture in minimal change nephrotic syndrome on rat kidney capillaries. *Nephron*. 1989;51: 73–76.
284. Kobayashi Y, Aizawa A, Takizawa T, et al. DNA methylation changes between relapse and remission of minimal change nephrotic syndrome. *Pediatr Nephrol*. 2012;27:2233–2241.
285. Liu LL, Qin Y, Cai JF, et al. Th17/treg imbalance in adult patients with minimal change nephrotic syndrome. *Clin Immunol*. 2011;139:314–320.
286. Yap HK, Cheung W, Murugasu B, et al. Th1 and Th2 cytokine mRNA profiles in childhood nephrotic syndrome: evidence for increased IL-13 mRNA expression in relapse. *J Am Soc Nephrol*. 1999;10:529–537.
287. Lai KW, Wei CL, Tan LK, et al. Overexpression of interleukin-13 induces minimal-change-like nephropathy in rats. *J Am Soc Nephrol*. 2007;18:1476–1485.
288. Yu CC, Fornoni A, Weins A, et al. Abatacept in B7-1-positive proteinuric kidney disease. *N Engl J Med*. 2013;369:2416–2423.
289. Delville M, Baye E, Durrbach A, et al. B7-1 blockade does not improve Post-transplant nephrotic syndrome caused by recurrent FSGS. *J Am Soc Nephrol*. 2016;27:2520–2527.
290. Kristensen T, Ivarsen P, Povlsen JV. Unsuccessful treatment with abatacept in recurrent focal segmental glomerulosclerosis after kidney transplantation. *Case Rep Nephrol Dial*. 2017;7:1–5.
291. Garin EH, Reiser J, Cara-Fuentes G, et al. Case series: CTLA4-IgG1 therapy in minimal change disease and focal segmental glomerulosclerosis. *Pediatr Nephrol*. 2015;30:469–477.
292. Reiser J, von Gersdorff G, Loos M, et al. Induction of B7-1 in podocytes is associated with nephrotic syndrome. *J Clin Invest*. 2004;113:1390–1397.
293. Clement LC, Avila-Casado C, Mace C, et al. Podocyte-secreted angiopoietin-like-4 mediates proteinuria in glucocorticoid-sensitive nephrotic syndrome. *Nat Med*. 2011;17:117–122.
294. Cara-Fuentes G, Segarra A, Silva-Sanchez C, et al. Angiopoietin-like-4 and minimal change disease. *PLoS ONE*. 2017;12:e0176198.
295. Novelli R, Gagliardini E, Ruggiero B, et al. Any value of podocyte B7-1 as a biomarker in human MCD and FSGS? *Am J Physiol Renal Physiol*. 2016;310:F335–F341.
296. Gee HY, Ashraf S, Wan X, et al. Mutations in EMP2 cause childhood-onset nephrotic syndrome. *Am J Hum Genet*. 2014;94:884–890.
297. Schmid H, Henger A, Cohen CD, et al. Gene expression profiles of podocyte-associated molecules as diagnostic markers in acquired proteinuric diseases. *J Am Soc Nephrol*. 2003;14:2958–2966.
298. Hingorani SR, Finn LS, Kowalewska J, et al. Expression of nephrin in acquired forms of nephrotic syndrome in childhood. *Pediatr Nephrol*. 2004;19:300–305.
299. Jeampierre C, Denamur E, Henry I, et al. Identification of constitutional WT1 mutations, in patients with isolated diffuse mesangial sclerosis, and analysis of genotype/phenotype correlations by use of a computerized mutation database. *Am J Hum Genet*. 1998;62: 824–833.
300. Shih NY, Li J, Karpitskii V, et al. Congenital nephrotic syndrome in mice lacking CD2-associated protein. *Science*. 1999;286:312–315.
301. Winn MP, Conlon PJ, Lynn KL, et al. A mutation in the TRPC6 cation channel causes familial focal segmental glomerulosclerosis. *Science*. 2005;308:1801–1804.
302. Bierzyńska A, Soderquest K, Dean P, et al. NephroS, tUKsoNS: MAGI2 mutations cause congenital nephrotic syndrome. *J Am Soc Nephrol*. 2016.
303. Gee HY, Saisawat P, Ashraf S, et al. ARHGDIA mutations cause nephrotic syndrome via defective RHO GTPase signaling. *J Clin Invest*. 2013;123:3243–3253.
304. Gee HY, Zhang F, Ashraf S, et al. KANK deficiency leads to podocyte dysfunction and nephrotic syndrome. *J Clin Invest*. 2015;125: 2375–2384.
305. Genovese G, Friedman DJ, Pollak MR. APOL1 variants and kidney disease in people of recent African ancestry. *Nat Rev Nephrol*. 2013;9:240–244.
306. Tzur S, Rosset S, Shemer R, et al. Missense mutations in the APOL1 gene are highly associated with end stage kidney disease risk previously attributed to the MYH9 gene. *Hum Genet*. 2010;128: 345–350.
307. Beckerman P, Bi-Karchin J, Park AS, et al. Susztak, K: transgenic expression of human APOL1 risk variants in podocytes induces kidney disease in mice. *Nat Med*. 2017;23:429–438.
308. Chang JW, Pardo V, Sageshima J, et al. Podocyte foot process effacement in postreperfusion allograft biopsies correlates with early recurrence of proteinuria in focal segmental glomerulosclerosis. *Transplantation*. 2012;93:1238–1244.
309. Wu J, Zheng C, Fan Y, et al. Downregulation of microRNA-30 facilitates podocyte injury and is prevented by glucocorticoids. *J Am Soc Nephrol*. 2014;25:92–104.
310. Debiec H, Guigonis V, Mougenot B, et al. Antenatal membranous glomerulonephritis due to anti-neutral endopeptidase antibodies. *N Engl J Med*. 2002;346:2053–2060.
311. Stanescu HC, Arcos-Burgos M, Medlar A, et al. Risk HLA-DQ α 1 and PLA(2)r1 alleles in idiopathic membranous nephropathy. *N Engl J Med*. 2011;364:616–626.
312. Hoxha E, Beck LH Jr, Wiech T, et al. An indirect immunofluorescence method facilitates detection of thrombospondin type 1 domain-containing 7A-specific antibodies in membranous nephropathy. *J Am Soc Nephrol*. 2017;28:520–531.
313. Hoxha E, Wiech T, Stahl PR, et al. A mechanism for cancer-associated membranous nephropathy. *N Engl J Med*. 2016;374:1995–1996.

314. Stahl R, Hoxha E, Fechner K. PLA2R autoantibodies and recurrent membranous nephropathy after transplantation. *N Engl J Med.* 2010;363:496–498.
315. Seitz-Polski B, Payre C, Ambrosetti D, et al. Prediction of membranous nephropathy recurrence after transplantation by monitoring of anti-PLA2R1 (m-type phospholipase A2 receptor) autoantibodies: a case series of 15 patients. *Nephrol Dial Transplant.* 2014;29:2334–2342.
316. Hoxha E, Harendza S, Pinnschmidt H, et al. PLA2R antibody levels and clinical outcome in patients with membranous nephropathy and non-nephrotic range proteinuria under treatment with inhibitors of the renin-angiotensin system. *PLoS ONE.* 2014;9:e110681.
317. Hoxha E, Thiele I, Zahner G, et al. Phospholipase A2 receptor autoantibodies and clinical outcome in patients with primary membranous nephropathy. *J Am Soc Nephrol.* 2014;25:1357–1366.
318. Hoxha E, Harendza S, Pinnschmidt H, et al. M-type phospholipase A2 receptor autoantibodies and renal function in patients with primary membranous nephropathy. *Clin J Am Soc Nephrol.* 2014;9:1883–1890.
319. Kanigherla D, Gummadova J, McKenzie EA, et al. Anti-PLA2R antibodies measured by ELISA predict long-term outcome in a prevalent population of patients with idiopathic membranous nephropathy. *Kidney Int.* 2013;83:940–948.
320. Meyer-Schweisinger C, Lambeau G, Stahl RA. Thrombospondin type-1 domain-containing 7A in idiopathic membranous nephropathy. *N Engl J Med.* 2015;372:1074–1075.
321. Godel M, Grahammer F, Huber TB. Thrombospondin type-1 domain-containing 7A in idiopathic membranous nephropathy. *N Engl J Med.* 2015;372:1073.
322. Tomas NM, Meyer-Schweisinger C, von Spiegel H, et al. A heterologous model of thrombospondin type 1 domain-containing 7A-associated membranous nephropathy. *J Am Soc Nephrol.* 2017.
323. Spicer ST, Tran GT, Killingsworth MC, et al. Induction of passive heymann nephritis in complement component 6-deficient PVG rats. *J Immunol.* 2007;179:172–178.
324. Leenaerts PL, Hall BM, Van Damme BJ, et al. Active Heymann nephritis in complement component C6-deficient rats. *Kidney Int.* 1995;47:1604–1614.
325. Ronco P, Debiec H. Pathophysiological advances in membranous nephropathy: time for a shift in patient's care. *Lancet.* 2015;385:1983–1992.
326. Kerjaschki D, Schulze M, Binder S, et al. Transcellular transport and membrane insertion of the C5b-9 membrane attack complex of complement by glomerular epithelial cells in experimental membranous nephropathy. *J Immunol.* 1989;143:546–552.
327. Schulze M, Donadio JV Jr, Pruchno CJ, et al. Elevated urinary excretion of the C5b-9 complex in membranous nephropathy. *Kidney Int.* 1991;40:533–538.
328. Cybulsky AV. Membranous nephropathy. *Contrib Nephrol.* 2011;169:107–125.
329. Kitzler TM, Papillon J, Guillemette J, et al. Complement modulates the function of the ubiquitin-proteasome system and endoplasmic reticulum-associated degradation in glomerular epithelial cells. *Biochim Biophys Acta.* 2012;1823:1007–1016.
330. Ruggenenti P, Pertuccci E, Cravedi P, et al. Role of remission clinics in the longitudinal treatment of CKD. *J Am Soc Nephrol.* 2008;19:1213–1224.
331. Yamazaki M, Fukusumi Y, Kayaba M, et al. Possible role for glomerular-derived angiotensinogen in nephrotic syndrome. *J Renin Angiotensin Aldosterone Syst.* 2016;17(4).
332. Wennmann DO, Hsu HH, Pavenstadt H. The renin-angiotensin-aldosterone system in podocytes. *Semin Nephrol.* 2012;32:377–384.
333. Hayashi K, Sasamura H, Nakamura M, et al. Renin-angiotensin blockade resets podocyte epigenome through Kruppel-like factor 4 and attenuates proteinuria. *Kidney Int.* 2015;88:745–753.
334. Ilatovskaya DV, Palygin O, Levchenko V, et al. The role of angiotensin II in glomerular volume dynamics and podocyte calcium handling. *Sci Rep.* 2017;7:299.
335. Tian D, Jacobo SM, Billing D, et al. Antagonistic regulation of actin dynamics and cell motility by TRPC5 and TRPC6 channels. *Sci Signal.* 2010;3:ra77.
336. Campbell KN, Raji L, Mundel P. Role of angiotensin II in the development of nephropathy and podocytopathy of diabetes. *Curr Diabetes Rev.* 2011;7:3–7.
337. Guess A, Agrawal S, Wei CC, et al. Dose- and time-dependent glucocorticoid receptor signaling in podocytes. *Am J Physiol Renal Physiol.* 2010;299:F845–F853.
338. Ransom RF, Lam NG, Hallett MA, et al. Glucocorticoids protect and enhance recovery of cultured murine podocytes via actin filament stabilization. *Kidney Int.* 2005;68:2473–2483.
339. Xing CY, Saleem MA, Coward RJ, et al. Direct effects of dexamethasone on human podocytes. *Kidney Int.* 2006;70:1038–1045.
340. Wada T, Pippin JW, Marshall CB, et al. Dexamethasone prevents podocyte apoptosis induced by puromycin aminonucleoside: role of p53 and Bcl-2-related family proteins. *J Am Soc Nephrol.* 2005;16:2615–2625.
341. Mallipattu SK, Guo Y, Revelo MP, et al. Kruppel-like factor 15 mediates glucocorticoid-induced restoration of podocyte differentiation markers. *J Am Soc Nephrol.* 2017;28:166–184.
342. Fujii Y, Khoshnoodi J, Takenaka H, et al. The effect of dexamethasone on defective nephrin transport caused by ER stress: a potential mechanism for the therapeutic action of glucocorticoids in the acquired glomerular diseases. *Kidney Int.* 2006;69:1350–1359.
343. Ohashi T, Uchida K, Uchida S, et al. Dexamethasone increases the phosphorylation of nephrin in cultured podocytes. *Clin Exp Nephrol.* 2011;15:688–693.
344. Uchida K, Suzuki K, Iwamoto M, et al. Decreased tyrosine phosphorylation of nephrin in rat and human nephrosis. *Kidney Int.* 2008;73:926–932.
345. Nijenhuis T, Sloan AJ, Hoenderop JG, et al. Angiotensin II contributes to podocyte injury by increasing TRPC6 expression via an NFAT-mediated positive feedback signaling pathway. *Am J Pathol.* 2011;179:1719–1732.
346. Wang Y, Jarad G, Tripathi P, et al. Activation of NFAT signaling in podocytes causes glomerulosclerosis. *J Am Soc Nephrol.* 2010;21:1657–1666.
347. Schlendorff J, Del Camino D, Carrasquillo R, et al. TRPC6 mutations associated with focal segmental glomerulosclerosis cause constitutive activation of NFAT-dependent transcription. *Am J Physiol Cell Physiol.* 2009;296:C558–C569.
348. Faul C, Donnelly M, Merscher-Gomez S, et al. The actin cytoskeleton of kidney podocytes is a direct target of the antiproteinuric effect of cyclosporine A. *Nat Med.* 2008;14:931–938.
349. Konigshausen E, Sellin L. Recent treatment advances and new trials in adult nephrotic syndrome. *Biomed Res Int.* 2017;2017:7689254.
350. Fornoni A, Sageshima J, Wei C, et al. Rituximab targets podocytes in recurrent focal segmental glomerulosclerosis. *Sci Transl Med.* 2011;3:85ra46.
351. Muller-Deile J, Schiffer M. Podocyte directed therapy of nephrotic syndrome—can we bring the inside out? *Pediatr Nephrol.* 2016;31:393–405.
352. Tian X, Ishibe S. Targeting the podocyte cytoskeleton: from pathogenesis to therapy in proteinuric kidney disease. *Nephrol Dial Transplant.* 2016;31:1577–1583.
353. Ma H, Togawa A, Soda K, et al. Inhibition of podocyte FAK protects against proteinuria and foot process effacement. *J Am Soc Nephrol.* 2010;21:1145–1156.
354. Kang YS, Li Y, Dai C, et al. Inhibition of integrin-linked kinase blocks podocyte epithelial-mesenchymal transition and ameliorates proteinuria. *Kidney Int.* 2010;78:363–373.
355. Schiffer M, Teng B, Gu C, et al. Pharmacological targeting of actin-dependent dynamin oligomerization ameliorates chronic kidney disease in diverse animal models. *Nat Med.* 2015;21:601–609.
356. Vogelbacher R, Wittmann S, Braun A, et al. The mTOR inhibitor everolimus induces proteinuria and renal deterioration in the remnant kidney model in the rat. *Transplantation.* 2007;84:1492–1499.
357. Letavernier E, Legendre C. mToR inhibitors-induced proteinuria: mechanisms, significance, and management. *Transplant Rev (Orlando).* 2008;22:125–130.
358. Sandhu S, Wiebe N, Fried LF, et al. Statins for improving renal outcomes: a meta-analysis. *J Am Soc Nephrol.* 2006;17:2006–2016.
359. Douglas K, O'Malley PG, Jackson JL. Meta-analysis: the effect of statins on albuminuria. *Ann Intern Med.* 2006;145:117–124.
360. Yang HC, Ma LJ, Ma J, et al. Peroxisome proliferator-activated receptor-gamma agonist is protective in podocyte injury-associated sclerosis. *Kidney Int.* 2006;69:1756–1764.
361. Liu HF, Guo LQ, Huang YY, et al. Thiazolidinedione attenuate proteinuria and glomerulosclerosis in Adriamycin-induced nephropathy rats via slit diaphragm protection. *Nephrology (Carlton).* 2010;15:75–83.
362. Yuan Y, Huang S, Wang W, et al. Activation of peroxisome proliferator-activated receptor-gamma coactivator 1alpha ameliorates

132.e8 SECTION I – NORMAL STRUCTURE AND FUNCTION

- mitochondrial dysfunction and protects podocytes from aldosterone-induced injury. *Kidney Int.* 2012;82:771–789.
363. Kanjanabuch T, Ma IJ, Chen J, et al. PPAR-gamma agonist protects podocytes from injury. *Kidney Int.* 2007;71:1232–1239.
364. Li Z, Zhang Y, Ying Ma J, et al. Recombinant vascular endothelial growth factor 121 attenuates hypertension and improves kidney damage in a rat model of preeclampsia. *Hypertension.* 2007;50:686–692.
365. Huber TB, Edelstein CL, Hartleben B, et al. Emerging role of autophagy in kidney function, diseases and aging. *Autophagy.* 2012;8:1009–1031.

BOARD REVIEW QUESTIONS

1. Which glomerular structure is not involved in regulating glomerular filtration?
 - a. Glomerular endothelial cells
 - b. Parietal epithelial cells
 - c. Podocytes
 - d. Mesangial cells
 - e. Glomerular basement membrane

Answer: b

Rationale: Glomerular filtration is regulated by the coordinate interaction of glomerular endothelial cells, podocytes, and mesangial cells. Podocytes and glomerular endothelial cells comprise the glomerular filtration barrier. Together, both cells allow for a size- and charge-selective glomerular filtration due to their specialized three-dimensional structure, extensive glycocalyx coating, and synthesis of the unique glomerular basement membrane. Mesangial cells regulate glomerular filtration by means of contraction and release of vasoactive substances and maintain the health of glomerular endothelial cells. Parietal epithelial cells built the Bowman's capsule to prevent leakage of the primary urine to the tubulointerstitium and are not primarily involved in glomerular filtration. They can, however, contribute to glomerular scarring and are thought to constitute a potential reservoir for podocytes in development, maturation, and eventually in adulthood.

2. A 26-year-old female patient presents with swollen legs for the past week. She has been using ibuprofen 800 mg 3× a day for 1 month for a shoulder injury. Her examination is significant for a blood pressure of 130/90 mm Hg and 3+ lower extremity edema. Urinalysis: exhibits 4+ protein, no blood, 24-h urine protein: 10.8 g, no hematuria, Serum creatinine 0.9 mg/dL (eGFR >60 mL/min).

What is the most likely glomerular location causing this clinical picture?

- a. Mesangial cells (i.e., IgA nephritis)
- b. Glomerular basement membrane (i.e., Alport syndrome)
- c. Glomerular endothelial cell (i.e., eclampsia)
- d. Parietal epithelial cell (i.e., rapid progressive glomerulonephritis)
- e. Podocyte (i.e., minimal change disease)

Answer: e

Rationale: The predominant symptom of massive proteinuria without hematuria in the setting of preserved renal function is characteristic of primary podocyte injury such as in minimal change disease. In this case, minimal change disease might be a result of the use of nonsteroidal antiinflammatory drugs. Mesangial cell, glomerular basement membrane, and glomerular endothelial cell involvement usually presents with mild to strong hematuria with characteristic dysmorphic erythrocytes. Parietal epithelial cell involvement is reflected by the formation of glomerular scars.

3. Which of the following are podocyte antigens in adult membranous nephropathy?
 - a. suPAR
 - b. Neutral endopeptidase (NEP)
 - c. Phospholipase A2 receptor (PLA₂R1)
 - d. Nephrin
 - e. Thrombospondin type-1 domain-containing 7A (THSD7A)

Answers: c and d

Rationale: NEP, PLA₂R, and THSD7A are all podocyte antigens associated with membranous nephropathy, however, NEP is only found in rare cases of antenatal membranous nephropathy caused by alloimmunization due to vertical transfer of antibodies from a genetically NEP-deficient mother. Autoantibodies to PLA₂R1 and THSD7A are typically found in adult membranous nephropathy. PLA₂R1 is highly specific for membranous nephropathy and is found in 70% of patients with membranous nephropathy and is associated with disease activity. Autoantibodies to THSD7A are found in 5% of patients with membranous nephropathy and are strongly associated with the tumors.

Metabolic Basis of Solute Transport

Prabhleen Singh | Scott Culver Thomson | Alicia Ann McDonough

CHAPTER OUTLINE

| |
|--|
| THERMODYNAMIC APPROACH TO METABOLISM AND TRANSPORT, 133 |
| ENERGY AND THE SODIUM PUMP, 134 |
| CELL POLARITY AND VECTORIAL TRANSPORT, 136 |
| METABOLIC SUBSTRATES FUELING ACTIVE TRANSPORT ALONG THE NEPHRON, 137 |

| |
|---|
| NEPHRON-REGION-SPECIFIC METABOLIC CONSIDERATIONS, 143 |
| CONTROL OF RENAL OXYGENATION, 145 |
| RENAL OXYGENATION AND METABOLISM DURING NORMAL PERTURBATIONS AND DISEASE, 149 |
| SUMMARY, 155 |

Metabolism refers to the entire set of interconnected chemical reactions within living organisms that form and maintain tissue and govern the storage and release of energy in order to sustain life. This chapter is dedicated to one aspect of kidney metabolism—namely, the storage, release, and utilization of energy by the nephron as it transforms the glomerular filtrate into urine.

How much energy is required to make the urine? Of the major body organs, the kidney consumes the second highest amount of oxygen per gram of tissue (2.7 mmol/kg/min vs. 4.3 mmol/kg/min for the heart).¹ Most of the potential energy provided by renal oxidative metabolism is committed to epithelial transport, which determines the volume and composition of the urine. It has been asserted that, because the kidney reabsorbs 99% of the glomerular filtrate, it must use a lot of energy. But this logic is incorrect. The minimum net energy required for reabsorption does not depend on the amount of fluid that is reabsorbed. Forming a volume of urine with a solute composition equal to that of the body fluid from which it is formed is the thermodynamic equivalent of partitioning a bucket into two compartments by the use of a divider, which requires no net energy. On the other hand, energy is required to form a urine that differs in solute composition from that of the body fluids (i.e., plasma). To appreciate this, consider that the hypothetical remixing of urine with plasma would cause the formation of entropy, known as mixing entropy. Thus, energy is required to form urine from plasma and attain a state of reduced entropy. The minimum amount of energy required for this is equal to the temperature multiplied by the decrease in mixing entropy associated with the differential solute composition of urine versus plasma.

This chapter provides an overview of the interdependence of renal solute transport and renal metabolism, including (1) the role of the sodium pump, Na⁺-K⁺-adenosine triphosphatase (ATPase), in epithelial transport; (2) the metabolic substrates

fueling active transport along the nephron and regional metabolic considerations; (3) the role of renal blood flow, the glomerular filtration rate (GFR), and tubuloglomerular feedback in controlling fluid and electrolyte filtration and tissue oxygenation; (4) the amount of oxygen consumed per sodium reabsorbed (Q_{O₂}/T_{Na}); and (5) the metabolic efficiency of transport during normal perturbations and disease.

THERMODYNAMIC APPROACH TO METABOLISM AND TRANSPORT

THERMODYNAMIC ANALYSIS OF KIDNEY FUNCTION

Interest in kidney metabolism antedates most knowledge of the kidney's inner workings or of biochemistry. The theoretical minimum amount of energy required to make urine was determined from the laws of equilibrium thermodynamics nearly a century ago. For a human in balance on a typical diet, the cost of converting the glomerular filtrate into urine by an idealized process that is 100% efficient, infinitely slow, completely reversible, involves no back-leak, and generates no entropy and heat is about 0.5 cal/min/1.73 m².² In reality, the kidney consumes more than 50-fold this amount of energy. On this basis alone, one might argue that the kidney is horribly inefficient, even after one subtracts the cost of the kidney maintaining itself. On the other hand, added costs are imposed by the requirement to make urine in a finite amount of time, the need for flexibility to rapidly alter the volume and composition of the urine, the stoichiometric constraints of biochemistry, the known limits on the thermodynamic efficiency of oxidative phosphorylation, and the intrinsic permeabilities of tissues to electrolytes, gases, and urea.

The thermodynamic requirement may be a small fraction of the actual expenditure, but before one concludes that

the body is unconcerned with thermodynamics, it may be noted that the thermodynamic energy required of the kidney to maintain salt and nitrogen balance with consumption of a typical diet is minimized with the usual water intake of 1 to 2 L/day. This suggests that the human body evolved to minimize the thermodynamic energy requirements of the kidney.

Moreover, the thermodynamic cost of excreting urea declines as blood urea nitrogen (BUN) concentration increases. Thus, as BUN rises in kidney disease, less energy is required to maintain the nitrogen balance. In kidney disease, the urine composition is also restricted to a narrower range. Using a classical thermodynamic approach, Newburgh suggested that the composition of the urine and the body fluids in kidney disease is determined by the available free energy; he noted that the declining flexibility of the diseased kidney to vary the urine composition could be predicted from the reduced free energy available for transport.³

APPLICATION OF THE LAWS OF THERMODYNAMICS TO KIDNEY FUNCTION

The macroscopic laws of equilibrium thermodynamics apply to kidney metabolism; any theory of metabolism is necessarily incorrect if it violates these laws. The laws of thermodynamics essentially describe transitions of a system from one state to another. The first law of thermodynamics states that total energy is conserved during any process that occurs in a closed system. When a system is open to its environment, the combined energy of the system + environment remains constant. When the total internal energy, temperature, pressure, and volume of a system remain constant, any process that yields a change in free energy also yields reciprocal changes in entropy. Doing work on the system is equivalent to adding free energy to the system, which determines the upper limit of how much useful work the system can do against its environment.

The first law stipulates that total energy is conserved throughout any process but provides no other indication of whether a given process will occur spontaneously. The glomerular filtrate contains a mixture of salt and urea. The tubule partitions this into urine and reabsorbate. The urine has a different ratio of urea to salt than the reabsorbate, so the entropy has decreased. But the total internal energy of the combined urine and reabsorbate is the same as the original filtrate. Hence, the first law would be satisfied if the urine were to form spontaneously from the filtrate. The fact that NaCl and urea never sort themselves spontaneously into regions of higher and lower concentration is a consequence of the second law of thermodynamics, which states that all spontaneous processes generate entropy. Conversely, all spontaneous processes dissipate free energy and will cease when the supply of free energy is exhausted. It is possible to reduce entropy or elevate free energy in a system, but only if the system imports energy from its surroundings, in which case, there will be an increase in entropy of the surroundings that exceeds the decrease in entropy of the system. Some processes in the kidney, such as conversion of chemical to mechanical energy by the Na⁺-K⁺-ATPase, are highly efficient and generate almost no entropy. Other processes, such as the countercurrent multiplier, are inefficient and generate a lot of entropy. As a rule, those processes

that generate the least entropy work over short distances and short times.

The laws of equilibrium thermodynamics determine the direction of any spontaneous process, but they do not address the rate of change. Hence the laws of equilibrium thermodynamics are not adequate for a full description of a living system that is displaced from equilibrium and characterized by flow of matter and energy within the system itself, as well as between the system and its environment. Thermodynamic principles are extended to incorporate time as a variable by the theory of nonequilibrium thermodynamics. Nonequilibrium thermodynamics entails certain assumptions and approximations that make it more of a tool and less of an edifice than classical equilibrium thermodynamics, but the theory performs well in many areas of physiology, including transport physiology. Basically, the theory asserts that the flow of any extensive property (e.g., mass, volume, charge) is the product of a driving force and a proportionality constant, which has units of conductance. It applies to both macro- and micro-processes involved in forming the urine. Examples include all mechanisms for secondary active transport and the conversion of chemical to translational free energy by ATPases.

ENERGY AND THE SODIUM PUMP

Na⁺-K⁺-ATPase, also referred to as the sodium pump, is a ubiquitous plasma membrane protein that transports intracellular sodium out of the cell and extracellular potassium into the cell, thereby generating opposite concentration gradients for sodium and potassium ions across the cell membrane. This process of separating sodium from potassium across the cell membrane is fueled by the hydrolysis of adenosine triphosphate (ATP).^{4,5} Each cycle of the pump consumes 1 ATP molecule while transporting 3 Na⁺ and 2 K⁺ ions across the cell membrane. The hydrolysis of ATP and the associated transport of ions are mutually dependent^{4,5} and constitute an example of primary active transport. In this process there is nearly full conversion from chemical to mechanical energy, with minimal dissipation. The translational energy that develops after ATP hydrolysis results from electrostatic repulsion between the product ions, ADP and Pi, in accordance with Coulomb's law. Although this energy could be dissipated through subsequent collisions, such events are unlikely over very short time scales and short distances. For a relative kinetic energy of the phosphate of 0.6 eV, for example, the phosphate ion moves about 0.1 nm in 0.3 ps. If no other collisions occur in that short time interval, the phosphate can then transfer its entire kinetic energy to the sodium pump in the form of a molecular strain. Given the intrinsic free energy of ATP hydrolysis, the pump can generate gradients that store up to approximately 0.6 eV of electrochemical potential per 3 Na⁺ plus 2 K⁺ ions. For a typical cell in a typical environment, about 0.4 eV is required to cycle the pump against the existing Na and K gradients, which means that cells tend to operate with some reserve to further reduce their sodium or increase their potassium concentrations.

STRUCTURE OF THE SODIUM PUMP

The sodium pump is composed of an α catalytic subunit, which hydrolyzes ATP and transports Na⁺ and K⁺ across the

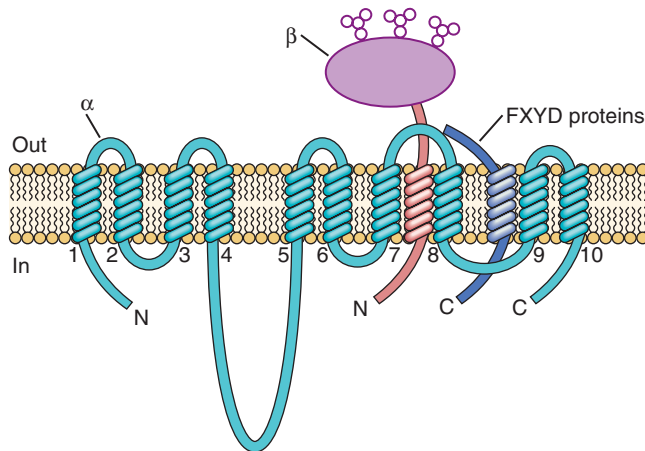


Fig. 5.1 $\text{Na}^+\text{-K}^+$ -ATPase is composed of a catalytic α -subunit (teal), an obligatory β -subunit (pink), and tissue-specific FXYD proteins (blue). The α -subunit has 10 transmembrane segments. It hydrolyzes ATP, is phosphorylated in the large cytoplasmic loop, and transports sodium and potassium. The β -subunit is a type II glycoprotein that is located close to M7/M10 and interacts with the extracellular loop between transmembrane segments M7 and M8 and with intracellular regions of the α -subunit.³ FXYD proteins are type I membrane proteins that interact with M9 with the β -subunit,⁴ and in the case of FXYD1 with the intracellular lipid surface and the cytoplasmic domain of the α -subunit [5•]. (From Geering K. Functional roles of Na,K -ATPase subunits. *Curr Opin Nephrol Hypertens.* 2008;17[5]:526–532.)

membrane, a β -subunit that is critical for functional maturation and delivery of $\text{Na}^+\text{-K}^+$ -ATPase to the plasma membrane, and an FXYD protein that can modulate the kinetics of $\text{Na}^+\text{-K}^+$ -ATPase in a tissue-specific manner⁶ (Fig. 5.1). There are multiple isoforms of each subunit. The $\alpha 1\beta 1$ heterodimer is likely the exclusive $\text{Na}^+\text{-K}^+$ -ATPase in renal epithelia,⁷ whereas several FXYD protein subunits are expressed differentially along the nephron.^{6–9} Biophysical models describing the turnover of the sodium pump through its functional cycle are described in a review by Horisberger.⁴

OTHER ADENOSINE TRIPHOSPHATASES

Besides $\text{Na}^+\text{-K}^+$ -ATPase, additional ion-translocating ATPases are expressed in renal epithelia along the nephron,¹⁰ including $\text{H}^+\text{-K}^+$ -ATPase,^{11,12} Ca^{2+} -ATPases,¹³ and H^+ -ATPases.^{14,15} These transport ATPases play important roles in maintaining urinary acidification and calcium homeostasis as discussed in Chapters 6, 7, and 9. These ATPases do not contribute significantly to the reabsorption of the bulk of the filtrate.

PUMP LEAK PROCESS AND THE SODIUM POTENTIAL

For a cell in a steady state, the pumping of ions by the $\text{Na}^+\text{-K}^+$ -ATPase must be offset by an equal and opposite diffusion of those ions back across the cell membrane. The back-leak of ions is an example of electrodiffusion. This diffusion of ions generates an electric field to retard diffusion of the most mobile charged species, thereby transferring free energy from the chemical potential of the mobile species to an electrical potential acting on the less mobile species.

If the electric field is constant within the cell membrane, then the electrical potential difference across the membrane is given by the Goldman voltage equation, which is shown here for a membrane that is permeable to Na, K, and Cl:

$$\psi = \frac{RT}{F} \ln \left(\frac{P_K[K]_o + P_{Na}[Na]_o - P_{Cl}[Cl]_o}{P_K[K]_i + P_{Na}[Na]_i - P_{Cl}[Cl]_i} \right)$$

where P_X is the permeability to X, $[X]_o$ is the concentration of X outside the cell, and $[X]_i$ is the concentration inside the cell. If the permeability to one ion dominates the others, then the membrane voltage approaches the Nernst potential for that ion and the free energy is transferred to electrochemical potential of the other ions. If chloride is not actively transported, then the second law of thermodynamics dictates that no free energy exists in the chloride gradient. Thus, for a membrane that actively transports Na and K and is primarily permeable to K, the membrane voltage approaches the Nernst potential for K and the free energy provided by active transport is all transferred to the transmembrane Na difference.

To summarize, because cell membranes are generally more permeable to potassium than to sodium, potassium diffusion contributes more to the cell voltage than sodium diffusion, even though three sodium ions leak into the cell for every two potassium ions that leak out. Thus, diffusion of potassium out of the cell dominates the cell voltage, making it negative. The negative cell voltage, in turn, neutralizes the net driving force for further potassium egress and augments the net driving force for sodium entry. Because cell membranes are poor capacitors, an imperceptible charge imbalance suffices to form the entire membrane voltage. This allows the transmembrane concentration differences for sodium and potassium to remain nearly equal and opposite despite the much greater permeability to potassium. The net outcome of this pump-leak process is that electrochemical potential, which originates with ATP hydrolysis, becomes concentrated in the transmembrane sodium gradient, whereas potassium resides near electrochemical equilibrium.

HARNESSING THE SODIUM POTENTIAL FOR WORK

The difference in electrochemical potential for sodium across the cell membrane is available to drive the unfavorable passage of other solutes across the membrane by a variety of exchangers and cotransporters. Examples include the proximal tubule Na^+/H^+ exchanger, sodium-glucose cotransporters (SGLTs), the basolateral Na/α -ketoglutarate (α -KG) cotransporter, the furosemide-sensitive $\text{Na}-\text{K}-2\text{Cl}$ cotransporter, (NKCC2), and the thiazide-sensitive $\text{Na}-\text{Cl}$ cotransporter (NCC). Generically, transport that directly uses free energy from the sodium gradient to drive uphill flux of another solute is referred to as secondary active transport¹⁶ (α -KG cotransport in Fig. 5.2). Tertiary active transport refers to the net flux of a solute against its electrochemical potential gradient coupled indirectly to the Na^+ gradient (three transport processes working in parallel). An example of tertiary active transport is the uptake of various organic anions from the peritubular blood into the proximal tubular cell by the so-called organic anion transporters (OATs). Energy from the sodium gradient is converted into a gradient for α -KG to diffuse out of the cell

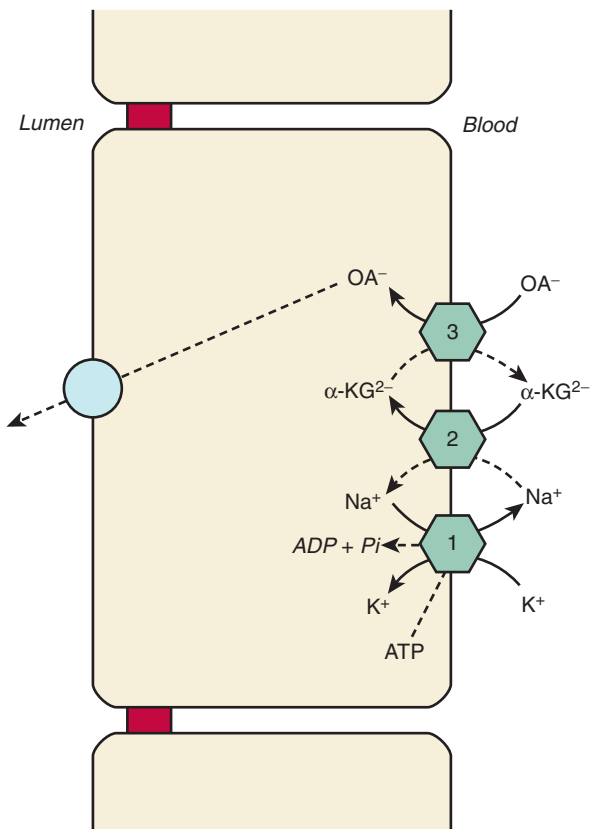


Fig. 5.2 Different modes of active uphill transport as exemplified by organic acid (OA) secretion in proximal tubule epithelial cells. Transport across the basolateral membrane involves three steps functioning in parallel. Primary active transport (1) of Na and K by $\text{Na}^+\text{-K}^+$ -ATPase coupled to the hydrolysis of ATP establishes the inwardly directed Na gradient. Secondary active transport (2) of α -ketoglutarate ($\alpha\text{-KG}$) with Na on an Na/ α -KG cotransporter uses the inwardly directed Na gradient to drive $\alpha\text{-KG}$ into the cell. Tertiary active transport (3) of OA with $\alpha\text{-KG}$ on an OA/ α -KG antiporter uses the outward downhill transport of $\alpha\text{-KG}$ to drive the inward uphill transport of OA. The $\alpha\text{-KG}$ is recycled through the Na/ α -KG cotransporter, which thus links the uphill transport of OA to the generation of the Na gradient by the $\text{Na}^+\text{-K}^+$ -ATPase. Ultimately OAs are secreted down the OA concentration gradient into the tubular lumen. (From Dantzler WH, Wright SH. The molecular and cellular physiology of basolateral organic anion transport in mammalian renal tubules. *Biochim Biophys Acta*. 2003;1618[2]:185–193.)

by Na/ α -KG cotransport. OATs use this potential difference to exchange α -KG for another organic anion¹⁷ (see Fig. 5.2).

For tubular cells that actively reabsorb chloride, free energy is transferred from the Na potential to drive apical chloride entry and raise cell chloride above equilibrium. In the proximal tubule, the energy for apical chloride entry is derived circuitously via sodium-hydrogen exchange that is coupled to oxalate, formate, or hydroxyl ion transport (see Chapter 5). In the thick ascending loop of Henle (TALH) and distal convoluted tubule (DCT), the energy transfer occurs by direct cotransport with Na via NKCC2 or NCC. In each case, raising cell chloride above equilibrium provides a driving force for chloride to diffuse out of the cell across the basolateral membrane, which is permeable to chloride. Raising cell chloride also makes the basolateral membrane voltage less negative, as is apparent from the Goldman equation. Because luminal voltage is the sum of voltage steps across the

basolateral and apical membranes, raising cell chloride in a cell with basolateral chloride conductance will raise the lumen voltage (make it more positive), thus providing free energy that can either be dissipated by the intercellular back-leak of chloride, which would increase entropy, or be applied to do the useful work of cation reabsorption, which would decrease entropy. The kidney uses the latter mechanism of energy transfer to augment Na reabsorption in the proximal tubule as well as calcium and magnesium reabsorption in the TALH.

For cells that express ENaC, opening these channels will depolarize the apical membrane, as can be seen from the Goldman equation. K ions, which enter the cell via the basolateral Na pump, can leave the cell by K conductances in either basolateral or apical membranes. Depolarizing the apical membrane will increase the fraction of K ions leaving by way of the apical membrane conductance. This represents the transfer of free energy from the $\text{Na}^+\text{-K}^+$ -ATPase and the apical Na potential to the useful work of K secretion.

CELL POLARITY AND VECTORIAL TRANSPORT

The polar arrangement of transporters in renal cells is essential for vectorial transport. Wherever it is expressed along the nephron, the sodium pump, which removes sodium from the cell, is restricted to the basolateral membrane. Meanwhile, the variety of exchangers, cotransporters, and sodium channels through which sodium enters the tubular cell are restricted to the apical membrane. These include the principal Na^+/H^+ exchanger (NHE3) and SGLTs in the proximal tubule, the NKCC2 in the thick ascending limb (TAL) of the loop of Henle, the NCC in the distal convoluted tubule, and epithelial sodium channels in the connecting tubule and collecting duct (see Chapter 5). These apical sodium transporters effect secondary active transport coupled to the primary active transporter, $\text{Na}^+\text{-K}^+$ -ATPase.

Close coordination of sodium uptake across the apical membrane with sodium extrusion across the basolateral membrane is required to avoid osmotic swelling and shrinking of the cell. Assuming ATP is not limiting for basolateral exit, the magnitude of transepithelial transport is a function of (1) the number of transporters in the plasma membrane, which can be varied by changes in synthesis or degradation rates and/or trafficking between intracellular and plasma membranes, and (2) the activity per transporter, which can be varied by covalent modification (e.g., phosphorylation or proteolysis) or protein–protein interaction (e.g., $\text{Na}^+\text{-K}^+$ -ATPase kinetics are influenced by FXYD subunit association).⁶ The rate of apical sodium entry is also subject to influence by the availability of substrates for cotransport. For example, the amount of sodium–glucose cotransport depends on the availability of glucose in proximal tubular fluid, and the sodium entry at a given point along the TAL is subject to variations in the local chloride concentration, because NKCC2 has a relatively low affinity for chloride.

Many factors and hormones known to regulate renal sodium reabsorption (including angiotensin II, aldosterone, dopamine, parathyroid hormone, and blood pressure) act in parallel to affect the activity, distribution, or abundance of apical transporters and basolateral sodium pumps.^{7,18} The

molecular basis of this apical–basolateral crosstalk is not clearly understood, especially in the light of close cell volume control; however, there is evidence for a role of elevated cellular calcium level in response to depressed sodium transport.¹⁹ There is also recent evidence for a salt-inducible kinase that responds to slight elevations in cell Na and Ca,²⁰ as well as evidence for coupling of Na⁺-K⁺-ATPase to apical channel activity.²¹

METABOLIC SUBSTRATES FUELING ACTIVE TRANSPORT ALONG THE NEPHRON

Mitchell has noted that:

“Biochemists generally accept the idea that metabolism is the cause of membrane transport.”

The underlying idea of the hypothesis put forward here is that if the processes that we call metabolism and transport represent events in a sequence, not only can metabolism be the cause of transport, but also transport can be the cause of metabolism. Thus, we might be inclined to recognize that transport and metabolism, as usually understood by biochemists, may be conceived advantageously as different aspects of one and the same process of vectorial metabolism.²²

METABOLISM BASICS

Detailed accounts of cellular metabolism are provided in many excellent texts²³; nonetheless, an abbreviated overview

relevant to renal metabolism is warranted. Substrates enter the kidney by renal blood flow (RBF) and GFR and enter renal epithelial cells by substrate transporters, often facilitated by the inward-directed Na⁺ gradient created by the sodium pump (see Fig. 5.2), as discussed thoroughly in Chapter 8. Oxygen is likewise delivered by RBF to the epithelial cells. Once in the cell, substrates face one of three fates: (1) transport across the epithelium back into the blood (reabsorption); (2) conversion into another substrate (e.g., lactate to pyruvate); or (3) oxidization to CO₂ in the process of cellular ATP production.²⁴ This section traces the roadmap that connects substrates to production of ATP in the mitochondrion and to ATP utilization by the sodium pump, and the feedback connections between production and utilization.

Renal epithelia, except in the descending and thin ascending limbs of the loop of Henle, are packed with mitochondria (see Chapter 2). All the pathways of fuel oxidation take place in the mitochondrial matrix, except for glycolysis, which occurs in the cytosol. Substrates in the cytosol can freely cross the outer mitochondrial membrane through integral membrane porins. These substrates, as well as adenosine diphosphate (ADP) and phosphate (the building blocks of ATP), cross the inner mitochondrial membrane into the mitochondrial matrix via specific substrate transporters driven by their respective concentration gradients or by the H⁺ gradient created by the electron transport chain (ETC; Fig. 5.3).

As illustrated in Fig. 5.4, amino acids, fatty acids, and pyruvate are metabolized to acetyl-coenzyme A and enter the citric acid cycle. With each turn of the cycle, three molecules of reduced nicotinamide adenine dinucleotide

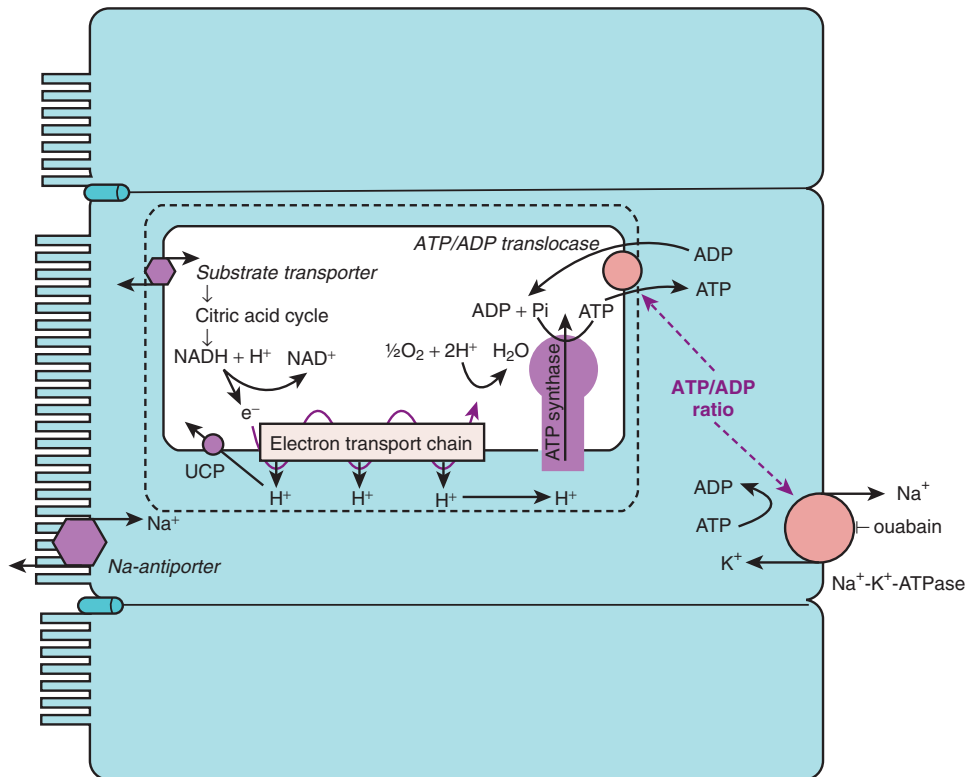


Fig. 5.3 Whittam model. Coupling of ATP utilization by Na⁺-K⁺-ATPase to ATP production by mitochondrial oxygen consumption (Q_{O₂}). Hydrolysis of ATP produces ADP plus inorganic phosphate (Pi), which lowers the ATP/ADP ratio, a signal to increase ADP uptake into the mitochondria and increase ATP synthesis.

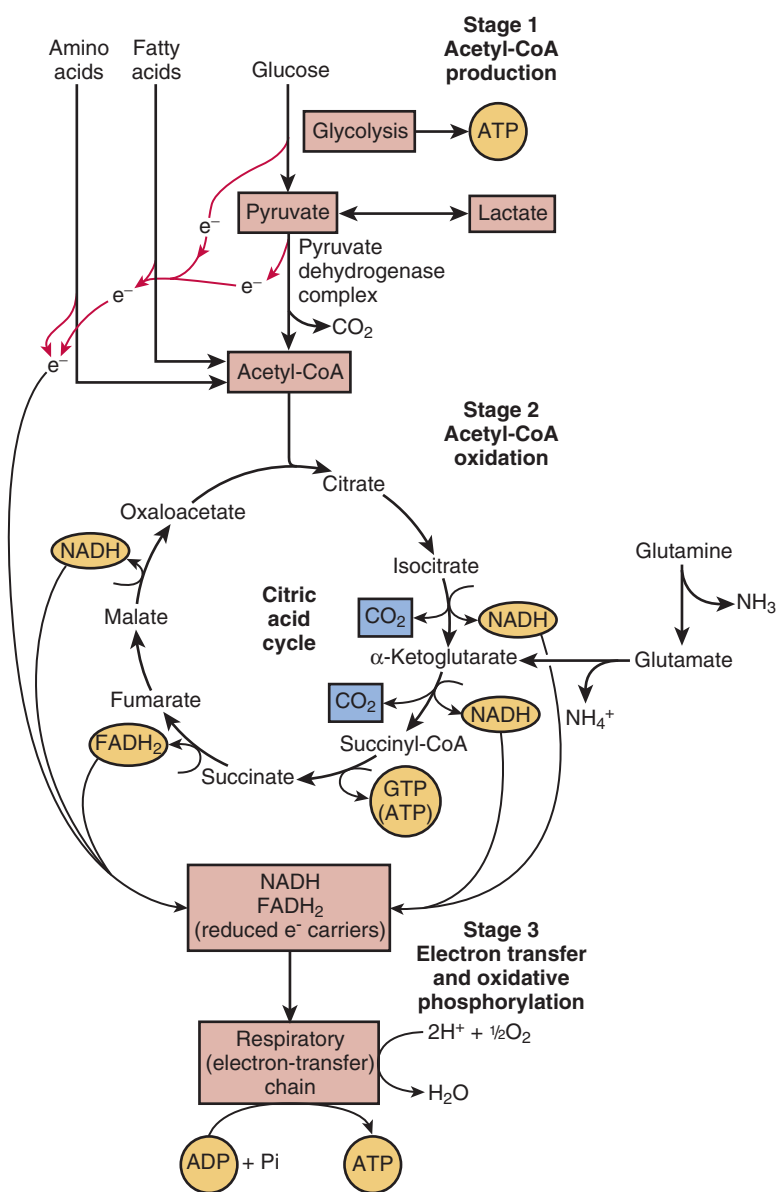


Fig. 5.4 Catabolism of proteins, fats, and carbohydrates in three stages of cellular respiration. Stage 1: oxidation of fatty acids, glucose, and some amino acids yields acetyl-coenzyme A (CoA). Stage 2: oxidation of acetyl groups in the citric acid cycle includes four steps in which electrons are abstracted. Stage 3: electrons carried by reduced nicotinamide adenine dinucleotide (NADH) and reduced flavin adenine dinucleotide (FADH₂) are funneled into a chain of mitochondrial (or, in bacteria, plasma membrane-bound) electron carriers (the respiratory chain) that ultimately reduces O₂ to H₂O. This electron flow drives the production of ATP. Also indicated are two proximal tubule pathways: (1) oxidation of lactate through pyruvate and acetyl-CoA, and (2) glutamine conversion to glutamate and α-ketoglutarate in the mitochondria with the production of two molecules of NH₃, which is the main source of NH₃ secreted during acidosis. (Modified from Nelson DL, Cox MM. *Lehninger principles of biochemistry*, 5th ed. New York: WH Freeman; 2008.)

(NADH), one molecule of reduced flavin adenine dinucleotide (FADH₂), one molecule of guanosine triphosphate (GTP) or ATP, and two molecules of CO₂ are released in oxidative decarboxylation reactions (Table 5.1). Electrons carried by NADH and FADH₂ are transferred into the mitochondrial electron transport chain, a series of integral membrane complexes located within the inner mitochondrial membrane, where the electrons are sequentially transferred, ultimately to oxygen, which is reduced to H₂O. NADH and FADH₂ oxidation provoke the transport of H⁺ from the matrix to the inner mitochondrial space.

The release of the potential energy stored in the H⁺ gradient across the inner mitochondrial membrane provides the driving force for ATP synthesis from ADP by the ATP synthase: H⁺ is transported into the matrix coupled to the production of ATP from ADP and inorganic phosphate (Pi) (see Fig. 5.3). These are the fundamental pieces of the chemiosmotic mechanism of oxidative phosphorylation proposed by Peter Mitchell in 1961.²² The newly synthesized ATP is extruded from the matrix into the intermembrane space via the ADP–ATP countertransporter known as adenine nucleotide translocase and then exits the mitochondria

Table 5.1 Adenosine Triphosphate (ATP) Yield From Metabolism of One Glucose Molecule

| Process | Direct Product | Final ATP |
|--|--|----------------|
| ATP Yield from Complete Oxidation of Glucose | | |
| Glycolysis | 2 NADH (cytosol) | 5 ^a |
| | 2 ATP | 2 |
| Pyruvate oxidation (two per glucose) | 2 NADH (mitochondrial matrix) | 5 |
| Acetyl-coenzyme A oxidation in citric acid cycle (two per glucose) | 6 NADH (mitochondrial matrix) 2 FADH ₂ | 18 4 |
| Total yield per glucose | | 30 |
| ATP Yield from Glycolysis of Glucose | | |
| Glycolysis | 2 ATP, 2 NADH | 2 |

^aVia malate-aspartate shuttle.

across the permeable outer membrane. In the cytosol, ATP is available to bind to ATPases such as plasma membrane Na⁺-K⁺-ATPase.

In summary, the flow of electrons through the ETC generates a proton gradient across the inner mitochondrial membrane that provides the energy to drive ATP synthesis from ADP + Pi by ATP synthase and is also sufficient to extrude the ATP across the mitochondrial membrane.²³ Thus, the oxidation of substrates is coupled to ATP synthesis by an electrochemical proton gradient. This coupling can be influenced by uncoupling protein isoforms (UCPs) located in the mitochondrial inner membrane and expressed in a tissue-specific manner. Simply stated, UCPs create a proton leak that dissipates the proton gradient available to drive oxidative phosphorylation (see Fig. 5.3). It has been reported that UCP-2 is expressed in the renal proximal tubule and TAL (not in glomerulus or the distal nephron) and that its expression is elevated in kidneys of diabetic rats.²⁵ However, the physiologic consequences of the expression and regulation of UCP in kidneys has not been explored much experimentally.

WHITTEM MODEL

In the early 1960s, the coupling between active transport, respiration, and Na⁺-K⁺-ATPase activity was recognized by Whittam and Blond,^{69,70} who tested the idea that inhibition of active ion transport at the plasma membrane would cause a fall in oxygen consumption (QO₂) in the mitochondria. Using brain or kidney samples studied in vitro, they demonstrated that inhibition of Na⁺-K⁺-ATPase activity by removal of sodium or addition of the sodium pump-specific inhibitor ouabain (neither of which directly inhibits mitochondrial respiration) markedly reduced QO₂, which led the investigators to conclude that an extramitochondrial ATPase, sensitive to Na⁺ and ouabain, as well as to K⁺ and Ca⁺⁺, is one of the pacemakers of respiration of the kidney cortex.^{26,27}

A careful study by Balaban and colleagues two decades later²⁸ used a suspension of renal cortical tubules to reexamine this Whittam model (see Fig. 5.3) in more detail by measuring

the redox state of mitochondrial nicotinamide adenine dinucleotide (NAD), cellular ATP and ADP concentrations, ATP/ADP ratio, and QO₂ in the same samples. If transport and respiration are assumed to be coupled, inhibition of transport is predicted to provoke a mitochondrial transition to a resting state²⁹ accompanied by an increase in NADH/NAD⁺ (reduced to oxidized NAD), increase in [ATP], decrease in [ADP] and [Pi], increase in ATP/ADP ratio, and decrease in QO₂. Stimulation of active transport would provoke the opposite pattern: decreased NADH, ATP, and ATP/ADP ratio, and increased QO₂. Predictably, incubating the renal cortical tubule suspension with the Na⁺-K⁺-ATPase inhibitor ouabain caused a 50% decline in QO₂, reduction of NAD to NADH, and a 30% increase in the ATP/ADP ratio, all evidence for coupling of mitochondrial ATP production to ATP consumption via Na⁺-K⁺-ATPase. Similarly, in tubules deprived of K⁺ (which is required for Na⁺-K⁺-ATPase turnover), adding 5 mmol/L K⁺ increased QO₂ by more than 50%, oxidized NADH to NAD⁺, and decreased the cellular ATP/ADP ratio by 50%. These results provide evidence for the coupling of both Na⁺-K⁺-ATPase and ATP production via ATP synthase to the cellular ATP/ADP ratio (see Fig. 5.3).

ENERGY REQUIREMENTS AND SUBSTRATE USE ALONG THE NEPHRON

In all renal epithelial cells from the proximal convoluted tubule to the inner medullary collecting duct (IMCD), the basolateral sodium pump uses the hydrolysis of ATP to drive primary active transport of Na⁺ out of and K⁺ into the cell, and the gradients created are used to drive coupled transport of ions and substrates across both the apical and basolateral membranes.

Despite consistent distribution and function, the relative abundance of Na,K-ATPase as a function of tubular location along the nephron is highly variable. Na,K-ATPase activity, ouabain binding, and Na,K-ATPase subunit abundance have been studied in dissected tubules and with imaging techniques. Na,K-ATPase expression patterns and ouabain binding patterns along the nephron are very similar.^{10,30} The pronounced differences in activity can largely be accounted for by differences in sodium pump number measured either by ouabain binding or by immunoblot of subunits in dissected nephron segments (Fig. 5.5).³¹

The patterns of Na⁺-K⁺-ATPase protein expression and activity as a function of tubule length are what is to be expected from what is understood of the physiology of the nephron segments: moderate levels are expressed in the proximal tubule where two-thirds of the sodium is reabsorbed across a leaky epithelium, and lower levels are expressed in the straight than in the convoluted segments, reflecting the amount of sodium transported in these two regions. Very low levels are detected in the thin limbs of the loop of Henle, whereas high levels are expressed in the medullary and cortical TAL ("diluting segments") that must reabsorb a significant fraction of NaCl without water against an increasingly steep transepithelial gradient. The Na⁺-K⁺-ATPase activity and expression in the DCT, which is responsible for reabsorbing another 5% to 7% of the filtered load against a very steep transepithelial gradient, is very high. In the collecting duct, which reabsorbs a smaller fraction of Na⁺ via channels electrically coupled to the secretion of K⁺ or H⁺ and has variable

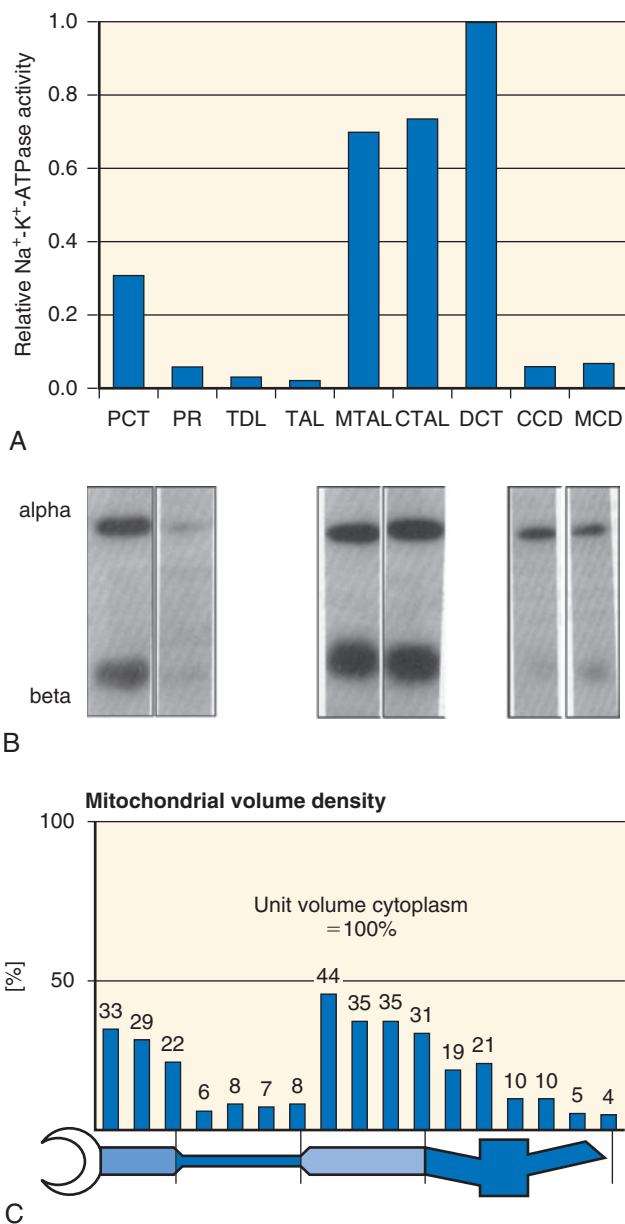


Fig. 5.5 (A) Relative levels of $\text{Na}^+\text{-K}^+$ -ATPase activity measured in individual segments of the rat nephron. (Data are normalized to that of the distal convoluted tubule and expressed per unit length of tubule segment.) (B) Detection of $\text{Na}^+\text{-K}^+$ -ATPase α_1 - and β_1 -subunits along the nephron. Tubule segments 40 mm long were resolved by sodium dodecyl sulfate–polyacrylamide gel electrophoresis and subjected to immunoblotting with subunit-specific antisera. Blots placed below corresponding tubule label indicated in (A). (C) Morphologic analysis of mitochondrial density relative to a unit of cytoplasm. CCD, Cortical collecting duct; CTAL, cortical thick ascending limb of the loop of Henle; DCT, distal convoluted tubule; MCD, outer medullary collecting duct; MTAL, medullary thick ascending limb of the loop of Henle; PCT, proximal convoluted tubule; PR, pars recta (proximal straight tubule); TAL, thin ascending limb of the loop of Henle; TDL, thin descending limb of the loop of Henle. ([A] redrawn from Katz AI, Doucet A, Morel F. $\text{Na}^+\text{-K}^+$ -ATPase activity along the rabbit, rat, and mouse nephron. *Am J Physiol.* 1979;237:F114–F120; [B] based on data from McDonough AA, Magyar CE, Komatsu Y. Expression of $\text{Na}^+\text{-K}^+$ -ATPase alpha- and beta-subunits along rat nephron: isoform specificity and response to hypokalemia. *Am J Physiol.* 1994;267:C901–C908; [C] based on data from Pfaller W, Rittinger M. Quantitative morphology of the rat kidney. *Int J Biochem.* 1980;12[1-2]:17–22.)

H_2O permeability, the $\text{Na}^+\text{-K}^+$ -ATPase is quite low, albeit sufficient to drive sodium reabsorption in this region. The distribution of the ATP-producing mitochondria along the nephron, reported as percent of cytoplasmic volume,³² parallels the distribution of the ATP-consuming sodium pumps but is somewhat less variable, ranging from 10% or less of the cell volume in the thin loop of Henle and medullary collecting duct to 20% in the cortical collecting duct (CCD) and proximal straight tubule to 30% to 40% of cell volume in the proximal tubule and TAL³² (Fig. 5.5C).

Determining which substrates support ATP production and $\text{Na}^+\text{-K}^+$ -ATPase activity along the nephron has been the subject of many studies and reviews.^{24,33,34} To obtain nephron-specific information, investigators have dissected nephron segments and assayed for either metabolic pathway enzyme distribution or examined how specific substrates affected ATP levels. Although these *in vitro* approaches lack the *in vivo* realities of blood flow, tubular flow, and autocrine-paracrine, hormonal, and nervous system inputs that are evident in the whole kidney, the studies do provide information about the metabolic potential of each segment under defined conditions.

Isolated nephron segments had been reported to have low levels of cellular ATP, so Uchida and Endou³⁵ reasoned that if the segments were incubated with fuels that could be used by the segment, their ATP levels should increase toward physiologic levels. They examined a range of substrates for their ability to maintain cellular ATP levels in microdissected glomeruli and nephron segments (excluding thin sections of loop of Henle and papillary duct). The substrates studied (all at 2 mmol/L) included L-glutamine, D-glucose, β -hydroxybutyrate (HBA), and DL-lactate. Because the preincubation did not fully deplete the TAL and distal nephron segments of ATP, the ionophore monensin was included in the incubation with the substrate to dissipate the Na^+ gradient and promote ATP consumption.

The change in ATP per millimeter of tubule (or glomerulus) as a function of substrate addition, shown in Fig. 5.6, illustrates that each segment had a distinct ability to use these substrates. Lactate was very effective at maintaining ATP levels in all nephron segments tested, notably in the proximal tubule. The S1, S2, and S3 segments of the proximal tubule all used glutamine effectively as a fuel, which is consistent with the role of the proximal tubule in ammoniagenesis. Glutamine is the main amino acid oxidized by the proximal tubule, where it is deaminated and converted to α -KG, yielding 2 NH_3 molecules that are secreted during acidosis, as illustrated in Fig. 5.4 and discussed in Chapter 9. Glutamine is not a preferred fuel in the more distal nephron segments. Glucose is completely reabsorbed along the proximal tubule yet, glucose is not an effective metabolic fuel for the S1 or S2 regions of the proximal tubule. In contrast, all of the more distal segments tested readily used glucose to maintain cellular ATP. The ketone HBA was used effectively in all nephron segments tested; however, in S1 and S2 of the proximal tubule the capacity of HBA to support ATP production was far less than that provided by glutamine or lactate.

The distribution along the nephron of numerous enzymes involved in metabolic pathways, collated from many studies, has been summarized by Guder and Ross.³³ Their description of glycolytic (Fig. 5.7A) and gluconeogenic (Fig. 5.7B) enzymes along the rat nephron^{36–38} demonstrates very low

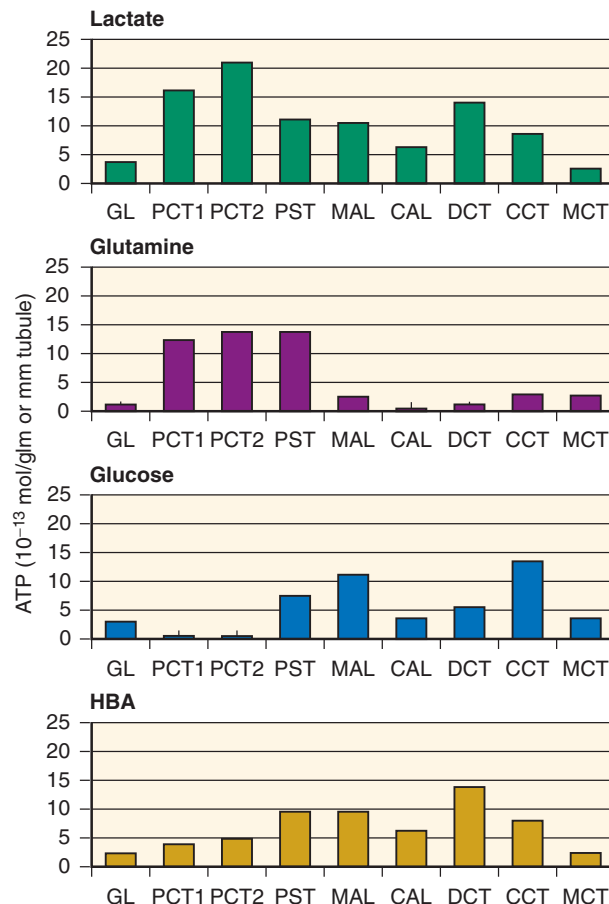


Fig. 5.6 ATP production in glomeruli and dissected nephron segments as a function of substrates. In glomeruli and PCT1, PCT2, and PST segments, the values equal the differences in ATP content between samples incubated with and without each substrate for 30 minutes. In MAL, CAL, DCT, CCT, and MCT, the values equal the differences in ATP content between samples incubated with and without each substrate in the presence of monensin (10 pg/mL) for 15 minutes. CAL, Cortical ascending limb; CCT, cortical collecting tubule; DCT, distal convoluted tubule; GL, glomerulus; MAL, medullary thick ascending limb; MCT, medullary collecting tubule; PCT1, early proximal convoluted tubule; PCT2, late proximal convoluted tubule; PST, proximal straight tubule. (Data from Uchida S, Endou H. Substrate specificity to maintain cellular ATP along the mouse nephron. *Am J Physiol*. 1988;255:F977–F983.)

glycolytic potential in the proximal tubule and high glycolytic potential from medullary ascending limb to medullary collecting tubule. In contrast, gluconeogenic enzymes are found almost exclusively in the proximal tubule.

In summary, the proximal tubule reabsorbs glucose and can synthesize glucose biosynthetically but does not metabolize glucose. There are both practical and theoretical explanations for the lack of glucose metabolism in this segment. The proximal tubule is specialized to reabsorb the filtered load of glucose from the tubular fluid back into the blood. Because of the enormous load of glucose moving through these cells, a proximal tubule hexokinase would need to have exceedingly low affinity for glucose, which would be difficult to regulate. In contrast, more distal regions of the nephron such as the loop of Henle and distal nephron normally have little or no

glucose in their tubular fluid, have no Na-glucose cotransporters in their apical membranes, and cannot synthesize glucose, but these regions use glucose delivered via RBF as a metabolic fuel (which could be provided by gluconeogenesis in the proximal tubule during fasting). A summary of substrate preferences along the nephron is provided in Fig. 5.8.³⁴

RENAL GLUCONEOGENESIS AND LACTATE HANDLING

In a review of renal gluconeogenesis, Gerich and colleagues³⁹ comment that the kidney can be considered two separate organs, because the proximal tubule makes and releases glucose from noncarbohydrate precursors, whereas glucose utilization occurs primarily in the medulla. Because the kidney is both a consumer and a producer of glucose, net arteriovenous glucose differences across the kidney can be uninformative, because glucose consumption in the medulla can mask glucose release by the cortex.

Gerich and colleagues³⁹ also make the case that the kidney is a significant gluconeogenic organ in normal humans based on the following: (1) in humans fasted overnight, proximal tubule gluconeogenesis can be as much as 40% of whole-body gluconeogenesis³⁹; (2) during liver transplantation, endogenous glucose release falls to only 50% of control levels by 1 hour after liver removal⁴⁰, and (3) pathologically in type 2 diabetes, renal glucose release is increased by about the same fraction as hepatic glucose release.⁴¹ Zucker diabetic fatty rats also exhibit marked stimulation of gluconeogenesis compared with their lean litter mate controls.⁴²

Lactate can reach the nephron by filtration or blood flow and can also be produced along the nephron. Within the kidney, lactate can be (1) oxidized to produce energy with generation of CO₂, a process that consumes oxygen but generates ATP; or (2) converted to glucose via gluconeogenesis in the proximal tubule, a process that consumes oxygen and ATP. This is shown in Fig. 5.9. Studies by Cohen⁴³ in an isolated whole kidney perfused with just lactate as substrate demonstrated a change in ¹⁴C-lactate utilization as a function of its concentration in the perfusate: at low concentrations, all the lactate was oxidized (detected as CO₂) in order to fuel transport and basal metabolism; when lactate in perfusate was raised above 2 mmol/L some of the lactate was used for synthesis of glucose (gluconeogenesis); and at high lactate in perfusate the metabolic and synthetic rates approach maximum, and some lactate is conserved (reabsorbed). However, it is not the normal circumstance that lactate is the sole substrate, and it is now appreciated that the metabolism of lactate is affected by the presence of other substrates—for example, lactate uptake and oxidation are inhibited in the presence of fatty acids.^{24,44}

The kidney's ability to convert lactate to glucose provides evidence that it can participate in cell-cell lactate shuttle, also known as the Cori cycle.⁴⁵ This cycle is important when oxidative phosphorylation is inhibited in vigorously exercising muscle, which becomes hypoxic. In the muscle, pyruvate is reduced to lactate to regenerate NAD⁺ from NADH, which is necessary for ATP production by glycolysis to continue. Lactate is released into the blood and can be taken up by tissues capable of gluconeogenesis, such as the liver and kidney. In the proximal tubule, the lactate that is not oxidized can be converted to glucose, and because this substrate is

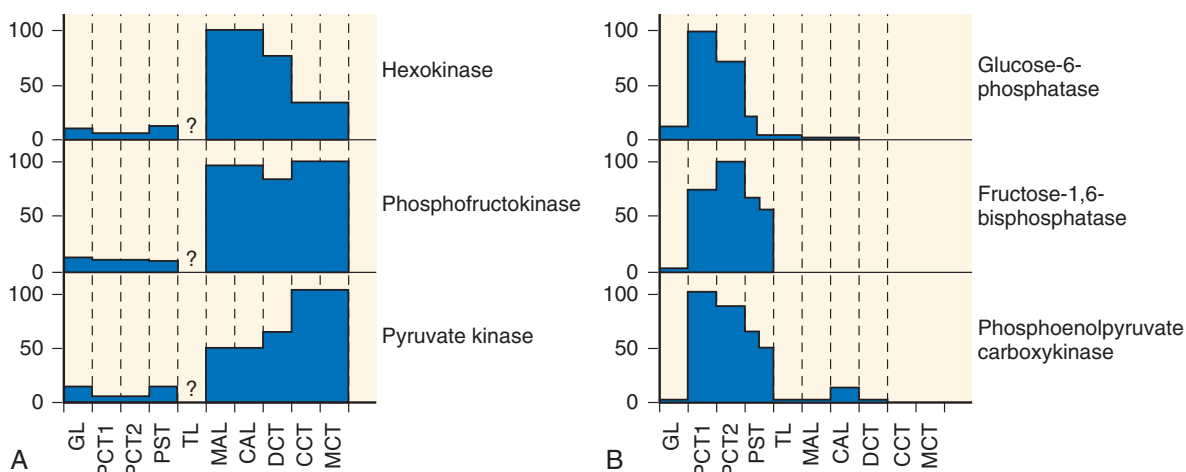


Fig. 5.7 Distribution of glycolytic and gluconeogenic enzymes along the rat nephron. Nephron segments were dissected from fed (A) and starved (B) rats, respectively. The activity of hexokinase, phosphofructokinase, pyruvate kinase, glucose-6-phosphatase, fructose 1,6-bisphosphatase, and phosphoenolpyruvate carboxykinase was determined in individual segments. Enzyme activities are expressed as a percentage of the maximal value observed, based on the original activity per gram of dry weight. CAL, Cortical ascending limb; CCT, cortical collecting tubule; DCT, distal convoluted tubule; GL, glomerulus; MAL, medullary thick ascending limb; MCT, medullary collecting tubule; PCT1, early proximal convoluted tubule; PCT2, late proximal convoluted tubule; PST, proximal straight tubule; TL, loop of Henle, thin limbs. (Modified from Guder WG, Ross BD. Enzyme distribution along the nephron. *Kidney Int.* 1984;26[2]:101–111.)

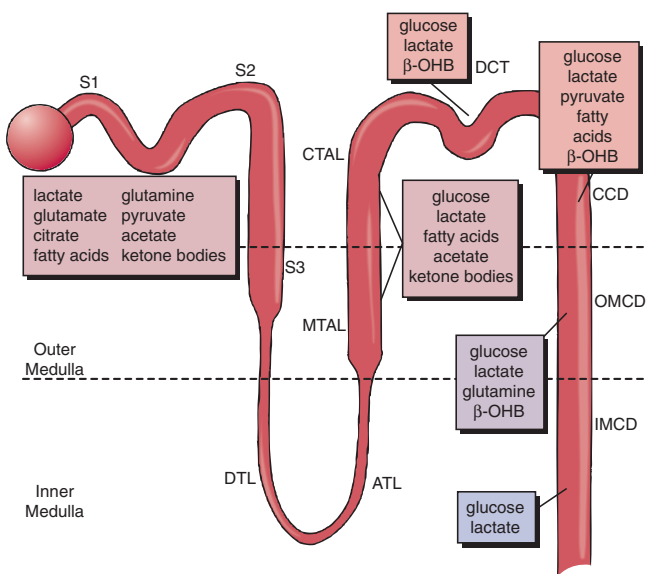


Fig. 5.8 Substrate preferences along the nephron. Summary of preferred substrates to fuel active transport in nephron segments as gleaned primarily from studies using oxygen consumption (Q_O_2), ion fluxes, radioactive carbon (^{14}C)-labeled carbon dioxide generation from ^{14}C -labeled substrates, ATP contents, and reduced nicotinamide adenine dinucleotide fluorescence. ATL, Ascending thin limb; β -OHB, β -Hydroxybutyrate; CCD, cortical collecting duct; CTAL, cortical thick ascending limb of the loop of Henle; DCT, distal convoluted tubule; DTL, descending thin limb; IMCD, inner medullary collecting duct; MTAL, medullary thick ascending limb of the loop of Henle; OMCD, outer medullary collecting duct; S1, S2, S3, successive segments of proximal tubule. (From Kone BC. Metabolic basis of solute transport. In: Brenner and Rector's the kidney, 5th ed. St Louis: Saunders; 2008.)

not used by the proximal tubule, glucose will be reabsorbed back into the blood, where it will be available for metabolism by the exercising muscle. Overall, this cycle is metabolically costly: glycolysis produces 2 ATP molecules at a cost of 6 ATP molecules consumed in the gluconeogenesis. Thus, the

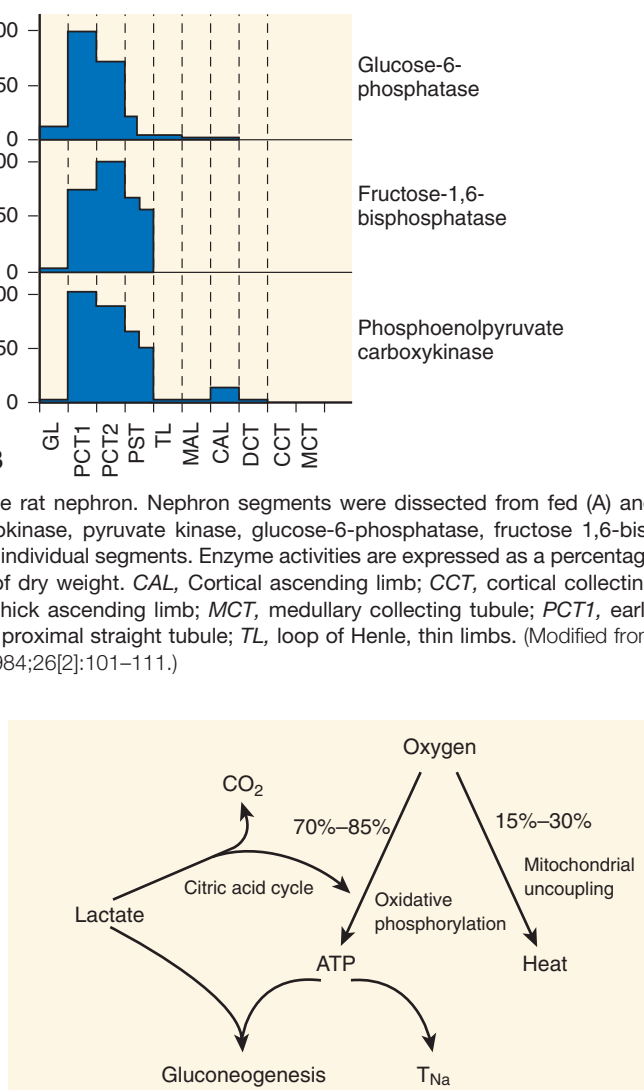


Fig. 5.9 Fate of lactate and oxygen in renal metabolism. Oxygen can be used to generate ATP via oxidative phosphorylation or heat if mitochondrial uncoupling occurs. Lactate can act as a substrate for gluconeogenesis, which consumes energy, or can enter into the citric acid cycle to generate energy. ATP is either used for Na^+ transport (T_{Na}) or consumed in the process of gluconeogenesis.

Cori cycle is an energy-requiring process that shifts the metabolic burden away from the exercising muscle during hypoxia. This cell-cell lactate shuttle could also operate within the kidney between nephron segments that produce lactate anaerobically and the proximal tubule.

Renal medullary lactate concentration was explored in a 1965 study in rats by Scaglione and colleagues⁴⁶ to test the idea that the medulla used glycolysis in the low-oxygen environment. Medullary lactate concentration is a function of delivery via the blood flow, production in the medulla, and removal by the blood flow, because there is no gluconeogenesis in this region to consume lactate. Because of the countercurrent arrangement of the vasa recta, lactate would be expected to concentrate in the medulla somewhat. The study results indicated that lactate concentration was twice as high in the inner medulla as in the cortex and

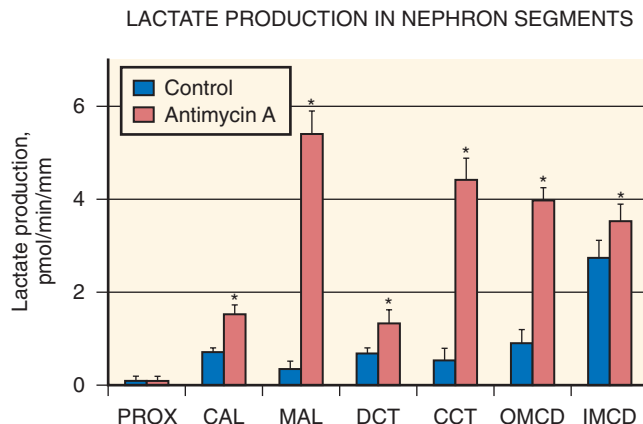


Fig. 5.10 Lactate production by rat nephron segments under control conditions and in the presence of antimycin A. *CAL*, Cortical ascending limb; *CCT*, cortical collecting tubule; *DCT*, distal convoluted tubule; *IMCD*, inner medullary collecting duct; *MAL*, medullary thick ascending limb; *OMCD*, outer medullary collecting duct; *PROX*, proximal tubule. (From Bagnasco S, Good D, Balaban R, et al. Lactate production in isolated segments of the rat nephron. *Am J Physiol*. 1985;248:F522–F526.)

that during osmotic diuresis the medullary lactate doubled, whereas cortical lactate remained unchanged. The authors postulated that increased medullary lactate was evidence for increased glycolysis during osmotic diuresis because the diuresis and increased flow through the vasa recta would be expected to decrease medullary lactate if synthesis rates were unchanged. Sodium delivery to the distal nephron would also increase during osmotic diuresis and the accompanying increased Na^+ reabsorption could drive the increased glycolysis.

Twenty years later, Bagnasco and colleagues⁴⁷ studied lactate production along the nephron in dissected rat nephron segments incubated *in vitro* with glucose with or without an inhibitor of oxidative metabolism, antimycin A. The only pathway for lactate production in the kidney is from pyruvate via lactate dehydrogenase. Proximal tubules produced no lactate with or without antimycin A. The distal segments all produced lactate, and the production was significantly increased (approximately 10-fold in TAL) during antimycin A incubation (Fig. 5.10), which led the authors to conclude that significant amounts of lactate can be produced by anaerobic glycolysis during anoxia in the distal segments. The IMCD, a region with low oxygen tension under control conditions, had high levels of lactate production even without antimycin A, which indicates that it is primed for anaerobic glycolysis.

NEPHRON-REGION-SPECIFIC METABOLIC CONSIDERATIONS

PROXIMAL TUBULE

Studies carried out in a number of laboratories provide evidence that sodium transport and gluconeogenesis compete for ATP in the proximal convoluted tubule.^{48–50} Friedrichs and Schoner⁴⁹ studied both processes in rat renal tubules

and slices and found that ouabain inhibition of Na^+/K^+ -ATPase increased renal gluconeogenesis by 10% to 40% depending on the substrate, and that stimulating Na^+/K^+ -ATPase activity with high extracellular K^+ inhibited gluconeogenesis. The authors concluded that inhibition of the sodium pump induced a higher energy state of the cell, which would favor energy-requiring synthetic processes.

Nagami and Lee⁵⁰ used an isolated perfused mouse proximal tubule preparation to address this issue. When tubules were perfused at higher rates, delivering more sodium to the proximal tubule, the glucose production rate was decreased by 50%, whereas when tubules were incubated with ouabain in the bath or perfused with amiloride (to inhibit apical transport), the glucose production rate increased above that seen in nonperfused tubules. These authors also verified that the reduction in glucose production seen at elevated perfusion rates does not result from increased glucose utilization and is not dependent on the presence of specific substrates. Related to the topic of proximal tubule gluconeogenesis, two studies suggest that the blood glucose-lowering effects of sodium glucose cotransporter isoform 2 (SGLT2) inhibitors are due, in part, to reduced proximal gluconeogenesis: inhibiting SGLT2-mediated glucose uptake in diabetic mice reduced gluconeogenic gene expression, including PEPCK, a principal regulator of gluconeogenesis.^{51,52}

Recent studies and mathematical models have evaluated the effects of inhibiting proximal tubule transport routes on metabolism and transport efficiency (sodium transport/oxygen consumption, $T_{\text{Na}}/\text{QO}_2$) discussed further under the section regarding metabolic cost of sodium reabsorption. Proximal tubule transport, T_{Na} , is the sum of transcellular reabsorption (e.g., via Na^+/H^+ exchanger isoform 3 [NHE3]) and sodium glucose cotransporter isoform 2 (SGLT2), and paracellular reabsorption (e.g., via claudin 2 [cldn2]). Mathematical models predict that $T_{\text{Na}}/\text{QO}_2$ is 80% higher in the S3 segment of the proximal tubule due to the larger paracellular contribution to T_{Na} , which is highly energy efficient. In these models, inhibiting NHE3 (the main sodium transporter in the proximal tubule), or Na,K -ATPase reduced T_{Na} , QO_2 , and transport efficiency.⁵³ Inhibiting SGLT2 also lowered T_{Na} but increased QO_2 in part by activating NHE3 and SGLT1 and in part by blunting the driving force for paracellular transport of Na^+ due to tubular glucose buildup.^{51,53} Regarding paracellular reabsorption, QO_2 is markedly increased in proximal tubule claudin-2 null mice as T_{Na} is shifted from the energy efficient paracellular route to the Na,K -ATPase driven transcellular routes. Consequently, cldn2 mice exhibit medullary hypoxia and increased susceptibility to tubular injury.^{54,55} How (or if) the increase in the metabolic cost of transport affects metabolic pathways and substrate utilization in the proximal tubule remains to be determined.

THICK ASCENDING LIMB

The TAL has a very high rate of Na^+ transport against a steep concentration gradient, very high levels of Na^+/K^+ -ATPase activity and expression, and, perhaps not unexpectedly, 40% of its cytosolic volume occupied by mitochondria (see Fig. 5.5). Although the TALs have a far greater capacity for anaerobic metabolism than the proximal tubules, this region still requires oxidative metabolism to maintain cellular ATP levels and active Na^+ reabsorption.^{35,56}

CORTICAL COLLECTING DUST

CCD metabolism is particularly interesting because it is made up of distinctly different cell types: principal cells that reabsorb sodium and intercalated cells that can secrete bicarbonate (HCO_3^-). Hering-Smith and Hamm microperfused rabbit CCD and measured Na^+ reabsorption (with 22Na^+) from lumen to bath, and HCO_3^- transport by microcalorimetry in the presence of substrates and with or without inhibitors. Both Na^+ reabsorption and HCO_3^- secretion were inhibited by antimycin A, which provides evidence for dependence on oxidative phosphorylation. However, neither was dependent on either glycolysis or the hexose-monophosphate shunt pathways. A small component of Na^+ transport was supported by endogenous substrates. Na^+ reabsorption was supported best by a mixture of basolateral glucose and acetate, whereas HCO_3^- secretion was fully supported by either glucose or acetate. HCO_3^- secretion (but not Na^+ transport) was supported to some extent by luminal glucose. In sum, this study indicates that principal cells and intercalated cells have distinct metabolic phenotypes.

MEDULLARY COLLECTING DUCT

Medullary collecting ducts contribute to final urinary acidification. Comparing the outer medullary collecting duct (OMCD) with the CCD, Hering-Smith and Hamm⁵⁷ found that bicarbonate secretion in the OMCD could be fully supported by endogenous substrates. This region has far less sodium transport and few mitochondria (see Fig. 5.5). Stokes and colleagues⁵⁸ isolated IMCDs and examined their metabolic characteristics. In the absence of exogenous substrate, IMCD can maintain cellular ATP and respire normally, which is evidence for the presence of significant endogenous substrate. In the presence of rotenone, an inhibitor of oxidative phosphorylation, glycolysis increased 56%, which provides evidence for anaerobic metabolism, as supported by enzymatic profiles. Inhibition of sodium pump activity reduced QO_2 by 25% to 35%, which provides evidence for a requirement

for a linkage between sodium pump activity and oxidative metabolism.

In studies that examined the metabolic determinants of K^+ transport in isolated IMCD,¹² glucose increased both oxygen consumption and cell K^+ content by more than 10%, whereas an inhibitor of glycolysis promoted a release of cell K^+ . Nor could cell K^+ content be maintained during inhibition of mitochondrial oxidative phosphorylation. Thus, in the IMCD, both glycolysis and oxidative phosphorylation are required to maintain optimal Na^+-K^+ -ATPase activity to preserve cellular K^+ gradients. Given the low PO_2 and low density of mitochondria in this region, the collecting ducts have a higher reliance on anaerobic metabolism, but still take advantage of oxidative metabolism to fully support transport.

SEXUAL DIMORPHIC PATTERN OF TRANSPORTERS ALONG THE NEPHRON AND METABOLIC CONSIDERATIONS

For 30 years, sex differences in renal hemodynamics, including lower GFR and higher RVR in females, and similar blood pressures between sexes, have been recognized in experimental rodents.⁵⁹ Immunoblots coupled to physiologic assays in rats indicate that females, versus males, exhibit a distinct transporter profile of lower proximal transporters' abundance and HCO_3^- reabsorption coupled to higher distal NCC and ENaC activation⁶⁰ (Fig. 5.11). This shift in T_{Na} from the energetically efficient PT to the costlier distal nephron is predicted to decrease sodium transport energy efficiency ($T_{\text{Na}}/\text{QO}_2$) in females. A rationale for this downstream shift in T_{Na} can be found in female biology. Pregnancy, and even more so lactation, represent major challenges to fluid homeostasis in females. The proximal tubule, which is shorter at baseline in females versus males,⁶¹ lengthens during lactation, driving a proportional increase in T_{Na} in a region where transport efficiency is very high due to paracellular T_{Na} .^{61,62} These significant sex- and reproduction-dependent differences in renal transport function likely necessitate differences in nephron region-specific metabolism that warrant serious future consideration.

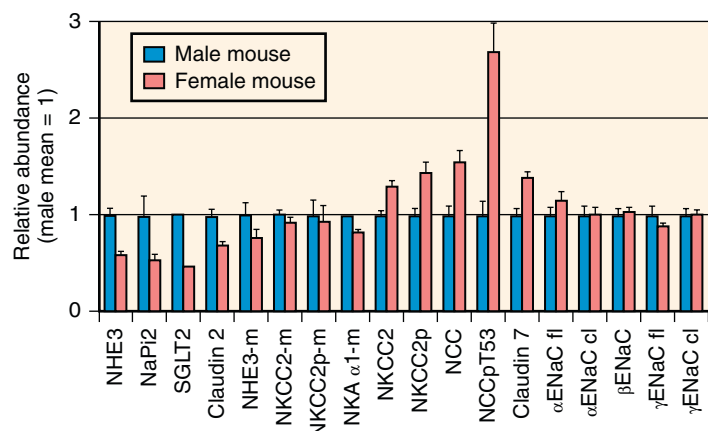


Fig. 5.11 Profile of renal sodium transporter protein abundance in female C57BL/6 mice expressed relative to abundance in male mice (defined as 1.0). Cortical and medullary (-m) samples were detected by immunoblot: Na^+/H^+ exchanger isoform 3 (NHE3), Na^+ -phosphate cotransporter isoform 2 (NaPi2), Na^+ -glucose cotransporter (SGLT2), claudin 2, $\text{Na}^+-\text{K}^+-2\text{Cl}^-$ cotransporter isoform 2 (NKCC2 and activated phosphorylated form NKCC2p), Na,K -ATPase α catalytic isoform, Na^+-Cl^- cotransporter (NCC and activated phosphorylated form NCCp), claudin 7, epithelial Na^+ channel α,β,γ subunits full length (fl), and activated cleaved (cl) forms. (Adapted from Veiras et al.⁶⁰ and Pastor-Soler and Hallows KR¹⁹².)

CONTROL OF RENAL OXYGENATION

The kidneys are faced with the challenge of maintaining intrarenal oxygen levels so as to avoid both hypoxia, which leads to energy failure, and hyperoxia, which promotes oxidant damage.⁶³ Determinants of renal oxygenation and tissue oxygen tension (Po_2) include (1) RBF and oxygen content of arterial blood; (2) the oxygen consumed by the cells; and (3) arterial-to-venous (AV) oxygen shunting, which entails the diffusion of oxygen from preglomerular arteries to postglomerular veins without being available to the cell for consumption.

RENAL BLOOD FLOW, OXYGEN CONSUMPTION, AND AV OXYGEN SHUNTING

The kidney enjoys a high blood flow, nearly 25% of the cardiac output, which is needed to sustain GFR. Compared with other major body organs, renal QO_2 (product of RBF and renal oxygen extraction) per gram of tissue is high, second only to the heart (2.7 mmol/kg/min vs. 4.3 mmol/kg/min for the heart).¹ Renal QO_2 is largely driven by the high RBF because renal oxygen extraction itself is low. Although RBF is high and renal oxygen extraction is low, the renal cortex is vulnerable to hypoxia.⁶⁴ It has been hypothesized that renal AV oxygen shunting is an adaptation to prevent hyperoxia in the setting of the high renal perfusion needed to sustain GFR. However, such shunting can be detrimental in conditions of oxygen demand-supply mismatch.⁶³

The phenomenon of O_2 shunting from descending to ascending vasa recta in the medulla has been accepted,⁶⁵ yet little else is known regarding the location of shunting in the cortex or its impact on oxygenation. Evidence for AV O_2 shunting in the kidney cortex was provided when it was shown, using oxygen-sensing microelectrodes, that the oxygen tension is substantially higher in the renal vein (50 mm Hg) than in efferent arterioles (45 mm Hg) or tubules (40 mm Hg).^{67,68} The fraction of oxygen subject to preglomerular AV O_2 shunting and impact on delivery of O_2 to the renal cortex was recently examined by independent groups using computer model simulations. A 2015 study concluded that preglomerular O_2 shunting was negligible and unlikely to impact renal oxygenation.⁶⁹ The issue was raised that the model may not have sufficiently considered the impact of wrapped artery–vein pairs (with short diffusion and no O_2 sink) that would facilitate AV O_2 shunting.⁷⁰ A 2017 study examining the preglomerular AV O_2 shunting concluded that although the AV shunting would have only a small impact under baseline conditions, it would exacerbate hypoxia during renal ischemia.⁷¹

Noting the similarity of tissue Po_2 in the kidney and in other organs, some have argued that the renal AV O_2 shunt is an adaptive mechanism for preventing the exposure of cortical tubules to toxic levels of oxygen while permitting a high RBF, which is needed for clearance.⁷² As mentioned earlier, there is substantial shunting of oxygen from descending to ascending vasa recta in the renal medulla due to countercurrent flow in these vessels. Countercurrent flow in “hairpin loops” formed by the vasa recta facilitates the recycling of solutes to the inner medulla, where a high osmolarity is essential to the formation of concentrated urine

(see Chapter 10). As an inherent consequence of this countercurrent mechanism for maintaining a medullary osmotic gradient, there arises a negative oxygen gradient from cortex to inner medulla, where Po_2 falls to 10 mm Hg.⁷³ This results from the combination of slow blood flow through the vasa recta, O_2 consumption by active transport in the outer medullary TAL, and diffusion of O_2 from descending to ascending vasa recta.⁷³ This leaves the medullary tissue at the brink of hypoxia, especially the stripe of outer medulla where the S3 segment of the proximal tubule and medullary TAL lie, making these segments most vulnerable to ischemic injury as they reabsorb significant fractions of filtered Na^+ .

Consideration of O_2 transport was incorporated into a mathematical model of the rat outer medulla by Chen and colleagues.^{74,75} The model takes into account fine details of the medullary anatomy, which includes positioning of the long descending vasa recta in the center of vascular bundles and the positioning of the TAL and collecting ducts at some distance from those vascular bundles. The model predicts steeply declining O_2 gradients from vascular bundles to the corresponding TALs and a compromise between the TAL and inner medulla with respect to the provision of oxygen.⁷⁶

In most organs, tissue oxygen can be stabilized by metabolic regulation of blood flow. In such an arrangement, vasoactive end products of metabolism due to increased metabolic activity and oxygen utilization produce a signal that results in more blood flow to that organ. A unique feature of renal oxygenation is that the kidney cannot rely on this simple mode of metabolic autoregulation because, unlike other organs that receive blood solely to supply the metabolic needs of the organ, the kidney also receives blood to perform the functions of glomerular filtration and tubule transport.

RBF creates its own demand because it determines GFR, which in turn determines the rate of sodium reabsorption, which is the main determinant of QO_2 .^{77,78} If the kidneys were to modulate RBF as a means of stabilizing renal O_2 content, this would create a vicious cycle of positive feedback in which increased O_2 delivery would increase O_2 consumption, which would call for more O_2 delivery. Positive feedback is inherently destabilizing, so this arrangement alone could not work to stabilize either RBF or renal O_2 content. Hence, the kidney is compelled to invoke mechanisms that are more complex. There are two generic routes for the kidney to stabilize its O_2 content. One is to dissociate RBF from GFR. The other is to alter the metabolic efficiency of Na^+ transport (Table 5.2). Further details are discussed shortly.

Ultimately, the rate at which the kidney consumes oxygen must be linked to GFR. This is true because the main use

Table 5.2 Mechanisms for Changing the Amount of Oxygen Consumed per Work Performed

- Dissociate glomerular filtration rate from renal blood flow.
- Alter the amount of O_2 consumed per Na^+ reabsorbed.
- Shift transport between tubular segments that make more or less use of passive reabsorption.
- Alter back-leak permeability of the tubule.
- Change the coupling ratio of adenosine triphosphate generated to O_2 consumed by mitochondria.

of oxygen is to support the reabsorption of the filtered sodium, which is linked to GFR by glomerulotubular balance (GTB). GTB describes the direct effect of the filtered load on tubular reabsorption, and it operates in all nephron segments, although the mechanism differs between segments. In the proximal tubule, shear strain tied to increased tubular flow exerts torque on the apical microvilli, which leads to upregulation of apical sodium transporters.^{79,80} In cases in which filtration fraction increases, the parallel increase in peritubular capillary oncotic pressure will increase the Starling force driving fluid reabsorption. In the TAL, flux through NKCC2 is limited by chloride concentration, which declines more slowly along the TAL at high flow rates. But although GTB applies to net reabsorption, increased flow rate in the tubule also shortens the time that a given sodium ion is exposed to the reabsorptive machinery. This leads to the prediction that GTB can do no better than maintain constant fractional reabsorption.⁷⁸

TUBULOGLOMERULAR FEEDBACK

Significant fluctuations in RBF, GFR, and filtered Na^+ load would overwhelm the kidney's ability to accurately match Na^+ and volume output to input and compromise homeostasis of extracellular fluid volume. This does not normally occur because RBF and GFR are tightly controlled by the tubuloglomerular feedback (TGF) mechanism (described in detail in Chapter 3). In short, if RBF and/or GFR increases and GTB maintains a constant fractional reabsorption along the proximal tubule, an increasing amount of salt will be delivered to the macula densa, which sets off the TGF response. Specifically, increases in apical NaCl delivery or flow to this region provoke the cells of the macula densa to release ATP into the interstitium surrounding the afferent arterioles. This response is dependent on the basolateral Na^+/K^+ -ATPase to maintain the inward-directed Na^+ gradient.⁸¹ ATP release is via maxi-anion channels.⁸² Some fraction of the released ATP is converted to adenosine by local ecto-nucleoside triphosphate diphosphohydrolase 1 (ecto-NTPDase1) and ecto-5'-nucleotidase.⁸³ This adenosine activates A_1 adenosine receptors on the afferent arteriole, causing vasoconstriction. The arteriolar constriction reduces RBF and GFR in concert until Na^+ delivery to the macula densa is realigned. Thus, an inverse relationship is established between tubular NaCl load and the GFR of the same nephron.⁷⁷

Due to the time it takes for information to pass through the TGF system, the system is prone to oscillate with a period of around 30 seconds. Rhythmic oscillations of kidney PO_2 occur at the same frequency as TGF-mediated oscillations in tubular flow. This illustrates the simultaneous influence of TGF over minute-to-minute tubular flow rate and oxygen levels in the kidney.⁸⁴

Adenosine mediates TGF as a vasoconstrictor. Adenosine-mediated vasoconstriction is unique to the afferent arteriole. In all other beds where adenosine is vasoactive, it exerts a vasodilatory effect mediated by A_2 receptors. In addition to adenosine receptors, the afferent arteriole expresses $\text{P}_{2\text{x}}$ purinergic receptors that also mediate a vasoconstrictor response, in this case to interstitial ATP. These $\text{P}_{2\text{x}}$ receptors are essential to pressure-mediated RBF autoregulation,⁸⁵ but adenosine A_1 receptors are sufficient to explain the TGF response.⁸³

Adenosine also plays an important role in stabilizing medullary energy balance through local adjustments in blood flow and transport along with other autocrine and paracrine factors, including vasodilatory prostaglandins and nitric oxide, which increase medullary blood flow while inhibiting sodium transport in the TAL.^{48,86,87} Adenosine, in particular, is a case study in local metabolic regulation by negative feedback in the medulla. When ATP levels decline, adenosine is released from TAL cells into the renal interstitium, where it binds to adenosine A_1 receptors and inhibits Na^+ reabsorption in the TAL and IMCD. This has the effect of increasing PO_2 by reducing QO_2 . The same pool of adenosine also activates vascular adenosine A_2 receptors in the deep cortex and medullary vasa recta to increase blood flow.^{88,89}

By these mechanisms, the TAL looks after its own interest. But because TAL sodium reabsorption normally exceeds the urinary sodium excretion by 40-fold, any significant decline in TAL reabsorption must be compensated for by increasing active transport somewhere else or by reducing GFR through TGF. Activation of A_1 receptors in the glomerulus, proximal tubule, or TAL contributes to lessening the amount of work imposed on the hypoxic outer medulla, whereas activating A_2 receptors in the vasa recta supports O_2 delivery to the medulla (summarized in Fig. 5.12).

METABOLIC COST OF SODIUM REABSORPTION

The cost of renal sodium transport can be estimated from the sodium pump stoichiometry and the amount of oxygen required to produce ATP. Sodium pump stoichiometry dictates that hydrolysis of one ATP molecule is coupled to the transport of 3 Na^+ ions out of the cell and 2 K^+ ions into the cell,⁴ and oxidative metabolism generates approximately 6 ATP molecules per O_2 molecule consumed (see Table 5.1 and Fig. 5.4). In the 1960s, several investigators undertook measuring the metabolic cost of tubular reabsorption in various species of mammals. There is fair consensus among four oft-cited studies published between 1961 and 1966 that the relationship between QO_2 and T_{Na} is linear and that the kidney reabsorbs 25 to 29 Na^+ ions per molecule of O_2 consumed in the process.^{90–93} A representative figure from one of these studies is shown in Fig. 5.13.

If one assumes that kidney mitochondria make 6 molecules of ATP per molecule of O_2 , the kidney must then reabsorb 4 to 5 Na^+ per ATP molecule. This exceeds the 3:1 stoichiometry of the Na^+/K^+ -ATPase, which was known at the time (reviewed in Burg and Good).⁹⁴ Because there are thermodynamic difficulties with the idea of an undiscovered basolateral sodium pump capable of forcing 5 Na^+ from a tubular cell with energy from a single ATP molecule, it was surmised that a considerable fraction of overall sodium reabsorption must be passive and paracellular, as is now accepted.

It was later suggested, by Cohen⁴³ and others, that these calculated ratios of $\text{QO}_2/\text{T}_{\text{Na}}$ actually underestimate the true efficiency of sodium reabsorption because a fraction of the oxygen consumed during Na^+ transport is also spent metabolizing organic substrates that enter the cell by Na cotransport. The most important example of this is lactate, which is converted to glucose in the proximal tubule via the Cori cycle. The capacity for renal gluconeogenesis from lactate is large, and it has been estimated that the kidney can consume

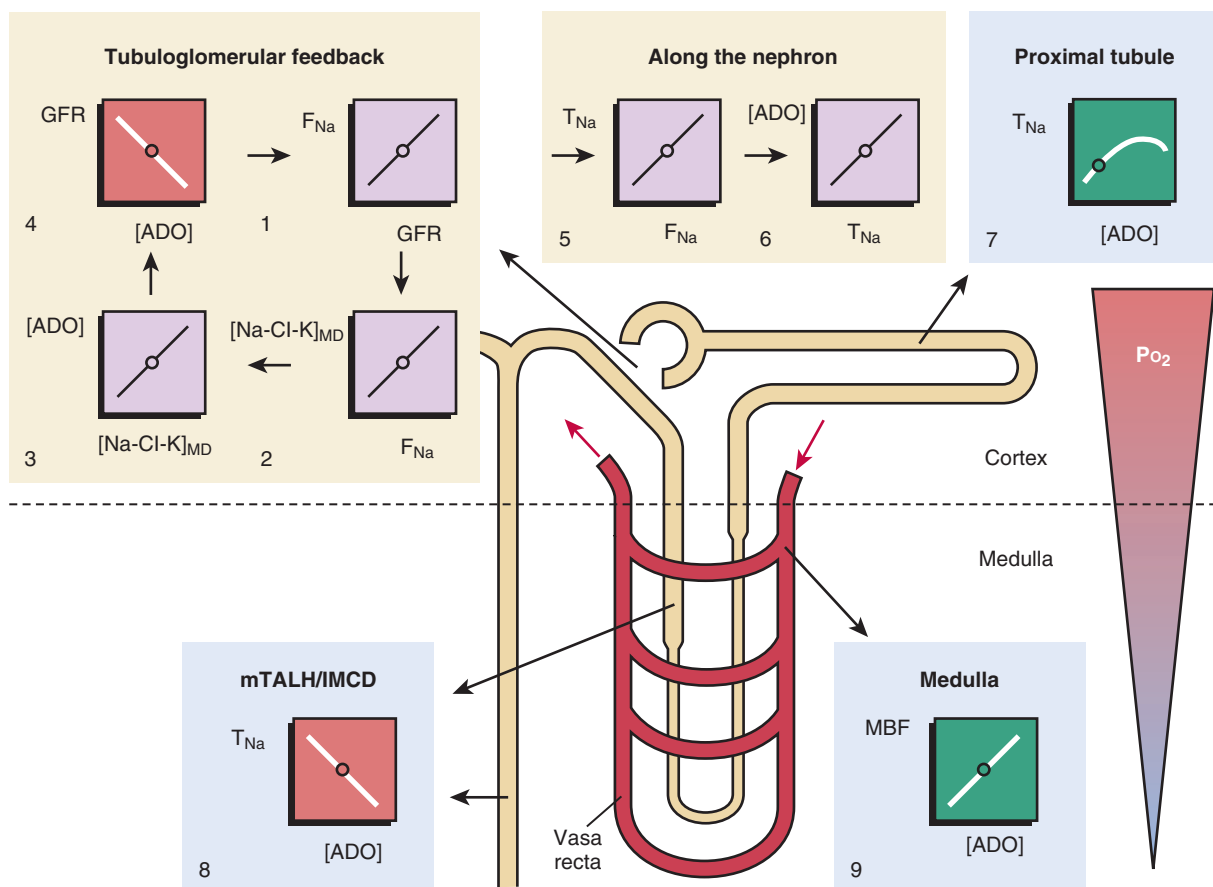


Fig. 5.12 Role of extracellular adenosine (ADO) in protecting the renal medulla from hypoxia. The line plots illustrate the relationships between the given parameters. Small circles on these lines indicate ambient physiologic conditions. (1) A rise in glomerular filtration rate (GFR) increases the Na^+ load (F_{Na}) to the tubular system in cortex and medulla. (2) This rise in F_{Na} increases the salt concentration sensed by the macula densa ($[Na\text{-Cl-K}]_{MD}$). (3) The increase in $[Na\text{-Cl-K}]_{MD}$, in turn, enhances local ADO. (4) ADO lowers GFR and thus F_{Na} , which closes a negative feedback loop and thus provides a basis for an oscillating system. (5) F_{Na} determines Na^+ transport work (T_{Na}) and O_2 consumption in every nephron segment, and thus oscillations in F_{Na} may help protect the medulla. (6) A rise in T_{Na} increases ADO along the nephron. (7) In the cortical proximal tubule, ADO stimulates T_{Na} and thus lowers the Na^+ load to segments residing in the medulla. (8) In contrast, ADO inhibits transport work in the medulla, including medullary thick ascending limb (mTAL) and inner medullary collecting duct (IMCD). (9) In addition, ADO enhances medullary blood flow (MBF), which increases O_2 delivery and further limits O_2 -consuming transport in the medulla. (Modified from Vallon V, et al. Adenosine and kidney function. *Physiol Rev*. 2006;86:901–940.)

up to 25% as much energy converting lactate to glucose as it spends reabsorbing sodium.⁴³

The metabolic cost of active sodium transport is expected to vary along the nephron. As reviewed earlier, the overall stoichiometry of Na^+ reabsorbed to O_2 consumed is estimated at 25 to 30 (microequivalents Na^+ /micromoles O_2).^{90,92} This ratio translates to 5 Na^+ reabsorbed for every ATP molecule consumed, which is much higher than the ratio of 3 Na^+ to every ATP molecule predicted by sodium pump stoichiometry. In fact, one might expect a ratio lower than 3 because of the basal metabolic functions of the kidney that are independent of sodium transport (i.e., insensitive to the $\text{Na}^+\text{-K}^+$ -ATPase inhibitor ouabain) (Fig. 5.14) and because of tubular back-leak.

One reason for this higher than expected efficiency of sodium reabsorption is that the kidney can leverage excess free energy in the gradients created by primary and secondary active transport to drive passive paracellular reabsorption of sodium chloride. The paracellular route in the proximal

tubule responsible for sodium reabsorption is the tight junction protein channel claudin-2.⁹⁵ Free energy for paracellular reabsorption is available in the mid-proximal tubule and early TAL.⁹⁴ In the proximal tubule, the driving force for the passive transport develops as a result of the preferential absorption of bicarbonate over chloride earlier in the tubule.^{96,97}

The decline in tubular bicarbonate concentration is paralleled by a rise in chloride concentration as water follows Na^+ , HCO_3^- , and organic osmoles across the leaky proximal tubule (see Chapter 5). This favorable lumen-to-blood Cl^- gradient drives passive paracellular chloride reabsorption. The transepithelial voltage that arises from electrodiffusion of chloride, in turn, drives passive sodium reabsorption. Because the NaCl reflection coefficient is less than that for NaHCO_3 in this region,⁹⁶ coupled sodium chloride reabsorption also occurs secondary to solvent drag.⁹⁸ Although estimates vary, this passive reabsorption may increase the number of Na^+ ions reabsorbed to O_2 molecules consumed in the proximal tubule from 18 to 48.⁹⁹ As discussed in a previous section,

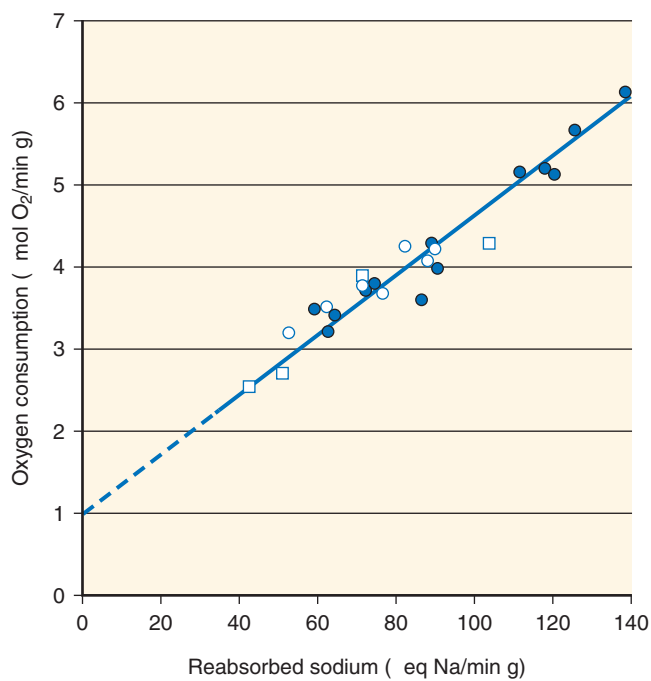


Fig. 5.13 Oxygen consumption as a function of net sodium reabsorption in whole dog kidney. Filled circles, control; open circles, hypoxia; squares, hydrochlorothiazide. The slope of the line fitted to the data points represents QO_2/T_{Na} and is approximately 1/28. (Modified from Thurau K. Renal Na-reabsorption and O₂-uptake in dogs during hypoxia and hydrochlorothiazide infusion. *Proc Soc Exp Biol Med*. 1961;106:714–717; and Mandel LJ, Balaban RS. Stoichiometry and coupling of active transport to oxidative metabolism in epithelial tissues. *Am J Physiol*. 1981;240[5]:F357–F371.)

Components of renal epithelial oxygen consumption

| | |
|-------------------------------|---|
| (Q _{O₂}) | Ouabain sensitive <ul style="list-style-type: none"> • Primary active transport <ul style="list-style-type: none"> - Na⁺-K⁺-ATPase • Coupled transport <ul style="list-style-type: none"> - Secondary Na-coupled transport - Tertiary coupled transport |
| | Ouabain insensitive (basal) <ul style="list-style-type: none"> • Primary and secondary active transport <i>not</i> coupled to Na⁺-K⁺-ATPase • Cell repair, growth • Synthetic functions <ul style="list-style-type: none"> - Lipid synthesis - Gluconeogenesis • Substrate interconversions |

Fig. 5.14 A large fraction of renal epithelial oxygen consumption (Q_{O₂}) in renal cells is sensitive to the Na⁺-K⁺-ATPase-specific inhibitor ouabain, and this Q_{O₂} drives primary active transport and transport coupled to sodium pump activity. The fraction of renal oxygen consumption that does not change in the presence of ouabain is, by definition, independent of Na⁺-K⁺-ATPase activity in the cell and is roughly equivalent to the basal Q_{O₂}, which fuels transport not coupled to sodium gradients, cell repair and growth, biosynthesis, and substrate interconversions.

blunting paracellular reabsorption in the claudin-2-null mouse increases the oxygen consumption cost of T_{Na} by shifting it from paracellular to transcellular reabsorption, supporting the idea that paracellular transport is required for energy efficiency of oxygen utilization in the service of the large fraction of Na⁺ reabsorption that occurs in the proximal tubule.⁵⁵

Simultaneously blocking both cytosolic and membrane carbonic anhydrase with acetazolamide reduces bicarbonate reabsorption and Q_{O₂} in a 16:1 molar ratio as expected for simple coupling to the sodium pump.¹⁰⁰ But inhibiting bicarbonate reabsorption with a membrane-specific carbonic anhydrase inhibitor, which acidifies the tubular lumen, paradoxically increases Q_{O₂} both *in vivo* and in isolated proximal tubules, an effect that is prevented by also blocking the apical Na⁺/H⁺ exchanger NHE3.¹⁰¹ A simple explanation is lacking for why increasing the cell-to-lumen proton gradient should increase Q_{O₂} in the proximal tubule, but these results establish the phenomenon *in vitro* and *in vivo*.

The early portion of the TAL is also capable of paracellular Na⁺ reabsorption. In this region, Na⁺ can be transported transcellularly by the apical Na-K-2Cl cotransporter or apical Na⁺/H⁺ exchanger, secondary to a high density of Na⁺-K⁺-ATPase extruding Na⁺ across the basolateral membranes. In addition, Na⁺ can be reabsorbed paracellularly as long as there is a lumen-positive transepithelial voltage sufficient to overcome the force for back diffusion associated with an unfavorable concentration difference. A lumen-positive voltage develops in the TAL because the apical membrane has a high concentration of K⁺ channels, whereas the basolateral membrane has both K⁺ and Cl⁻ channels. As predicted by the Goldman-Hodgkin-Katz voltage equation, the chloride conductance causes the basolateral membrane potential to be less negative than the apical membrane potential, which results in a positive transepithelial gradient.^{102,103}

Further along the nephron in the distal tubule and collecting duct, the tubular fluid sodium concentration is too low to allow paracellular reabsorption of sodium. In those segments, a lower limit on the cost of Na⁺ reabsorption is set by the 3 Na⁺/1 ATP ratio of the sodium pump. Although active transport of sodium is a pacemaker for renal respiration, there are ways to reset the relationship of Q_{O₂} to sodium pump activity. Examples of this were provided by Silva and Epstein, who measured both O₂ consumption and Na⁺-K⁺-ATPase activity in rat kidney slices in which an increase in the latter had been induced by prior treatment of the animals with triiodothyronine (T₃), methylprednisolone, potassium loading, or subtotal nephrectomy. Although each of these maneuvers increased *ex vivo* sodium pump activity, only T₃ and methylprednisolone increased Q_{O₂}.¹⁰⁴

It has also been shown that the thermogenic effect of catecholamines, normally associated with brown fat and striated muscle, also occurs in the kidney, which responds to dopamine infusion with a near doubling of overall metabolic rate, but minimal change in sodium reabsorption.¹⁰⁵ Dopamine inhibits Na⁺ reabsorption in the proximal tubule,^{106,107} thereby shifting the reabsorptive burden to less efficient downstream segments. However, heat accumulates in both cortex and medulla during dopamine infusion, which suggests that the mechanism may be a direct effect of catecholamines on renal metabolism. In addition, an increase in RBF

by dopamine could be responsible for the increased renal oxygen consumption, which is the product of RBF and renal oxygen extraction.

Weinstein and Szyjewicz^{108,109} also examined QO_2/T_{Na} using 10% body weight short-term saline expansion as another way to inhibit proximal Na^+ reabsorption in rats. This maneuver reduced fractional Na^+ reabsorption by 30% in the proximal tubule, leading to a GTB-mediated increase in net reabsorption downstream of the proximal tubule. Yet overall QO_2 did not increase but actually fell. It was conjectured that energy for this increase in downstream reabsorption was derived anaerobically, but the full details of this remain to be clarified. It appears that the energy cost of transport in the proximal versus distal nephron during inhibition of proximal tubule transport depends on the nature of the stimulus provoking the change in transport as well as the metabolic environment.

Energetic efficiency of Na^+ reabsorption is highly variable along the nephron, in large part due to the presence of paracellular pathways for reabsorption in “leaky” epithelia such as the proximal tubule that can take advantage of favorable concentration and electrochemical gradients to reabsorb Na^+ without requiring ATP hydrolysis. Thus, if proximal reabsorption is lower (as in females) or reduced, the shift of T_{Na} to more distal sites should provoke an increase in QO_2 driven by higher active uphill transcellular Na^+ reabsorption. The example of the cldn-2 null mouse is provided earlier as an example.⁵⁵ Layton et al. now provide computational models that assess how shifting T_{Na} from one region to another or inhibiting T_{Na} in a region-specific manner alters overall QO_2 .^{110,111} In this model, increasing single-nephron GFR did not alter the efficiency of reabsorbing Na^+ in the proximal tubule (T_{Na}/QO_2) while it increased T_{Na}/QO_2 downstream secondary to higher paracellular T_{Na} due to higher luminal $[Na^+]$. This finding suggests that the proximal S3 segment and medullary thick ascending limb (which are vulnerable to hypoxia) are buffered from higher QO_2 in response to increased flow and substrate delivery.¹¹⁰ When the model was applied to an examination of the effects of inhibiting individual transporters, the impact of inhibiting the proximal tubule NHE3 was most pronounced, not unexpected given the fact that the NHE3 reabsorbs 36% of filtered Na^+ at baseline. Overall, inhibiting NHE3 by 80% reduced GFR by 30% (mediated by TGF) and reduced whole kidney T_{Na}/QO_2 by 20%, explained by far less proximal paracellular T_{Na} and the shift of T_{Na} to less efficient distal regions. Interestingly, the model predicts that NHE3 and NKCC2 inhibition increase CNT and CD ENaC-mediated T_{Na}/QO_2 secondary to increased luminal Na^+ . Inhibition of NKCC2, NCC, or ENaC, although changing urine volume, Na^+ and K^+ excretion as predicted, did not change whole kidney T_{Na}/QO_2 .¹¹¹

RENAL OXYGENATION AND METABOLISM DURING NORMAL PERTURBATIONS AND DISEASE

The kidneys have developed multiple mechanisms to minimize changes in oxygen delivery and to cope with a reduction in Po_2 . Some of these are specific to the kidney, whereas others are generic to many tissues as discussed next.

PHYSIOLOGIC REGULATION: FILTRATION FRACTION AND QO_2/T_{Na}

As reviewed earlier, there are two generic routes for the kidney to achieve a stable content of O_2 : dissociation of RBF from GFR, and alteration of QO_2/T_{Na} (see Table 5.2). Both routes are subject to regulation. Dissociating RBF from GFR equates to changing the glomerular filtration fraction. This can work to stabilize kidney O_2 because lowering the filtration fraction increases the ratio of supply to demand for O_2 . For nephrons in filtration equilibrium, this requires independent control of the afferent and efferent arterioles, which can be achieved by modulating relative activities of purinergic, angiotensin, nitric oxide, and other signaling systems in the glomerulus. A full discussion of glomerular hemodynamics is available in Chapter 3, but a few features are noted here.

To begin, filtration fraction can be lowered by constricting the afferent arteriole (which reduces net O_2 delivery) or dilating the efferent arteriole (which increases net O_2 delivery). Constricting the afferent arteriole confers initial energy savings by reducing GFR faster than RBF, but there is diminishing return as O_2 delivery declines toward the basal requirement. Dilating the efferent arteriole reduces GFR only when glomerular capillary pressure is low to begin with, such as during hypotension or with high afferent resistance.¹¹² When angiotensin II acts on the afferent and efferent arterioles to stabilize GFR in the face of low blood pressure or high upstream resistance by preferentially constricting efferent arterioles, the kidney is accepting a decrease in the ratio of O_2 supply to O_2 demand. Conversely, adenosine signaling in the glomerulus decreases filtration fraction and so manages to stabilize nephron function without compromising the O_2 supply–demand balance. Adenosine in the nanomolar range constricts the afferent arteriole via high-affinity A_1 adenosine receptors. Higher adenosine concentration dilates the efferent arteriole via low-affinity A_2 adenosine receptors. Interstitial adenosine concentration rises as more NaCl is delivered into the nephron. The prototype for this is the TGF signaling through the macula densa, although other sources are not precluded (see Fig. 5.12). When the kidney is operating in the domain of modest distal delivery, increasing the TGF signal constricts the afferent arteriole. When the kidney is operating in the domain of high distal delivery, further increase causes the efferent arteriole to dilate,¹¹³ which can be viewed as a shift in priority toward maintaining the O_2 supply as the supply diminishes.

The second generic means for stabilizing kidney O_2 is to alter QO_2/T_{Na} . As mentioned earlier, studies in the 1960s established the linear relationship between QO_2 and T_{Na} . Each adopted a similar standard, which was to express suprabasal renal QO_2 as a function of T_{Na} . Suprabasal O_2 consumption was obtained by subtracting from total O_2 consumption the amount required for basal metabolism. The latter was determined by various methods. One method was to plot QO_2 against T_{Na} and then extrapolate to the y -intercept to obtain basal QO_2 . Another approach was to reduce renal perfusion pressure to the point that glomerular filtration ceased, then ascribe the residual measured QO_2 to basal metabolism. These approaches for obtaining basal O_2 consumption have their unique limitations, and both require the dubious assumption that basal metabolism is static under most conditions and is unaffected by T_{Na} per se. Nonetheless,

these studies attempted to measure and incorporate the contribution of basal QO_2 to the total QO_2 . In the recent literature, the ratio of total QO_2 to T_{Na} has been represented as an index of metabolic efficiency of transport, ignoring the contribution of basal QO_2 to the total QO_2 . This can lead to inaccuracies as estimates of basal metabolism have varied widely in the published literature, indicating its susceptibility to different experimental conditions.¹¹⁴ For example, the proximal tubule can devote considerable energy to gluconeogenesis, especially in the postabsorptive or fasting states, and in diabetes.^{41,115,116} In light of the fact that oxygen can be diverted to do other work, an increase in $\text{QO}_2/T_{\text{Na}}$ is not necessarily due to “decreased transport efficiency.”

The specific factors contributing to this $\text{QO}_2/T_{\text{Na}}$ stoichiometry as well as to the basal metabolic rate in the kidney have been the subject of numerous reviews.^{117,118} It is theoretically possible to alter $\text{QO}_2/T_{\text{Na}}$ in a number of ways (see Table 5.2):

1. Transport could be shifted from the proximal tubule, where efficient use of energy from the Na^+/K^+ -ATPase drives passive transport, to other segments where all Na^+ reabsorbed passes through the Na^+/K^+ -ATPase.
2. Tubular back-leak permeability could change, which would affect the number of times that a given Na^+ ion must be reabsorbed to escape excretion into the urine.
3. The ratio of ATP produced per O_2 consumed could be altered by the regulated activity of UCPs (see Fig. 5.3).²⁵
4. ATP could be diverted to gluconeogenesis, such as during fasting.

The same neurohumoral factors that exert well-known effects on glomerular hemodynamics and O_2 supply, including nitric oxide, angiotensin II, adenosine, and catecholamines, also appear to participate in the regulation of kidney metabolism and QO_2 by the tubule. It has been shown^{119,120} that the administration of nonselective nitric oxide synthase (NOS) inhibitors increases $\text{QO}_2/T_{\text{Na}}$. Other experiments suggested that NOS-1 is the specific isoform that regulates this action *in vivo*.¹¹⁹ The changes in QO_2 with NOS inhibition may occur due to (1) a shift in the site of sodium reabsorption to a less efficient nephron segment; (2) decreased efficiency of transport in the proximal tubule (i.e., decrease in the passive component of reabsorption); or (3) less efficient use of O_2 by mitochondria. For example, nitric oxide given directly to a proximal tubular cell is both a proximal diuretic¹²¹ and a competitive inhibitor of O_2 flux through the ETC in mitochondria.¹²²

Most effects of nitric oxide are mediated by cyclic guanosine monophosphate, but the mitochondrial effect is presumed to occur through the competitive inhibition of cytochrome *c* oxidase.^{122–124} Studies in normal rats,¹²⁵ in rats with experimental diabetes,¹²⁶ and in rats with untreated hypertension^{127,128} have found an antagonistic relationship between nitric oxide and angiotensin II in terms of both glomerular hemodynamics and tubular reabsorption. Specifically, systemic NOS blockade causes renal vasoconstriction and activation of TGF, which can be prevented by angiotensin II blockers.

A similar antagonistic relationship appears to exist in control of kidney metabolism as well. Angiotensin II was recently shown to be capable of increasing QO_2 despite lowering T_{Na} .¹²⁹ Rats and mice with angiotensin-induced hypertension exhibit stimulation of sodium transporters from

the cortical TAL to the CD, in regions with higher $\text{QO}_2/T_{\text{Na}}$, and inhibition or no stimulation of sodium transporters in the proximal nephron, where $\text{QO}_2/T_{\text{Na}}$ is lower.^{130,131} Studies in spontaneous hypertensive rats have suggested opposing effects of angiotensin II and nitric oxide on the $\text{QO}_2/T_{\text{Na}}$ ratio in the kidney.¹³² Rats with angiotensin-induced hypertension demonstrated an increased $\text{QO}_2/T_{\text{Na}}$ that was reversed by a mimetic of superoxide dismutase, which is consistent with the theory that many angiotensin II effects are mediated by upregulating the activity of reduced nicotinamide adenine dinucleotide phosphate (NADPH) oxidase.¹²⁹ In addition, there is evidence that angiotensin II contributes to mitochondrial dysfunction and oxygen consumption in aging rats.¹³³

There is also evidence for a self-contained, intrarenal renin-angiotensin system that operates independently of the systemic renin-angiotensin system (RAS).^{134–137} It is possible to dissociate tubular and whole-kidney angiotensin II in the regulation of proximal reabsorption and salt homeostasis.¹³⁷ For example, a low-salt diet activates the systemic RAS and increases renal sodium reabsorption without any measurable increase in intrarenal synthesis of angiotensin II,¹³⁸ whereas a high-salt diet has a predictable inhibitory effect on plasma and whole-kidney angiotensin II but, surprisingly, leads to increased angiotensin II content of proximal tubular fluid. This finding explains why the tonic influence of endogenous angiotensin II over proximal reabsorption fails to decline with consumption of a high-salt diet. Thus, whereas the systemic RAS is oriented toward salt homeostasis, it appears that the tubular angiotensin II system is oriented toward a stable salt delivery beyond the proximal tubule.¹³⁷

The role of angiotensin II in kidney metabolism is implicated in the ablation/infarction remnant kidney model of chronic kidney disease (CKD). Oxygen consumption factored for nephron number or T_{Na} has been shown to be elevated in this model^{139–141} and lowered by various treatments including angiotensin blockade.¹³⁹ A connection has also been established recently between local accumulation of the Krebs cycle intermediate succinate and activation of the RAS.¹⁴² Succinate can accumulate extracellularly when oxygen supply does not match demand. In the extracellular fluid, it can bind to its G protein-coupled receptor, GPR91. Po_2 in the juxtaglomerular region is reduced in the hyperglycemia of diabetes, and succinate levels are very high in urine and renal tissue of diabetic animals. Inhibition of the Krebs cycle’s succinate dehydrogenase complex causes robust renin release. This effect is amplified in high-glucose conditions or with added succinate. In summary, GPR91-mediated signaling in the juxtaglomerular apparatus could modulate glomerular filtration rate and RAS activity in response to changes in metabolism (especially after a meal when glucose level is elevated). Pathologically, GPR91-mediated signaling could link metabolic diseases (such as diabetes) with RAS activation, systemic hypertension, and organ injury.

HYPOXIA AND ISCHEMIA

Intrarenal hypoxia has been proposed as a final common pathway to progression of CKD.¹⁴³ In late stages of CKD, rarefaction of capillaries and other structural changes have been implicated in the decrease in oxygen supply leading to hypoxia. However, intrarenal hypoxia has been demonstrated in the early stages before any structural changes.¹⁴⁴ High

Q_{O_2}/T_{Na} has been postulated to be the etiology of tubular hypoxia in the early stages of CKD.¹³⁹ In early experimental diabetes, decreased tissue oxygen tension (P_{O_2}) has also been demonstrated prior to any structural changes associated with diabetic nephropathy.¹⁴⁵ Various forms of kidney injury, acute and chronic, have demonstrated tissue hypoxia in early and late stages as discussed later in the chapter.

Blood oxygen level-dependent magnetic resonance imaging (BOLD MRI) has been used to measure blood flow, oxygen tension, and regional tissue oxygenation in kidney cortex and medulla in humans with hypertension. The following were compared: kidneys with atherosclerotic renal artery stenosis, the kidneys contralateral with the stenotic kidneys, and kidneys in individuals with essential hypertension with no accompanying stenosis.^{146,147} In the stenotic kidneys, as expected, tissue volume was decreased and blood flow was compromised; however, there was no significant decrease in P_{O_2} in the cortex or deep medulla compared with the contralateral kidney in the same person or compared with kidneys in individuals with essential hypertension. This led the authors to postulate that there was reduced oxygen consumption in the stenotic kidneys. Consistent with this interpretation, furosemide-suppressible Q_{O_2} in the medulla was significantly less in the stenotic kidney than in the contralateral kidney or kidneys in individuals with essential hypertension.¹⁴⁷ The association between tissue hypoxia and renal damage has also been assessed in patients with renal artery stenosis.¹⁴⁸

In diabetic and nondiabetic CKD patients, intrarenal hypoxia correlates with renal pathology.^{149,150} Alterations in renal oxygenation in acute transplant rejection have also been described.¹⁵¹ Recently, the effect of sodium intake on renal tissue oxygenation was investigated.¹⁵² In brief, 1 week of low- Na^+ intake increased renal medullary oxygenation in both normotensive and hypertensive subjects, whereas a high- Na^+ diet reduced medullary oxygenation. Another recent study in patients with CKD and hypertension compared with healthy controls revealed tight regulation of renal oxygenation at rest but altered response to furosemide in both CKD and hypertension groups, suggesting early metabolic changes in hypertension.^{153,154} In many of these studies, furosemide was administered to inhibit tubular reabsorption, which improved medullary oxygenation, demonstrating the significant role of Na reabsorption-driven Q_{O_2} , even in established disease with structural alterations, which impact oxygen delivery.

Assessment of tissue hypoxia in acute kidney injury has largely been described in animal studies. Studies in an ischemia–reperfusion model in rats and pigs demonstrated reduced oxygenation and persistent tissue hypoxia in the early stages after reperfusion,^{155,156} which was more prominent in the outer medullary regions. These studies were limited to early stages after reperfusion (3–4 hours post ischemia). Assessment of tissue oxygenation in later stages could provide important information regarding the role of hypoxia in repair or recovery from AKI and/or transition to CKD. In animal studies of sepsis associated AKI, variability in tissue oxygenation has been reported depending on the animal model, species, or time point after injury.^{157–161} However, increased renal oxygen extraction despite reduction in GFR and filtered load has been described,^{160,161} indicating inefficiency of oxygen utilization and/or changes in basal metabolism of tubular cells. Clinical studies assessing renal oxygenation in AKI are

limited. However, in a set of elegant studies in postcardiac surgery patients with or without AKI, increased renal O_2 extraction and Q_{O_2}/T_{Na} was demonstrated in the AKI group.¹⁶² Improvement in renal oxygenation with loop diuretics due to reduction in tubular transport related Q_{O_2} was also demonstrated.¹⁶³

HYPOXIA-INDUCIBLE FACTOR

One of the major transcription factors mediating the cellular adaptation to hypoxia is the oxygen-sensitive, hypoxia-inducible factor (HIF).¹⁶⁴ A great body of work by Semenza have described the role of HIF as a primary oxygen sensor and regulator of cellular oxygen homeostasis.^{164–167} It accumulates in hypoxic cells, where it acts to regulate gene expression. HIF consists of a labile α subunit (HIF1 α , HIF2 α , HIF3 α) and a constitutive β subunit. These subunits heterodimerize to form a transcriptional complex that translocates to the nucleus and binds to hypoxia response elements of various hypoxia responsive genes.^{168,169} HIF1 α and HIF2 α have been well studied, have similar structures, and have significant overlap in their actions on target genes; however, some target genes appear to be exclusively under the regulation of one or the other. Their renal tissue expression patterns also differ, with predominant expression of HIF1 α in the tubular epithelial cells and HIF2 α in the interstitial fibroblasts and peritubular endothelial cells in the hypoxic kidney.^{170,171} There is limited information regarding the function and actions of HIF-3 α .

During adaptation to hypoxia, HIF1 α and 2 α regulate the expression of many genes that regulate oxygen delivery and consumption. Changes that culminate in a rise in erythropoiesis, vasodilation, and tissue vascularization all increase oxygen delivery.^{172,173} Another set of responses conserve energy by decreasing substrate movement into the tricarboxylic acid cycle, increasing cellular glucose uptake and glycolytic enzymes to increase anaerobic ATP production and shifting the cell towards glycolytic metabolism.¹⁶⁷ HIF-1 α also has significant effects on mitochondrial metabolism; specifically, it diminishes NADH supply to the ETC, induces a subunit switch in complex IV of ETC to optimize its efficiency in hypoxia, and represses mitochondrial biogenesis and respiration.^{174,175} Finally, HIF-1 α also induces mitochondrial autophagy as an adaptive metabolic response to prevent increased levels of reactive oxygen species (ROS) generation and cell death.¹⁷⁶

Recently, HIF-1 α has also been recognized as a regulator of salt transport. High-salt intake increased HIF-1 α expression in the renal medulla.¹⁷⁷ Inhibition of HIF-1 α in the renal medulla decreased medullary blood flow, and blunted urine flow and urinary Na excretion. In the presence of HIF-1 α inhibitor, rats on a high-salt intake developed positive cumulative salt balance and higher blood pressure. Thus, medullary HIF-1 α inhibition on a high-salt intake leads to resetting of pressure natriuresis, Na retention, and salt-sensitive hypertension.¹⁷⁸ HIF-1 α expression has been reported in the medulla in a normal rat,¹⁷⁹ where selective inhibition of medullary HIF-1 induced significant tubulointerstitial damage. Interestingly, HIF-1 expression appeared to correlate with salt transport—an increase noted after an increase in medullary workload and a decrease in expression noted after inhibiting Na transport in the TAL by furosemide administration, which also increased medullary P_{O_2} .¹⁷⁹

HIF activity is regulated by proteasomal degradation during normoxia by von Hippel-Lindau-E3 ubiquitin ligase complex after being hydroxylated by prolyl 4 hydroxylase domains (PHD). Of the three main identified PHDs (1, 2, and 3), PHD2 is the main enzyme that targets HIF for degradation under normoxia.¹⁷⁰ All three PHDs are expressed in the kidney and are found predominantly in the distal convoluted tubule, collecting duct, and podocytes, and levels are depressed during ischemia and reperfusion.^{169,170} HIF activity is also regulated by factor inhibiting HIF (FIH), which inhibits its transcriptional activity by hydroxylating an asparagine residue within the transactivation domain and prevents the binding of coactivators to the HIF transcriptional complex.¹⁶⁶

A tremendous amount of progress has been made in understanding how HIF helps to maintain O₂ homeostasis, and the study of this factor in the kidney under normal physiologic and pathophysiologic conditions. Particularly, the role of HIF stabilization and activation in the kidney to stimulate erythropoietin production has been targeted therapeutically. Structural analogs of 2-oxyglutarate, which are the substrates used by PHDs for HIF hydroxylation, have been developed to reversibly inhibit PHD activity. These analogs are in phase 2 and 3 clinical trials for treatment of anemia by endogenous erythropoietin production in CKD.¹⁸⁰ Recently, the efficacy of Vadarustat, an oral PHD inhibitor, was evaluated in a 20-week, double-blind, randomized, placebo-controlled, phase IIb study in patients with stage 3–5 CKD.¹⁸¹ Hemoglobin levels were increased and maintained in the treatment arm without major adverse effects. Moreover, increased iron mobilization was also reported in patients treated with Vadarustat. Another oral PHD inhibitor, Roxadustat, was evaluated in an open-label, phase IIb study in patients with CKD using different starting doses and frequencies of administration for 16 or 24 weeks.¹⁸² The various dosing regimens were well tolerated and effective in achieving target hemoglobin levels, without the need for additional iron supplementation. The same agent has also shown effectiveness in patients on incident hemodialysis or peritoneal dialysis.¹⁸³ A third agent, GSK1278863, was evaluated in both CKD patients not on dialysis and ESRD patients on dialysis in a 4-week, phase IIa study.¹⁸⁴ It was safe and well tolerated in both populations and produced dose-dependent increases in hemoglobin concentrations in the CKD patients, whereas only the higher dose was effective in maintaining hemoglobin concentrations in the ESRD patients on dialysis. The ease of administration, lower peak plasma erythropoietin levels, and beneficial effects on iron homeostasis make these oral HIF stabilizers attractive alternatives for anemia management in CKD. However, longer-duration trials to study efficacy and safety of these agents in CKD and ESRD patients are needed.

ADENOSINE MONOPHOSPHATE-ACTIVATED PROTEIN KINASE

The energy status of the cell can be detected by the ultrasensitive 5'-adenosine monophosphate (AMP)-activated protein kinase (AMPK), which is a ubiquitously expressed, highly conserved, key energy sensor and regulator of cellular metabolic activity.¹⁸⁵ AMPK consists of a heterotrimer of a catalytic subunit ($\alpha 1$ or $\alpha 2$), together with a beta ($\beta 1$ or $\beta 2$) and a gamma ($\gamma 1$, $\gamma 2$, or $\gamma 3$) regulatory subunit.¹⁸⁵ Cellular energy stress, which can be due to a variety of conditions, such as

nutrient or glucose deprivation, exercise, hypoxia, or ischemia, is detected as a rising concentration of AMP and an increase in the AMP/ATP ratio. AMPK is activated by phosphorylation of the α catalytic subunit on threonine-172 (Thr172) by upstream kinases.¹⁸⁶ The binding of AMP to the γ -regulatory subunit of AMPK increases its activity in three ways: (1) conformational change in AMPK, which allows enhanced phosphorylation of the α catalytic subunit on Thr172 by upstream kinases, thus, activating AMPK; (2) inhibition of dephosphorylation of the catalytic subunit; and (3) direct allosteric activation. These three effects, working in concert, render the system exquisitely sensitive to changes in AMP, and all are antagonized by ATP; thus the importance of the AMP/ATP ratio. AMPK acts as a metabolic checkpoint to facilitate metabolic adaptation to cellular energetic stress by triggering ATP producing pathways such as fatty acid oxidation, glucose uptake, and glycolysis, while inhibiting ATP consuming pathways such as fatty acid synthesis, protein synthesis, and potentially active transport¹⁸⁷ (see Fig. 5.15). AMPK also promotes cellular autophagy, an energy conserving survival mechanism in low energy states by inhibiting mTOR.^{188,189}

There is abundant AMPK expression in the kidney, but the understanding of its impact on energy metabolism and transport in the kidney is just emerging. The role of AMPK

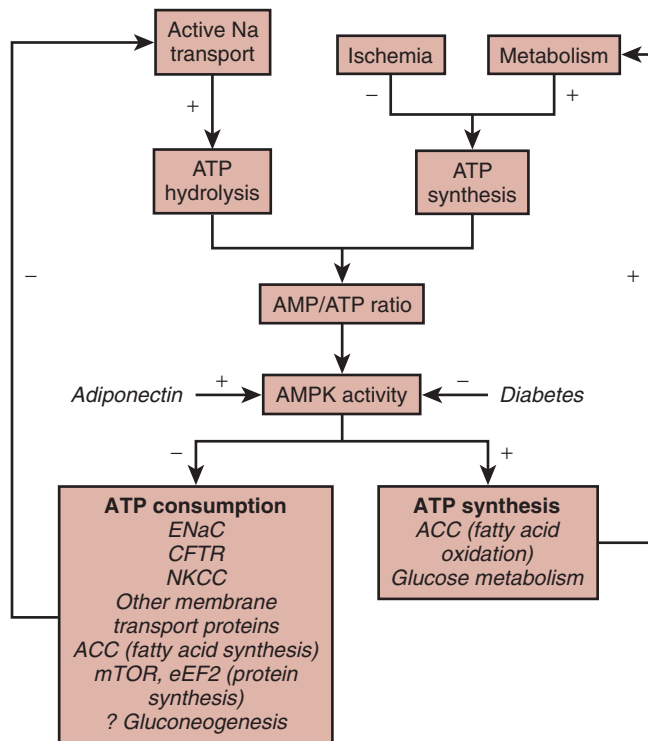


Fig. 5.15 Proposed role of adenosine monophosphate-activated protein kinase (AMPK) in the kidney in coupling catabolic pathways requiring ATP hydrolysis (primarily sodium transport) with metabolic pathways leading to ATP synthesis (primarily fatty acid and glucose oxidation). +, Activating pathway; -, inhibitory pathway. ACC, acetyl-CoA carboxylase. (From Hallows KR, et al. Role of the energy sensor AMP-activated kinase in renal physiology and disease. *Am J Physiol Renal Physiol.* 2010;298:F1067–F1077.)

in ion transport in the kidney has been recently reviewed.^{190,191} Overall, AMPK becomes activated when ATP is limiting, that is, when the AMP/ATP ratio increases, and once activated it decreases ATP consumption and increases ATP synthesis. In the kidney, sodium transport is the major energy-consuming process and there is increasing evidence regarding the role of AMPK in sodium transport in the kidney and other epithelial cells. AMPK has been shown to inhibit the activity of various transport proteins in the lung, gut, and kidney, including epithelial Na channel (ENaC) in the kidney collecting duct, Na-K-2Cl cotransporter (NKCC2) in the thick ascending limb, and Na⁺-K⁺-ATPase in the alveolar epithelial cells, particularly during hypoxia (as reviewed^{191,192}). Hallows and colleagues have determined that AMPK activation depresses transport mediated by the cystic fibrosis transmembrane conductance regulator, the epithelial sodium channel, the vacuolar H⁺-ATPase, and NKCC (see Fig. 5.15). A key question is whether renal AMPK activation suppresses Na⁺-K⁺-ATPase activity along the nephron. AMPK activation has been reported to inhibit lung cell Na⁺-K⁺-ATPase transport activity mediated by endocytosis,¹⁹³ but AMPK activation had no apparent effect on skeletal muscle Na⁺-K⁺-ATPase activity or distribution,¹⁹⁴ which leaves the question open for the kidney, where one report demonstrates that inhibition of AMPK induces the endocytosis of Na⁺-K⁺-ATPase in Madin-Darby canine kidney cells.¹⁹⁵

AMPK expression in the kidney is seen mainly in the cortical thick ascending limb and macula densa cells, and in some distal convoluted tubules and collecting ducts.¹⁹⁶ Recently, AMPK expression in the proximal tubule has also been reported.¹⁹⁷ Differing results in pAMPK expression in response to high salt intake has been observed with increased pAMPK in one study¹⁹⁶ and reduced expression in another.¹⁹⁸ In vivo, pharmacologic activation of AMPK in rats fed a high salt diet was shown to enhance TGF response and reduce sodium reabsorption in the proximal and distal tubule but had no effects on these parameters in rats fed a normal salt diet.¹⁹⁸ Whether these effects are driven by a change in cellular metabolism that results in an increase in AMP/ATP levels is not clear. Consumption of a high salt diet does decrease the fraction of the filtered load of Na⁺ that is absorbed. Given the effect of AMPK activation in inhibiting transporters, the findings suggest that AMPK participates in salt and water homeostasis. The AMPK pathway may provide another important layer of regulation between ATP production by mitochondria and ATP consumption by transporters. In the Whittam model illustrated in Fig. 5.3, increased active transport provokes a decrease in the ATP/ADP ratio, which drives increased ATP production by the mitochondria. When ATP production by the mitochondria becomes limiting, however, AMPK is likely to be activated, which would drive a reduction in ATP consumption by active membrane transporters. Thus, AMPK may regulate the coupling of ion transport and energy metabolism in the kidney.

Regulation of glucose and lipid metabolism by AMPK in pathophysiologic conditions such as diabetic nephropathy and CKD has been elucidated in recent publications. In animal models of CKD, diabetes, and obesity, reduced AMPK activity has been described.^{199–202} Endogenous AMPK activation by targeting adiponectin (adipose tissue-derived cytokine) as well as pharmacologic AMPK activation (metformin, AICAR) has been shown to improve glucose and lipid

homeostasis in diabetes and obesity-associated kidney disease. In a recent paper, significant changes in renal metabolism with the deletion of a major upstream AMPK activator, liver kinase B1 (LKB1), in kidney distal tubules were observed.²⁰³ Expression of AMPK and other key regulators of metabolism were significantly diminished and accompanied by tubular epithelial injury and interstitial fibrosis. In cultured epithelial cells, loss of LKB1 was associated with diminished fatty acid oxidation and glycolysis, leading to energy depletion and apoptotic cell death. In human kidney samples, lower levels of phosphorylated LKB1 and AMPK $\alpha 2$ subunit were seen in CKD patients. Thus, the important role of AMPK in regulating kidney metabolism is being increasingly recognized.

Acute renal ischemia provokes a rapid and powerful activation of AMPK, but its functional role in the response to ischemia remains unclear. There is conflicting evidence in the literature regarding the effects of AMPK activation in renal ischemia-reperfusion injury.^{204–207} Similarly, while several studies show a beneficial effect of AMPK activation in myocardial ischemia-reperfusion, there are some conflicting studies demonstrating deleterious effects of AMPK activation in ischemic injury in the heart and brain (as reviewed¹⁸⁵). Hence, the effects of AMPK activation are likely to be time, tissue, and cell-dependent. Whether AMPK abundance or its phosphorylation is higher in the hypoxia-prone medulla than in the cortex has not yet been investigated, nor have studies been conducted examining the effect of AMPK activation on renal gluconeogenesis or glycolysis.^{193–195}

TUBULAR METABOLISM

Until recently there were limited studies exploring cellular metabolism in pathophysiologic conditions. Several recent publications have highlighted metabolic alterations in various forms of CKD. Moreover, alterations in glucose and fatty acid metabolism as early events in the course of diabetic and other forms of CKD place metabolic reprogramming central to the pathophysiology of CKD.

In mouse models of autosomal dominant polycystic kidney disease (ADPKD) and in kidney tissue from patients with ADPKD, defective glucose metabolism—specifically, increased aerobic glycolysis—was observed.²⁰⁸ Moreover, treatment with 2-deoxyglucose, an inhibitor of glycolysis, lowered kidney weight, volume, cystic index, and proliferation rates in mouse models of ADPKD.²⁰⁹ This phenotypic feature of enhanced aerobic glycolysis, also known as Warburg effect, is typically seen in proliferating cancer cells. In these mice models of PKD gene inactivation, there was inhibition of liver kinase B1 (LKB1)-AMPK axis along with activation of mTOR complex I pathway, leading to increased glycolysis.²⁰⁸

Besides altered glucose metabolism, changes in fatty acid metabolism in the kidney have been described in CKD. In a recent paper, Kang et al. described reduced levels of enzymes and regulators involved in fatty acid oxidation in mouse models of fibrosis.²¹⁰ In transcriptional analyses of microdissected human kidney samples from patients with diabetic or hypertensive CKD changes in fatty acid metabolism, β -oxidation, amino acid catabolism, and carbohydrate metabolism were observed. Genes related to fatty acid metabolism and their key transcriptional regulator complex, PPARA-PPARGC1A, were markedly lower in CKD samples compared with samples obtained from people with normal kidney function. This was

associated with higher lipid accumulation in renal tubular epithelial cells. Key regulators of glucose utilization were also lower in CKD samples. Using elegant experiments with genetic and pharmacologic approaches, the reduction in fatty acid oxidation was shown to be directly implicated in the pathogenesis of renal fibrosis in CKD. Although lipid accumulation in tubular cells in CKD patients has been reported before, these findings showed convincingly that it is the reduction in fatty acid oxidation rather than just the accumulation of lipid in tubular cells that plays a role in the development of renal fibrosis.

Metabolic reprogramming has also been recently reported in diabetic CKD.²¹¹ As discussed earlier, proximal tubules are largely dependent on mitochondrial oxidative metabolism for energy with limited glycolytic capacity. Under physiologic conditions, proximal tubules mainly use fatty acids, lactate, and glutamine as substrates for energy generation. In diabetes, there are increases in plasma concentration of glucose and fatty acids. These changes are also found intracellularly in various tissues including the kidneys, particularly proximal tubules. In an elegant study, Sas et al. provided a comprehensive assessment of substrate metabolism in diabetes using a systems-based approach that included transcriptomics, metabolomics, and metabolic flux analyses to determine alterations in glucose and fatty acid metabolism.²¹¹ In the kidney cortex in a type 2 diabetic mouse model (db/db mice), transcriptomic and metabolomic profiling demonstrated an increase in glycolysis, fatty acid β -oxidation, and tricarboxylic acid (TCA) cycle flux. Increased renal metabolism was associated with increased protein acetylation, which is a nutrient sensing posttranslational modification. There was also evidence for mitochondrial dysfunction as discussed later. Remarkably, transcriptomic analysis of kidney biopsy samples in patients with type 2 diabetes identified significant enrichment of many pathways involved in fatty acid, glucose, and amino acid metabolism and network analysis showed results similar to those obtained in db/db mice. In another cohort of type 1 diabetic patients enrolled in the Finnish Diabetic Nephropathy (FinnDiane) Study, increased glycolytic (hexose-6-phosphates, 2,3-phosphoglycerate) and TCA cycle metabolites (succinate, fumarate, malate) were detected in the urine compared with healthy control subjects. Urine samples from a subset of patients from the Family Investigation of Nephropathy and Diabetes (FIND) study, showed increased glycolytic intermediates at baseline in diabetic subjects compared with control subjects. TCA cycle intermediates in the urine were also elevated in diabetic subjects and predicted diabetic kidney disease progression, demonstrating their potential as prognostic biomarkers of diabetic kidney disease progression. These and previously discussed studies highlight the adaptive and maladaptive metabolic reprogramming and its role in the pathophysiology of diabetic and nondiabetic CKD.

MITOCHONDRIAL DISORDERS

Given the central role of mitochondria in producing ATP via oxidative phosphorylation, it is not surprising that genetic mutations affecting mitochondrial function have renal manifestations. Moreover, several lines of investigation support the significant role of early mitochondrial dysfunction in the pathophysiology of acute and chronic kidney diseases. The

mitochondrial genome is distinct from the nuclear genome, and it encodes 13 of the 88 protein subunits of ETC complexes I through V as well as 22 mitochondrial-specific transfer RNAs (tRNAs) and two RNA components of the translational apparatus. The nuclear genome encodes the remaining respiratory chain subunits as well as most of the mitochondrial DNA replication and expression components.

Disorders affecting mitochondrial oxidative phosphorylation can arise from mutations in either mitochondrial genes or nuclear genes encoding respiratory chain components or ancillary factors involved in maintenance of ETC function or the overall number of mitochondria.²¹² The incidence of genetic mitochondrial disorders is estimated at about 1 in 5000 births, with the most common affecting the sequence of a mitochondrial tRNA for leucine. Such mutations affect mitochondrial function in all tissues. Symptoms are evident before 2 months of age, and the number of organ systems affected increases with age.

Impairment of mitochondrial oxidative phosphorylation results in increased levels of reducing equivalents (NADH, FADH), which, in the mitochondria, transform acetoacetate to 3-hydroxybutyrate and, in the cytosol, transform pyruvate to lactate. Thus, elevated levels of lactic acid, ketone bodies, and impaired redox status are suggestive of a mitochondrial defect disorder.²¹³ If the genetic cause of the impairment can be pinpointed, then an appropriate therapy, if available, can be implemented to treat these life-threatening disorders; for example, coenzyme Q₁₀ enzyme defects can be treated with coenzyme Q₁₀ supplementation.²¹²

Myopathies and cardiomyopathies are the most common manifestations of mitochondrial disease, and central nervous system symptoms, including encephalopathies, are very common. Renal system impairment can be present but is not seen without other system deficiencies and is usually reported in children. Although glomerular disease and tubulointerstitial nephropathy have both been reported, the most frequently observed is impairment of proximal tubule reabsorption, known as de Toni–Debré–Fanconi syndrome, in which there are urinary losses of bicarbonate, amino acids, glucose, phosphate, uric acid, potassium, and water. All of these symptoms can be explained by a lack of ATP to fuel Na⁺-K⁺-ATPase sufficiently to drive transepithelial transport. The symptoms can range from mild to more severe and present in the neonatal period in most patients. Biopsy specimens show tubular dilations, casts, dedifferentiation, and cellular vacuolization. At the cellular level there are enlarged mitochondria. Supplements of sodium bicarbonate, potassium, vitamin D, phosphorus, and water are called for if these symptoms are evident.^{212,213}

Significant changes in mitochondrial function in diabetic kidneys have been described and recently reviewed in detail.^{214,215} Early changes in mitochondrial energetics, increased mitochondrial fragmentation, and reduced levels of PGC1a have been described in diabetic kidneys. In diabetic nephropathy, increased metabolism has been shown to be associated with mitochondrial dysfunction.²¹¹ Assessment of oxidative phosphorylation in mitochondria isolated from renal cortices of 24-week-old control and diabetic mice showed increased proton leak and diminished mitochondrial ATP production. Additionally, total mitochondrial capacity was decreased in diabetic mitochondria, and the expression of mitochondrial uncoupling protein 2 was increased fourfold.

In renal cortices from diabetic mice, expression of proteins in complexes I, II, III, and complex IV subunit cytochrome *c* oxidase subunit 4 (COX4) were significantly decreased at 24 weeks. The results of these studies suggested that dysfunction of ETC proteins in mitochondria from diabetic kidneys lead to less efficient ATP production and compensatory increases in glucose and fatty acid metabolic flux. This may be the primary metabolic abnormality in the diabetic kidney cortex as it precedes other markers of renal injury. Another study compared urine metabolites in patients with diabetes, but with or without CKD and in healthy controls.²¹⁶ Bioinformatic analyses revealed that 12 of the 13 differentially expressed metabolites were linked to mitochondrial metabolism. Kidney sections in patients with diabetes and CKD showed lower expression of mitochondrial proteins and lower gene expression of PGC1a, which is a major regulator of mitochondrial biogenesis. Urine exosomes in these patients also showed less mitochondrial DNA. Evidence of mitochondrial dysfunction in nondiabetic CKD is also emerging. Early changes in mitochondrial function and structure in animal models of CKD has been reported.²¹⁷ In patients with CKD, mRNA levels of several mitochondrial enzymes and transcription factors were found to be lower, although no differences in mitochondrial copy number was seen.²¹⁸ In another clinical study, mitochondrial DNA copy number was evaluated in peripheral blood in a population cohort.²¹⁸ Participants with higher mitochondrial DNA copy numbers had a lower rate of prevalent diabetes and lower risk of incident CKD, even after adjusting for various risk factors for CKD.

The role of mitochondrial dysfunction in AKI has received significant attention. Several publications have elucidated the underlying mechanisms of mitochondrial dysfunction in various etiologies of AKI (reviewed in details²¹⁵). In ischemic and nephrotoxic AKI, decreased mitochondrial mass, disruption of cristae, and significant mitochondrial swelling has been observed.²¹⁹ In ischemic AKI, increase in mitochondrial NADH and dissipation of mitochondrial membrane potential in proximal tubules has been demonstrated.²²⁰ In ischemic and myoglobinuric AKI, reduction in various ETC proteins in the proximal tubule was shown.²²¹ Other studies have uncovered the crucial role of mitochondrial biogenesis using stimulators of PGC1α, master regulator of mitochondrial biogenesis in recovery from ischemic AKI²²² and sepsis-associated AKI.¹⁵⁸ The role of mitochondrial dynamics has also been elucidated in some forms of AKI. In an elegant study, Brooks et al. described the disruption of mitochondrial dynamics and its pathogenic role in ischemic and nephrotoxic AKI.²¹⁹ Mitochondrial fragmentation was shown to precede tubular cell injury and death and pharmacologic inhibition of Drp1 prevented fragmentation and ameliorated AKI. Further highlighting the role of mitochondrial dysfunction, several pharmacologic targets to improve mitochondrial function in AKI and CKD have been investigated and found to be effective.²²³

SUMMARY

Most of the energy consumed by the kidney is traceable to the energy requirements for sodium reabsorption. Although all sodium reabsorption is linked to Na⁺-K⁺-ATPase, efficiency is achieved by leveraging Na⁺-K⁺-ATPase into transepithelial chloride or voltage gradients that allow some sodium to be reabsorbed without passing through the Na⁺-K⁺-ATPase itself. ATP production in the proximal tubule is solely by aerobic metabolism, whereas the medullary segments have additional capacity to produce energy by glycolysis. Transport activity regulates metabolism, metabolism may be rate limiting for transport, and the efficiency of transport can be made to vary at multiple levels from back-leak permeability to the efficiency of mitochondrial respiration. With regard to metabolic autoregulation, the kidney faces a particular challenge because the usual mechanism for delivering more oxygen to the kidney also increases the demand for that oxygen. Several intermediaries have been identified as parts of the complex network of interactions between transport and metabolism that allow the kidney to meet this challenge while balancing the risk of hypoxia against the risk of oxygen toxicity. A partial list of these includes adenosine, nitric oxide, prostaglandins, angiotensin II, dopamine, succinate, uncoupling proteins, HIF, and AMPK. A multiscale systems model that incorporates these elements along with renal anatomy to recapitulate renal metabolism is expected in the future.

 Complete reference list available at ExpertConsult.com.

KEY REFERENCES

24. Mandel LJ. Metabolic substrates, cellular energy production, and the regulation of proximal tubular transport. *Annu Rev Physiol*. 1985;47:85–101.
48. Epstein FH. Oxygen and renal metabolism. *Kidney Int*. 1997;51: 381–385.
60. Veiras LC, Girardi ACC, Curry J, et al. Sexual dimorphic pattern of renal transporters and electrolyte homeostasis. *J Am Soc Nephrol*. 2017;28:3504–3517.
78. Thomson SC, Blantz RC. Glomerulotubular balance, tubuloglomerular feedback, and salt homeostasis. *J Am Soc Nephrol*. 2008; 19:2272–2275.
95. Yu ASL. Paracellular transport and energy utilization in the renal tubule. *Curr Opin Nephrol Hypertens*. 2017;26:398–404.
165. Semenza GL. Hypoxia-inducible factors in physiology and medicine. *Cell*. 2012;148:399–408.
180. Sugahara M, Tanaka T, Nangaku M. Prolyl hydroxylase domain inhibitors as a novel therapeutic approach against anemia in chronic kidney disease. *Kidney Int*. 2017;92:306–312.
185. Steinberg GR, Kemp BE. AMPK in health and disease. *Physiol Rev*. 2009;89:1025–1078.
210. Kang HM, Ahn SH, Choi P, et al. Defective fatty acid oxidation in renal tubular epithelial cells has a key role in kidney fibrosis development. *Nat Med*. 2015;21:37–46.
211. Sas KM, Kayampilly P, Byun J, et al. Tissue-specific metabolic reprogramming drives nutrient flux in diabetic complications. *JCI Insight*. 2016;1:e86976.

REFERENCES

- Cohen N, Kamm DE. *Renal metabolism: relation to renal function*. In: Brenner BM, Rector FC, eds. *The Kidney*. 2nd ed. Philadelphia: W.B. Saunders; 1981.
- Rapoport S, Brodsky WA, West CD. Excretion of solutes and osmotic work of the resting kidney of hydropenic man. *Am J Physiol*. 1949;157:357–362.
- Newburgh JD. The changes which alter renal osmotic work. *J Clin Invest*. 1943;22:439–446.
- Horisberger JD. Recent insights into the structure and mechanism of the sodium pump. *Physiology (Bethesda)*. 2004;19:377–387.
- Skou JC. The identification of the sodium pump. *Biosci Rep*. 2004;24:436–451.
- Geering K. FXYD proteins: new regulators of Na-K-ATPase. *Am J Physiol Renal Physiol*. 2006;290:F241–F250.
- Feraile E, Doucet A. Sodium-potassium-adenosinetriphosphatase-dependent sodium transport in the kidney: hormonal control. *Physiol Rev*. 2001;81:345–418.
- Arystarkhova E, Donnet C, Munoz-Matta A, et al. Multiplicity of expression of FXYD proteins in mammalian cells: dynamic exchange of phospholemmann and gamma-subunit in response to stress. *Am J Physiol Cell Physiol*. 2007;292:C1179–C1191.
- Geering K. Functional roles of Na,K-ATPase subunits. *Curr Opin Nephrol Hypertens*. 2008;17:526–532.
- Katz AI. Distribution and function of classes of ATPases along the nephron. *Kidney Int*. 1986;29:21–31.
- Gumz ML, Lynch IJ, Greenlee MM, et al. The renal H+-K+-ATPases: physiology, regulation, and structure. *Am J Physiol Renal Physiol*. 2010;298:F12–F21.
- Kone BC, Kikeri D, Zeidel ML, et al. Cellular pathways of potassium transport in renal inner medullary collecting duct. *Am J Physiol*. 1989;256:C823–C830.
- Magyar CE, White KE, Rojas R, et al. Plasma membrane Ca²⁺-ATPase and NCX1 Na⁺/Ca²⁺ exchanger expression in distal convoluted tubule cells. *Am J Physiol Renal Physiol*. 2002;283:F29–F40.
- Valles P, Lapointe MS, Wysocki J, et al. Kidney vacuolar H⁺-ATPase: physiology and regulation. *Semin Nephrol*. 2006;26:361–374.
- Wagner CA, Finberg KE, Breton S, et al. Renal vacuolar H⁺-ATPase. *Physiol Rev*. 2004;84:1263–1314.
- Aronson PS. Identifying secondary active solute transport in epithelia. *Am J Physiol*. 1981;240:F1–F11.
- Dantzler WH, Wright SH. The molecular and cellular physiology of basolateral organic anion transport in mammalian renal tubules. *Biochim Biophys Acta*. 2003;1618:185–193.
- McDonough AA. Mechanisms of proximal tubule sodium transport regulation that link extracellular fluid volume and blood pressure. *Am J Physiol Regul Integr Comp Physiol*. 2010;298:R851–R861.
- Lapointe JY, Garneau L, Bell PD, et al. Membrane crosstalk in the mammalian proximal tubule during alterations in transepithelial sodium transport. *Am J Physiol*. 1990;258:F339–F345.
- Sjostrom M, Stenstrom K, Eneling K, et al. SIK1 is part of a cell sodium-sensing network that regulates active sodium transport through a calcium-dependent process. *Proc Natl Acad Sci U S A*. 2007;104:16922–16927.
- Muto S, Asano Y, Seldin D, et al. Basolateral Na⁺ pump modulates apical Na⁺ and K⁺ conductances in rabbit cortical collecting ducts. *Am J Physiol*. 1999;276:F143–F158.
- Mitchell P. Coupling of phosphorylation to electron and hydrogen transfer by a chemi-osmotic type of mechanism. *Nature*. 1961;191:144–148.
- Nelson DL, Cox, Michael M. *Lehninger Principles of Biochemistry*. New York: W.H. Freeman and Company; 2008.
- Mandel LJ. Metabolic substrates, cellular energy production, and the regulation of proximal tubular transport. *Annu Rev Physiol*. 1985;47:85–101.
- Friederich M, Nordquist L, Olerud J, et al. Identification and distribution of uncoupling protein isoforms in the normal and diabetic rat kidney. *Adv Exp Med Biol*. 2009;645:205–212.
- Blond DM, Whittam R. The regulation of kidney respiration by sodium and potassium ions. *Biochem J*. 1964;92:158–167.
- Whittam R. Active cation transport as a pace-maker of respiration. *Nature*. 1961;191:603–604.
- Balaban RS, Mandel LJ, Soltoff SP, et al. Coupling of active ion transport and aerobic respiratory rate in isolated renal tubules. *Proc Natl Acad Sci U S A*. 1980;77:447–451.
- Chance B, Williams GR. The respiratory chain and oxidative phosphorylation. *Adv Enzymol Relat Subj Biochem*. 1956;17:65–134.
- Katz AI, Doucet A, Morel F. Na-K-ATPase activity along the rabbit, rat, and mouse nephron. *Am J Physiol*. 1979;237:F114–F120.
- McDonough AA, Magyar CE, Komatsu Y. Expression of Na(+)-K(+)ATPase alpha- and beta-subunits along rat nephron: isoform specificity and response to hypokalemia. *Am J Physiol*. 1994;267:C901–C908.
- Pfaller W, Rittinger M. Quantitative morphology of the rat kidney. *Int J Biochem*. 1980;12:17–22.
- Guder WG, Ross BD. Enzyme distribution along the nephron. *Kidney Int*. 1984;26:101–111.
- Kone BC. Metabolic basis of solute transport. In: Brenner BM, ed. *Brenner and Rector's The Kidney*. 8th ed. Philadelphia: Saunders; 2008.
- Uchida S, Endou H. Substrate specificity to maintain cellular ATP along the mouse nephron. *Am J Physiol*. 1988;255:F977–F983.
- Burch HB, Narins RG, Chu C, et al. Distribution along the rat nephron of three enzymes of gluconeogenesis in acidosis and starvation. *Am J Physiol*. 1978;235:F246–F253.
- Schmid H, Mall A, Scholz M, et al. Unchanged glycolytic capacity in rat kidney under conditions of stimulated gluconeogenesis. Determination of phosphofructokinase and pyruvate kinase in microdissected nephron segments of fasted and acidotic animals. *Hoppe Seylers Z Physiol Chem*. 1980;361:819–827.
- Schmidt U, Marosvari I, Dubach UC. Renal metabolism of glucose: anatomical sites of hexokinase activity in the rat nephron. *FEBS Lett*. 1975;53:26–28.
- Gerich JE, Meyer C, Woerle HJ, et al. Renal gluconeogenesis: its importance in human glucose homeostasis. *Diabetes Care*. 2001;24:382–391.
- Joseph SE, Heaton N, Potter D, et al. Renal glucose production compensates for the liver during the anhepatic phase of liver transplantation. *Diabetes*. 2000;49:450–456.
- Meyer C, Stumvoll M, Nadkarni V, et al. Abnormal renal and hepatic glucose metabolism in type 2 diabetes mellitus. *J Clin Invest*. 1998;102:619–624.
- Eid A, Bodin S, Ferrier B, et al. Intrinsic gluconeogenesis is enhanced in renal proximal tubules of zucker diabetic fatty rats. *J Am Soc Nephrol*. 2006;17:398–405.
- Cohen JJ. Relationship between energy requirements for Na⁺ reabsorption and other renal functions. *Kidney Int*. 1986;29:32–40.
- Gullans SR, Brazy PC, Dennis VW, et al. Interactions between gluconeogenesis and sodium transport in rabbit proximal tubule. *Am J Physiol*. 1984;246:F859–F869.
- Brooks GA. Cell-cell and intracellular lactate shuttles. *J Physiol*. 2009;587:5591–5600.
- Scaglione PR, Dell RB, Winters RW. Lactate concentration in the medulla of rat kidney. *Am J Physiol*. 1965;209:1193–1198.
- Bagnasco S, Good D, Balaban R, et al. Lactate production in isolated segments of the rat nephron. *Am J Physiol*. 1985;248:F522–F526.
- Epstein FH. Oxygen and renal metabolism. *Kidney Int*. 1997;51:381–385.
- Friedrichs D, Schoner W. Stimulation of renal gluconeogenesis by inhibition of the sodium pump. *Biochim Biophys Acta*. 1973;304:142–160.
- Nagami GT, Lee P. Effect of luminal perfusion on glucose production by isolated proximal tubules. *Am J Physiol*. 1989;256:F120–F127.
- Vallon V, Gerasimova M, Rose MA, et al. SGLT2 inhibitor empagliflozin reduces renal growth and albuminuria in proportion to hyperglycemia and prevents glomerular hyperfiltration in diabetic akita mice. *Am J Physiol Renal Physiol*. 2014;306:F194–F204.
- Sasaki M, Sasako T, Kubota N, et al. Dual regulation of gluconeogenesis by insulin and glucose in the proximal tubules of the kidney. *Diabetes*. 2017;66:2339–2350.
- Layton AT, Vallon V, Edwards A. Modeling oxygen consumption in the proximal tubule: effects of NHE and SGLT2 inhibition. *Am J Physiol Renal Physiol*. 2015;308:F1343–F1357.
- Pei L, Solis G, Nguyen MT, et al. Paracellular epithelial sodium transport maximizes energy efficiency in the kidney. *J Clin Invest*. 2016;126:2509–2518.
- Pei L, Solis G, Nguyen MT, et al. Paracellular epithelial sodium transport maximizes energy efficiency in the kidney. *J Clin Invest*. 2016;126:2509–2518.
- Chamberlin ME, Mandel LJ. Na⁺-K⁺-ATPase activity in medullary thick ascending limb during short-term anoxia. *Am J Physiol*. 1987;252:F838–F843.

155.e2 SECTION I – NORMAL STRUCTURE AND FUNCTION

57. Hering-Smith KS, Hamm LL. Metabolic support of collecting duct transport. *Kidney Int.* 1998;53:408–415.
58. Stokes JB, Grupp C, Kinne RK. Purification of rat papillary collecting duct cells: functional and metabolic assessment. *Am J Physiol.* 1987;253:F251–F262.
59. Munger K, Baylis C. Sex differences in renal hemodynamics in rats. *Am J Physiol.* 1988;254:F223–F231.
60. Veiras LC, Girardi ACC, Curry J, et al. Sexual dimorphic pattern of renal transporters and electrolyte homeostasis. *J Am Soc Nephrol.* 2017;28:3504–3517.
61. Oudar O, Elger M, Bankir L, et al. Differences in rat kidney morphology between males, females and testosterone-treated females. *Ren Physiol Biochem.* 1991;14:92–102.
62. Arthur SK, Green R. Fluid reabsorption by the proximal convoluted tubule of the kidney in lactating rats. *J Physiol.* 1986;371:267–275.
63. O'Connor PM, Anderson WP, Kett MM, et al. Renal preglomerular arterial-venous O₂ shunting is a structural anti-oxidant defence mechanism of the renal cortex. *Clin Exp Pharmacol Physiol.* 2006;33:637–641.
64. Layton AT. Recent advances in renal hypoxia: insights from bench experiments and computer simulations. *Am J Physiol Renal Physiol.* 2016;311:F162–F165.
65. Zhang W, Edwards A. Oxygen transport across vasa recta in the renal medulla. *Am J Physiol Heart Circ Physiol.* 2002;283:H1042–H1055.
66. Deleted in review.
67. Schurek HJ, Jost U, Baumgartl H, et al. Evidence for a preglomerular oxygen diffusion shunt in rat renal cortex. *Am J Physiol.* 1990;259:F910–F915.
68. Welch WJ, Baumgartl H, Lubbers D, et al. Nephron pO₂ and renal oxygen usage in the hypertensive rat kidney. *Kidney Int.* 2001;59:230–237.
69. Olgac U, Kurtcuoglu V. Renal oxygenation: preglomerular vasculature is an unlikely contributor to renal oxygen shunting. *Am J Physiol Renal Physiol.* 2015;308:F671–F688.
70. Evans RG, Smith DW, Khan Z, et al. Letter to the editor: The plausibility of arterial-to-venous oxygen shunting in the kidney: it all depends on radial geometry. *Am J Physiol Renal Physiol.* 2015;309:F179–F180.
71. Lee CJ, Ngo JP, Kar S, et al. A pseudo-three-dimensional model for quantification of oxygen diffusion from preglomerular arteries to renal tissue and renal venous blood. *Am J Physiol Renal Physiol.* 2017;313:F237–F253.
72. Evans RG, Gardiner BS, Smith DW, et al. Intrarenal oxygenation: unique challenges and the biophysical basis of homeostasis. *Am J Physiol Renal Physiol.* 2008;295:F1259–F1270.
73. Neuhofer W, Beck FX. Cell survival in the hostile environment of the renal medulla. *Annu Rev Physiol.* 2005;67:531–555.
74. Chen J, Edwards A, Layton AT. A mathematical model of O₂ transport in the rat outer medulla. II. Impact of outer medullary architecture. *Am J Physiol Renal Physiol.* 2009;297:F537–F548.
75. Chen J, Layton AT, Edwards A. A mathematical model of O₂ transport in the rat outer medulla. I. Model formulation and baseline results. *Am J Physiol Renal Physiol.* 2009;297:F517–F536.
76. Edwards A. Modeling transport in the kidney: investigating function and dysfunction. *Am J Physiol Renal Physiol.* 2010;298:F475–F484.
77. Blantz RC, Deng A, Miracle CM, et al. Regulation of kidney function and metabolism: a question of supply and demand. *Trans Am Clin Climatol Assoc.* 2007;118:23–43.
78. Thomson SC, Blantz RC. Glomerulotubular balance, tubuloglomerular feedback, and salt homeostasis. *J Am Soc Nephrol.* 2008;19:2272–2275.
79. Du Z, Duan Y, Yan Q, et al. Mechanosensory function of microvilli of the kidney proximal tubule. *Proc Natl Acad Sci U S A.* 2004;101:13068–13073.
80. Wang T, Weinbaum S, Weinstein AM. Regulation of glomerulotubular balance: flow-activated proximal tubule function. *Pflugers Arch.* 2017;469:643–654.
81. Lorenz JN, Dostanic-Larson I, Shull GE, et al. Ouabain inhibits tubuloglomerular feedback in mutant mice with ouabain-sensitive alphal Na₊K₊-ATPase. *J Am Soc Nephrol.* 2006;17:2457–2463.
82. Bell PD, Lapointe JY, Sabirov R, et al. Macula densa cell signaling involves ATP release through a maxi anion channel. *Proc Natl Acad Sci U S A.* 2003;100:4322–4327.
83. Schnermann J, Briggs JP. Tubuloglomerular feedback: mechanistic insights from gene-manipulated mice. *Kidney Int.* 2008;74:418–426.
84. Schurek HJ, Johns O. Is tubuloglomerular feedback a tool to prevent nephron oxygen deficiency? *Kidney Int.* 1997;51:386–392.
85. Nishiyama A, Majid DS, Taher KA, et al. Relation between renal interstitial ATP concentrations and autoregulation-mediated changes in renal vascular resistance. *Circ Res.* 2000;86:656–662.
86. Herrera M, Ortiz PA, Garvin JL. Regulation of thick ascending limb transport: role of nitric oxide. *Am J Physiol Renal Physiol.* 2006;290:F1279–F1284.
87. Lear S, Silva P, Kelley VE, et al. Prostaglandin E2 inhibits oxygen consumption in rabbit medullary thick ascending limb. *Am J Physiol.* 1990;258:F1372–F1378.
88. Vallon V. P2 receptors in the regulation of renal transport mechanisms. *Am J Physiol Renal Physiol.* 2008;294:F10–F27.
89. Vallon V, Muhlbauer B, Osswald H. Adenosine and kidney function. *Physiol Rev.* 2006;86:901–940.
90. Kiil F, Aukland K, Refsum HE. Renal sodium transport and oxygen consumption. *Am J Physiol.* 1961;201:511–516.
91. Knox FG, Fleming JS, Rennie DW. Effects of osmotic diuresis on sodium reabsorption and oxygen consumption of kidney. *Am J Physiol.* 1966;210:751–759.
92. Thurau K. Renal Na-reabsorption and O₂-uptake in dogs during hypoxia and hydrochlorothiazide infusion. *Proc Soc Exp Biol Med.* 1961;106:714–717.
93. Torelli G, Milla E, Faelli A, et al. Energy requirement for sodium reabsorption in the in vivo rabbit kidney. *Am J Physiol.* 1966;211:576–580.
94. Burg M, Good D. Sodium chloride coupled transport in mammalian nephrons. *Annu Rev Physiol.* 1983;45:533–547.
95. Yu ASL. Paracellular transport and energy utilization in the renal tubule. *Curr Opin Nephrol Hypertens.* 2017;26:398–404.
96. Fromter E, Rumrich G, Ullrich KJ. Phenomenologic description of Na⁺, Cl⁻ and HCO₃⁻ absorption from proximal tubules of rat kidney. *Pflugers Arch.* 1973;343:189–220.
97. Neumann KH, Rector FC Jr. Mechanism of NaCl and water reabsorption in the proximal convoluted tubule of rat kidney. *J Clin Invest.* 1976;58:1110–1118.
98. Andreoli TE, Schafer JA, Troutman SL, et al. Solvent drag component of Cl⁻ flux in superficial proximal straight tubules: evidence for a paracellular component of isotonic fluid absorption. *Am J Physiol.* 1979;237:F455–F462.
99. Mathisen O, Monclair T, Kiil F. Oxygen requirement of bicarbonate-dependent sodium reabsorption in the dog kidney. *Am J Physiol.* 1980;238:F175–F180.
100. Ostensen J, Stokke ES, Hartmann A, et al. Low oxygen cost of carbonic anhydrase-dependent sodium reabsorption in the dog kidney. *Acta Physiol Scand.* 1989;137:189–198.
101. Deng A, Miracle CM, Lortie M, et al. Kidney oxygen consumption, carbonic anhydrase, and proton secretion. *Am J Physiol Renal Physiol.* 2006;290:F1009–F1015.
102. Hebert SC. Roles of Na-K-2Cl and Na-Cl cotransporters and ROMK potassium channels in urinary concentrating mechanism. *Am J Physiol.* 1998;275:F325–F327.
103. Hebert SC, Andreoli TE. Ionic conductance pathways in the mouse medullary thick ascending limb of henle. The paracellular pathway and electrogenic Cl⁻ absorption. *J Gen Physiol.* 1986;87:567–590.
104. Silva P, Torretti J, Hayslett JP, et al. Relation between Na-K-ATPase activity and respiratory rate in the rat kidney. *Am J Physiol.* 1976;230:1432–1438.
105. Johannessen J, Lie M, Mathisen O, et al. Dopamine-induced dissociation between renal metabolic rate and sodium reabsorption. *Am J Physiol.* 1976;230:1126–1131.
106. Aperia A, Bertorello A, Seri I. Dopamine causes inhibition of Na⁺-K⁺-ATPase activity in rat proximal convoluted tubule segments. *Am J Physiol.* 1987;252:F39–F45.
107. Aperia AC. Intrarenal dopamine: a key signal in the interactive regulation of sodium metabolism. *Annu Rev Physiol.* 2000;62:621–647.
108. Weinstein SW, Szymewicz J. Individual nephron function and renal oxygen consumption in the rat. *Am J Physiol.* 1974;227:171–177.
109. Weinstein SW, Szymewicz J. Single-nephron function and renal oxygen consumption during rapid volume expansion. *Am J Physiol.* 1976;231:1166–1172.
110. Layton AT, Vallon V, Edwards A. A computational model for simulating solute transport and oxygen consumption along the nephrons. *Am J Physiol Renal Physiol.* 2016;311:F1378–F1390.

111. Layton AT, Laghmani K, Vallon V, et al. Solute transport and oxygen consumption along the nephrons: effects of Na^+ transport inhibitors. *Am J Physiol Renal Physiol.* 2016;311:F1217–F1229.
112. Thomson SC, Blantz RC. Biophysical basis of glomerular filtration. In: Alpern RJ, Herbert SC, eds. *Seldin and Giebisch's The Kidney Physiology and Pathophysiology*. Elsevier/Academic Press; 2007:565–588.
113. Ren Y, Garvin JL, Carretero OA. Efferent arteriole tubuloglomerular feedback in the renal nephron. *Kidney Int.* 2001;59:222–229.
114. Evans RG, Harrop GK, Ngo JP, et al. Basal renal O_2 consumption and the efficiency of O_2 utilization for Na^+ reabsorption. *Am J Physiol Renal Physiol.* 2014;306:F551–F560.
115. Ekberg K, Landau BR, Wajngot A, et al. Contributions by kidney and liver to glucose production in the postabsorptive state and after 60 h of fasting. *Diabetes.* 1999;48:292–298.
116. Mithieux G, Gautier-Stein A, Rajas F, et al. Contribution of intestine and kidney to glucose fluxes in different nutritional states in rat. *Comp Biochem Physiol B Biochem Mol Biol.* 2006;143:195–200.
117. Mandel LJ, Balaban RS. Stoichiometry and coupling of active transport to oxidative metabolism in epithelial tissues. *Am J Physiol.* 1981;240:F357–F371.
118. Soltóff SP. ATP and the regulation of renal cell function. *Annu Rev Physiol.* 1986;48:9–31.
119. Deng A, Miracle CM, Suarez JM, et al. Oxygen consumption in the kidney: effects of nitric oxide synthase isoforms and angiotensin II. *Kidney Int.* 2005;68:723–730.
120. Laycock SK, Vogel T, Forfia PR, et al. Role of nitric oxide in the control of renal oxygen consumption and the regulation of chemical work in the kidney. *Circ Res.* 1998;82:1263–1271.
121. Yip KP. Flash photolysis of caged nitric oxide inhibits proximal tubular fluid reabsorption in free-flow nephron. *Am J Physiol Regul Integr Comp Physiol.* 2005;289:R620–R626.
122. Beltran B, Mathur A, Duchen MR, et al. The effect of nitric oxide on cell respiration: a key to understanding its role in cell survival or death. *Proc Natl Acad Sci U S A.* 2000;97:14602–14607.
123. Borutaite V, Brown GC. Rapid reduction of nitric oxide by mitochondria, and reversible inhibition of mitochondrial respiration by nitric oxide. *Biochem J.* 1996;315(Pt 1):295–299.
124. Kovisto A, Pittner J, Froelich M, et al. Oxygen-dependent inhibition of respiration in isolated renal tubules by nitric oxide. *Kidney Int.* 1999;55:2368–2375.
125. De Nicola L, Blantz RC, Gabbai FB. Nitric oxide and angiotensin II. Glomerular and tubular interaction in the rat. *J Clin Invest.* 1992;89:1248–1256.
126. De Nicola L, Blantz RC, Gabbai FB. Renal functional reserve in the early stage of experimental diabetes. *Diabetes.* 1992;41:267–273.
127. De Nicola L, Blantz RC, Gabbai FB. Renal functional reserve in treated and untreated hypertensive rats. *Kidney Int.* 1991;40:406–412.
128. De Nicola L, Keiser JA, Blantz RC, et al. Angiotensin II and renal functional reserve in rats with Goldblatt hypertension. *Hypertension.* 1992;19:790–794.
129. Welch WJ, Blau J, Xie H, et al. Angiotensin-induced defects in renal oxygenation: role of oxidative stress. *Am J Physiol Heart Circ Physiol.* 2005;288:H22–H28.
130. Gonzalez-Villalobos RA, Janjoulia T, Fletcher NK, et al. The absence of intrarenal ACE protects against hypertension. *J Clin Invest.* 2013;123:2011–2023.
131. Nguyen MT, Lee DH, Delpire E, et al. Differential regulation of Na^+ transporters along nephron during ANG II-dependent hypertension: distal stimulation counteracted by proximal inhibition. *Am J Physiol Renal Physiol.* 2013;305:F510–F519.
132. Welch WJ, Baumgartl H, Lubbers D, et al. Renal oxygenation defects in the spontaneously hypertensive rat: role of AT1 receptors. *Kidney Int.* 2003;63:202–208.
133. Adler S, Huang H, Wolin MS, et al. Oxidant stress leads to impaired regulation of renal cortical oxygen consumption by nitric oxide in the aging kidney. *J Am Soc Nephrol.* 2004;15:52–60.
134. Kobori H, Nangaku M, Navar LG, et al. The intrarenal renin-angiotensin system: from physiology to the pathobiology of hypertension and kidney disease. *Pharmacol Rev.* 2007;59:251–287.
135. Navar LG, Harrison-Bernard LM, Imig JD, et al. Intrarenal angiotensin II generation and renal effects of AT1 receptor blockade. *J Am Soc Nephrol.* 1999;10(suppl 12):S266–S272.
136. Rohrwitter A, Morgan T, Dillon HF, et al. Elements of a paracrine tubular renin-angiotensin system along the entire nephron. *Hypertension.* 1999;34:1265–1274.
137. Thomson SC, Deng A, Wead L, et al. An unexpected role for angiotensin II in the link between dietary salt and proximal reabsorption. *J Clin Invest.* 2006;116:1110–1116.
138. Shao W, Seth DM, Prieto MC, et al. Activation of the renin-angiotensin system by a low-salt diet does not augment intratubular angiotensinogen and angiotensin II in rats. *Am J Physiol Renal Physiol.* 2013;304:F505–F514.
139. Deng A, Tang T, Singh P, et al. Regulation of oxygen utilization by angiotensin II in chronic kidney disease. *Kidney Int.* 2009;75:197–204.
140. Harris DC, Chan L, Schrier RW. Remnant kidney hypermetabolism and progression of chronic renal failure. *Am J Physiol.* 1988;254:F267–F276.
141. Nath KA, Croatt AJ, Hostetter TH. Oxygen consumption and oxidant stress in surviving nephrons. *Am J Physiol.* 1990;258:F1354–F1362.
142. Toma I, Kang JJ, Sipos A, et al. Succinate receptor GPR91 provides a direct link between high glucose levels and renin release in murine and rabbit kidney. *J Clin Invest.* 2008;118:2526–2534.
143. Nangaku M. Chronic hypoxia and tubulointerstitial injury: a final common pathway to end-stage renal failure. *J Am Soc Nephrol.* 2006;17:17–25.
144. Manotham K, Tanaka T, Matsumoto M, et al. Evidence of tubular hypoxia in the early phase in the remnant kidney model. *J Am Soc Nephrol.* 2004;15:1277–1288.
145. Ries M, Basseau F, Tyndal B, et al. Renal diffusion and BOLD MRI in experimental diabetic nephropathy. Blood oxygen level-dependent. *J Magn Reson Imaging.* 2003;17:104–113.
146. Gloviczki ML, Glockner JF, Lerman LO, et al. Preserved oxygenation despite reduced blood flow in poststenotic kidneys in human atherosclerotic renal artery stenosis. *Hypertension.* 2010.
147. Carey RM. Are kidneys not ischemic in human renal vascular disease? *Hypertension.* 2010.
148. Inoue T, Kozawa E, Okada H, et al. Noninvasive evaluation of kidney hypoxia and fibrosis using magnetic resonance imaging. *J Am Soc Nephrol.* 2011;22:1429–1434.
149. Yin WJ, Liu F, Li XM, et al. Noninvasive evaluation of renal oxygenation in diabetic nephropathy by BOLD-MRI. *Eur J Radiol.* 2012;81:1426–1431.
150. Sadowski EA, Fain SB, Alford SK, et al. Assessment of acute renal transplant rejection with blood oxygen level-dependent MR imaging: initial experience. *Radiology.* 2005;236:911–919.
151. Pruijm M, Hofmann L, Maillard M, et al. Effect of sodium loading/depletion on renal oxygenation in young normotensive and hypertensive men. *Hypertension.* 2010;55:1116–1122.
152. Pruijm M, Hofmann L, Piskunowicz M, et al. Determinants of renal tissue oxygenation as measured with BOLD-MRI in chronic kidney disease and hypertension in humans. *PLoS ONE.* 2014;9:e95895.
153. Pruijm M, Hofmann L, Vogt B, et al. Renal tissue oxygenation in essential hypertension and chronic kidney disease. *Int J Hypertens.* 2013;2013:696598.
154. Legrand M, Almac E, Mik EG, et al. L-NIL prevents renal microvascular hypoxia and increase of renal oxygen consumption after ischemia-reperfusion in rats. *Am J Physiol Renal Physiol.* 2009;296:F1109–F1117.
155. Siegmund M, van Bommel J, Stegenga ME, et al. Aortic cross-clamping and reperfusion in pigs reduces microvascular oxygenation by altered systemic and regional blood flow distribution. *Anesth Analg.* 2010;111:345–353.
156. Bullen A, Liu ZZ, Hepokoski M, et al. Renal oxygenation and hemodynamics in kidney injury. *Nephron.* 2017;137:260–263.
157. Tran M, Tam D, Bardia A, et al. PGC-1alpha promotes recovery after acute kidney injury during systemic inflammation in mice. *J Clin Invest.* 2011;121:4003–4014.
158. Wang Z, Holthoff JH, Seely KA, et al. Development of oxidative stress in the peritubular capillary microenvironment mediates sepsis-induced renal microcirculatory failure and acute kidney injury. *Am J Pathol.* 2012;180:505–516.
159. Heemskerk AE, Huisman E, van Lambalgen AA, et al. Renal function and oxygen consumption during bacteraemia and endotoxaemia in rats. *Nephrol Dial Transplant.* 1997;12:1586–1594.
160. Porta F, Takala J, Weikert C, et al. Effects of prolonged endotoxemia on liver, skeletal muscle and kidney mitochondrial function. *Crit Care.* 2006;10:R118.

155.e4 SECTION I – NORMAL STRUCTURE AND FUNCTION

162. Redfors B, Bragadottir G, Sellgren J, et al. Acute renal failure is NOT an “acute renal success”—a clinical study on the renal oxygen supply/demand relationship in acute kidney injury. *Crit Care Med.* 2010;38:1695–1701.
163. Sward K, Valsson F, Sellgren J, et al. Differential effects of human atrial natriuretic peptide and furosemide on glomerular filtration rate and renal oxygen consumption in humans. *Intensive Care Med.* 2005;31:79–85.
164. Semenza GL. Regulation of oxygen homeostasis by hypoxia-inducible factor 1. *Physiology (Bethesda)*. 2009;24:97–106.
165. Semenza GL. Hypoxia-inducible factors in physiology and medicine. *Cell*. 2012;148:399–408.
166. Semenza GL. Oxygen sensing, hypoxia-inducible factors, and disease pathophysiology. *Annu Rev Pathol*. 2014;9:47–71.
167. Semenza GL. Oxygen sensing, homeostasis, and disease. *N Engl J Med*. 2011;365:537–547.
168. Gunaratnam L, Bonventre JV. HIF in kidney disease and development. *J Am Soc Nephrol*. 2009;20:1877–1887.
169. Haase VH. Hypoxia-inducible factors in the kidney. *Am J Physiol Renal Physiol*. 2006;291:F271–F281.
170. Haase VH. Mechanisms of hypoxia responses in renal tissue. *J Am Soc Nephrol*. 2013;24:537–541.
171. Rosenberger C, Mandriota S, Jurgensen JS, et al. Expression of hypoxia-inducible factor-1alpha and -2alpha in hypoxic and ischemic rat kidneys. *J Am Soc Nephrol*. 2002;13:1721–1732.
172. Haase VH. Regulation of erythropoiesis by hypoxia-inducible factors. *Blood Rev*. 2013;27:41–53.
173. Tanaka T, Nangaku M. Angiogenesis and hypoxia in the kidney. *Nat Rev Nephrol*. 2013;9:211–222.
174. Papandreou I, Cairns RA, Fontana L, et al. HIF-1 mediates adaptation to hypoxia by actively downregulating mitochondrial oxygen consumption. *Cell Metab*. 2006;3:187–197.
175. Wheaton WW, Chandel NS. Hypoxia. 2. Hypoxia regulates cellular metabolism. *Am J Physiol Cell Physiol*. 2011;300:C385–C393.
176. Zhang H, Bosch-Marce M, Shimoda LA, et al. Mitochondrial autophagy is an HIF-1-dependent adaptive metabolic response to hypoxia. *J Biol Chem*. 2008;283:10892–10903.
177. Li N, Chen L, Yi F, et al. Salt-sensitive hypertension induced by decoy of transcription factor hypoxia-inducible factor-1alpha in the renal medulla. *Circ Res*. 2008;102:1101–1108.
178. Wang Z, Zhu Q, Xia M, et al. Hypoxia-inducible factor prolyl-hydroxylase 2 senses high-salt intake to increase hypoxia inducible factor 1alpha levels in the renal medulla. *Hypertension*. 2010;55:1129–1136.
179. Manotham K, Tanaka T, Ohse T, et al. A biologic role of HIF-1 in the renal medulla. *Kidney Int*. 2005;67:1428–1439.
180. Sugahara M, Tanaka T, Nangaku M. Prolyl hydroxylase domain inhibitors as a novel therapeutic approach against anemia in chronic kidney disease. *Kidney Int*. 2017;92:306–312.
181. Pergola PE, Spinowitz BS, Hartman CS, et al. Vaddadustat, a novel oral HIF stabilizer, provides effective anemia treatment in nondialysis-dependent chronic kidney disease. *Kidney Int*. 2016;90:1115–1122.
182. Provenzano R, Besarab A, Sun CH, et al. Oral hypoxia-inducible factor prolyl hydroxylase inhibitor roxadustat (FG-4592) for the treatment of anemia in patients with CKD. *Clin J Am Soc Nephrol*. 2016;11:982–991.
183. Besarab A, Chernyavskaya E, Motylev I, et al. Roxadustat (FG-4592): correction of anemia in incident dialysis patients. *J Am Soc Nephrol*. 2016;27:1225–1233.
184. Holdstock L, Meadowcroft AM, Maier R, et al. Four-week studies of oral hypoxia-inducible factor-prolyl hydroxylase inhibitor GSK1278863 for treatment of anemia. *J Am Soc Nephrol*. 2016;27:1234–1244.
185. Steinberg GR, Kemp BE. AMPK in health and disease. *Physiol Rev*. 2009;89:1025–1078.
186. Hardie DG. AMP-activated protein kinase: maintaining energy homeostasis at the cellular and whole-body levels. *Annu Rev Nutr*. 2014;34:31–55.
187. Gwinn DM, Shackelford DB, Egan DF, et al. AMPK phosphorylation of raptor mediates a metabolic checkpoint. *Mol Cell*. 2008;30:214–226.
188. Klionsky DJ. Autophagy. *Curr Biol*. 2005;15:R282–R283.
189. Meley D, Bauvy C, Houben-Weerts JH, et al. AMP-activated protein kinase and the regulation of autophagic proteolysis. *J Biol Chem*. 2006;281:34870–34879.
190. Hallows KR. Emerging role of AMP-activated protein kinase in coupling membrane transport to cellular metabolism. *Curr Opin Nephrol Hypertens*. 2005;14:464–471.
191. Hallows KR, Mount PF, Pastor-Soler NM, et al. Role of the energy sensor AMP-activated protein kinase in renal physiology and disease. *Am J Physiol Renal Physiol*. 2010;298:F1067–F1077.
192. Pastor-Soler NM, Hallows KR. AMP-activated protein kinase regulation of kidney tubular transport. *Curr Opin Nephrol Hypertens*. 2012;21:523–533.
193. Vadasz I, Dada LA, Briva A, et al. AMP-activated protein kinase regulates CO₂-induced alveolar epithelial dysfunction in rats and human cells by promoting Na,K-ATPase endocytosis. *J Clin Invest*. 2008;118:752–762.
194. Zheng D, Perianayagam A, Lee DH, et al. AMPK activation with AICAR provokes an acute fall in plasma [K⁺]. *Am J Physiol Cell Physiol*. 2008;294:C126–C135.
195. Alves DS, Farr GA, Seo-Mayer P, et al. AS160 associates with the Na⁺,K⁺-ATPase and mediates the adenosine monophosphate-stimulated protein kinase-dependent regulation of sodium pump surface expression. *Mol Biol Cell*. 2010;21:4400–4408.
196. Fraser S, Mount P, Hill R, et al. Regulation of the energy sensor AMP-activated protein kinase in the kidney by dietary salt intake and osmolality. *Am J Physiol Renal Physiol*. 2005;288:F578–F586.
197. Li H, Thali RF, Smolak C, et al. Regulation of the creatine transporter by AMP-activated protein kinase in kidney epithelial cells. *Am J Physiol Renal Physiol*. 2010;299:F167–F177.
198. Huang DY, Gao H, Boini KM, et al. In vivo stimulation of AMP-activated protein kinase enhanced tubuloglomerular feedback but reduced tubular sodium transport during high dietary NaCl intake. *Pflugers Arch*. 2010;460:187–196.
199. Lee MJ, Feliers D, Mariappan MM, et al. A role for AMP-activated protein kinase in diabetes-induced renal hypertrophy. *Am J Physiol Renal Physiol*. 2007;292:F617–F627.
200. Decleves AE, Zolkipli Z, Satriano J, et al. Regulation of lipid accumulation by AMP-activated kinase [corrected] in high fat diet-induced kidney injury. *Kidney Int*. 2014;85:611–623.
201. Li H, Satriano J, Thomas JL, et al. Interactions between HIF-1alpha and AMPK in the regulation of cellular hypoxia adaptation in chronic kidney disease. *Am J Physiol Renal Physiol*. 2015;309:F414–F428.
202. Dugan LL, You YH, Ali SS, et al. AMPK dysregulation promotes diabetes-related reduction of superoxide and mitochondrial function. *J Clin Invest*. 2013;123:4888–4899.
203. Han SH, Malaga-Dieguez L, Chinga F, et al. Deletion of Lkb1 in renal tubular epithelial cells leads to CKD by altering metabolism. *J Am Soc Nephrol*. 2016;27:439–453.
204. Lieberthal W, Tang M, Zhang L, et al. Susceptibility to ATP depletion of primary proximal tubular cell cultures derived from mice lacking either the alpha1 or the alpha2 isoform of the catalytic domain of AMPK. *BMC Nephrol*. 2013;14:251.
205. Mount PF, Gleich K, Tam S, et al. The outcome of renal ischemia-reperfusion injury is unchanged in AMPK-beta1 deficient mice. *PLoS ONE*. 2012;7:e29887.
206. Pan JS, Huang L, Belousova T, et al. Stanniocalcin-1 inhibits renal Ischemia/reperfusion injury via an AMP-activated protein kinase-dependent pathway. *J Am Soc Nephrol*. 2014.
207. Wang LT, Chen BL, Wu CT, et al. Protective role of AMP-activated protein kinase-evoked autophagy on an in vitro model of ischemia/reperfusion-induced renal tubular cell injury. *PLoS ONE*. 2013;8:e79814.
208. Rowe I, Chiaravalli M, Mannella V, et al. Defective glucose metabolism in polycystic kidney disease identifies a new therapeutic strategy. *Nat Med*. 2013;19:488–493.
209. Chiaravalli M, Rowe I, Mannella V, et al. 2-deoxy-d-glucose ameliorates PKD progression. *J Am Soc Nephrol*. 2016;27:1958–1969.
210. Kang HM, Ahn SH, Choi P, et al. Defective fatty acid oxidation in renal tubular epithelial cells has a key role in kidney fibrosis development. *Nat Med*. 2015;21:37–46.
211. Sas KM, Kayampilly P, Byun J, et al. Tissue-specific metabolic reprogramming drives nutrient flux in diabetic complications. *JCI Insight*. 2016;1:e86976.
212. Di Donato S. Multisystem manifestations of mitochondrial disorders. *J Neurol*. 2009;256:693–710.
213. Niaudet P, Rotig A. The kidney in mitochondrial cytopathies. *Kidney Int*. 1997;51:1000–1007.
214. Forbes JM, Thorburn DR. Mitochondrial dysfunction in diabetic kidney disease. *Nat Rev Nephrol*. 2018;14:291–312.

215. Bhargava P, Schnellmann RG. Mitochondrial energetics in the kidney. *Nat Rev Nephrol.* 2017;13:629–646.
216. Sharma K, Karl B, Mathew AV, et al. Metabolomics reveals signature of mitochondrial dysfunction in diabetic kidney disease. *J Am Soc Nephrol.* 2013;24:1901–1912.
217. Thomas JL, Pham H, Li Y, et al. Hypoxia-inducible factor-1alpha activation improves renal oxygenation and mitochondrial function in early chronic kidney disease. *Am J Physiol Renal Physiol.* 2017;313:F282–F290.
218. Tin A, Grams ME, Ashar FN, et al. Association between mitochondrial DNA copy number in peripheral blood and incident CKD in the atherosclerosis risk in communities study. *J Am Soc Nephrol.* 2016;27:2467–2473.
219. Brooks C, Wei Q, Cho SG, et al. Regulation of mitochondrial dynamics in acute kidney injury in cell culture and rodent models. *J Clin Invest.* 2009;119:1275–1285.
220. Hall AM, Rhodes GJ, Sandoval RM, et al. In vivo multiphoton imaging of mitochondrial structure and function during acute kidney injury. *Kidney Int.* 2013;83:72–83.
221. Funk JA, Schnellmann RG. Persistent disruption of mitochondrial homeostasis after acute kidney injury. *Am J Physiol Renal Physiol.* 2012;302:F853–F864.
222. Jesinkey SR, Funk JA, Stallons LJ, et al. Formoterol restores mitochondrial and renal function after ischemia-reperfusion injury. *J Am Soc Nephrol.* 2014;25:1157–1162.
223. Szeto HH. Pharmacologic approaches to improve mitochondrial function in AKI and CKD. *J Am Soc Nephrol.* 2017;28:2856–2865.